UNSW SYDNEY | Australia's Global University

Australian Centre for Advanced Photovoltaics
Australia-US Institute for Advanced Photovoltaics

Annual Report 2016

Table of Contents

1. Director's Report

Solar photovoltaics involves the direct generation of electricity from sunlight, when it shines upon devices known as solar cells. Silicon is the most common material used to make these photovoltaic cells, similarly to its key role in microelectronics, although several other photovoltaic materials are being actively investigated.

During 2016, it became very clear that photovoltaics now provides the lowest cost option for electricity production yet developed. In August 2016, bids were submitted for the long-term supply of electricity in Chile using solar photovoltaics at US$29.10/MWh, appreciably lower than from any other bidding technology including coal, where the corresponding bid was nearly twice as high at US$57/MWh (itself quite low by international standards, with Bloomberg estimating the cost of electricity from a new black coal plant in Australia in 2016 at an appreciably higher AUD$120/MWh).

The following month (September 2016) an even lower bid of US$24.20/MWh was made for the supply of photovoltaic-generated electricity in Abu Dhabi, lower than even the short-run marginal cost of generation from many existing Australian black coal plants. There are two exciting aspects to these developments. One is that photovoltaic costs will continue to decrease, with analysts expecting module prices to reduce by over 10% in 2017, with further reductions over the coming decade. The other is that Australia has played a major role in achieving past cost reductions and is expected to play a key role in future cost reductions through the activities of the Australian Centre for Advanced Photovoltaics (ACAP), documented in this 2016 Annual Report.

The transformation of the manufacturing industry that has led to the recent low costs was spearheaded by multiple Australian joint ventures in Asia. Complementing this, as Prime Minister Malcolm Turnbull reported in his speech to the United Nations Climate Change Conference in Paris at the end of 2015, Australian researchers have "held the world record for solar cell efficiency for 30 of the last 32 years" with the majority of the world's solar cells soon to use technology developed by Australian researchers. The latter refers to the Australian-developed PERC cell (Passivated Emitter and Rear Cell) technology, accounting for 15–20% solar cell production capacity in 2016, with rapidly accelerating market share. ACAP researchers are working closely with manufacturers to further increase PERC performance while reducing costs.

This is the fourth annual ACAP report also incorporating that of the Australia–US Institute for Advanced Photovoltaics (AUSIAPV), supported by the Australian Government through the Australian Renewable Energy Agency (ARENA). ACAP encompasses the activities of Australian-based researchers while, through synergistic research activities with US partners, AUSIAPV aims to significantly accelerate photovoltaic development beyond that achievable by Australia or the US individually. This objective is to be reached by leveraging development of "over the horizon" photovoltaic technology, providing a pipeline of improved technology for increased performance and ongoing cost reduction.

A second aim is to provide high quality training opportunities for the next generation of photovoltaic researchers, particularly through enhanced collaborations between Australian and US researchers, with one targeted outcome being to consolidate Australia's position as the photovoltaic research and educational hub of the Asia-Pacific manufacturing region.

ACAP/AUSIAPV came into being on 1 February 2013 after the signing of a Head Agreement between the University of New South Wales (UNSW) and ARENA. During 2013, related Collaboration Agreements were signed between UNSW and the other ACAP nodes, Australian National University (ANU), University of Melbourne (UoM), Monash University, University of Queensland (UQ) and CSIRO (Materials Science and Engineering, Melbourne), and additionally with the ACAP industrial partners, Suntech Research and Development, Australia (SRDA) (partnership now transferred to Wuxi Suntech Power Co., Ltd.), Trina Solar Ltd, BlueScope Steel and BT Imaging. Our major international partners include the NSF-DOE Engineering Research Center for Quantum Energy and Sustainable Solar Technologies (QESST) and the US National Renewable Energy Laboratory (NREL), as well as the Molecular Foundry, Berkeley, Stanford University, Georgia Institute of Technology and the University of California, Santa Barbara. Two additional agreements were signed in 2016 with Australian-based partners, PV Lighthouse and Dyesol.

This report covers the period from 1 January to 31 December 2016. Over the past four years, both ACAP and AUSIAPV have moved quickly to establish a high profile within the international research community. Following on from the world record 24.4% energy conversion efficiency rear-junction cell developed at ANU during 2013, a system based on splitting focused sunlight into different colour bands, designed and fabricated at UNSW with performance then certified by US partner NREL, became, in late 2014, the first in history to convert sunlight to electricity with over 40% energy conversion efficiency.

In 2016, an outstanding seven more world records were achieved. The earlier 40% efficiency was increased to 40.6% for the conversion of concentrated sunlight in a 200 cm^2 aperture system, with 34.5% confirmed for a standard non-concentrating (one-sun) photovoltaic 30 cm^2 minimodule using a similar approach, also based on splitting sunlight into its spectral components. This efficiency was well above the previously best value of 24%. Two additional world-record results were confirmed for "thin-film" cells made from the compound CZTS (Cu_2ZnSnS_4), based on "earth abundant", relatively benign materials. The first of these records, early in 2016, was the demonstration of 7.6% efficiency for a 1 cm^2 CZTS cell with the second, towards the end of the year, an outright record of 9.5% efficiency for a smaller area cell.

CZTS is promising in its own right as a thin-film solar cell material in competition with silicon or for combining with silicon to form high performance tandem cell stacks, where different cells in the stack respond to the different colours in sunlight, increasing conversion efficiency. This dual possibility also applies to cells made from organic-inorganic lead halide perovskite materials that have emerged, only recently since 2012, as another thin-film contender. An efficiency of 18% was independently confirmed for a 1.2 cm^2 perovskite cell, the highest ever for a cell of this size, as was the 12.1% efficiency for a much larger 16 cm^2 device. A minimodule of a similar size consisting of four cells, also briefly held the record of 11.5% efficiency for such a device.

These perovskite world records are the first significant outcomes of a new ACAP initiative that commenced during 2016, involving a coordinated perovskite program spanning all ACAP nodes. This collaboration has seen synergistic effects arising from the different node competencies quickly pushing combined capabilities to the cutting edge, as demonstrated by the above results. ACAP is well positioned to maximise Australian benefits from exploitation of this new technology, should it prove competitive. Similar benefits from collaborations facilitated by ACAP are also becoming apparent, particularly with silicon and organic cell programs.

These and several other key achievements during 2016 are summarised in the highlight pages immediately following my report. More detailed results described in the body of this 2016 Annual Report contributed to making 2016 an extremely successful year for both ACAP and AUSIAPV. These results also undoubtedly contributed to the very positive outcome of ACAP's mid-term review conducted in July with the Review Committee's report made available in October.

I would like to thank ARENA for the ongoing financial support and also for the very effective involvement of ARENA personnel in supporting the ACAP/AUSIAPV program, both informally and via the ACAP National Steering Committee and the AUSIAPV International Advisory Committee. I would additionally like to thank, in particular, all researchers affiliated with the Institute for their contributions to the broad range of progress reported in the following pages.

Finally, I am pleased to be able to report that ACAP/AUSIAPV has taken another major step towards attaining its significant long-term objectives by achieving all fourth-year milestones, on time and within budget. We look forward to similar progress in 2017 and in subsequent years.

Martin Green
Director

2. Highlights

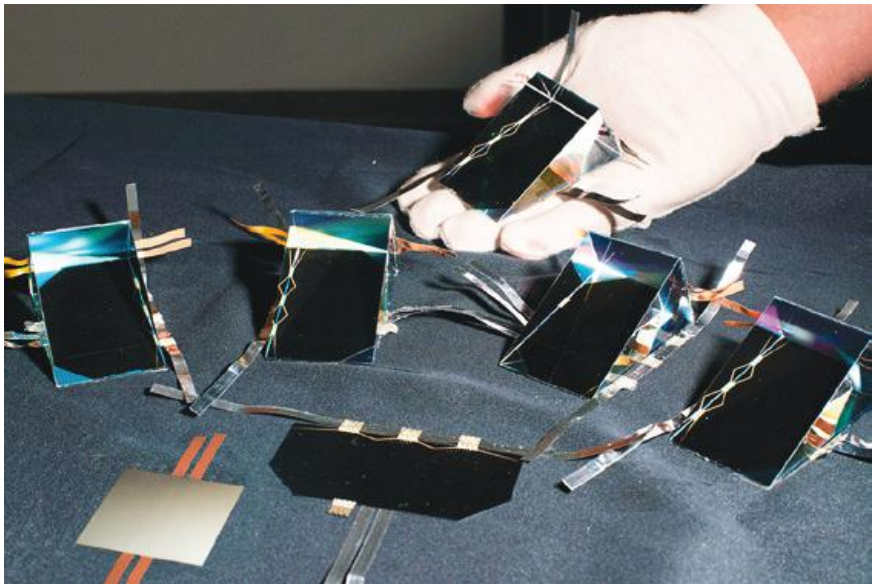

Figure 2.1: Dr Mark Keevers and colleagues at UNSW have developed a new solar cell configuration which has pushed the sunlight-to-electricity conversion efficiency to 34.5%.

New World Record for Conversion of Unconcentrated Sunlight

A new solar cell configuration developed at the UNSW node has pushed sunlight-to-electricity conversion efficiency to 34.5%, establishing a new world record for unconcentrated sunlight, confirmed by ACAP partner the US National Renewable Energy Laboratory (NREL). The record was set by Dr Mark Keevers and Prof Martin Green, using a 28 cm^2 four-junction mini-module, built around a silica prism, that steers the incoming rays onto a four-junction receiver. The mini-module combines a silicon cell on one face of the prism, with a triple-junction (indium gallium phosphide, indium gallium arsenide and germanium) tandem cell on another, while the sunlight enters through the third. Some of the infra-red band of incoming sunlight, unused by the triple-junction cell, is reflected from this cell and directed onto the silicon cell. The aim is to scale the device up to 800 cm^2 while maintaining similar efficiency.

In late news, the Museum of Applied Arts & Sciences (Sydney's "Powerhouse Museum") has featured the record-breaking mini-module mentioned in the first highlight item, above, in its popular displays.

Record 7.6% and 9.4% Efficiency CZTS Cell

The UNSW node team, led by Dr Xiaojing Hao, have achieved the world's highest efficiency rating for a 1 cm^2 area copper-zinc-tin-sulphur (CZTS) thin-film solar cell. ACAP partner, the US's NREL, confirmed this world-leading 7.6% efficiency in March 2016. Unlike most of its thin-film competitors, CZTS cells are made from abundant materials and CZTS avoids the toxicity issues associated with two of its thin-film rivals, known as CdTe (cadmium-telluride) and CIGS (copper-indium-gallium-selenide). Cadmium and selenium are toxic, while tellurium and indium are rare. In addition, CZTS can be stacked as a thin-film on top of silicon cells to ultimately improve the overall performance. UNSW is collaborating with a number of large companies keen to develop applications, including for building integration, well before it reaches its target 20% efficiency. A further step towards this efficiency was made later in 2016 with 9.5% efficiency confirmed for a smaller area 0.24cm^2 cell, also a record for a cell of this size.

Figure 2.2: The UNSW node team have developed the solar thin-filmed CZTS solar cells with world-leading 7.6% efficiency.

Record Perovskite Cells

As announced at the Asia-Pacific Solar Research Conference in Canberra in December 2016, the UNSW node team, led by Dr Anita Ho-Baillie, has achieved the highest efficiency rating with the largest perovskite solar cells to date. A 12.1% efficiency rating for a 16 cm^2 perovskite solar cell, the largest single perovskite photovoltaic cell certified with the highest energy conversion efficiency, was independently confirmed by an international testing centre, Newport Corporation, in Bozeman, Montana. The new cell is more than 10 times larger than the current certified high efficiency perovskite solar cells on record. The same team also achieved an 18% efficiency rating on a 1.2 cm^2 single perovskite cell, and 11.5% for a 16 cm^2 four-cell perovskite mini-module, both independently certified by Newport.

Perovskite is a structured compound, where a hybrid organic-inorganic lead or tin halide-based material acts as the light-harvesting active layer. They are the fastest-advancing solar technology to date, and are attractive because the compound is potentially cheap to produce, at low temperatures, and simple to manufacture, and can even be sprayed onto surfaces. Although perovskites hold much promise for cost-effective solar energy, they are currently sensitive to temperature and moisture, allowing them to last only a few months without protection. As part of its current research program, ACAP is trying to extend perovskite cell durability. The project's goal is to lift perovskite solar cell efficiency to 26%.

High Impact Papers

An additional nine papers published under the ACAP program in 2016 have already been identified as making a large impact at the international level. These have been classified as "Highly Cited Papers", earning a ranking within the top 1% in their field. Six of these have earned the additional distinction of being identified as "Hot Papers", within the top 0.1% in their field. This is a disproportionately high number relative to the ACAP total and brings the total to 32 papers earning the "Highly Cited" distinction over the first four years of ACAP operation.

Five of the 2016 "Highly Cited Papers" were based on results generated in ACAP program strand PP2: "Organic and Earth-Abundant Thin-Film Cells". The first of these, with lead author Naveen Kumar Elumalai affiliated with the UNSW Sydney node, elaborates the governing mechanisms affecting the V_{OC} of organic solar cells and analyses the interdependencies between the factors influencing this parameter, highlighting potential research strategies to improve it. Another with lead author Dian Wang, also affiliated with the UNSW Sydney node, addresses the key topic of stability issues relevant to perovskite solar cells. This paper has the

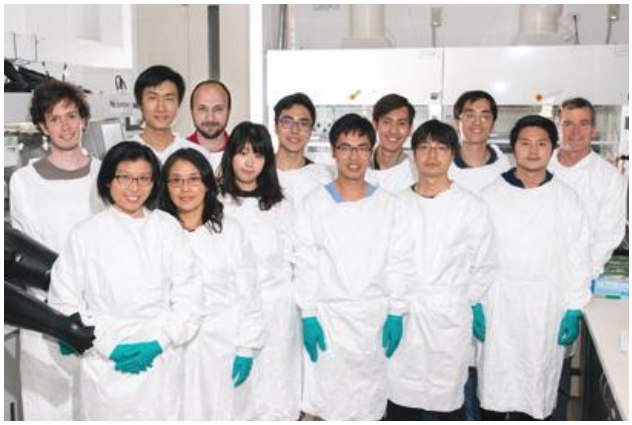

Figure 2.3: The team that developed the record perovskite cells.

additional distinction of being identified as a "Hot Paper" (within the top 0.1% in its field). Another with lead author Xiaoming Wen, also with UNSW Sydney node affiliation, studies defect trapping states and carrier recombination dynamics in organic-inorganic halide perovskites using steady state and time-resolved photoluminescence. A fourth, another "Hot Paper", with lead author Young Chan Kim from the Korean Research Institute for Chemical Technology, but with co-authors Jae Sun Yun, Anita Ho-Baillie, Shujuan Huang and Martin Green from the UNSW Sydney node, addresses the beneficial effects of incorporating PbI_2 into organo-lead halide perovskite solar cells. The final highly cited paper in the PP2 strand, with lead author Xiaolei Liu, also with the UNSW Sydney node affiliation, but additionally involving Duke University, North Carolina, addresses CZTS cell technology, focusing on the following three key aspects of the device and providing suggestions for their improvement and for future research: the interface between the CZTS absorber and the Mo back contact; bulk defects and grain boundaries; and the interface between the CZTS absorber and the buffer layer.

Two "Highly Cited Papers" were based on results generated in ACAP program strand PP1: "Silicon Cells". The first, a "Hot Paper", with lead author Evan Franklin, affiliated with the ANU node, but also involving ACAP partners PV Lighthouse and Trina Solar, documents the 24.4% interdigitated back contact (IBC) result obtained earlier in the ACAP program. A second "Hot Paper" with Andres Cuevas, affiliated with the ANU node as one co-author, reviews high efficiency silicon photovoltaics from a device-engineering perspective, discusses key factors responsible for the success of the classic dopant-diffused silicon cell, analyses two high efficiency device architectures, the IBC and the silicon heterojunction cell, and, finally, summarises pathways for further efficiency improvements and cost reduction.

The final two "Highly Cited Papers" arose from collaboration between AUSIAPV partners, UNSW and Colorado-based NREL, documenting recent efficiency

improvements in photovoltaics across a range of technologies, including the recent UNSW 40.6% sunlight to electricity concentrator submodule, the 34.5% one-sun minimodule, record 7.6% and 9.5% CZTS cell results, 11.5% for a perovskite minimodule and the record 21.3% result for multicrystalline silicon obtained by ACAP industrial partner, Trina Solar, using UNSW-developed PERC (Passivated Emitter and Rear Cell) technology. Both papers also received the additional "Hot Paper" distinction, being within the top 0.1% in their field.

The article, "High efficiency rubidium incorporated perovskite solar cells by gas quenching" by a UNSW team of Meng Zhang, Jae Sung Yun, Qingshan Ma, Jianghui Zheng, Cho-Fai Jonathan Lau, Xiaofan Deng, Jincheol Kim, Dohyung Kim, Jan Seidel, Martin Green, Shujuan Huang and Anita Ho-Baillie, was among the most read articles in American Chemical Society's ACS Energy Letters for February 2017. The team applied gas quenching to fabricate perovskite films incorporating rubidium for high efficiency perovskite solar cells achieving 20% power conversion efficiency on a 65 mm^2 device.

From a slightly different perspective, Australia published 3.7% of all papers between 2013-2016 with "Perovskite Solar Cell" included in the title, but 9.5% in the highest impact category of "Hot Papers", according to the Web of Science. Similarly, Australia published 7.4% of all papers with "Silicon Solar Cell" in the title over the same period, but a massive 13.3% in the top category of "Highly Cited Papers", if perovskite and graphene papers are excluded. All the papers in the most highly cited category had ACAP authorship in both cases.

Opposition Leader Bill Shorten Visits ACAP Nodes

The Monash, ANU and UNSW nodes of ACAP all hosted visits by the Leader of the Opposition in the lead-up to the 2016 Federal Election.

Figure 2.4: Dr Mark Keevers, UNSW, explains the record-performance spectrum-splitting prismatic mini-module to Leader of the Opposition, Hon Bill Shorten MP, and Member for Kingsford Smith, Hon Matt Thistlethwaite MP on the roof of the Tyree Energy Technologies Building at UNSW on 2 July 2016.

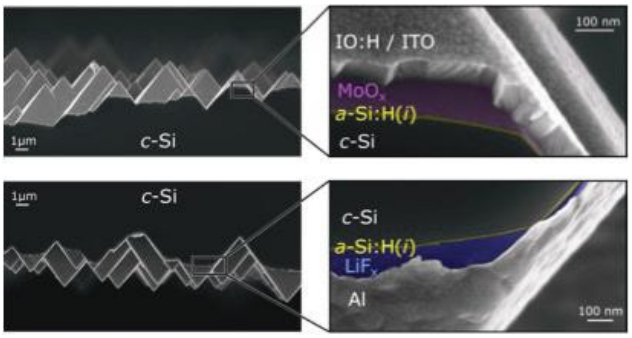

Figure 2.5: ANU's dopant-free heterocontact silicon solar cells with efficiencies of ~20%

Novel Silicon Solar Cells with Passivating Contacts

Most photovoltaic systems are based on crystalline silicon solar cells, which keep getting cheaper and better. Further progress hinges upon the use of "passivating contacts" to selectively transport electrons and holes towards the cell's terminals. As an example, ANU PhD student Di Yan has developed 21.1% efficient cells with a rear passivating contact based on a tunnelling oxide coated with polysilicon. In an alternative pathway, ACAP is investigating a wide range of materials, many of them transparent, that can be deposited at low temperatures, thus simplifying the fabrication of high efficiency silicon solar cells. Recently, ANU's James Bullock and collaborators from the University of California at Berkeley and École Polytechnique Fédérale de Lausanne in Switzerland have demonstrated a dopant-free silicon cell, referred to as a DASH (dopant free asymmetric heterocontact) cell, with an efficiency of 19.4%. PhD students Thomas Allen and James Bullock, with co-workers, have applied materials like lithium fluoride, calcium and titanium oxide to make first-of-a-kind n-type silicon solar cells with partial-area rear contacts, achieving efficiencies in the range of 20.6% to 21.8%. See Section 6.7 for more information.

Direct Observation of Intrinsic Twin Domains in Tetragonal $CH_3NH_3PbI_3$

Organic-inorganic hybrid perovskites are exciting candidates for next generation solar cells, with $CH_3NH_3PbI_3$ being one of the most widely studied. While there have been intense efforts to fabricate and optimise photovoltaic devices using $CH_3NH_3PbI_3$, critical questions remain regarding the crystal structure that governs the unique properties of the hybrid perovskite material. A team with membership from CSIRO, the Melbourne Centre for Nano Fabrication, Monash University and Wuhan University of Technology has provided direct and unequivocal evidence, by using transmission electron microscopy, for the existence and crystallography of twin domains in tetragonal methylammonium lead tri-iodide

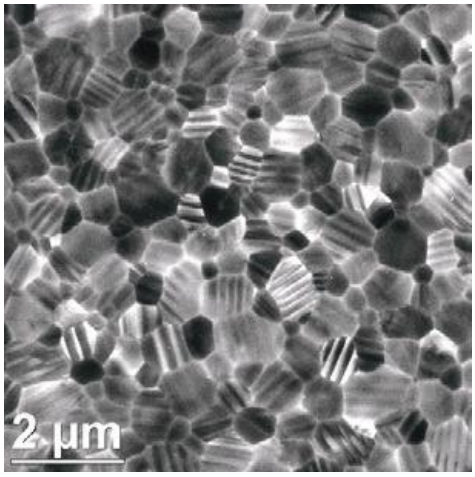

Figure 2.6: Crystallographic twin in hybrid perovskite materials. Bright field TEM image of a $CH_3NH_3PbI_3$ thin film at room temperature shows clearly twinning bands in perovskite grains.

($CH_3NH_3PbI_3$) thin films used for solar cell applications. These twins have eluded observation so far, possibly due to their very fragile nature under the electron beam, as well as the inherent instability of the material itself. Given the scale of these domains is comparable to the thickness of typical methylammonium lead iodide perovskite layers used in solar cells, and given that the twinning transition temperature lies within the operational temperature range of solar cells, these twin domains are likely to play an important role in the functional performance of perovskite solar cells. A report of this work has now been published in *Nature Communications*.

In-doped TiO_x Electron Transport Layers for Efficient Perovskite Cells and Perovskite-Silicon Tandems

Achieving high efficiency perovskite cells requires careful optimisation of both the perovskite active layer and the carrier-selective transport layers on either side. In an effort to improve both the fill-factor and voltage of perovskite cells, ANU PhD student Jun Peng developed a simple, one-step solution-based method for producing high quality In-doped TiO_x films as the electron transport layer. The process requires only a minor modification to the standard method used for depositing compact TiO_2 electron transport layers, so can be readily adopted by other groups. The electronic properties of the TiO_x films produced in this way (specifically conductivity and energy level alignment) can be tuned by varying the indium doping concentration in the precursors, providing significant efficiency gains compared to perovskite solar cells made with commonly used pure-TiO_2 transport layers.

Using the optimised transport layers, steady-state efficiencies of 17.9% for $CH_3NH_3PbI_3$–based cells and 19.3% for mixed-cation/mixed-halide cells were measured at ANU, corresponding to absolute efficiency gains of 4.4% and 1.2% respectively compared to TiO_2-based control cells. In addition, a steady-state efficiency of 16.6% was achieved for a semi-transparent perovskite cell and used to demonstrate a four-terminal perovskite-silicon tandem cell with a steady-state efficiency of 24.5% measured at ANU.

Compositional and Structural Engineering of Perovskites for Efficient and Stable Solar Cells

A critical hurdle to the commercial fabrication of perovskite solar cells is their limited stability. The popular methylammonium lead iodide (MAPI) perovskite is known to degrade following exposure to humidity, heat, oxygen and UV radiation; processes that have been linked partly to the presence of the organic (MA) cation. Compositional engineering of perovskites by partial substitution of the organic cation and other components provides a wide parameter space to optimise their physical and chemical properties. In this work, ANU PhD student The

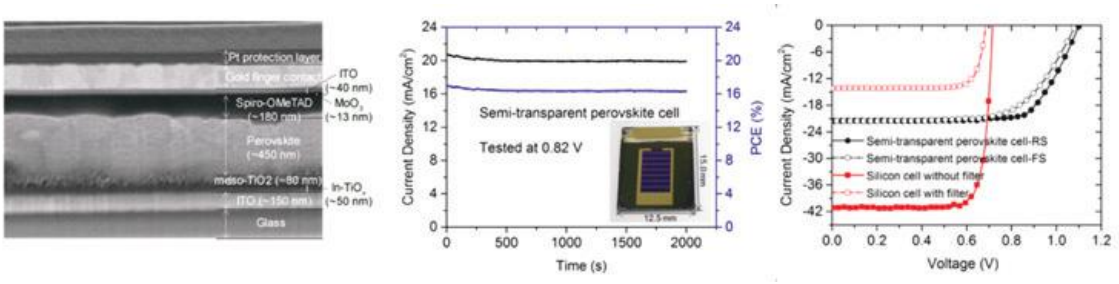

Figure 2.7: In-doped TiO_x electron transport layers for thin-film perovskite cells and perovskite-silicon tandems.

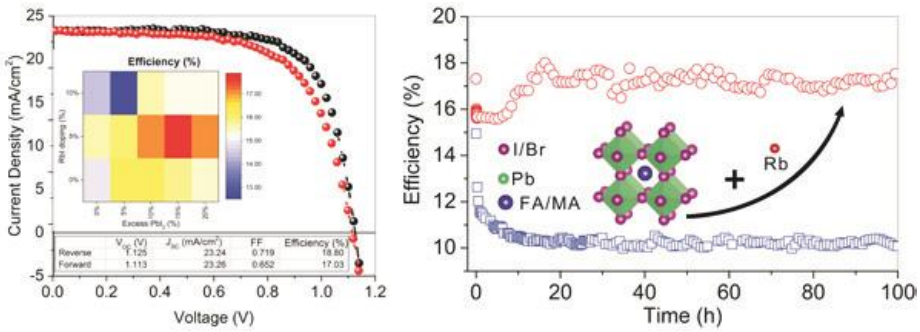

Figure 2.8: ANU reported in-house performance of a RbI-doped perovskite cells with highest efficiency of 18.8%.

Duong reported the impact of substitutional doping with rubidium iodide (RbI) to control the phase formation and crystallisation of mixed-cation, mixed-halide perovskites. High quality, single-phase films were obtained through systematic optimisation of RbI and PbI_2 ratios in the precursor solutions, supported by a combination of cathodoluminescence and X-ray diffraction studies. The RbI-doped perovskite cell gave efficiency of up to 18.8%, based on ANU measurements. Notably, these cells exhibited significantly improved thermal/photo stability compared to un-doped cells, ascribed mainly to the effect of RbI on the structure and compositional change of perovskite. The study demonstrated the potential of rubidium as an alternative cation for use in high efficiency perovskite cells.

Martin Green delivers Ian Wark Lecture

In November 2016, ACAP Director Prof Martin Green was announced the 2016 Ian Wark Medal receipient by the Australian Academy of Science. The award recognises research which contributes to the prosperity of Australia. “Professor Green is an acknowledged world-leader in the field of photovoltaics. He has published extensively and influentially, made many highly significant contributions to the knowledge base of the field, and successfully established a world-class research hub that is responsive to Australian needs in the photovoltaics industry. Several generations of his group’s technology have been successfully commercialised including, most recently, the PERC (Passivated Emitter and Rear Cell) that produced the first 25% efficient silicon cell in 2008 and accounted for the largest share of new manufacturing capacity added worldwide in 2014. His fundamental and applied research has led to, and will continue to lead to, significant economic benefits both in Australia and worldwide.”

‘Lab-to-Fab’ Translation of Perovskites

CSIRO has continued to work on ‘lab-to-fab’ translation of perovskites using its bespoke mini-slot die coating suite and range of pilot printing lines. For two-step (sequential) perovskite deposition on glass, spiro-MeOTAD was substituted with an in-house developed hole transport material (HTM), resulting in excellent results compared

Figure 2.9: The Australian Academy of Science awarded the 2016 Ian Wark Medal and Prof Green delivered the Ian Wark Lecture at a black tie dinner in Sydney.

with printing of spiro-MeOTAD. Efficiencies up to 14.7% (glass, 0.1 cm^2) and up to 9% for larger area devices (glass, 1 cm^2) have been demonstrated. Notably, these results have also been translated to roll-to-roll printed devices on flexible substrate (ITO/PET) yielding a power conversion efficiency of 11% (0.1 cm^2). This is an excellent outcome for ambient deposition via a potentially industry-relevant process on a flexible substrate, providing a promising grounding for further scale-up.

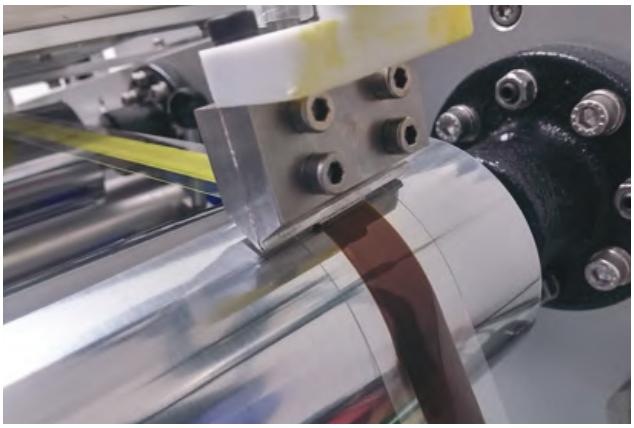

Figure 2.10: Roll-to-roll printing of photovoltaic devices on flexible substrate at CSIRO.

Figure 2.11: ANU's Tom Allen accepting his Student Award at the 32nd European Photovoltaic Solar Energy Conference in Munich in June 2016.

Student Awards at the 31st European Photovoltaic Solar Energy Conference, Amsterdam

Mr Thomas Allen of the Australian National University won a Best Paper Award at the 31st European Photovoltaic Solar Energy Conference, Amsterdam as lead author of, "Calcium Contacts to n-Type Crystalline Silicon Solar Cells". The entries were reviewed and scored by the conference's international Scientific Committee, made up of more than 200 leading research and industry experts from the global PV community. The winning paper was about direct metallisation of lightly doped n-type crystalline silicon, which is known to routinely produce non-Ohmic (rectifying) contact behaviour. This contribution demonstrated that low resistance Ohmic contact to n-type c-Si wafers can be achieved by incorporating a thin layer of the low work function metal calcium between the silicon surface and an overlying aluminium capping layer.

Mr Mohsen Goodarzi, also from ANU, won another Best Paper Award at the same conference as primary author

Figure 2.12: Mohsen Goodarzi of ANU, at the presentation of his Student Award at the 32nd European Photovoltaic Solar Energy Conference in Munich in June 2016.

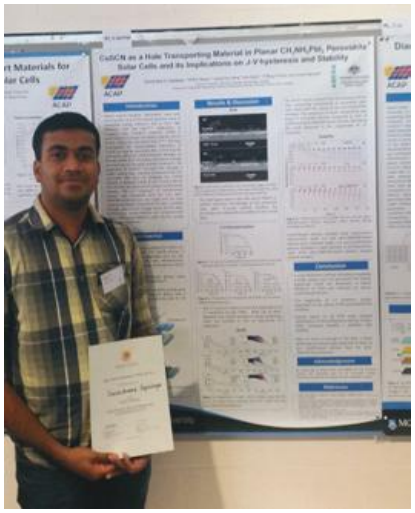

Figure 2.13: Gaveshana Sepalage with his winning poster.

of, "Modelling and Characterization of Multicrystalline Silicon Blocks by Quasi-Steady-State Photoconductance". Mohsen's research focuses on silicon material characterisation at the ingot level. This provides invaluable information about contamination, as well as providing immediate feedback on silicon crystalline growth quality.

Awards at Third Asia-Pacific Solar Research Conference, Canberra

Monash University's Mr Gaveshana Anuradha Sepalage won the 2016 Wal Read Memorial Prize for Best Poster at the Third Asia-Pacific Solar Research Conference, Canberra, as lead author for "CuSCN as a Hole Transporting Material in Planar $CH_3NH_3PbI_3$ Perovskite Solar Cells and its Implications on J-V hysteresis and Stability".

The 2016 Women in Solar Prize at that conference went to UNSW's Ms Yu Jiang for Best Poster for "Nanostructured Metal Oxide Electrochemical Capacitors for Rapid Response Module-Level Buffering of Silicon Photovoltaic Power". Photovoltaic modules can exhibit high variances in their power output due to the intermittence of illumination.

Silicon PV Conference Award 2016 to ANU's Jason Cui

The annual Silicon PV Conference is a very important meeting of silicon photovoltaics researchers, held in the Colorado Rocky Mountains. This paper, "Titanium oxide: a re-emerging optical and passivating material for silicon solar cells", by Jason Cui et al., was judged to be among the ten best presented. It demonstrated effective passivation of a variety of crystalline silicon surfaces by a thin layer of thermal atomic layer deposited (ALD) titanium oxide (TiO_2).

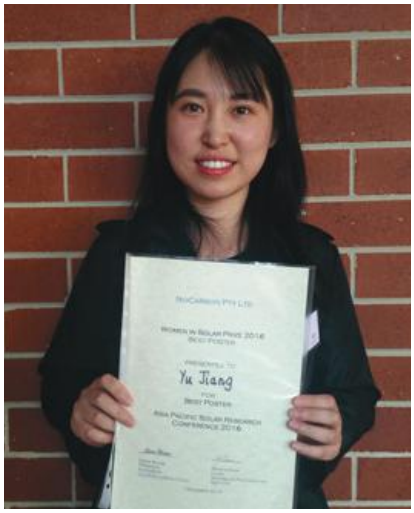

Figure 2.14: Yu Jiang after the Asia-Pacific Solar Research Conference presentation ceremony.

Figure 2.15: Jason Cui (third from left) at the Silicon PV Conference prize ceremony in Colorado.

IEEE PVSC Young Professional Award to Bram Hoex

Dr Bram Hoex, based at the UNSW node, was presented with the sought-after PVSC Young Professional Award at the 2016 IEEE Photovoltaics Specialists Conference (PVSC), in Portland, Oregon, in June 2016. The award recognises people who have made significant contributions to the science and technology of photovoltaic energy conversion, including work on PV materials, devices, modules and/or systems. Additionally, the award recipient has demonstrated significant promise as a leader in the field. Bram is an example of the next generation of Australian-based solar researchers whose careers are benefiting from the support and international linkages provided by ACAP.

Figure 2.16: Bram Hoex receives the IEEE PVSC Young Professional Award in Portland, Oregon.

Pierre Verlinden Lauded with William Cherry Award

Dr Pierre Verlinden, the Principal Investigator for ACAP's Collaborating Industry Participant, Trina Solar and an active and valued representative at ACAP's committee meetings, has been awarded the 2016 IEEE William R. Cherry Award, the most prestigious research award within the international photovoltaics community. The award was presented in June 2016 at the opening ceremony of the 43rd IEEE Photovoltaic Specialists Conference in Portland, Oregon.

This brings to four the number of ACAP-affiliated researchers who have received this award, with Professors Martin Green, Allen Barnett and Stuart Wenham as previous awardees. The only other organisation that can boast a similar number of awardees is ACAP partner, the US NREL.

Figure 2.17: Dr Pierre Verlinden, Principal Investigator for ACAP's Collaborating Industry Participant, Trina Solar and an active and valued representative at ACAP's committee meetings.

3. Organisational Structure and Research Overview

The Australian Centre for Advanced Photovoltaics (ACAP) coordinates the activities of the Australian partners in the Australia–US Institute for Advanced Photovoltaics (AUSIAPV), established to develop the next generations of photovoltaic technology and to provide a pipeline of opportunities for performance increase and cost reduction. The Australian partners in ACAP are UNSW, ANU, University of Melbourne, Monash University, University of Queensland and CSIRO, plus our industrial partners Suntech Power, Trina Solar, BlueScope Steel, BT Imaging, PV Lighthouse and Dyesol. AUSIAPV links ACAP with US-based partners, specifically the National Science Foundation and Department of Energy–supported Engineering Research Center for Quantum Energy and Sustainable Solar Technologies (QESST), based at Arizona State University, the National Renewable Energy Laboratory (NREL), Sandia National Laboratories, Lawrence Berkeley National Laboratory, Stanford University, Georgia Institute of Technology and University of California, Santa Barbara. These national and international research collaborations provide a pathway for highly visible, structured photovoltaic research collaboration between Australian and American researchers, research institutes and agencies, with significant joint programs based on the clear synergies between the participating bodies.

AUSIAPV/ACAP is driving significant acceleration of photovoltaic development beyond that achievable by institutes acting individually, with significant leveraging of past and current funding. This program is supported by the Australian Government through the Australian Renewable Energy Agency (ARENA). The Australian Government, through ARENA, is supporting Australian research and development in solar photovoltaic and solar thermal technologies to help solar power become cost competitive with other energy sources. (The views expressed herein are not necessarily the views of the Australian Government, and the Australian Government does not accept responsibility for any information or advice contained within this report.)

The AUSIAPV/ACAP organisational chart is shown in Figure 3.1. The international activities of AUSIAPV are coordinated by an International Steering Committee with membership drawn from ARENA, the US Department of Energy (DOE), ACAP and the ACAP National Steering Committee, QESST and NREL. The International Steering Committee is also charged with identifying opportunities for synergistic photovoltaic research initiatives between Australia and the US and for facilitating staff and student exchanges. Some examples of current international activities are reported in Section 6 of this report.

As well as these collaborative activities, the major partners in AUSIAPV, specifically ACAP, QESST and NREL, conduct their own largely independent research programs meeting the specific research and training objectives of their major supporters and sponsors. In the case of ACAP, research is milestone driven with annual milestone targets established under the Funding Agreement with ARENA. ACAP is managed by a Management Committee, which consists of the node directors or delegates from each of the nodes. The Management Committee takes advice from the National Steering Committee, with an independent Charter, but with membership including a representative of ARENA and NREL, the ACAP and QESST directors, and other members drawn from industrial partners.

As indicated in Figure 3.1, the ACAP program is organised under five Program Packages (PP1–PP5), each supported by multiple nodes. PP1 deals with silicon wafer-based cells, by far the dominant photovoltaic technology commercially, and likely to remain so for at least the next 10 years. Here the challenge is to continue to reduce manufacturing costs, while maintaining or preferably, improving, energy conversion efficiency. PP1 focuses on three main areas: cells made from solar grade silicon, rear contact cells and silicon-based tandem cells, both monolithic and mechanically stacked.

PP2 involves collaborative research into a range of organic, organic-inorganic hybrid cells and “earth abundant” thin-film materials, including Si and Cu_2ZnSnS_4 (CZTS), as well as more futuristic “third-generation” approaches. Recently, the relatively new photovoltaic material, the organic-inorganic perovskites, has been included within the scope and additional funding provided from 2016 to expand and intensify the research on these materials and devices. The program now has the overall goal of demonstrating efficiency above 16% for these new thin-film cells of above 1 cm^2 area and of demonstrating the feasibility of costs below the US Department of Energy SunShot targets for cost reductions.

PP3, optics and characterisation, targets experimental demonstration that theoretical conversion limits can be increased by the use of structures that have a high local density of optical states, with particular emphasis on thin-film organic and inorganic solar cells.

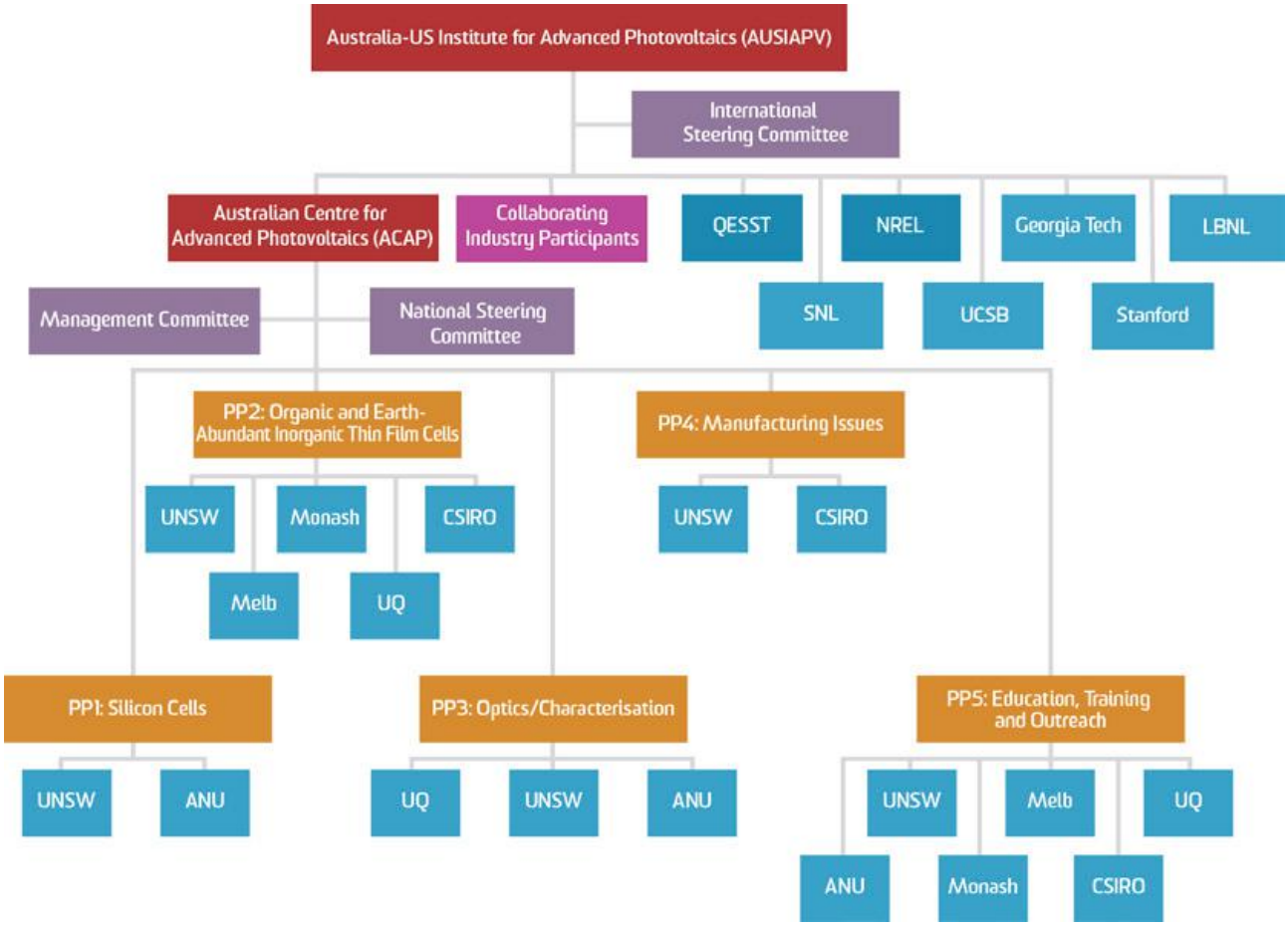

Figure 3.1: Organisational chart.
Collaborating Industry Participants are involved in collaborative research as well as in the Advisory and Steering Committees.

PP4, manufacturing issues, aims at delivery of a substantiated methodology for assessing manufacturing costs of the different technologies under investigation by ACAP. The overall cost target is to undercut the US Government's SunShot targets, for one or more of the technologies, in at least one major SunShot targeted application, as deduced by a substantiated costing methodology.

Additional targets for PP1–PP4 relate to the established academic measures assessing research performance, specifically the number and quality of publications, with strong collaboration being encouraged by placing emphasis on publications involving authors from multiple nodes within the Australian-based Centre or the Australia–US Institute, on invited keynote and plenary presentations, on patent applications and on indicators of commercial interest, such as the number of projects jointly supported by industry, with active commercialisation of key developments for at least one technology by Year Eight.

PP5 involves education, training and outreach. ACAP has specific targets for the number of researchers in different categories benefiting from the infrastructural support it provides and for the quality and number of researcher exchanges. Additionally, a significant number of major outreach events are targeted for each year. As well as major events such as those reported in the PP5 section of this annual report, other outreach activities include public lectures on material relevant to ACAP activities, newspaper and magazine articles, responses to governmental calls for submissions, visits by policy developers and their advisors, information papers prepared and presentations to both policy developers and their advisors.

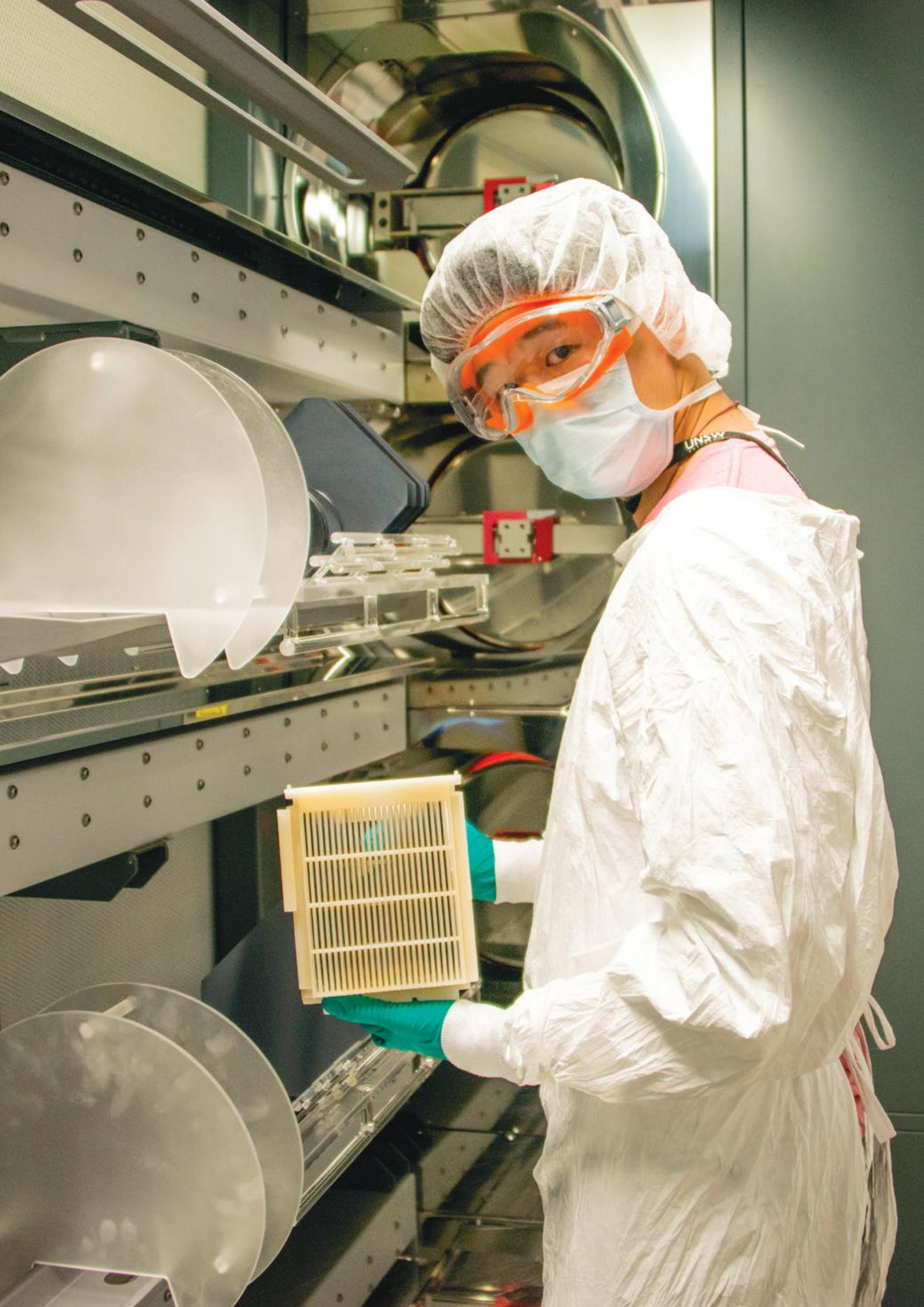
UNSW

4. Affiliated Staff and Students

University of New South Wales

Green, Martin (Centre Director)
Corkish, Richard (Centre Chief Operating Officer)

Academic Staff and Senior Researchers
Egan, Renate (Node Leader)
Bagnall, Darren
Barnett, Allen
Bremner, Stephen
Conibeer, Gavin
Edwards, Matthew
Hao, Xiaojing
Ho-Baillie, Anita
Huang, Shujuan
Keevers, Mark
König, Dirk (until 22 Dec 2016)
Lennon, Alison
Mehrvarz, Hamid
Perez-Wurfl, Ivan
Shrestha, Santosh
Trupke, Thorsten
Uddin, Ashraf
Varlamov, Sergey (until Jul 2016)
Watt, Muriel (until Oct 2016)
Wen, Xiaoming
Wenham, Stuart
Young, Trevor

ECR and Postdoctoral Fellows
Chan, Catherine
Cui, Hongtao
Edwards, Matthew
Feng, Yu
Hallam, Brett
Hsiao, Pei-Chieh (from Jul 2016)
Huang, Jialiang (from Jul 2016)
Ishwara, Thilini
Jiang, Yajie (from Sep 2016)
Johnson, Craig
Juhl, Matthias (from Jul 2016)
Kampwerth, Henner
Li, Zhongtian (from Jul 2016)
Liu, Fangyang
Liu, Ziheng (from Sep 2016)
Ma, Fajun (from Jul 2016)
Mai, Ly
Mehrvarz, Hamid
Mitchell, Bernhard
Ouyang, Zi (until Dec 2016)
Patterson, Robert
Pillai, Supriya
Puthen-Veettil, Binesh (until Dec 2016)
Romer, Udo (from Jul 2016)
Song, Ning (from Jul 2016)
Sugianto, Adeline
Tayebjee, Murad (until Sep 2016)
Wen, Xiaoming
Western, Ned (from Jul 2016)
Yan, Chang (from Oct 2016)
Zhang Tian (from Jul 2016)
Zhang, Meng (from Nov 2016)

PhD Students
Abdullah, Taufiq Mohammad
Allen, Vincent
An, Xin Rui (until Mar 2016)
Borojevic, Nino (until Mar 2016)
Cao, Wenkai
Chan, Kah Howe
Chang, Nathan
Chen, Ran
Chen, Sheng
Chen, Weijian
Chen, Zihan
Chung, Daniel
Chung, Simon
Colwell, Jack Killian
Concha Ramon, Bruno Gustavo
Conrad, Brianna
Dai, Xi
Deng, Xiaofan
Disney, Claire
Dumbrell, Robert
Evans, Rhett
Fung, Tsun Hang
Gupta, Neeti
Han, Jianshu (until Mar 2016)
Hsiao, Pei-Chieh (until Jul 2016)
Htoo, Thwin
Hu, Yicong
Hungerford, Soe Yoko
Jia, Xuguang
Jiang, Yajie (until Sep 2016)
Jiang, Yu
Juhl, Mattias (until Jul 2016)
Kim, Jincheol
Kim, Kyung Hun
Kim, Taehyun
Lambert, Daniel
Lau, Cho Fai Jonathan
Lee, Chang-Yeh
Li, Dun
Li, Hongzhao
Li, Yang

Li, Zhongtian (until Jul 2016)
Liao, Anqi
Liao, Yuanxun
Limpert, Steven
Lin, Shu (until Mar 2013)
Lin, Ziyun
Liu, Ziheng (until Sep 2016)
Lu, Zhong
Lunardi, Marina Monteiro
Ma, Qingshan
Mahboubi Soufiani, Arman
Mahmud, Md Arafat
Mitchell, Bernhard
Nampalli, Nitin
Noh, Shinyoung
Nomoto, Keita
Pakhuruddin, Mohd (until Mar 2016)
Park, Jongsung
Pu, Aobo
Rodriguez, John (until Mar 2013)
Shen, Chao
Sheng, Rui
Shi, Lei
Soeriyadi, Anastasia
Song, Ning (until Jul 2017)
Soon, Matthew
Sun, Kaiwen
Teng, Peinan
To, Alexander
Upama, Mushfika Baishakhi
Vargas Castrillon,Carlos Andre
Wang, Bo
Wang, Dian
Wang, Hongfeng
Wang, Kai
Wang, Li
Wang, Lu
Wang, Pei
Wang, Qian
Wang, Sisi
Wang, Xi
Western, Ned (until Jul 2016)
Wu, Lingfeng
Wu, Qiyuan
Xia, Hongze (until Mar 2016)
Xu, Cheng
Xu, Xiaoqi
Xue, Chaowei
Yan, Chang (until Oct 2016)
Yang, Chien-Jen
Yang, Jianfeng
Yao, Yao
Yao, Yu
Ye, Qilin
Yi, Chuqi
Yuan, Lin
Yun, Jae Sung
Zafirovska, Iskra
Zhang Tian (until Jul 2016)
Zhang, Haixiang
Zhang, Pengfei
Zhang, Qiuyang
Zhang, Yi
Zhang, Zewen
Zhang, Zhilong,
Zhao, Jing
Zhao, Xin
Zhou, Zibo

Masters Students
Kobamoto, Naoya
Lin, Ye
Wang, Li
Wilkinson, Ben
Zhang, Zhilong
Zhou, Fangzhou (until Mar 2016)

Honours Students
Azumi, Khairul
Carlaw, Raymond
Chan, Kai-Yuen Kevin
Chen, Daniel
Choi, Helen Na Eun
Choi, Tae
Chung, Ellie
Fung, Tsun
Gong, Sihong
Huang, Wister
Kim, Jiyun
Kim, Moon Yong
Kwok, Aaron
Lee, Minwoo
Lei, Ting
Li, Hongxue
Liang, Brian
Lin, Wenguang
Liu, Dunkang
Phua, Benjamin
Rim, Hyun
Shin, Suk
Sun, Heng
Sun,Tian
Wang, Xu Ying
Zhou, Yuchao
Zhu, Jinyi

Australian National University

Academic Staff and Senior Researchers
Bi, Qunyu
Blakers, Andrew (Node Leader)
Catchpole, Kylie
Chern Fong, Kean
Chowdury, Dibakar

Cuevas, Andres
Fell, Andreas
Franklin, Evan
Lal, Niraj
Macdonald, Daniel
Rougieux, Fiacre
Samundsett, Christian
Stocks, Matthew
Weber, Klaus
White, Tom
Zin, Soe (until Jun 2016)

ECR and Postdoctoral Fellows
Baker-Finch, Simeon
Ernst, Marco
Grant, Nick
Hargreaves, Stuart
Kumar, Hemant
Sieu Phang, Pheng
Walter, Daniel
Yang, Xinbo (until Jun 2016)

PhD Students
Allen, Thomas Gerald
Barugkin, Chog Basnet, Robin
Bullock, James
Cong, Jin Jin
Fu, Xiao
Grant, Dale
Han, Young-Joon
Kho, Teng Choon
Lim, Siew Yee
Liu, Anyao
Nguyen, Hieu
Osorio Mayon, Yahuitl
Phang, Pheng Peng, Jun
Phang, Sieu
Qiaoke Baerhujin (aka Chog Barugkin)Qiaoke
Ratcliff, Thomas
Sio, Hang Cheong
Sun, Chang
Wu, Huiting
Wu, Nandi
Wu, Yiliang
Zhang, Xinyu
Zheng, Peiting

CSIRO (Manufacturing, Melbourne)

Academic Staff and Senior Researchers
Wilson, Gerry (Node Leader)
Scholes, Fiona (Node Leader)
Chantler, Regine
Faulks, Andrew
Fell, Chris
Gao, Mei
Ramamurthy, Jyothi
Vak, Doojin
Weerasinghe, Hasitha

ECR and Postdoctoral Fellows
Aury, Clement
Fievez, Mathilde
Han, Hyun-Gyu
Qin, Tianshi
Sears, Kallista
Song, Seyeong
Weerasinghe, Hasitha

University of Melbourne

Academic Staff and Senior Researchers
Ghiggino, Ken (Node Leader)
Goerigk, Lars
Holmes, Andrew
Jones, David
Wong, Wallace

ECR and Postdoctoral Fellows
Kumar, John
Lai, Yuying
Lu, Shirong
Subbiah, Jegadesian

PhD Students
Banal, James
Belic, Ognjnen
Dkhissi, Yasmina
Farooq, Umer
Gao, Can
Geraghty, Paul
Hong, Quentin
Lee, Calvin
Lovel, Mathew
Masoomi, Saghar
Mitchell, Valerie
Novakovic, Sacha
Saker-Neto, Nicolau
Saxena, Sonam
Schwartz, Kyra
Song, Aaron

Masters Students
Duan, Ruoyu
Fabig, Thomas
Jameel, Mohammed A.
Kartika, Monica
Seow, Jia Yi
Vu, Khuyen
Wang, Hao-Tian
Zhang, Bolong

Monash University

Academic Staff and Senior Researchers
Cheng, Yi-Bing (Node Leader)
Bach, Udo
Spiccia, Leone

ECR and Postdoctoral Fellows
Fürer, Sebastian
Huang, Wenchao
Li, Feng
Lu, JianFeng
Meyer, Steffen
Pascoe, Alexander

PhD Students
Benesperi, Iacopo
Jiang, Liangcong
Lin, Xiongfeng
Milhuisen, Rebecca
Pai, Narendra
Rothmann, Mathias
Sepalage, Anuradha
Xiao, Manda

Masters Student
Bhargava, Rishabh

Honours Students
Gu, Qinying
Paz, Simon

University of Queensland

Academic Staff and Senior Researchers
Burn, Paul (Node Leader)
Meredith, Paul (Node Leader)

ECR and Postdoctoral Fellows
Armin, Ardalan
Donaghey, Jenny (until February 2016)
Fang, Yuan (until April 2016)
Jin, Hui
Stoltzfus, Dani (until January 2017)
Shaw, Paul

PhD Students
Kim, Il Ku (Benjamin) (until January 2016)
Li, Xin (until October 2016)
Lin, Qianqian (until September 2016)
Stolterfoht, Martin (until April 2016)
Yazmaciyan, Aren (until 27 January 2017)
Zhang, Shanshan
McGregor, Sarah

QESST

Honsberg, Christiana
Augusto, Andre
Bertoni, Mariana
Bowden, Stuart
Buonassisi, Tonio
Burrell, Anthony
Goodnick, Stephen
Jensen, Mallory
Mitchell, John
Peters, Ian Marius
Fraser, Matthew
Saenz, Delia
Tumas, William

National Renewable Energy Laboratory

Basore, Paul (until Jun 2016)
Emery, Keith
Friedman, Dan
Geisz, John
Johnston, Steve
Haegel, Nancy
Kopidakis, Nikos (until Sept 2016)
Levi, Dean
Osterwald, Carl
Page, Mathew
Reid, Obadiah
Rumbles, Garry
Schnabel, Manuel
Stradins, Paul
Teeter, Glenn
Wilson, Gregory
Woodhouse, Michael
Young, Mathew

Molecular Foundry, Lawrence Berkeley National Laboratories

Chen, Teresa
Javey, Ali
Knapstein, Jessie
Neaton, Jeffrey

Stanford University

McGehee, Mike
Dauskardt, Reinhold
Rolston, Nick

Georgia Technology Institute

Kippelen, Bernard
Jradi, Fadi

Marder, Seth
Reichmanis, Elsa
Rohatgi, Ajeet
Samuel, Graham
Upadhyaya, Ajay

University of California, Santa Barbara

Bazan, Gui
Nguyen, Quyen

Wuxi Suntech Power Co. Ltd.

Chen, Rulong
Zhou, Min

Trina Solar

Verlinden, Pierre

BT Imaging

Bardos, Robert
Maxwell, Ian
Trupke, Thorsten

BlueScope Steel

Nolan, David
Zappacosta, Dion

PV Lighthouse

Abbott, Malcolm
McIntosh, Keith

Dyesol Pty Ltd.

Milliken, Damion
Thompson, Gordon

5. Research Reports

PP1 Silicon Cells

Overview

Silicon solar cells constitute about 93% of the worldwide solar photovoltaic (PV) electricity market. This share is unlikely to change much over the next five years. In 2016, new silicon PV and wind electricity generation capacity was installed at a greater rate than the sum of new fossil, nuclear, hydro and other renewable generation capacity combined. Reasons for silicon's dominance include silicon abundance, moderate cost, low toxicity, high and stable cell efficiency, robustness, bankability, highly advanced and widespread knowledge of silicon, and extensive and sophisticated supply chains.

This Program Package (PP1) addresses silicon wafer-based cells and has efficiency targets, increasing over the planned eight-year period of ACAP operation, for cells formed from solar-grade silicon, all-rear contact cells and tandem structures that include silicon.

PP1.1 Solar-grade silicon

Solar-grade silicon feedstocks offer a low-cost alternative to the standard electronic-grade feedstocks used today. There is a potential cost reduction from US$20/kg to US$10/kg for silicon material, leading to a 10% reduction in module production cost. Research into fabricating high efficiency cells from wafers of low-cost upgraded metallurgical-grade (UMG) silicon wafers is being carried out through a collaboration between ANU (cell fabrication), UNSW (defect hydrogenation) and Apollon Solar (solar-grade silicon supplier). The aim is to demonstrate that the use of less pure solar-grade silicon does not reduce cell efficiency. The key outcome in 2016 was a world-first demonstration of a solar cell above 21% efficiency for a device made with 100% solar-grade silicon, supplied by Apollon Solar. A specially developed fabrication sequence to maintain wafer quality during thermal processing was used. The highest efficiency achieved was 21.1%, compared with 21.9% for a co-processed cell using electronic-grade silicon. The next step is to demonstrate efficiencies above 23%, taking advantage of the UNSW process for optimised defect hydrogenation.

Solar cells tend to lose some of their initial performance when exposed to sunlight, a process termed light-induced degradation (LID). The mechanism for this has been poorly understood, and current passivation techniques for eliminating LID are slow and relatively ineffective. An understanding of the defect and a method for accelerating boron-oxygen (B-O) defect formation has been developed, which allows generation then complete elimination of B-O-related LID in p-type silicon, in a treatment that lasts for 10 seconds during cell manufacture and the passivation remains stable against standard industry stability testing. The treatment efficacy has been demonstrated on industrial solar cells, and methods for integrating the process into industrial tools are being developed and commercialised by UNSW in partnership with ANU. Typical absolute efficiency gain on industrial cells is 1% absolute (5–6% relative).

PP1.2a Rear contact silicon cells

Work continued on improving interdigitated back contact (IBC) silicon solar cells, with collaboration and support from PV Lighthouse, ACAP and Trina Solar. Further improvements in surface passivation were achieved via ONO passivation, reaching 24.7% IBC cell efficiency, indicating the possibility of efficiencies beyond 25%, provided a sufficiently high bulk lifetime at the end of device fabrication. The path forward is therefore in identifying and replacing processes which degrade wafer lifetime such as deposition of high-stress films, and boron diffusions. Exploratory work to replace boron diffusion was initiated. Improved bulk and surface quality allowed lifetimes of 50 ms to be obtained. Careful analysis of optical losses allowed improved understanding of remaining losses. A path to 25–26% efficiency has been identified.

PP1.2b Passivated contacts

Today's record silicon solar cells use "passivated contacts" to selectively transport electrons and holes towards the cell's terminals. We are developing several passivated contact technologies to open new pathways for the next generation of silicon photovoltaics. In a high temperature approach, we have completed the optimisation of boron doped polysilicon/tunnelling oxide contacts, and we have implemented a unique double-interlayer structure underneath an n+ polysilicon film to achieve a 21.1% efficient cell. In a low temperature approach, we are investigating a wide range of materials, many of them transparent, that have either a very high or a very low work function. Using lithium fluoride and molybdenum oxide we demonstrated the first dopant-free asymmetric heterocontact silicon solar cell (DASH) having a conversion efficiency close to 20%. We have also made 20.3% efficient solar cells with LiF_x or calcium partial-area rear contacts (PaRC), thus demonstrating implementation on n-type silicon the already popular p-type silicon cell structure. These novel, dopant-free technologies have

the advantages of simplifying the fabrication of high efficiency silicon solar cells and being ideally suited to perovskite/silicon tandem devices.

PP1.3a Silicon tandem cells (monolithic)

Tandem cells offer realistic efficiencies above 30% even in non-concentrator applications. In the monolithic approach, a wide bandgap top cell is grown on a silicon cell, with the two cells operating in series. Several different technologies are being pursued: three for stacking III-V cells on silicon, each with a distinct approach for matching to the smaller atomic spacing of silicon and two technologies involving materials that are either already lattice matched to silicon or do not require good crystal quality for high performance. Highlights in 2016 include that the structure and fabrication process have been improved for top and bottom cells; tandem efficiency of 23.8% has been reported under 7.2X concentration outdoor measurement; and a pathway to achieve 32.9% at 20X and 35.8% at 400X has been determined. Using a different approach, in 2016, a 23.2% efficient cell using Pd nano-particles for bonding triple-junction InGaP/GaAs cells to crystalline Si cells was demonstrated. The aim is to demonstrate multi-junction III-V/Si tandem without epitaxial growth on a crystalline Si template while achieving high performance. The use of bonding allows two-terminal configuration to be achieved without the additional wiring that would otherwise be required in a mechanically stacked four-terminal tandem.

PP1.3b Silicon tandem cells (mechanically stacked)

In a mechanically stacked tandem system, a high bandgap top cell is independently operated in conjunction with a standard silicon bottom cell. Two approaches, involving series or parallel connection of top and bottom cells, enable high annual energy yields under simulation of real weather conditions. Each approach involves scaling the area of the top cell relative to the bottom cell to enable voltage or current matching. This area scaling enables the use of a much wider range of top cell bandgaps with ideal four-terminal efficiencies approached for a broad range of bandgaps. GaAs cells developed in a related ACAP collaboration project will be paired with silicon to demonstrate the potential for efficiencies well above 30%.

PP1.1 Solar-grade Silicon

Lead Partner
ANU

ANU Team
Prof Daniel Macdonald, Dr Fiacre Rougieux

ANU Students
Peiting Zheng, Chang Sun, Rabin Basnet

UNSW Team
Prof Stuart Wenham, Assoc Prof CheeMun Chong, Dr Brett Hallam, Dr Catherine Chan, Dr Malcolm Abbott

UNSW Students
Sisi Wang, Ran Chen, John Fung

Industry Partners
Apollon Solar (France)

Funding Support
ARENA, ARC, ANU

Aim

The use of low-cost solar-grade silicon materials is likely to play an important role in achieving further cost reductions for photovoltaic modules. However, to create a compelling case for the industrial application of such solar-grade materials, it is necessary to demonstrate that the resulting cell efficiencies are almost indistinguishable from those obtained when using standard silicon wafers. In support of this broader objective, the aims for the previous period were: to continue to increase the efficiency of solar cells made with solar-grade wafers in the laboratory at ANU; to develop a new cell process with a selectively doped front surface to allow higher efficiency potential; and to further optimise the deactivation of the boron-oxygen defect in these devices through collaboration with colleagues at UNSW.

Progress

We have continued to make good progress during the reporting period, with the key achievement being an independently confirmed cell efficiency of 21.1% using n-type Czochralski-grown (Cz) wafers grown from 100% solar-grade silicon, also known as upgraded metallurgical-grade (UMG) silicon, supplied by our industry partner Apollon Solar. This represents a world record efficiency for this class of material, passing our previous record of 20.9% achieved in 2015.

There were a number of Actions identified in the previous Activity Plan. Progress against each of these is described below.

1. Further development of our cell fabrication process. Our previous cell process was not compatible with efficiencies above 22%, even on high quality electronic-grade wafers. This was due primarily to recombination in the front surface boron diffused regions, at the metal contacts, and at the cell edges. A major effort in 2016 was the development of a new solar cell fabrication process with the following features: a 'selective emitter' structure for the front side, with varying boron dopant concentrations under and between the metal fingers; optimised metallisation processes that reduce recombination and shading losses; and reduced edge losses by using a dielectric edge barrier rather than the previous mesa-etch approach. Modelling shows that these changes should enable solar cells with efficiencies well over 23%. The first batch of solar cells with this new process is currently being completed, with test structures indicating open-circuit voltages of over 700 mV on electronic-grade wafers.

2. Reducing the impact of the boron-oxygen (B-O) defect. Our work in 2015 showed that advanced hydrogenation through illuminated annealing to form and passivate the B-O defects could only partially eliminate this important defect on our previous devices, causing the solar cells to degrade under normal operating conditions. Through working with the team at UNSW in 2016, the latter has shown that the presence of sufficient atomic hydrogen in the correct charge state can, not only passivate such B-O defects, but that once completed, the passivation remains stable against standard industry stability testing. We have since found that this partial deactivation in our devices is due to the lack of a SiN firing step in our previous cell process, which is necessary to introduce sufficient hydrogen into the device. Our new cell process has a dedicated SiN firing step and should allow the first-time demonstration of almost complete defect deactivation in these devices. In parallel with this work, UNSW and ANU are working together to commercialise this advanced hydrogenation technology, and are applying the technology to the various low-cost wafer types from industry leaders GCL, LONGi, 1366 Technologies and Elkem as well as Apollon Solar. UNSW and ANU are also working together with various tool manufacturers (Schmid, DR Laser, Kelong Wei, Asia NeoTech and Meyer Burger Technology) to make the new advanced hydrogenation technology available to all cell manufacturers for large-scale manufacturing.

3. Solar-grade cells with efficiencies above 21.5%. During the reporting period we achieved a new record efficiency of 21.1% (independently confirmed at Fh-ISE CalLab, Germany). Figure PP1.1.1 shows the quantum efficiency and reflectance data for two of the best UMG cells and a control electronic-grade (FZ) device, indicating that there is very little difference between the performance of the solar-grade and the electronic-grade devices. These cells were made using the cell process developed in the earlier stages of this project, known as a PERL cell (Passivated Emitter and Rear Locally-diffused). A photograph of a 2cm x 2cm UMG PERL cell is shown in Figure PP1.1.2. We expect that the use of our new selective emitter PERL process will enable efficiencies on UMG wafers of over 21.5% in the coming reporting period.

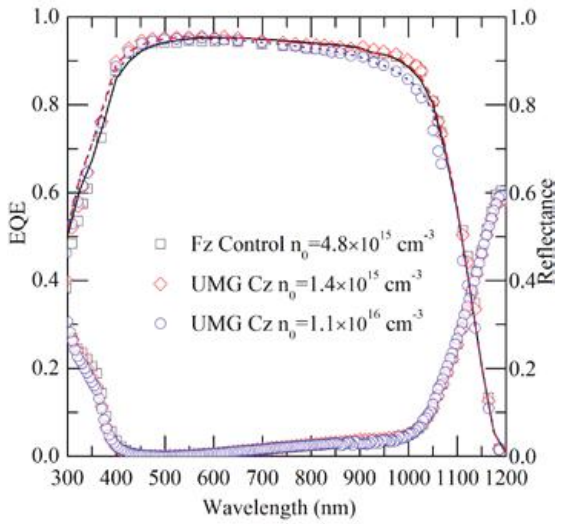

Figure PP1.1.1: External quantum efficiency (EQE) and front reflectance of two UMG cells with different base doping, and a control electronic-grade FZ cell.

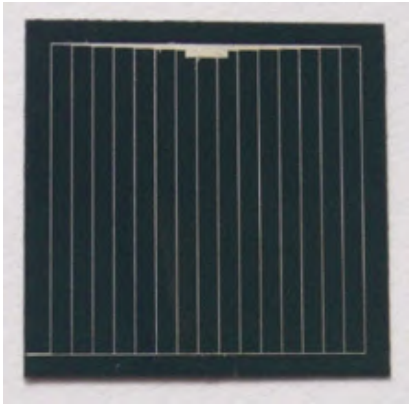

Figure PP1.1.2: Photograph of a 2cm × 2cm solar-grade silicon UMG PERL cell fabricated at ANU.

Highlights

- Fabrication of a 21.1% efficient (independently confirmed) n-type solar-grade silicon cell, the highest efficiency reported to date for this class of material.
- Development of a high efficiency cell fabrication process for solar-grade wafers that allows high carrier lifetimes after phosphorus diffusion to be maintained through to the final device. This device structure features a selectively doped boron diffused front surface, which is compatible with efficiencies above 23% in principle.
- Discovery that the partial deactivation of the boron-oxygen defect in previous UMG cells made at ANU was due to the lack of a firing step in the cell fabrication. This insight points the way to much improved deactivation of this important defect in future devices, which should lead to UMG cells that are stable over many years of operation.
- Application of the advanced hydrogenation technology to a range of new and low-cost wafer types being developed by industry leaders GCL, LONGi 1366 and Apollon Solar.
- Development of commercial tools for the large-scale manufacturing of the advanced hydrogenation technology.

Future Work

Future work will aim to achieve confirmed solar-grade cell efficiencies of over 21.5% by March 2018. In order to achieve this, we will optimise the new selective emitter cell fabrication sequence, and, in particular, optimise the advanced hydrogenation technology for these devices such as through annealing/illumination conditions for permanently deactivating the boron-oxygen defect.

References

Liu, A. Y., Sun, C., Markevich, V. P., Peaker, A. R., Murphy, J. D. and Macdonald, D., 2016, “Gettering of interstitial iron in silicon by plasma-enhanced chemical vapour deposited silicon nitride films”, J. Appl. Phys. 120, 193103.

P. Zheng, P., Rougieux, F. E., Samundsett, C., Yang, X., Wan, Y., Degoulange, J., Einhaus, R., Rivat P. and Macdonald, D., 2016, “Upgraded Metallurgical-Grade Silicon Solar Cells with Efficiency above 20%”, Appl. Phys. Lett. 108, 122103.

Sun, C., Nguyen, H.T., Rougieux, F.E. and Macdonald, D., 2016, “Characterization of Cu and Ni precipitates in n- and p-type Czochralski-grown silicon by photoluminescence”, 6th International Conference on Crystalline Silicon Photovoltaics (SiPV), Chambery, France.

Sun, C., Rougieux, F.E., and Macdonald, D., 2016, “Reassessment of the recombination properties of aluminium-oxygen complexes in n- and p-type Czochralski-

grown silicon", Phys. Stat. Sol. B: Basic Solid State Physics, 253, 2079-2084.

Zheng, P., Fiacre.E.Rougieux, F.E., Samundsett, C., Yang, X., Wan, Y., Degoulange, J., Einhaus, R., Rivat P. and Daniel Macdonald, D., "Simulation of 20.96% efficiency n-type Czochralski UMG silicon solar cell", 6th International Conference on Crystalline Silicon Photovoltaics (SiPV), Chambery, France

Zheng, P., Rougieux, F.E., Zhang, X., Degoulange, J., Einhaus,R., Rivat, P. and Macdonald, D., 2016 , "21.1% UMG Silicon Solar Cells", IEEE J. Photovoltaics, 7, 58 – 61.

PP1.2 Rear Contact Silicon Cells

PP1.2a Rear Contact Silicon Cells

Lead Partner
ANU

ANU Team
Prof Andrew Blakers, Dr Evan Franklin, Dr Matthew Stocks, Dr Kean Fong, Dr Ngwe Zin, Dr Er-Chien Wang, Dr Thomas Ratcliff

ANU Students
Teng Choon Kho

Industry Partners
PV Lighthouse – Dr Keith McIntosh

Funding Support
ACAP, ARENA

Aim
The objectives of PP1.2a are twofold: to develop very high efficiency laboratory-based silicon solar cells; and, in parallel, to develop cell fabrication techniques and processes compatible with industrially feasible low-cost implementation of interdigitated back contact (IBC) solar cells. IBC cells, by their very nature, are both inherently capable of very high efficiencies owing to superior optics compared to conventional cell architectures and owing to an improved ability to tailor fabrication processes to meet specific goals of cell features. However, such cells are also characterised by more complex and expensive fabrication processes. The target for the end of the program is to fabricate cells using any techniques with efficiencies of 26% or above, and in parallel to produce cells using industrially applicable techniques, and by doing so meeting an informal or internal efficiency target of 24% or above.

1. **Progress** Fabrication of IBC solar cells

- The advancements made in 2015 led to the fabrication of a 24.7% IBC solar cell as was reported in January 2016. The measurement was done in-house, but it was referenced against a certified reference cell from Fraunhofer CalLab. The I-V curve of the champion cell is presented in Figure 1.2a.1, with the following I-V parameters:

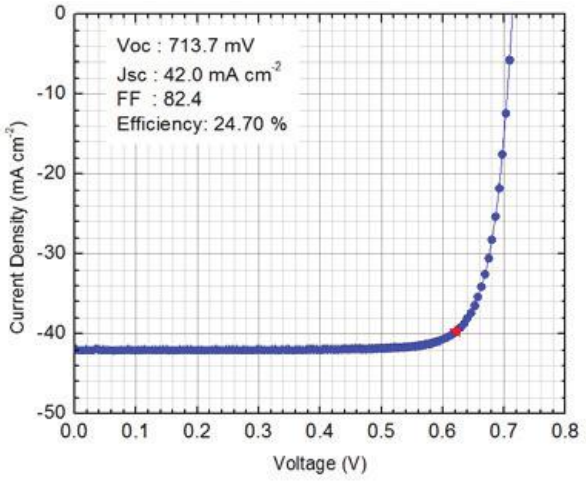

Figure PP1.2a.1: I-V measurement of the champion IBC cell, with 24.7% cell efficiency. Measurement was an in-house measurement, referenced against a certified calibration cell from Fraunhofer CalLab.

  - V_{OC}: 713.7 mV
  - J_{SC}: 42.0 mAcm^{-2}
  - FF: 82.3%
  - Efficiency: 24.7%

- The batch from which the 24.7% cell was measured was fabricated with a newly developed "thermal-SiO_2/PECVD SiN_x/PECVD SiO_x" referred to as an ONO stack. The film is capable of excellent ambipolar passivation qualities, boasting extremely low J_0 values of approximately 0.1 fAcm^{-2} on planar undiffused surfaces, and approximately 3 fAcm^{-2} on textured surfaces with either light phosphorus or undiffused. An interesting feature of this film is the ability to tune its charge density by corona charging, and it can be made permanent by a 250°C annealing immediately thereafter. Experiments on test samples have shown excellent stability of the modified charge density, retaining an excellent surface passivation after the samples were stored in ambient conditions for one year. The 24.7% cell was subjected to the same treatment of corona charging and annealing, a process deemed to be non-damaging to the surface passivation of the devices and it is a low risk process.

Current – voltage (IV) measurement of the devices immediately after the charging process shows a slight increase in V_{OC} and efficiency. However, after a 250°C sintering, the fill factor (FF) of the devices degraded significantly. The V_{OC}, J_{SC} and pseudo FF of the devices after sintering remained unchanged to the charged state, suggesting that the drop in FF was unrelated to the surface passivation. Further analysis reveals a significantly higher series resistance consistent with delamination of contact fingers. Figure 1.2a.2 presents the IV measurements on one of the cells in the batch, demonstrating the slight improvement after corona charging, followed by the degradation after a 250°C sintering on the devices. Since the devices were significantly degraded, they were not sent for third party measurement. The champion cell efficiency of 24.7% was measured prior to corona charging.

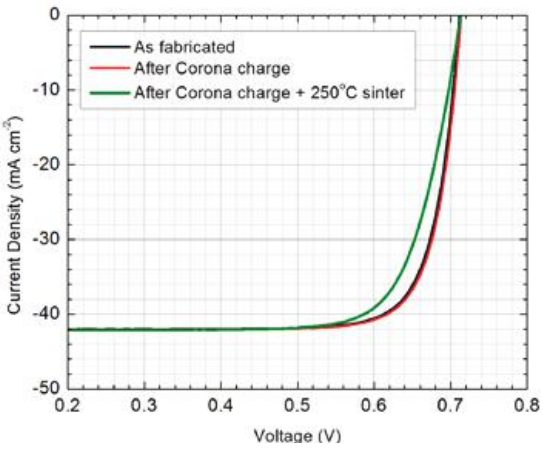

Figure PP1.2a.2: I-V measurements of ONO passivated cells, showing a slight improvement after corona charging, and a significant degradation to the FF after 250°C sintering.

- An in-depth analysis was done to obtain better understanding of the main factors contributing towards the high efficiency as well as to explain some discrepancy between the cell results and the simulated results. The main findings of the study are as follows:
  - High V_{oc}: The cells in the batch have a relatively high average V_{OC} of 712.3 mV across 12 cells. The main contributing factor for such high V_{OC} is due to the use of ONO as the surface passivation layer. This dielectric layer was developed as part of this project in 2015, boasting the capability to achieve immeasurably low J_0 values of approximately 0.1 fAcm^{-2} on planar undiffused surfaces, and approximately 3 fAcm^{-2} on textured surfaces. This film was used over both diffusion polarities on the rear surface as well as the front textured surface, also functioning as the front anti-reflection coating.
  - Sustained J_{sc}: The use of ONO rather than SiN_x/SiO_x for previous batcheswas motivated by the significant improvements to the front surface passivation. However, the addition of the thin thermal oxide layer incurs a slight penalty to reflection loss of the device. We estimated an additional reflection loss of approximately 0.2 mAcm^{-2}. However, the improvement to the front surface passivation from 5 to 3 fAcm^{-2} provided a boost to collection efficiency, thus making up for the reflection loss.
  - Improved FF: The wafers used in the cell fabrication are high resistivity (100 Ohm cm) n-type wafers. The motivation for using such high resistivity is the promise of a higher bulk lifetime, therefore the ability to fabricate thicker cells with a high photo-generation current, and excellent collection efficiencies. However, numerous batches of cells fabricated in 2014 and 2015 using this material have suffered from low FF, identified to be caused by a combination of poor bulk lifetime at the end of fabrication, and the increased internal resistive loss of the cells. After extensive experimentation in 2015, we developed a fabrication sequence with the inclusion of a blanket light phosphorus diffusion which enabled us to retain very high bulk lifetimes. The addition of a light phosphorus diffusion across the entire rear surface of the wafer also acted as a minority carrier flow path, further reducing the internal ohmic losses and improving the carrier collection efficiency. Photo-conductance decay (PCD) measurements of the cells before metal contact formation (after all high temperature steps), indicated a bulk lifetime of 40 ms!

- Among the biggest challenges for the year of 2015 was development of a better understanding of high resistivity n-type float zone (FZ) wafers, with the mission of retaining high lifetime at the end of processing. We established that careful control of the temperature process and retaining a phosphorus doped surface throughout high temperature steps are crucial to retaining bulk lifetimes above 30 ms, contributing towards the fabrication of 24.7% (in-house measured) IBC solar cells in late 2015. Several modified IBC fabrication sequences were trialled in 2016, but did not provide further improvements to the record device efficiency. Once again, we identified the problem to be associated with having low bulk lifetime at the end of device fabrication:
  - The modified IBC sequence for high bulk lifetime was only successful on a small percentage of wafers within an FZ ingot. We found that many wafers would still have significantly reduced bulk lifetime at the end of the IBC process sequence, revealed as concentric circular patterns under

photoluminescence (PL) imaging. Such low lifetime 'rings' are consistent with observation of vacancy related defects created during the FZ crystal growth process. Attempts to identify the affected wafers prior to device fabrication have been unsuccessful as no correlation was found to the wafer resistivity, or initial bulk lifetime of the wafer. Through careful experimentation, we established that an initial 1100°C oxidation for 60 minutes at the start of wafer processing would 'cure' the defects, and does not negatively impact the bulk lifetime of wafers which did not have such defects. The 1100°C oxidation has been incorporated into the cell fabrication, as part of the wafer preconditioning sequence. Figure 1.2a.3 presents a PL image demonstrating the aforementioned effect. All quarters in the figure have a light phosphorus diffusion and SiO_2 surface passivation, with the difference that the bottom two wafers were initially subjected to 1100°C oxidation for 60 minutes.

– Tube furnace diffusion of boron dopants into small openings in dielectrics have been observed to have disproportional effects on effective electronic lifetime, and hence ultimately cell efficiency, compared with large area boron diffusions. Acquiring an improved understanding of the detailed outcomes of boron diffusions in small openings may prove to be a key factor in retaining high bulk lifetimes, and high cell efficiencies for IBC cell structures with small localised doping and contacting. One area of new work which will help in this respect is the development of new methods for characterising doping characteristics at micron resolution via micro-photoluminescence spectroscopy (μ-PLS). A quantitative assessment of doping (surface concentration and depth) can be inferred from the shape of the emission spectrum. Subsequent scanning of the excitation source across a larger area allows a 2D map to be constructed. In Figure 1.2a.4 below we show 2D maps representing the quantity of dopants introduced for diffusions into dielectric openings of 30, 40 and 50 μm. In this instance we show simply the ratio of PLS dopant peak to underlying silicon band-to-band peak, prior to any subsequent analysis which would resolve surface dopant density and diffusion depth and which is the subject of a journal paper under preparation for publication in early 2017. Even from this raw data map we can see, perhaps somewhat unexpectedly, the considerable influence that opening size has on spatially resolved doping characteristics. The 'flat' area in the middle of the largest opening is consistent with the PLS signal observed for a diffusion into a large area, with less dopant signal observed near the edges of openings and for smaller openings generally.

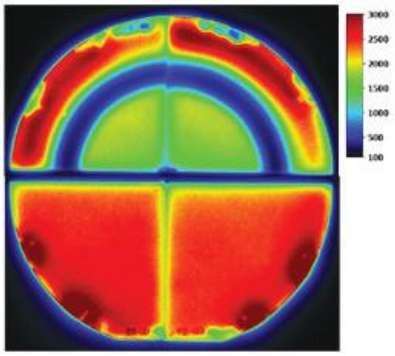

Figure PP1.2a.3: PL image of a wafer where the bottom half has been subjected to 1100°C oxidation for 60 minutes followed by phosphorus diffusion and oxidation on all four quarters.

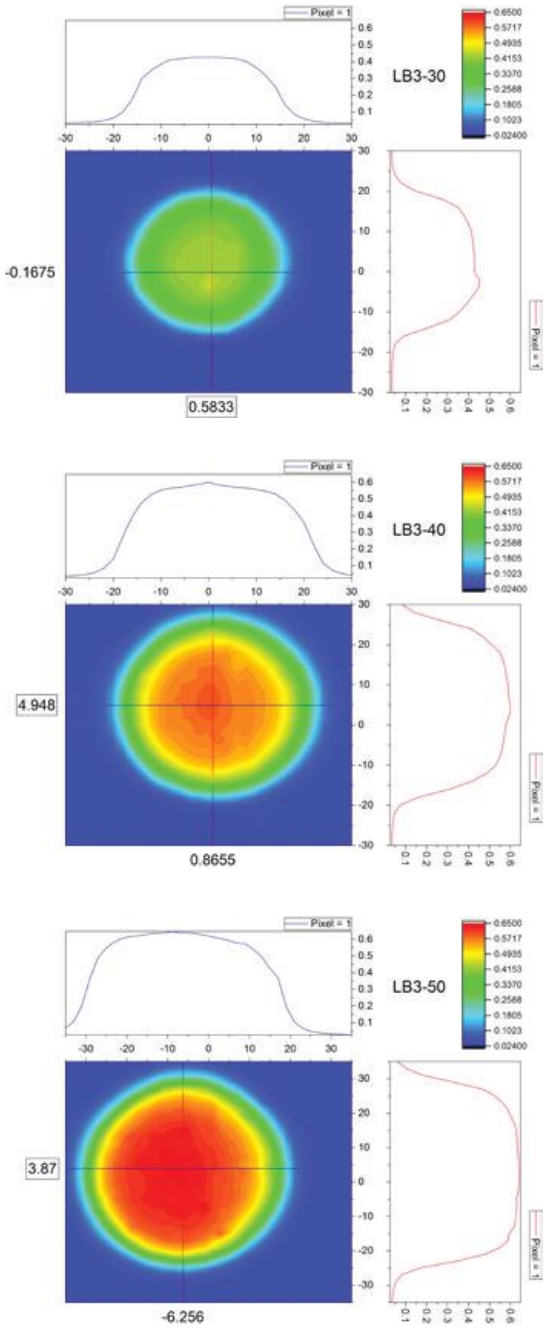

Figure PP1.2a.4: 2D scanned maps of ratio of PLS dopant peak to PLS band–band peak intensity, for boron diffusions into 30 μm, 40 μm and 50 μm (top, middle, bottom) dielectric mask openings.

2. Further development of LPCVD Si_3N_4-based surface passivation film stack

- A J_0 of 4 fAcm^{-2} was achieved using thermal SiO_2/LPCVD Si_3N_4, passivation on a light phosphorus diffused surface (400 Ω/sq). This is an improvement over the previous 6 fAcm^{-2} which was previously achieved on undiffused surface. The motivation to optimise thermal SiO_2/LPCVD Si_3N_4 for light phosphorus diffused surface is related to the improved understanding of wafer lifetime through high temperature processes, and of FF loss of IBC devices where the presence of light phosphorus diffusion blanketing the entire rear surface area improves the FF significantly. This passivation stack has been applied to the most recent batches of IBC cells, achieving a measured V_{OC} of 715 mV.

3. Progress on edge-region passivation

- Since establishing the significance of edge-region losses of small area IBC devices, several edge-passivation schemes have been trialled. The most promising method which allowed keeping the cell still housed on the wafer was to form a physical trench along the perimeter of the active cell area. The process involves the use of laser to ablate SiO_2/LPCVD Si_3N_4 dielectric along the cell perimeter, and to then etch the exposed silicon via tetramethylammonium hydroxide (TMAH) etching. This forms a trench with very thin silicon in between two angled side walls of a (111) plane. The exposed surfaces are passivated along with the front surface using PECVD SiN_x. The biggest challenge in its implementation is balancing the trade-off between mechanical strength and the effectiveness of the geometrical structure to provide electrical isolation. Several batches of IBC cells have had mechanical failures of the structure, either broken wafers or cracks observed along the isolation trench under PL imaging. Analysis of PL images of ongoing batches of cells have shown excellent surface passivation of the sloped walls and that good carrier isolation was achieved. As an example, Figure 1.2a.5 shows the PL images of two adjacent cells on the same wafer under a 2 cm x 2 cm aperture mask; one with edge passivation along the top and bottom edges, and one without. It is observed that the cell with edge passivation shows relatively higher PL counts near the edges. A batch is due for completion and exhibits promising bulk and effective lifetimes above 20 ms and 10 ms respectively.

4. Development of photoluminescence spectroscopy (PLS) method for analysis and assessment of rounded rear texture cells

- The past 12 months included a concerted effort to apply photoluminescence spectroscopy (PLS) to characterise light trapping in textured silicon wafers.

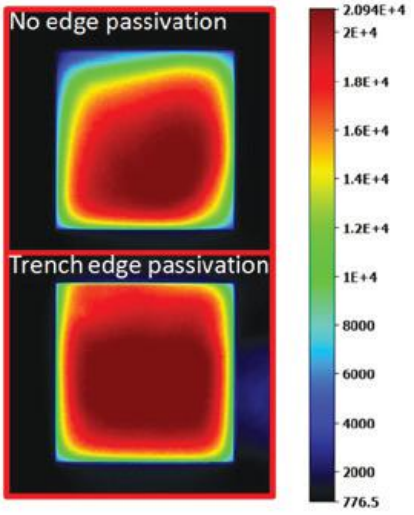

Figure PP1.2a.5: PL images of 2 cm x 2 cm IBC cells through a 2 cm x 2 cm aperture mask. The two cells are adjacent cells on the wafer. The cell on the bottom image has edge passivation on the top and bottom edges.

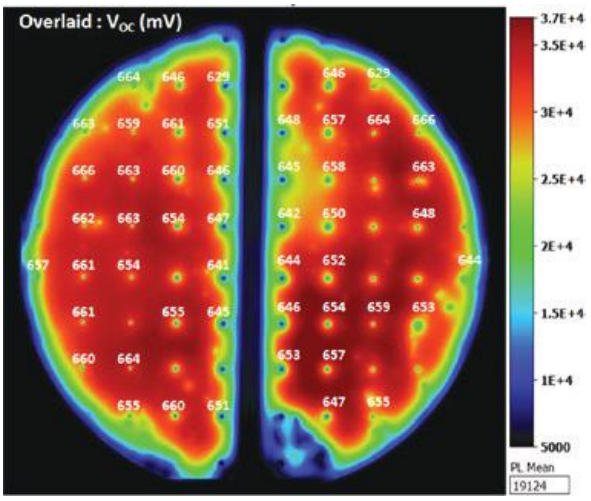

Figure PP1.2a.6: PL image of MIS contact screening test structure. Visible dots of various sizes are the MIS contacts, and inlaid text is the measured V_{OC} under 1-sun illumination intensity.

If successful, PLS would offer a relatively quick way to characterise light trapping, thereby allowing the evaluation of a large variety of surface morphologies to find those best suited to high efficiency IBC solar cells. It was found that the application of PLS to textured wafers introduces significant systematic error for four major reasons: (i) the incident laser light is reflected by the texture towards the detector introducing an 'optical-background signal' that is much greater than the electrical-background signal measured during a conventional zeroing procedure; (ii) the large optical background led to a poor signal-to-noise at short wavelengths, preventing the conventional approach of calibrating the measurement with the sample's external reflection; (iii) the long optical pathlength of a textured wafer combined with the high laser intensity led to significant free-carrier absorption, which could not be neglected as is usually assumed; and (iv) a combination of the

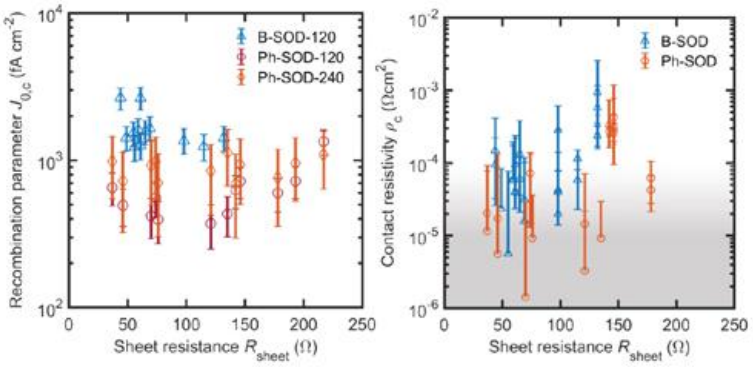

Figure PP1.2a.7: Recombination current prefactor, $J_{0,C}$, and contact resistivity, for combined region of laser doped, passivated and laser contact–opened localised small features as function of sheet resistance achieved via laser doping from phosphorus and boron spin-on-dopant with 248 nm excimer laser.

detector's focal area, the laser's non-uniformity, and the strong wavelength dependence of the optical pathlength led to a wavelength-dependent collection area, preventing the calibration of the measurement at a single wavelength. Clearly, a PLS measurement on a textured wafer is much more complicated than on a planar wafer. Methods to circumvent or mitigate these sources of error were devised and evaluated. ANU's PLS system can now accurately measure the light trapping of a textured wafer but only when there is a reference wafer with a very similar texture and known light-trapping characteristics. A journal article describing the complications of applying PLS to textured wafers is in preparation.

5. Investigation of diffusionless metal-insulator-silicon (MIS) carrier selective contacts

- The most significant factors preventing improvements of device efficiency for the last 12 months are due to the constraints of high temperature processing and the boron diffusion process, both of which reduce the bulk lifetimes of the wafer. Such constraints are not unique to ANU as is obvious from the fact that all single crystalline Si solar cells with confirmed efficiencies above 25% with the exception of Sunpower and heterojunction cells have been made with doped polysilicon (either in situ or ion implanted) instead of traditional furnace diffusions. Unavailability of in situ doped silicon deposition at ANU makes it impossible to follow such a route, however, this prompted the investigation into diffusionless MIS contacts as a boron diffusion replacement. In order to trial a large range of available combinations of dielectrics and metals, a fast screening method was established. The method involves fabricating a number of MIS contact dots of various sizes on a high lifetime wafer, with excellent surface passivation on all other surfaces, and a well-characterised dot contact on the other side. Phtoconductance decay (PCD) measurements and PL images are taken at various steps of fabrication to keep track of the local recombination rates, and the Suns-V_{OC} as well as the 1-sun Light IV which is measured at the end. Extracted series resistance, V_{OC} and PL images from the different dot sizes provide a first order approximate of the contact resistivity. Figure 1.2a.6 presents the PL image of the test structure featuring Al_2O_3/Pd MIS contacts, achieving a V_{OC} of ~670 mV but with a rather high contact resistivity. Progress of the screening as well as refinement of the screening method is expected to be a major agenda in the next 12 months.

6. Analysis and improvement of laser patterning and doping for IBC cells

- There is strong incentive still to fabricate high efficiency cell structures, such as IBC cells, using industrially applicable laser processing – local doping and local contact opening. Such a cell fabrication process can be achieved without full wafer high temperature processing, thus eliminating expensive processing steps while also giving resilience to material defects formed via thermal processing. Following success in 2015 with fabrication of 22.8% efficient all laser doped IBC cells, work continues at a low level on development of these cells. Characterisation of localised features formed by laser doping, passivation and subsequent laser ablation and metallisation has been conducted in 2016 via novel test structures and PL analysis techniques. Some of this work is currently under review for publication in J-PV, and forms the basis for the current batch of cells being fabricated at ANU.
Figure 1.2a.7 shows the key parameters for localised doped and contacted features that can be used in point doped and contact cell structures – the combined (passivated and metallised laser doped) region-averaged recombination current prefactor, $J_{0,C}$, and the contact resistivity, $\rho_{C.}$, as a function of sheet resistance measured using a range of different laser parameters. The analysis shows on the one hand that low damage and low contact resistivity can be achieved using this two-step diffusion laser patterning process, and on the other hand that this can be achieved for a wide range of laser parameters and resultant sheet resistances. Cell simulations, based on the best selection of laser parameters plus currently measured optical and electronic properties of ANU

IBC cells, indicate cell efficiencies of up to 24% can be achieved. On the basis of this characterisation, work will continue in 2017 towards achieving a conventional diffusion-free, all laser doped IBC cell with an efficiency in this range.

7. Design of IBC cells tailored for use as bottom cell in 4-terminal tandem structure

- An efficiency of 26.4 ± 0.7% was measured on a 4 terminal perovskite-Si tandem solar cell using an ANU fabricated IBC solar cell as the bottom cell (Duong et al., 2017). The top layer perovskite cell has a significantly higher bandgap, and thus utilises the low wavelength light, while passing the long wavelength light onto the bottom silicon IBC cell. The excellent light-trapping qualities and excellent quantum efficiency QE at long wavelengths makes the IBC cells ideal for this application, as is illustrated in Figure 1.2a.8 from a previous journal publication featuring a 24.5% tandem, also achieved by using ANU IBC cells as the bottom cell. There is significant room for further improvements to the long wavelength response of the bottom IBC cell. For instance, this can be achieved by increasing the thickness of the Si cell, incorporation of improved light trapping such as rear texturing, and optimising the front anti-reflection coating for long wavelength lights. Fabrication of several thick IBC cells are currently underway, thus further improvements to the tandem stack are likely in the near future.

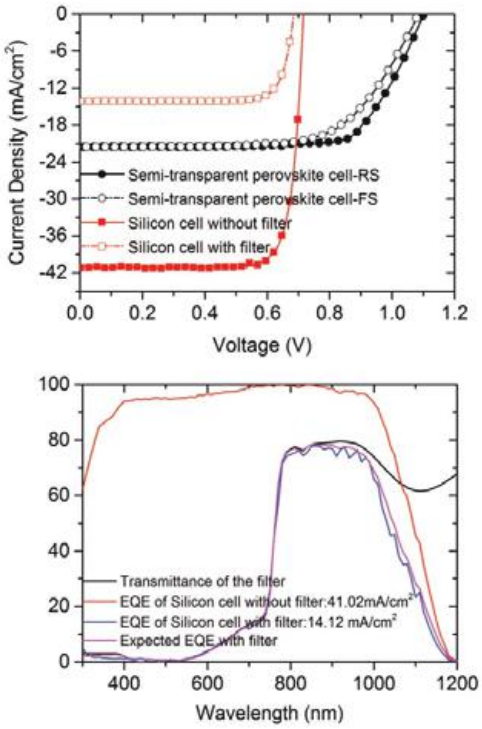

Figure PP1.2a.8: (Top) I-V data of perovskite and silicon cell and (Bottom) EQE measurement of silicon cell with and without top layer perovskite.

Highlights

- 26% perovskite-Si tandem solar cell measured.
- Improvement of rear surface passivation to 4 $fAcm^{-2}$.
- Al_2O_3/Pd diffusionless MIS contact on test structure demonstrating 670 mV.

Future Work

Work over the next 12-month period will be spread across several major areas;

- Evolutionary improvements to existing IBC cell baseline. An in-depth study is underway into lifetime degradation induced by boron diffusion. We aim to gain further understanding of the effects, and to then incorporate the learnings into upcoming batches of IBC cells. Furthermore, we expect further improvements to surface passivation, optical enhancement, edge passivation, and overall understanding of IBC devices from ensuing investigations and device simulations.
- MIS contact as a boron diffusion replacement. We aim to screen through a wide range of MIS contacts to identify promising candidates as substitutes for boron diffusion p+ contact. In the process, we will continue to refine the methodology to provide fast and effective screening.
- All laser doped IBC cells. We aim to consolidate the learnings and fabricate several batches of all laser doped IBC solar cells. We anticipate efficiency greater than 23.5% within the next 12 months.
- Perovskite-Si tandem cells. Optical modelling and device simulations will be employed to further investigate optimisation of Si IBC cells as a bottom cell in the perovskite-Si tandem. Learnings from the study will be implemented in subsequent batches of tandem IBC cell fabrication.

Reference

Duong et al., 2017, Rubidium multi-cation perovskite with optimised bandgap for perovskite-silicon tandem, Advanced Energy Materials (in press)

PP1.2b Passivated Contacts

Lead Partner
ANU

ANU Team
Prof Andres Cuevas, Dr Di Yan, Dr Yimao Wan, Dr Xinyu Zhang, Mr Christian Samundsett

ANU Students
Thomas Allen

ACAP Team
Dr James Bullock

Academic Partners
École polytechnique fédérale de Lausanne (EPFL), University of California Berkeley

Funding Support
ARENA, ARC, ANU

Aim

Crystalline silicon solar cells keep getting cheaper and better. Today's record-setting solar cells use "passivated contacts" to selectively transport electrons and holes towards the cells' terminals. There is a strong motivation for bringing such passivated contacts to the broader PV industry, and this small project, with synergistic support from other sources of funding, aims to do that. The Cuevas Research Group at ANU, together with collaborators at University of California Berkeley and EPFL in Neutâchel, Switzerland, is following a two-pronged approach at developing novel silicon solar cells that incorporate passivated contacts. Part of our work is on the well-proven high temperature approach of depositing a silicon film onto an ultrathin dielectric layer (or layers), so that quantum mechanical tunnelling can take place. We also pursue a low temperature approach, based on depositing materials that have either a very high or a very low work function, which makes them selective to the transport of holes or electrons, respectively.

Progress

Progress in both the high temperature and low temperature approaches during 2016 has been truly remarkable, and part of it is described in separate reports (projects 6.7 and 6.9) detailing our collaboration with University of California Berkeley and EPFL in Neuchâtel, including the demonstration of a dopant-free asymmetric heterocontact silicon solar cell (DASH) with a conversion efficiency approaching 20%.

As lead author, Mr Thomas Allen completed the investigation of gallium oxide as an alternative to aluminium oxide. On the high temperature, polysilicon contact front, Dr Di Yan, has completed the development of boron doped polysilicon/tunnelling contacts. He has also improved on last year's results with a 21.1% efficient cell that uses a novel double-interlayer structure underneath an n^+ polysilicon film. In the alternative, low temperature pathway, we have investigated a wide range of materials, many of them transparent, that can be deposited at low temperatures, thus simplifying the fabrication of high efficiency silicon solar cells. As lead authors, Dr James Bullock, Dr Yimao Wan, Dr Xinyu Zhang and Mr Thomas Allen, with co-workers, have explored materials like lithium fluoride, magnesium fluoride, magnesium oxide, copper oxide, magnesium and calcium. With some of them we have made n-type cells with a full-area rear contact, and with others we have made solar cells with a partial-area rear contact (PaRC), thus reproducing on n-type silicon, for the first time, the advanced cell structure that is becoming popular on p-type silicon. We have convincingly demonstrated these novel n-type Si PaRC devices with efficiencies above 20%.

Plasma-enhanced atomic layer deposited gallium oxide

Advances in the passivation of p-type and p^+ surfaces have been one of the main developments in crystalline silicon solar cell technology in recent years, enabling significant progress in p-type solar cells with partial rear contacts, and n-type cells with front side boron diffusions. As an alternative to the commonly used aluminium oxide (Al_2O_3), we have explored gallium oxide (Ga_2O_3), a relatively similar material, with the added advantage that it may be made conductive by doping. We did attempt such doping via sequential deposition of SnO_2 and Ga_2O_3, but the work was discontinued due to disappointing results and the limited time and resources. This year we demonstrated improvements in the passivation of p-type and boron diffused p^+ surfaces with plasma-enhanced atomic layer deposited (PEALD) gallium oxide (Ga_2O_3) with the addition of plasma-enhanced chemical vapour deposition (PECVD) silicon nitride (SiN_x). On 1.6 Ωcm p-type wafers we measured an improvement in the upper limit surface recombination velocity ($S_{eff\ UL}$) from 2.5 cms^{-1} to 1.4 cms^{-1}, before and after SiN_x capping respectively. We also showed an improvement in the passivation of boron diffused p^+ surfaces over previously reported data, measuring a recombination parameter (J_0) of 26 $fAcm^{-2}$ on a Ga_2O_3 passivated 85 Ω/sq boron diffusion, approaching the Auger limit of ~21 $fAcm^{-2}$ for this diffusion. In addition, we performed initial studies on the thermal stability of the Ga_2O_3/SiN_x stack, which indicate that it is compatible with conventional screen-printed metallisation firing procedures.

Passivated electron and hole contacts based on doped polysilicon and thin dielectrics

Further work on n-type solar cells with a rear n^+ polysilicon contact led to an improvement in the

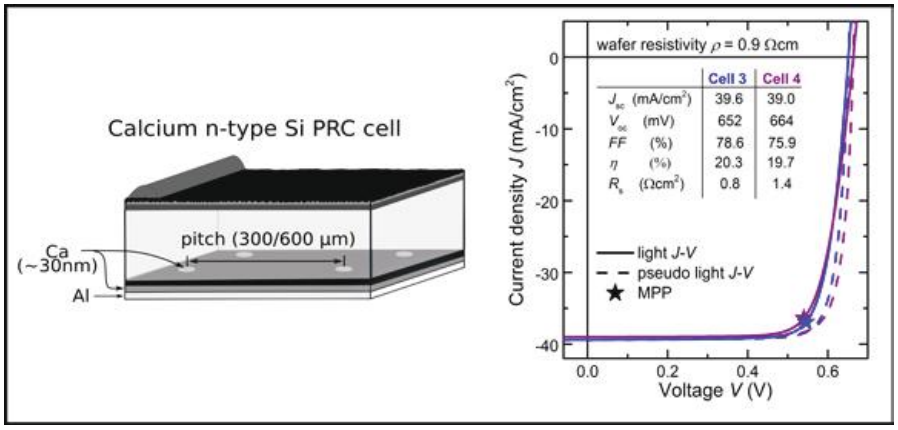

Figure PP1.2b.1: n-type Si solar cell with a calcium-based partial-area rear contact.

conversion efficiency from 20.8% to 21.1%. This still falls short of the real potential of these contacts and, to address that, a new cell design has been made and a more advanced fabrication process is being implemented in our lab. The mentioned progress was related to the development of a novel passivating contact structure based on a double SiN_x/SiO_x interfacial layer, intrinsic hydrogenated amorphous silicon (a-Si:H) and subsequent $POCl_3$ diffusion. The impact of the thickness of SiN_x film was explored in terms of contact resistance and recombination. PL spectra taken before and after the thermal diffusion process indicated that the top a-Si:H layer becomes partially crystallised and, most likely, heavily doped with phosphorus. An important result is that for the optimised diffusion temperature of 850°C, the recombination current parameter J_{0c} and the contact resistivity are no longer sensitive to the SiN_x thickness, in the range that we have investigated. The electron-selective passivating contact with a SiN_x/SiO_x double interlayer achieves a recombination current parameter of ~4 $fAcm^{-2}$ and a contact resistivity of ~140 mΩ cm^2 for the n = 2.5 SiN_x, with thickness from 5 to 13 nm. This passivating contact has been applied to the rear side of n-type silicon solar cells, achieving V_{OC} = 672.4 mV, FF = 80.3% and efficiency = 21.1%. One cell presented a high open circuit voltage of 680 mV.

A technique to make poly-Si (p^+)/SiO_x contacts for crystalline silicon solar cells based on doping PECVD intrinsic amorphous silicon (a-Si) by means of a thermal BBr_3 diffusion process has been developed. The thickness of the a-Si layer and the temperature of the boron diffusion have been optimised in terms of suppressing carrier recombination and transport losses. Different interfacial layers were studied, including ultrathin SiO_x grown either chemically or thermally, and stacks of SiO_x and SiN_x. While the double SiO_x/SiN_x interlayers did not achieve the desired performance, both kinds of single SiO_x layers produced satisfactory passivating contacts, with both a low recombination current and a low contact resistivity. By adjusting the boron diffusion temperature, recombination current parameter J_0 values of ~16 $fAcm^{-2}$ to ~30 $fAcm^{-2}$ have been obtained for structures with initial a-Si thicknesses of 36–46 nm, together with a contact resistivity of ~8 mΩcm^2.

Low resistance hole contacts on crystalline silicon via nitrogen-doped copper oxide films

We have explored the application of transparent nitrogen-doped copper oxide (CuO_x:N) films deposited by reactive sputtering to create hole-selective contacts for p-type crystalline silicon (c-Si) solar cells. We found, for the first time, that CuO_x:N directly onto c-Si is able to form an ohmic contact. X-ray photoelectron spectroscopy (XPS) and Raman spectroscopy measurements were used to characterise the structural and physical properties of the CuO_x:N films. Both the oxygen flow rate and the substrate temperature during deposition were found to have a significant impact on the film composition, as well as on the resulting contact resistivity. After optimisation, a low contact resistivity of ~10 mΩcm^2 has been established. This result offers significant advantages over conventional contact structures in terms of the carrier transport and device fabrication.

Calcium-based contacts for n-type silicon solar cells

The direct metallisation of lightly doped n-type c-Si routinely produces a non-ohmic (rectifying) contact behaviour. This has inhibited the development of n-type c-Si solar cells with PaRC, an increasingly popular cell design for high performance p-type c-Si solar cells. In this research we demonstrated that low resistance ohmic contact to n-type c-Si wafers can be achieved by incorporating a thin layer of the low work function metal calcium (ϕ ~2.9 eV) between the silicon surface and an overlying aluminium capping layer. Using this approach contact resistivities of ρ_c ~2 mΩcm^2 can be realised on undiffused n-type silicon wafers, thus enabling PaRC cell designs on n-type silicon without the need for a phosphorus diffusion. Integrating the Ca/Al stack into a PaRC solar cell architecture fabricated on a lightly doped (N_D = 4.5x10^{14} cm^{-3}) n-type wafer resulted in a device efficiency of η = 17.6% where the Ca/Al contact comprised only ~1.26% of the rear surface. We then

achieved an improvement in this cell structure to an efficiency of η = 20.3% by simply increasing the wafer doping by an order of magnitude to N_D = 5.4x10^{15} cm^{-3}.

Magnesium/amorphous silicon passivating contacts for n-type crystalline silicon solar cells

Among the metals, magnesium has one of the lowest work functions, with a value of 3.7 eV. This makes it very suitable to form an electron-conductive cathode contact for silicon solar cells. We have experimentally demonstrated an amorphous silicon/magnesium/aluminium (a-Si:H/Mg/Al) passivating contact for silicon solar cells. The conduction properties of a thermally evaporated Mg/Al contact structure on n-type c-Si were investigated, achieving a low resistivity ohmic contact to moderately doped n-type c-Si (~5 × 10^{15} cm^{-3}) of ~0.31 Ωcm^2 and ~0.22 Ωcm^2 for samples with and without an amorphous silicon passivating interlayer, respectively. Application of the passivating cathode to the whole rear surface of n-type front junction c-Si solar cells led to a power conversion efficiency of 19% in a proof-of-concept device. The low thermal budget of the cathode formation, its dopant-less nature, and the simplicity of the device structure enabled by the Mg/Al contact open up possibilities in designing and fabricating low-cost silicon solar cells.

Highlights

- 21.1% efficient silicon solar cell with a novel SiN_x/SiO_x/polysilicon double-interlayer passivated contact.
- n-type silicon solar cells with partial-area rear contacts, achieving conversion efficiencies over 20%.
- Best student paper award of the 31st European Photovoltaic Solar Energy Conference (Allen, 2016).
- Best PhD thesis award at the ANU Solar Oration and APVI conference (James Bullock, 2016).

Future Work

Solar cell technologies based on the deposition of junction-forming materials on c-Si wafers offer great promise to reduce fabrication costs, while increasing performance, spurring a wave of technological change in silicon photovoltaics. During 2017 we will investigate a broader range of materials and stacks, optimising their carrier-selective, surface-passivating properties. This work will include strong collaboration with University of California Berkeley, EPFL, KAUST and UNSW. The latter collaboration will focus on the scientific characterisation of passivated contacts. A second, high temperature, strand of the project will capitalise on our n$^+$ and p$^+$ polysilicon contact technology and will focus on improving the efficiency of solar cells made in our lab.

Actions

1. Explore additional selective contact materials by low temperature deposition, both for electrons and holes.
2. Make solar cells using such materials, both with partial and full area rear contacts.
3. Continue the development of advanced n$^+$ and p$^+$ polysilicon/tunnelling contacts.
4. Implement n$^+$ and p$^+$ polysilicon contacts on newly designed solar cells.

References

Allen, T.G., Zheng, P., Vaughan, B., Barr, M., Wan, Y., Samundsett, C. and Bullock, J., "Low resistance TiO2-passivated calcium contacts to for crystalline silicon solar cells", 43rd IEEE Photovoltaic Specialists Conference, Portland, 6-10 Jun 2016, pp. 230.

Allen, T.G., Bullock, J., Zheng, P., Vaughan, B., Barr, M., Wan, Y., Samundsett, C., Walter, D., Javey A., and Cuevas, A., "Calcium contacts to n-type crystalline silicon solar cells", Progress in Photovoltaics: Research and Applications, 2016. DOI: 10.1002/pip.2838.

Wan, Y., et al., 2016, "A magnesium/amorphous silicon passivating contact for n-type crystalline silicon solar cells", Appl. Phys. Lett. 109, 113901.

Yan, D., et al., 2016, Solar Energy Materials and Solar Cells 152, 73.

Zhang, X., Cuevas, A., Bullock, J., "Characterisation of sputtering deposited amorphous silicon films for silicon heterojunction solar cells", 43rd IEEE PVSC, Portland, U.S. , 6-10 Jun 2016, 73

Zhang, X., Wan, Y.M., Bullock, J. Allen, T., Cuevas, A., 2016, "Low resistance Ohmic contact to p-type crystalline silicon via nitrogen-doped copper oxide films", Appl. Phys. Lett. 109, 52102.

PP1.3 Silicon Tandem Cells

The world's best laboratory silicon cell efficiency is now 26.6% and commercial cells are expected to come close to this as the industry continues to scale and mature. To improve on this, research needs to address the losses that stop silicon cells from achieving the theoretical photovoltaic limit of 33%.

Stacking cells on silicon in a tandem structure brings the limiting performance even closer to the theoretical limits for such stacks, due both to silicon's near ideal bandgap in this role and to a reduction in the significance of Auger effects as generation is split between multiple devices. For three cells stacked on silicon, the limiting efficiency exceeds 50%, over 70% relatively higher than for the limit for a single cell.

The large and vigorous silicon photovoltaic industry will continue to perfect the production and reduce the cost of

high quality wafers, as well as other aspects of silicon cell processing. Combined with the large potential efficiency gains outlined above, this suggests that one possible evolutionary path for silicon wafer-based cells would be to use a silicon cell as a substrate for the deposition of thin, high performance, wide-bandgap cells on its top surface, much the same way as an antireflection coating layer or a heterojunction emitter structure is deposited in present commercial cell sequences.

The AUSIAPV work programs target higher efficiencies by addressing silicon tandem cell technologies as monolithic devices (built on the same substrate) or with cells mechanically stacked.

PP1.3a Silicon Tandem Cells (Monolithic)

Five strands under Program Package 1.3a aim, for the first time, to successfully mate the commercially dominant PV technology based on silicon solar cells with other promising PV materials, including the III-V semiconductors, the chalcogenides and perovskite technologies.

Of the Group III-V materials of interest, only GaP offers a good lattice match to silicon, with the other III-V semiconductors as used in high performance III-V cells having about 4% mismatch, being better matched to Ge. One strategy of PP1.3a(i) is to take advantage of the miscibility between Si and Ge to grow a series of Si_xGe_{1-x} buffer layers on Si, with x steadily decreasing. In this way, the lattice constant can be changed from that of Si to that of Ge after growth of a micron or more of buffer material. High quality III-V cells can then be grown on the Ge surface.

A parallel approach PP1.3a(ii) is to take advantage of the similar miscibility of GaP and GaAs by growing a series of GaP_xAs_{1-x} buffer layers on Si with x again steadily decreasing, allowing a transition from the Si lattice constant to that of GaAs. An advantage in this case is that the material in the buffer layer has a much higher bandgap than silicon, allowing the silicon substrate to participate as an active cell in the stack.

Working with US- and Australian-based collaborators, with additional project support leveraged beyond that able to be provided from SRI funding, an efficiency of over 24% with one or more of these approaches is anticipated in the first four years of the ACAP operation. Options for reducing the thickness and cost of any buffer layers, or finding other ways of reducing costs, will be the target of the second phase of activities during years 5 to 8, with a targeted cell efficiency of 32%.

Two more adventurous approaches to building high quality tandem cells on silicon wafers are also being explored. PP1.3a(iii) targets an atomically abrupt Si/Ge transition, where the lattice mismatch is taken up in a single atomic layer, which is thermodynamically feasible since it is a low energy configuration. UNSW has filed patent applications on approaches that have given promising results of this type. This would allow the Ge layer to be very thin, creating negligible absorption loss or, alternatively, thick enough to be used as an active cell in a novel “out-of-sequence tandem”.

The second of these more adventurous approaches (PP1.3a(iv)) is the investigation of silicon tandem cells using chalcogenides as the upper cells in the stack. Although the established chalcogenide cell materials (copper indium gallium selenide (CIGS) and CdTe) have shown high efficiency potential, they are not lattice-matched to silicon and have problems for long-term use arising from the use of toxic and/or scarce materials.

More promising for the long term are devices made from materials based on the CZTS (CuZnSnS) system. Despite the relatively small effort so far devoted to the development of this material, solar cells using it have already demonstrated energy conversion efficiency above 12%. Moreover, the lattice constant of CZTS and that of related alloys are a close match to silicon and the CZTS bandgap, at circa 1.5 eV, is almost ideal for the lower cell in a two-cell stack on silicon. Moreover, alloying with related compounds to replace, for example, Zn or Sn by lighter elements, such as Fe(ii) or Si, will increase the bandgap making values such as the 1.7 eV required for a one-cell stack or the circa 2 eV required for the top cell in a two-cell stack on silicon also accessible in a highly compatible materials system.

Another parallel strand of activity (PP1.3a(v)) involves investigation of materials systems that do not require lattice matching to silicon.

Finally, PP1.3a(vi) takes the approach of using Pd nano-particles for bonding a triple-junction InGaP/GaAs cell to a crystalline Si cell. The aim is to demonstrate multi-junction III-V/Si tandem without epitaxial growth on a crystalline Si template while achieving high performance. The use of bonding allows two-terminal configuration to still be achieved without the additional wiring that would otherwise be required to interconnect a mechanically-stacked four-terminal tandem.

PP1.3a(i) III-V Cells on Silicon Using SiGe Buffer Layers

Lead Partner
UNSW
UNSW Team
Prof Allen Barnett, Dr Ivan Perez-Wurfl

UNSW Students
Li Wang, Brianna Conrad, Martin Diaz, Xin Zhao, Dun Li, Anastasia Soeriyadi

Academic Partners
Yale University, University of Delaware, QESST at Arizona State University

Industry Partners
Veeco, AmberWave

Funding Support
ARENA, USASEC

Aim

Development and demonstration of GaAsP/SiGe tandem solar cell grown on silicon with a target efficiency greater than 24% and show the pathways to more than 35%.

Progress

Great progress has been achieved for this GaAsP/SiGe tandem device on Si substrateThe next quantum step for silicon solar cell efficiency will be a high bandgap solar cell on top of the silicon solar cell. III-V solar cells grown on Si substrates are promising choice due to the demonstrated high conversion efficiency. The efficiency limit for a two-junction structure constrained to a silicon bottom cell is 42.5% (Green, 2013). However, the challenge is the lattice mismatch between epitaxially grown III-V materials and Si. This mismatch leads to a high threading dislocation density (TDD) which results in a reduced open circuit voltage (V_{OC}) (Geisz et al., 2006). A GaAsP/SiGe tandem solar cell has the potential efficiency of 40% (Schmieder et al., 2012). This work reported here is based on the success of growing Si_xGe_{1-x} graded buffer layers to make the lattice constant transition from Si to GaAsP. The SiGe is designed as a high quality bottom cell to form a dual-junction tandem solar cell. A simplified GaAsP/SiGe tandem structure on Si along with a cross-sectional scanning electron microscope (SEM) micrograph is presented in Figure PP1.3a.1.

The structure of the SiGe bottom cell has been improved by adding a 250 nm thick back surface field (BSF) layer, which enables a V_{OC} increase. The highest V_{oc} of 354 mV has been achieved on a SiGe cell (Li et al., 2016a) by adding another BSF layer. J_{SC} of the bottom cell has also been boosted by adding back surface texturing to increase the optical path length of reflected near-bandgap photons and an SiO_2/Al back reflector at the Si rear surface. The highest J_{SC} of 20.3 $mAcm^{-2}$ (Li et al., 2016b) under a GaAsP top cell has been realised by thinning the Si substrate to 150 nm and adding an improved anti-reflection coating (ARC). Applying these light trapping techniques (optical texturing, back surface reflector and thinning Si substrate) to a tandem device, the J_{SC} of the bottom cell has been increased to 14.5 $mAcm^{-2}$ (Wang et al., 2016a) and 14.7 $mAcm^{-2}$ (Conrad et al., 2016) (active area), respectively. The fill factor (FF) of the bottom cell can be further increased by reducing the series resistance (Zhao et al., 2017a). Optical absorption of $Si_{1-x}Ge_x$ graded buffer layers has been analysed to better understand the current contribution of the bottom cell (Li et al., 2016c).

SiGe bottom cell grown on silicon was also separately fabricated. Rear surface texturing was applied on Si back surface. A 200 nm SiO_2 layer was then deposited on the back surface as a back surface reflector. Next, openings were made with photolithography and hydrofluoric acid (HF) etching on SiO_2 layer. This was followed by Al back metal contact evaporation. Ti/Pd/Ag front contacts were deposited on the front. Then the SiGe cell was isolated by reactive-ion etching (RIE). A single layer SiN_x ARC is deposited on the front surface to reduce the front reflection. The fabricated bottom cell is illustrated in Figure PP1.3a.2(a).

Top GaAsP cell J_{SC} has been increased due to a newly designed top grid, which reduces the metal shading percentage. Optimising the window layer thickness and ARC thickness would potentially enable the GaAsP top cell to achieve a J_{SC} of 20.8 $mAcm^{-2}$ (Soeriyadi et al., 2016a). The fill factor of the top cell has also been enhanced due to newly designed top cell geometry to reduce the series resistance. The optical characterisation of III-V alloys has been conducted (Conrad et al., 2017a). Spatially resolved EL and PL coupling of a dual-junction solar cell has been analysed (Soeriyadi et al., 2016b), and

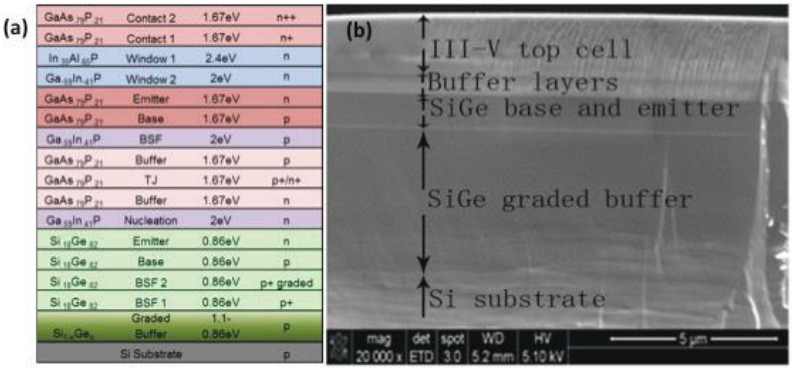

Figure PP1.3a.1: (a) Diagram of an improved GaAsP on SiGe/Si tandem structure showing the layers; and (b) Cross-sectional SEM of GaAsP/SiGe grown on Si with labelled main regions.

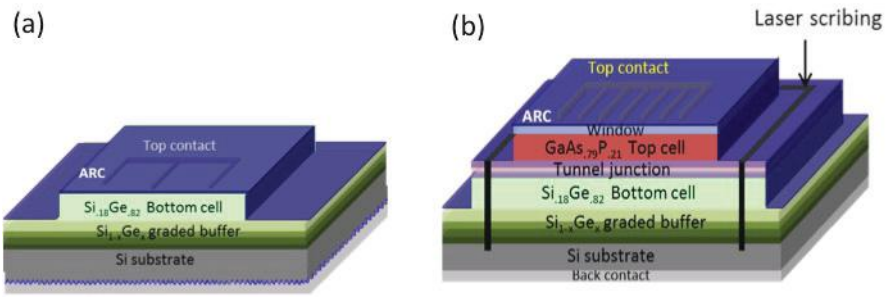

Figure PP1.3a.2: (a) Cross-section of fabricated bottom cell; and (b) Top cell in the tandem structure.

some parameters of each sub-cell have been extracted using a three-terminal device design (Soeriyadi et al., 2016c).

The fabricated top cell in the tandem structure is illustrated in Figure 1.3a.2(b). Al was deposited as the rear metal contact to the Si substrate. Ni/AuGe/Au was evaporated for the front contact grid on the heavily doped contact layer. Both metal contacts were annealed at 350°C for 1 minute by rapid thermal processing (RTP). The contact layer was selectively etched by wet chemistry (NH_4OH: H_2O_2: H_2O=7:35:160) using the front metal grid as a protection mask. The top cell was isolated by two steps. First, we used wet chemical etchants (HNO_3: HCL: H_2O=1:1:1) to etch through the window layer. Second, we switched to wet chemical etchants (NH_4OH:H_2O_2:H_2O=7:35:160) which selectively stops at the BSF layer of the GaAsP top cell. Next the SiN_x/SiO_2 ARC stack was deposited by PECVD. Finally, we used Lee laser to scribe around the top cell on the BSF surface. This was to short-circuit the bottom cell since the laser scribes as deep as around 40 um measured by Dektak, such that the top cell can be measured and analysed in this tandem structure without a middle metal contact.

The GaAsP top cell and the SiGe bottom cell were measured independently, in order to measure the efficiency of the combined best individual sub-cells from our presently available materials.

IV measurements were conducted outdoors on a clear day using a sun tracker (STR-22G Sun Tracker, EKO instrument) as shown in Figure 1.3a.3. An optical lens was used to measure the IV performance under different concentrations. The top cell was measured under the sunlight directly, and the bottom cell was measured under a 750 nm long pass filter in order to simulate the condition of being beneath the GaAsP top cell, since GaAsP (with a bandgap of 1.67 eV) absorbs the light with wavelength shorter than 750 nm.

IV measurements have been conducted for the top cell and bottom cell individually. Light JV curves of top cell and bottom cell under 7.2X illuminations are shown in Figure PP1.3a.4. Concentration ratio of the top cell is determined using 1-sun J_{SC} of 20.1 and 17.4 $mAcm^{-2}$ for top cell and bottom cell, respectively, under direct light as introduced above. The efficiencies (active area) under 1X of the top cell and bottom cell are 18.7% and 3.0%, respectively, such that the tandem efficiency (active area) totals 21.7%. The peak efficiency (active area) of the top cell is 20% under 7.2X; the active area efficiency of the bottom cell is 3.8% under the 7.2X. Therefore the tandem active area efficiency of 23.8% is calculated under 7.2X. All the parameters are listed in Table PP1.3.1. Any uncertainties in the calculations and measurements were propagated throughout the calculations arriving to a conservative bound for the calculated efficiency of ±1% absolute.

A realistic efficiency for this GaAsP/SiGe on an Si tandem device can be predicted using the best measured individual parameters, as listed in Table PP1.3a.2. The sum of the best measured individual sub-cell (GaAsP and SiGe) V_{OC} is 1.54V and 1.79V under 1× and 20× (Wang et al., 2015a and Zhao et al., 2015a), respectively. The best measured FF of a two-terminal (2-T) tandem device is around 83% (Schmieder et al., 2012a). The best measured J_{SC} of the top cell and the bottom cell is 20.1 and 20.3 $mAcm^{-2}$, respectively, as mentioned above, such that the 2-T tandem J_{SC} will achieve 20.1 $mAcm^{-2}$. This leads to a 2-T efficiency of around 25.7% at 1X. By summing up the measured V_{OC} of each sub-cell under 20X, the tandem V_{OC} of the tandem device will be 1.79V, and with the measured FF of 80%, the 2-T efficiency will achieve approximately 28.8% at 20X. By further improving

Figure PP1.3a.3: Outdoor IV measurement set up on sun tracker.

the material quality with the TDD below 10^{-6} cm^{-2}, tandem V_{OC} will be 1.7V and 1.87V under 1X and 20X, respectively. With the aid of improving light-trapping techniques and optimising window layer and ARC thicknesses, targeted 20.8 $mAcm^{-2}$ will be realised for each sub-cell. In addition, with further decreasing series resistance, FF of 83% will be kept under concentrated illuminations. Therefore, the GaAsP/SiGe tandem device on Si will achieve efficiencies of 29.3% and 32.3% under 1X and 20X, respectively. With two-axis trackers for 400X, the voltage of tandem will be boosted to 2.04V, using the same tandem FF of 83% . The efficiency (active area) may reach 35.8% with all these improvements.

Highlights

- The structure and fabrication process have been improved for top and bottom cells.
- Tandem efficiency of 23.8% has been reported under 7.2X concentration outdoor measurement.
- Pathway to achieve 32.9% at 20X and 35.8% at 400X has been outlined.

Future Work

Demonstrate a world-record efficiency (target 26%) with independent certification.

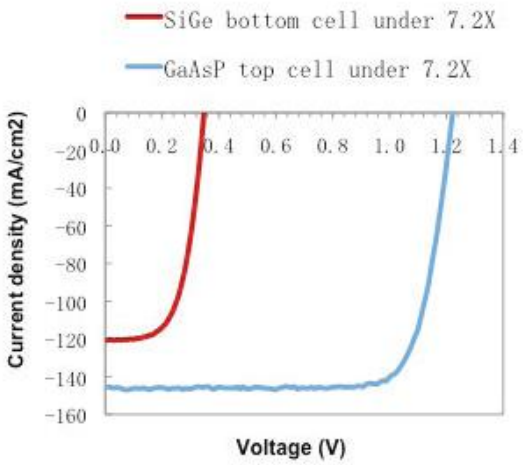

Figure PP1.3a.4: JV curve of top cell and bottom cell under 7.2X illuminations.

References

Conrad, B., et al., 2016a, "Improved GaAsP/SiGe Tandem on Silicon Outdoors and Under Concentration", 43rd IEEE PVSC

Conrad, B., et al., 2017a, "Optical characterisation of III-V alloys grown on Si by spectroscopic elliposometry. Solar Energy Materials and Solar Cells. 162, 7–12.

GaAsP-SiGe dual junction solar cell on a Si substrate", Solar Energy Materials & Solar Cells, 159, 86–93.

Geisz, J. F., et al., 2006, "Lattice-mismatched GaAsP solar cells grown on silicon by OMVPE,", Photovoltaic Energy Conversion, Conference Record of the 2006 4th World Conference., 1, 772–775.

Green, M., 2013, "Silicon solar cells: State-of-the-art", Phil. Trans. R. Soc. A, 371, 1996.

Device	Concentration ratio X	Jsc (mA/cm2)	Voc (V)	FF	Efficiency (full area)	Efficiency (active area)
Top cell	1	20.1	1.12	80.9	18.2%	18.7%
Bottom cell	1	16.7	0.278	61.2	2.84%	3%
Tandem cell	1				21%	21.7%
Top cell	7.2	146.2	1.22	0.79	19.4%	20.0%
Bottom cell	7.2	125.2	0.344	0.60	3.6%	3.8%
Tandem cell	7.2	/	/	/	23.0%	23.8%

Table PP1.3a.1: Parameters of top cell and bottom cell under 1X and 7.2X concentrations.

# of SUN	Condition	Voc	Jsc	FF	Product of best Voc*Jsc*FF full area	Product of best Voc*Jsc*FF active area
		(V)	(mA/cm2)	(%)	(%)	(%)
1X	Measured	1.54	20.1	83	25.7	26.4
	Predicted	1.7	20.8	83	29.3	29.7
20X	Measured	1.79	402 (20.1)	80	28.8	29.3
	Predicted	1.87	416 (20.8)	83	32.3	32.9
400X	Predicted	2.04	8320 (20.8)	83	35.2	35.8

Table PP1.3a.2: Summary of measured and predicted individual best parameters of tandem cell.

Li, D., et al., 2015a, "Optical constants of silicon germanium films grown on silicon substrates", Solar Energy Materials and Solar Cells, 140, 69–76.

Li, D., et al., 2016a, "Performance improvement for epitaxially grown SiGe on Si solar cell by optimizing the back surface field", Phys. Status Solidi RRL, 10, 735–738.

Li, D., et al., 2016b, "Performance improvement for epitaxially grown SiGe on Si solar cell using a compositionally graded SiGe base", Applied Physics Letters, 109.

Li, D., et al., 2016c, "Optical absorption of graded buffer layers and short circuit current improvement in SiGe solar cells grown on silicon substrates", Solar Energy Materials & Solar Cells, 157, 973–980.

Schmieder, K. J., et al., "Analysis of tandem III-V/SiGe devices grown on Si," 38th IEEE PVSC.

Schmieder, K., et al., 2012, "Analysis of tandem III-V/SiGe devices grown on Si", 38th IEEE PVSC.

Soeriyadi, A., et al., 2016a, "Increased Spectrum Utilisation with GaAsP/SiGe Solar Cells Grown on Silicon Substrates", MRS Advances, 1–6.

Soeriyadi, A., et al., 2016b, "Spatially Resolved EL and PL Coupling of a Dual Junction Solar Cell", 43rd IEEE PVSC.

Soeriyadi, A., et al., 2016c., "Solar cell parameters extraction of subcells in a dual junction system through a three terminal device design", PVSEC-26.

Wang, L., et al., 2015a, "Material and device improvement of GaAsP top solar cells for GaAsP/SiGe tandem solar cells grown on Si substrates", IEEE Journal of Photovoltaics, 5(6), 1800–1804.

Wang, L., et al., 2016a, "Current and efficiency improvement for a GaAsP/SiGe on Si tandem solar cell device achieved by light trapping techniques", Physica Status Solidi –– Rapid Research Letters, 10(8), 596–599.

Zhao, X., et al., 2015a, ""Material and device analysis of SiGe solar cells in a GaAsP-SiGe dual junction solar cell on Si substrate," Solar Energy Materials & Solar Cells, 134, 114–121.

Zhao, X., et al., 2017a, "Short circuit current and efficiency improvement of SiGe solar cell in a

PP1.3a (ii): III-V Cells on Silicon Using GaAsP Buffer Layers

Please refer to Section 6.16.

PP1.3a(iii) III-V Cells on Silicon Using Atomically Abrupt Si/Ge Transition

Lead Partner
UNSW

UNSW Team
Dr Xiaojing Hao, Dr Anita Ho-Baillie, Prof Martin Green, Prof Gavin Conibeer, Dr Stephen Bremner, Dr Ziheng Liu, Dr Hamid Mehrvarz

UNSW Students
Shinyoung Noh, Chuqi Yi

NREL Team
Dr Dan Friedman

Academic Partners
Korea Advanced Nano Fab Center (KANC),Institute of Nuclear Energy Research (INER), Taiwan
Tianjin Institute of Power Sources (TIPS), China
Applied Physics Division, National Institute of Standards and Technology (NIST), USA
Helmholtz-Zentrum Berlin (HZB), Germany

Industry Partners
Shinshin, Epistar

Funding Support
ARENA, ARC

Aim

This project aims to build low-cost high efficiency Si/III-V tandem cells by using the sputtered heteroepitaxial Ge/Si. The high quality sputtered heteroepitaxial Ge/Si will be used as a virtual Ge substrate or interconnecting layer for integrating Si wafers with overlying III-V solar cells. For the latter, an atomically abrupt Si/Ge transition is used, where the lattice mismatch is taken up in a single atomic layer, which is thermodynamically feasible since it is a low energy configuration.

Progress

Good progress has been made on the novel methods developed in this project for reducing defects in the virtual Ge. The methods are (i) laser annealing and (ii) aluminium assisted crystallisation of Ge on Si.

It has been previously demonstrated that threading dislocation density (TDD) in Ge deposited on Si by DC magnetron sputtering can be effectively reduced by laser annealing to a range of 106–107 cm^2 in a large area. By laser scanning the sample, the Ge layer is melted and recrystallised laterally following the laser beam at a high speed. Due to the lateral regrowth, Ge acts as the crystallisation seed instead of Si. This changes the mechanism from Ge/Si heteroepitaxy to Ge/Ge homo-epitaxy. In addition, the high recrystallisation speed results in the vacancies super-saturation which will induce the dislocations climbing and moving to the lateral surface. As a result, Ge films with low TDD are obtained after diode laser annealing. However, the melting and regrowth process is also accompanied by the overheating issue which can induce the line pattern on Ge surfaces

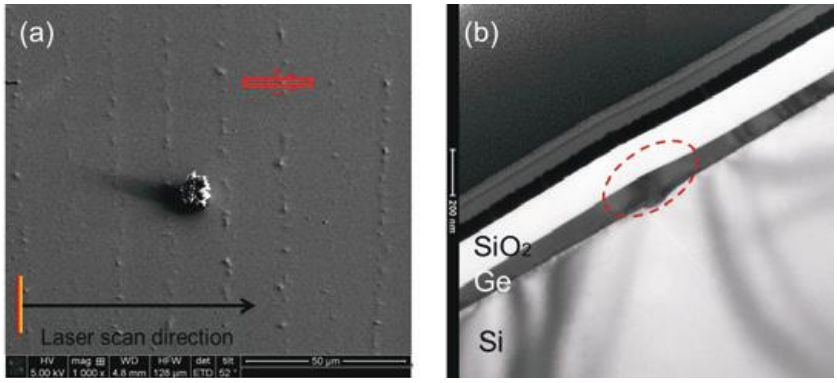

Figure PP1.3a.5: (a) Plan-view scanning electron microscop (SEM); and (b) cross-sectional TEM images of the Ge sample after laser annealing at melting temperature. The circled part is line pattern induced by overheating.

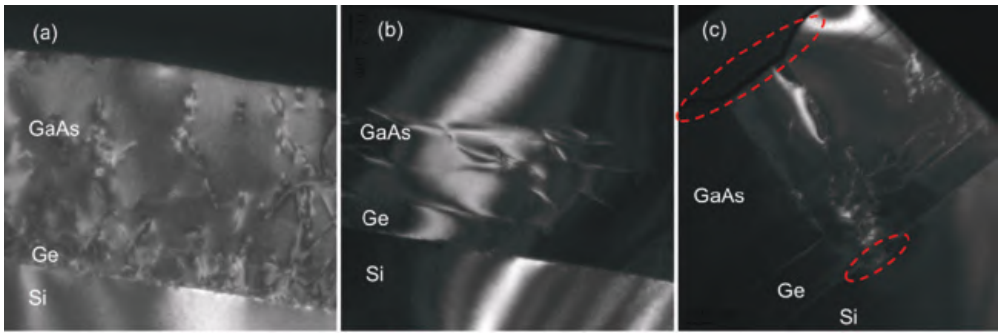

Figure PP1.3a.6: Dark-field cross-sectional TEM images of GaAs films grown on different virtual Ge substrates (a) as-deposited Ge, (b) laser treated Ge smooth part, and (C) laser treated Ge with line pattern part.

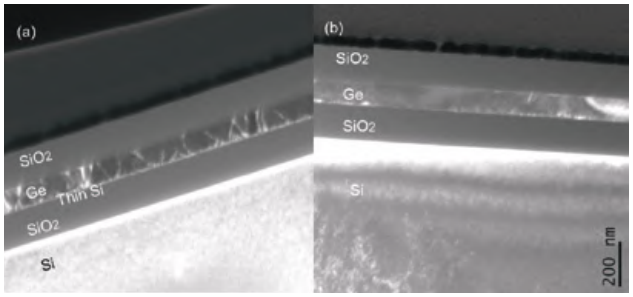

Figure PP1.3a.7: Dark-field cross-sectional TEM images of Ge films grown on SOI substrate (a) before and (b) after laser annealing

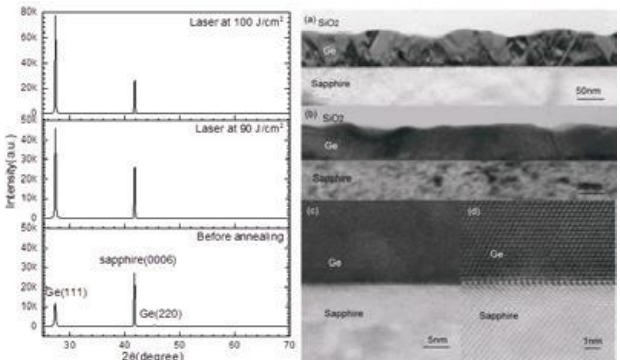

Figure PP1.3a.8: (a) XRD 2θ-Ω profiles of the Ge samples before and after laser annealing at 90 J/cm^2 and 100 J/cm^2; and (b) TEM images of the Ge sample (a) before annealing, (b) after laser annealing, (c) magnified and (d) atomic-resolution images of the Ge/sapphire interface showing good epitaxy.

and the diffusion of Si into Ge (Figure PP1.3a.5) which pose challenges to the subsequent growth of group III-V materials.

Since both the TDD and surface roughness are critical for the following III-V deposition on virtual Ge substrates, the surface pattern will degrade the quality of GaAs films. Figure PP1.3a.6 shows the dark-field cross-sectional transmission electron microscope (TEM) images of GaAs films grown on different virtual Ge substrates. Compared with the as-deposited one, the laser-treated Ge gives much lower defect density in the GaAs films. However, the pattern part induces quite a lot of defects which could grow laterally within the GaAs film.

Laser annealing was applied on Ge grown on SOI (Si on insulator) substrate to prove that the surface pattern

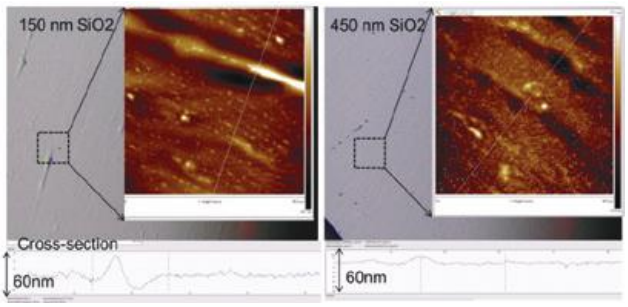

Figure PP1.3a.9: AFM data of the Ge surfaces after laser treatments with SiO_2 capping of 150 nm and 450 nm.

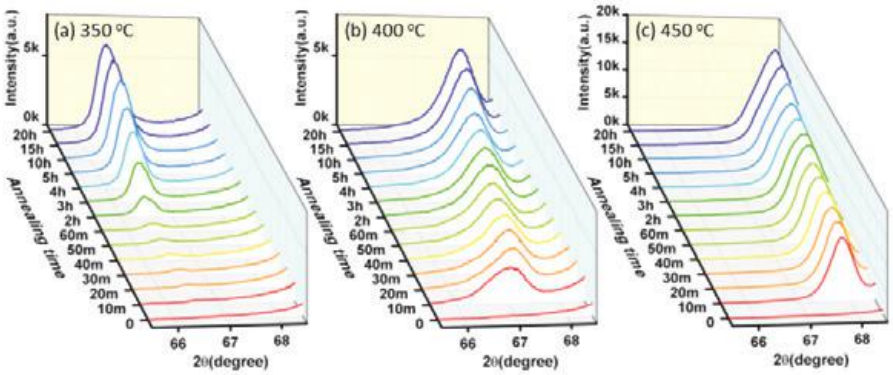

Figure PP1.3a.10: In situ XRD results: 2θ–Ω profiles around (400) order of the Si_xGe_{1-x} annealed at (a) 350°C (b) 400°C and (c) 450°C for various times.

is due to the Si and Ge interdiffusion induced by overheating. As shown in Figure PP1.3a.7, there is no surface roughening after laser treatment because the amount of Si is limited. The effects of laser scanning speed and laser power on the surface roughness have been investigated. However, the line pattern on the surface still exists.

One method to solve the surface pattern issue is to insert a barrier layer below Ge to prevent the Si and Ge interdiffusion and therefore minimise the surface roughening. Thin SiO_2 barrier layers with thicknesses between 0.5 nm and 3 nm have been introduced prior to Ge depositions. The results show that the SiO_2 layers at these thicknesses are not thick enough to prevent the Si and Ge interdiffusion, but have already interrupted the Ge epitaxy from Si. A barrier layer such as Al_2O_3 that can maintain the epitaxy growth of Ge is required. As both the two epitaxial growth processes are difficult to achieve, we start with the epitaxy of Ge on sapphire (Al_2O_3) substrates. The x-ray diffraction (XRD) and TEM results indicate that high quality single crystalline Ge on sapphire are achieved after laser annealing (Figure PP1.3a.8). The next step could be epitaxial growth of Al_2O_3 on Si and to finally obtain the Ge/Al_2O_3/Si structure.

Another approach to minimise the surface pattern is capping layer engineering. Our recent work shows that the capping layer can dramatically affect the property of the surface pattern. With the thickness of the SiO_2 capping layer increasing from 150 nm to 450 nm, the height of the surface line pattern is significantly reduced from 50 nm to 10 nm (Figure PP1.3a.9). The optimisation of the capping layer thickness, use of different types of dielectric layers, and various dopings of the capping layer are to be conducted to minimise the surface pattern.

In this project, aluminium-assisted crystallisation is also investigated as an option for Ge epitaxial growth on Si because the temperature required for Ge crystallisation is reduced with the presence of aluminium (Al). This is because the covalent bonds of the Ge and Si are weakened when in contact with Al. As a result of the bond weakening, these Si and Ge atoms have relatively high mobility and tend to lower the Gibbs energy of the system by crystallising at sites of low energy. The higher mobility of the Ge atoms may help to eliminate the growth of dislocations and improve the Ge film quality.

An aluminium-assisted crystallisation process can involve the deposition of a stack of Al and Ge layers on the Si substrate at room temperature to form an Si/Al/Ge structure. After thermal annealing at temperatures around 400°C for 1 hour, the layer exchange happens and epitaxial Si_xGe_{1-x} layers are obtained.

To further investigate the mechanism of Si_xGe_{1-x} epitaxial growth on Si by aluminium-assisted crystallisation, we have conducted an in situ XRD to study the effect of annealing time at different temperatures. The Si content of the Si_xGe_{1-x} films rises with increasing annealing temperature due to the reduced critical thickness for crystallisation. The switch of growth rate observed in XRD results (Fig. PP1.3a.10 and Fig. PP1.3a.11) and changes of microstructures revealed in TEM measurements (Fig. PP1.3a.12) suggest that the evolution of the Si_xGe_{1-x} films with time can be divided into two stages: Si_xGe_{1-x} epitaxial growth on Si through layer exchange and Si_xGe_{1-x} diffusion into Si substrate. The time required for complete layer exchange decreases with elevating temperature. After the completion of layer exchange, the Si_xGe_{1-x} diffuses into the Si substrate with prolonged annealing time. The Si content of the epitaxial Si_xGe_{1-x} film keeps increasing with time throughout the process. This increase is rapid during the layer exchange but is gradual during the diffusion into Si substrate. These results suggest that the Si content of the Si_xGe_{1-x} films can be controlled by the annealing temperature and duration.

Highlights

- Developed understanding of the laser-induced crystallisation.
- Developed understanding of the surface roughening caused by the laser annealing process.
- Devised strategies for reducing surface roughening and Si diffusion into the Ge layer caused by the laser annealing process.

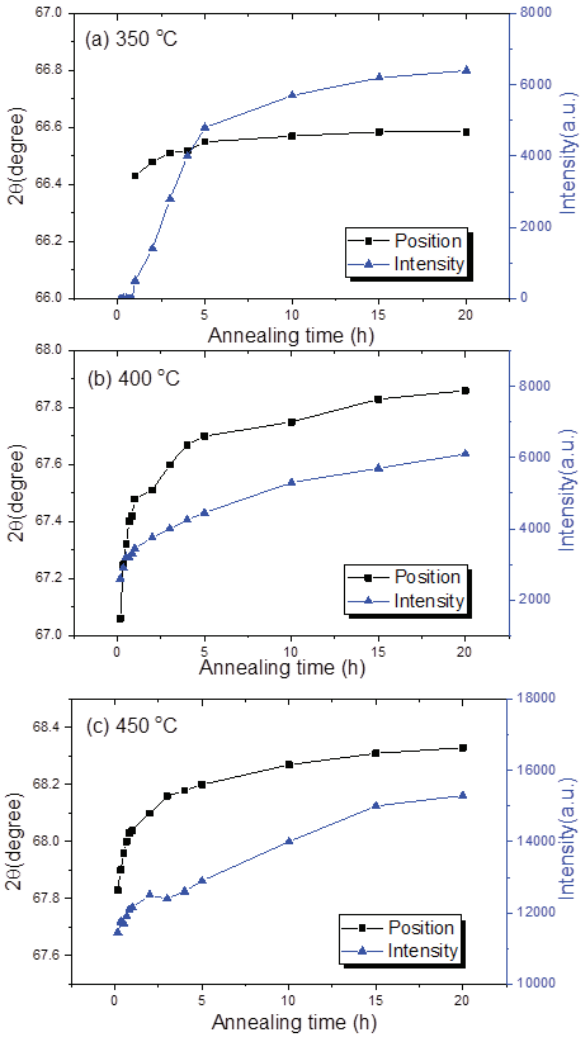

Figure PP1.3a.11: In situ XRD peak data as a function of annealing time at (a) 350°C (b) 400°C and (c) 450°C.

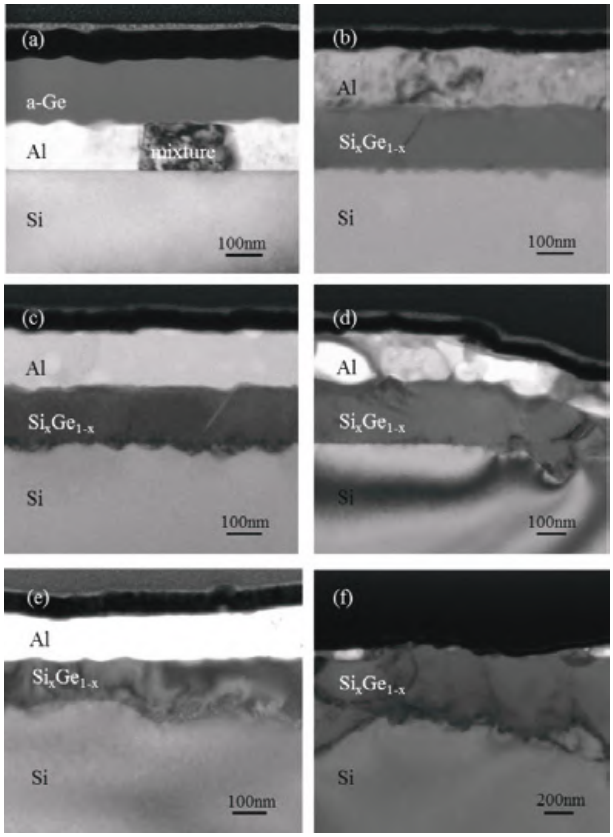

Figure PP1.3a.12: Cross-sectional TEM images of the Si_xGe_{1-x} samples annealed at 350°C for (a) 1 h and (b) 20 h; at 400°C for (c) 1 h and (d) 20 h; at 450°C for (e) 1 h and (f) 20 h.

- Preliminary work has started using capping layer to reduce surface roughening during laser annealing process.
- Developed understanding of the mechanism of Si_xGe_{1-x} epitaxial growth on Si by aluminium-assisted crystallisation.

Future Work

The aim of future work is to improve the laser annealing process to reduce surface roughening and Si diffusion into the Ge layer caused by the laser annealing process. The use of capping layer, such as different types, different thicknesses, and the introduction of dopants into the capping layer will be investigated.

Other future work may include the investigation of a combined process of aluminium-assisted crystallisation and laser annealing to capitalise on the advantages from both processes. The combined process may lower the crystallisation temperature and therefore the laser power required thereby avoiding Si diffusion into the Ge layer.

This includes investigation of the use of capping layer to "smooth" the Ge layer.

References

Liu, Z., Hao, X., Huang, J., Ho-Baillie, A. and Green, M.A., 2016, "Dislocation density reduction of virtual Ge substrates by CW diode laser treatment", 43rd IEEE Photovoltaic Specialists Conference, Portland, 2382.

Liu, Z., Ho-Baillie, A., Hao, X., Huang, J. and Green, M.A., 2016, "Virtual Ge Substrates with Low Threading Dislocation Density Produced by CW Laser Induced Recrystallization", 2016, MRS Spring Meeting, Phoenix.

Liu, Z., Hao, X., Huang, J., Li, W., Ho-Baillie, A. and Green, M.A., 2016, "Diode laser annealing on Ge/Si (100) epitaxial films grown by magnetron sputtering", Thin Solid Films, 609, 49.

Liu, Z., Hao, X., Ho-Baillie, A. and Green, M.A., 2017, "In situ X-ray diffraction study on epitaxial growth of Si_xGe_{1-x} on Si by aluminium-assisted crystallization", J.Alloys and Compounds, 695, 1672 .http://dx.doi.org/10.1016/j.jallcom.2016.10.315.

PP1.3a(iv) Chalcogenide on Silicon Tandem Cells

Lead Partner
UNSW

UNSW Team
Dr Xiaojing Hao, Prof Martin Green, Dr Jialiang Huang, Dr Ouyang Zi, Dr Fajun Ma

UNSW Students
Aobo Pu, Jongsung Park, Xu Liu, Chang Yan, Kaiwen Sun

NREL Team
Dr Glenn Teeter, Dr Mathew Young, Dr Steve Johnston

Academic Partners
Colorado School of Mines (A/Prof Brian Gorman)

Funding Support
ACAP, ARENA

Aim

Chalcogenide semiconductors are promising as absorber materials for solar cells due to their direct bandgaps, high absorption coefficient (>$10^4 cm^{-1}$), high energy conversion efficiency potential and high stability. As an ideal candidate to substitute for toxic and rare elements in CIGS, CZTS (Cu_2ZnSnS_4), a quaternary absorber material with a bandgap of 1.5 eV has been identified. This bandgap energy is close to the optimal bandgap for a single-junction solar cell of 1.35 eV, and is also optimal for a middle cell in a three-cell tandem with a Si bottom cell. Bandgap tuning of CZTS by substituting a lower atomic number group IV element for some of the Sn, Ag for Cu, allows exploration of CZTS-based cells for the top cell in a CZTS/Si stack for a two- or three-cell tandem. The combination of optimal bandgap as a middle cell, and tunable bandgap as a top cell for a three-cell stack and low lattice mismatch shows that this material system is well suited for the top cell on Si cells. The aim of the present project is to work with NREL and CSU, which has world-leading expertise on I-II-VI chalcogenide solar cells and characterisation, to exploit the complementary synergies to develop a new generation of Si wafer cell technology by using chalcogenide materials, with performance of the Si cell substantially improved by deposition of thin layers of high performance chalcogenide cells on its surface to produce tandem devices.

Progress

Significant progress has been made in improving the efficiency of CZTS/Si tandem cells by increasing the CZTS solar cells' efficiency and designing tandem cells with CZTS (family) cells and Si cells.

Highlighted research progress is mainly in the following aspects.

The efficiency of base-line pure sulphide CZTS solar cells has been improved. The highest in-house measured CZTS cell efficiency is 9.7% and certified performance by NREL is 9.5% (Figure PP1.3a.13). In addition to the main manufacturing stream of CZTS made from sputtering method, CZTS prepared from nanocrystal ink was also developed as a low-cost alternative. Combined Li and Na doping of CZTS was identified as more effective in obtaining high performance CZTS solar cells than Na doping only (Figure PP1.3a.14). This will be tested in our future work in the sputtering manufactured CZTS solar cells.

Alternative transparent conductive electrode (Ag NW) was developed replacing traditional transparent conductive oxide (TCO) (i.e. indium tin oxide (ITO) and aluminium-doped zinc oxide (AZO)) and beyond 7% efficient CZTS solar cells with Ag NW electrode was demonstrated (Figure PP1.3a.15). Traditional transparent conducting oxides (TCOs), ITO and AZO, will cause significant red wavelength light absorption through free carrier absorption (Figure PP1.3a.16). A novel highly transparent and conductive hybrid Ag NW structure composed of thin ITO/Ag NW/thin ZnO was developed, enabling improved lateral conductivity and mechanical adhesion, reduced reflection and Ag oxidisation. In order to avoid the temperature-induced alteration on the underneath heterojunctions/solar cells, highly transparent and conductive Ag NW were developed as the front electrode, without any heat treatment, and integrated within CZTS solar cells. CZTS solar cells with Ag NW show increased J_{SC} and FF, with an average 1% increase in the efficiency compared with the reference cells with ITO electrodes (Figure PP1.3a.15).

With the established TCAD simulation model and the measured properties of our fabricated CZTS solar cells (by NREL and UNSW), the key factors responsible for the voltage loss were identified and prioritised. For our champion cells, the cell performance loss is still dominated by the heterojunction interface recombination (Figure PP1.3a.17). The second key factor contributing to the performance loss is the disorder issue of the CZTS absorber (Figure PP2.2b.3).

With the champion CZTS solar cell and screen-printed Si wafer solar cell, beyond 15% four-terminal CZTS/Si

tandem cells were demonstrated by spectrum splitting (Table PP1.3a.1, Figure PP1.3a.18). Please note the CZTS solar cell used ITO as the front electrode, which will be replaced by Ag NW in future work to reduce its parasitic absorption and improve the optical gain in both CZTS and underneath Si cells. In addition, it is notable that the average open circuit voltage of our CZTS solar cells with $Zn_xCd_{1-x}S$ buffer is about 750 mV (Figure PP1.3a.19), higher than the 669 mV of the 9.7% efficient CZTS solar cell used in this tandem case. This is because the added buffered solution changes the ratio of Zn/Cd, resulting in a band alignment shifted from the optimised range used for the CZTS cells with 750 mV open circuit voltage. In a similar way, with the high bandgap CIGS solar cell provided by Solar Frontier, the demonstrated best four-tandem cells by spectrum splitting method are CIGS

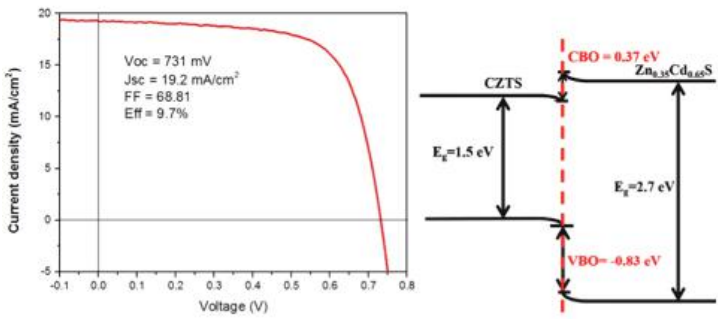

Figure PP1.3a.13: J-V curve of in-house measured 9.7% efficiency CZTS solar cells (left) with better aligned conduction band offset at heterojunction interface (right).

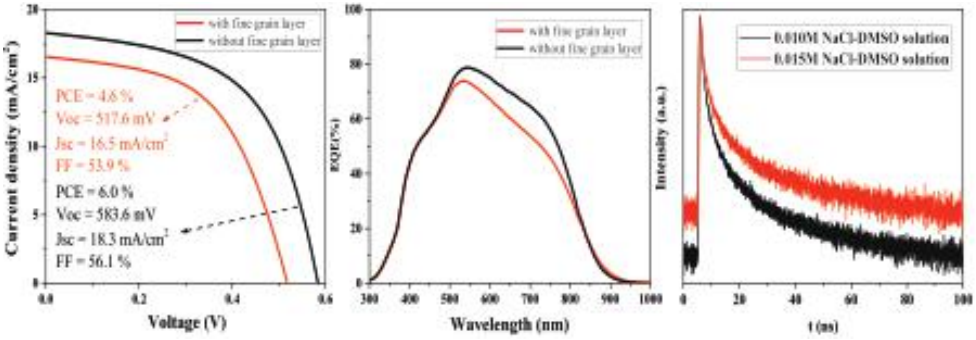

Figure PP1.3a.14: (a) Photovoltaic performance of a CZTS solar cell with the typical bi-layer structure; (b) External quantum efficiency spectral response of the same device; and (c) TRPL transient of the complete solar cells made from different NaCl-DMSO solutions at room temperature.

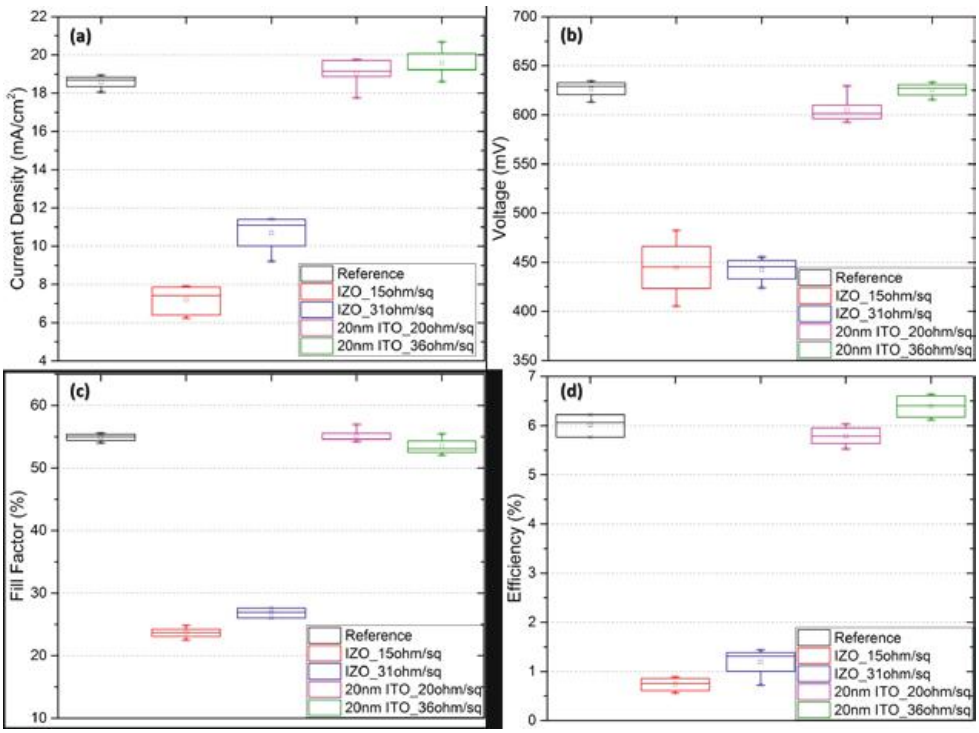

Figure PP1.3a.15: J-V characteristics of CZTS devices with different types of electrodes. (The numbers of samples measured were between 10 and 15 for each device, sample labelling with IZO and 20 nm ITO is the type of substrates, and numbered ohm/sq is R_{sheet} of the hybrid electrodes).

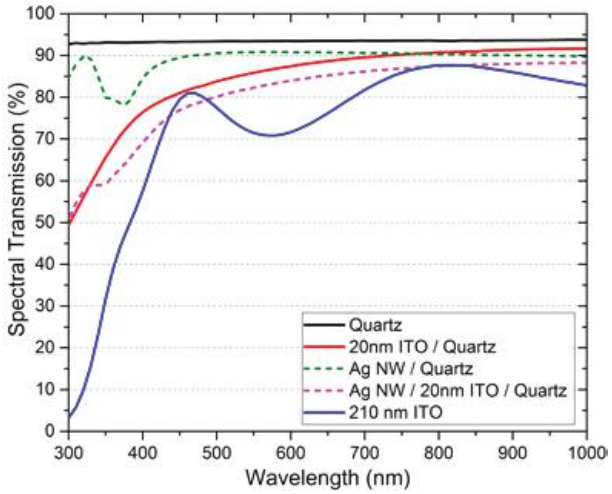

Figure PP1.3a.16: Transmission spectra of Quartz, 20 nm ITO/ Quartz, 210 nm ITO / Quartz and (solid lines), AgNW network on quartz and AgNW network on 20 nm ITO / Quartz (dash lines).

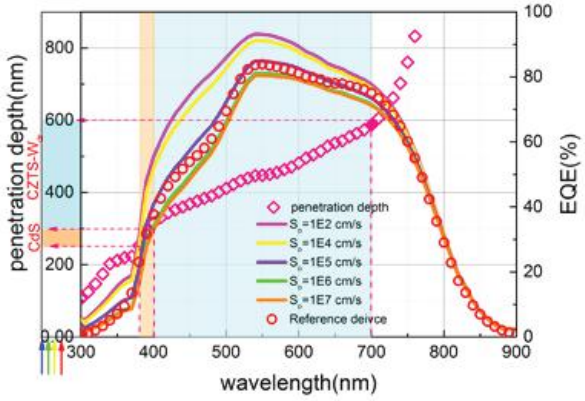

Figure PP1.3a.17: At right-side y-axis, simulated EQE for different interface velocities spanning from 10^2 cms^{-1} to 10^7 cms^{-1} (coloured lines) is displayed as well as measured EQE on the device (red dot). At left-side y-axis, penetration depth (pink diamond), till 36% intensity, as a function of wavlength is shown. And according to this, the parts of the spectrum collected by CdS buffer and CZTS depletion region are depicted in light orange and light cyan, respectively.

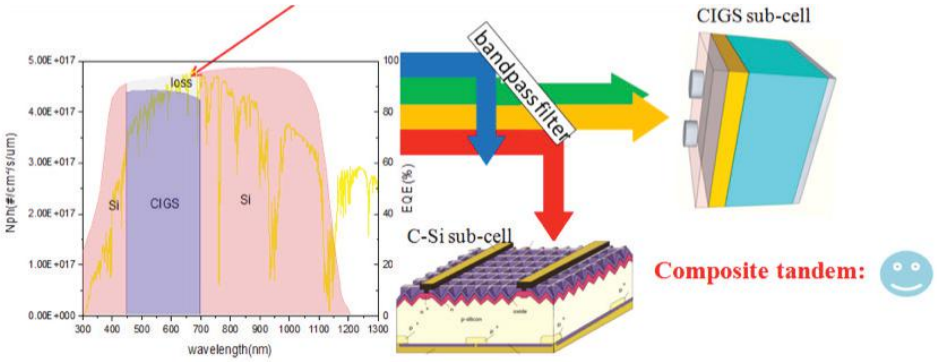

Figure PP1.3a.18: Schematic of four-terminal tandem cells by spectrum splitting approach.

(pure sulphide)/SP-Si (17.49%, +2.88 diff%), CIGS/PERC-Si (19.72%, +3.79 diff%), CIGS/PERL-Si (23.35%, +4.7 diff%).

Highlights

- Base-line efficiency of CZTS solar cells has been significantly improved with the in-house highest efficiency of 9.7% and certified highest efficiency of 9.5%.
- Demonstrated beyond 15% efficiency CZTS/SP-Si tandem solar cells and 17.49% CIGS/SP-Si tandem solar cells.
- Developed low temperature treated transparent and conductive Ag NW front electrode and demonstrated beyond 7% efficient CZTS solar cells with Ag NW electrode.
- Identified the key factors limiting CZTS device performance

Future Work

Future work in 2017 will be focused on (1) further improving the efficiency of CZTS solar cells, in particular the open circuit voltage; (2) Integrating the highly transparent and conductive Ag NW in chalcogenide/ Si tandem cells; (3) demonstrating beyond 20% chalcogenide/Si tandem cells.

References

Crovetto, A., Yan, C., Sun, K., Hao, X.J., Estelrich, R., Canulescu, S., Stamate, E., Pryds, N., Hansen, O., and Schou, J., "Ultra-thin Cu_2ZnSnS_4 solar cell by pulsed laser deposition", Solar Energy Materials and Solar Cells. (revised version submitted).

Crovetto, A., Yan, C., Zhou, F., Stride, J., Schou, J., Hao, X.J., and Hansem, O., "Lattice-matched Cu_2ZnSnS_4/ CeO2 solar cell with open circuit voltage boost", Applied Physics Letters, 2016, vol. 109, issue 23, 2016, DOI: 10.1063/1.4971779.

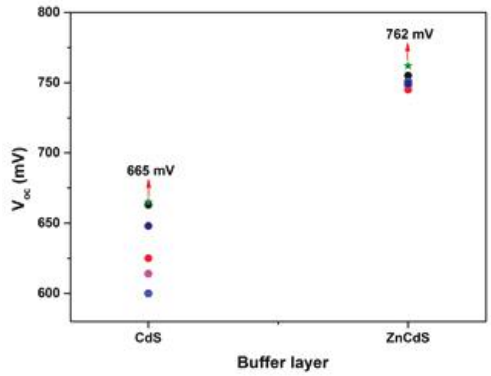

Figure PP1.3a.19: J-V curves of CZTS device with different buffer layers.

device name	Voc(mV)	Jsc(mA/cm²)	FF(%)	PCE(%)
Newport-c12 with filter	629	7.37mA/cm²	69%	3.2%
PERC Si with filter	603	31mA/cm²	78%	14.60%
Composite Eff%	17.81			
SP Si with filter	579	27mA/cm²	78%	12.37%
Composite Eff%	15.58			

Table PP1.3a.1: Performance of demonstrated four-terminal CZTS/Si tandem solar cells.

Liu, F., Chang, Y., Sun, K., Park, J., Green, M. A., and Hao, X.J., "8.4% ultrathin CZTS thin film solar cells", Advanced Function Materials (submitted).

Liu, F., Yan, C., Huang, J., Sun, K., Zhou, F., Stride, J., Green, M., and Hao, X.J., 2016, "Nanoscale microstructure and chemistry of Cu_2ZnSnS_4/CdS interface in kesterite Cu_2ZnSnS_4 solar cells", Advanced Energy Materials, 2016. 1600706, (1–10).

Liu, X., Feng, Y., Cui, H., Liu, F., Hao, X.J., Coniber, G., Mitzi, D. B., and Green, M., 2016, "The current status and future prospects of kesterite solar cells: a brief review", Progress in Photovoltaics: Research and Applications, 2016, DOI: 10.1002/pip.2741.

Liu, X., Huang, J., Zhou, F., Liu, F., Stride, J.A., and Hao, X.J., "Spatial grain growth and composition evolution during sulfurizing meta-stable wurtzite Cu_2ZnSnS_4 nanocrystal-based coating", Chemistry of Materials, (in press).

Liu, X., Huang, J., Zhou, F., Liu, F., Sun, K., Yan, C., Stride, J.A., and Hao X.J., 2016 "Understanding the key factors of enhancing phase and compositional controllability for 6% efficient pure-sulfide Cu_2ZnSnS_4 solar cells prepared from quaternary wurtzite nanocrystals", Chemistry of Materials, 2016, DOI: 10.1021/acs.chemmater.5b04620.

Park, J., Zi, O., Yan, C., Sun, K., Sun, H., Liu, F., Green, M. A., and Hao X.J., "Hybrid Ag nanowire-ITO as transparent conductive electrode for kesterite Cu_2ZnSnS_4 solar cells", Solar Energy Materials and Solar Cells. (submitted).

Pu, A., Ma, F., Yan, C., Huang, J., Sun, K., Green, M., and Hao X.J., 2017, "Sentaurus modelling of 6.9% Cu_2ZnSnS_4 device based on comprehensive electrical & and optical characterisation", Solar Energy Materials and Solar Cells, 160 (2017), 372–381.

Sun, K., Yan, C., Liu, F., Huang, J., Zhou, F., Stride, J., Green, M., and Hao X.J., 2016, "Over 9% efficient kesterite Cu_2ZnSnS_4 solar cell fabricated by using $Zn_{1-x}Cd_xS$ buffer layer", Advanced Energy Materials, 2016, 1600046, (1–6).

Yan, C., Liu, F., Sun, K., Song, N., Stride, J. A., Zhou, F., Hao, X.J., and Green M. A., 2016, "Boost efficiency of pure sulphide CZTS solar cell via In/Cd-based hybrid buffer", Solar Energy Materials and Solar Cells, 144, 700–706, 2016.

Yan, C., Sun, K., Liu, F., Huang, J., Zhou, F., and Hao, X.J., 2017, "Boost Voc of pure sulphide kesterite solar cells via a double CZTS layer stacks", Solar Energy Materials and Solar Cells, 160 (2017), 7–11.

Yan, C., Sun, K.W., Johnson, S., Liu, F., Huang, J., Pu, A., Sun, K.,L., Zhou, F., Puthen-Veettil, B., Stride, J. A., Green, M. A., and Hao, X.J., "Beyond 11% efficient sulphide kesterite $Cu_2Zn_xCd_{1-x}SnS_4$ solar cell: role of cadmium alloying"., ACS Energy Letters (submitted).

Zhao, L., Di, Y., Yan, C., Liu, F., Cheng, Z., Jiang, L., Hao, X.J., Lai, Y. and Li, J., 2016, "In-situ growth of SnS absorbing layer by reactive sputtering for thin film solar cells", RSC Advances, 6(5): 4108–4115, 2016.

PP1.3a(v) Non-Epitaxial Tandem Cells on Silicon – Perovskite/Si Tandem

Lead Partner
UNSW

UNSW Team
Dr Anita Ho-Baillie, Dr Shujuan Huang, Dr Xiaoming Wen, Dr Xiaojing Hao, Dr Jae S. Yun, Dr Meng Zhang, Dr Yajie Jiang, Dr Mark Keevers, Dr Trevor Young, Prof Martin Green

UNSW Students
Rui Sheng, Qingshan Ma, Sheng Chen, Adrian Shi, Arman M. Soufiani, Jincheol Kim, Cho Fai Jonathan Lau, Xiaofan Deng, Ning Song, Benjamin Wilkinson, Nathan Chang, Jianghui Zheng, Daseul Lee, Yongyoon Cho

Monash Team
Prof Udo Bach, Prof Yi-Bing Cheng, Prof Leone Spiccia, Dr Yong Peng, Dr Fuzhi Huang, Dr Wei Li, Dr Yasmina Dkhissi

Monash Students
Liangcong Jiang, Qicheng Hou

ANU Team
Dr Mulmudi Hemant Kumar, Dr Heping Shen, Dr Tom White, Prof Klaus Weber, Prof Kylie Catchpole

ANU Students
The Duong, Jun Peng, Daniel Jacobs, Yiliang Wu

Other Partners
Dr Nochang Park, Korean Electronics Technology Institute
Korea Research Institute of Chemical Technology (KRICT)
Ulsan National Institute of Science and Technology
School of Materials Science and Engineering, UNSW
School of Physics, UNSW

Some of these tasks have been conducted under the ARENA RND075 program in collaboration with Monash University, Australian National University, Arizona State University, Suntech Power Co. Ltd. and Trina Solar Energy Co. Ltd.

Aim

Investigate material systems where epitaxial growth on a crystalline template is not required for good cell performance. One such material system is organic metal halide perovskite.

Progress

In 2016, significant progress has been made towards high efficiency tandem. Since the demonstrations of split spectrum tandems at 23% (Sheng et al., 2015; Duong, et al., 2016), the team improved on the four-terminal perovskite/Si solar tandem device (produced by stacking) with 24.5% efficiency measured in-house in 2016 (Peng et al., 2016).

Optical analyses of various tandem structures that use different electron and hole transport layers have been carried out to determine parasitic reflection and absorption losses (Jiang et al., 2016; Grant et al., 2016) and we continue to make good in progress in demonstrating semi-transparent perovskite cells with "inverted" polarity using PEDOT:PDD as a hole-transporting material (HTM) and PCBM as an electron-transporting material (ETM) that are compatible with the polarity of commercial Si solar cells that have n-type polarity on the illuminated side and p-type polarity on the rear side.

A low temperature ETM, comprising a combination of SnO_2 with C60, for two-terminal silicon/perovskite tandem cells is under development.

A new stability testing protocol that involves multiple 12-hour cycles of darkness and illumination has been developed. The "fatigue" behaviour in planar $CH_3NH_3PbI_3$ perovskite solar cells is observed. It is found that cell efficiency decreases by > 50% after storage in the dark for 12 hours under open circuit conditions. The efficiency drop can be recovered during the 12-hour illumination period. The recovery rate slows down in successive illumination/darkness cycles. Fatigue is dependent on cell temperature and therefore is likely to be attributed to ion migration (Huang et al., 2016). Further work is underway and shows that fatigue behaviour changes with cell structure (e.g. using different ETM and HTM) and can be recovered.

Highlights

- Measured 24.5% four-terminal perovskite/Si solar tandem device produced by stacking.
- Achieved world record conversion efficiency for a 16 cm^2 single monolithic perovskite solar cell at 12.1% efficiency independently certified.
- Demonstrated the largest perovskite cell (1.2 cm^2) at 18.1% (certified).
- Achieved 11.5% efficiency (certified) for a 16 cm^2 four-parallel cell module.

Future Work

- Exploration of alternative perovskite materials including fabrication of solar devices, modelling of material properties and characterisations for better understanding of the materials and device operation including loss mechanisms and factors affecting stability.
- Study of various perovskite/Si monolithic tandem cell designs. Fabrication of perovskite/Si tandem cells under various terminal configurations.
- Stability study and encapsulation strategies for perovskite/Si tandem technology, extending to large areas.

References

Grant, D.T. et al., 2016, Optics Express, 24 (22), A1454–A1470.

Huang, F. Z. et al., 2016, Nano Energy, vol. 27, pp. 509–514.

Peng, J. et al., 2016, Advanced Energy Materials, 1601768 doi:10.1002/aenm.201601768.

Sheng, R. et al., 2015, J. Phys. Chem. Lett., 6, 3931−3934.

Duong, T. et al., 2016, IEEE J. Photovolt., 6(6), 1432.

Jiang, Y. et al., 2016, J. Mater. Chem. C, 4, 5679–5689.

PP1.3a(vi) Non-Epitaxial Tandem Cells on Si – Two-Terminal III-V/Silicon Tandem via Bonding

Lead Partner
UNSW

UNSW Team
Dr Anita Ho-Baillie, Dr Hamid Mehrvarz, Prof Martin Green

NREL Team
Dr Glenn Teeter, Dr Mathew Young, Dr Steve Johnston

Academic Partners
Fukushima Renewable Energy Institute, National Institute of Advanced Industrial Science and Technology (AIST), Japan

Funding Support
ARENA, New Energy and Industrial Technology Development Organization (NEDO) under Ministry of Economy, Trade and Industry (METI), Japan.

Aim

The aim is to demonstrate multi-junction III-V/Si tandem without epitaxial growth on a crystalline Si template while achieving high performance. The use of bonding allows two-terminal configuration to still be achieved avoiding the additional interconnection required in a mechanical stacked tandem that often requires a four-terminal configuration.

Progress

In this work, we demonstrate a triple-junction tandem consisting of InGaP/GaAs cells by AIST on UNSW's crystalline Si sub-cell using the "Smart Stack" approach developed by AIST. The advantages of the choice of a Si sub-cell include abundance, low cost, non-toxicity, proven technology and ideal bandgap as a bottom cell in a multi-junction tandem. A conversion efficiency of 23.2% was measured.

For the fabrication of PERL Si cells at UNSW, a double-sided polished, FZ 1.5 Ω-cm p-type <100>Si wafer with a thickness of 400 μm was used to prepare a bottom cell. A phosphorus ($POCl_3$) diffused n^{++} emitter was formed on the front side. Boron (BBr_3) diffused p^{++} regions were formed locally on the rear for metal contact (Al/Ti/Pd/Ag). The rest of the non-contacted rear was passivated by thermally grown and annealed SiO_2.

On the un-passivated n^{++} front side of this Si bottom cell, a Pd NP array was formed at AIST. Figure PP1.3a.20(a) shows a typical scanning electron microscopy (SEM) image of such a Pd NP array on the Si bottom cell. Pseudohexagonally patterned Pd NPs were observed, whose size, inter-particle distance, density and surface coverage, were ~40 nm, ~100 nm, ~1×10^{10} cm^{-2}, and ~12%, respectively.

An AIST's tandem InGaP/GaAs cell was grown on a GaAs growth substrate by metal-organic chemical vapour deposition. The thicknesses of InGaP and GaAs absorption layers were 0.35 and 0.5 μm, respectively. In order to allow the release of the device part from the growth substrate afterwards, an AlAs sacrificial layer was also grown between the substrate and cell. After an AuGeNi top electrode was deposited by electron beam evaporation, the entire sample was immersed into aqueous HF. Due to the selective etching of the AlAs layer by HF, the cell was separated from the substrate as a free-standing thin-film (i.e., epitaxial lift-off (ELO)).

The ELO InGaP/GaAs top cell was deposited on the Pd NP–decorated Si bottom cell which was wet with H_2O. The resulting pre-stack was pressed lightly using manual hand-press equipment at room temperature for 3 hours. A stable contact was formed between the bottommost layer of the ELO cell and the Pd NPs during the evaporation of the H_2O. As a result, a target smart stack InGaP/GaAs/Si (E_g = 1.89/1.42/1.12 eV) structure was obtained. Finally, a SiO_2/TiO_2 (100/70 nm) anti-reflection coating (ARC) was deposited by sputtering. The final structure (cross-section) and photo of the smart stack cell are shown in Figure PP1.3a.20(b) and (c) respectively.

The photovoltaic performance was investigated under AM1.5G solar spectrum illumination. A light-shielding mask was applied to the fabricated InGaP/GaAs/Si smart stack cell to restrict the light illumination within the grid electrode of the top cell (note that the size of the bottom cell is larger than that of the top cell, as shown in Figure PP1.3a.20(b)). In this case, the designated area of the cell was 0.1448 cm^2. Figure PP1.3a.21(a) shows the resulting J-V characteristics. The short-circuit current density (J_{SC}), open-circuit voltage (V_{OC}), and fill factor (FF), were 10.46 $mAcm^{-2}$, 2.81 V and 0.790, respectively, which resulted in the efficiency of 23.2%.

The EQE spectra of the smart stack cell as well as each sub-cell were summarised in Figure PP1.3a.21(b). Over 70–80% EQEs were observed across the 450–1000 nm wavelength range as a total device. As for the sub-cells, it was revealed that the EQE of the Si bottom cell already starts to increase at the wavelength of around 600 nm because of the thinness of the GaAs layer (0.5 μm). This design was intentional to adjust the current matching between the InGaP/GaAs top and Si bottom cells, although there is room for improvement. Indeed, the photogenerated J_{SC} of the InGaP, GaAs, and Si subcells, calculated from the corresponding spectra, were 11.1, 10.5 and 9.2 $mAcm^{-2}$, respectively, suggesting that the overall performance of the smart stack cell is mainly

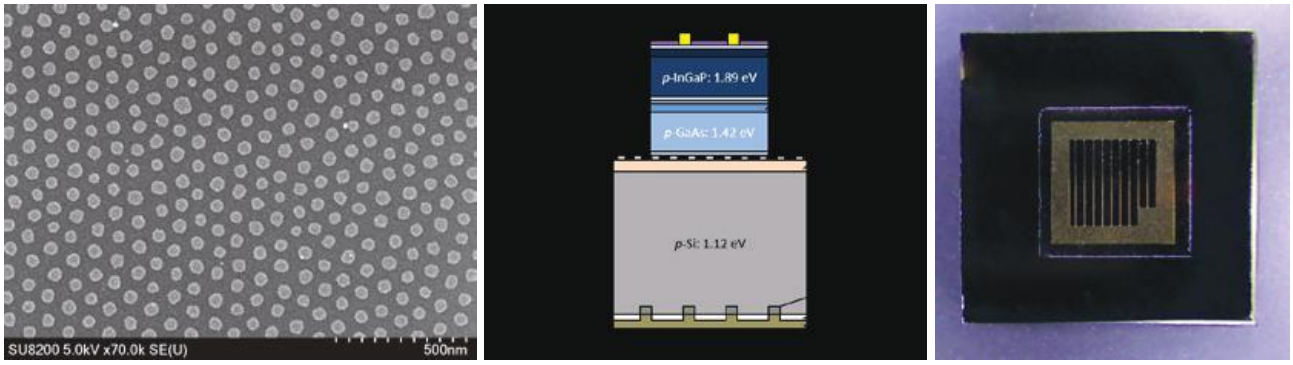

Figure PP1.3a.20: (a) SEM image of the Pd NP array formed on the front side of the Si bottom cell; (b) Schematic cross-section of the InGaP/GaAs/Si smart stack cell; and (c) Photo of InGaP/GaAs/Si smart stack cell.

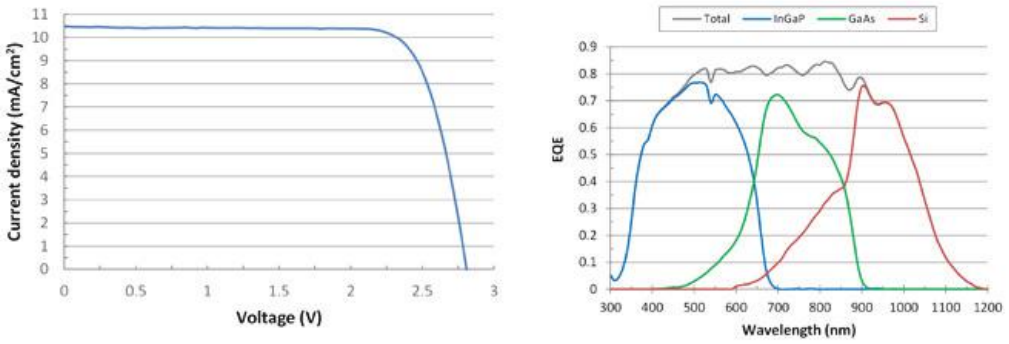

Figure PP1.3a.21: (a) J-V characteristics of the InGaP/GaAs/Si smart stack cell; and (b) EQE spectra of the InGaP/GaAs/Si smart stack cell and sub-cells.

limited by the Si bottom cell due to optical loss from high reflection from a planar device and lack of light trapping in the bottom cell.

Highlights

A triple-junction cell consisting of InGaP/GaAs and crystalline Si sub-cells based on AIST's smart stack approach is demonstrated achieving an energy conversion efficiency of 23.2%.

Future Work

The EQE measurement of the smart stack cell suggested that the overall performance is limited by the Si bottom cell (the lowest photogenerated J_{SC}). Therefore, higher efficiencies are feasible through the further optimisation of the design such as surface treatment on the top surface, to reduce front reflection, which can also enhance light trapping in the bottom cell to improve current matching.

Reference

Mizuno, H., Makita, K., Tayagaki, T., Mochizuki, T., Takato, H., Sugaya, T., Mehrvarz, H., Green, M. and Ho-Baillie, A., 2016, "A 'Smart Stack' Triple-Junction Cell Consisting of InGaP/GaAs and Crystalline Si", 43rd IEEE Photovoltaic Specialists Conference Portland, 1923–1925.

PP1.3b Silicon Tandem Cells (Mechanically Stacked)

An alternative approach to implementing silicon tandem cells is mechanical stacking with independent connection to each cell in the stack. This removes constraints upon the matching of current, lattice constant and thermal expansion coefficient, albeit at the cost of additional mounting and interconnection costs. The best available silicon and wide bandgap cells can be separately optimised and mounted together.

Current proof-of-concept work is focused on reflector-based architectures to direct long wavelength light to the silicon cell. This enables the use of commercially available conventional GaAs cells as the top cell in the stack. Design of the mounting, optics and interconnection is critical to maximising performance. Longer term design preferences are for transparent top cells which offer more flexibility in the application of the tandem structure.

Other work related to this topic is also reported in Section 6.1 of this report.

Lead Partner
ANU

ANU Team
Dr Matthew Stocks, Prof Andrew Blakers, A/Prof Klaus Weber, Dr Thomas White

Monash Team
Prof Udo Bach, Prof YiBing Cheng

Funding Support
ARENA, ANU

Aim

Demonstrate potential of mechanically stacked tandems to increase silicon module efficiency.

Progress

The major activity has been the extension of the annual yield modelling to area adjusted series connected cells. Area adjusted series connected tandem cells were proposed by Bailie (2015) for perovskite-silicon devices. The area of the top cell is scaled to ensure that the current of the top cell matches that of the silicon. This can be seen schematically in Figure PP1.3b.1.

The scaling is achieved by determining the current densities of the top and bottom cells under a reference condition, typically illumination with the AM1.5G spectrum under Standard Test Conditions (STC). The area of the top cell is then scaled inversely proportional to the ratio of the top cell to bottom cell current. Cells with bandgaps close to silicon (<1.7 eV) are smaller than the silicon cell while those with high bandgaps are scaled larger due to their lower relative current density. Since the total area of the top cells and bottom cells needs to be identical, the number of top cells connected in series is inversely scaled to the area of the top cell multiplied by the total number of bottom cells.

The ideal four-terminal and typical series connected arrangement, without area scaling, devices were then simulated with a year of real spectral data for this configuration. High annual energy yields for the area scaled configuration were found for a wide range of bandgaps as show in Figure PP1.3b.2. These yields were between 5 and 10% below those of the ideal four-terminal results. Interestingly, the series connected tandem without scaling (red line in Figure PP1.3b.2) achieved the highest annual yields with a bandgap above the expected optimum. This suggests the real spectrum was, on average, more blue rich than the AM1.5G spectrum leading to better matching with a relatively smaller (matched) top cell area.

While not as promising as the series-parallel approach reported last year (Stocks, 2016), both results indicate that there are alternative interconnection schemes that enable bandgaps other than the “ideal” 1.7 eV to be usefully used in a mechanically stacked configuration with silicon.

Highlight

Simulation of high annual energy yield for wide range of bandgaps for area-adjusted tandem devices.

Future Work

- Interconnection and testing of the GaAs/Si tandem. GaAs cell developed under the NREL collaboration in Section 6.8.
- Comparison of annual yield for four-terminal, series-parallel and a broader range of device parameters.

References

Bailie, C., Christoforo, M., Mailoa, J., Bowring, A., Unger, E., Nguyen, W., Burschka, J., Pellet, N., Lee, J., Grätzel, M., Noufi, R., Buonassisi, T., Salleo, A. and McGehee, M., 2015, “Semi-transparent perovskite solar cells for tandems with silicon and CIGS”, Energy Environ. Sci., 8(3), 956–963.

Stocks, M., Loo, Y.X. and Lal, N.N., 2016, “Free the Bandgap!”, Proc. EU PVSEC, 223–227.

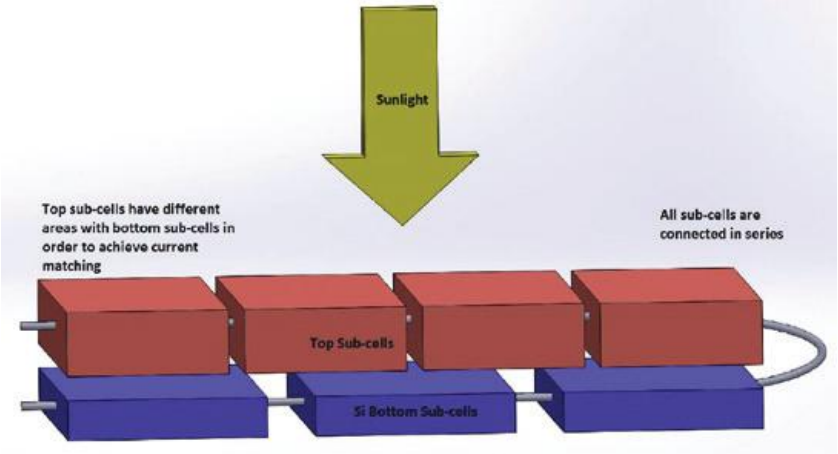

Figure PP1.3b.1: Schematic of the area adjusted series connected tandem configuration.

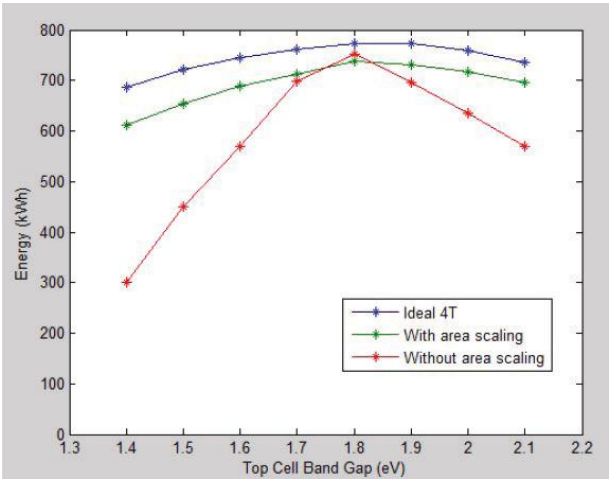

Figure PP1.3b.2: Annual energy yield versus bandgap area adjusted series connected tandems.

PP2 Thin-Film, Third Generation and Hybrid Devices

Overview

Program Package 2 (PP2) encompasses research into a range of next generation cell technologies with the overall goals of demonstrating efficiency above 16% for cells of greater than 1 cm² area and of demonstrating the feasibility of significantly reduced costs. The program is divided into tasks to address the key materials groups: organic solar cells (OPV), organic-inorganic hybrid cells, "Earth-abundant" inorganic thin-film materials, "third generation" approaches and the hot topic of organic-inorganic perovskites.

Great progress has been made in 2016 in a number of target areas including setting new international records for large-area cell efficiency in CZTS and perovskite technologies.

The thin-film organic photovoltaics task (PP2.1) aims to identify and address roadblocks in organic photovoltaics to enable cost-effective, mass manufacture of modules using this technology. The research targets lower cost materials and/or processes compared to those of conventional cells or, alternatively, applications such as flexible or partly transparent cells for which conventional cells are not well suited. In 2016, OPV research focused on fundamental materials investigations and scaling and reproducibility of manufacturing processes (PP2.1c) in partnerships between UoM, Monash, UQ and CSIRO.

Significant progress was made at UoM in working with a newly developed OPV molecular donor, with efficiency over 10% achieved on devices > 1 cm², in line with targets (PP2.1f) and over 11.5% on smaller devices.

Over 2016, CSIRO added new printing capacity, with the commissioning of four new slot-die coaters. Translating the promising new donor OPV cell materials to the CSIRO's mini slot-die coater processes resulted in a power conversion efficiencies (PCE) of 6% (glass, 0.1 cm²) in preliminary trials (PP2.1c).

Thin films of the compound semiconductor Cu_2ZnSnS_4 (CZTS) form the focus of PP2.2. In 2016, the team established a confirmed 7.6% to set a new world record efficiency for CZTS solar cells (total cell area 1 cm²) and established a second world record efficiency for small area CZTS solar cells of 9.5% (total cell area 0.24 cm²), breaking the previous 9.1% record set by Toyota in 2014. Further, continuous improvements were achieved in the development of CZTS thin-film solar cells on stainless steel, with an efficiency of 6.2% achieved; showing continuous improvement from last year's early results of 4% (and 2.1% in 2014).

Work on advanced third generation devices forms the focus of PP2.4. Hot carrier cells are a topic of particular interest given their long-term potential with efforts directed to understanding fundamentals as well as to implementing the different elements required for their successful implementation. Advances in work on both absorbers and contacts are reported in this section.

A new work program was started in 2016, to advance the organohalide perovskite technologies, addressing scale and durability. The work program was established as an internal project within ACAP and outcomes are reported under PP2.5.

Advances in 2016 include:

- 18.1% efficiency for a 1.2 cm² cell, up from 12% in the 2015 report. This is the largest certified perovskite cell at that energy conversion efficiency.
- 11.5% efficiency for a 16 cm² four-parallel-cell module.

This remarkable progress has been achieved through collaborative efforts in:

- developing the understanding of the factors limiting the performance of perovskite solar cells, including the origin of hysteresis, and developed models for slow transient response
- advancing techniques in transmission electron microscopy (TEM) to reduce artefacts caused by electron beam damage and make it a useful diagnostic tool
- developing methodologies to fabricate uniform, pinhole- free perovskite films for large area perovskite solar devices ranging from 1 cm² to 25 cm² in area, resulting in certified record results achieved on 1 cm² cells, 1.2 cm² cells, 16 cm² cells and 16 cm² modules
- translation of batch printing on glass to roll-to-roll printing on flexible substrate has been successful.

PP2.1 Organic Photovoltaic Devices

PP 2.1a Organic Bulk Heterojunction Solar Cells

Lead Partner
UNSW

UNSW Team
A/Prof Ashraf Uddin, Dr Matthew Wright, Dr Naveen Kumar Elumalai, Dr Supriya Pillai

UNSW Students
Mushfika Baishakhi Upama, Cheng Xu, Arafat Mahmud, Dian Wang, Kah Chan, Faiazul Haque

Funding Support
ACAP, ARENA, ARC, UNSW

Aim

The overall aim of this project is to fabricate highly stable and efficient organic solar cells in the Organic Photovoltaics (OPV) lab at UNSW.

Our research activities are mainly focused on the following three areas:

- morphology control and light trapping in organic solar cells
- interface engineering of buffer layers
- semi-transparent organic solar cells

Progress

We are working on fundamental issues involved in the morphology control of light absorbing organic films for OPV devices which includes control of electronic structure at film interfaces, exciton dissociation and carrier transport properties for efficient photovoltaic operation. We also employed an ab-initio (density functional theory – DFT) method which is considered to be a valuable tool to obtain insight into the charge separation (exciton dissociation) and transport process as well as the photochemical stability of organic molecules – a major challenge for organic PV. This method helps us to find robust and electronically suitable molecules which determine the morphology of OPV devices. The key issues of polymer design include engineering the bandgap and energy levels to achieve high J_{SC} and V_{OC}, enhancing planarity to attain high carrier mobility, and materials processability and stability. All of these issues are correlated with each other.

Furthermore, we have investigated the plasmonic enhancement of bulk heterojunction OPV cells with incorporated thin silver (Ag) nanoparticle film. Such films consist of plasmon-active and size-variable Ag nanostructures. Incorporation of plasmon-active Ag nano-material is shown to enhance light absorbance in the photoactive layer. Consequently, enhancements of external quantum efficiency at red wavelengths are observed. This plasmonic enhancement needs to be optimised further in order to improve the photo conversion efficiency of OPV cells. Similarly SiO_2-coated Ag nanoparticles are also studied for their effect on both electronic and optical properties in the organic solar cells.

We have also designed and developed a new inverted OPV device to address the challenge of improving the device stability without compromising the efficiency. In line with this approach, we achieved highly efficient OPV devices with high power conversion efficiency of ~11.3% complemented with good device lifetime of ~3–5 months without any encapsulation in ambient conditions. Compared to traditional/conventional device structures which only last for a few days, our devices with inverted architecture possess extended lifetime lasting for months. The device structure and current-voltage characteristics are shown in Figure PP2.1.1.

Investigation of device degradation mechanism

The burn-in loss mechanism in organic solar cells is also investigated using photothermal deflection spectroscopy (PDS) technique. This method enables the in-depth evaluation of short-term degradation of organic devices under continuous illumination. The PDS technique facilitates: (i) measurement of absorption features in the sub-bandgap region in polymer–polymer and polymer–fullerene blend film; (ii) measurement of weak absorption near the band-edge where it's very difficult for traditional methods. Absorption spectra of P3HT:PC71BM and PTB7:PC71BM films using PDS is shown in Figure PP2.1.2.

In PTB7-based devices, sub-bandgap absorption is attributed to sub-bandgap disorder and trap state formation, which causes severe J_{SC} loss under illumination. This study is also the first report of a sub-bandgap defect study of PTB7 using PDS technique.

The magnitude of the PL signal increases in the aged film, indicating increased radiative recombination of excitons and less effective charge separation between

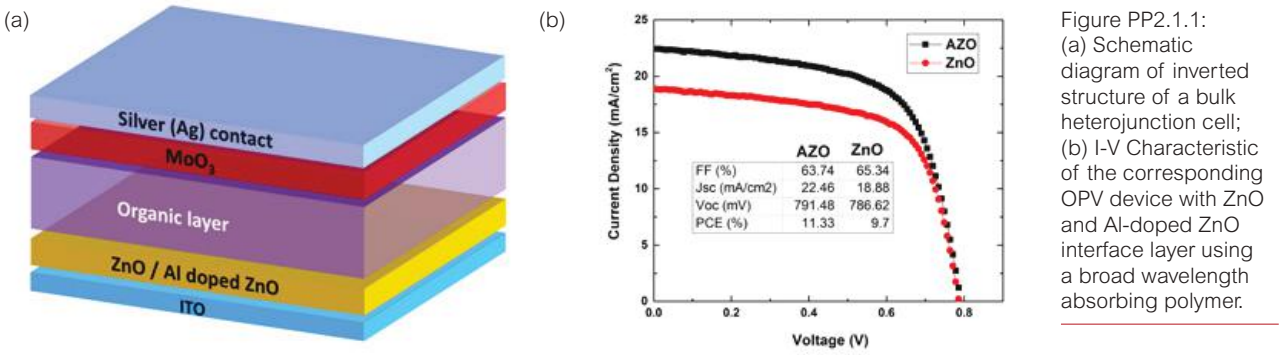

Figure PP2.1.1: (a) Schematic diagram of inverted structure of a bulk heterojunction cell; (b) I-V Characteristic of the corresponding OPV device with ZnO and Al-doped ZnO interface layer using a broad wavelength absorbing polymer.

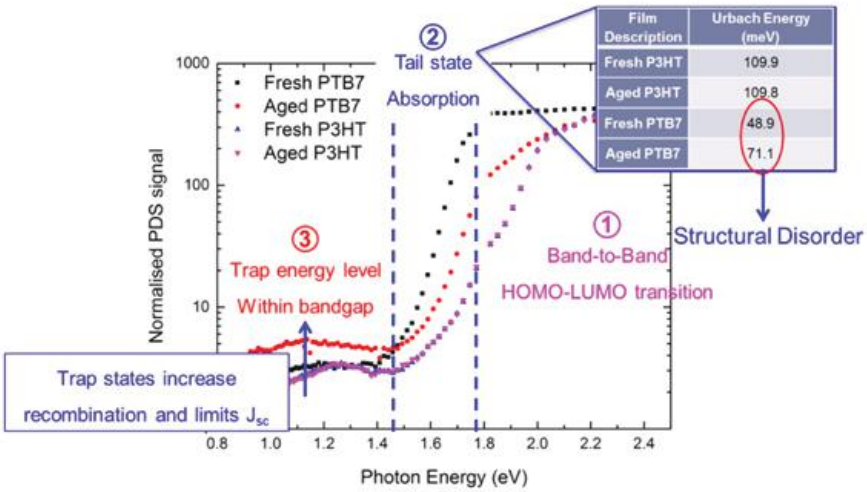

Figure PP2.1.2: Absorption spectra of P3HT:PC71BM and PTB7:PC71BM films using.
The energy level description across three distinct regions is also explained.

donor polymer and acceptor fullerene. The aggregates formed during photo-aging may serve as electron traps and recombination centres in aged PTB7. No change in sub-bandgap absorption was observed in P3HT:PC71BM films. We believe that the formation of these trap states is the mechanism underpinning the severe initial degradation in PTB7-based devices.

Semitransparent organic solar cells

A highly efficient bulk heterojunction semitransparent inverted organic solar cell has been developed that incorporates D/M/D electrode (MoO_3/Ag/MoO_3) and polymer–fullerene blend (PTB7:PC71BM) as the photo-absorbing layer. The device combines the simple construction of D/M/D electrode and high efficiency of PTB7:PC71BM solar cells. The change in device transparency was studied by varying the active layer thickness and outer MoO_3 layer thickness. Changing these parameters also affects the amount of absorbed photons and, hence, the photocurrent density. By tuning the active layer thickness, the average device efficiency increased from 3.8% to 4.7%. An impressive PCE of 5% was achieved for the best device at an average visible transmittance (AVT) of 18.3%. Devices with an AVT of 25%, which is considered as a requirement for window applications, achieved a PCE of 3.82%.

Highlights

- Developed our understanding of donor/acceptor morphology in low bandgap polymer-based bulk heterojunction solar cells.
- Investigated the effect of interfacial layers on efficiency enhancement in OPVs.
- Developed semitransparent organic solar cells with colour rendering index and transparency.

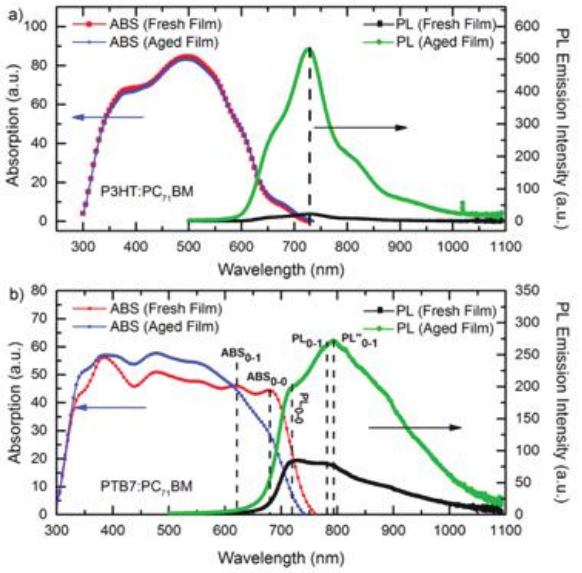

Figure PP2.1.3: (a) PL emission spectra (right) and absorption spectra (left) of fresh and aged P3HT:PC71BM (1:1) film; (b) PL emission spectra (right) and absorption spectra (left) of fresh and aged PTB7:PC71BM (1:1.5) film. The black dashed vertical lines identify the absorption and PL emission peak positions. The absorption displayed in this figure is measured using reflection/transmission measurements from a UV/VIS spectrometer.

Future Work

- Continued investigation into morphology control of donor/acceptor materials in bulk heterojunction solar cells.
- Extended lifetimes study and degradation mechanism in OPV devices.
- Exploit light trapping prospects in organic solar cells by plasmonic nanoparticles.
- Develop highly efficient semitransparent OPV devices with high AVT.

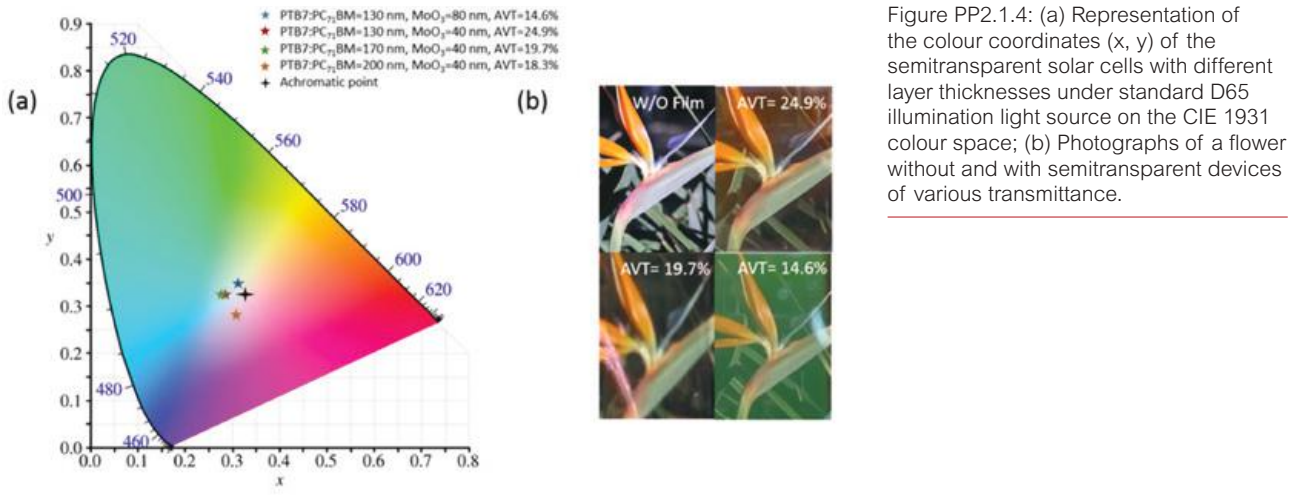

Figure PP2.1.4: (a) Representation of the colour coordinates (x, y) of the semitransparent solar cells with different layer thicknesses under standard D65 illumination light source on the CIE 1931 colour space; (b) Photographs of a flower without and with semitransparent devices of various transmittance.

References

Chan, K.H., Elumalai, N.K., Tayebjee, M.J.Y., Uddin, A. and Pillai, S., 2017, "Dark carrier dynamics and electrical characteristics of organic solar cells integrated with Ag-SiO_2 core-shell nanoparticles", Synthetic Metals, 223, 34–42

Upama, M.B., Wright, M., Elumalai, N.K., Mahmud, M.A., Wang, D., Chan, K.H., Xu, C., Haque, F. and UddinDDIN, A., 2017a, "High performance semitransparent organic solar cells with 5% PCE using non-patterned MoO_3/Ag/MoO_3 anode", Current Applied Physics, 17, 298–305

Upama, M.B., Wright, M., Elumalai, N.K., Mahmud, M.A., Wang, D., Chan, K.H., Xu, C., Haque, F. and Uddin, A., 2017b, "Optical modelling of P3HT:PC71BM semi-transparent organic solar cell", Optical and Quantum Electronics, 49, 28

Upama, M.B., Wright, M., Puthen-Veettil, B., Elumalai, N.K., Mahmud, M.A., Wang, D., Chan, K.H., Xu, C., Haque, F. and Uddin, A., 2016, "Analysis of burn-in photo degradation in low bandgap polymer PTB7 using photothermal deflection spectroscopy", RSC Advances, 6, 103899–103904

PP 2.1b Organic-Inorganic Base Solar Cells

Lead Partner
UNSW

UNSW Team
A/Prof Ashraf Uddin, Dr Naveen Kumar Elumalai, Dr Matthew Wright

UNSW Students
Arafat Mahmud, Dian Wang, Mushfika Baishakhi Upama, Cheng Xu, Faiazul Haque

Industry Partner
Future Solar Technology

Funding Support
ACAP, ARENA, ARC, UNSW

Aim

Organic-inorganic hybrid perovskite structures have evolved from their predecessors (dye-sensitised solar cells) experiencing a steep progress in terms of power conversion efficiency (PCE) starting with 3.8% in 2009 and achieving 22% in 2016, by using an all-solid-state thin-film architecture. The emergence of perovskite solar cells has created a lot of attention not only because of their rapidly increased efficiency, but also due to the flexibility in material growth and architecture. On the way to high efficiency, much effort has been directed towards perovskite film deposition, structure optimisation, and interface manipulation.

The aim of the organic-inorganic hybrid solar cell project is to:

- test novel perovskite materials along with charge transfer buffer layers including metal oxide nanostructures and polymers for improved photon harvesting and stability
- employ low temperature solution-processed techniques for device fabrication – compatible with flexible substrates and roll-to-roll (R2R) manufacturing
- establish reproducible benchmark devices against which future improvements can be evaluated
- develop robust device structures to simultaneously improve stability and device efficiency
- develop and characterise tandem solar cells with perovskite and organic solar cells concatenated together.

Progress

Tandem solar cells

The project involves two parallel device fabrication and optimisation streams: (i) Perovskite solar cells; (ii) organic solar cells. The optimised functional units developed under streams (i) and (ii) are then concatenated on top of each other via an interconnection layer (ICL) to make a fully functional tandem solar cell. As an example, the designs of perovskite solar cell (stream 1), organic solar cell (stream 2) and tandem solar cell structure are shown in Figure PP2.1b.1.

The fabrication of tandem solar cells with the abovementioned configuration necessitates the deposition of the perovskite layer via thermal evaporation – in order to maintain the structural integrity of the bottom layer. We are also working on other possible device structures to build the tandem solar cell without using thermal evaporation, which is quite a challenge. We are currently evaluating several options and working on solution processable material systems to fabricate the targeted tandem solar cells.

Highlights

- Investigation of novel perovskite materials and electron interfacial materials.
- Use of advanced characterisation techniques to evaluate the charge transport properties in the bulk and interfaces.
- Development of highly efficient and robust interconnection layers for developing the organic-perovskite tandem solar cells.

Future Work

- Establish reproducible benchmark devices for future improvements.
- Test novel perovskite materials to improve thermal and moisture stability of the devices.
- Evaluate novel interfacial layers including polymers for improved charge selectivity and collection across the electrodes.
- Investigate interfacial compatibility with inorganic and organic materials, develop highly functional metal oxide nanostructures, self-assembling materials for surface modification, quantum dots etc. to improve the PCE and stability.
- Develop state-of-the-art interconnection layers for fabricating organic-perovskite tandem solar cells.

References

Mahmud, M.A., Elumalai, N.K., Upama, M.B., Wang, D., Chan, K.H., Wright, M., Xu, C., Haque, F. and Uddin, A., 2017, “Low temperature processed ZnO thin film as electron transport layer for efficient perovskite solar cells”, Solar Energy Materials and Solar Cells, 159, 251–264.

Mahmud, M.A., Elumalai, N.K., Upama, M.B., Wang, D., Wright, M., Chan, KH., Xu, C., Haque, F. and Uddin, A., 2016, “Single Vs Mixed Organic Cation for Low Temperature Processed Perovskite Solar Cells”, Electrochimica Acta, 222, 1510–1521.

Mahmud, M.A., Elumalai, N. K., Upama, M. B., Wang, D., Wright, M., Sun, T., Xu, C., Haque, F. and Uddin, A., 2016, “Simultaneous enhancement in stability and efficiency of low-temperature processed perovskite solar cells”, RSC Advances, 6, 86108-86125

Mahmud, M. A., Elumalai, N.K., Upama, M.B., Wang, D., Haque, F., Wright, M., Howe Chan, K., Xu, C. and Uddin, A., 2016, “Enhanced stability of low temperature processed perovskite solar cells via augmented polaronic intensity of hole transporting layer”, physica status solidi (RRL) – Rapid Research Letters, 10, 882–889.

Figure PP2.1b.1: Schematic device structures of perovskite solar cell (stream 1), organic solar cell (stream 2) and their tandem structure are shown.

PP2.1c Printing and Scale-Up

Lead Partner
CSIRO

CSIRO Team
Dr Fiona Scholes, Dr Gerry Wilson, Dr Doojin Vak, Dr Hasitha Weerasinghe, Dr Mei Gao, Dr Andrew Scully, Mr Andrew Faulks, Ms Jyothi Ramamurthy, Dr Kallista Sears, Dr Tianshi Qin, Mrs Régine Chantler
CSIRO Students
Ms Mathilde Fievez, Mr Clement Aury, Mr Hyun-Gyu Han, Ms Seyeong Song, Mr Xiaojin Peng

UoM Team
Dr David Jones

Georgia Tech Team
Prof Samuel Graham

Stanford University Team
Prof Reinhold H. Dauskardt

Stanford University Student
Haotian Wang

Academic Partners
Chimie Paris Tech, France; Ulsan National Institute of Science and Technology (UNIST), Korea; Dongguk University, Korea; Wuhan University of Technology, China; UoM

Funding Support
ARENA, CSIRO, Chinese Science Council

Aim

The overall aim of this sub-package is to address challenges associated with scale-up of printed solar films. The activities are articulated around the key research areas of organic photovoltaics (OPV) and perovskite PV, with a uniting theme of 'lab-to-fab' translation, i.e. accelerating the translation of laboratory-based small-scale results to larger-scale devices using industry-relevant manufacturing methods. These activities include expansion of CSIRO's lab-to-fab translation tools, as well as exploration of different materials for enhanced performance and a more robust printing process, thereby accelerating progress towards roll-to-roll printed solar devices.

Progress

Expansion of lab-to-fab translation tools

CSIRO's custom-developed mini slot-die coating capabilities were significantly expanded in 2016 with the commissioning of four new mini slot-die coaters. The design of these units was refined from previous versions, with additional functionality incorporated in selected units (e.g. thermal control). The units also offer significant improvements in ease of operation, making them more amenable to utilisation by collaborators.

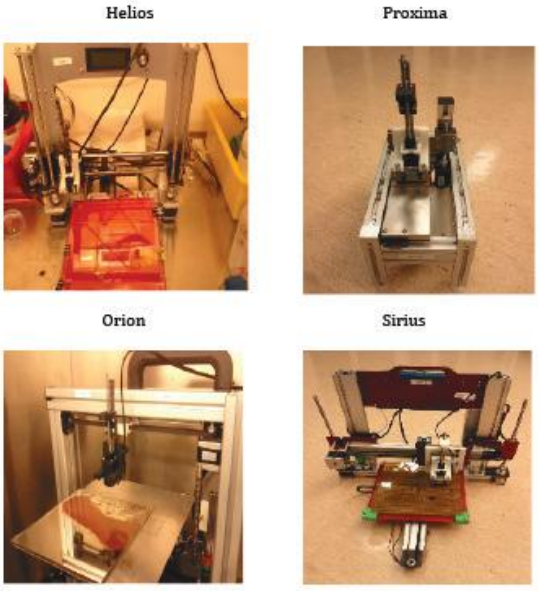

Figure PP2.1c.1: CSIRO's new, improved mini slot-die coaters.

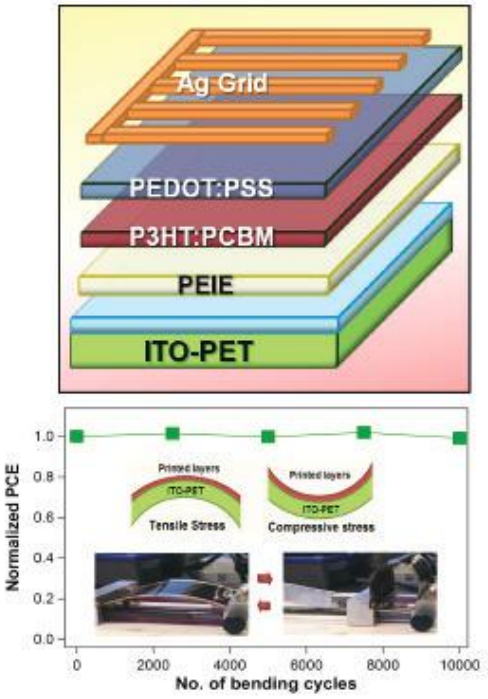

Figure PP2.1c.2: Schematic structure of the PEIE-based OPV modules (top); and PCE as a function of bending cycles at a radius of curvature of 1.5 cm. Inset illustrates the two different bending modes and the bending test being conducted on a flexible PEIE-based module (bottom).

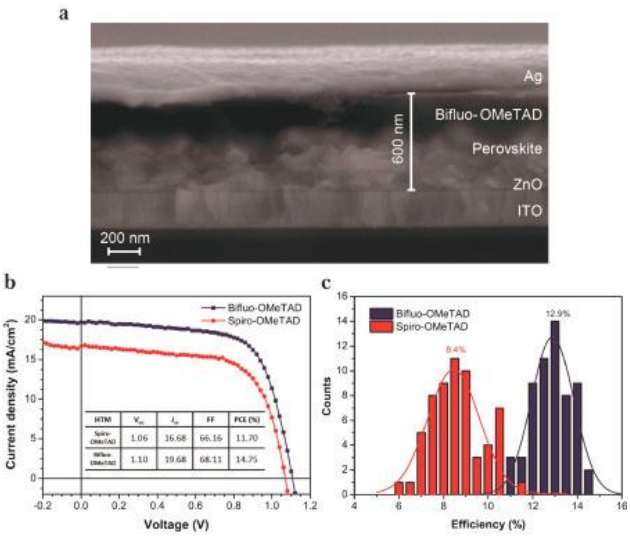

Figure PP2.1c.3: (a) Cross-section SEM images of slot-die coated PSC using bifluo-OMeTAD as an HTM; (b) Current density-voltage curve of PSCs with HTMs bifluo-OMeTAD and spiro-OMeOTAD. The device was measured at reverse scan with AM 1.5 G one-sun illumination; (c) Statistical distribution of efficiencies of perovskite solar cells with HTMs bifluo-OMeTAD and spiro-OMeOTAD. The average efficiency of PSCs employing bifluo-OMeTAD is 12.9%, while the average efficiency of PSCs employing spiro-OMeOTAD is 8.4%.

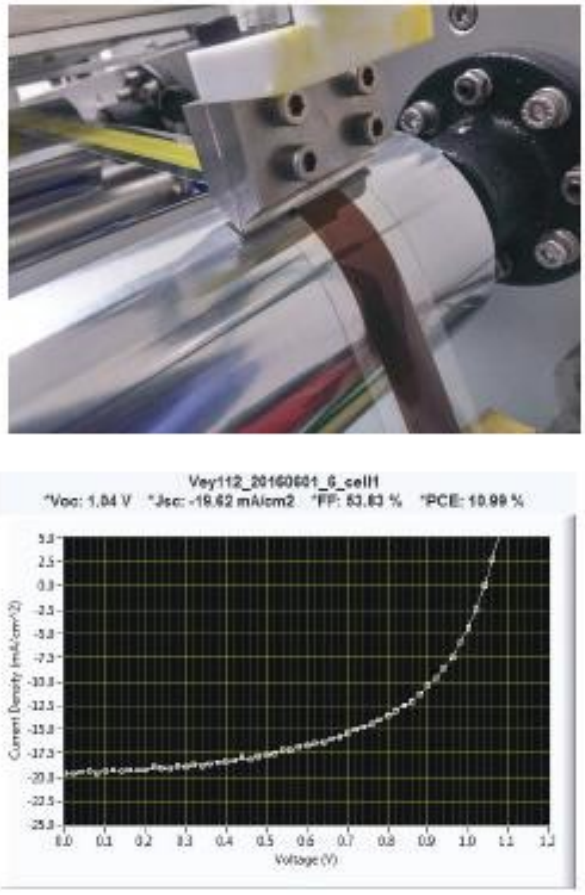

Figure PP2.1c.4: (top) R2R printing of flexible perovskite solar cells with two-step process; (bottom) current density-voltage curve of perovskite solar cell fabricated via R2R printing on ITO/PET conducted in air (ITO/PET/ETL(printed)/perovskite (printed)/HTL(printed)/MoO_3 (evaporated)/Ag (evaporated)). The device was measured under AM 1.5 G one-sun illumination at cell area of 0.1 cm^2.

Organic and perovskite PV – provision of printed films to collaborators

CSIRO is the only ACAP partner printing OPV and perovskite photovoltaics. For research purposes, several rolls of printed OPV and perovskite PV on 25 mm ITO/PET (0.1 cm^2 devices) with different degrees of encapsulation have been provided to US collaborators, in particular for interface delamination studies by Stanford University, and fracture and encapsulation studies by Georgia Tech (see below).

Organic PV – lab-to-fab translation

CSIRO's lab-to-fab translation tools have already been utilised for work with ACAP partners at UoM. Their OPV donor material, BQR, demonstrated high performance on the laboratory scale by spin-coating (glass, 0.1 cm^2). This material was then translated to CSIRO's mini slot-die coaters, resulting in a PCE of 6% (glass, 0.1 cm^2). This represents 60% of the performance achieved by spin-coating. This preliminary effort indicates that additional optimisation studies may result in further improvements in performance.

Organic PV – PEIE to enhance performance of flexible modules

The performance of flexible OPV modules depends on intrinsic material properties as well as film-forming characteristics. This motivated CSIRO to explore a commercial polymer, PEIE, as a replacement for ZnO for printed OPV modules. We have already shown that using PEIE as the electron transport layer results in a 20% improvement in efficiency over ZnO on flexible modules. In 2016, CSIRO worked with collaborators in the US (Stanford, Georgia Tech) to measure interfacial adhesion and mechanical stability to bending (10,000 cycles @ 1.5 cm radius). Improved interfacial strength and good mechanical qualities were demonstrated, confirming that PEIE is a good candidate for future scale-up efforts (Weerasinghe, 2016).

Perovskite PV – lab-to-fab translation

CSIRO have utilised its lab-to-fab tools to investigate translation of exciting developments in perovskite PV performance by spin-coating to printing. CSIRO have focused on both one-step and two-step deposition processes with planar structures (i.e. no TiO_2) and ambient processing (i.e. in air). Spiro-MeOTAD has been shown to be an excellent hole transport material (HTM) for spin-coated perovskite PV, however its poor film-

forming properties on perovskites by slot-die coating result in an inhomogeneous film due to slower drying when printed. For two-step deposition on glass, spiro-MeOTAD was substituted with an in-house developed HTM, bifluo-OMeTAD (Qin, 2017), resulting in excellent results compared with printing of spiro-MeOTAD. PCEs up to 14.7% (glass, 0.1 cm^2) and up to 9% for larger area devices (glass, 1 cm^2) have been demonstrated.

The above results were also translated to roll-to-roll (R2R) printed devices on ITO/PET, yielding a PCE of 11% at 0.1 cm^2 (Figure PP2.1c.4). This is a very promising outcome for ambient deposition via an industry-relevant process on a flexible substrate, providing an excellent grounding for further scale-up.

CSIRO has also commenced investigations on printing perovskite PV via the one-step process. While this is, in principle, the preferred approach due to its simplicity, the formation of defect-free perovskite layers via one-step deposition has proved to be challenging, especially when fabricated in air. CSIRO has addressed this through studies of p-i-n junctions prepared by one-step deposition of mixed cations and halides [$MA_{0.17}FA_{0.83}Pb(I_{0.83}Br_{0.17})_3$] treated with a newly developed quenching agent. Device hysteresis was reduced, a 12% PCE was demonstrated and, to date, film stability appears to be excellent after four months ambient exposure. Early work to translate these results to R2R printing on ITO/PET resulted in a PCE of 2–3%, which is a promising start for future work.

Perovskite PV – large-area characterisation

In order to measure flexible perovskite modules without encapsulation, CSIRO's large-area solar simulator was relocated into a glove box to enable measurements to be made in the absence of, and in comparison with, additional ambient exposure.

Highlights

- Expansion of lab-to-fab translation tools through design, construction and installation of four new mini slot-die coaters.
- Provision of printing OPV and perovskite PV to ACAP collaborators.
- Collaboration with UoM ACAP partners demonstrating a promising start for a new OPV material using CSIRO's lab-to-fab translation tools.
- Excellent perovskite PV results demonstrated by industry-relevant printing methods in ambient conditions (two-step perovskite deposition):
  - 14.7% PCE, slot-die, glass, 0.1 cm^2
  - 9% PCE, slot-die, glass, 1 cm^2
  - 11% PCE, R2R printed, flexible ITO/PET, 0.1 cm^2.
  - Promising early results for one-step perovskite deposition in ambient conditions.

References

Qin, T., et al., 2017, Nano Energy 31, 210–217.

Weerasinghe, H.C., et al., 2016, Solar Energy Materials & Solar Cells 152, 133–140.

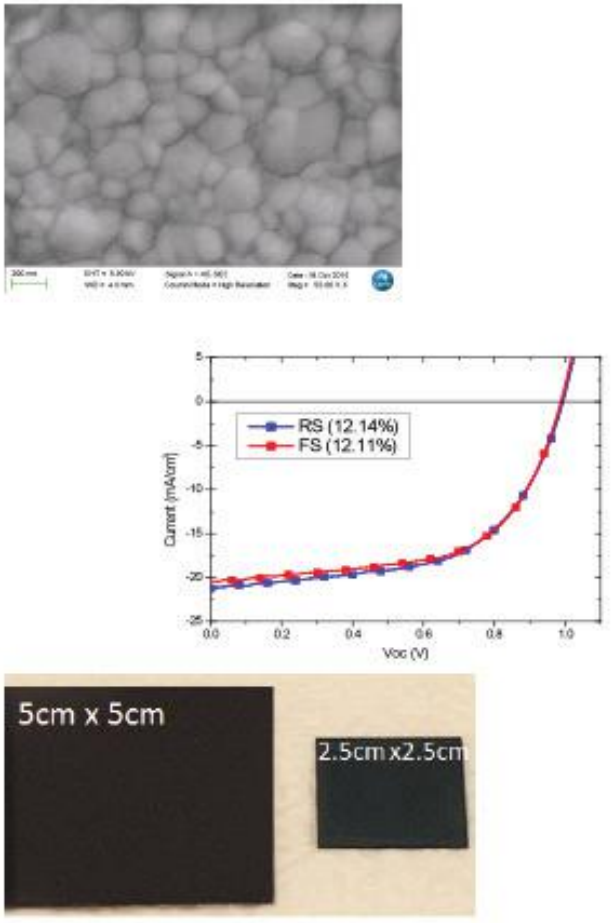

Figure PP2.1c.5: (top) SEM image of air-stable one-step process perovskite crystal surface; (middle) current density-voltage characteristics of the cell scanned at forward and reverse direction; (bottom) optical image of a large-scale film prepared by the same preparation method.

PP2.1d OPV Industrially Relevant Solvent Systems

Lead Partner
UoM

UoM Team
Dr David Jones, Dr Wallace Wong

UoM Students
Ms Valerie Mitchell, Mr Nickolas Hui, Mr Nicolau Saker Neto

Academic Partners
University of Bayreuth, Prof Mukundan Thelakkat, Dr Sven Huettner

Funding Support
ARENA, UoM, ARC (Future Fellowship)

Aim

Commercialisation of emerging technologies requires performance profiles sufficiently high to allow confidence that translation to large-scale modules will give commercial performance. For organic solar cells being developed within ACAP key materials properties are: (1) high power conversion efficiency (> 10%); (2) material stability during processing; (3) processability in industrial relevant solvent systems; and (4) new device architectures requiring new materials.

For organic solar cells it is expected that efficiencies for printed modules of between 8% and 10% power conversion efficiency would provide a commercial performance. Therefore, lab-based devices with an efficiency of > 10% power conversion efficiency will be required.

Research is focused on the development of high performance p- and n-type organic semiconductor materials, triplet host materials, understanding degradation mechanisms in OPV devices, block copolymers for solvent compatibility and new materials for luminescent solar concentrators.

In this package one key materials property required for commercialisation will be examined, the processability in industrial-relevant solvent systems.

Research is focused on the development of block copolymers for compatibility with industrially relevant solvents.

Progress

The first pure amphiphilic block-copolymers, where side-chain engineering has replaced the alkyl side-chains on the acceptor block with tetraethylene glycol (TEG) side-chains to promote the use of various solvents have been synthesised. The new materials show excellent solubility in non-chlorinated solvents and have been processed from industrially relevant and acceptable solvent systems. The block copolymers show excellent morphology control in thin films.

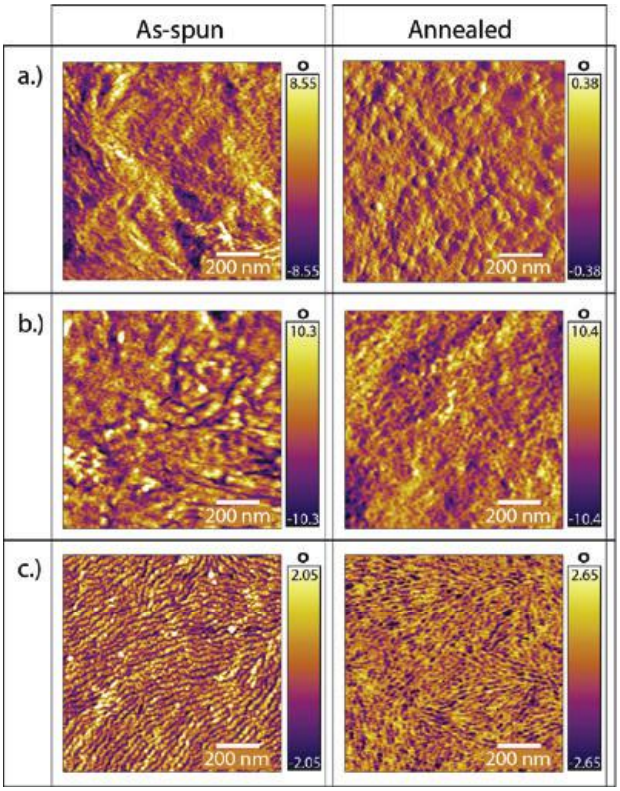

Figure PP2.1d.1: AFM image detailing the enhanced phase separation for conjugated block copolymers when deposited from industrially relevant solvent systems. Tapping mode AFM of films of (a) Donor-Acceptor (1:1) polymer blend, (b) Donor-Acceptor and block copolymer (1:1:1) blend, and (c) conjugated block copolymer (P3HT-*b*-PF_{TEG}T6BT) deposited from 2% bromoanisole in xylene before and after annealing.

Highlights

- The new amphiphilic conjugated block copolymers show enhanced solubility in industrially acceptable solvents.
- We have demonstrated excellent morphology development for these new materials with domain sizes of the order of 20 nanometres.

Future Work

New high performance amphiphilic conjugated block copolymers have been synthesised and are currently being examined in devices.

References

Mitchell, V.D., Wong, W.W.H., Thelakkat, M. and Jones, D. J., 2016, "The synthesis and purification of amphiphilic conjugated donor–acceptor block copolymers", Polymer J., DOI: 10.1038/pj.2016.97.

Subbiah, J., Mitchell, V.D., Hui, N.K.C., Jones, D.J. and Wong, W.W.H., "A Green Route to Conjugated Polyelectrolyte Interlayers for High Performance Solar Cells", Submitted for publication.

Mitchell, V.D., Gann, E., Huettner, S., Singh, C.R., Subbiah, J., Graser, A., Thomsen, L., McNeill, C.R., Thelakkat, M. and Jones, D.J., "The Morphological and Device Evaluation of Amphiphilic Block Copolymers for Organic Photovoltaic Applications", Submitted for publication.

PP2.1e OPV High Performance Materials

Lead Partner
UoM

UoM Team
Dr David Jones, Dr Wallace Wong, Dr Jegadesan Subbiah

UoM Students
Paul Geraghty, Calvin Lee, Sonam Saxena, Bolong Zhang, Nicolau Saker-Neto, Saghar Massomi, Sacha Novakovic, Can Gao, Khuyen Vu, Jia Yi Seow, Ruoyu Duan

Academic Partners
Georgia Institute of Technology, Prof Seth Marder, Dr Fadi Jradi

Funding Support
ARENA, ACAP, UoM, ARC (Future Fellowship)

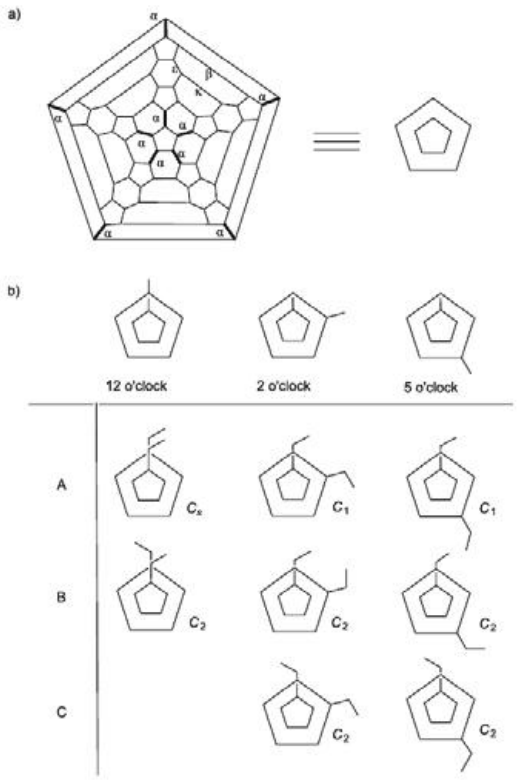

Figure 2.1e.1: (a) Schlegel diagram of C_{70}; (b) Illustrations of three regioisomers of $IC_{70}BA$ and their geometrical isomers.

Aim

Development of high performance p- and n-type organic semiconductors, interface modifiers, luminescent solar concentrator materials, up-conversion and singlet fission materials for organic solar cells.

Progress

A better understanding of structure performance properties for bis-substituted fullerenes in organic solar cells was developed after careful separation of the regioisomers and geometric isomers of IC70BA. The best performance in organic solar cells was associated with highly symmetrical 2 o'clock-B isomer (Figure PP2.1e.1(b)), as indicated by 1H-NMR and UV-Vis spectroscopy. The large variation in performance of the different isomers implies there is a significant benefit in looking for new, high yielding routes to the preferred isomers as previously demonstrated for C_{60} analogues.

Development of bottlebrush copolymers continued with the examination of synthetic methods to access n-type bottlebrush-polymer blocks incorporating the high performance polymer N2200 (naphthalenediimide-bithiophene-based polymer). The next step is to combine the previously synthesised p-type brush polymer (based on poly-3-hexylthiophene) with the new n-type brush polymer to generate the bottlebrush block-copolymer, Figure PP2.1e.3.

A significant program has been initiated to scale-up the synthesis of small molecule p-type donors, based on the benzodithiophene-terthiophene-rhodanine (BTR) scaffold, for use in high performance organic solar cells and for extended collaborations within the ACAP network, including printing programs. Benzodithiophene- quaterthiophene -rhodanine (BQR) (Figure PP2.1e.4) has been especially promising in providing highly thermally stable organic solar cells with an excellent performance profile, see Figure PP2.1e.5. BQR has been extensively examined through extensive collaborations through the ACAP network and with key US partners,. A full structure property relationship study on analogues of BQR is currently underway and results will be reported in the next period.

Extensive work is being devoted to the development of new synthetic methods to access key asymmetric building blocks to enable controlled polymerisation of desired conjugated polymers. Research on singlet fission, up-conversion, luminescent solar concentrators, exponential polymerisation through iterative coupling, n-type organic semiconductors, and stabilised nanoparticles is ongoing and will be reported at a later date.

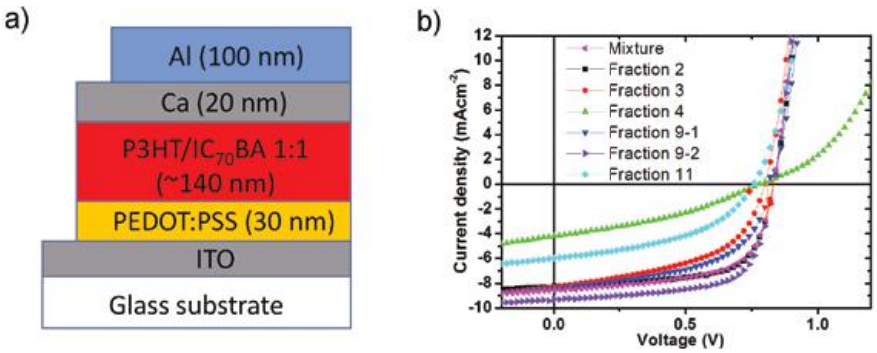

Figure PP2.1e.2: Schematic diagram of the architecture of bulk heterojunction (BHJ) solar cell devices (a) and *J–V* curves of the devices containing P3HT and each $IC_{70}BA$ fractions (b).

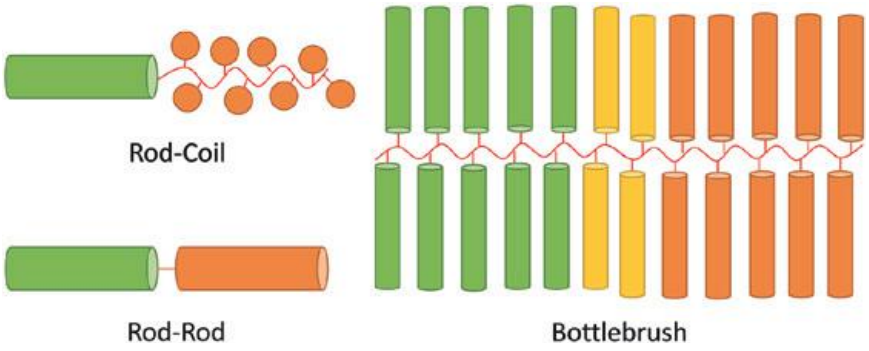

Figure PP2.1e.3: Illustrations of block copolymer structures. The components in green are electron donor materials and electron acceptors are coloured orange. Electron donor and acceptor materials as well as mixtures (yellow) can be easily incorporated into the bottlebrush material to give di-block or tri-block bottlebrushes.

Highlights

- The exceptional properties of benzodithiophene-X-rhodanine (BXR) high performance p-type organic semiconductors have been probed with materials being sent to ACAP collaborators for detailed analysis.
- BQR has been identified as an ideal candidate for synthetic scale-up for detailed characterisation and print trials.
- Synthesis of a high performance luminescent solar concentrator using non-aggregating dyes.
- Identification of the differential performance of bis-adducts of C_{70} in organic solar cells demonstrated the need for a regioselective synthesis.
- Development of a regioselective synthesis of C_{70} fullerene bis-adducts.
- Development of synthetic methods for the synthesis of well-defined bottlebrush polymers for morphology control in organic solar cells.

Future Work

- The importance of an association between a high temperature nematic liquid crystalline phase in p-type organic semiconductors and improved organic solar cell performance will be probed.
- Characterisation of a series of BTR/BQR analogues will be completed to investigate structure-property relationships and the energy landscape of high performance p-type organic solar cells.
- The high performance p-type organic semiconductor BQR will be synthesised on a large scale for print trials and to enable deeper collaboration with ACAP and AUSIAPV partners.
- The synthesis of a series of n-type organic semiconductors will be completed and materials characterised.
- New singlet fission and up-conversion materials will be developed and characterised.
- Synthetic methodologies to desymmetrised building blocks will be developed to enable controlled assembly of polymers or molecular materials.

References

Banal, J., 2016, “Spectral downshifting by molecular aggregates in planar concentrators for solar energy conversion”, PhD Thesis, UoM

Banal, J.L., Soleimaninejad, H., Jradi, F.M., Liu, M., White, J.M., Blakers, A.W., Cooper, M.W., Jones, D.J., Ghiggino, K.P., Marder, S.R., Smith, T.A. and Wong, W.W.H., 2016, “Energy Migration in Organic Solar Concentrators with a Molecularly Insulated Perylene Diimide”, J. Phys. Chem. C, 120, 12952–12958.

Gao, M., Subbiah, J., Geraghty, P.B., Chen, M., Purushothaman, B., Chen, X., Qin, T., Vak, D., Scholes, F.H., Watkins, S.E., Skidmore, M., Wilson, G.J., Holmes, A.B., Jones, D.J. and Wong, W.W.H., 2016, “Development of a High-Performance Donor–Acceptor Conjugated Polymer: Synergy in Materials and Device Optimization”, Chem. Materials, 28, 3481–3487.

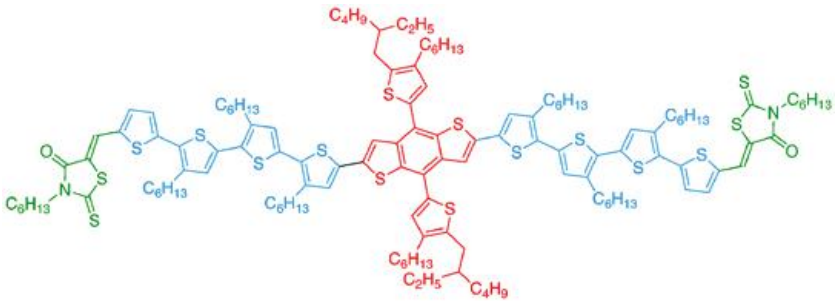

Figure PP2.1e.4: Chemical structure of the high performance p-type organic donor material BQR.

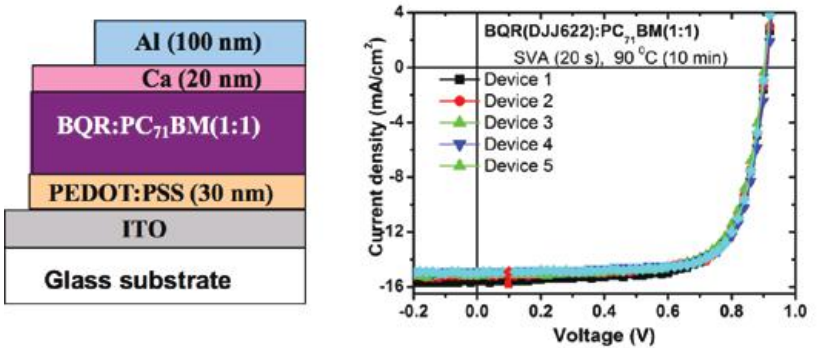

Figure PP2.1e.5: Schematic diagram of the architecture of BQR containing BHJ solar cell devices (a) and *J*–*V* curves of a batch of devices containing BQR and PC71BM (b). An average PCE of 9.8 ± 0.4% was recorded for this batch of devices with a best efficiency of 10.2%.

Geraghty, P.B., Lee, C., Subbiah, J., Wong, W.W.H., Banal, J.L., Jameel, M.A., Smith, T.A. and Jones, D.J., 2016, "High performance p-type molecular electron donors for OPV applications via alkylthiophene catenation chromophore extension", Beilstein J. Org. Chem., 12, 2298–2314.

Van As, D., Subbiah, J., Jones, D.J. and Wong, W.W.H., 2016, "Controlled Synthesis of Well-Defined Semiconducting Brush Polymers"," Macromol. Chem. Phys., 217, 403–413.

Vu, K.uyen, 2016, "Toward the synthesis of Semi-conducting brush polymer for organic solar cells", Master of Science Thesis, UoM

Zhang, B., Subbiah, J., Jones, D.J. and Wong, W.W., 2016, "Separation and identification of indene-C70 bisadduct isomers", Beilstein J. Org. Chem., 12, 903–911.

Zhang, B., White, J.M., Jones, D.J. and Wong, W.W.H., 2015, "Regioselective synthesis of fullerene multiadducts via tether-directed 1,3-dipolar cycloaddition", Org. Biomol. Chem., 13, 10505–10510.

PP2.1f OPV Device Architectures

Lead Partner
UoM

UoM Team
Dr David Jones, Dr Jegadesan Subbiah

UoM Students
Mr Haotien Wang

Funding Support
ARENA, UoM

Aim

A key aspect of the current program is to ensure OPV device performance is measured against the common standard over a 1 cm^2 area, rather than the typical 0.1 cm^2 normally used for OPV. The key outcome is then to translate the performance for developed or known materials to the larger area with minimal performance loss. To reach the project milestone of a device with >10% PCE for a 1 cm^2 area was expected to require materials improvement in the active layer, interface modifiers and device architecture.

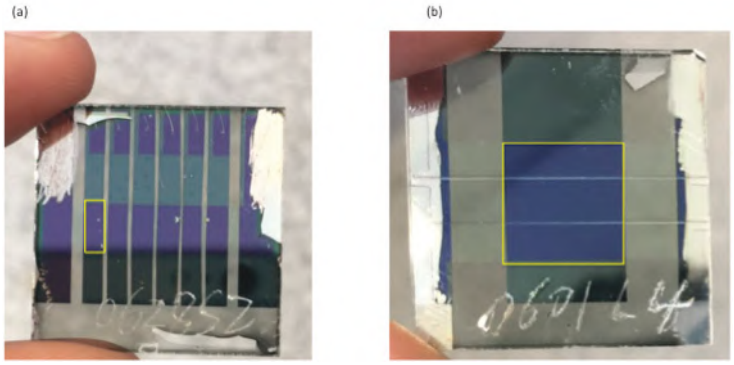

Figure PP2.1f.1: Photograph of (a) 0.1 cm^2 PTB7:PC71BM devices, and (b) 1 cm^2 PTB7:$PC_{71}BM$ devices with two lines Ag for enhanced charge collection (inverted structure). Active area is shown inside of the yellow rectangles. (Photo by Haotian Wang)

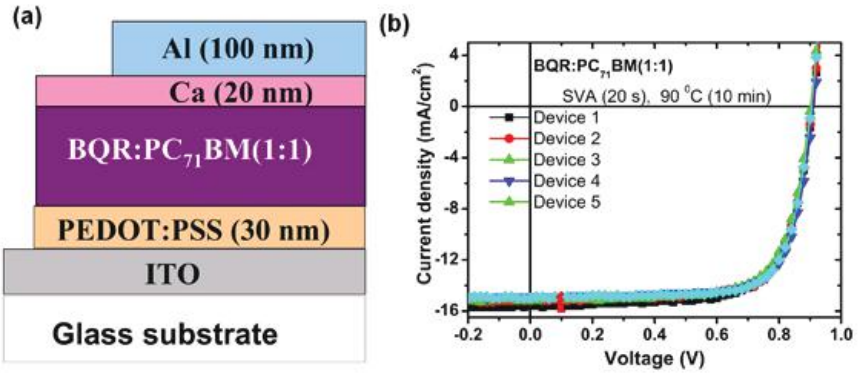

Figure PP2.1f.2: Device architecture (a) and J-V curves (b) for the optimised BQR/PC71BM containing organic solar cells.

Progress

Large area devices (milestone of >10 % PCE for devices >1 cm^2):

1. The conductivity of the transparent conducting oxide (TCO) is low resulting in significant series losses in larger area devices. The problem was overcome by accessing high conductivity indium tin oxide (ITO).
2. The active layer must perform optimally with low series losses, excellent light absorption and ease of processing. In this case we have used a commercial high performing polymer (PTB7) in a ternary blend with our molecular donor (BQR) to boost performance.
3. Our molecular donors have excellent performance in small area devices, however issues with the commercially available interlayer has restricted performance in larger devices so new substrates have been sourced and these modifications will be reported in the next period.
4. The combination of the above modifications resulted in small area device efficiencies of >11.5% PCE, while for large area ternary devices containing BQR with power conversion efficiencies of >10% PCE and up to 10.5% PCE (submitted to CSIRO Energy Technology in Newcastle for certification).

Device Stability:

1. In previous research with our BQR molecular donors, we demonstrated our devices are thermally stable up to 120°C for 20 minutes without significant loss of performance (not yet fully optimised), and are therefore printable. Device optimisation using a combination of solvent vapour and thermal annealing has delivered small area devices with an average of 9.8% PCE and a best of 10.2% PCE, see Figure PP2.1f.2.

Highlights

- Thermally stable devices have been assembled using the new BQR molecular donor with the best efficiencies now >10% PCE.
- BQR is currently being synthesised on a large scale for print trials and for distribution to AUSIAPV partners for collaborative projects.
- Organic solar cells with >10% PCE (1 cm^2) have been assembled and submitted for evaluation.

References

Geraghty, P.B., Lee, C., Subbiah, J., Wong, W.W.H., Banal, J.L., Jameel, M.A., Smith, T.A. and Jones, D.J., 2016, "High performance p-type molecular electron donors for OPV applications via alkylthiophene catenation chromophore extension", Beilstein J. Org. Chem., 12, 2298–2314.

Wang, H., 2016, "Large Area Organic Solar Cells: Fabrication and Optimization", Masters, UoM.

PP2.1g OPV Characterisation

Lead Partner
UoM

UoM Team
Prof Kenneth Ghiggino, Dr David Jones, Dr Wallace Wong

UoM Students
Ms Kyra Schwarz, Mr Paul Geraghty, Mr Paul Hibbert

ACAP Partner
UQ

UQ Team
Prof Paul Meredith, Dr Ardalin Armin

Academic Partners
NIST (USA), Dr Lee Richter, Dr Sebastian Engmann

Funding Support
ARENA, ARC, UoM, UQ

Aim

The key aim of this package is to better understand the fundamental process occurring in solar cells so that the device architectures can be improved, and the fundamental process occurring in devices so that materials design can be improved.

Progress

The key aspects of the work in the reporting period were to; (i) examine the fundamental processes involved in exciton formation and charge separation when BTR or BQR were incorporated into the active layer; (ii) examine fundamental processes involved in exciton formation and charge separation in polymer nanoparticles; (iii) model and map processes in OPV devices or LSCs.

Active OPV devices containing BTR show only modest resistance to thermal stress once formed with a rapid decrease in PCE with exposure to heat. The solution to this problem has been to increase the chromophore length generating BQR which shows significantly improved thermal stability. This suggests that diffusion coefficients for BTR were too high leading to excess crystallisation and phase separation. We have used transient absorption (TA) spectroscopy to examine the changes in exciton formation and charge separation for BTR and BQR containing thin films, so that we can then compare these processes before and after solvent vapour annealing or thermal annealing. These TA studies on BQR are currently underway, with results for BTR now published, where we have demonstrated marked differences between annealed and unannealed films. Rapid exciton formation and charge separation is seen in solvent vapour annealed devices with the loss of a signal assigned to a triplet species in the un-annealed films. The role of spin in the performance of BTR devices was elucidated.

Researchers at UQ have led a program on the detailed characterisation of charge regeneration in BTR containing active layers. It has been determined that the charge recombination in BTR-PC71BM active layers is very slow, possibly leading to the high performance of this class of materials.

Work completed in collaboration with NIST has mapped the in situ structural changes for BTR/PC71BM films during annealing to map impact of crystallisation on device performance. Using in situ wide and small angle X-ray techniques the crystal growth parameters were followed indicating an Ostwald-type ripening process with

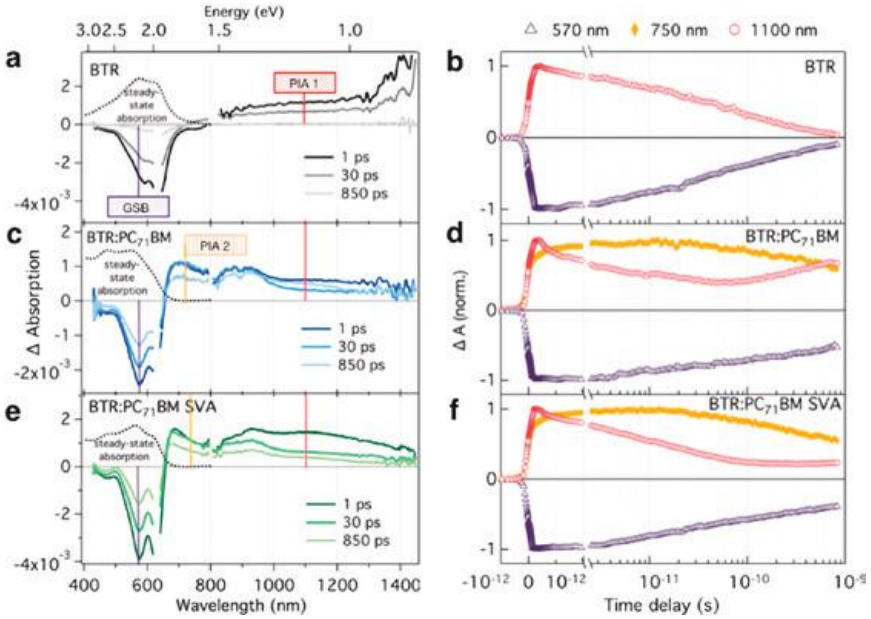

Figure PP2.1g.1: Thin-film transient absorption measurements with 630 nm excitation at 6 μJ/cm² of (a) and (b) BTR, (c) and (d) BTR:PC71BM as-cast, and (e and (f) BTR:PC71BM after SVA. Spectral slices are shown in (a), (c), and € at 1, 30 and 850 ps, with ground-state absorption spectra also shown for comparison (black dotted lines). Kinetic profiles are shown in (b), (d) and (f) of the ground-state bleach (GSB) at 570 nm (open triangles), photo-induced absorption 2 (PIA 2) at 750 nm (closed diamonds), and photo-induced absorption 1 (PIA 1) at 1100 nm (open squares).

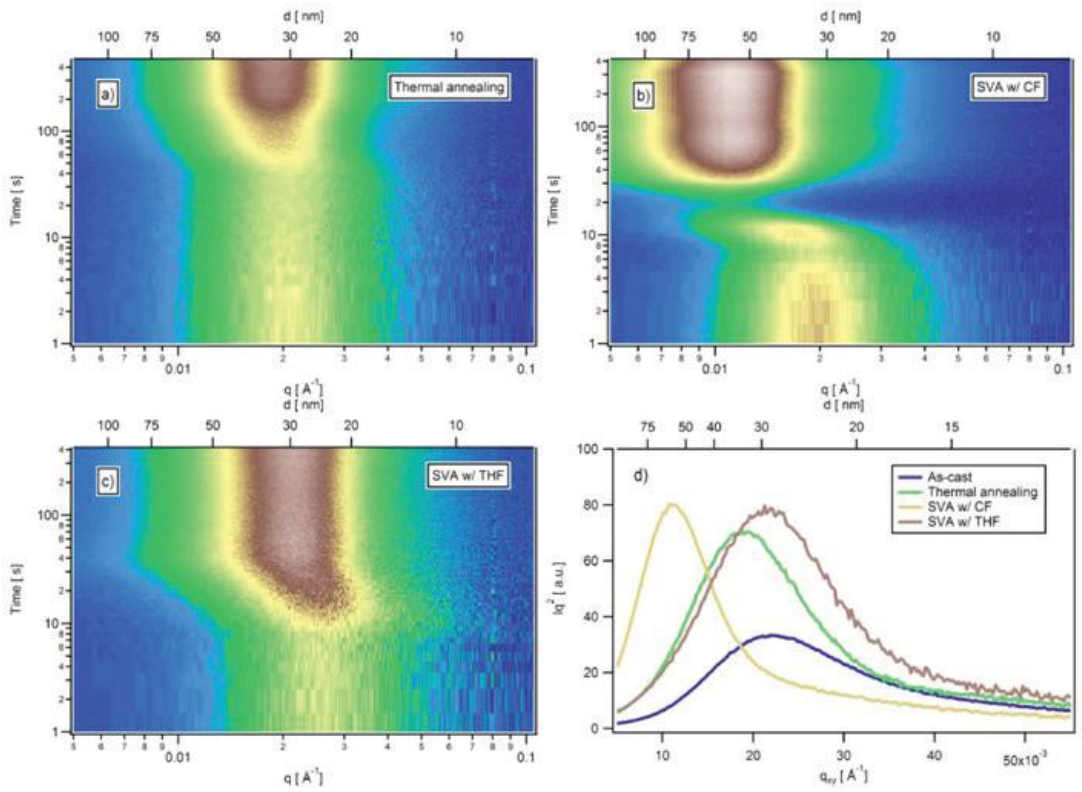

Figure PP2.1g.2: Evolution of the q2-weighted background corrected GISAXS intensity near the sample horizon (qz z 0, a-c) for a BTR/PC71BM BHJ film. The data corresponds to a BHJ film during (a) thermal annealing, (b) during 15 s SVA with chloroform (CF), and (c) during 30 s SVA with tetrahydrofuran (THF). The background corrected scattering intensity after annealing is shown in (d), domain size is indicated along the top of (d).

overgrowth of crystallites during thermal annealing. For the optimal solvent vapour annealing with tetrahydrofuran (THF) a domain size of around 30 nm was measured, while after thermal annealing an overgrowth of the domains was measured at 60–50 nm. It is well known that large domains do not allow exciton diffusion to the internal donor-acceptor (p-n) interface required for charge separation. This directly correlates with the observed trends in device performance.

Highlights

- The new molecular material BTR has been shown to have remarkably slow recombination kinetics allowing performance to be maintained in films up to 350 nm thickness, ideal for printing.
- TA spectroscopy on films containing BTR have identified the involvement of triplet states in as-cast films. Upon solvent vapour annealing as the device performance improves the triplet signal is lost.
- Chromophore chain extension of BTR-generated BQR with improved thermal stability in devices and, after optimisation, improved device performance over BTR.
- In situ X-ray characterisation of printed films (doctor bladed).

References

Armin, A., Subbiah, J., Stolterfoht, M., Shoaee, S., Xiao, Z., Lu, S., Jones, D. J., and Meredith, P., 2016, “Reduced Recombination in High Efficiency Molecular Nematic Liquid Crystalline: Fullerene Solar Cells”, Advanced Energy Materials, p. 1600939, DOI: 10.1002/aenm.201600939.

Banal, J. L., , Soleimaninejad, H., Jradi, F. M., Liu, M., White, J. M., Blakers, A. W., Cooper, M. W., Jones, D. J., Ghiggino, K. P., Marder, S. R., Smith, T. A., and Wong, W. W. H., 2016, “Energy Migration in Organic Solar Concentrators with a Molecularly Insulated Perylene Diimide”, The Journal of Physical Chemistry C, Vol. 120(24), pp. 12952–-12958, 2016. DOI: 10.1021/acs.jpcc.6b04479.

Banal, J. L., Zhang, B., Jones, D. J., Ghiggino, K. P., and Wong, W. W., 2016, “Emissive Molecular Aggregates and Energy Migration in Luminescent Solar Concentrators”, Acc. Chem. Res., DOI: 10.1021/acs.accounts.6b00432.

Engmann, S., Ro, H. W., Herzing, A., Snyder, C. R., Richter, L. J., Geraghty, P. B., and Jones, D. J., 2016, “Film morphology evolution during solvent vapor annealing of highly efficient small molecule donor/acceptor blends”, J. Mater. Chem. A, Vol. 4(40), pp. 15511-–15521, DOI: 10.1039/c6ta05056e.

Schwarz, K. N., Geraghty, P. B., Jones, D. J., Smith, T. A., and Ghiggino, K. P., 2016, "Suppressing Subnanosecond Bimolecular Charge Recombination in a High-Performance Organic Photovoltaic Material", The Journal of Physical Chemistry C, Vol. 120 (42), pp. 224002-–24010, DOI: 10.1021/acs.jpcc.6b08354.

PP2.1h Elucidating the Role of Donor and Acceptor in Photocurrent Generation

Lead Partner
UQ

UQ Team
Dr Dani Stoltzfus, Dr Andrew Clulow, Prof Ian Gentle, Dr Ravi Nagiri, Prof Paul Burn, Prof Paul Meredith

Ulm University, Germany Team
Prof Peter Bäuerle

Funding Support
ARENA, ACAP, UQ

Aim

The aim of this program is to understand how light absorption in organic semiconducting materials can contribute to current generation in donor-acceptor organic solar cells.

Progress

In the reporting period activity focused on two key areas:

1. State-of-the-art single-junction organic photovoltaic devices contain a bulk heterojunction active layer comprising a blend of donor and acceptor materials. In the best devices near 100% internal quantum efficiencies (IQE) have been achieved, resulting in overall power conversion efficiencies (PCE) of around 10%. For efficient solution-processed devices comprising narrow optical gap polymers and fullerene acceptors the polymer donor to acceptor ratio often falls between 1:1 and 1:4 by weight, corresponding to 50 weight per cent (wt%) to 20 wt% of the donor. However, there have been a number of recent reports of moderately efficient donor:fullerene solar cells in which the wt% of the donor is significantly lower (a few per cent). Such devices can have a large and similar open-circuit voltage (≈1.0 V) independent of the choice of donor and a key feature of these devices is that they operate by the Channel II mechanism for charge generation as the concentration of the donor is low and thus it only provides a small contribution to the optical density of the film. However, the use of wt% in these studies is in some ways misleading due to the significantly different molecular weights of the donor materials – it is the number of molecules and not just the weights of each material that is important. While there have been a number of explanations as to how such devices work when the donor is apparently below the percolation threshold there is still much uncertainty as to the exact mechanism of how they operate. We have studied the effect of dendrimer donor content on solar cell performance. We find that low donor content cells containing the dendrimer 42T (see Figure PP2.1h.1), can give rise to large open circuit voltages of up to 0.92 V and a PCE of 3.5%. We find that the use of mol% for blend ratios is a more meaningful measure than wt% for materials with defined molecular weight, as it is the ratio of molecules present in the bulk heterojunction and the volume they occupy in the film that governs the presence (or absence) of percolation pathways, and hence efficient charge transport and extraction. We further found that the ratio of components in the casting solution does not necessarily correlate to that in the film (Stoltzfus et al., 2016a).
2. The most common method for evaluating new materials and their blends is to fabricate and test organic solar cells to empirically determine the optimum blend ratio and processing conditions. The present understanding is that optimised two-component bulk heterojunction films incorporating

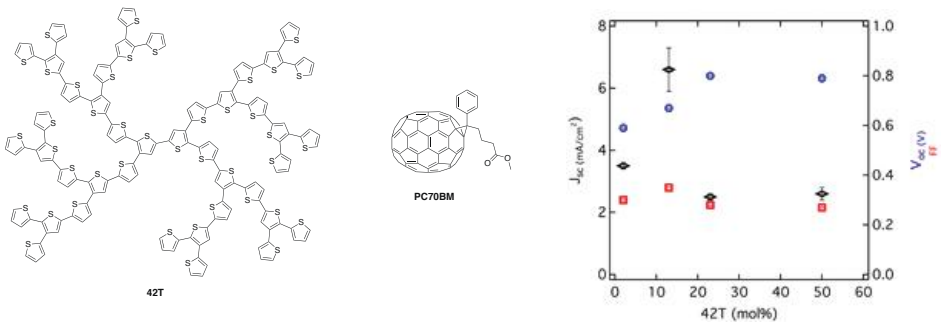

Figure PP2.1h.1: Structures of the dendrimeric donor 42T and acceptor PC70BM and photovoltaic characteristics of 42T:PC70BM cells under AM1.5G at 100 mW/cm^2 illumination: FF (red), Voc (blue) and J_{SC} (black) versus 42T mol% of the casting solution.

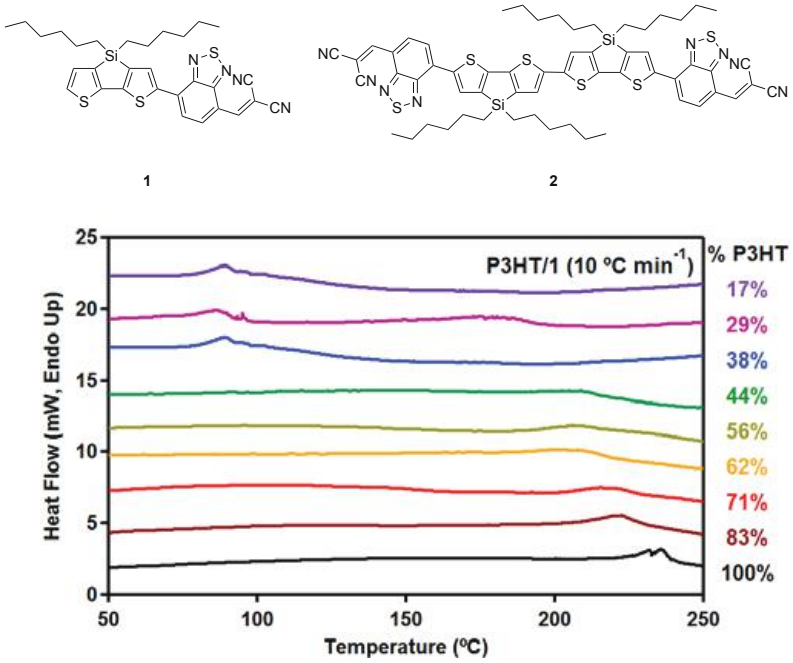

Figure PP2.1h.2: Structure of the monomer and dimer acceptors and first heating thermograms for blends of acceptor 1 with P3HT. Traces are offset for clarity.

polymer donors are three phase systems comprising pure donor, pure acceptor and intermixed phases. There have now been a small number of reports that aim to determine the optimised blend ratio in a predictive manner based on the thermal properties of the blended materials. In particular two component blends containing poly(3-alkylthiophene)s (P3ATs) and electron acceptors such as the [6,6]-phenyl-C61 (or C71)-butyric acid methyl esters (PCBMs) or a small molecule non-fullerene acceptor such as 2-[(7-(9,9-di-*n*-propyl-9*H*-fluoren-2-yl)benzo[c]-[1,2,5] thiadiazol-4-yl)methylene]malononitrile were found to form a eutectic composition, and the blend ratio that gave the best device performance was hypoeutectic with respect to the polymer. We have continued to develop the predictive concept in exploring the thermal properties and crystallinity of blends of poly(3-*n* hexylthiophene) (P3HT) with the non-fullerene acceptors 1 or 2 (see Figure PP2.1h.2). We have found that the blends of these materials do not exhibit eutectic phases, with the morphology of the film strongly dependent on whether the monomer or dimer is used. Diffractometry measurements showed that dimerisation of chromophore 1 to give dimer 2 profoundly altered the crystalline properties of the non-fullerene acceptors and consequently those of the blends with P3HT, leading to only moderate solar cell performance with both acceptors but for opposite reasons – in one case too crystalline and the other too amorphous. The results thus add to our understanding of the important role of eutectic phases and crystallinity in non-fullerene-based organic solar cells.

Highlights

- Development of new understanding of low donor content solar cell performance.
- Development of methodology for evaluating new materials based on thermal properties.

References

Stoltzfus, D., et al., 2016a, Appl. Phys. Lett. 109, 103302.

Stoltzfus, D., et al., 2016b, Macromolecules 49, 4404.

PP2.1i Characterising the Factors that Affect Photocurrent Collection in Sub-Module Cells

Lead Partner
UQ

UQ Team
Dr Hui Jin, Dr Dani Stoltzfus, Dr Ardalan Armin, Dr Jenny Donaghey, Dr Andrew Clulow, Prof Ian Gentle, Prof Paul Burn, Prof Paul Meredith

Funding Support
ARENA, ACAP, UQ

Aim

The aim of this program is to understand how photocurrent can be effectively collected in sub-module organic and Earth-abundant solar cells to facilitate through the development of new materials and device architectures. Note: this report should be read in conjunction with Section 2.5.

Progress

In addition to the previously reported perovskite solar cells we have made progress in the following areas during the reporting period:

High dielectric constant organic semiconductors for enhanced exciton separation and reduced geminate recombination: The low dielectric constants of conventional organic semiconductors leads to poor charge carrier photogeneration in homojunction organic solar cells due to large exciton binding energies. This fact necessitates the use of high and low electron affinity organic semiconductor (acceptor and donor) blends in a heterojunction architecture. It has been suggested that increasing the organic semiconductor dielectric constant could lower the exciton binding energy and facilitate more efficient free carrier generation and maybe also decrease geminate recombination from the charge transfer state. However, the role of the low frequency and optical frequency regime dielectric constants has not been elucidated. To test this hypothesis we designed, synthesised and characterised a series of model non-polymeric and polymeric materials with short glycol or alkyl solubilising groups to study the effect on dielectric constant. We found that glycolation increased the low frequency dielectric constant while the optical frequency dielectric constant appears to be dependent on the size of the delocalised chromophore and their packing in thin film. It was also found that the materials with the higher optical frequency dielectric constant had higher internal quantum efficiencies near the optical gap than materials that do not. The results are still being fully analysed in preparation for submission work.

Highlight

- Creation of high dielectric constant organic semiconductors at low and optical frequencies by glycolation and engineering the chromophore and film density.

Future Work

Future work in PP2.1i will include:

- Activities associated with the perovskite studies reported in Section 2.5.
- Further development of high dielectric materials.
- Development of devices with alternative transparent conducting electrodes.

PP2.2 Thin-Film Inorganic (CZTS)

PP2.2b CZTS Cells on Soda Lime Glass

Lead Partner
UNSW

UNSW Team
Dr Xiaojing Hao, Prof Martin Green, Dr Fangyang Liu, Dr Hongtao Cui, Dr Jialiang Huang, Dr Fajun Ma

UNSW Students
Yuanfang Zhang, Chang Yan, Xiaolei Liu, Fangzhou Zhou, Xu Liu, Jongsung Park, Aobo Pu, Kaiwen Sun, Heng Sun

Industry Partner
China Guodian Corporation

Funding Support
ACAP, ARC, China Guodian Corporation

Aim

All successfully commercialised non-concentrating photovoltaic technologies to date are based on silicon or chalcogenides (semiconductors containing Group VI elements, specifically Te, Se and S). The successful chalcogenide materials, CdTe and Cu(In,Ga)Se2, can be regarded as “synthetic silicon” where the balance between atoms in these materials provides the same average number of valence band electrons as in silicon, resulting in the same tetrahedral coordination. Cd and Se are toxic while Te and In are among the 12 most scarce elements in Earth’s crust. These factors would seem to clearly limit the long-term potential of the established chalcogenide technologies. By delving more deeply into the Periodic Table, an alternative option can be uncovered with the same number of valence band electrons on average but involving only Earth-abundant, non-toxic elements.

Kesterite Cu_2ZnSnS_4 (CZTS) compound semiconductor has emerged, based on such reasoning, as a promising candidate for thin-film solar cells. Analogous to the chalcopyrite structure of CIGS, CZTS shares similar optical and electrical properties. CZTS has a bandgap of around 1.5 eV, a large absorption coefficient of over $10^4 cm^{-1}$. Notable is that the bandgap of the CZTS family can be tuned to span a wide range beyond 2.25 eV, even above the accessible range of the highest efficiency III-V cells. This makes the material suitable for tandem cells (see Section PP1.3a(iv)). For thin-film solar cells, energy conversion efficiency up to 12.6% and 9.5% have been achieved so far for CZTS(e) and CZTS solar cells by IBM and UNSW, respectively.

ACAP’s work in the CZTS area takes the sputtering fabrication direction, a low-cost, high-throughput and up-scalable manufacturing process which has been used in the commercialised CIGS solar cells. Work in this strand

includes the development of high efficiency CZTS solar cells on soda lime glass.

Progress

CZTS solar cell performance loss mechanisms have been analysed by established Sentaurus TCAD device simulation based on the combination of experimental characterisation results and empirical data from literature (see Table PP2.2b.1). The effective lifetime is introduced and the impact of interface velocity and CZTS bulk Shockley-Read-Hall (SRH) lifetime on device effective lifetime is studied (see Figure PP2.2b.1). The bandgap fluctuation of the fabricated CZTS is estimated (see Figure PP2.2b.2). It is identified that heterojunction interface recombination, together with disorder-induced bandgap fluctuation contributed to 97% of V_{OC} loss (see Figure PP2.1b.3). The model further forecast that, with the heterojunction interface problem alone settled, the device V_{OC} could be boosted to above 900 mV. Furthermore, device V_{OC} could even reach to 1 eV when mitigation of these two problems comes to fruition. Relevant strategies have been developed with a focus on the interface engineering and disorder issue of the CZTS absorber.

One of the key interface engineering strategies at back contact results in significant improvement in the quality of CZTS absorber (see Figure PP2.1b.4). The improved absorber quality solves the traditional problems of voids, secondary phases and highly resistive MoS_x. A confirmed world record 7.6% efficiency CZTS solar cell was achieved based on this technology, which is recorded in the Solar Cell Efficiency Tables (version 48).

In 2015, a novel $Zn_xCd_{1-x}S$ buffer was developed to engineer the conduction band alignment. By X-ray photoelectron spectroscopy (XPS) analysis, it is deduced that the original cliff-like conduction band offset (CBO) between CdS/CZTS can be shifted towards a spike form when introducing a $Zn_xCd_{1-x}S$ buffer (see Figure PP2.1b.5). As the surface plays an important role determining the analysed CBO and the surface of CZTS is greatly affected by the stoichiometry of CZTS, the effect of Zn content on the performance of CZTS/$Zn_xCd_{1-x}S$ was analysed. The Zn content range giving beyond 9% efficiency CZTS solar cells was identified (see Figure PP2.1b.6). The recipe for the SILAR process for the development of $Zn_xCd_{1-x}S$ was re-examined. The addition of a buffered solution into the SILAR process was found effective in further improving the CZTS cell performance. A confirmed world record 9.5% efficiency CZTS solar cell was obtained (see Figure PP2.1b.7), which breaks the 9.1% previous record set by Toyota and is recorded in the Solar Cell Efficiency Tables (version 49).

A Cd-free buffer of ZnSnO was explored by collaborating with Nanyang Technological University, the initial test yielding beyond an 8% CZTS solar cell. More analysis is currently under investigation.

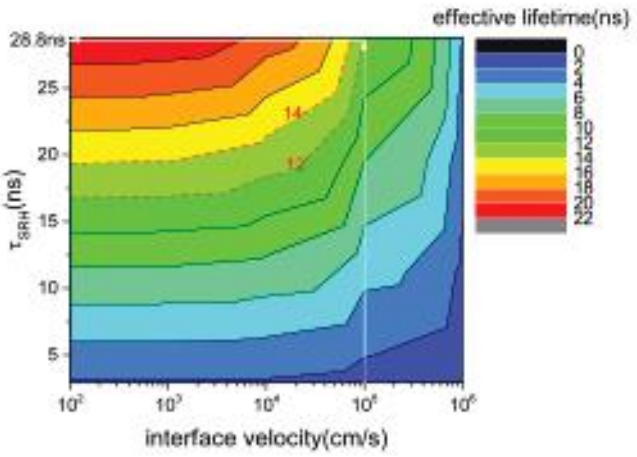

Figure PP2.2b.1: Impact of interface velocity and CZTS bulk SRH lifetime on device effective lifetime is depicted as contour colour map. The zone of effective lifetimes as predicted by time-resolved photoluminescence (TRPL) is shown between two marked lines.

Strategies for passivating the heterojunction interface were also explored. Among various passivation materials, Al2O3 and SnO are found more effective in improving the V_{OC} of CZTS/CdS-based solar cells (see Figures PP2.1b.8 and PP2.1b.9). This result agrees with our device simulation. More analysis is planned for the coming year.

Disorder arising from the close atomic radius of Cu and Zn has been recognised as one of the major reasons for the band tailing issues. We explored the alloying of Cd or Ag partially replacing Zn and Cu, respectively to reduce the disorder issue. PDS was applied to investigate the urbach energy which is expected to be affected by the disorder issue. A smaller urbach energy was observed in the Cd-alloyed CZTS compared with that of CZTS (see Figure PP2.1b.10). This characterisation gives the direct evidence of the reduction in the band tailing by Cd-alloying. An 11.5% efficiency CCZTS (Cd-alloyed CZTS) was achieved, which to our knowledge is the highest reported in the world (see Figure PP2.1b.11).

Performance loss mechanisms were re-examined on CZTS solar cells and Cd-alloyed CZTS solar cells. Further device analysis (JVT) shows that the recombination is still dominated at the interface in both CZTS/ $Zn_xCd_{1-x}S$-based solar cells and Cd-alloyed CZTS/CdS-based solar cells.

Highlights

- Performed detailed analysis on the performance loss mechanisms of CZTS solar cells by TCAD device simulation.
- Established the confirmed world record 7.6% efficiency CZTS solar cell (total cell area 1cm^2), which is recorded in the Solar Cell Efficiency Tables (version 48 and version 49).
- Established the confirmed world record 9.5% efficiency CZTS solar cell (total cell area 0.24 cm^2),

which breaks the previous 9.1% record set by Toyota and is recorded in the Solar Cell Efficiency Tables (version 49).

Future Work

Future work in 2017 will be focused on improving the efficiency of CZTS solar cells to beyond 10%. Strategies will be developed to reduce the V_{OC} deficit. Characterisations will be focused on CZTS absorber to identify effective strategies to improve its quality (disorder, bandgap fluctuation, lifetime, etc.).
Demonstrate effective strategies to reduce the disorder degree of CZTS by alloying with other elements and demonstrated 11.5% Cd-alloyed CZTS solar cells.

References

Cui, H., Lee, C-Y., Gong, S., Liu, X. and Hao, X.J., 2015, "Chemical composition control of evaporated Cu_2ZnSnS_4 Solar cells", Journal of Solar Energy Research Updates, 2 (2).

Liu, F., Tong, Z., Sun, K., Yan, C., Jiang, L., Hao, X.J. and Li J., 2016, "Modification of absorber quality and Mo-back contact by a thin Bi intermediate layer for kesterite Cu_2ZnSnS_4 Solar Cells", Solar Energy Materials and Solar Cells, 144:537–543.

Liu, F., Yan, C., Huang, J., Sun, K., Zhou, F., Stride, J., Green, M.A. and Hao, X.J., 2016, "Nanoscale microstructure and chemistry of Cu_2ZnSnS_4/CdS interface in kesterite Cu_2ZnSnS_4 solar cells", Advanced Energy Materials, DOI: 10.1002/aenm.201600706.

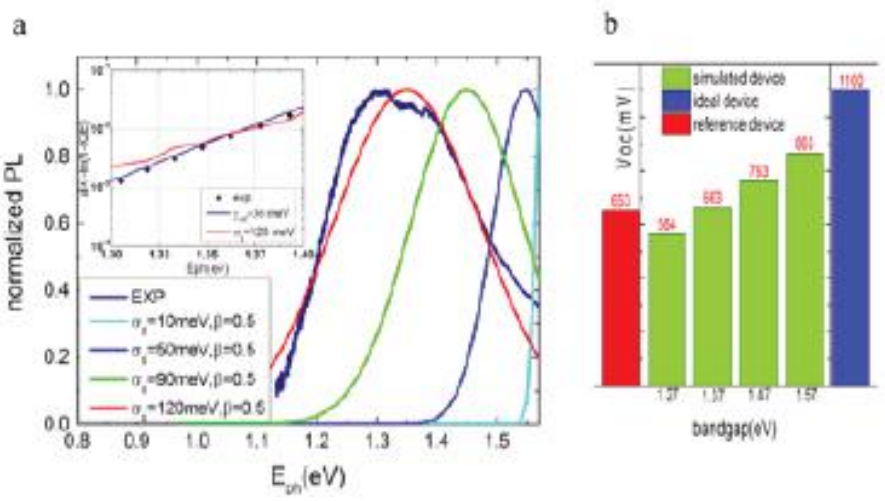

Figure PP2.2b.2: (a) Simulated room temperature PL spectra (coloured lines) for different standard deviation of bandgap fluctuation from 10 meV to 120 meV are displayed as well as measured data (navy dot) on the device. The inset graph shows absorption coefficient vs. Eph below bandgap energy for the device and fitted based on bandgap model; (b) The simulated V_{OC} (green) at various electronic bandgaps. All simulated V_{OC} here are extracted from a model with 1E5 cm/s interface velocity. The measured V_{OC} from the device (red) and ideal V_{OC} (blue) without interface recombination and bandgap reduction are also shown as a comparison reference.

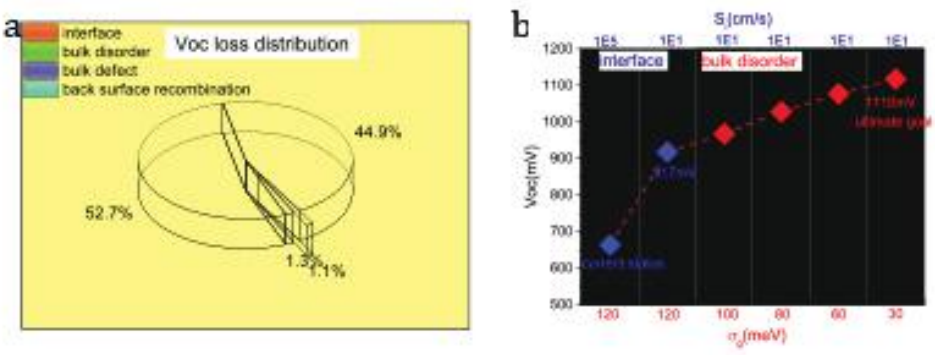

Figure PP2.2b.3: (a) Fraction of V_{OC} loss pertains to mechanisms including heterojunction interface, bulk disorder, bulk deep level defects and back contact recombination parametrised into device model. The V_{OC} loss is calculated comparing it to that of an ideal device without any loss mechanisms; (b) Device V_{OC} evolution map predicted by improving hetero-interface and bulk disorder properties (Si and σg).

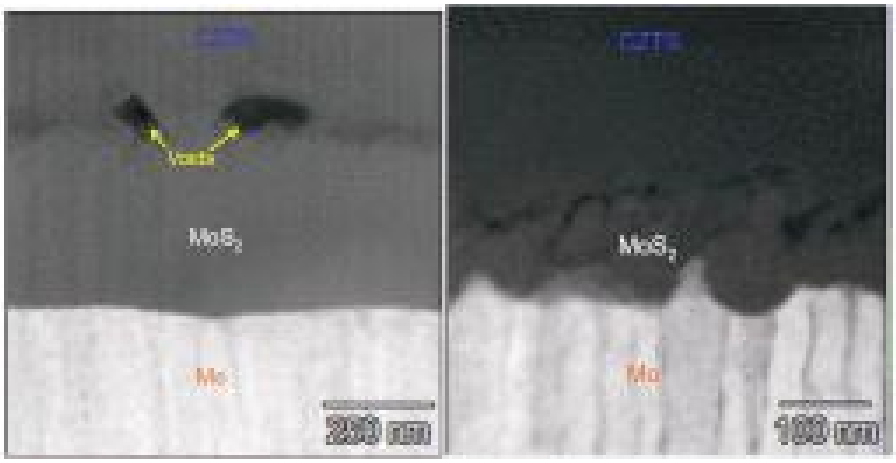

Figure PP2.2b.4: Cross-sectional TEM images for back contact regions of CZTS devices with (left) and without (right) back contact modification.

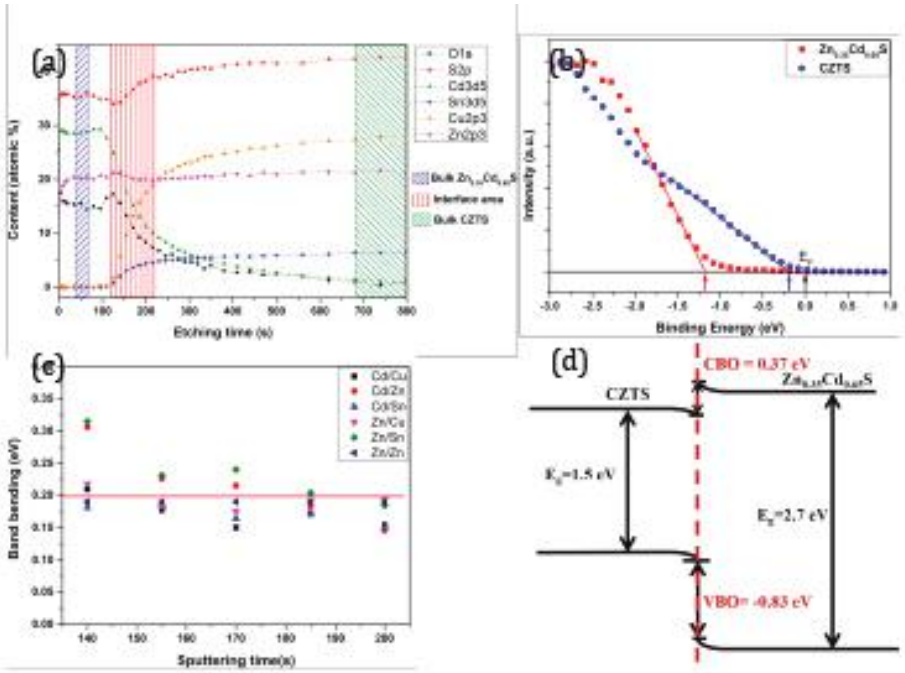

Figure PP2.2b.5: (a) The XPS composition profile from CZTS/$Zn_{0.35}Cd_{0.65}S$ to CZTS as a function of sputtering time. According to composition profile, the blue, red and green area can be regarded as bulk $Zn_{0.35}Cd_{0.65}S$, interface and bulk CZTS area, respectively; (b) Normalised valence band (VB) data of CZTS/$Zn_{0.35}Cd_{0.65}S$ heterojunctions measured by XPS. Binding energies are measured with respect to the Fermi energy (E_F); (c) Band bending as a function of sputtering time shown for six data sets; (d) Schema of the band alignment at CZTS/$Zn_{0.35}Cd_{0.65}S$ interface. Values of the valence and conduction band offsets (VBO, CBO) and bandgap (Eg) are indicated.

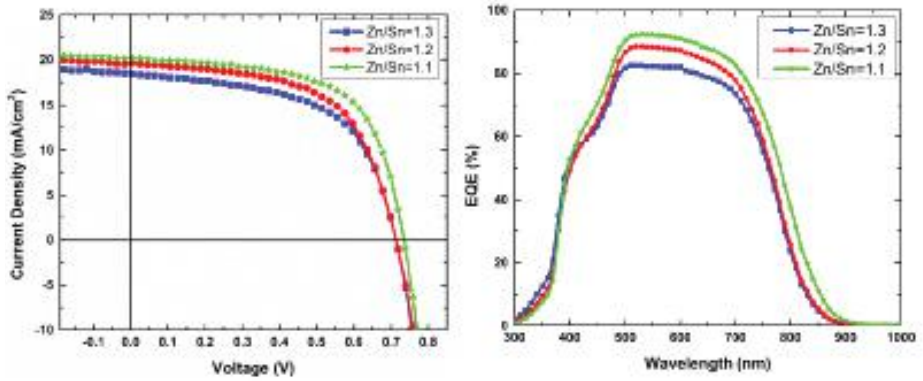

Figure PP2.2b.6: Current density-voltage (J-V) (left), external quantum efficiency (EQE) curves (right) of devices with ZnCdS buffer fabricated from absorbers of different composition.

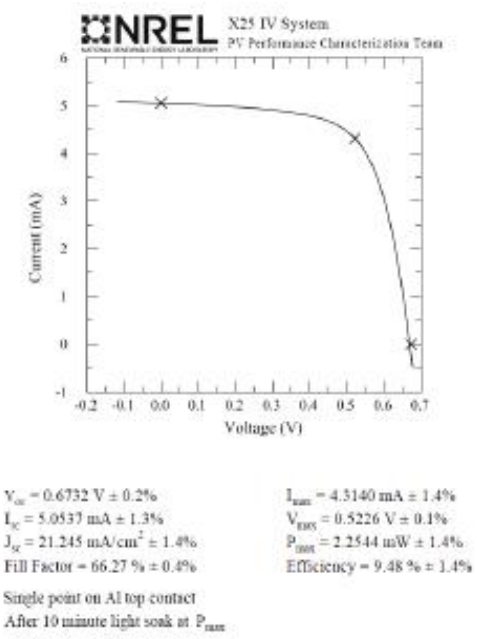

Figure PP2.2b.7: Certified J-V curve of 9.5% CZTS solar cells.

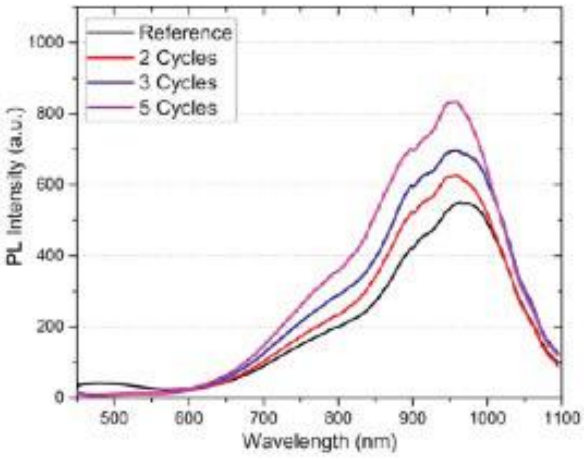

Figure PP2.2b.8: PL spectra of CZTS with various thickness of Al_2O_3 showing effective passivaton effect.

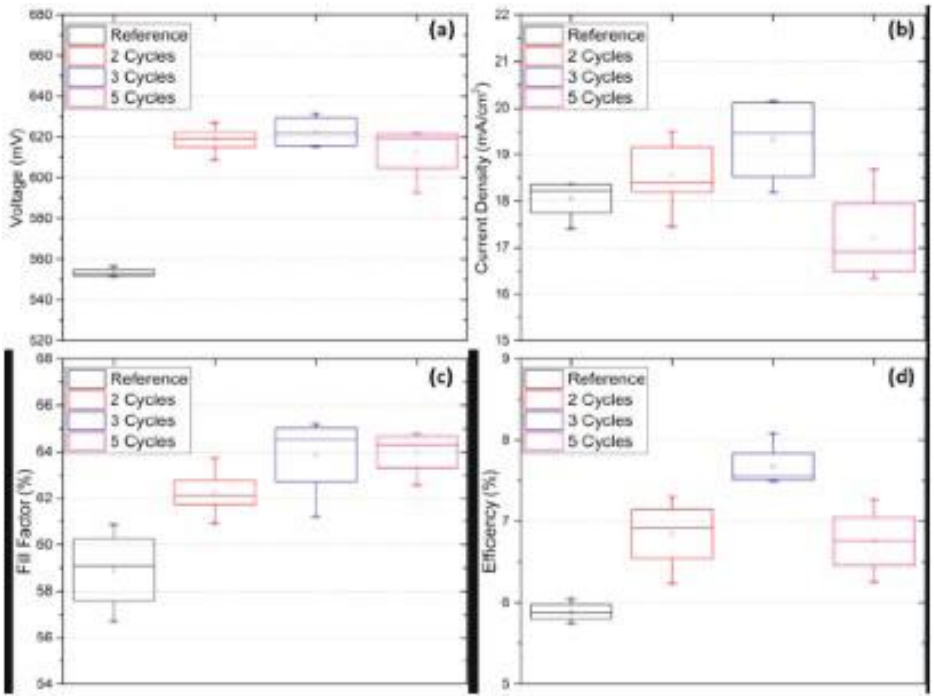

Figure PP2.2b.9: J-V characteristics of the CZTS/CdS devices with different cycles of ALD-Al_2O_3 on absorber layer. (The numbers of samples plotted in the figure were 8–10 for each device.)

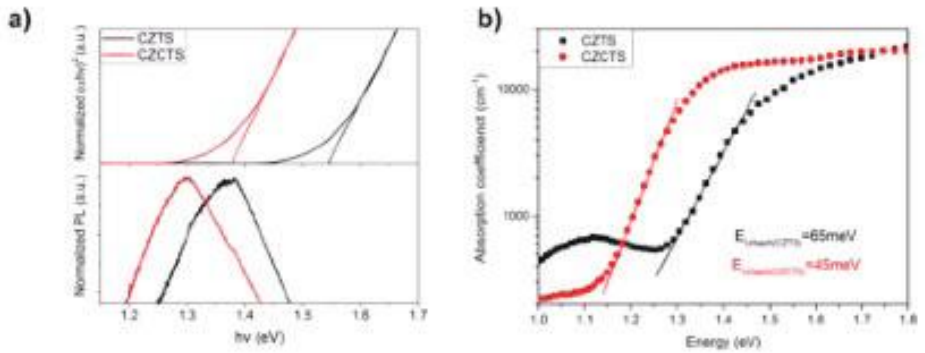

Figure PP2.2b.10: (a) Normalised Tauc plots created from UV-VIS transmission and reflectance measurements (top), and normalised PL spectra (bottom) of CZTS and CZCTS thin films; (b) Absorption coefficienct obtained from PDS measurement. The inverse of the slope from the linear part below the bandgap energy provides the Urbach energy (EU) of the devices.

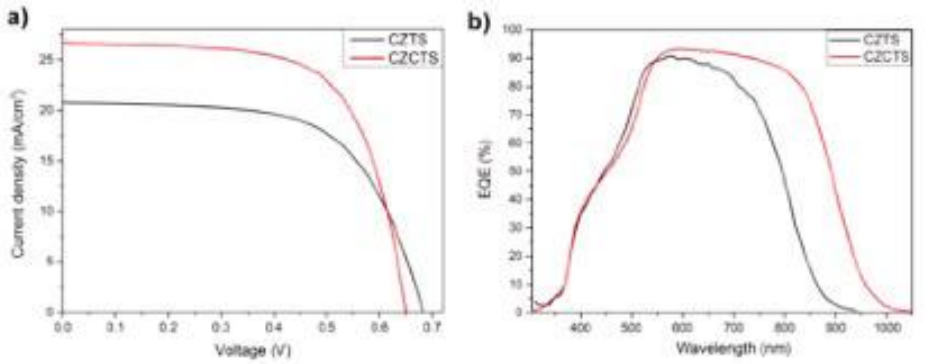

Figure PP2.2b.11: (a) J-V curves, and (b) EQE curves of CZTS and champion CZCTS devices.

CZTS layer parameters	Symbol	Value/Unit	Remark
Temperature	K	300	
Electron affinity	χ	3.9eV	Calc from CBO of [16]
Optical bandgap	$E_{g,opt}$	1.57eV	From QE
Relative dielectric constant	$\varepsilon_r/\varepsilon_0$	7	Reported from [19]
Conduction band density of states	N_C	$2.2\times10^{18}cm^{-3}$	[5]
Valence band density of states	N_V	$1.8\times10^{19}cm^{-3}$	[5]
Electron mobility	μ_e	1.02-1.25$cm^2/V/s$	Calc from TRPL&EBIC
Hole mobility	μ_h	0.5-1$cm^2/V/s$	Measured from hall-effect
Free Carrier concentration	N_A	$1.42\times10^{16}cm^{-3}$	Measured from C-V

Table PP2.2b.1: Key electrical parameters used in CZTS layer of Sentaurus model.

Liu, X., Feng, Y., Cui, H., Liu, F., Hao, X.J., Coniber, G., Mitzi, D.B., Green, M., 2016, "The current status and future prospects of kesterite solar cells: a brief review", Progress in Photovoltaics: Research and Applications, DOI: 10.1002/pip.2741.

Liu, X., Zhou, F., Song, N., Huang, J., Yan, C., Liu, F., Sun, K., Stride J.A., Hao, X.J. and Green M.A., 2015, "Exploring the application of quaternary metastable wurtzite nanocrystal in pure-sulfide Cu_2ZnSnS_4 solar cells by forming nearly micron-sized large grains", Journal of Materials Chemistry A, vol. 3, 23185–23193, DOI:10.1039/C5TA05813A.

Pu, A., Ma, F., Yan, C., Huang, J., Sun, K., Green, M. and Hao, X.J., 2017, "Sentaurus modelling of 6.9% Cu_2ZnSnS_4 device based on comprehensive electrical & optical characterisation", Solar Energy Materials and Solar Cells, 160 (2017), 372–381.

Sun, K., Yan, C., Liu, F., Huang, J., Zhou, F., Stride, J., Green, M. and Hao, X.J., 2016, "Over 9% efficient kesterite Cu_2ZnSnS_4 solar cell fabricated by using $Zn_{1-x}Cd_xS$ buffer layer", Advanced Energy Materials, DOI: 10.1002/aenm.201600046.

Yan, C., Liu, F., Sun, K., Song, N., Stride, J.A., Zhou, F., Hao, X.J. and Green M.A., 2016, "Boost efficiency of pure sulphide CZTS solar cell via In/Cd-based hybrid buffer", Solar Energy Materials and Solar Cells, 144, 700–706.

Yan, C., Sun, K., Liu, F., Huang, J., Zhou, F. and Hao X.J., 2017, "Boost Voc of pure sulphide kesterite solar cells via a double CZTS layer stacks", Solar Energy Materials and Solar Cells, 160, 7–11.

Zhao, L., Di, Y., Yan, C., Liu, F., Cheng, Z., Jiang, L., Hao, X.J., Lai, Y. and Li J., 2016, "In-situ growth of SnS absorbing layer by reactive sputtering for thin film solar cells", RSC Advances, 6(5): 4108–4115.

Zhou, F., Zeng, F., Liu, X., Liu, F., Song, N., Yan, C., Pu, A., Park, J., Sun, K. and Hao, X.J., 2015, "Improvement of J_{SC} in Cu_2ZnSnS_4 solar cell by using a thin carbon intermediate layer at Cu_2ZnSnS_4/Mo interface", ACS Applied Materials & Interfaces, 7(41): 22868–22873, DOI: 10.1021/acsami.5b05652.

PP2.2c CZTS Solar Cells on Stainless Steel

Lead Partner
UNSW

UNSW Team
Dr Xiaojing Hao, Prof Martin Green, Prof Gavin Conibeer, Dr Yansong Shen, Dr Fangyang Liu, Dr Jialiang Huang, Heng Sun

UNSW Students
Chang Yan, Kaiwen Sun

Industry Partner
Baosteel

Funding Support
ACAP, ARC, Baosteel

Aim

Cu_2ZnSnS_4 (CZTS), which consists of Earth-abundant and non-toxic constituents, is an ideal material for low-cost thin-film solar cells. To date, most of the CZTS solar cells are fabricated on rigid soda lime glass (SLG) with a typical thickness of 2~3 mm. Actually, the utilisation of flexible and lightweight substrates such as stainless steel can reduce cost by roll-to-roll manufacturing, opening new application fields. The aim of this project is to work with Baosteel to exploit technologies of kesterite (CZTS) coated architectural stainless steel for BIPV. The developed technology would be compatible with existing commercial equipment options for high-volume production. The measurable target of this project would be to increase the CZTS cell efficiency on stainless steel surfaces to around 10% but at a lower cost. This will be achieved by an integrated and synergistic effort combining materials growth and advanced characterisation, growth kinetics modelling, device fabrication and characterisation, and simulation.

Progress

The major differences between CZTS on SLG and CZTS on stainless steel are: (1) no sodium supply in the case of stainless steel which is a must-have for high performance CZTS solar cells; (2) Fe diffusion into CZTS in the case of stainless steel which is known as a killer for CZTS solar cells; and (3) surface property such as roughness might be different. While transferring the CZTS technology from SLG to stainless steel, the above three key issues will have to be addressed. In 2016, the progress associated with the above three key issues are summarised as follows.

Evaluation of the use of low-cost enamelled steel for CZTS solar cell: It was confirmed it is the high roughness of enamelled steel that limits CZTS absorber quality and device performance (see Figures PP2.2c.1, PP2.2c.2 and PP2.2c.3). Though surface polish processes such as mechanical and chemical polish can reduce the roughness, the additional cost might be a concern for future application. With optimised CZTS preparation process on Baosteel enamelled steel with a focus on morphology, composition, phase and crystallinity, we demonstrated a 3% efficient CZTS solar cell device on enamelled steel (see Figure PP2.2c.4).

Development of knowledge – effect of alkali elements on properties of CZTS absorber and associated device performance: Two ways of Na supply were developed, i.e. Na via additional NaF layer (see Figure PP2.2c.5) or via Na containing Mo back contact. Introducing NaF significantly affects the microstructure of CZTS film and associated device performance (see Figures PP2.2c.6 and PP2.2c.7). In order to create a similar growth mechanism of CZTS on stainless steel to that on SLG, the Na containing Mo back contact was considered. Five different structures combining a Ti barrier layer, Mo:Na layer and Mo stacking layers are studied (see Figure PP2.2c.8). The best back contact configuration was identified to be the Mo capping layer / Mo-Na layer/Mo combination. Though Na can be effectively introduced into CZTS by both ways, the preferred U-shape usually

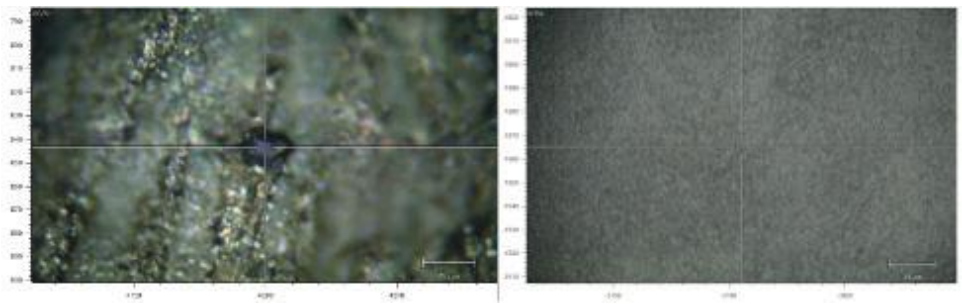

Figure PP2.2c.1: Optical images of CZTS on enamelled steel (left) and glass (right) showing much rougher and inhomogeneous morphology of CZTS on enamelled steel.

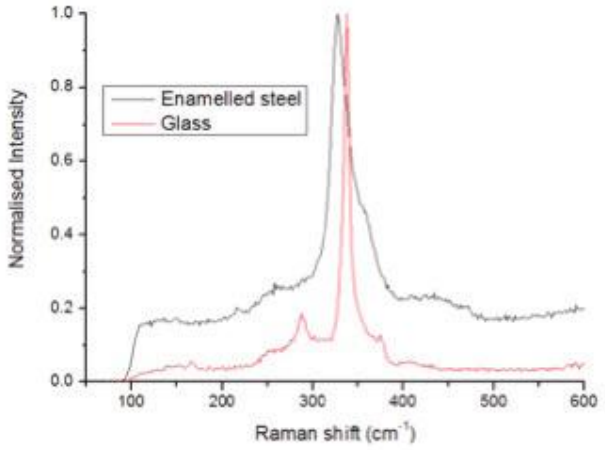

Figure PP2.2c.2: Raman spectra of CZTS films on enamelled steel and on glass showing CZTS on enamelled steel has worse crystallinity.

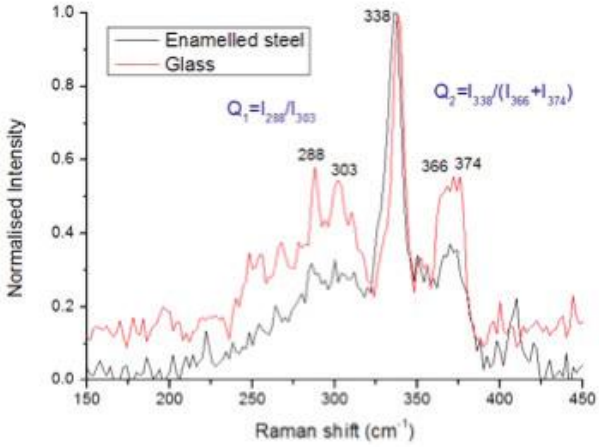

Figure PP2.2c.3: Raman spectra of CZTS films on enamelled steel and on glass showing CZTS on enamelled steel yields higher Cu/Zn disorder from low wave number of the main peak and Q1< 1.

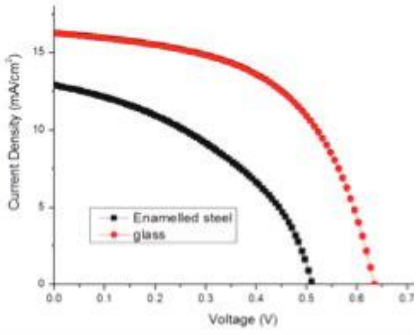

Figure PP2.2c.4: J-V curves of CZTS solar cells on enamelled steel and on glass demonstrating 3% efficiency CZTS solar cells on enamelled steel.

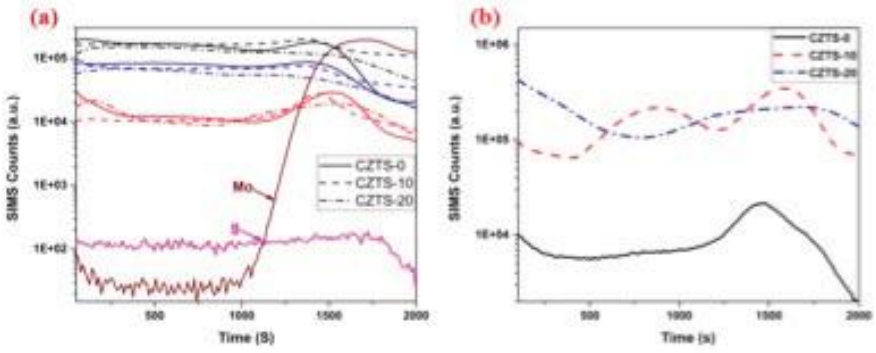

Figure PP2.2c.5: SIMS depth profile of CZTS films with different thickness of NaF layer on stainless steel: 0 nm NaF (CZTS-0), 10 nm NaF (CZTS-10) and 20 nm NaF (CZTS-20). (a) Cu, Zn, Sn and S of all samples overlaid with Mo and S signals shown for depth reference; (b) Na signals of the three samples.

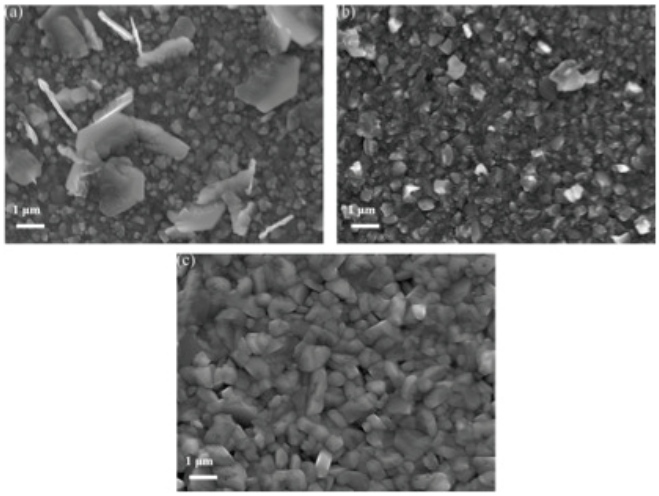

Figure PP2.2c.6: Plane-view SEM images of CZTS films with 0 nm NaF (a), 10 nm NaF (b) and 20 nm NaF (c) on stainless steel substrates.

shown in the CZTS on SLG is not formed here with much less Na at surface region (see Figure PP2.2c.9). Further optimisation for U-shape Na distribution is required.

Ion soaking with different ions is developed and employed for defect passivation: Soaking CZTS into various ions before buffer deposition was explored with various ions such as Cd_2^+, Zn_2^+ etc. Cd_2^+ ion soaking is found to be the best one for efficiency enhancement. Detailed characterisation is underway.

Developed strategies of know-how to achieve CZTS solar cells on steel with efficiency beyond 6%: With the identified back contact configuration of Mo capping layer / Mo-Na layer/Mo combination and ion soaking, we demonstrated 6% efficiency CZTS solar cells on stainless steel (see Figure PP2.2c.10).

Highlights

- Demonstrated 3% efficiency CZTS solar cells on enamelled steel.
- Demonstrated 6.2% efficiency CZTS solar cells on flexible stainless steel.
- Developed CZTS surface treatment strategies.
- Developed two ways of introducing Na in the CZTS film.

Future Work

Future work in 2017 will be focused on improving the efficiency of CZTS solar cells to beyond 8%. Strategies will be developed to further improve the CZTS absorber quality, to obtain the ideal U-shape sodium distribution typically present in high efficiency CZTS/CIGS solar cells, and to improve the voltage of CZTS solar cells.

References

Sun, K., Liu, F., Yan, C., Zhou, F., Huang, J., Stride, J.A. and Hao, X., 2016, "Influence of sodium incorporation on kesterite Cu_2ZnSnS_4 solar cells fabricated on stainless steel substrates", Solar Energy Materials and Solar cells, 157:565–571, DOI: 10.1016/j.solmat.2016.07.036.

Liu, F., Sun, H., Yan, C., Sun, K., Zhang, Y.F., Shen, Y., Green, M. and Xiaojing Hao, X., "Sodium-doped molybdenum back contacts for flexible kesterite Cu_2ZnSnS_4 solar cells on stainless steel", Solar Energy Materials and Solar cells (submitted).

Liu, F., Sun, H., Yan, C., Sun, K., Zhang, Y.F., Shen, Y., Green, M. and Xiaojing Hao, X., "Ion-soaking: an effective way of improving the efficiency of Cu_2ZnSnS_4 solar cells on stainless steel", ACS Applied Materials & Interfaces (in preparation).

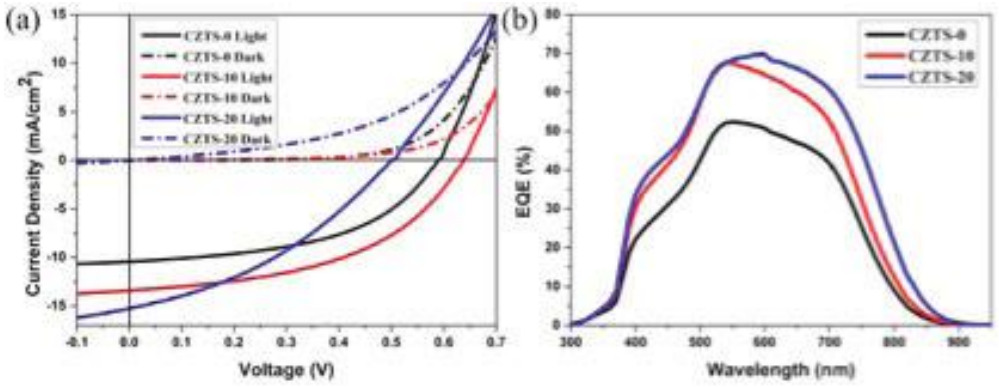

Figure PP2.2c.7: (a) J-V characteristics, and (b) EQE of CZTS devices on stainless steel using absorbers with different NaF thickness.

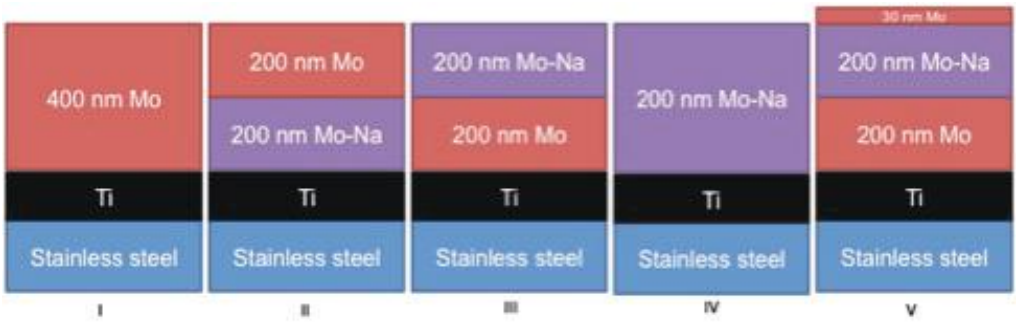

Figure PP2.2c.8: Five different back contact configurations. (The layers are not drawn to scale.)

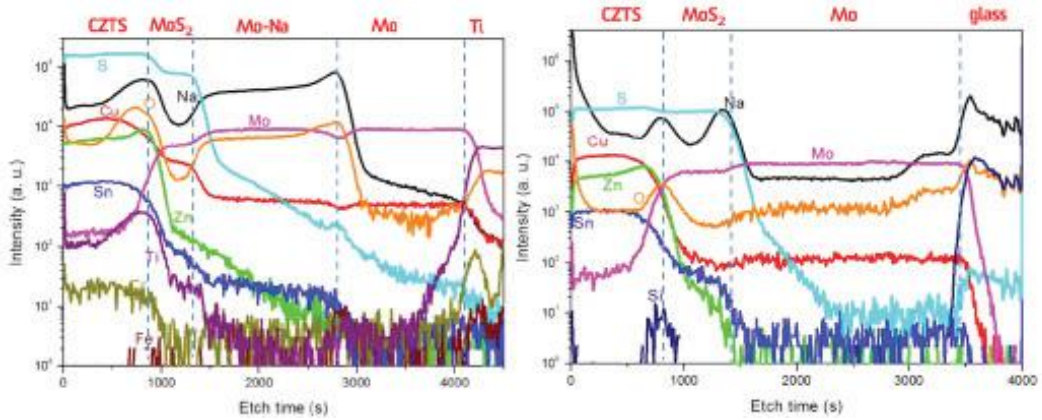

Figure PP2.2c.9: TOF-SIMS depth compositional profiles of relevant elements for CZTS absorbers on type V configuration on stainless steel (left) and on glass (right).

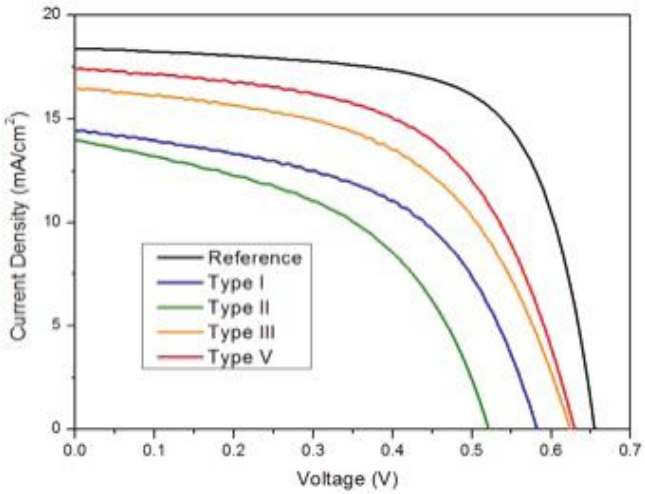

Figure PP2.2c.10: J-V and EQE curves of devices based on four configurations and reference on SLG.

Liu, F., Sun, K., Yan, C., Zhou, F., Huang, J., Shen, Y., Hao,X. and Green, M., 2016, "Kesterite Cu_2ZnSnS_4 thin film solar cells on enamelled steel substrates", The 4th BAJC Conference, Hobart.

Sun, K., Liu, F., Yan, C., Zhou, F., Huang, J., Shen, Y., Hao, X. and Green, M., "Sodium doping kesterite Cu_2ZnSnS_4 solar cells fabricated on stainless steel substrates", The 4th BAJC Conference 2016, Hobart.

PP2.4a Hot Carrier Cells

PP2.4a(i) Model Phonon Dispersion in Bulk Materials and Nanostructures

Lead Partner
UNSW

UNSW Team
Dr Shujuan Huang, Dr Santosh Shrestha, Prof Gavin Conibeer, Dr Robert Patterson

UNSW Students
Hongze Xia, Jianfeng Yang, Bo Wang

Funding Support
ARENA

Aim

Develop models of phonon dynamics, electron-phonon interaction and efficiency models to be fully consistent and predictive of real material systems.

Progress

Modelling of hot carrier absorber

Multiple quantum wells (MQWs) have shown significantly longer hot carrier (HC) lifetimes compared to their counterparts and therefore are promising candidates for HC absorber. Moreover, high quality and controlled growth of III-V MQWs can be achieved with molecular beam epitaxy (MBE). Therefore, InN/$In_xGa_{1-x}N$ and GaAs/AlAs MQWs and superlattices (SL) have been studied as the absorber of the HC solar cell. Such structures will exploit the significant hot-phonon-bottleneck effects observed in MQWs. Nitride-based structures have large phonon bandgaps which can effectively stop Klemens decay. Lattice mismatch between the well and barrier materials is very small which facilitates high quality growth of these structures. The one-dimensional (1-D) superlattice structure ensures a continuous electronic energy spectrum and hence a broad-band absorption. The absorption is further enhanced by the small electronic bandgap of InN.

The dispersion relations of phonon modes in superlattices have been computed with a 1-D atomic-plane model. Since the epitaxial growth is intended to be along the high-symmetrical $\Gamma-A$ direction for both InN and $In_xGa_{1-x}N$ layers, the periodicity of MQW-SL and hence the Brillouin zone-folding is along this direction. For simplicity we assumed that the mode frequency of each zone-folded mini-band only depends on the vertical component of the wave-vector (i.e. along $\Gamma-A$). The reason for this assumption partly comes from the high concentration of electron-emitted polar phonons around the zone-centre, where the dispersions are relatively flat compared to the mini-gaps. In wurtzite structure periodic atomic planes with alternating elements align perpendicular to the $\Gamma-A$ direction. If only considering the vertical component of wave-vectors, all atoms in one atomic plane vibrate in phase and can be treated as one uniform displacement. The phononic model adopted here treats a 1-D chain with an equal length of the superlattice periodicity, taking into account the plane-to-plane force constants. The plane-to-plane force constants are calculated by adopting the conventional Keating potentials for all bonds. A sample phononic dispersion relation is shown in Figure PP2.4a.1. The electronic structures, involving the wave funtions and energies of all the states, can be calculated by using the Kronig-Penney model for superlattices. In equilibrium conditions space charges occur in the well layers (negative) and in the barrier layers (positive) due to the difference of their electron affinities. The electron affinity of InGaN is significantly lower than that of InN, giving a larger offset of the conduction band edge rather than that of the valence band edge. A sample electronic dispersion relation is shown in Figure PP2.4a.2.

The calculation of the rate of polar interaction between hot electrons (here emission by holes is not of concern) and polar phonons is based on the Frohlich-type Hamiltonian and the first order perturbation theory. A hot reservoir of electrons at 1000K is assumed, with heat transferred to the cold reservoir of lattice modes at 300K. The energy relaxation times referring to the polar phonon emission are illustrated in Figure PP2.4a.3, for all the MQW-SL configurations, i.e. for different well and barrier thicknesses and different barrier materials. 18×18 combinations of the thicknesses are sampled for representing all the possible structures from 2 nm to 9 nm. The number of combinations comes from the fact that a complete well/barrier layer should include an integer number of unit cells. Figure PP2.4a.3 is generated by interpolating the relaxation time data of the sampling combinations.

The energy relaxation times of high-lying longitude optical phonons are demonstrated in Figure PP2.4a.4, for different combinations of well and barrier thicknesses. For Indium mole fraction x=0 (left figure), the contrast of relaxation times is larger than that for the case for x=0.2 (right figure); this is reasonable as the higher Indium content in the barrier layer would make the structure closer to bulk InN. Both figures show the same trend with different barrier/well thicknesses: the relaxation time increases with thicker well layers and thinner barrier layers, in spite of some irregular local variations. The regular variation mainly results from the change of numbers of InN-like modes and InGaN-like modes.

To explain the variation, we need to first examine the phonon dispersions of the MQW-SL. Taking x=0 as an example, the left figure in Figure PP2.4a.1 shows the dispersions of an InN/GaN SL structure, with six layers of nitrogen atoms inside each layer (the same for both the InN layer and the GaN layer). From the number of atomic layers involved we could expect the same number of high-lying optical modes which are InN-like and GaN-like respectively. The GaN-like optical phonon modes (blue colour: solid line for longitudinal optical (LO), dashed line for transverse optical (TO)) have much higher frequencies than the InN-like optical modes (green colour), for the bond force constants of GaN are larger than for InN and the atomic mass of Ga is smaller than In. There are also four branches (orange colour: two of LO and two of TO) corresponding to the interfacial modes (IF), with frequencies between GaN-like modes and InN-like modes. From the right figure of Figure PP2.4a.1, the vibrations can be seen to be almost completely confined in the respective layers, for InN-like and GaN-like optical modes. For IF, most of the vibrational energy is within the first and second nitrogen atoms from the interface, and hence has little overlap with InN-like or GaN-like modes.

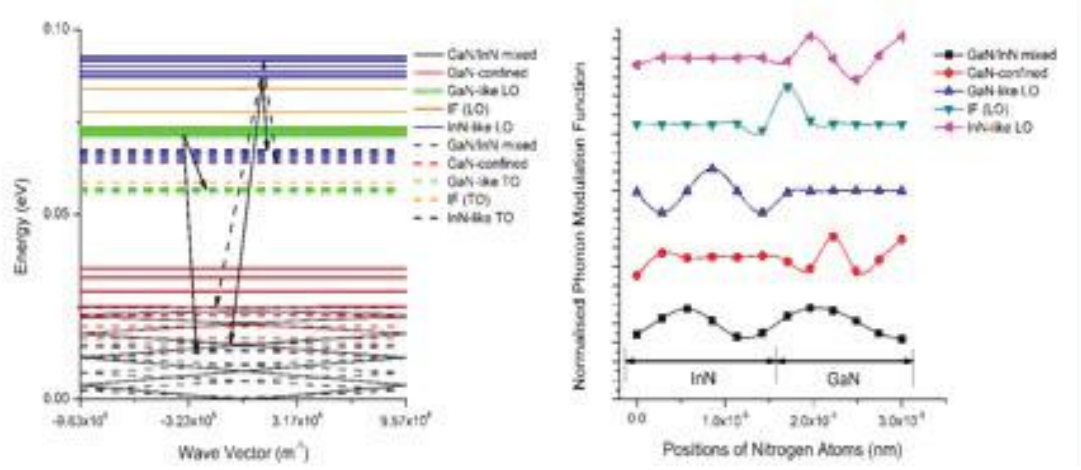

Figure PP2.4a.1: The left figure indicates the phonon decay paths and the sample dispersion for an SL structure with three layers of unit cells inside each layer (barrier or well). The right figure shows the phonon modulation function of a representative mode from each category of modes, computed from the eigenfunctions of the lattice dynamic equation. The transverse modes have similar modulation functions and hence only that part of the longitude modes is shown.

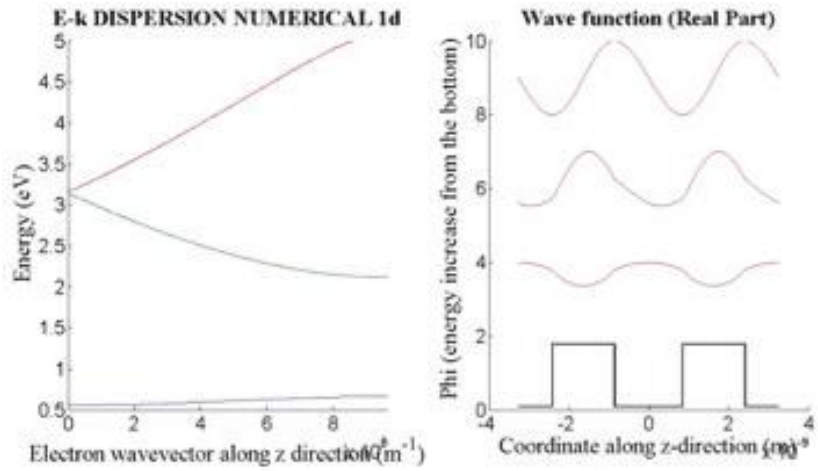

Figure. PP2.4a.2: The electronic dispersion relation and the zone-centre wave functions for an SL structure with three layers of unit cells inside each layer (barrier or well). The wave-vector is along the Gamma-A crystal direction.

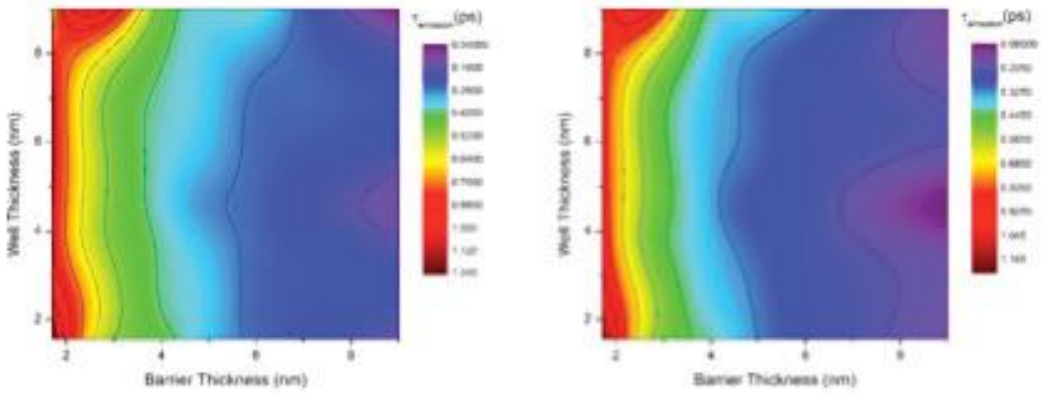

Figure. PP2.4a.3: Energy relaxation times of the hot electron system (1000K), in the reservoir of phonons (300K), with superlattice structures of different well/barrier thicknesses and $In_xGa_{1-x}N$ compositions (Left: x=0, Right: x=0.2).

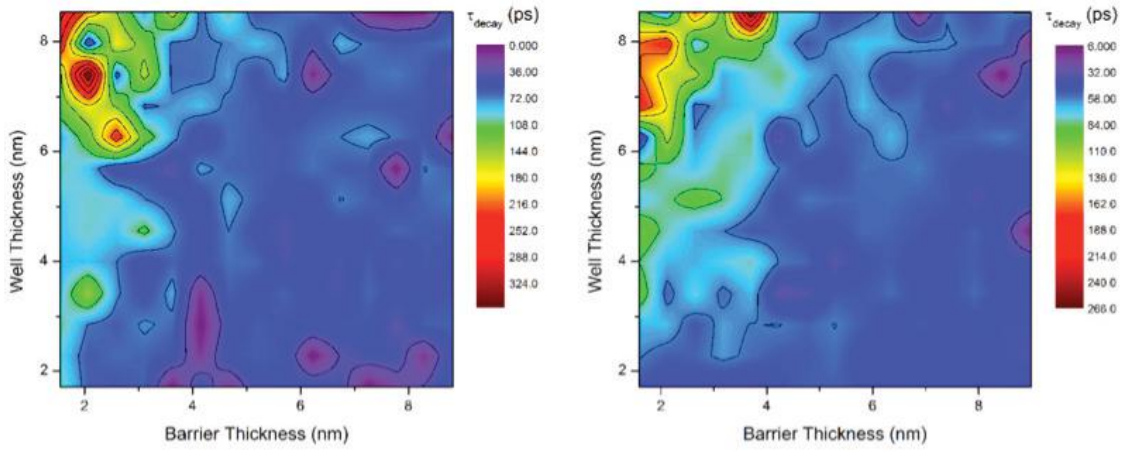

Figure. PP2.4a.4: Energy relaxation times of the high-lying LO phonon system (1000K), in the reservoir of 1000K high-lying phonons and 300K low-lying phonons, with superlattice structures of different well/barrier thicknesses and $In_xGa_{1-x}N$ compositions (Left: x=0, Right: x=0.2).

Considering all three-phonon processes, only the Ridley channel and the Shrivistava-Barman channel (decaying into a high-lying optical phonon and a low-lying optical phonon) are allowed due to the energy conservation law. As in wurtzite-structured SL, the difference between the acoustic branches and the low-lying optical branches becomes almost indistinguishable with both having partial optical-like characters. These low-lying branches can be separated into two categories: GaN-confined modes (red lines) and GaN-InN mixed modes (grey lines). In fact the InN-like low-lying modes sit within the allowed frequency band of GaN, hence vibrations in GaN layers are excited too. Therefore no InN-confined modes exist in the low-lying branches. Among all allowed three-phonon processes, GaN-like optical modes can decay into both types of low-lying modes (see the solid arrow and the dashed arrow in Figure PP2.4a.1), while InN-like optical modes can only decay into the mixed modes as they only overlap with the mixed modes. Besides, the energy gap between GaN-like LO modes and GaN-like TO modes is relatively large; hence the resulting low-lying phonons have relatively high energies, compared to the decayed low-lying phonons from the InN-like modes. Since the low-lying branches with high energies are generally flatter, leading to a larger joint density of states of transition, the decay rates of GaN-like LO modes could be enhanced further. Due to the two reasons explained above the GaN-like LO modes decay faster than the InN-like LO modes. Therefore with a thicker well layer (or a thinner barrier layer), the energy relaxation time of the high-lying LO phonon system becomes longer, for it introduces more InN-like modes (or fewer InGaN-like modes).

According to Figure PP2.4a.4 the relaxation time of high-lying phonons could go up to 300 ps, which is significantly longer than the bulk value of around 1 ps.

And according to Figure PP2.4a.3 the relaxation time of hot electrons (if phonons are completely thermalised) can go up to more than 1 ps, this is also much longer than the bulk value. Combining these two, an optimised MQW-SL structure should involve a thin barrier layer and a thick well layer. The contrast in phonon energies between the well and the barrier also needs to be large, indicating a small Indium content in the barrier. In addition, such a structure could potentially prevent hot phonons diffusing out, which makes it even more attractive than bulk materials.

Highlights

- Model of phonon dispersions of phonon dispersions of multiple quantum wells.
- Calculation of hot carrier relaxation times up to 300 ps.

Future Work

Refine models to incorporate a wider range of materials and structures. Incorporate superlattice defects in models. Both of these need increased computation power. Incorporate higher level modelling approaches to interface with ab initio input parameters and thus decrease computational intensity.

References

Feng, Y., et al., 2012, Applied Physics Letters 100, 053502.

Feng, Y., Xia, H., et al., 2015, Physica E: Low-Dimensional Systems and Nanostructures 74, 625–629.

Hirst, L. and Ekins-Daukes, N.J., 2011, Progress in Photovoltaics 19, 286–293.

PP2.4a(ii) Investigate HC Absorber Using Bulk Materials

Lead Partner
UNSW

UNSW Team
Dr Santosh Shrestha, Prof Gavin Conibeer

UNSW Students
Simon Chung, Neeti Gupta

Funding Support
ARENA

Aim

- Investigate HC absorber using bulk materials.
- Determine appropriate bulk materials for slowed carrier cooling through reduced phonon modes.
- Fabricate materials of high quality and characterise for carrier cooling.

Progress

The HC solar cell aims to operate by absorbing a wide range of photon energies in the hot carrier absorber (HCA) and then extracting these carriers while they are still hot through energy selective contacts (ESCs). One of the critical requirements of the absorber is the slow carrier cooling properties (Conibeer et al., 2015). It allows the collection of carriers before they thermalise on the band edges, i.e. while they have high energies ("hot carriers"). Hence higher voltages can be extracted from the cell. In most semiconductors hot carrier cooling time is of the order of a few picoseconds. However, the carrier cooling rate needs to be significantly slower to achieve high efficiencies.

The photo-generated hot carriers primarily lose their energies by scattering hot electrons with zone centre optical phonons (Othonos, 1998) and optical phonons lose their energies, predominantly, by decaying into two acoustic phonons of half the energy and opposite momenta of the original phonon, i.e. via Klemens decay mechanism (Klemens, 1966). Another decay route, which is much less efficient than Klemens mechanism, is via Ridley mechanism where an optical phonon decays into optical phonon with a lower energy and an acoustic phonon (Pomeroy et al., 2005). If the lifetime of optical phonons is long enough, they can transfer their energies to the carriers and return them to 'hot' state.

Klemens mechanism is restricted in materials where the minimum energy gap between the optical and acoustic phonons (phononic bandgap) is higher than the maximum acoustic phonon energy (Conibeer et al., 2010). Ridley mechanism is also suppressed in such materials with

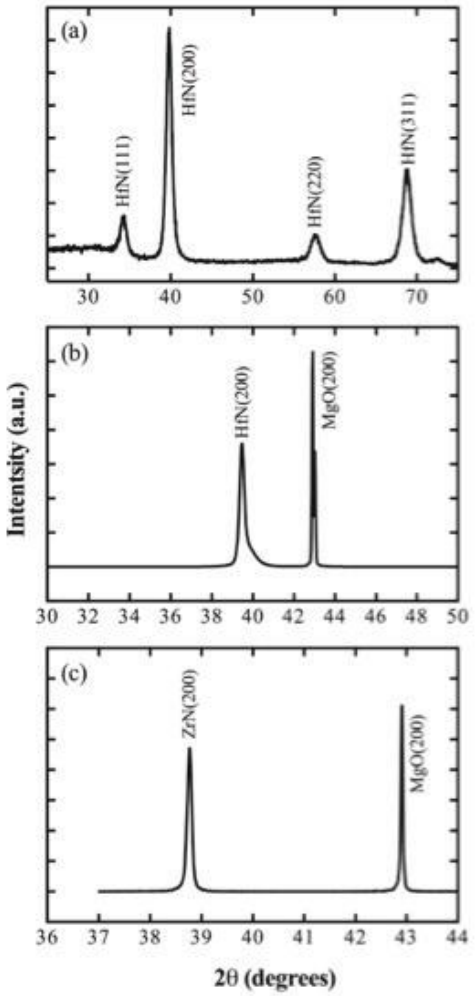

Figure PP2.4a.5: XRD spectra of (a) HfN film deposited on Si (100) substrate; (b) HfN film deposited on MgO (100) substrate; and (c) ZrN film deposited on MgO (100) substrate.

large phonon bandgap and/or narrow dispersion of optical modes. For binary compounds phonon energies can be approximated from a 1-D force constant model treating the atoms as simple harmonic oscillators (Misra, 2010). Using this model, it can be calculated that the minimum of $M/m > 4$ is necessary to produce such a large phononic bandgap to prevent Klemens decay, where is M and m are the mass of the heavier and lighter atom, respectively. Potential absorber materials should also have a small dispersion of optical modes to suppress Ridley decay and small electronic bandgap so that a large fraction of incident solar radiation can be absorbed. For large-scale production, abundance also needs to be relatively large.

Using the above model a range of materials have been investigated for their suitability as slow carrier cooling materials. HfN and ZrN show very large phononic bandgaps. A large phononic bandgap and small dispersion of optical modes have also been reported

(Saha et al., 2010; Shanavas et al., 2016). The abundance of these materials is also relatively large. While HfN and ZrN are metallic, Hf_3N_4 and Zr_3N_4 have relatively small bandgaps, ~0.9 eV and 1 eV, respectively (Bazhanov et al., 2005).

Hafnium nitride and zirconium nitride films were deposited by sputtering. Process parameters such as radio frequency power, substrate temperature and Ar/N_2 were varied to optimise quality of the films. Results of X-ray diffraction (XRD) on selected HfN films grown on silicon and MgO substrates are shown in Figure PP2.4a.5(a) and (b), respectively. The films were deposited at 450°C. Peaks corresponding to the HfN and substrates are labelled. It can be deduced that the HfN film preferentially grows in [100] direction on Si (100) and epitaxially on MgO (100) substrate. Growth of better crystal quality on MgO substrate can be attributed to smaller lattice mismatch between HfN and MgO. XRD spectra of ZrN film (see Figure PP2.4a.5(c)) also show preferential growth in (100) direction on MgO (100) substrate. Compositional analysis shows that most of the films are metal-rich.

Carrier cooling properties of these materials have been investigated by transient absorption (TA) spectroscopy. For these measurements HfN and ZrN films grown on quartz were used as transmitted signal is detected in this method. The TA measurements were performed using a 400 nm excitation pump source with 100 fs duration and 1 kHz repetition rate. White light continuum was used as the probe beam and detected by a polychromator charge coupled device.

In Figures PP2.4a.6 and PP2.4a.7 TA results of typical HfN film are shown. In Figure PP2.4a.6, TA spectra at various time delays are shown. The changes in optical density, ΔOD, before and after the pump are plotted as a function of probe wavelength. The spectra show an excited state absorption peak around 440 nm and a bleaching peak around 730 nm. In Figure PP2.4a.7, time evolution of ΔOD at a particular wavelength is plotted as a function of time delays. The data has been fitted with single exponential fit which is shown by the red curves. From the fit decay time constant of about 2900±1200 ns can be extracted. For ZrN the extracted decay time constant is a bit lower (470±84 ps). These values are about two orders of magnitude larger than that for typical semiconductors. As mentioned earlier, for TA measurements films grown on quartz substrates were used in which crystal quality was inferior to that grown on silicon and MgO substrates. Carrier decay time can be expected to be longer in better crystal quality.

Highlights

- Good quality hafnium and zirconium nitride films have been deposited with sputtering.
- Very long carrier thermalisation time has been observed in the above materials.

Future Work

The future work would include optimisation of the quality of HfN and ZrN films. Films will be deposited using atomic layer deposition (ALD) which is expected to give better quality materials which can further increase the carrier thermalisation rate. Materials with different compositions will be deposited to study their effects on the thermalisation time.

References

Bazhanov, D.I., Knizhnik, A.A., Safonov, A.A., Bagatur'yants, A.A., Stoker, M.W. and Korkin, A.A., 2005, J. Appl. Phys., 97, 044108.

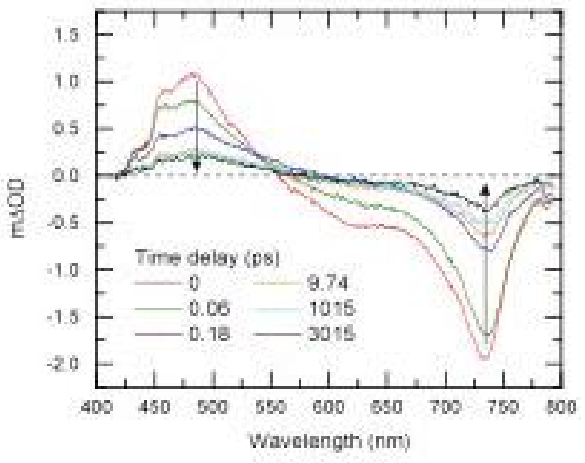

Figure PP2.4a.6: Transient absorption spectra of a typical HfN sample deposited at 450°C in visible range.

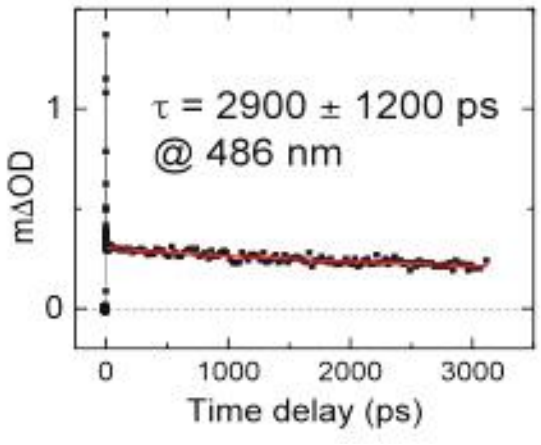

Figure PP2.4a.7: Δ*OD* as a function of delay time measured at 730 nm for samples deposited at 500°C. The red curve are the exponential fits.

Conibeer, G., Patterson, R., Huang, L., Guillemoles, J.F., Kőnig, D., Shrestha, S. and Green, 2010, M.A., 2010, Sol. Energy Mater. Sol. Cells, 94, 1516.

Conibeer, G., Shrestha, S., Huang, S., Patterson, R., Xia, H., Feng, Y., Zhang, P., Gupta, N., Tayebjee, M., Smyth, S., Liao, Y., Lin, S., Wang, P., Dai, X., and Chung, S., 2015, Sol. Energy Mater. Sol. Cells, 135, 124.

Klemens, P.G., 1966, Phys. Rev., 148, 845.

Misra, P., 2010, Physics of Condensed Matter (Academic Press), p. 44.

Othonos, A., 1998, J. Appl. Phys. Reviews, 83, 1789.

Pomeroy, J.W., Kuball, M., Lu, H., Schaff, W.J., Wang, X. and, Yoshikawa, A., 2005, Appl. Phys. Lett. 86, 223501.

Saha, B., Acharya, J., Sands, T. D. and Waghmare, U.V., 2010, J. Appl. Phys., 107, 033715.

Shanavas, K. V., Lindsay, L. and, Parker, D. S., 2016, Scientific Reports 6, doi:10.1038/srep28102.

PP2.4a(iii) Investigate HC Absorber Using Nanostructures

Lead Partner
UNSW

UNSW Team
Dr Shujuan Huang, Dr Santosh Shrestha, Prof Gavin Conibeer

UNSW Students
Zhilong Zhang, Wenkai Cao, Yi Zhang

Funding Support
ARENA

Aim

- Investigate hot carrier (HC) absorber using nanostructures.
- Measure carrier cooling rates in a range of quantum well (QW) nanostructures obtained from collaborators to determine carrier cooling mechanisms.
- Fabricate quantum dot (QD) nanostructure arrays from colloidal nanoparticles to modulate phonon dispersions.

Progress

Slowed carrier cooling in MQWs

An alternative route to achieve a phonon bottleneck and hence reduce carrier cooling rates is to arrange for reflection of phonons from interfaces in double-interface narrow cavities. This can possibly lead to long relaxation times in multiple quantum wells (Rosenwaks, 1993; Hirst, 2011). Such structures could be created as previously with InGaAs wells and GaAsP barriers, or with InN wells and InGaN barriers. The difficult growth of the nitride alloys, however, may lead to dislocations in the material and thence uncontrollable aspects of phonon behaviour. Indium gallium nitride alloys, fairly close in lattice constant to InN, have large phonon bandgaps, and large electronic bandgaps, suggesting their use in barriers for MQW absorber structures.

GaAs/AlAs MQW samples grown by MBE are used to comprehensively investigate these mechanisms behind the reduction of carrier cooling. A series of samples in which the well thickness is varied with constant barrier thickness is compared with a series in which the barrier thickness is varied at constant well thickness. Photoluminescence and XRD data are presented which indicate reasonably uniform material quality across the series. Time resolved photoluminescence, utilising time correlated single photon counting, is used to measure the carrier temperature with time after excitation and hence indicate carrier cooling rates. Comparison of the trends in the various series of samples is used to elucidate some insight into the nature of the reduced carrier cooling mechanisms.

Time resolved photoluminescence (tr-PL) was carried in order to investigate the carrier dynamics on a nanosecond timescale, where the time resolution is 66 ps and excitation wavelength is 640 nm. (This excitation energy is chosen to be between the GaAs and AlAs bandgaps and hence only absorbed in the GaAs wells.) The tr-PL intensity is the spectrally integrated PL for a 20 nm spectral width around the corresponding peak position.

Figure PP2.4a.8 shows the intensity of the integrated tr-PL signal as a function of both emitted photon wavelength and time since excitation in ns, for the series of samples with L_W increasing from 2, 8, 12 to 30 nm and with common L_B of 40 nm.

Figure PP2.4a.9 shows tr-PL for the series of samples with L_B decreasing from 40, 5 to 2 nm and with common L_W of 30 nm.

Vertical slices through the plots in Figures PP2.4a.8 and PP2.4a.9 are used to generate full spectrum tr-PL curves at specific time delays for each sample, with TRPL intensity plotted in logarithmic form to find the linear carrier cooling region within the high energy tail. An exponential fit to this linear portion then gives the time-dependent carrier temperature. In order to improve the reliability of the fitting results, the linear portion used excludes the high signal noise region for the small number of data points at very high energies. The corresponding carrier temperature is therefore mainly extracted from radiative recombination of e1-lh1.

The carrier temperatures from these “high energy tail fittings” are plotted as a function of time delay in Figure

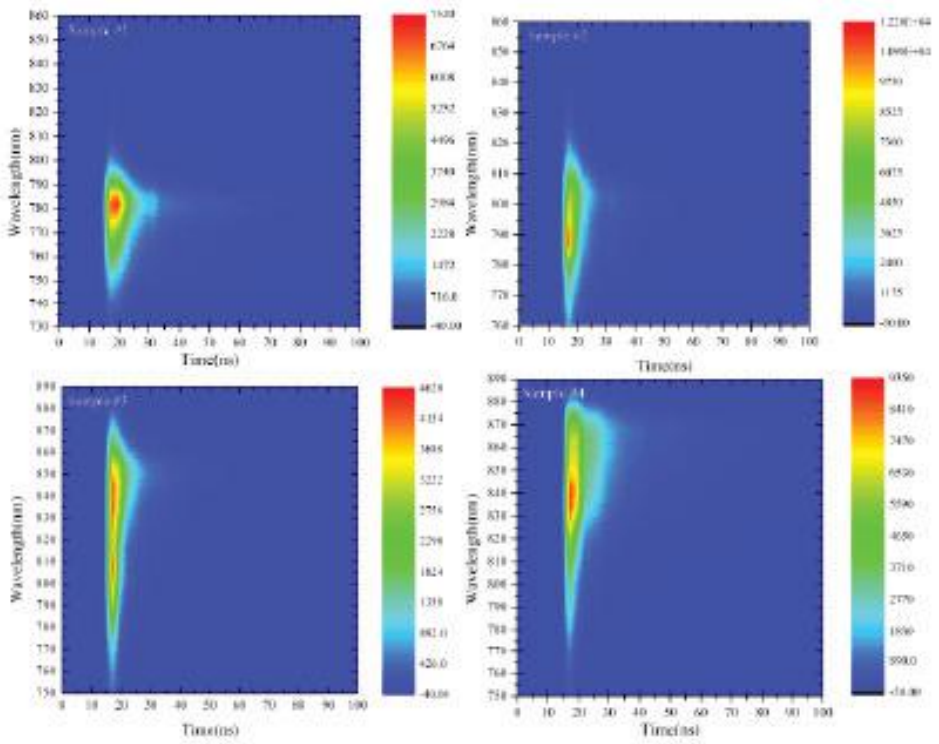

Figure PP2.4a.8: Tr-PL intensity as a function of wavelength and of time for samples 1 to 4 with the same L_B but increasing L_W.

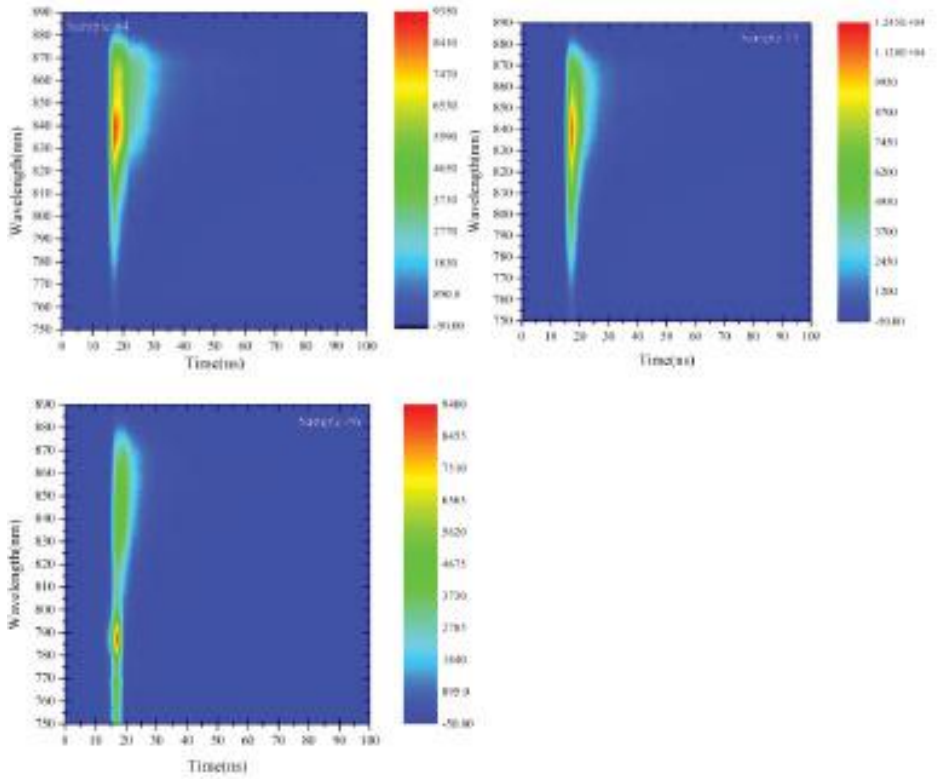

Figure PP2.4a.9: Tr-PL intensity as a function of wavelength and of time for samples 4, 5 and 6 with the same L_W but decreasing L_B.

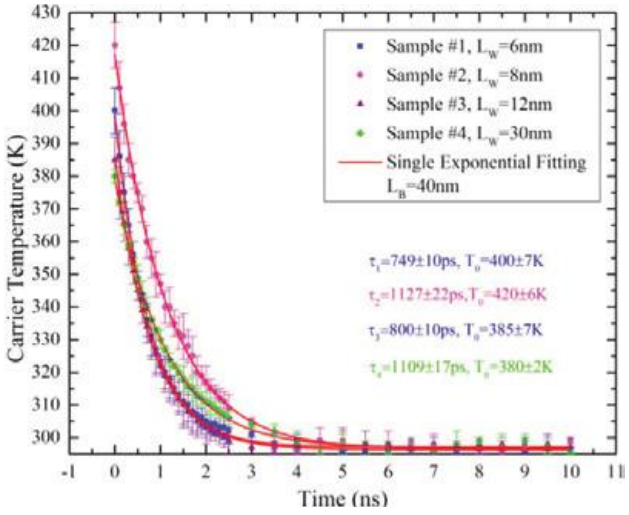

Figure PP2.4a.10: Carrier temperature evolution from "high energy tail fitting" for samples 1 to 4 with increasing QW L_W, but fixed L_B.

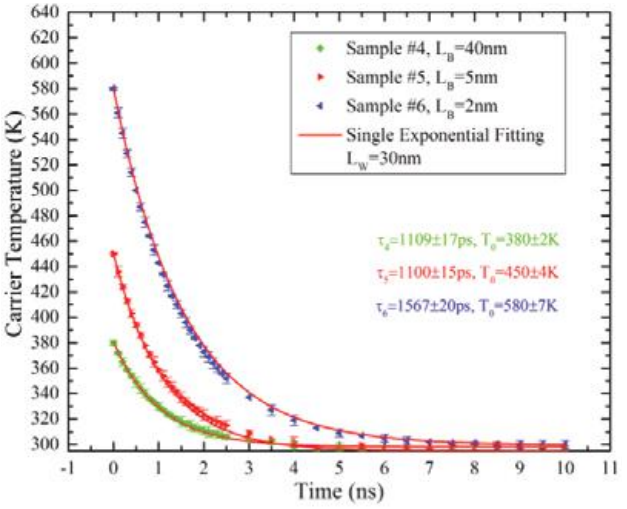

Figure PP2.4a.11: Carrier temperature evolution from "high energy tail fitting" for samples 4, 5 and 6 with decreasing QW L_B, but fixed L_W.

PP2.4a.10 for each of the samples with different QW thickness and in Figure PP2.4a.11 for those with different barrier thickness. A single exponential fit to each of these curves then also gives the carrier temperature decay time constant for each QW thickness.

The results in Figures PP2.4a.10 and PP2.4a.11 all show thermalisation times of hundreds of picoseconds, which is much longer than that of bulk materials. This is consistent with the long times seen in the other work on MQW carrier temperatures in the above references. The much higher temperatures and hot carrier lifetimes observed as the barrier thickness decreases in Figure PP2.4a.11 are highly indicative of strong phonon bottleneck increasing to suppress carrier relaxation and increase temperature and of delocalisation of electrons and holes with thin barriers leading to longer lifetimes.

Highlights

- High carrier temperatures, 300K above ambient, measured in MQWs with tr-PL.
- Temperatures increase with thin barriers between MQWs.
- Hot carrier lifetimes increase with thin barriers.

Future Work

- Fabricate and measure MQWs with varying numbers of wells. This will allow a determination of the effect of interfaces on reflecting and confining phonons.
- Investigate devices based on these MQW systems.

References

Conibeer, G., Zhang, Y., Shrestha, S. and Bremner, S., 2016, Proc of PVSEC Singapore, October.

Guillemoles, J.-F.G., Conibeer, G. and Green, M.A., 2006, Proc. 21st European Photovoltaic Solar Energy Conference, p. 234.

Hirst, L., Führer, M., LeBris, A., Guillemoles, J-F., Tayebjee, M., Clady, R., Schmidt, T., Wang, Y., Sugiyama, M. and Ekins-Daukes, N., 2011, Proc. 37th IEEE PV Specialists Conference, Seattle.

Hirst, L.C., Führer, M., Farrell, D.J., Le Bris, A., Guillemoles, J.-F., Tayebjee, M.J.Y., Clady, R., Schmidt, T.W., Sugiyama, M., Wang, Y., Fujii, H. and Ekins-Daukes, N.J., 2012, Proc. of SPIE 8256, 82560X.

Rosenwaks, Y., Hanna, M.C., Levi, D.H., Szmyd, D.M., Ahrenkiel, R.K. and Nozik, A.J., 1993, Phys. Rev. B 48(19), 14675.

PP2.4a(iv) Investigate Energy Selective Contacts

Lead Partner
UNSW

UNSW Team
Dr Santosh Shrestha, Yuanxun Liao, Dr Shujuan Huang, Prof Gavin Conibeer

UNSW Students
Wenkai Cao, Qiuyang Zhang

Funding Support
ARENA, UNSW

Aim

- Investigate double barrier resonant tunnelling structures as energy selective contacts for hot carrier solar cells
- Fabricate high quality energy selective contacts.

Progress

Energy selective contacts (ESCs) are crucial requirements for the hot carrier (HC) solar cell. They allow carrier extraction with minimum entropy gain and energy loss. Double barrier resonant tunnelling structures (DBRs) consisting of quantum well (QW) and quantum dot (QD) have been investigated for ESCs. Such structures are expected to give conduction of carriers strongly peaked at the discrete energy levels, and lower at other energies. Evidence of resonance tunnelling can be demonstrated by negative differential resistance (NDR) in I-V measurements (Shrestha et al., 2010). The resonant energy can be varied by optimising the barrier and well thicknesses and also using different material combinations. This allows optimisation of ESC to operate at optimal energy extraction point.

ESC structures have been investigated using Ge, Si QWs and PbS QDs and Al_2O_3 barriers. Ge- and Si-based structures were fabricated by sputtering. For the PbS-based structures, Al_2O_3 layers were deposited by atomic layer deposition (ALD). PbS QDs were chemically synthesised and transferred to the first Al_2O_3 layer by Langmuir-Blodgett method.

Figure PP2.4a.12 shows results of I-V measurements on selected ESC structures at different temperatures. I-V measurements on Al_2O_3/ Ge QW/Al_2O_3 at 300K and 90K are shown. For this structure, Al_2O_3 was 0.5 nm and Ge QW was 4 nm thick. In both measurements, NDR features can be observed around 0.85 V. Similar NDR features have also been observed for Si- and PbS-based devices. The voltage and current resolution was 3 mV and 1 pA for these measurements. FWHM, peak to valley current ratio (PVCR) and quality factor (QR = PVCR/FWHM) of the NDR peaks are shown in Figure PP2.4a.12. PVCR and QR increase at low temperature.

The observed NDR peaks are reasonably narrow (FWHM~30 mV), which demonstrates good energy selectivity. Ideally hot carriers need to be extracted at a discrete energy through mono-energetic contacts for optimum efficiency, although in this case the power output from the device would be minimum. In practical HC solar cell devices the width of the ESC, ∂E, has to be finite to extract the carriers and should be kept as small as possible. A rough estimate of $\partial E \sim 25$ mV has been recommended as a reasonable value (Conibeer et al., 2010). The observed FWHM is about 30 mV, which is only slightly larger than the value suggested above. This suggests that these structures can be used as ESCs for HC solar cells.

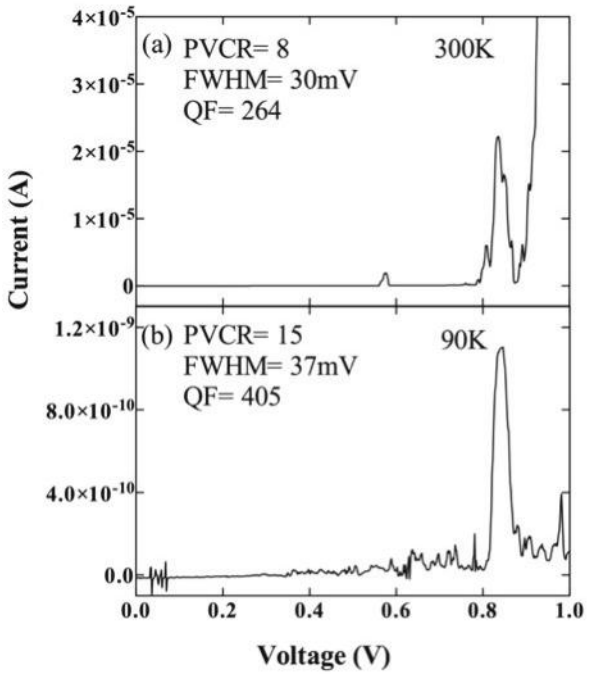

Figure PP2.4a.12: I-V curves measurement on Al_2O_3/ Ge QW/ Al_2O_3 at (a) 300K and (b) 90K.

Highlights

- New material combinations identified for double barrier resonant tunnelling structures.
- Low temperature and room temperature NDR.
- A large peak-to-valley ratio of the NDR.

Future Work

Further work is planned to study the variation of resonance energy with the thickness of QW, diameter of QDs and barrier thickness. It is also planned to investigate triple barrier structures with asymmetric wells for improved selection and carrier rectification.

References

Conibeer, G.J. et al., 2003, "Selective energy contacts for potential application to hot carrier solar PV cells", Proc. 3rd World Conference on Photovoltaic Energy Conversion, Japan, pp. 2730–2733.

Shrestha, S.K., Aliberti, P. and Conibeer, G.J., 2010, Sol. Energy Mater. Sol. Cells. 94, 1546–1550.

PP2.4a(v) Fabricate Complete Hot Carrier Devices

Lead Partner
UNSW

Figure PP2.4a.13: Hot carrier solar cell devices based on different contact structures.

UNSW Team
Dr Santosh Shrestha, Dr Shujuan Huang, Dr Yuanxun Liao, Prof Gavin Conibeer

UNSW Students
Simon Chung, Yi Zhang, Wenkai Cao, Xi Dai

Funding Support
ARENA, UNSW

Aim

Integrate hot carrier (HC) absorber and energy selective contacts to fabricate complete hot carrier devices.

Progress

Fabrication of complete HC solar cell devices have been investigated by integrating the most promising absorber and contacts. Different device structures have been investigated. A few examples of device structures are shown in Figure PP2.4a.13. For the absorber HfN thin film and GaAs/AlAS MQWs have been used. HfN and ZrN thin films were deposited by sputtering and GaAs/AlAs MQWs were deposited by MBE. Carrier selective contacts have been implemented by either band contact, or double barrier structure (DBR) using QW or QDs. DBR structures have been fabricated as discussed in PP2.4a(iv). Photovoltaic characteristics of these devices have been measured with current-voltage (I-V) curve in dark and light. Preliminary results show power generation from these devices under illumination.

Highlights

- Device structures for complete HC solar cells employing absorber and contacts identified.
- Most promising device structures have been fabricated.

PP2.4b Silicon Nanostructure Tandem Cells

PP2.4b(i) Optimisation of Homojunction Si QD Device

Lead Partner
UNSW

UNSW Team
Dr Ivan Perez-Wurfl, Prof Gavin Conibeer

UNSW Students
Terry Yang, Xuguang Jia, Ziyun Lin

Funding Support
ARENA

Aim

The focus of our research activities during this period has been on characterisation and modelling to be applied on Si quantum dot (QD) materials and solar cells.

Progress

The operating principle of a tandem cell is to divide the solar spectrum into sub-spectra and convert the energy contained in each sub-spectrum into electrical energy, using solar cells optimally tuned to operate in those sub-spectra based on their energy bandgap. The so called “bandgap tuning” can be achieved in all-silicon solar cells using silicon nanocrystals. Taking advantage of quantum confinement effects, reducing particle size allows us to engineer the energy bandgap of the material, in this case, silicon. This project aimed to optimise the operation of an Si QD homojunction cell in readiness for its use in a tandem device.

The material used in this work, as previously published, was deposited via RF sputtering onto a silicon wafer covered with thermal SiO_2 with a thickness of 750 nm as shown in the scanning electron microscope (SEM) image in Figure PP2.4b.11. The SiO_2 layer was used to electrically isolate the nanocrystal thin film from the Si wafer to exclude the possible contribution from the wafer

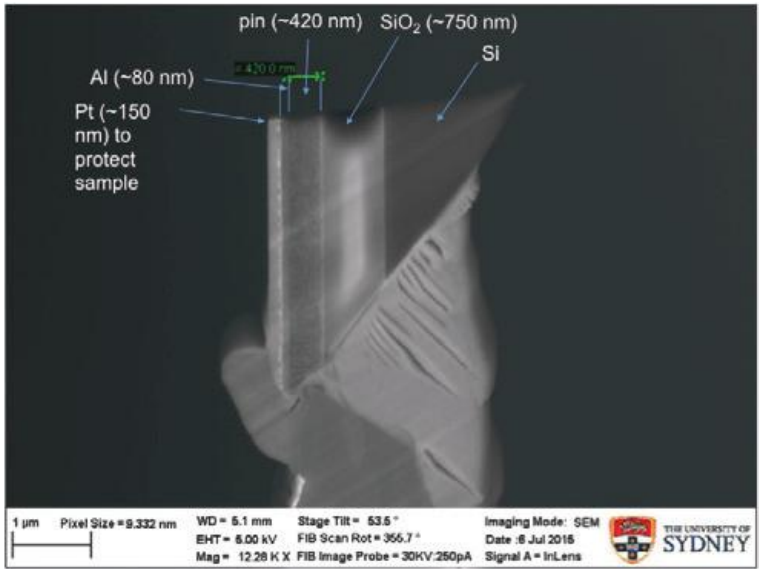

Figure PP2.4b.1: SEM image of the Si QD diode.

substrate. The sputtered thin film contained alternating layers of 4 nm silicon-rich oxide) SRO and 2 nm SiO_2. The unit structure made of an SRO layer and an SiO_2 layer will be addressed as a bilayer. The volume ratio of Si in the SRO layer, expressed as a percentage, is defined as the ratio between the deposition rate (nm/min) of Si and the sum of the deposition rate of Si and SiO_2 as reported in our earlier work. The volume ratio of Si in SRO presented as a percentage is 70.6% ($SiO_{0.37}$) and the overall stoichiometry of the bilayers is $SiO_{0.76}$ in the reported device. A 1-nm SiO_2 layer was deposited on the diode for the purpose of protection. The structure of the device is shown in Figure PP2.4b.12. As can be seen, 35 P_2O_5-doped bilayers were deposited first on the thick SiO_2 layer. They were followed by 15 undoped bilayers and then 20 boron-doped bilayers in deposition as reported earlier. To note, only SRO layers in the bilayer structure were doped. The distance between each electrode is 60 microns. The thin-film material was then annealed in an N_2 purged furnace at 1100°C for 1 hour.

The fabricated device has an open-circuit voltage, V_{OC}, of 367 mV and a short circuit current density, J_{SC}, of 0.04 mA/cm^2 at 25°C under the illumination of one sun. The current density is calculated based on the area of the mesa, as reported earlier in our work. The applied bias was limited to 40 V maximum (6600 V/cm) to prevent any damage due to high voltage across the device. From the inset of Figure PP2.4b.1, we can see that no current crowding effect occurs, up to an applied bias of 40 V. However, the high series resistance (3.24 ω cm^2) of the device limits the injected current, lowering the efficiency of emission from the NCs. The high resistance can be attributed to the lateral structure as shown in Figure PP2.4b.2, where the current passes through a very small cross-sectional area. The EL spectrum was detected by applying an external forward bias of up to 38 V, which generated a current of 7.3 Acm^{-2}. The figure shows a peak at 1.28 eV. No apparent change was noticed in the shape of the EL spectrum within the injected current density range from 2.0 Acm^{-2} (18 V) to 7.3 Acm^{-2} (38 V), but there was a 16 meV peak shift when the applied bias was increased from 18 V to 38 V. The EL peak intensity is proportional to the injected current. We can therefore safely assume that any shift of EL peaks much higher than 16 meV in this work does not depend on the injected current or the applied bias in the observed range. Interestingly, there is an obvious discrepancy between the EL and PL spectra. The PL spectrum (FWHM=0.20 eV) is broader than EL's (FWHM=0.14 eV) and it has a peak at 1.33 eV, as shown in Figure PP2.4b.3. This discrepancy contradicts the consistent PL and EL from size-separated Si NCs reported earlier. It also contradicts the EL-PL discrepancy observed in earlier work on Si NCs, where EL has a higher energy emission peak than PL. Assuming that the luminescence peak energy is inversely proportional to the square of the dimension of the photon-emitting NCs as given by the effective mass approximation (EMA), we can conclude that the discrepancy observed indicates that the EL and PL signals come from different sizes of NCs in the device. The excitation method (i.e. applied bias or illumination) determines which range of NCs is involved. With the NC size dispersion reported earlier, it can be assumed that there are two types of NCs in the material – optically active nanocrystals and electrically active nanocrystals. The optically active NCs are relatively smaller and physically isolated while the electrically active NCs are relatively larger and interconnected or in close proximity with each other. The effective bandgap of NCs varies

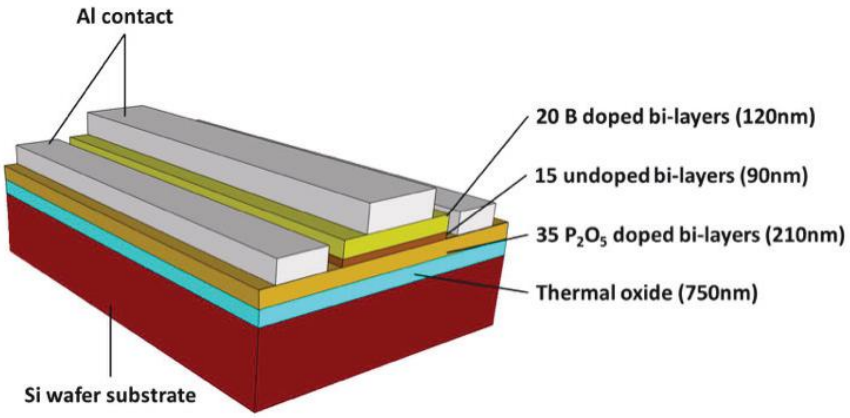

Figure PP2.4b.2: The lateral structure of the all-Si nanocrystal p-i-n diode.

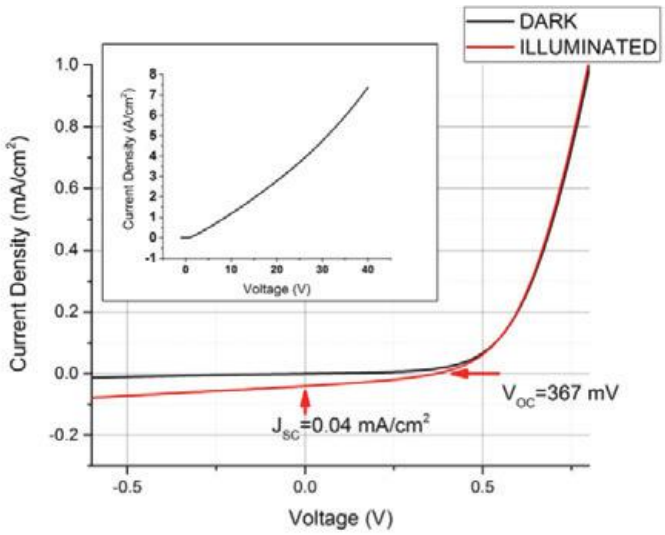

Figure PP2.4b.3: Current density-voltage relation of the all-Si NC p-i-n diode at 300K. The red curve was obtained under one-sun illumination, and shows V_{OC} of 367 mV and J_{SC} of 0.004 mAcm^{-2}. The black curve shows the dark J-V relation. The inset shows the dark J-V curve obtained under a forward applied bias of up to 40 V.

across space due to their distribution in size. We attribute the EL signal mainly to connected NCs (cNCs), because the applied bias injects carriers through the least resistant paths formed by cNCs and leave the isolated NCs (iNCs) uninvolved in recombination. In PL, however, both cNCs and iNCs whose effective bandgaps are lower than the incident photon energy (3.04 eV) are excited by the illumination. The absence of iNCs in EL emission leads to a lower energy peak and a narrower spectrum when compared to PL.

Highlights

- Fabrication of improved Si QD homojunction.
- First electroluminescence characterisation of Si QD cells.
- Successful model for two types of Si QDs – separated and connected QDs.

Future Work

In order for a tandem solar cell with silicon to work, a material with a higher bandgap namely around the 1.6–1.8 eV range is needed. Our Si QD material in this project, which allows us to tune the bandgap, is still a good candidate. However there are still some fundamental material properties that are severely limiting the efficiency of this type of solar cell as shown in the previous chapter.

This brings us to the question of how we can improve on our Si QD material properties in order for it to serve as the optimum top cell in an all-Si tandem solar cell with a crystalline silicon bottom cell. First, we must look at what an ideal Si QD material would look like in terms of its physical structure. Ideally, we want a QD array with:

- narrow size distribution
- close and evenly spaced Si QDs
- spherical Si QDs
- lower barrier height (e.g. using other matrix materials such as Si_3N_4 or SiC)
- well-passivated surfaces.

References

Li, D., Chen, Y.B. and Lu, M., 2012, "An effect of laser pre-annealing on the enhancement of light emission of Si nanocrystal thin film", Materials Letters, 89, 9–11.

Maier-Flaig, F., Rinck, J., Stephan, M., Bocksrocker, T., Bruns, M., Kübel, C., Powell, A.K., Ozin, G.A. and Lemmer, U., 2013, "Multicolor silicon light-emitting diodes (SiLEDs)", Nano Letters, 13(2), 475–480.

Wang, X.. Member, S. and Lundstrom, M., 2013, "On the Use of Rau s Reciprocity to Deduce E xternal Radiative Efficiency in Solar Cells", IEEE Journal of Photovoltaics, 3(2), 1–6.

Wu, L., Perez-wWurfl, I., Lin, Z., Jia, X., Zhang, T., Puthen-Veettil, B., Chien, T., Yang, J., Xia, H. and Conibeer, G., 2014, "Investigation on the effects of phosphine doping in Si nanocrystal material", Proc. 40th IEEE Photovoltaic Spec. Conf., Denver, 666–668.

Zacharias, M., Heitmann, J., Scholz, R., Kahler, U., Schmidt, M. and Bläsing, J., 2002, "Size-controlled highly luminescent silicon nanocrystals: A SiO/SiO_2 superlattice approach", Applied Physics Letters, 80(4), 661– 663.

PP2.4b(ii) Develop Heterojunction Devices

Lead Partner
UNSW

UNSW Team
Dr Ivan Perez-Wurfl, Prof Gavin Conibeer

UNSW Students
Xuguang Jia, Ziyun Lin, Lingfeng Wu

Funding Support
ARENA

Aim

Develop vertical device structures through investigation of conducting transparent layers for bottom contacts.

Progress

Aluminium-doped zinc oxide (AZO) superstrate n-i-p solar cell devices were fabricated as illustrated in Figure PP2.4b.4. These devices were fabricated by first depositing AZO and then sputtering high Si content SRO/SiO2 bilayers through a metallic mask with an n-i-p configuration. Then the samples were annealed at 1100°C using a special "pre-forming gas clean" annealing technique to allow the AZO to retain some of its conductivity.

Figure PP2.4b.5 shows the I-V curves of the AZO superstrate n-i-p solar cell devices in the dark before and after Al metallisation and with illumination (light). Figure PP2.4b.5(a) shows the I-V curves for the sample which was etched for 30 s in hydrofluoric acid to remove with 20 nm SiO_2 capping using tape to isolate the regions, whereas Figure PP2.4b.5(b) shows the I-V curves for the sample which was etched for 90 s in HF using photolithography to isolate the regions. From both figures (a) and (b) it can be seen that the AZO superstrate n-i-p solar cell devices do not produce rectifying junction responses (diode-like I-V curves) and are hence not strictly solar cells. The heavy cross-contamination and mixing of Al and Zn across the n-i-p region as seen from the ToF-SIMS results seem to have caused heavy shunting of the devices. From Figure PP2.4b.5(a) the graph shows a linear I-V response near the origin (0.00 V, 0.00 A) for all three curves which show a typical resistor type of device as a result of the heavy Al shunting. The curve starts deviating from the ideal linear response at higher voltages, but this could be due to a number of reasons such as high carrier injection or high field effects for which the exact nature cannot be deduced from I-V measurements alone. The resistance however can be estimated by the inverse of the gradients near the origin which were 7.1×10^5, 7.1×10^5 and 3.1×10^5 Ω for the dark I-V before and after Al metallisation and light I-V after Al metallisation respectively. The resistance as estimated by the inverse of the gradients near the origin were 9.6×10^3, 3.4×10^3 and 3.8×10^3 Ω for the dark I-V before and after Al metallisation and light I-V after Al metallisation respectively. The initial resistance of the sample with the SiO_2 cap removed using photolithography is lower than the sample using tape. However the conductivity improves much further once the Al is applied to the photolithography sample than the tape sample due to the higher initial sheet resistance of the AZO in the photolithography sample.

Suns-V_{oc} allows the measurement of the open-circuit voltage, V_{OC}, of a solar cell without the effect of series resistance and in turn can produce a pseudo light J-V curve using a separate reference cell to estimate the light-generated current. For both the AZO superstrate Si QD solar cell devices which were contacted as shown in Figure PP2.4b.4, there was no V_{OC} response which is what is expected if the device is in fact heavily shunted. A previous earlier sample which had a slight offset between the n and p layers because the B and P SRO/SiO_2 bilayers were deposited separately due to a slight misalignment with the metal mask was also tested. When this device was probed between the n and p layers on the very edge of the device it produced a Suns-V_{OC} of 93 mV, as shown in Figure PP2.4b.6. This suggested that the n-i-p regions in the devices still produced a rectifying junction although the V_{OC} was much lower than expected due to the heavy shunting.

Although this first demonstration of annealing Si QDs at 1100°C together with a TCO did not produce a working photovoltaic device, it still provided information to arrive

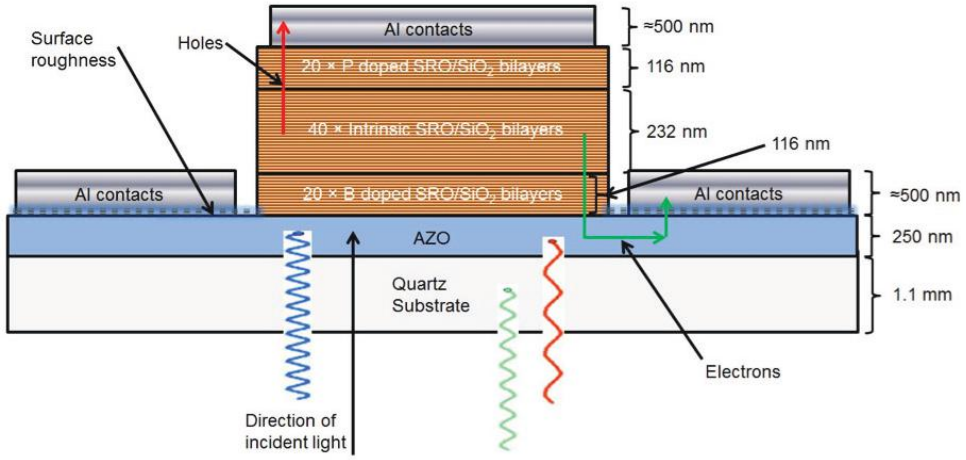

Figure PP2.4b.4: Schematic diagram of the final superstrate n-i-p Si QD solar cell device structure.

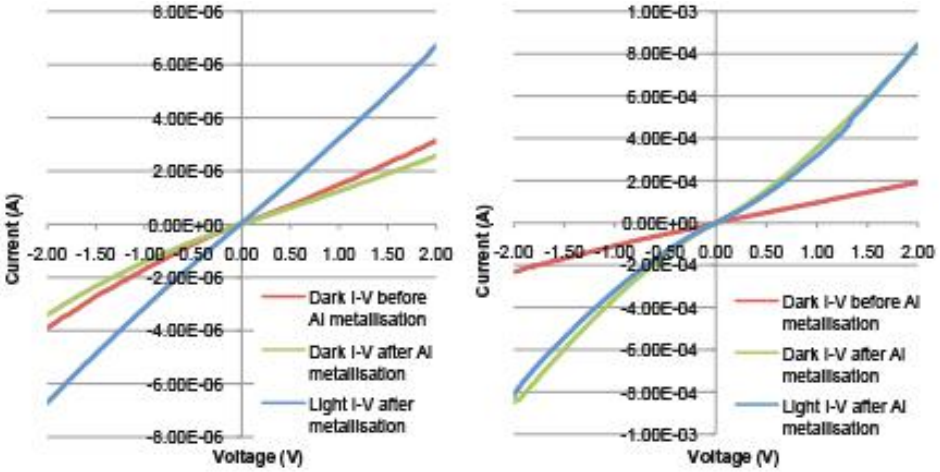

Figure PP2.4b.5: I-V curves of the AZO superstrate n-i-p solar cell devices in the dark before and after Al metallisation and with illumination (light). HF dip using (a) tape and (b) photolithography.

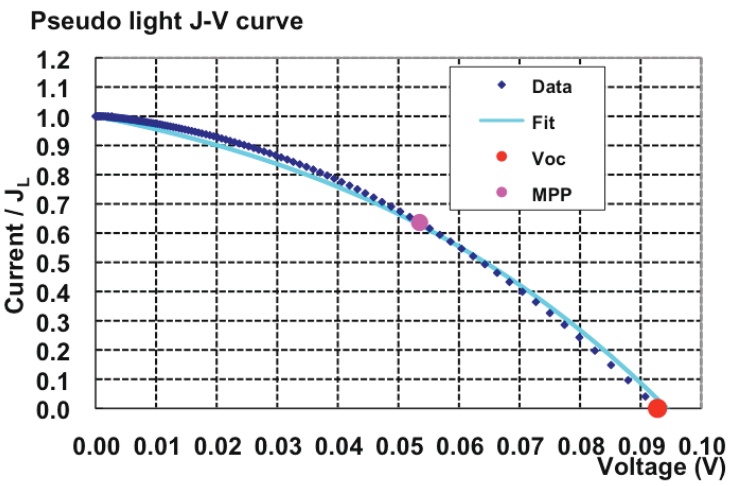

Figure PP2.4b.6: Suns-V_{OC} pseudo light J-V curve of the superstrate Si QD n-i-p solar cell device when contacted on the edge between the n and p layers from a sample with a slight offset.

at interesting and useful conclusions. The most important observation is that the contact between AZO and the B and P doped SRO/SiO_2 bilayers is ohmic believed to be due to the high doping or defects at both interfaces. If it were not for the inter-diffusion during the annealing stage, it seems that this could have been an excellent TCO for single-junction Si QD solar cells. This ohmic property could allow for other types of devices to be created with Si NC materials.

Highlights

- N-i-p devices grown on AZO superstrate.
- I-V and Suns-V_{oc} results for these AZO superstrate devices.

Future Work

- Improvement of the AZO deposition system.
- Investigation of the AZO/Si QD interface.

PP2.4b(iii) Model Absorption and Electrical Properties of Materials and Devices

Lead Partner
UNSW

UNSW Team
Dr Ivan Perez-Wurfl, Prof Gavin Conibeer

UNSW Students
Xuguang Jia, Tian Zhang

Funding Support
ARENA

Aim

Improvement of modelling and fitting optical absorption data for Si QD nanostructures.

Progress

Improving the spectrum fitting result via the "Hishikawa approach"

Based on the transfer matrix method, Hishikawa et al. provided a method to extract interference-free optical constants from the spectrum of transmittance (T) and reflectance (R) from (1-R)/T. In practice this approach is sensitive to the initial values of optical constants (n,k) due to the existence of multiple solutions. To address this limitation, we need reasonably well estimated initial values of *n* and *k* for the iteration to get the local solution near the approximate values. According to the non-linearly unconstrained optimisation theory, the optical constants (n,k) can be deduced via fitting the transmission/reflection spectra with a proper dispersion model. However, such a spectrum fitting method can only give a global optimal solution and its accuracy depends on the suitability of the physical dispersion model. The existing dispersion model may have some drawbacks due to the specific character of silicon nanocrystals. In this this study, we combine these two methods and apply spectrum fitting with a dispersion model first to obtain initial values and then use the "Hishikawa approach" to make fine adjustments and fix the mismatch induced by the global optimisation.

From Figure PP2.4b.7(a), it can be seen that experimental and calculated curves generally agree with each other except for a non-negligible mismatch of the transmission curves at ~700 nm peak. This is because in the F-B model, we only use six parameters (d, , A_i, B_i, C_i and E_g) to make a global fitting. Every physical model has its ideal assumptions and therefore limitations exist. Figure PP2.4b.7(b) shows that after the "Hishikawa approach" adjustment, the reflectance and transmittance spectra are fitted quite well with the peak mismatch fixed.

Application of spectroscopic ellipsometry (SE) on Si QD material

Spectroscopic ellipsometry (SE) is known as an effective technique to analyse the optical properties of thin films. It measures the intensity ratio of two distinct polarisations of reflected light incident on the sample's surface. The SE parameters are usually given as Ψ and Δ, which denote the amplitude ratio and phase shift of the perpendicularly polarised waves after reflection. To extract other optical information rather than these two abstract values, an appropriate optical model is needed. The SE data is generated based on the model and the model parameters are determined by minimising the difference between experimental data and generated data.

In the process of this modelling, the number of layers must be selected and the optical functions of each layer must be determined. Generally, there are two methods to simulate the properties of Si QD materials in SE modelling. One way is to build a multilayer structure with the same thickness as the sample layer. Another is to treat the whole multiple structure as a homogeneous material with the same dielectric function. The first approach, the multilayer structure, may give the information of each layer, but it cannot provide the properties when these multilayers act as a whole, especially if quantum confinement effects are expected in such material. Therefore, we treat the 30-bilayer Si QD material as one homogeneous semiconductor film. Then the structure of the sample will be simulated by a capping SiO_2 layer, a homogeneous mixture film and substrate layer.

Figure PP2.4b.8 shows the optical constants extracted from SE and SR spectra. It can be seen that they

correspond with each other. However, the extinction coefficient at short wavelength is not fitted well. We cannot ensure all optical properties from ellipsometry data alone since the optical function models are empirical and it is a global fitting method as mentioned before. Its accuracy highly depends on the function of the model we selected. On the other hand, the "Hishikawa approach" is a point by point fitting method to solve the transfer matrix. However, it does not consider the K-K relation and therefore the solutions for some points do not have physical meaning even when the initial values we use obey the K-K relation. Therefore, we cannot determine which method is better so far and we need to use both methods to extract the optical bandgap.

Highlights

- Improvement of the Hishikawa approach for fitting optical constants.
- Fitting of ellipsometry data for optical constants.

Future Work

Wider application of this more complete method of fitting optical data and a more sophisticated method for extraction of the optical bandgap.

References

Easwarakhanthan, T., et al., 2007, "Forouhi-Bloomer and Tauc-Lorentz optical dispersions applied using spectroscopic ellipsometry to plasma-deposited fluorocarbon films", Journal of Applied Physics, 101(7) 073102.

Hishikawa, Y., Nakamura, N., Tsuda, S., Nakano, S., Kishi, Y. and Kuwano, Y, 1991, "Interference-Free Determination of the Optical Absorption Coefficient and the Optical Gap of Amorphous Silicon Thin Films", Japanese Journal of Applied Physics, 30(5) 1008–1014.

PP2.4b(iv) Investigate Other Materials Based on Si or Ge QDs

Lead Partner
UNSW

UNSW Team
Dr Santosh Shrestha, Dr Ivan Perez-Wurfl, Prof Gavin Conibeer, Dr Binesh Puthen-Veettil, Dr Yuanxun Liao

UNSW Students
Terry Yang, Keita Nomoto

Funding Support
ARENA

Aim

Energy selective contacts based on group IV nanostructures.

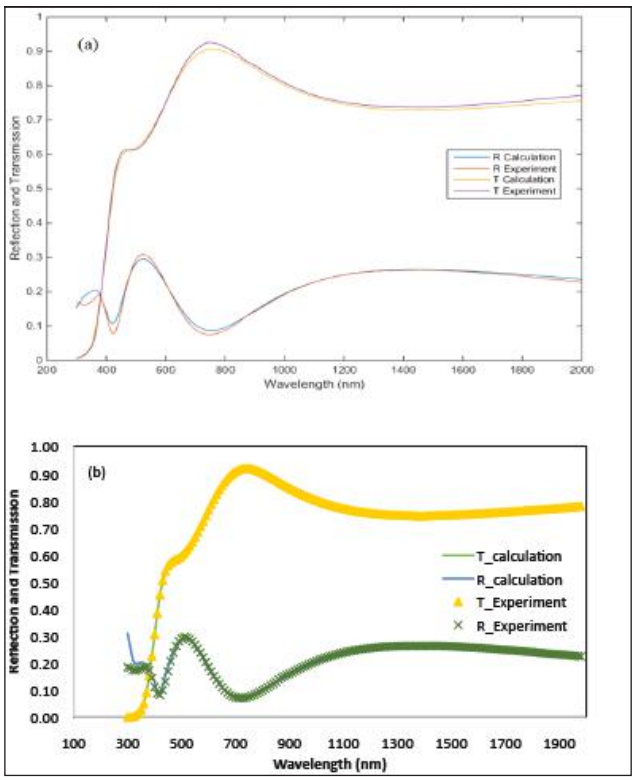

Figure PP2.4b.7: (a) Measured and calculated reflection and transmission spectra for 1 nm SRO, the parameters of the F-B model d, **n**(∞), A_i, B_i, C_i and E_g are 1.7362, 0.0528, 7.5413, 14.711, 1.9698 and 1.3923, respectively; (b) Improved fitting by "Hishikawa approach".

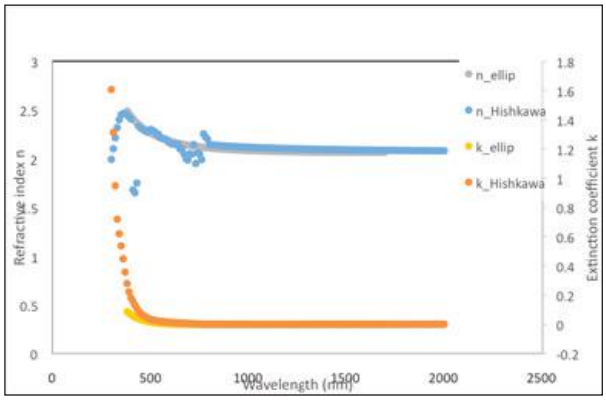

Figure PP2.4b.8: Optical constants of Si QD material from RT spectra and SE fitting.

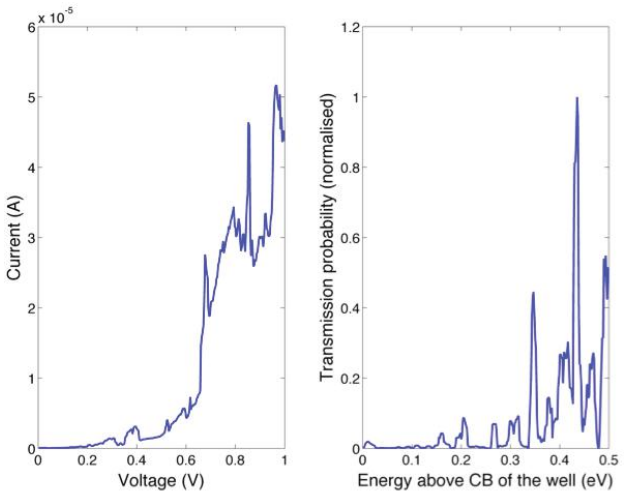

Figure PP2.4b.9: Room temperature–measured I-V characteristics (left) and calculated transmission (right) for the $Al_2O_3/Ge/Al_2O_3$ sample (1 nm Al_2O_3 and 3 nm Si).

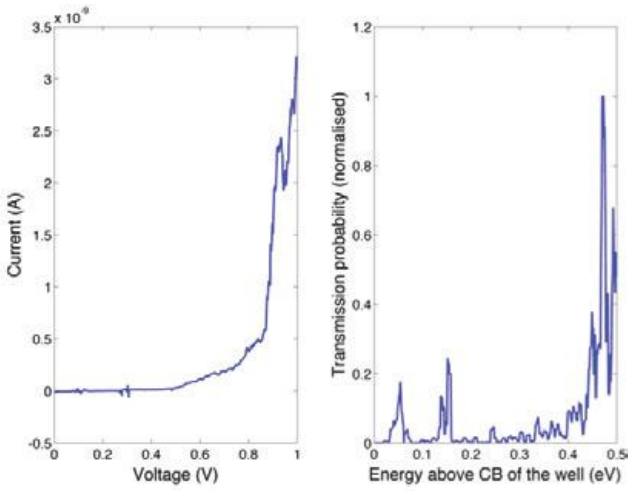

Figure PP2.4b.10: Room temperature–measured I-V characteristics (left) and calculated transmission (right) for the $Al_2O_3/Si/Al_2O_3$ sample (1 nm Al_2O_3 and 3 nm Si).

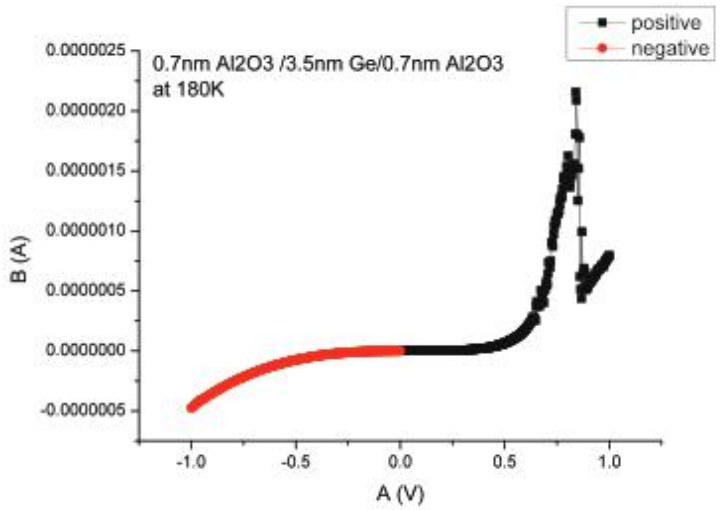

Figure PP2.4b.11: Results of I-V measurements on an $Al_2O_3/Ge/Al_2O_3$ resonant tunnelling structure.

Progress

Energy selective contacts based on group IV nanostructures for hot carrier solar cells

As reported in Section 2.4a(iv), energy selective contacts (ESCs) are essential for efficient hot carrier solar cell operation. In this work resonant tunnelling structures using thin-film materials based on Si and Ge nanostructures have been fabricated to produce rectifying ESCs which will be of importance for further hot carrier cell research.

ESCs based on quantum well resonant tunnelling structures have been studied. Two types of contacts have been investigated: $Al_2O_3/Si/Al_2O_3$ $Al_2O_3/Ge/Al_2O_3$. They are either grown on p-type or n-type silicon substrates. The group IV layer of Si or Ge is deposited by RF-sputtering. I-V measurements are carried out using a Lakeshore probe station.

The I-V profiles for the structures are shown in Figure PP2.4b.9 for an $Al_2O_3/Ge/Al_2O_3$ contact and Figure PP2.4b.10 for an $Al_2O_3/Si/Al_2O_3$ contact, with their corresponding calculated transmission probability profiles using an effective mass approximation. They clearly show resonant transmission peaks. For the $Al_2O_3/Ge/Al_2O_3$ sample, the main peak appears at 0.42 eV, while the second most significant peak is around 0.3 eV. For the $Al_2O_3/Si/Al_2O_3$ sample, the main peak is around 0.05 eV.

It is important for ESCs to exhibit asymmetric rectifying behaviour, so that carriers as well as energy are selected at the contact. Figure PP2.4b.11 shows results of I-V measurements on the $Al_2O_3/Ge/Al_2O_3$ structure measured in forward and reverse bias. In the positive voltage axis, a resonance peak can be observed around 0.8 V whereas in the negative voltage axis such a peak is not visible. This indicates extraction of electron/holes from the contact and clear rectification of carrier type.

Highlights

- Room temperature resonance in ESCs based on Si and Ge nanostructures.
- Rectifying behaviour in Al_2O_3 Ge nanostructure ESC structure.

Future Work

Improve resonance of ESCs. Investigate other material structures for ESCs. Apply to hot carrier devices.

PP2.5 Perovskites

UNSW Team
Prof Martin Green, Dr Anita Ho-Baillie (also Project Manager), Dr Shujuan Huang, Dr Trevor Young, Dr Jae Yun, Dr Yajie Jiang, Dr Meng Zhang

UoM Team
Prof Ken Ghiggino, Dr David Jones

Monash Team
Prof Udo Bach, Prof Yi-Bing Cheng, Prof Leone Spiccia, Dr Feng Li, Dr Alex Pascoe, Dr Steffen Meyer, Dr Jianfeng Lu

ANU Team
Prof Kylie Catchpole, Prof Klaus Weber, Dr Thomas White, Dr Daniel Walter, Dr Chog Barugkin, Dr Hemant Kumar Mulmudi, Dr Heping Shen

UQ Team
Prof. Paul Burn, Prof. Paul Meredith, Dr Mike Hambsch, Dr Ravi Chandra Raju Nagiri, Dr Ardalan Armin

CSIRO Team
Dr Gerry Wilson, Dr Fiona Scholes, Dr Mei Gao, Dr Doojin Vak, Dr Jyothi Ramamurthy, Dr Hasitha Weerasinghe, Dr Andrew Scully, Dr Anthony Chesman, Ms Regine Chantler, Mr Karl Weber, Mr Andrew Faulks, Dr Kallista Sears, Dr Dechan Angmo, Dr Askhat Jumabekov

Academic Partners
Prof Sang Il Seok (Korea Research Institute of Chemical Technology (KRICT), Ulsan National Institute of Science and Technology, Korea (UNIST))
Dr Stephen Moore and Dr Juan Alvarez Gaitan (Civil Engineering, UNSW)
Prof Joanne Etheridge (Monash Centre for Electron Microscopy)
Prof Nripan Mathews (Nanyang Technological University (NTU), Singapore), P.C. Harikesh (NTU), Dr Ghanshyam Pilania (Los Alamos National Laboratory (LANL)), Prof Rohan Mishra (Washington University)
The University of Toledo
Stanford University
Georgia Institute of Technology

Students
Qingshan Ma (UNSW), Sheng Chen (UNSW), Adrian Shi (UNSW), Jincheol Kim (UNSW), Xiaofan Deng (UNSW), Cho Fai Jonathan Lau (UNSW), Benjamin Wilkinson (UNSW), Jianghui Zheng (UNSW), Arman Mahboubi Soufiani (UNSW), Da Seul Lee (UNSW), Yongyoon Cho (UNSW), Jueming Bing (UNSW), Rui Sheng (UNSW), Nathan Chang (UNSW), Yecheng Zhou (UoM), Liancong Jiang (Monash), Wuqiang Wu (Monash), Mathias Uller Rothmann (Monash), The Duong (ANU), Jun Peng (ANU), Yiliang Wu (ANU), Xiao Fu (ANU), Daniel Jacobs (ANU), Dale Grant (ANU), Qianqian Lin (UQ)

Aim

Since the establishment of AUSIAPV/ACAP in 2012, mixed organic-inorganic halide perovskites have emerged as a new class of solar cell with potential as a material for the development of efficient, lower cost photovoltaic cells.

The potential of perovskites for PV cells as an absorber material lies in its ability to achieve good cell efficiencies, while being relatively cheap to produce and simple to manufacture (i.e. competitive cell efficiency at a lower cost).

A significant effort has been initiated internationally on this materials class, and ACAP has several unique advantages that place the proposed activities at the forefront of these international efforts. Foremost among these advantages are the different relevant perspectives that ACAP is able to offer given the expertise within the different groups constituting ACAP in the dye-sensitised, organic photovoltaics (OPV), inorganic thin-film and silicon cell and module areas, as well as the strong contacts to the commercial sector, and the coordination of this expertise and research effort made possible through the ACAP organisational structure.

To capture these research efforts within ACAP, a new program package for Perovskite Solar Cells under PP2 Thin-Film, Third Generation and Hybrid Devices with additional funding has been established to carry out focused and highly collaborative Australian research and industry effort in perovskite photovoltaics. The aim is to establish an internationally leading activity in this exciting new materials group and, consistent with the original intent of ACAP, the team will undertake highly innovative and competitive research with a strategic focus on PV technologies that targets breakthroughs in the cost of solar energy. With a focus on issues that need to be resolved to enable low-cost, full-scale production, the work would enhance the commercial viability of perovskites.

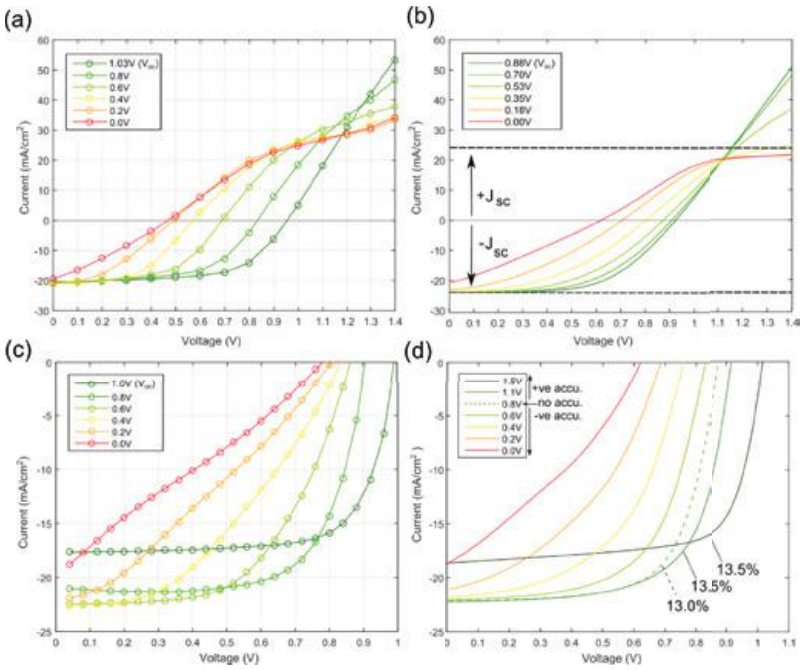

Figure PP2.5.1: Experimental (a) and (c) and modelled (b) and (d) hysteresis behaviour based on the hypothesis of ionic accumulation.

The research is divided into the following main areas:

- Thorough understanding of basic material and device properties by taking full advantage of the expertise, facilities and experience within the partner organisations. The project will undertake research in a diverse range of applications of perovskite materials and devices to develop a path to cost-effective, stable perovskite solar cells.
- Investigation of prospects for Pb-free perovskite materials.
- Understanding the stability of these materials and both material synthesis and encapsulation approaches to addressing present stability and durability issues.
- Development of tandem thin-film cells both within the perovskite material system and in combination with inorganic thin films (Si wafer tandems specifically excluded since they are covered by another ARENA project).
- Commercialisation of relevant research including improving the performance of reasonably large devices (> 1cm^2 in area) rather than on the tiny devices (< 0.1cm^2 in area) where a majority of international attention is focused. This task also includes the evaluation of manufacturing costs for the most promising of the fabrication approaches identified and scaling issues.
- Others aspects of perovskite solar cell research that are relevant but with different focuses are also reported. For the year 2016, highlights of some environmental impact studies will be reported.

Note that this section incorporates the following projects: PP1.3a(v), PP2.1j, PP3.1.

Progress

Materials and device properties

Hysteresis has been widely observed in perovskite solar cell current-voltage characteristics. A number of research activities using different characterisation techniques applied on various types of perovskite test structures and complete cells under various operating conditions have been carried out to provide insights into the origin of hysteresis. Models have also been developed to help predict performance behaviour under different operating conditions.

The team at ANU in collaboration with Monash have modelled the effect of mobile ion accumulation on TiO_2-based perovskite device performance, likely to be the main contributor to the notorious problem of current-voltage hysteresis in perovskite cells. S-shaped IV curves (see Figure PP2.5.1(a,b)) indicate that carriers are collected at the “wrong” electrode under negative ionic accumulation and high forward bias. The presence of this feature indicates a lack of selectivity at the electrodes, likely due to a high density of recombination centres at the perovskite interfaces, as shown in Figure PP2.5.1(c) and (d). Rapid scanned IV curves show the decisive influence of pre-biasing voltage. In this measurement and the accompanying simulation the instantaneous photocurrent is reduced following pre-biasing periods at large positive voltages, a phenomenon related to reports of “inverted hysteresis”, explicable in terms of “positive” ionic accumulation. Key findings from simultaneous measurements of photoluminescence emissions and open circuit voltage of perovskite solar cells suggest the presence of a majority carrier bottleneck at one or both of the perovskite/transport layer interfaces, combined with recombination at that

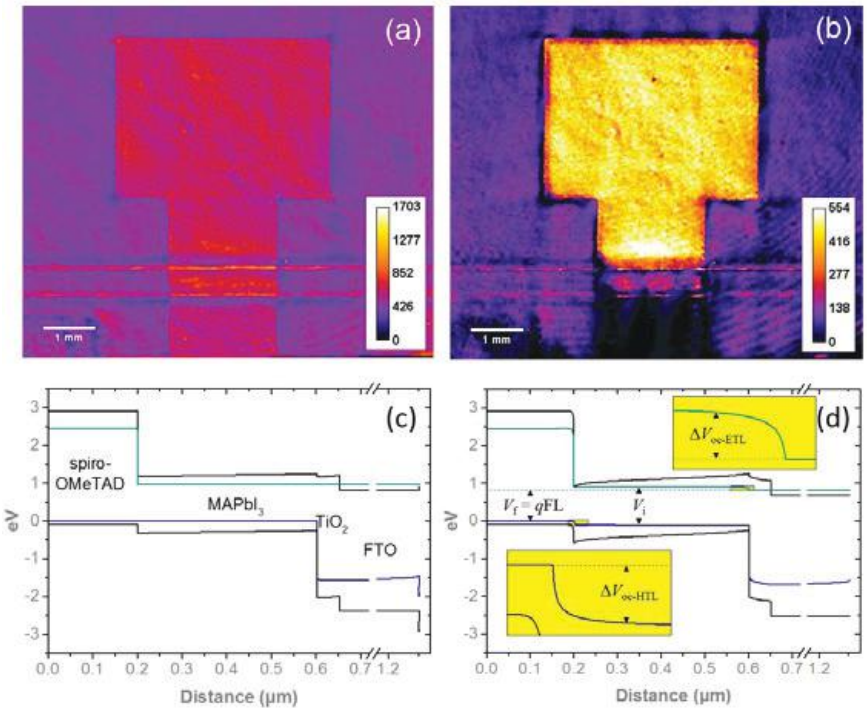

Figure PP2.5.2: PL images of a planar Perovskite Solar Cells. (a) Raw image of a planar structure PSC with 1 s exposure upon illumination; (b) image with background subtraction, SCAPS-1D simulation of the energy bands of a PSC under (c) stabilised open circuit conditions and (d) immediately after switching from stabilized short circuit to open circuit conditions. In the second case we observe a significantly reduced terminal voltage V_f compared with the internal voltage V_i due to the majority carrier barriers at the interfaces.

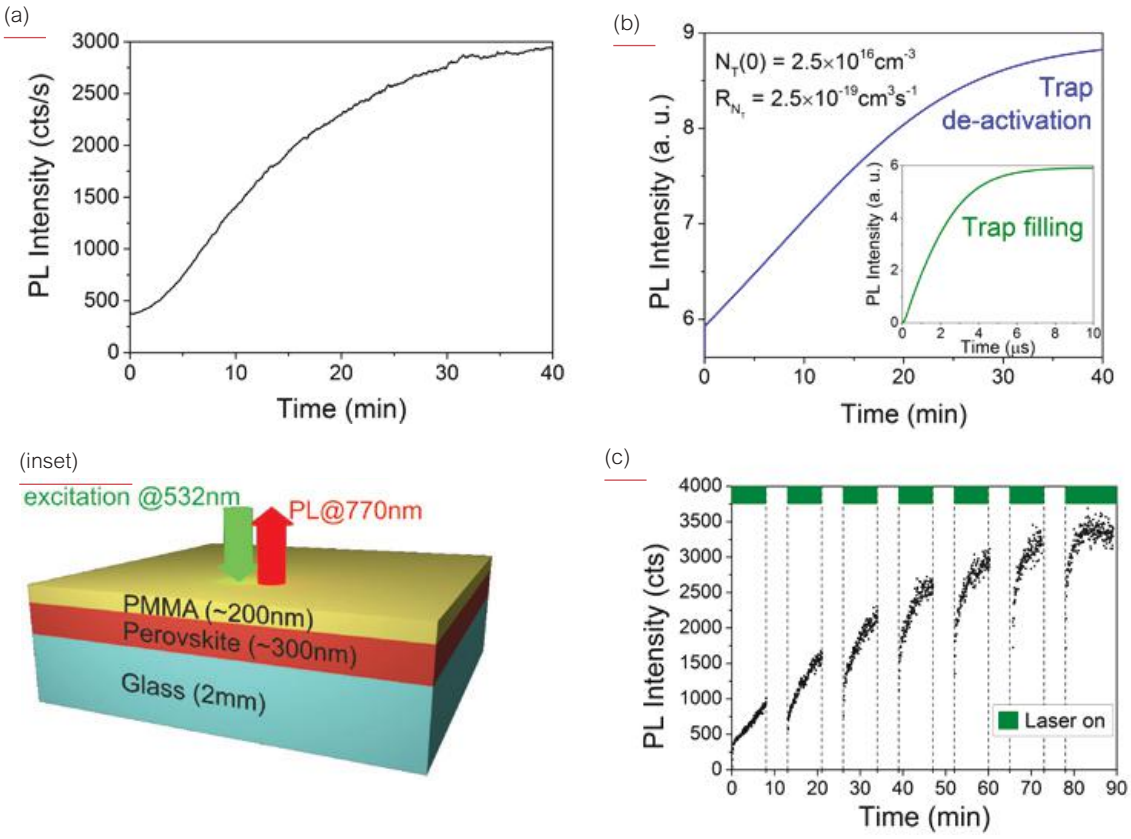

Figure PP2.5.3: (a) PL peak intensity as a function of laser exposure time. The laser intensity is approximately 150mWcm^{-2}. Inset is the schematic of the perovskite film measured in this experiment, (b) Modelled PL intensity enhancement with trap deactivation rates; the inset shows the initial rapid increase in PL during the first 10ms of illumination due to trap filling, (c) Single point PL intensity measurement with intervals of laser exposure. The laser source is turned on for 8 min and then turned off for 5 min in each cycle. The overall PL intensity is enhanced over a period of 90 min, while the enhanced PL always reduces to some extent during the dark time.

interface contributing to the observed hysteresis (Wu et al., 2016) (see Figure PP2.5.2). Work at ANU using confocal photoluminescence microscopy to investigate the time and spatial characteristics of light-induced trap deactivation in $CH_3NH_3PbI_3$ perovskite films (Fu et al. 2016) found that trap deactivation is characterised by a dramatic increase in PL emission during continuous laser illumination accompanied by a lateral expansion of the PL enhancement far beyond the laser spot. These observations are attributed to an oxygen-assisted trap deactivation process associated with carrier diffusion. This effect is modelled by adding a trap deactivation term to the standard semiconductor carrier recombination and diffusion models to reproduce the observed temporal and spatial dependence of laser-induced PL enhancement using realistic physical parameters. Another key finding is that trap deactivation is not permanent, with the traps appearing again once the illumination is turned off. This study provides new insights into recombination and trap dynamics in perovskite films that could offer a better understanding of perovskite solar cell performance (see Figure PP2.5.3). The modelling of the current-voltage hysteresis, and the enhancement in PL efficiency after light-soaking (Jacobs et al., 2016a) suggest that mobile ions are primarily responsible for hysteresis in perovskite cells. A quantitative model has also been developed for the theory of photo-induced defect deactivation, which is shown to be a viable explanation for the unusual light-soaking behaviour in $MAPbI_3$ films (see Figure PP2.5.4).

The team at UNSW have visualised and characterised the electric field–induced effects in laterally structured Au/fluorine-doped-tin-oxide (FTO)/$CH_3NH_3PbI_3$/FTO/Au samples via photoluminescence optical microscopy, in situ time-correlated single photon counting measurements and scanning electron microscopy (SEM) (see Figure PP2.5.5) (Jacobs et al., 2016b). Both irreversible and reversible responses are observed

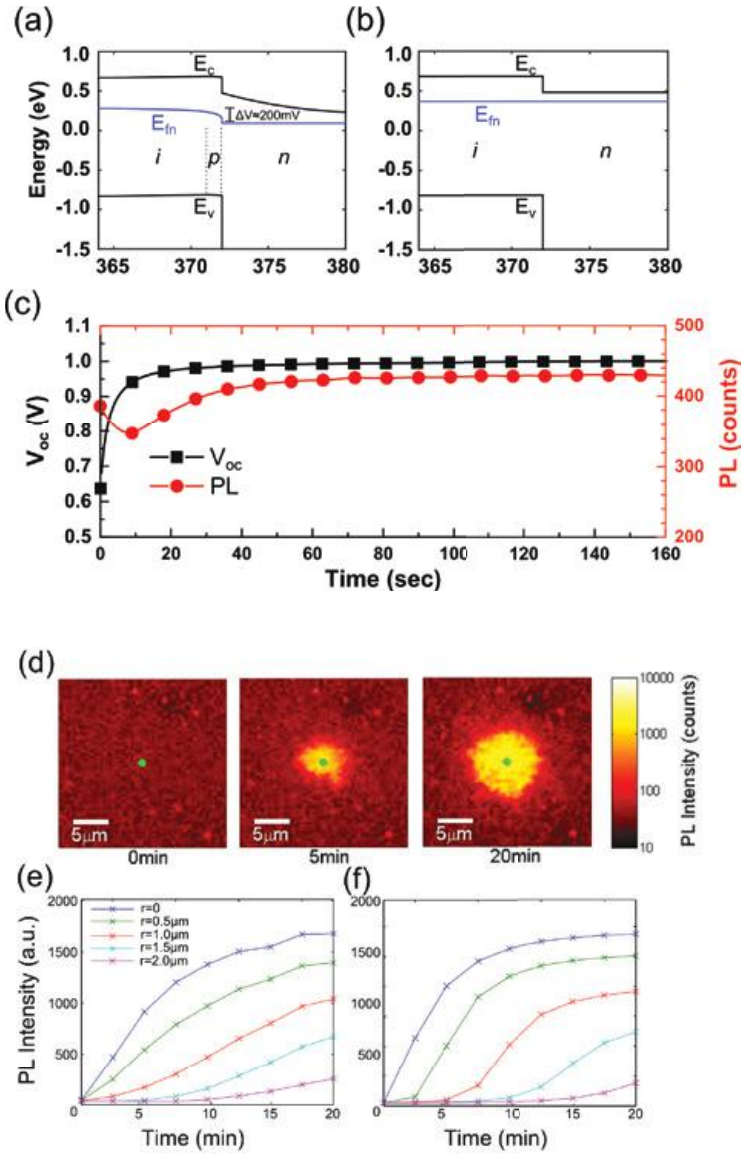

Figure PP2.5.4: (a) Band structure at the i-n interface (electron contact) with ions in their equilibrium position for short-circuit bias, measured at Voc and (b) without ions, (c) Measurements of Voc and PL intensity after biasing at short-circuit condition, (d) PL intensity of a partially encapsulated $MAPbI_3$ film measured as a function of time after exposure to 572nm laser light at an intensity of 80Wcm-2 with spot size ≈750nm, (e) Measured PL intensity shown at different radii, (f) Simulated PL intensity.

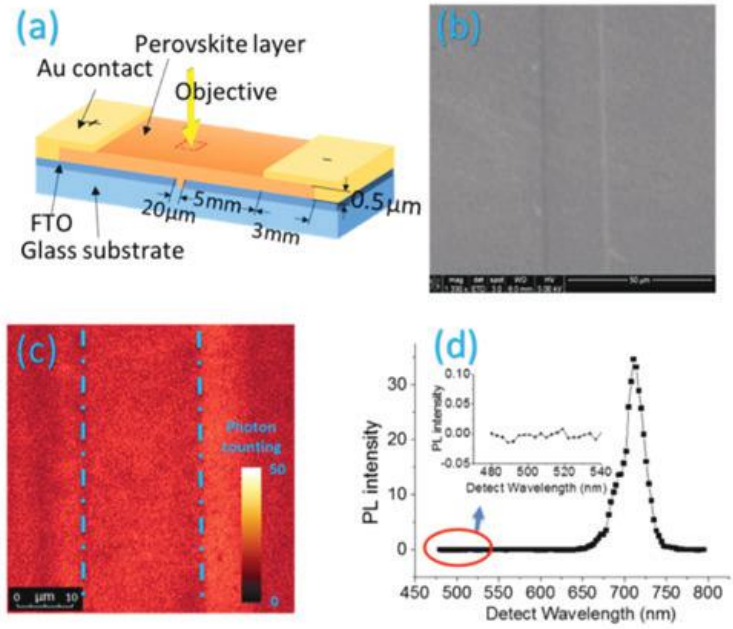

Figure PP2.5.5: (a) Schematic of laterally structured sample with a $CH_3NH_3PbI_3$ layer on the top (not to scale), (b) SEM image, (c) PL image and (d) PL spectrum of the $CH_3NH_3PbI_3$ sample before electrical bias (inset shows the zoomed PL spectrum for wavelength range of 480–540 nm). The two blue lines indicate the region of the perovskite in the ~20 nm wide gap between the FTO electrodes.

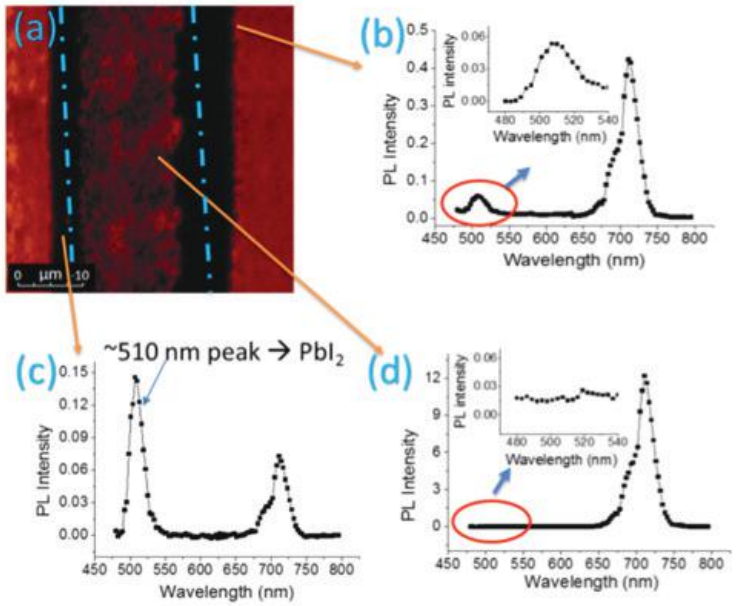

Figure PP2.5.6: Photoluminescence image of the pre-moisturised sample after 1 day recovery from 15 minutes biasing at 0.5 V /µm (a) and PL spectra measured at the quenching area near the cathode side (b), at the quenching area near the anode side (c), and at the recovered area between two electrodes (d). Insets in (b) and (d) show the zoomed PL spectra for wavelength range of 480–540 nm.

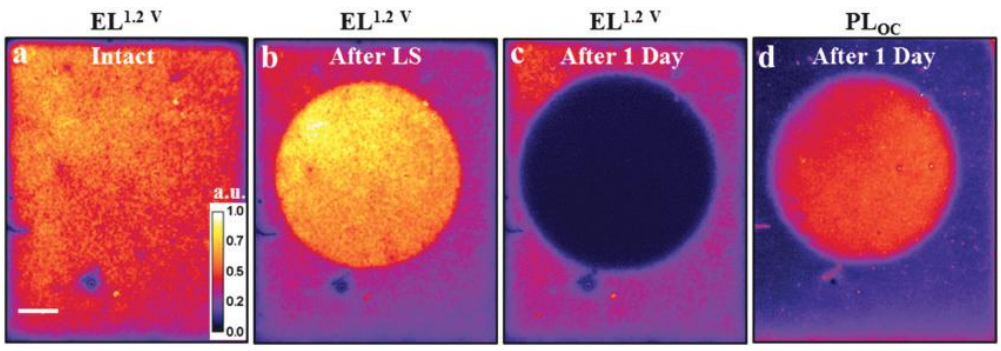

Figure PP2.5.7: Effect of light-soaking under open-circuit conditions on EL and PLOC behavior of PSC. Luminescence images illustrating the impact of 30 min light soaking, at one-sun simulated solar irradiance, on the EL performance of a cell at 1.2 V forward bias for fresh (a), immediately after J–V (b) and after one day (c) the PLOC image of the same device after one day storage in dark is presented in (d). The scale bar in (a) is 1 mm and applies to all the images in this figure. Luminescence intensity of all the images in (a)–(d) is in normalised form.

under different electric fields and humidity conditions. First, the irreversible response near both electrodes includes permanent photoluminescence quenching and morphology changes. Such changes are observed when the applied field is larger than a nominal value, which depends on the humidity conditions. The irreversible change is a result of perovskite decomposition, which is indicated by the appearance of a PbI_2 peak in the localised photoluminescence spectrum. It is shown that this moisture-assisted electric field–induced decomposition can be minimised by encapsulation. Second, a reversible response near the anode observed under a weak electric field, which is characterised by photoluminescence quenching and a reduced lifetime with negligible morphology change, is attributed to the migration and accumulation of mobile ions. The dominant mobile species is ascribed to be iodide ions by mobility calculations. Third, a slowdown of the irreversible response, i.e. decomposition within the bulk of the perovskite and away from the electrodes, is observed. This is because of the negative feedback between perovskite decomposition and ion accumulation, which offsets the field-induced effect in the perovskite bulk. This work demonstrates the effective use of photoluminescence microscopy revealing different mechanisms behind the observed instability of perovskite devices under different bias and moisture conditions that cause either reversible or irreversible changes (see Figure PP2.5.6). In another study (Deng et al., 2016), planar FTO/compact (c-) TiO_2/$CH_3NH_3PbI_3$/Spiro-OMeTAD/Au solar cells from Monash were investigated using fast and spatially resolved photo- and electroluminescence imaging at UNSW. It was found that regions that are exposed to light initially produce stronger electroluminescence signals than surrounding unilluminated regions, mainly due to a lower contact resistance and, possibly, higher charge collection efficiency (see Figure PP2.5.7). Over a period of several days, however, these initially illuminated regions appear to degrade more quickly despite the device being stored in a dark, moisture- and oxygen-free environment. Using transmission electron microscopy, this accelerated degradation is attributed to delamination between the perovskite and the titanium dioxide (TiO_2) layer (see Figure PP2.5.8) (Mahboubi Soufiani, 2017). An ion migration mechanism is proposed for this delamination process, which is in accordance with previous current-voltage hysteresis observations. These results provide evidence for the intrinsic instability of $CH_3NH_3PbI_3$-based devices under illumination and have major implications for the design of perovskite solar cells from the standpoint of long-term performance and stability.

At UNSW, Kelvin probe force microscopy (KPFM) has been used to characterise device operation within grain interiors and at grain boundaries, in particular the ion migration behaviour at different

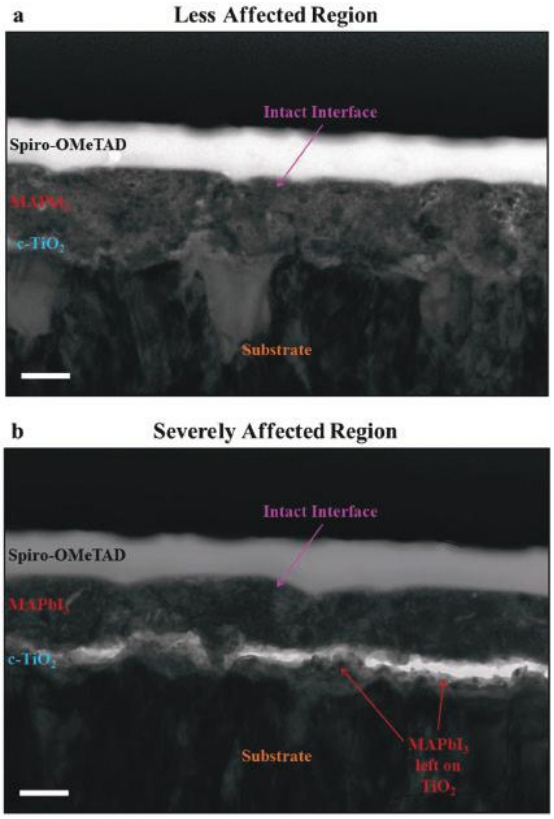

Figure PP2.5.8: High-resolution cross-sectional TEM images of the changes in the light-exposed regions of a cell. Panel (a) shows an interface which is affected less during light exposure and (b) a region severely affected and delaminated upon illumination. The scale bars are 200 nm.

regions. $(CH(NH_2)_2PbI_3)_{0.85}(CH_3NH_3PbBr_3)_{0.15}$ and $(FAPbI_3)_{0.85}(MAPbBr_3)_{0.15}$ perovskite test structures (FTO/c-TiO_2/meso-porus (mp-)TiO_2/perovskite) fabricated by Professor Sang Il Seok's group at UNIST and KRICT that produces the highest efficient perovskite solar cells have been studied using KPFM under various voltage bias and illumination conditions. It is found that ion migration is enhanced at the grain boundaries. Under illumination, the light-induced potential causes ion migration leading to a rearranged ion distribution. Such a distribution favours photo-generated charge-carrier collection at the grain boundaries (see Figure PP2.5.9) (Yun et al., 2016). Evidence for the temporary and permanent morphological changes due to the ion migration when bias voltage was applied under contact mode (short-circuit conditions) is also revealed under KPFM. Energy-dispersive X-ray (EDX) analysis confirmed that MA^+ and/or FA^+ ions and I^- ions participate in such migration. The role of excess PbI_2, when incorporated into high efficiency independently confirmed 19.7% $(FAPbI_3)_{0.85}(MAPbBr_3)_{0.15}$ device, is also investigated using KPFM. It is found that the presence of PbI2 in the perovskite reduces the effects of the ionic migration on charge separation (see Figure PP2.5.10) (Kim et al., 2015).

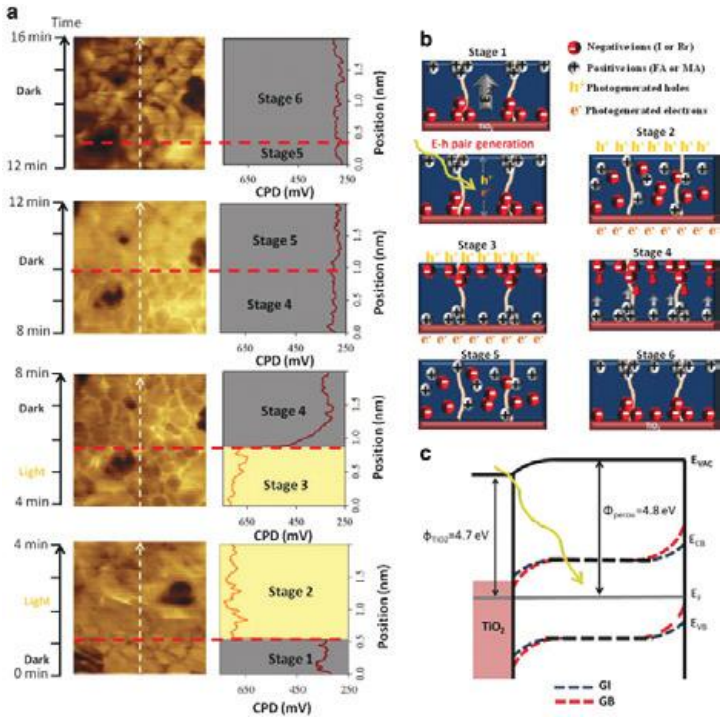

Figure PP2.5.9: Effect of light-induced potential and charge separation. (a) Contact potential difference spatial maps and the corresponding contact potential difference line profile (white line) over an area of 4 μm^2 in changing illumination conditions (ON = 0.3 Wm^{-2}; OFF = 0 Wm^{-2}) with time. (b) Schematic illustration of the ion movement based on results in a). Note that contact potential difference spatial maps are normalised with background subtraction in order to observe contrast between GBs and GIs, and contact potential difference profile displays absolute values. (c) Energy diagram of the perovskite layer under the influence of built-in potential (V_{bi}). ECB is the conduction band energy, EVB is the valence band energy, and EF is the Fermi level.

The team at UoM in collaboration with Monash have been working to determine whether the polarisation and capacitive charge in $CH_3NH_3PbI_3$ screens the external electric field that hinders charge transport. The screening effect is responsible for hysteresis in $CH_3NH_3PbI_3$ photovoltaic cells. A numerical model with these charges implemented (see Figure PP2.5.11) (Zhou et al., 2016), has been developed for perovskite solar cells to quantitatively reproduce experimental "anomalous" hysteresis current density-voltage (J-V) curves.

At Monash, advanced transmission electron microscopy (TEM) characterisation techniques have been developed for studying perovskite films. First, proper specimen preparation techniques have been developed whereby a film can be deposited onto the required grid that reliably resembles the films used in perovskite thin-film solar cells. Second, it has been found that the $CH_3NH_3PbI_3$ degrades when the incorrect TEM operating conditions are used on a number of levels including morphological, crystallographic and compositional, with the rate being dependent on the total number of electrons impinging on the material (see Figure PP2.5.12). The end product of the degradation of $CH_3NH_3PbI_3$ in the microscope is locally strained PbI_2 sitting within a surrounding perovskite-like lattice. This degradation product has caused confusion within the community, since its diffraction pattern shares many similarities with that of pristine $CH_3NH_3PbI_3$, as well as similar lattice spacings in a range of orientations. Third, under appropriate TEM operation conditions, crystallographic twin domains, which is a crystallographic phenomenon whereby two different crystal orientations growing adjacent to each other with a common mirror plane in between, is observed for $CH_3NH_3PbI_3$ perovskites. The twin domains have been confirmed using selected area electron diffraction (SAED). At room temperature $CH_3NH_3PbI_3$ exhibits crystallographic twinning across the {112} planes, forming striped domains passing through most grains, with widths of around 100–300 nm. These domains disappear after only a few minutes of very low electron beam dose rate (around 1 $eÅ^{-2}s^{-1}$), both from the bright field image and from the diffraction pattern, and thus cease to exist in the grains (see Figure PP2.5.13). This fragility explains why this phenomenon has not been described earlier. Interestingly, it was found that upon heating the film to 70°C, above the tetragonal-to-cubic phase transition temperature of 57°C, the twins disappeared, which corresponds nicely with the cubic phase not readily twinning. Upon cooling to room temperature, the twins reformed in some of the grains, most with the same orientation as the original twins (see Figure PP2.5.14). This indicates that the twins are induced in the grains following the cubic-to-tetragonal phase transition that happens during cooling after annealing, and it is therefore likely that the twins are found in most $CH_3NH_3PbI_3$ thin films that have undergone annealing. Furthermore, the existence of crystallographic twinning can help future X-ray diffraction refinements more reliably determine the space group of $CH_3NH_3PbI_3$, which is still an important fundamental question. The advanced TEM characterisation techniques developed at Monash and new observation of twinning domains open up opportunities for further investigations on material properties and their relationships to electrical properties and operation of perovskite devices.

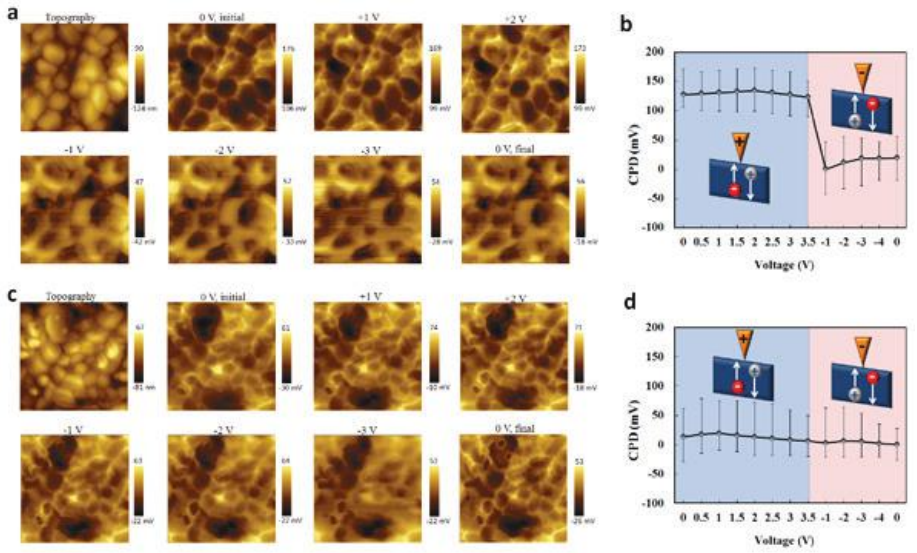

Figure PP2.5.10: Topography and CPD spatial maps over an area of 4 μm^2 with different bias voltages applied to the tip under 500 nm with 0.3 Wm^{-2} illuminations of the samples consisting of FTO/bl-TiO_2/mp-TiO_2/$(FAPbI_3)_{0.85}(MAPbBr_3)_{0.15}$:PbI_2. (a) Without and (c) with 5.7 mol% of PbI_2 incorporated in perovskite layer. Average CPD with maximum and minimum values as a function of various bias voltages applied to the tip under 500 nm with 0.3 Wm^{-2} illumination, (b) without and (d) with 5.7 mol% of PbI_2 incorporated.

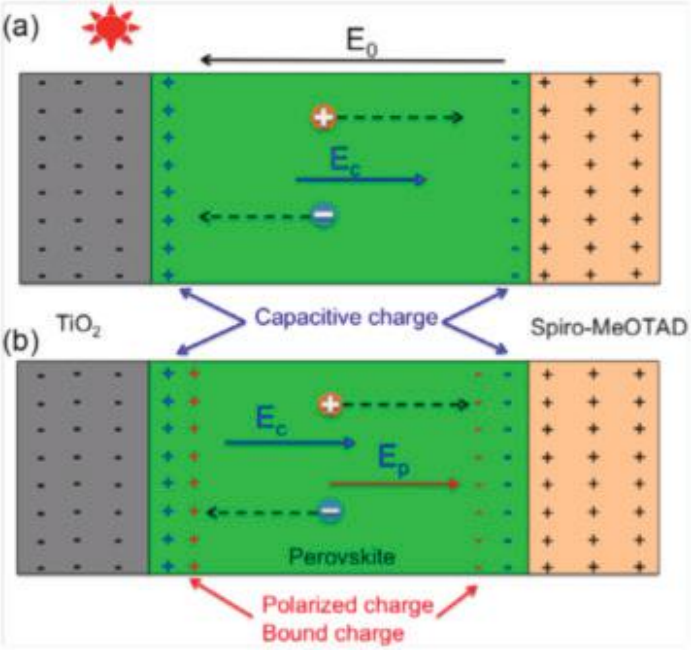

Figure PP2.5.11: Proposed mechanism of perovskite solar cells

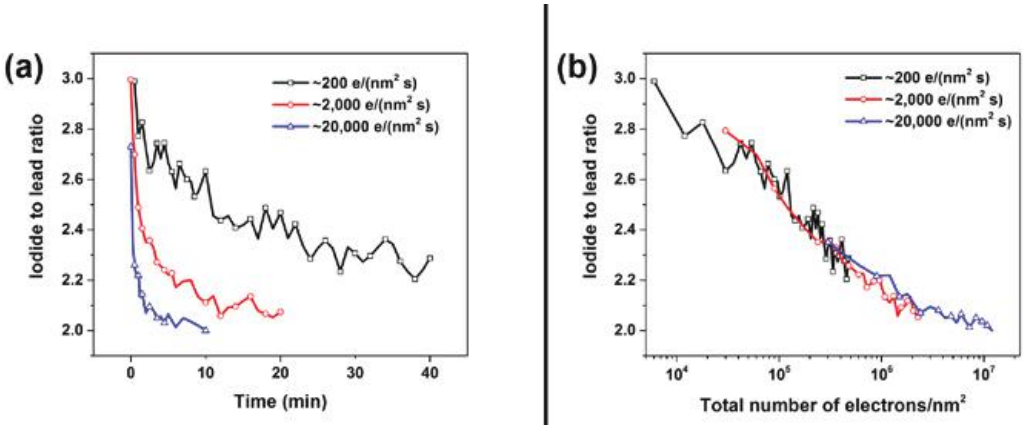

Figure PP2.5.12: Normalised iodide to lead ratios of a 300 nm $CH_3NH_3PbI_3$ thin film under a range of electron exposures as a function of (a) exposure time and (b) total electron dose.

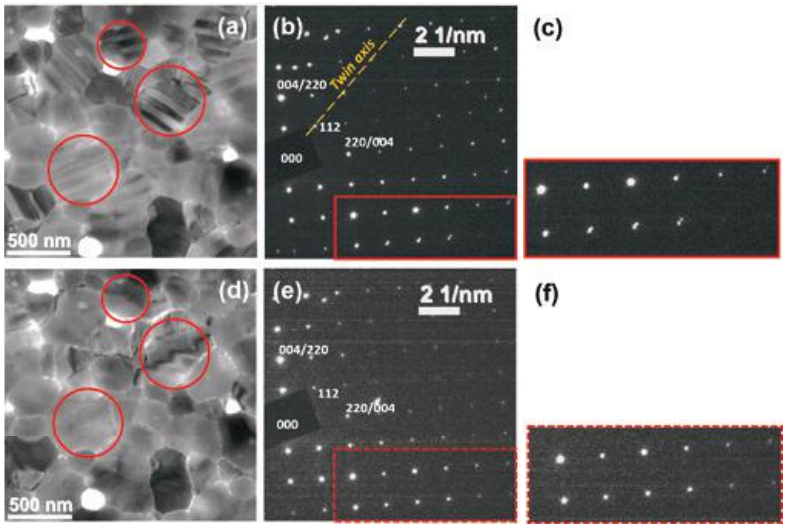

Figure PP2.5.13: (a) Bright field TEM image of pristine $CH_3NH_3PbI_3$ thin film at room temperature. A stripe contrast is visible through some of the grains (examples circled in red). (b) Near $_t$-oriented diffraction pattern taken from a grain exhibiting stripe contrast showing two single crystal patterns with a mirrored relationship. Coincident hh2h spots lie along the twin axis with all other spots from the two domains very slightly separated and the separation increasing away from the origin, as seen in the magnified region (solid red rectangle) in (c). (d–f) The same region as that in (a) and (b) but after extended electron beam exposure. The stripe contrast and 'split' spots are gone. All indexes are in the tetragonal phase.

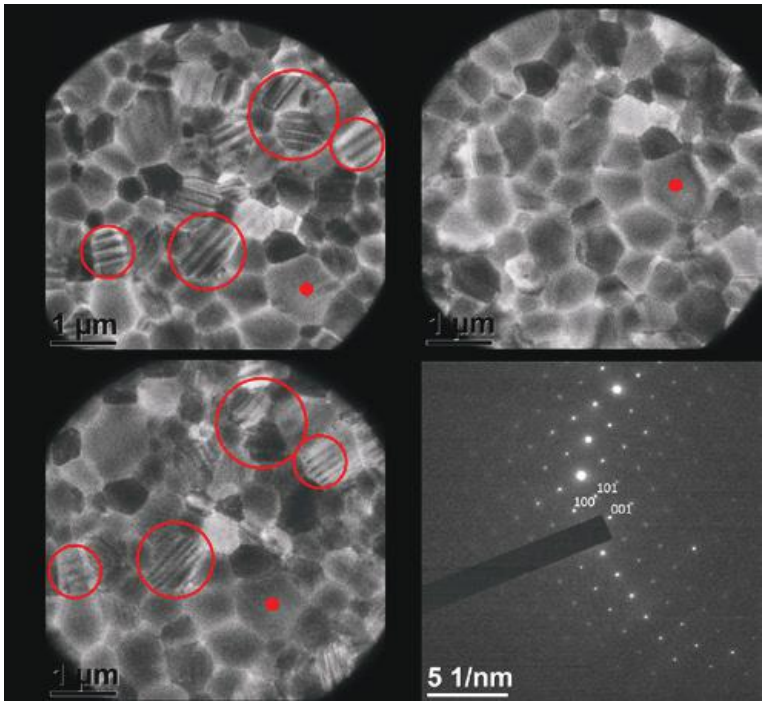

Figure PP2.5.14: (a–c) BF TEM images of the same area at the same orientation in a $CH_3NH_3PbI_3$ thin film (a) at room temperature, (b) sample holder heated to 70 °C for 10 minutes, and (c) cooled down to room temperature again. The same grain in these images is marked with a red dot as a reference for comparison. All of the striped twin domains disappear upon heating beyond the tetragonal-to-cubic transition temperature. Some twin domains reappear when the film is cooled to room temperature again, with some domains showing the same striped pattern as before heating (red circles). (d) SAED pattern from a grain at 70 °C showing no periodic diffraction spot "splitting" and thus no twinning. All indexes in (d) are in the cubic phase.

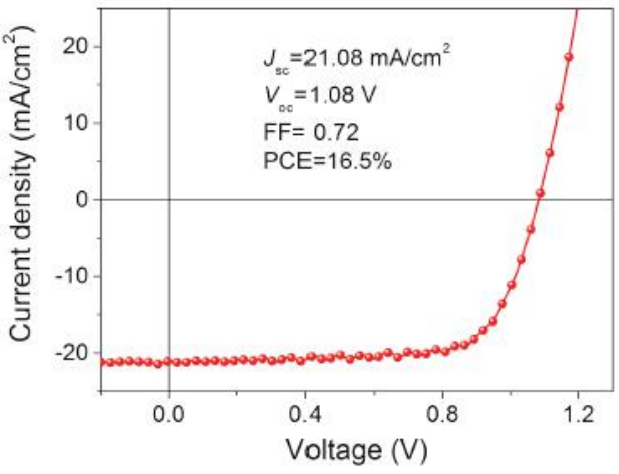

Figure 1 PP2.5.15: Current density–voltage (*JV*) curve under 1 sun illumination of the hero device with triarylamine/ITO anode.

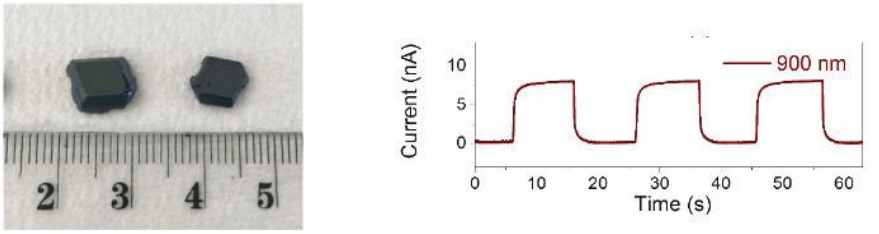

Figure PP2.5.16: (Left) $CH_3NH_3PbI_3$ single crystals. (Right) The below gap device performance of a single crystal organohalide perovskites photoresistor comprised of a $CH_3NH_3PbI_3$ photoresistors measured with a reverse bias of 0.5 V. The light intensity used for characterisation of the responsivity and photoresponse was kept at 0.2 mW cm^{-2}.

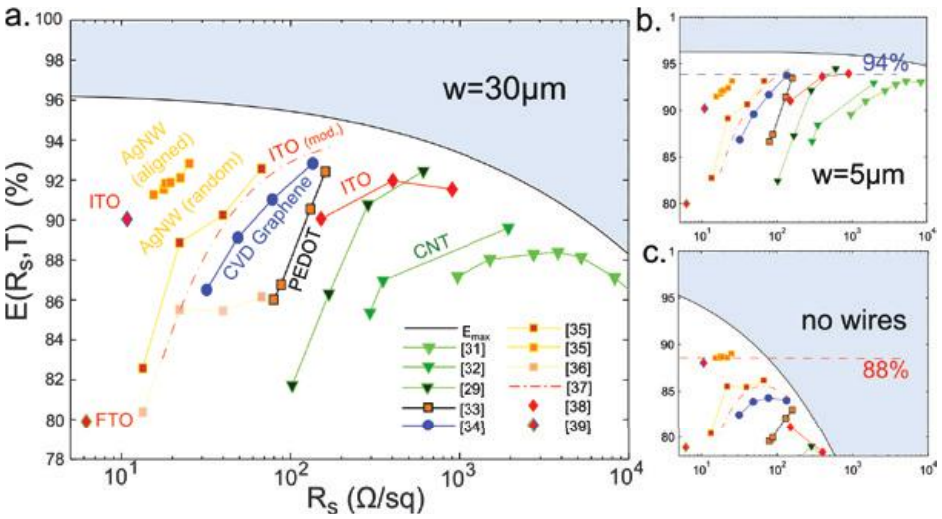

Figure PP2.5.17: Plots of the efficiency factor E calculated using experimental (R_s,T) data from the literature with varying wire thickness.

At UQ, an improved process for interlayer creation that involves the UV-ozone treatment of indium tin oxide (ITO) before deposition of the p-type material has been developed. The surface was found to be sufficiently hydrophilic to enable the deposition of a good quality perovskite layer for an "inverted" ITO/p-interlayer/$CH_3NH_3PbI_3$/PC60BM/LiF/Ag cell. Using the new interlayer deposition method it was possible to improve the average V_{OC} from 0.73 ± 0.25 V (bare ITO) to 1.02 ± 0.03 V. The highest V_{OC} reached 1.08 V and the champion cell delivered a power conversion efficiency (PCE) of 16.5 % with a J_{SC} of 21.08 $mAcm^{-2}$ and FF of 0.72 (see Figure PP2.5.15). The UQ team has also exploited the surface defects of perovskites to develop photodiode and photoresistor architectures with a sub-optical gap response (see Figure PP2.5.16) (Lin et al., 2016).

Team ANU also demonstrated the impact of metallisation on transparent conductor requirements, and in particular the crucial parameter of finger width (Jacobs et al., 2016b). It has been found that the usual requirement of 10 Ω/sq can be dramatically relaxed if the printing and embedding of wire widths below 30 mm becomes economical (see Figure PP2.5.17).

Organic hole transport materials (HTM) are commonly used in high efficiency hybrid organic-inorganic (perovskite) solar cells. Additives are typically added into these HTMs for improving cell performance making the cells but causing them to become more sensitive to moisture and oxygen resulting in low stability of device performance in the longer term. The team at Monash have investigated the use of inorganic hole transport materials such as CuSCN to improve stability and to reduce the cost of perovskite solar cells. The major obstacle for the application of CuSCN in planar structured devices is the solvent-induced damage of commonly used propyl sulphide on the perovskite film during the deposition of the HTM. A novel method of deposition was introduced to avoid this damage. A chlorobenzene layer was introduced onto the perovskite film before dropping the propyl sulphide solution that contained CuSCN. Rapid doctor blading under conditions that supported the evaporation of the solvent was continued until a thin layer of CuSCN was formed. A record performance of 9.6% was achieved for the planar CuSCN-based perovskite solar cells (see Figure PP2.5.18). According to the literature the J-V hysteresis has also been found to be dependent on the characteristics of the electron transport material adjacent to the perovskite film. In the study with the CuSCN layer, the J-V hysteresis was observed to be dependent on HTM. The J-V hysteresis phenomenon was studied using devices based on CuI, CuSCN and spiro-OMeTAD (see Figure PP2.5.19). Open circuit voltage decay (OCVD) provided insight into the slow process in the device and its dependence on the HTM (Sepalage et al., 2017). It is proposed that among the other factors, the deposition

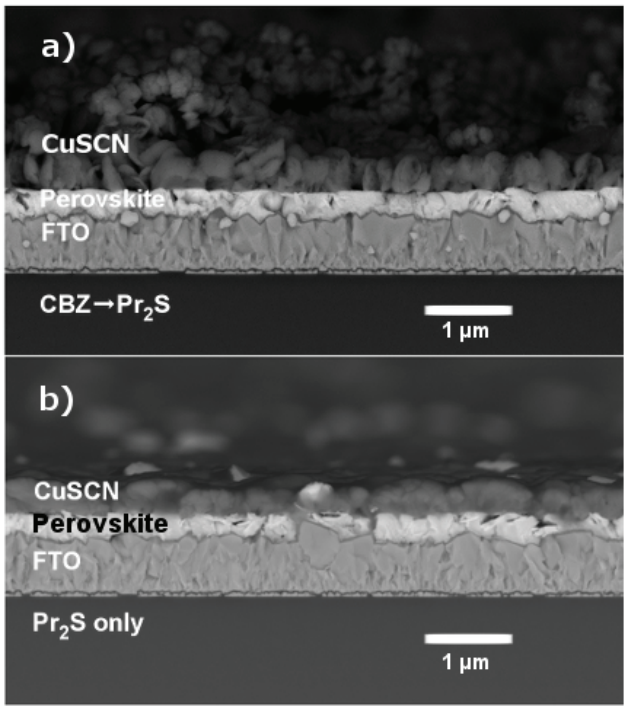

Figure PP2.5.18: Cross section images of perovskite solar cells made using different deposition techniques. (a) Novel deposition technique involving chlorobenzne (CBZ) and propyl sulphide (Pr_2S), (b) Method involving Pr_2S only.

technique and its impact on the interface of perovskite/HTM also affects the J-V hysteresis. This was supported by the observation of different magnitudes of J-V hysteresis of the CuI- and CuSCN-based devices despite their similar physicochemical properties. A combination of ion migration and defect assisted charge trapping may be the reason for J-V hysteresis.

At Monash, a novel architecture for quasi-interdigitated electrodes (QIDEs) has been developed which allows for the fabrication of back-contacted perovskite solar cells. The devices showed a stable power output of 3.2%. The design of the QIDEs avoids the defects that cause short-circuiting in conventional IDEs, while enhancing the collection area of the electrodes (see Figure PP2.5.20) (Jumabekov et al., 2016).

Lead-free perovskites

The team at ANU with collaborators at NTU, have worked on the development of a rubidium-based layered antimony perovskite. A simple solution process was developed to fabricate the layered antimony perovskite with the structure $A_3Sb_2I_9$ (see Figure PP2.5.21) (Harikesh et al., 2016). The study demonstrated that a smaller cation like rubidium can effectively stabilise the structure in its layered form. These findings may also be extended to lead-based perovskites to stabilise other reported unstable structures and to unlock a less explored genome of inorganic perovskites. The findings from cathodoluminescence prove the need for carefully tuned fabrication methodologies in antimony-based and other lead-free materials to obtain materials very close to stoichiometry as these may not be as tolerant to defects as lead (see Figure PP2.5.21) (Harikesh et al., 2016).

Device durability

The team at Monash have reported a new characterisation protocol of multiple 12-hour cycles of darkness and illumination, uncovering unique "fatigue" behaviour of perovskite solar cells. It is found that the cells' efficiencies decrease to 50% or less of the maximum value after storage in the dark for 12 hours under open circuit conditions. The solar cell performance was capable of recovering to its maximum value in the subsequent 12-hour illumination period, but the recovery rate slowed significantly with successive illumination/darkness cycles (see Figure PP2.5.22). This fatigue mechanism was strongly dependent on the cell temperature. The identification of this fatigue behaviour calls for the reported characterisation protocol to be an essential component of perovskite solar cell testing (Huang et al., 2016).

In other work, a novel strategy to improve the stability of perovskite materials and devices has been developed at Monash, by mixing diammonium (ethane-1,2-diammonium, EDA) and (methylammonium, MA) cations for mixed cation perovskites (see Figure PP2.5.23). Systematic tuning of the morphology, electronic structure, light absorption and photoluminescence properties was achieved by changing the stoichiometry of the diammonium ratio in the perovskite precursor. After optimisation, cells based on EDA/MA mixed cation perovskite reached 18.14% for the small area devices (aperture, 0.16 cm²) and 15.15% for the large area devices (aperture, 1.04 cm²) under 1 sun. In particular, the mixed cation perovskite films exhibited much improved stability at ambient conditions. The EDA2+/MA+-based perovskite solar cells lose only one-fourth of the initial PCE over 72 hours of operation at 50% relative humidity and 51°C under continuous 1 sun illumination, whereas the efficiencies of the $MAPbI_3$ devices degrade by more than 80% within the initial 15 hours of tests (see Figure PP2.5.24) (Sheng et al., 2015).

Tandem

One advantage of perovskites is that their bandgap can be tuned by varying the composition. Higher bandgap perovskites can be used as a "top" sub-cell for multi-junction thin-film tandems. At UNSW, the team is building on previous work of a higher bandgap device (e.g., $MAPbBr_3$ (Sheng, et al. 2015) (V_{OC}=1.45V) by vapour-assisted deposition and $CsPbIBr_2$ (Ma et al., 2016) using dual source thermal evaporation) and have now demonstrated a 7% $CsPbIBr_2$ device by spray-assisted deposition (Lau et al., 2016). The process involves the spraying of CsI on $PbBr_2$-coated-substrate followed by annealing of the $CsPbIBr_2$ film. It is demonstrated

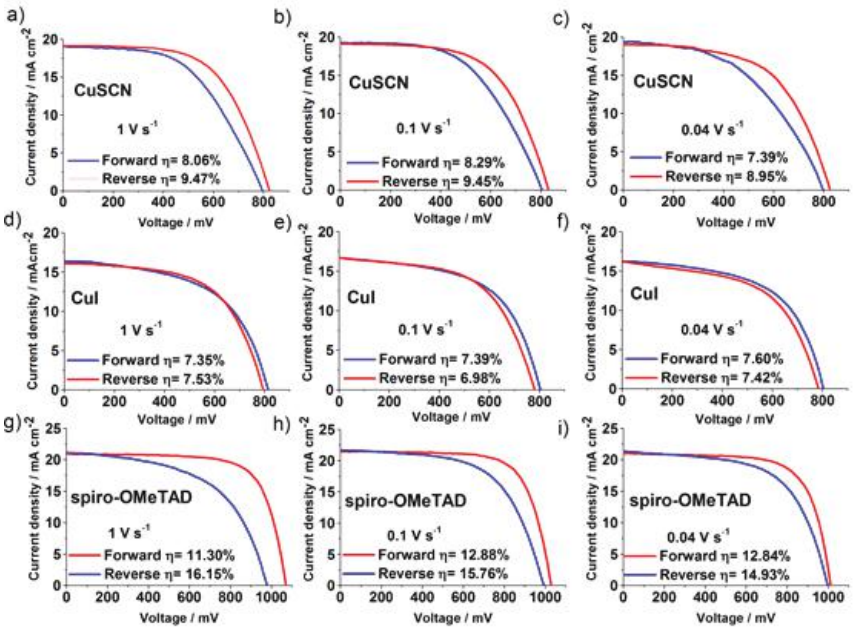

Figure PP2.5.19: Comparison of J-V hysteresis of different HTM-based devices at different scanning directions and rates.

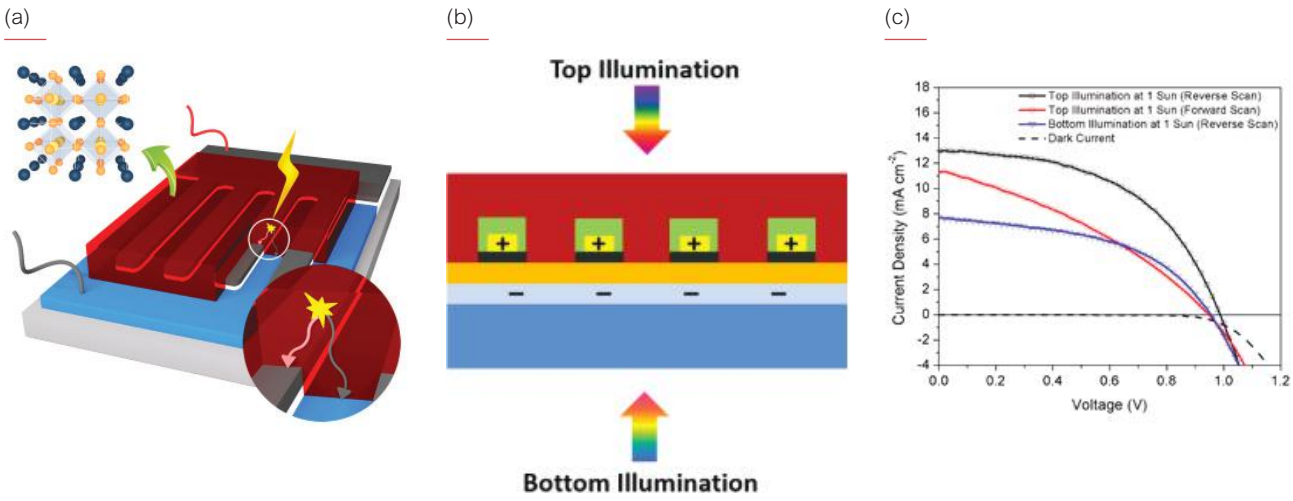

Figure PP2.5.20: (a) Illustration of back-contact perovskite solar cell. (b) Schematic of quasi-inter-digitated contacting scheme. (c) J–V characteristics of the back-contacted perovskite solar cell.

that both steps can be successfully conducted in air. This sequential processing of the $CsPbIBr_2$ film, overcomes the solubility problem of the bromide ion in the precursor solution that would otherwise occur in a single-step solution process. The higher bandgap (2.05 eV) $CsPbIBr_2$ film is thermally stable at 300°C and therefore can withstand more subsequent processes at elevated temperatures, e.g. for tandem cell fabrication. Figure PP2.5.25 shows the results of the study of the effects of substrate temperature during spraying, annealing temperature, and after optimisation of device performance.

Commercial prospects, up-scaling and manufacturing costs

At ANU, work has started on optimising fabrication processes to obtain uniform films for larger perovskite solar cells. PL imaging is employed to study the uniformity of the perovskite films deposited by a modified sequential and single-step deposition (see Figure PP2.5.26).

At UQ, through the application of optical modelling and in-house transparent conducting electrode deposition it was found that 2 cm² devices could be prepared with a reduced loss of efficiency relative to small laboratory test devices. Using the in-house higher conductivity (lower sheet resistance ~10 Ω/sq) ITO electrodes co-optimised for transmittance (thickness 135 nm), the team demonstrated a hero 2 cm² perovskite solar cell measured in a two-wire configuration with a scan averaged PCE of 12.4%, with J_{SC} = 20.4 $mAcm^{-2}$, V_{OC} = 1.02 V, and an improved FF of 0.61 (see Figure PP2.5.27). Compared with the large area devices on commercial

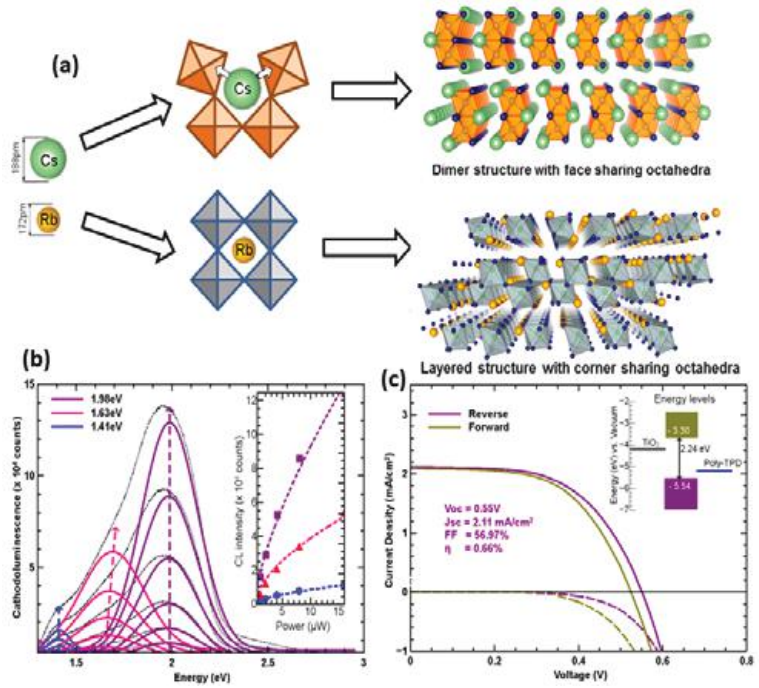

Figure PP2.5.21: (a) Schematic showing the influence of A (Cs, Rb) cation size on the structure of $A_3Sb_2I_9$, (b) variation of cathodoluminescence with fixed accelerating voltage (5 kV) and varying excitation power (in log scale). I_b is the beam current and I_{CL} is the CL intensity, (c) I–V curve under forward and reverse scans of the best device with the energy levels of $Rb_3Sb_2I_9$ shown in inset.

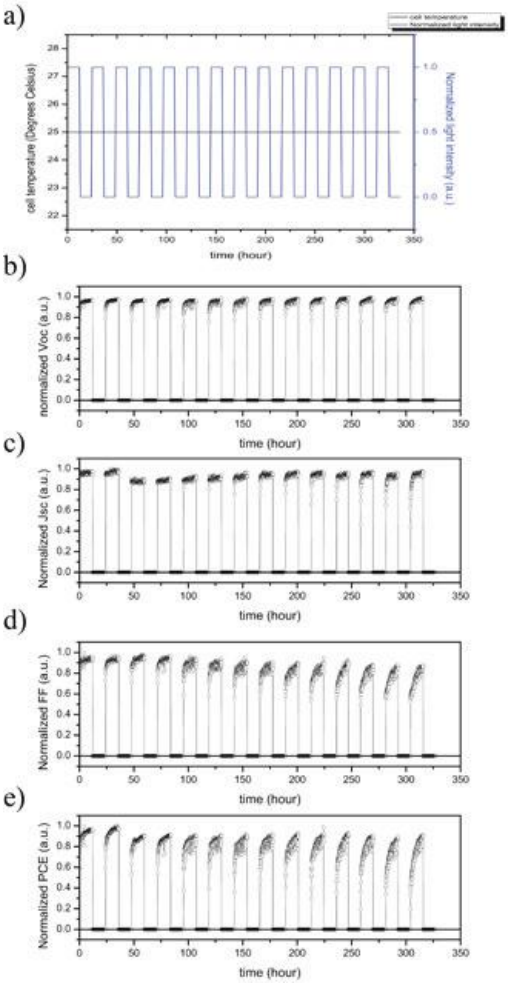

Figure PP2.5.22: Fatigue behaviour of planar $MAPbI_3$ perovskite solar cells.

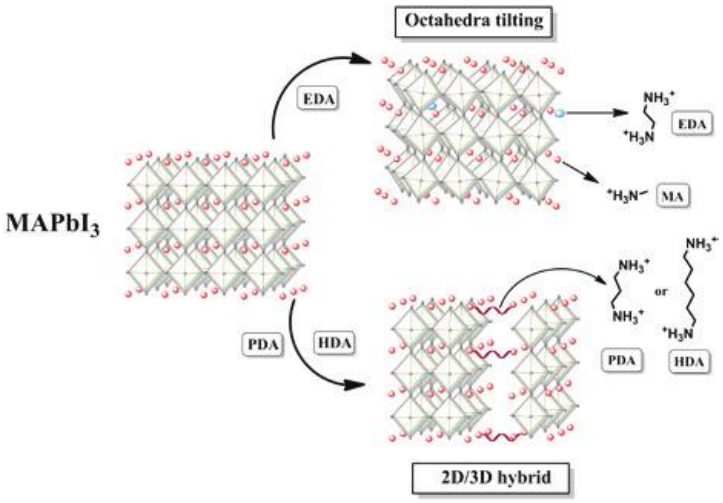

Figure PP2.5.23: Illustration of the role of di-ammonium cation in the mixed cation perovskite structure.

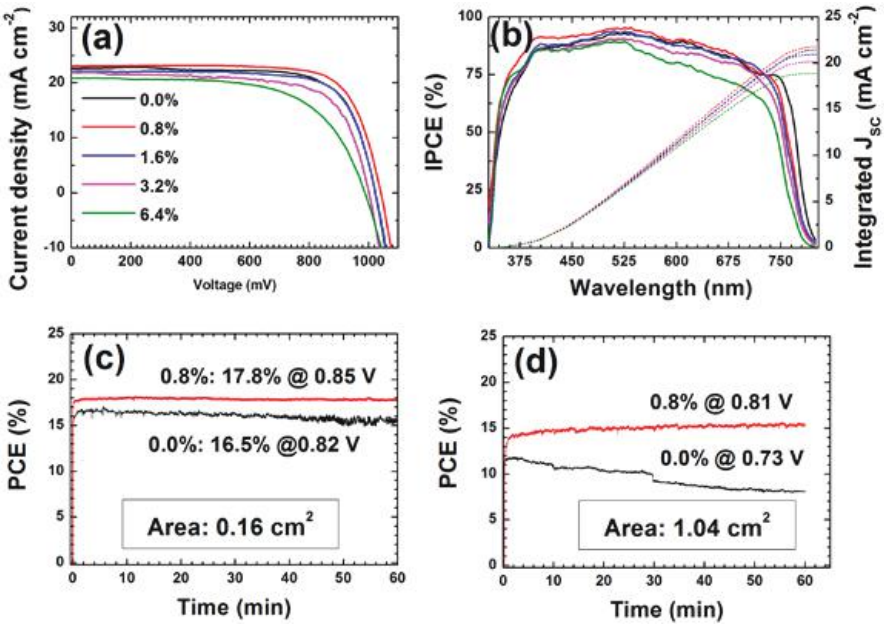

Figure PP2.5.24: The stability behaviour of mixed cation and $MAPbI_3$ only perovskite solar cells.

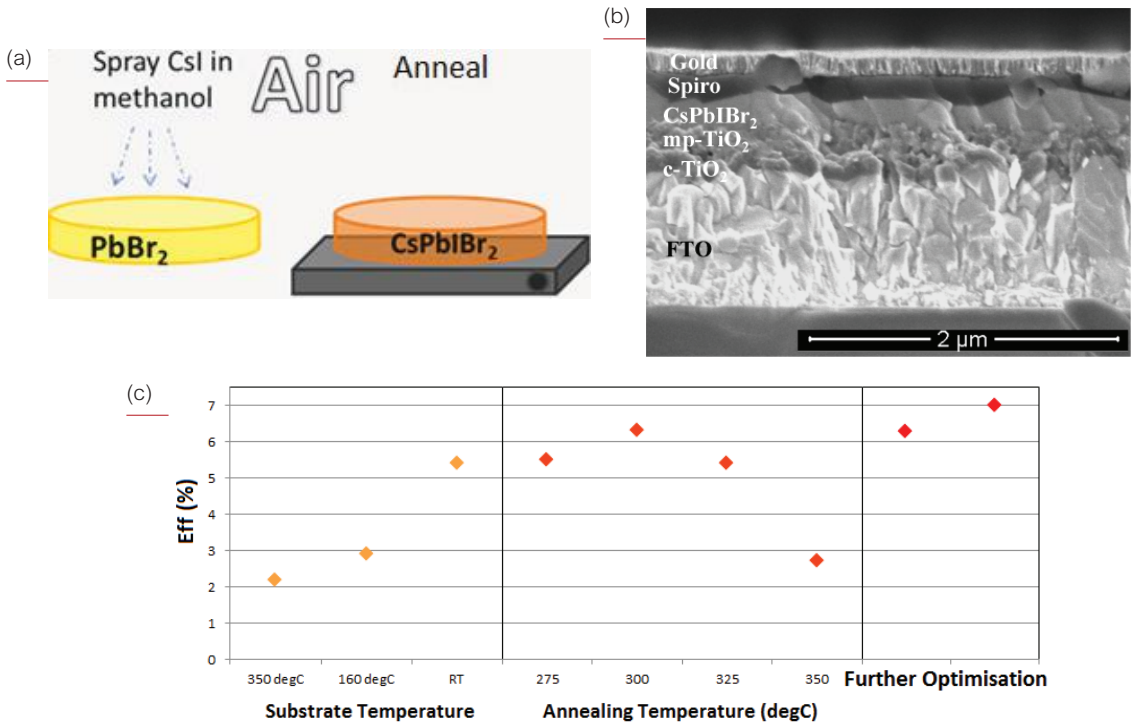

Figure PP2.5.25: (a) Schematic of process used to fabricate $CsPbIBr_2$ film. (b) Cross-sectional SEM image of an Au/spiro-OMeTAD/$CsPbIBr_2$/mp-TiO_2/bl-TiO_2/FTO device. (c) Cell efficiencies versus substrate temperature during spraying, annealing temperature and perovskite film thickness.

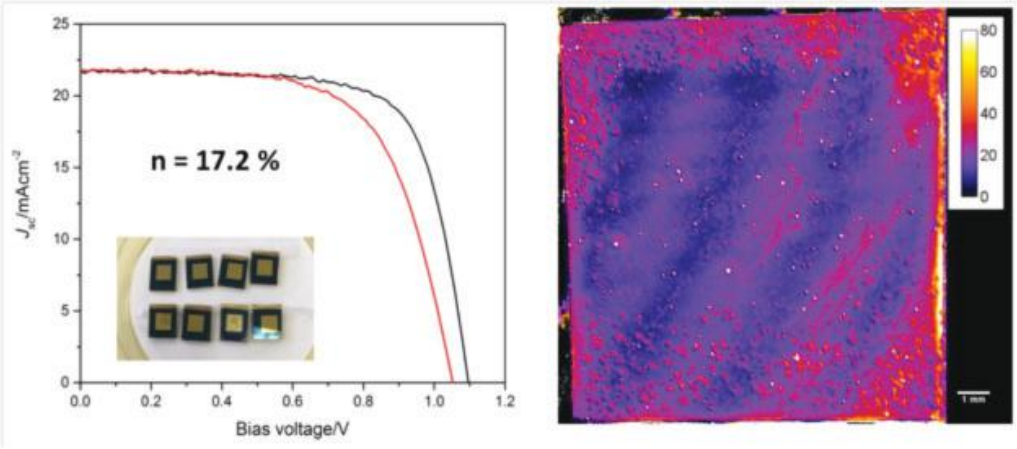

Figure PP2.5.26: J-V plots of large area (1cm^2) devices fabricated at ANU, PL imaging (right) is used to check the uniformity of the films.

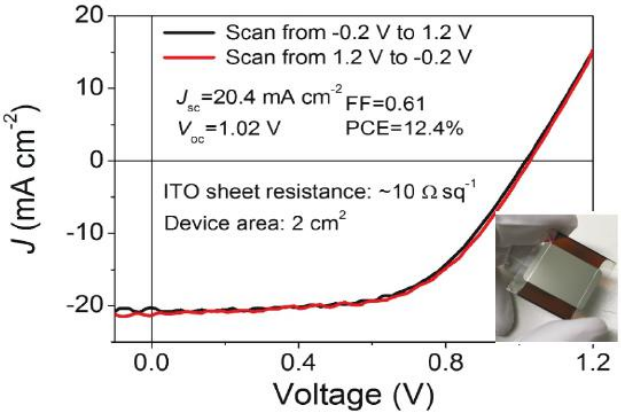

Figure PP2.5.27: Device performance of 'hero' large area (2 cm^2) solar cells: *JV* curves (forward scan from -0.2 V to 1.2 V and reverse from 1.2 V to -0.2 V with a scan rate of 0.2 V s^{-1}, measured with a two-wire configuration). Inset: Picture of cell.

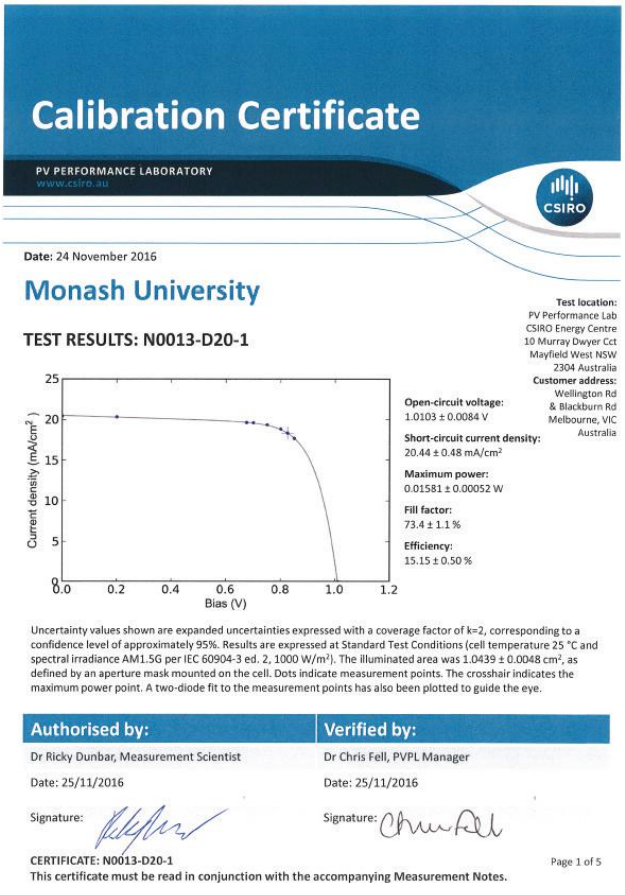

Calibration Certificate

PV PERFORMANCE LABORATORY
www.csiro.au

CSIRO

Date: 24 November 2016

Monash University

Test location:
PV Performance Lab
CSIRO Energy Centre
10 Murray Dwyer Cct
Mayfield West NSW
2304 Australia

Customer address:
Wellington Rd
& Blackburn Rd
Melbourne, VIC
Australia

TEST RESULTS: N0013-D20-1

Current density (mA/cm^2)
Bias (V)

Open-circuit voltage:
1.0103 ± 0.0084 V

Short-circuit current density:
20.44 ± 0.48 mA/cm^2

Maximum power:
0.01581 ± 0.00052 W

Fill factor:
73.4 ± 1.1 %

Efficiency:
15.15 ± 0.50 %

Uncertainty values shown are expanded uncertainties expressed with a coverage factor of k=2, corresponding to a confidence level of approximately 95%. Results are expressed at Standard Test Conditions (cell temperature 25 °C and spectral irradiance AM1.5G per IEC 60904-3 ed. 2, 1000 W/m^2). The illuminated area was 1.0439 ± 0.0048 cm^2, as defined by an aperture mask mounted on the cell. Dots indicate measurement points. The crosshair indicates the maximum power point. A two-diode fit to the measurement points has also been plotted to guide the eye.

Authorised by:	Verified by:
Dr Ricky Dunbar, Measurement Scientist	Dr Chris Fell, PVPL Manager
Date: 25/11/2016	Date: 25/11/2016
Signature:	Signature:

CERTIFICATE: N0013-D20-1
This certificate must be read in conjunction with the accompanying Measurement Notes.

Page 1 of 5

Figure PP2.5.28: Certification from CSIRO confirming power conversion efficiency for a 1.0 cm^2 device.

ITO electrodes, there was an almost 30% improvement in terms of PCE (Lin et al., 2017). In addition, perovskite devices with an aperture area of 25 cm² without relying on an interconnected strip design, making them more compatible with the c-Si cell geometry, have been manufactured and tested. Using aluminium grid lines with a thin aluminium oxide layer (produced using a simple plasma exposure) improved the wetting and film forming of the organohalide perovskite junction on top of the lines. The best devices employing these modified grids achieved power conversion efficiencies of up to 6.8% (Hambsch et al., 2016).

At Monash, a planar device using mixed EDA/MA ions has been certified by CSIRO PV Performance Laboratory at 15% efficiency on 1 cm² (see Figure PP2.5.28).

At UNSW, the team has developed a modified solution process that allows uniform perovskite films to be deposited over a large area (see Figure PP2.5.29). Following on the work from UQ, the effect of using metal grids in reducing series resistance of large area cells has been modelled (see Figure PP2.5.30) and verified experimentally (see Figure PP2.5.31). Using these approaches, world record conversion efficiencies were achieved for a 16 cm² single monolithic 12.1% efficient perovskite solar cell independently certified by Newport Corporation, Bozeman, Montana. In addition, an independently certified efficiency of 18.1% has been achieved for a 1.2 cm² cell. This is the largest certified perovskite cell at that energy conversion efficiency. As part of this work, a 16 cm² 4-parallel-cell module is also certified at 11.5% efficiency (see Figure PP2.5.32).

At CSIRO, an alternative hole transport layer has been developed that is suitable for printing. Bifluo-OMeTAD is used in the two-step printing of perovskite devices on glass in air. A PCE at 14.4% can be achieved for 0.1 cm² devices on glass that are printed in air. A PCE at 9.4% has been achieved on a larger 1 cm² device on glass. In this work, additives are also used to control morphology (see Figure PP2.5.33), for sequential deposition of the perovskite (see Figure PP2.5.34(a)), which requires careful matching of the perovskite conversion rate to print speed. For large-scale processing, a one-step perovskite deposition is preferred over a two-step perovskite process as the former is a simpler and faster process (see Figure PP2.5.34(b)). The challenge is to ensure the deposition process is air-stable. By mixing the cations and halides in the perovskites, a 0.1 cm² test device with the structure glass/ITO/PEDOT/perovskite/PCBM/Al deposited by a one-step spin coating process in air achieved a PCE of 12%. Films fabricated by this process have been shown to be stable in air for more than 1.5 months. The CSIRO team has also succeeded in translating the batch-printing (14.4% PCE, 0.1 cm² on glass) to roll-to-roll printing (on flexible substrate) (see Figure PP2.5.35(a)). A PCE at 11% can be achieved on a 0.1 cm² device printed in air on an ITO coated flexible polyethylene terephthalate (PET) substrate (see Figure PP2.5.35(b)). Further optimisation is underway that involves solvent engineering and the use of polymer additives. CSIRO has also upgraded its characterisation capability to allow measurement of an un-encapsulated large-scale flexible perovskite device inside a glove box. Other collaboration work includes interface de-lamination testing by Stanford University (Rolston et al., 2016) and fracture and encapsulation

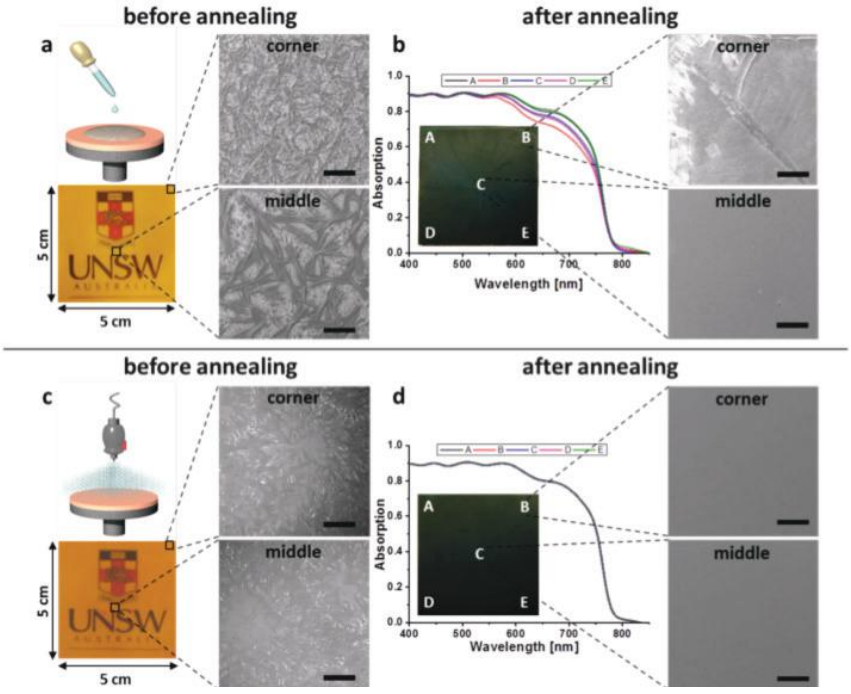

Figure PP2.5.29: Perovskite film on 5cm by 5cm FTO substrate. Schematic illustration, optical image and SEM images (at corner and centre positions) of film fabricated using the (a) conventional solution process and (c) modified solution process before annealing. (b) and (d) Optical image, SEM images (at different positions) and UV-visible absorption measurement (spot size of 0.45cm^2) of samples in (a) and (c) after annealing at 100 °C for 20 mins. The scale bar in SEM images is 150 μm.

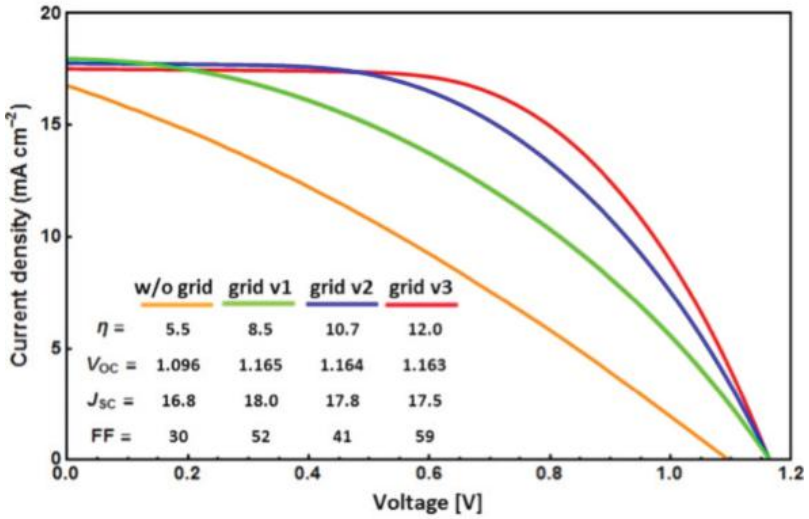

Figure PP2.5.30: Modelled J-V curves for a 16.0 cm^2 cell with different grid designs. The drop in J_{SC} is predominantly due the shading incurred through the use of a grid. The increase in FF due to reduced R_S results in improved efficiencies.

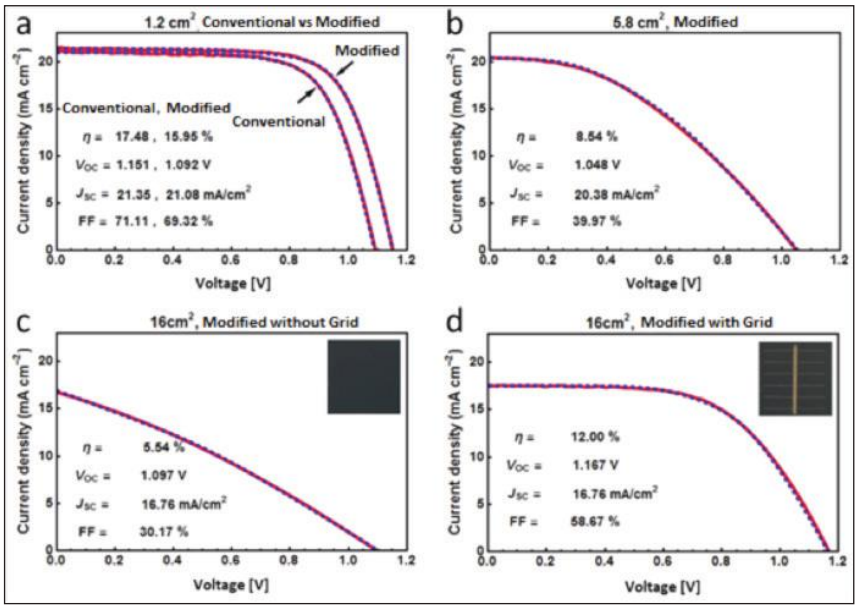

Figure PP2.5.31: The current density-voltage (J-V) curves for the best performing (a) 1.2 cm^2 devices using conventional and modified methods, (b) 5.8 cm^2 and (c) 16.0 cm^2 devices by modified process without a metal grid, and (d) 16.0 cm^2 device by modified process with a metal grid. Inset images in (c) and (d) are optical images of the devices. Dotted lines are fitted light J-V curve through "three-diode, two-cell" model.

Figure PP2.5.32: Certifications from Newport confirming power conversion efficiencies for (a) 1.2 cm^2 cell at 18.04%; (b) a singe 16 cm^2 perovskite cell at 12.1%; (c) a 16 cm^2 4-parallel-cell perovskite module at 11.5 %.

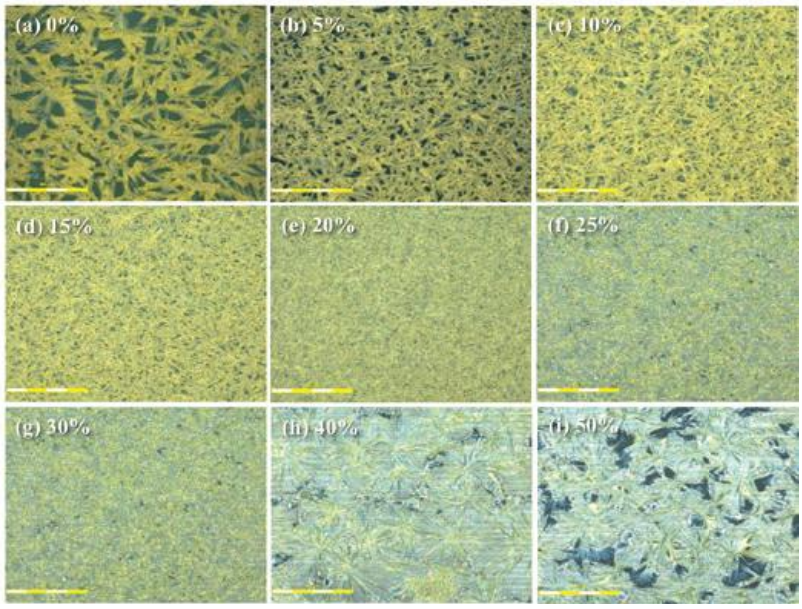

Figure PP2.5.33: Effect of the amount of additive on the morphology of printed perovskite film.

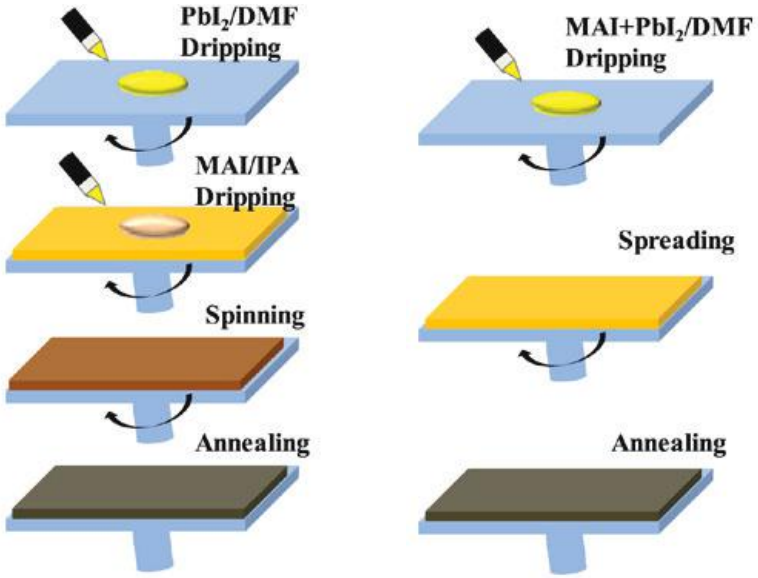

Figure PP2.5.34: Illustrations for (a) sequence deposition and (b) 1-step perovskite deposition processes.

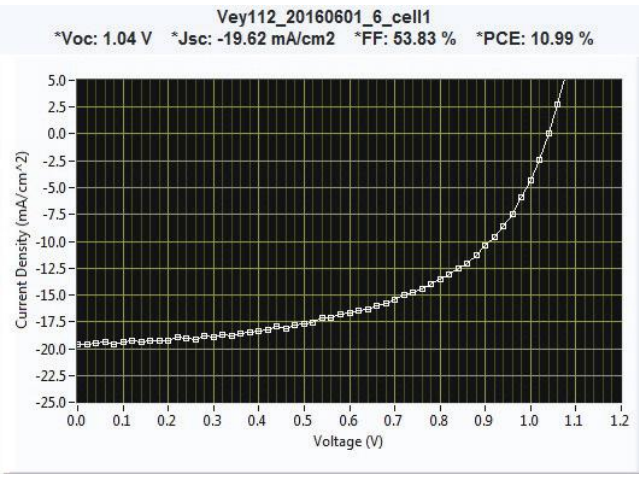

Figure PP2.5.35: (a) Tool used for roll-to-roll printing of perovskite solar cell on flexible substrate. (b) I-V curve of perovskite device roll-to-roll-printed on flexible substrate

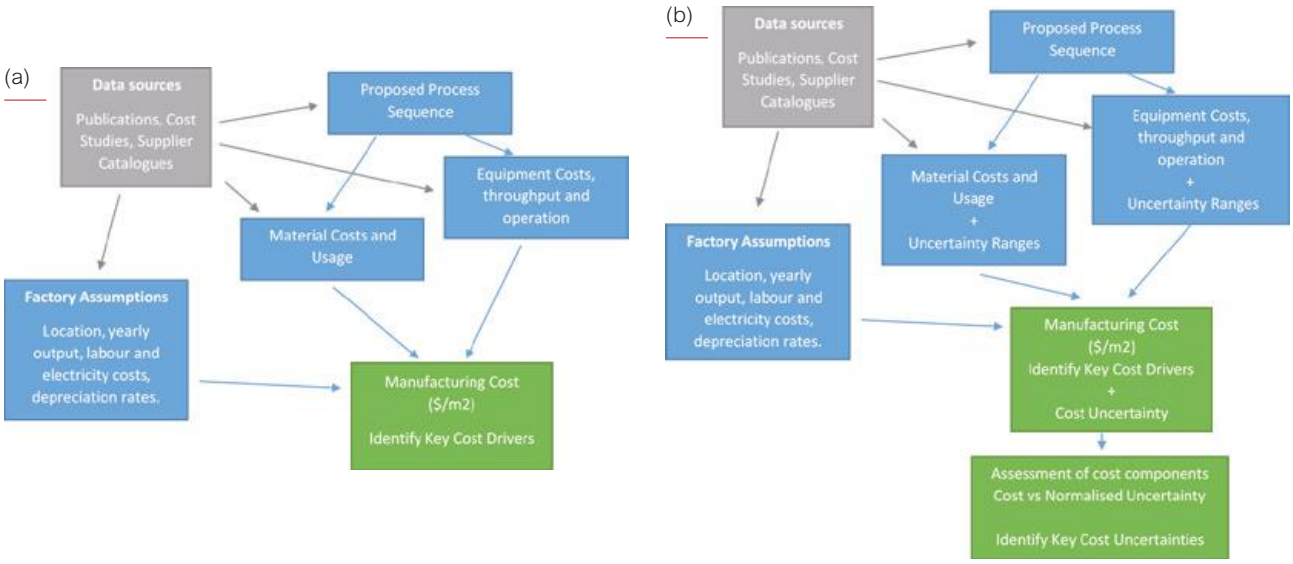

Figure PP2.5.36: An overview of (a) our costing process, and (b) our costing and uncertainty analysis process

A	B	C	L1	L2	Process Description	Equipment	Major materials
X	X	X	X		FTO Glass Receipt		FTO Glass
X	X				FTO patterning.	Laser	
X	X	X	X		Glass Cleaning	In-line glass Washer	acetone, ethanol, DI water
X	X				Sacrificial metal mask	Screen printer	Silver paste
X	X	X			TiO_2 Spray Pyrolysis	Spray pyrolysis tool	TAA, acetylacetone, ethanol
X	X				Chemical lift off	Chemical etch bath	HCl, DI water
		X	X		Pattern FTO and TiO_2	Laser	
X	X	X			Scaffold Print	Screen printer	TiO_2 ink, terpineol, ethylcellulose
X	X	X			Perovskite PbI_2 coat	Blade coater	PbI_2, DMF
X	X	X	X		Laser pattern PbI_2	Laser	
X	X	X			Dip coat MAI	Dip coater	MAI, isopropanol
X	X	X			Coat HTM	Blade coat	P3HT, chlorobenzene, Li-TFSI, tert-butylpyridine
X	X	X	X		Laser pattern HTM	Laser	
X					Evaporation of Gold contact	Evaporator	Gold, masks
	X	X			Evaporation of Silver contact	Evaporator	Silver, masks
X	X	X	X		Ribbon and encapsulate	Laminator and cure.	Ribbon, solder, glass, EVA, edge seal
X	X	X	X		J-box, test and package	Module tester	Junction box, packaging.

Table PP2.5.1 Definitions of process sequences A, B and C, and the two limit sequences L1 and L2. Note that sequence L2 is a 'Free' module, and so there are no processes included in that sequence.

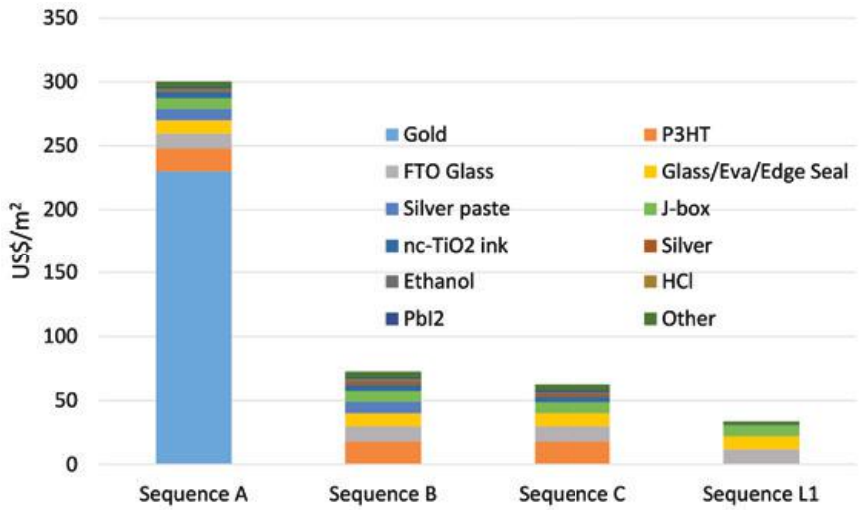

Figure PP2.5.37: Material cost breakdown. Both calculated using nominal input values for sequences A, B, C and L1.

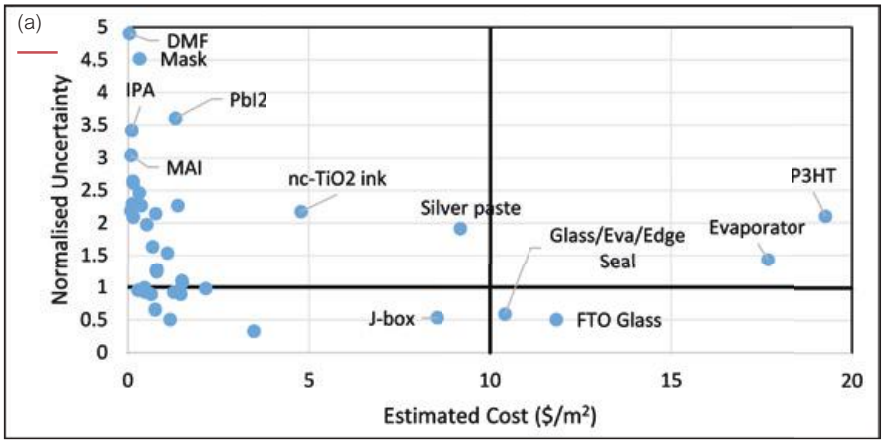

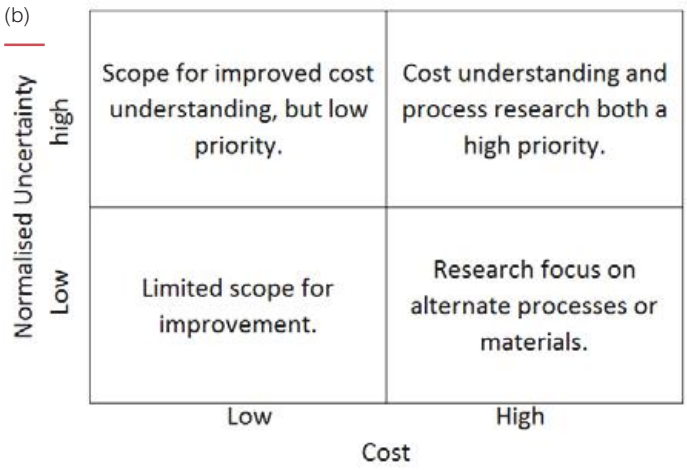

Figure PP2.5.38: (a) The normalised uncertainties as a function of median cost for the main cost components of sequence B, divided into four regions by solid black lines, and (b) the categorisation of different research priorities for each region.

	Seq B	Seq C	L1
10^{th} Percentile	100 (116)	87 (101)	42 (48)
Median	123 (142)	107 (126)	47 (54)
90^{th} Percentile	158 (183)	140 (162)	54 (61)

Table PP2.5.2 Total module cost (and minimum sustainable price) and uncertainty in $/m².

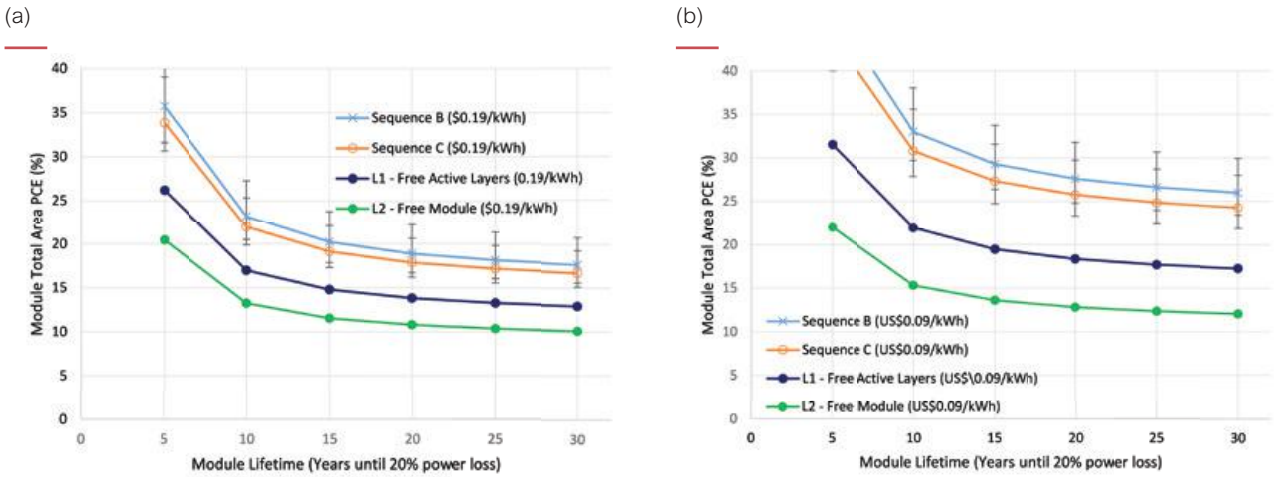

Figure PP2.5.39: (a) Required module total area PCE and as a function module lifetime for 2015 residential LCOE levels $0:19/kWh) for sequence B (blue), C (orange), L1 (dark blue) and L2 (green). (b) Required module total area PCE and as a function module lifetime for 2020 Sunshot LCOE targets ($0:09/kWh) for sequence B (blue), C (orange), L1 (dark blue) and L2 (green).

testing by Georgia Institute of Technology on CSIRO's printed flexible devices.

At UNSW, a method has been developed to estimate the manufacturing cost for evaluating the early stage of technology development (see Figure PP2.5.36), delivering both the manufacturing cost estimate as well as an uncertainty analysis that quickly highlights the opportunities for greatest cost improvement (see Figures PP2.5.37 and PP2.5.38) (Chang et al., 2017). This method has been applied to evaluate the costs of three process sequences for the large-scale production of organic-inorganic hybrid perovskite photovoltaic modules (see Table PP2.5.1). A process sequence (Seq C) that combines two demonstrated perovskite module sequences is estimated to cost $107/m² (uncertainty range $87 to $140/m²) (see TablePP2.5. 2), which is comparable with commercial crystalline silicon and cadmium telluride technologies (on a $/m² basis). A levelised cost of electricity calculation shows that this perovskite technology would be competitive in 2015 with incumbent photovoltaic technologies if a module power conversion efficiency of 18% and lifetime of 20 years could be achieved. Further analysis shows that if the cost of the active layers and rear electrode were reduced to zero (Seq L1), a module power conversion efficiency of 18% and lifetime of 20 years would be required to meet the 2020 SunShot levelised cost of electricity targets (see Figure PP2.5.39).

Other aspects

At UNSW, a life cycle assessment on perovskite solar cells and perovskite/Si tandems was carried out (Lunardi et al., 2017) with the aim of guiding research efforts towards cell designs with minimum environmental impact according to these criteria: global warming, human toxicity, freshwater eutrophication and ecotoxicity and abiotic depletion potential impacts and energy payback time. It is found that the replacement of the metal electrode with indium tin oxide or a metal grid reduces the environmental impacts significantly. Al, compared to Ag and Au gives better environmental outcomes, including energy payback time. The avoidance of using 2,2',7,7'-tetrakis(N,N-di-p-methoxyphenylamine)9,9'-spirobifluorene (Spiro-OMeTAD) and the reduction of solvent usage are also environmentally beneficial. Better environmental impacts are possible if perovskite materials become transparent and electrically conductive when they fail.

Highlights

We have developed an understanding of the factors limiting the performance of perovskite solar cells, including the origin of hysteresis, and developed models for slow transient response. While some of these responses are reversible due to ion migration and ion accumulation, some are non-reversible due to decomposition of the materials exacerbated by light illumination, voltage bias and the presence of moisture.

Kelvin probe force microscopy (KPFM) has been used to study high performing $(FAPbI_3)1\text{-}X(MAPbBr_3)X$ materials at the grain level revealing the roles of grain boundaries such as charge separation and enhancement of ion migration. The incorporation of excess PbI_2 changes the behaviour of ions at the grain boundaries reducing hysteresis in the JV characteristics.

Advanced transmission electron microscopy (TEM) has been developed to reduce artefacts caused by electron beam damage and make it a useful diagnostic tool. As a result, twin domains can be observed using the improved TEM technique and reversible disappearance and appearance of these domains can be observed in situ by varying the temperature allowing attribution of these observations to the cubic <-> tetragonal phase transition.

New contacting strategies (QIDEs), novel use of hole transparent materials (Bifluo-OMeTAD for large-scale printing, inorganic hole transport layers for low cost and better stability) have been demonstrated. A novel diammonium/mono-ammonium mixed cation perovskite has been synthesised producing improved photovoltaic performance and stability compared with the $MAPbI_3$ perovskite.

We have also uncovered the fatigue behaviour of $MAPbI_3$ perovskite solar cells and the importance of using diurnal (illumination) cycling to assess the long-term durability of perovskite solar cells.

Great progress has been made in the demonstration of > 1cm² devices. Various nodes have developed methodologies to fabricate uniform, pinhole free perovskite films for large area perovskite solar devices ranging from 1 cm² to 25 cm² in area. In particular, certified record results have been achieved on 1 cm² cells, 1.2 cm² cells, 16 cm² cells and 16 cm² modules. We have commenced work analysing resistive losses associated with transparent conductor and large area devices.

The translation of batch printing on glass to roll-to-roll printing on flexible substrate has been successful.

A method has been developed to estimate the manufacturing cost for evaluating the early stage of technology development. It has been shown to be an efficient and effective method delivering both the manufacturing cost estimate as well as an uncertainty analysis that quickly highlights the opportunities for greatest cost improvement. Large-scale manufacturing costs of three demonstrated perovskite module processing sequences have been evaluated.

Future Work

- We will link theoretical models to the design of new perovskite materials, predicting the behaviours of material modification, then verification by synthesis of the new materials.

- We will extend our hysteresis, slow response and stability studies from the $MAPbI_3$ perovskites and perovskite devices that were heavily researched in 2016 to other types of perovskites including mixed cation, mixed halide and two-dimensional/three-dimensional hybrid perovskites.
- We will develop further understanding of the roles of inter-layers on cell performance; on stability and on ion migration across the interface.
- We will develop a deeper understanding of the behaviour of mixed anion perovskites under light, electrical bias using luminescence spectroscopy such as photoluminescence, cathodoluminescence and EDX mapping under SEM.
- We will extend the use of KPFM characterisation on other types of perovskite materials and other types of material properties.
- We will expand the use of the TEM to other types of perovskites, particularly stable inorganic ones, as well as further study $MAPbI_3$. It will be of particular interest will be to investigate any correlation between grain orientation and grain performance (in conjunction with the use of KPFM), as well as the impact of annealing conditions on crystal- and microstructure, and individual grain performance using a range of electron microscope-based techniques, such as electron backscatter diffraction analysis (EBSD) and cathodoluminescence. Furthermore, mixed cation and mixed halide perovskites will be studied to characterise the effect the mixing of components has on the crystal- and microstructure. The study of inorganic perovskite films necessitates the development of a reliable method to deposit such films on TEM grids.
- We will develop further understanding of the mechanism behind fatigue behaviour of perovskite solar cells, thereby finding ways to reduce fatigue. We will expand the studies to other types of perovskites and other types of cell structures.

The fatigue behaviour of perovskite solar cells can be studied using photoluminescence and electroluminescence imaging systems. The imaging techniques will also be used for in situ imaging of perovskite films during annealing and for examining film uniformity for fabrication process optimisation.

- We will build on models developed for large area devices and continue to improve the efficiencies of large area devices.
- We will continue to develop fabrication techniques that are scalable.
- We will continue optimisation of printing processes, further scale-up and continue studies on the electrical stability and mechanical integrity of printed devices.

We will continue cost evaluation on roll-to-roll printing.

References

Chang, N. et al., 2017, "A Manufacturing Cost Estimation Method with Uncertainty Analysis and its Application to Perovskite on Glass Photovoltaic Modules", Prog. Photovolt. Res. Appl. Article DOI: 10.1002/pip.2871.

Deng, X. et al., 2016, "Electric field induced reversible and irreversible photoluminescence responses in methylammonium lead iodide perovskite", J. Mater. Chem. C,4, 9060–9068.

Fu, X. et al., 2016, "Photoluminescence study of time- and spatial-dependent light induced trap de-activation in $CH_3NH_3PbI_3$ perovskite films", Physical Chemistry Chemical Physics, 18(32), 22557–22564.

Hambsch, M. et al., 2016, "Efficient, monolithic large area organohalide perovskite solar cells", J. Mater. Chem. A, 4, 13830–13836.

Harikesh, P.C. et al., 2016, "Rb as an Alternative Cation for Templating Inorganic Lead-Free Perovskites for Solution Processed Photovoltaics", Chemistry of Materials, 28(20), 7496–7504.

Huang, F. et al., 2016, "Fatigue behavior of planar $CH_3NH_3PbI_3$ perovskite solar cells revealed by light on/off diurnal cycling", Nano Energy 27 509–514.

Jacobs, D. et al., 2016a, "Modelling of slow transient processes in organo-metal halide perovskites", 2016 International Conference on Numerical Simulation of Optoelectronic Devices (NUSOD).

Jacobs, D.A. et al., 2016b, "A re-evaluation of transparent conductor requirements for thin-film solar cells", Journal of Materials Chemistry A, 4(12), 4490–4496.

Jumabekov, A.N. et al., 2016, "Back-contacted hybrid organic-inorganic perovskite solar cells", J. Mater. Chem. C, 4, 3125.

Kim, Y.C. et al., 2015, "Beneficial Effects of PbI_2 Incorporated in Organo-Lead Halide Perovskite Solar Cells", Adv. Energy Mater., 1502104.

Lau, C.F.J. et al., 2016, "$CsPbIBr_2$ Perovskite Solar Cell by Spray-Assisted Deposition", ACS Energy Lett. 1, 573−577.

Lin, Q. et al, 2017, "Considerations for Upscaling of Organohalide Perovskite Solar Cell"s, Adv. Optical Mater., 5, 1600819.

Lin, Q. et al, 2016, "Near infrared photodetectors based on sub-gap absorption in organohalide perovskite single crystals", Laser Photonics Rev., 10, 1047–1053.

Lunardi, M. et al., 2017, "A life cycle assessment of perovskite/silicon tandem solar cells", Prog. Photovolt. Res. Appl., Article DOI: 10.1002/pip.2877.

Ma, Q. et al., 2016, "Hole Transport Layer Free Inorganic $CsPbIBr_2$ Perovskite Solar Cell by Dual Source Thermal Evaporation", Adv. Energy Mater., 1502202,

Mahboubi Soufiani, A. et al., 2017, "Lessons Learnt from

Spatially Resolved Electro- and Photoluminescence Imaging: Interfacial Delamination in $CH_3NH_3PbI_3$ Planar Perovskite Solar Cells upon Illumination", Adv. Energy Mater., 1602111.

Rolston, N. et al., 2016, "Mechanical integrity of solution-processed perovskite solar cells", Extreme Mechanics Letters, vol. 9, Part 3, 353–358.

Sepalage, G. et al., 2017, "A facile deposition method for CuSCN: Exploring the influence of CuSCN on J-V hysteresis in planar perovskite solar cells", Nano Energy, 32, 310–319.

Sheng, R. et al., 2015, "Methylammonium Lead Bromide Perovskite-Based Solar Cells by Vapor-Assisted Deposition", J. Phys. Chem. C, 119 (7), 3545–3549.

Wu, Y. et al., 2016, "On the Origin of Hysteresis in Perovskite Solar Cells", Advanced Functional Materials, 26(37), 6807–6813.

Yun, J.S. et al., 2016, "Critical Role of Grain Boundaries for Ion Migration in Formamidinium and Methylammonium Lead Halide Perovskite Solar Cells", Adv. Energy Mater., 6, 1600330.

Zhou, Y. et al., 2016, "Numerical analysis of a hysteresis model in perovskite solar cells", Computational Materials Science, 12622–12628, doi:10.1016/j.commatsci.2016.09.010.

PP3 Optics and Characterisation

Overview

Program Package 3, "Optics and Characterisation", targets experimental demonstration that previously accepted theoretical conversion limits can be increased by use of structures that have a high local density of optical states, with particular emphasis on thin-film organic and inorganic solar cells. Of special interest are devices thinner than the wavelength of light where there are opportunities for much stronger absorption of light than would normally be expected from the device thickness involved.

This year, the work previously reported under the heading of PP3.1, methods to characterise the optical and electrical properties of organic and other thin-film Earth-abundant solar cells, has been included in PP2.5, perovskites.

The work reported in PP3.2 studies plasmonic and nanophotonic light trapping for a range of cell structures. These methods are of particular interest for application in thin-film solar cells, where the films are too thin to allow the use of texturing for scattering the light, but might also be applied to wafer cells. Work at ANU and UNSW (PP3.2a) applies diffuse scattering rear reflectors, made by low-cost "Snow Globe Coating" of titanium dioxide particles, to boost cell efficiency by reduction of parasitic absorption. In addition, improved modelling methods were developed to compare plasmonic and textured light-trapping structures on silicon, showing that light trapping up to 96% of the Lambertian ideal may be achieved.

Sections PP3.2c, Plasmonics for Thin Film Photovoltaics, and PP3.2e, Novel Light Trapping in Si-based Solar Cells, are reported with Section 6.21.

A new set of optical constants for silver is now published and freely available online as an Excel file as an outcome of PP3.2d. This work was featured in the research highlights section of *Nature Photonics*. This project is now completed.

Task PP3.2f has developed and applied cutting-edge characterisation techniques for photovoltaics materials. Standard reflection-transmission (R/T) spectroscopy techniques are not sufficiently sensitive to measure the subtle effect of excitonic binding energy on absorption spectra. UNSW had some preliminary results in 2016 from a newly developed, customised system that is three orders of magnitude more sensitive to these spectral changes compared to standard systems. Observation of the very weak excitonic effect on the absorption spectrum of Si at 25°C is promising.

In addition, time- and spectral-resolved photoluminescence spectroscopy are being combined into one system and its capabilities have been extended to gain a better understanding of complex material characteristics. Initial measurements have successfully demonstrated spectral- and depth-resolved two-photon absorption at an excellent optical resolution.

PP3.2 Plasmonic and Nanophotonic Light Trapping

PP3.2a Photoluminescence Spectroscopy

Lead Partner
UNSW/ANU

ANU Team
A/Prof Kylie Catchpole, Dr Tom White, Dr Fiona Beck

ANU Students
Chog Barugkin, The Duong

UNSW Team
Dr Supriya Pillai

Academic Partner
FZ Juelich, Germany

Funding Support
ARENA, ACAP

Aim

- To use photoluminescence spectroscopy (PLS) to quantify nanophotonic light trapping in silicon wafers.
- To incorporate nanophotonic light trapping in solar cells and quantify their performance.

Progress

We have investigated the prototyping and development of a highly reflective dielectric back reflector for application in thin-film solar cells. The back reflector is fabricated by Snow Globe Coating (SGC), an innovative, simple and cheap process to deposit a uniform layer of TiO_2 particles which shows remarkably high reflectance over a broad spectrum (average reflectance of 99% from 500 nm to 1100 nm). We apply the highly reflective back reflector to tandem thin-film silicon solar cells and compare its performance with conventional ZnO:Al/Ag reflector. By using SGC back reflector, an enhancement of 0.5 $mAcm^{-2}$ in external quantum efficiency of the bottom solar cell

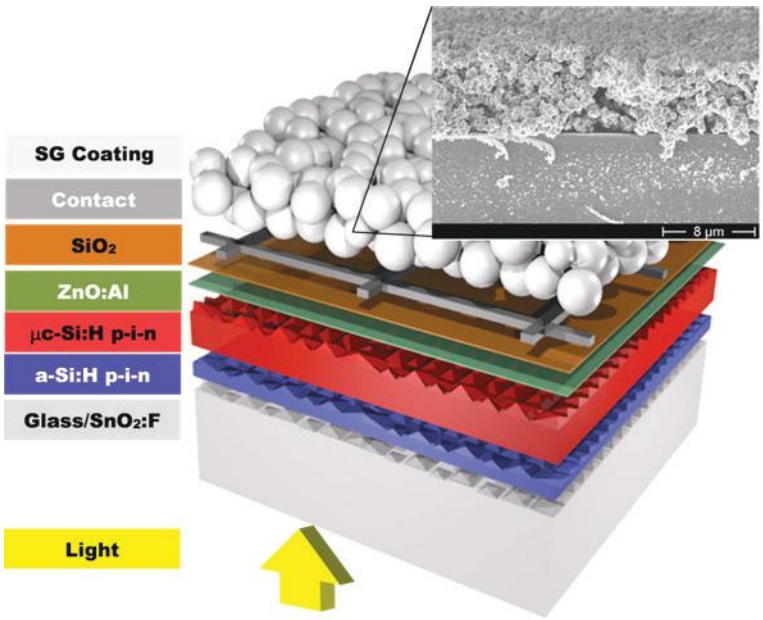

Figure PP3.2a.1: Three-dimensional schematic illustration of tandem thin-film silicon solar cell with hydrogenated amorphous silicon top solar cell and hydrogenated microcrystalline silicon bottom solar cell, deposited on Asahi U-type (SnO_2:F) coated glass substrate (not to scale). The back side structure consists of 80 nm sputtered ZnO:Al and evaporated SiO_2, cross-finger Ag contact and SGC TiO_2 as back reflector. A scanning electron microscopy image of SGC is presented on the top right side of the figure.

and an absolute value of 0.2% enhancement in overall power conversion efficiency are achieved. We also show that the increase in power conversion efficiency is due to the reduction of parasitic absorption at the back contact; that is, the use of the dielectric reflector avoids plasmonic losses at the reference ZnO:Al/Ag back reflector. The SGC process is compatible with other types of solar cells such as crystalline silicon, III–V, and organic photovoltaics. Due to its cost-effectiveness, stability and excellent reflectivity above a wavelength of 400 nm, it has high potential to be applied in industry.

Pigment-based diffuse reflectors (DRs) have several advantages over metal reflectors such as good stability, high reflectivity and low parasitic absorption. As such, DRs have the potential to be applied on high efficiency silicon solar cells and further increase the power conversion efficiency. In order to understand the potential of DRs for high efficiency silicon solar cells, we have combined PLS with a model incorporating the impact of front reflection, rear absorption and the angular distribution on the useful light absorption in silicon wafers. We have shown that plasmonic and textured light-trapping structures on silicon can achieve 96% of Lambertian light trapping.

Highlights

- Improved efficiency for thin-film silicon solar cells with a diffuse scattering rear reflector.
- Quantitative comparison of plasmonic and textured light-trapping structures on silicon, and 96% of Lambertian light trapping achieved.

Future Work

The future aims are to use optical design to minimise losses in perovskite-based solar cells and to use PLS measurements to quantify the quality of perovskite materials.

References

Barugkin, C., et al., 2016, “Highly Reflective Dielectric Back Reflector for Improved Efficiency of Tandem Thin-film Solar Cells”, Internat. J. Photoenergy, Vol. 2016, Article ID 7390974, http://dx.doi.org/10.1155/2016/7390974

Barugkin, C., et al., 2017, “Diffuse reflectors for improving light management in solar cells: a review and outlook”, J. Opt. 19, 014001

PP3.2d Optical Constants of Silver

Lead Partner
UNSW

UNSW Team
Dr Supriya Pillai, Dr Yajie Jiang, Prof Martin A. Green

Funding Support
ACAP, ARENA, UNSW

Aim

The data on the optical constants of silver available in literature is inconsistent and unreliable giving vastly different results (Jiang et al., 2015; Nash and Sambles, 1996 (N&S)). However measuring the optical properties of a layer while avoiding exposure to air is challenging.

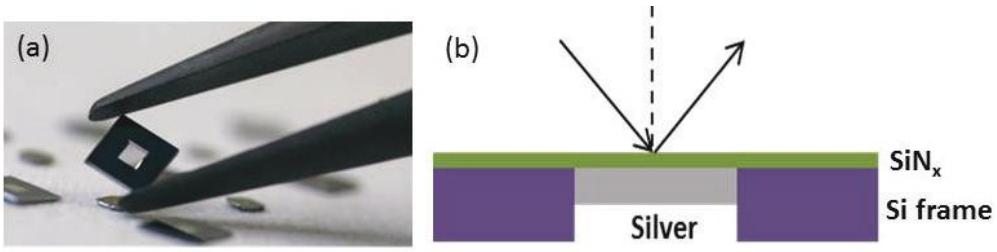

Figure PP3.2d.1: (a) Photograph of a typical membrane used in the study; and (b) A cross-sectional schematic the SiN_x membrane used in the experiment.

In this study we propose a novel method to measure the optical constants of silver in air without the problem of surface tarnishing and without the need for an ultra-high-vacuum atmosphere.

Progress

Surface tarnish layers form quickly when silver is exposed to air making it challenging to determine the optical constants from air exposed samples. Many previous studies were conducted with Ag exposed to air resulting in low accuracy data sets. The most widely used data sets of Palik (Palik, 1991)and Johnson and Christy (J&C) (Johnson and Christy, 1972) are inconsistent and unreliable. Hence a novel method of extracting the optical constants of thermally evaporated silver, by avoiding the air exposed side, was investigated. Interface measurement is one way to tackle this issue and will be used in this study, but interference from traditional substrates/superstrates (quartz etc.) can lead to errors in the fitting function. To circumvent the problem of incoherence of the superstrate layer mentioned above, a novel structure using an ultra-thin membrane has been proposed to measure the optical constants of silver. This method is particularly interesting as it avoids the air exposed side that might be tarnished and does not require an ultra-high-vacuum atmosphere to perform in situ measurements.

The samples used in the study were an SiN_x membrane supported on an Si wafer. The 5 mm x 5 mm membrane is held by a 10 mm x 10 mm silicon frame. The membrane can be treated as a top capping layer in our case if the measurement is taken in a "superstrate" configuration i.e. illumination is on the membrane side. This geometry results in a single coherent reflection from the protected Ag surface for ellipsometric analysis. A typical membrane used in this study is shown in Figure PP3.2d.1. For films deposited onto nitride, a short pre-treatment of the nitride (400°C, 15 minutes) was found optimal for preventing void formation in the Ag film. After deposition, a short low temperature anneal (200°C, 10 minutes) was found optimal, increasing grain size and reducing twin density as reported earlier. Ellipsometry and reflectance measurements were carried out to determine the optical constants immediately after deposition of silver film. The fitting process was accomplished using WVASE® which is spectroscopic ellipsometry software from J.A. Woollam Co. that allows building a model based on the sample structure and describing the property of target materials using different oscillators. Complementary techniques like the prism method were also used to check the accuracy of the data as well as demonstrating no strong dependence of Ag optical properties on the dielectric deposited.

An improved set of optical constants for silver was extracted using this method over a wide spectral range that could be used with confidence in simulations. The optical constants have now been tabulated and published (Jiang et al., 2016). Figure PP3.2d.2 shows the extracted n and k values for silver in comparison to those of Palik, N&S and J&C. Good agreement with N&S data was established which supports the reliability of the new data set.

Highlights

- A novel method of measuring the optical constants of silver was proposed using a silver nitride membrane.
- Demonstrated approaches to access the full capabilities of multiple-angle, spectrometric ellipsometry to generate an improved data set.
- Results are representative of overlayer-protected, untarnished silver films.
- A new set of optical constants for silver is now published and freely available online as excel file. Jiang, Y., Pillai, S. and Green, M.A., 2016, "Realistic Silver Optical Constants for Plasmonics", Sci. Rep, 6, 30605. (This article was featured in the research highlights section of Nature Photonics, "True Silver", 10, Sept 2016.)
- A second paper on the grain boundary effects on the optical constants has been accepted for publication in J. of Appl. Phys.

Future Work

This project is now complete.

References

Jiang, Y. et al., 2015, "Re-evaluation of literature values of

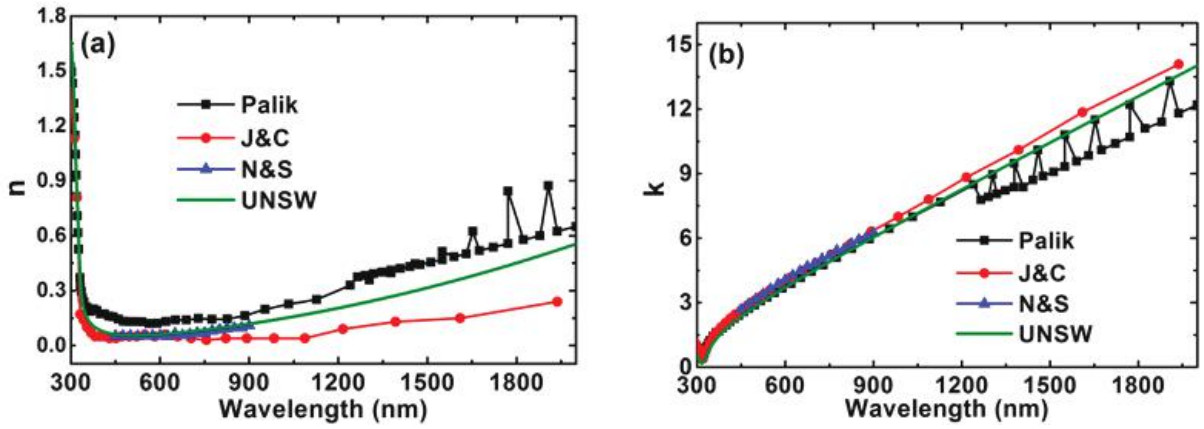

Figure PP3.2d.2: Comparison of extracted optical constants from this work (a) n and (b) k of silver in this work along with Palik's, J&C's and N&S's data for comparison.

silver optical constants", Optics Express, 23, 2133–2144.

Johnson, P.B. et al., 1972, "Optical Constants of the Noble Metals", Phys. Rev. B, 6, 4370–4379.

Nash, D. J. and Sambles, J. R., 1996, "Surface plasmon-polariton study of the optical dielectric function of silver", J. Modern Optics, 43, 81–91.

Palik, E.D., 1991, "Handbook of Optical Constants of Solids II", New York: Academic.

PP3.2f Characterisation of Photovoltaic Materials

PP3.2f(i) Excitonic Binding Energy Measurement

Lead Partner
UNSW

UNSW Team
Prof Martin A. Green, Dr Henner Kampwerth, Dr Binesh Puthen-Veettil

UNSW Student
XiaoQi Xu

Funding Support
ACAP, ARENA

Aim

The effect of excitonic binding energy on absorption spectra is subtle, but important for material and cell optimisation. Theoretical values for silicon, CZTS and perovskites need to be experimentally verified. Standard reflection-transmission (R/T) spectroscopy techniques are not sufficiently sensitive to measure this. UNSW is building a customised system that is three orders of magnitude more sensitive to these spectral changes compared to standard systems. The technique measures differential changes of the R/T spectrum by forming a lock-in signal between two wavelengths instead of measuring absolute intensities.

Progress

The system is set up and is presently being optimised for maximum sensitivity and repeatability. Preliminary results of the very weak excitonic effect on the absorption spectrum of Si at 25°C are promising.

Reference

Xu, X., Kampwerth, H., Puthen-Veettil, B. and Green, M.A., 2015, "A double beam wavelength modulation spectroscopy using two lock-in amplifiers", 25th International Photovoltaic Science and Engineering Conference, Busan, Korea.

PP3.2f(ii) Spectral-Resolved Two-Photon Microscopy

Lead Partner
UNSW

UNSW Team
Dr Michael Pollard, Dr Henner Kampwerth

UNSW Student
Robert Lee Chin

Funding Support
ACAP, ARENA

Aim

Time- and spectral-resolved photoluminescence spectroscopy are two of the most powerful characterisation techniques for photovoltaic materials. For a better understanding of complex material characteristics it is necessary to combine both techniques into one system. This would allow seamless parameter sweeps to study better electronic- and optical-band structures, various carrier lifetimes, defect characteristics and transport phenomena. Relative new materials such as perovskite and CZTS would benefit most from such a system.

Progress

The basic system that has been built between 2012 and 2015 through ARENA grant 1-GER010 has now been extended. A comprehensive microscopy system, a super-continuum laser and spectrometer have been added to the time-correlated single photon counting components and the widely tuneable optical parametric oscillator laser.

Highlights

Initial measurements have successfully demonstrated spectral- and depth-resolved two-photon absorption at an optical resolution of 17 μm FWHM. We are currently investigating the changes of emission spectrum that CZTS creates with varying excitation power.

Future Work

We intend to explore the new measurement capabilities on CZTS and multi-junction cells. Furthermore, we intend to couple the system with an H-cryostat for low temperature measurements.

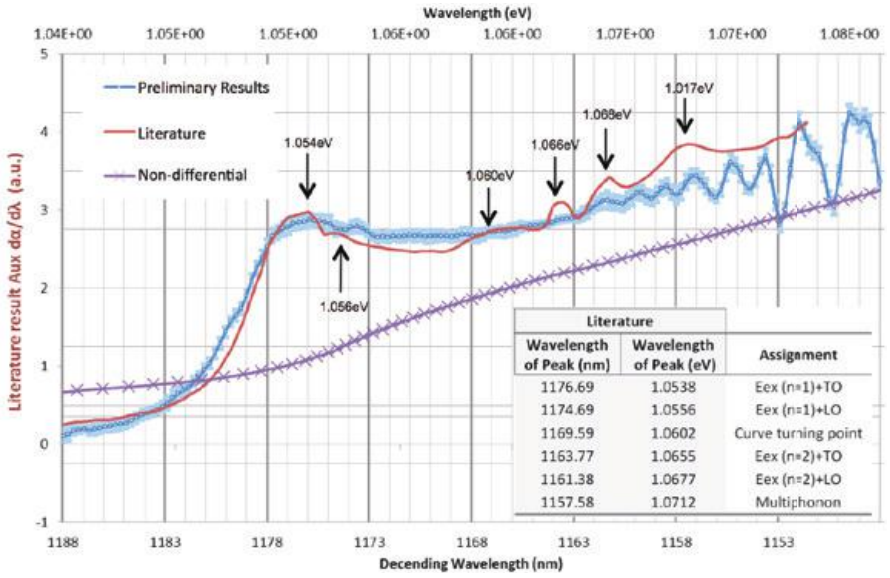

Figure PP3.2f.1: Absolute and differential absorption spectrum of Silicon at room temperature. The blue curve shows measurement data from the literature with possibly spurious peaks, where the blue data are our early preliminary measurements result before system optimisation. Numbers are theoretical values to be confirmed. The purple line is the absolute absorption spectrum which is insensitive to the subtle changes made visible in the differential spectrum.

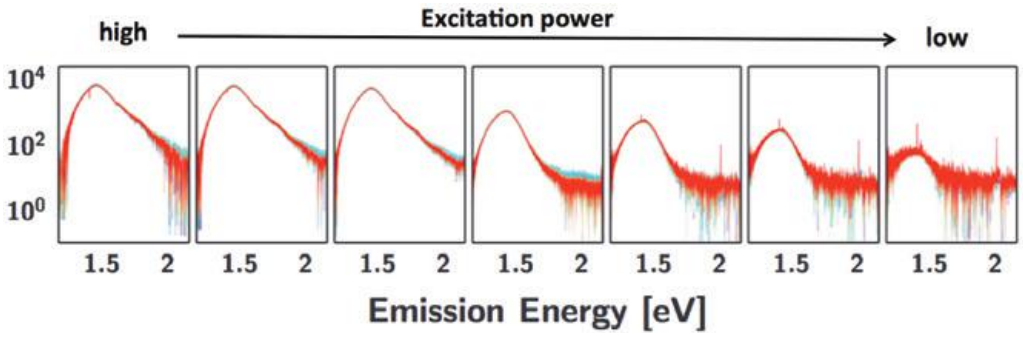

Figure PP3.2f.2: The figure shows the emission spectrum of a copper-poor CZTS sample at a spot size of 17 μm FWHM. The emission spectrum changes in shape with excitation intensity. (Here the detector noise at higher energies is to be neglected.) Currently we are investigating the causes for this spectral change and would like to extract physical parameters from it.

PP4 Manufacturing Issues

PP4.1 Cost Evaluations

Lead Partner
UNSW

UNSW Team
Dr Anita Ho-Baillie, A/Prof Renate Egan, Prof Martin Green

UNSW Student
Nathan Chang

ACAP Partners
NREL, CSIRO, ANU, Monash, UoM, UQ

Academic Partners
NREL, MIT

Overview

Energy from solar power is now cost competitive when compared to building new coal plants at residential, commercial and utility scale in many countries (Australia, Chile, Saudia Arabia). Advances in solar technologies contribute to the competitiveness through lowering the cost and improving the energy conversion efficiencies – as we are seeing now with the manufacturing deployment of PERC (Passivated Emitter and Rear Cell) technologies. The technologies being developed within ACAP aim to contribute to the ongoing improvements in cost and/or efficiency.

With a view to this increasingly competitive landscape, the manufacturing costing program within ACAP delivers methods for assessing module manufacturing costs for emerging technologies. The objectives are: (i) to quantify the potential of new technologies; (ii) to inform decision-making around research priorities; and (iii) to guide resources to cost ($) and performance (W) opportunities.

Targets for these manufacturing costs are set to a level such that the PV technology developed is internationally competitive, taking into consideration all aspects of the costs for PV manufacturing and will be competitive with other electricity generation options.

Consistent with the alignment of ACAP with US SunShot Initiative, the ACAP manufacturing costings are compared to the US Department of Energy targets for photovoltaics. The relevance of these cost reduction targets is that their achievement would be recognised as a very major technological advance internationally and would provide the stimulus needed to encourage serious investment in the new technology.

Sunshot Targets	Residential	Commercial	Utility
LCOE (USD/kWh)	0.09	0.07	0.06
System Cost (USD/Wp)	1.50	1.25	1.00
Degradation Rate			0.2%/year
System Lifetime			30 years
Module Cost			40c/Wp
Module Efficiency			20%

Table PP4.1.1: US SunShot targets for residential, commercial and utility-scale solar in 2020. The breakdown for utility-scale solar into module lifetime, cost and efficiency is shown. Costs are in USD.

The SunShot targets are thoroughly documented and regularly reviewed. The 2020 SunShot targets for the unsubsidised, levelised cost of electricity (LCOE) are shown in Table PP4.1.1, along with module targets for lifetime, cost and efficiency to reach these LCOE costs

The utility-scale PV system cost target for 2020 is $1/W and an LCOE of $0.06/kWh. To achieve this LCOE, the SunShot PV program has the following input targets:

- module cost to the end customer of $0.40/W
- module efficiency of 20%
- degradation rate of 0.2%/annum.

In late 2016, the SunShot Initiative proposed new 2030 targets for residential-, commercial- and utility-scale solar. These longer term values recognise the “transformative solar progress to date and the potential for further innovation” and reduce the average unsubsidised LCOE of utility-scale PV to 3¢/kWh, commercial-scale to 4¢/kWh and residential rooftop PV costs to 5¢/kWh by 2030 (SunShot, 2016).

The ACAP research program aims to contribute to meeting these cost targets through new materials and device developments, described in PP1, PP2 and PP3. The Manufacturing Issues program (PP4) provides the framework for comparing the manufacturability and competitiveness of the innovative technologies under investigation within the ACAP group.

Aim

Driven by a need to provide a framework for costing of new technologies, the aim of the PP4 program is to deliver a methodology for assessing manufacturing costs for the different technologies under investigation under the ACAP program. Modelling of cost and competitiveness, will help inform decisions around priority

areas for research giving consideration to potential benefit, risk, scale and capital cost.

The SunShot targets are used as benchmarks for comparison of the outcomes of the cost calculations. The aims for ACAP are to develop technologies with costs lower than the SunShot targets and ultimately to provide the stimulus needed to encourage serious investment in the new technology developments.

Progress

A key outcome of the efforts under PP4 is to provide a resource for assessing the cost of different processes with a view to informing research effort on the opportunities and key drivers and to understand how the technology fits on the costs and marketing roadmap for photovoltaics.

Building on the 2014 analysis of standard screen printing technology, in 2015, the manufacturing cost analysis activities included development of internal costing methodologies and then a cost analysis of one of the more mature ACAP technologies: liquid phase crystalline silicon on glass (LPCSG). In 2016, the costing methodology was further developed to take into account uncertainties associated with new technology developments, and four additional technologies were costed.

A costing methodology

Manufacturing cost estimation methods are commonly used in industry to optimise and incrementally improve performance and the cost of production. In ACAP, we are working on next generation technologies, where the processes are less refined and the costs less well understood. With solar becoming increasingly competitive, researchers are motivated to conduct an early assessment of the cost impact of new technologies to better direct research effort, but these assessments need to take into account the relative maturity of the emerging technology.

Within ACAP, we have developed novel methods for use during the early stages of process development to identify areas where cost reductions are necessary to bring an emerging PV technology to commercialisation and reduce the total time to commercialise a technology.

Normal practice in manufacturing costing is to apply a bottom-up analysis using commercial software packages. These calculators have limited application for new technology developments in that they do not take into account uncertainties in the expected processes and costs. At an early stage of development, it can be difficult to define final processes and challenging to obtain precise cost information from equipment and material suppliers.

Over 2016, significant improvements were made to the ACAP methodology for manufacturing cost analysis to account for uncertainties. The methods developed allow for cost calculations to be completed with a minimum time and effort while still providing useful conclusions such as the key cost drivers and opportunities for improvement. They can be used to identify the most significant sources of cost uncertainty which can be the focus of future cost analysis efforts (Chang et al., 2017).

To begin a cost analysis, a manufacturing process sequence is derived from consultations with the researchers developing the processes. Process sequences are documented that reflect the demonstrated research processes but are scaled to industrial throughput. The cost to manufacture is then calculated using a bottom-up 'Cost of Ownership' approach, considering costs such as materials, equipment, utilities, labour, building, maintenance and overheads. The main materials and suitable manufacturing tools are identified for each step, and the best available manufacturing cost data are obtained from various sources, such as publications, cost reports and price lists.

To account for uncertainties, for every cost parameter, a 'Nominal', 'High' and 'Low' value is determined. These data, together with other assumptions (such as factory yield, labour costs and depreciation schedules), are used to calculate the module manufacturing cost. Monte Carlo analysis is used to assess the impact of the uncertainty in each parameter. Typically 5,000 scenarios are generated. For each scenario, the value of each cost parameter is generated randomly according to its half normal distribution, and then the cost calculations are completed using these generated values. The distribution of the cost outputs from the 5,000 scenarios can then be analysed to understand the uncertainty of these cost estimates. Alternative process sequences can then be analysed and compared on both a median cost and cost uncertainty basis.

This costing methodology can be used iteratively as processes and knowledge develop.

With each iteration, the key cost drivers and the impact of the uncertainty from each parameter can be seen and can be used to inform research, resourcing and refining cost parameters to reduce uncertainty.

The analysis is used to develop a manufacturing cost in $/m^2 This allows the manufacturing cost to be calculated independently of the module efficiency, which remains uncertain in early development. The cost in $/W can be derived using additional assumptions, and uncertainties around efficiency. Estimates of the LCOE can then be derived using balance of systems inputs.

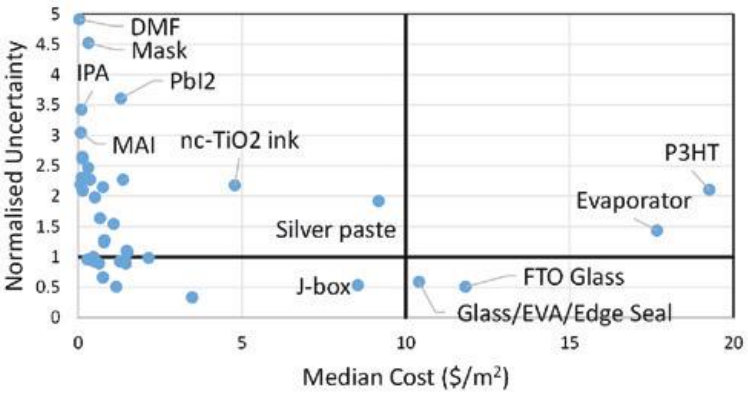

Figure PP4.1.1: Uncertainty / Cost Matrix for Perovskites on Glass. Identifying P3HT and the evaporator processes as being processes that are key cost drivers and also subject to significant uncertainty (Chang et al., 2017).

The costing can be extended to a market analysis to compare the proposed technology with the market offerings, in particular focusing on what efficiency and lifetime would be required to be competitive.

Costing: Perovskites on glass

There is significant international interest in the use of perovskites as the active material in solar cells. ACAP has responded to this opportunity with a new program in perovskites, described in PP2.5.

A manufacturing cost analysis has been carried out for three process sequences for the large-scale production of organic-inorganic hybrid perovskite on glass photovoltaic modules. The first pass of the costing analysis confirmed that the use of gold electrodes is prohibitive for any commercial outcome. Further costing assessed for alternatives and identified priority areas for research in reducing the cost or replacing the P3HT materials and the contact evaporation as shown in Figure PP4.1.1

The analysis identified a process sequence that combines two demonstrated perovskite module sequences to have an estimated cost of $107/m^2, which is comparable with commercial crystalline silicon and cadmium telluride technologies (on a $/m^2 basis).

An LCOE calculation showed that this perovskite technology would have been competitive with incumbent photovoltaic technologies in 2015 if a module power conversion efficiency of 18% and lifetime of 20 years had been achieved. Further analysis shows that even if the cost of the active layers and rear electrode were reduced to zero, a module power conversion efficiency of 18% and lifetime of 20 years would be required to meet the 2020 SunShot targets.

Costing: roll-to-roll perovskites printing

Perovskite photovoltaic cells are potentially compatible with roll-to-roll manufacturing processes developed by CSIRO, due to the low processing temperatures and solution-based approaches.

Roll-to-roll manufacturing is expected to be a much lower cost than more traditional processing on glass substrates, and the ACAP partners UNSW and CSIRO worked together to cost the current state-of-the-art roll-to-roll manufacturing sequence for perovskite solar cells, and explore the cost impacts of various process changes. In the analysis, the cost of roll-to-roll processing was compared with the perovskite on glass approach (modelled in in the previos section of this report) and two other proposed sequences, quantifying the benefit of roll-to-roll processing over that used in the perovskite on glass approaches.

The analysis shows that this cost is potentially much lower (on a $/m^2 basis) than the incumbent solar cell technologies in the market today. If the roll-to-roll perovskite manufacturing technology was able to match the lifetime and conversion efficiency of c-Si modules with the cost structure assumed in this work, then its cost advantage would give it a very significant market advantage. Lifetime and efficiency improvements remain the focus of research and will need to continue to demonstrate progress for the technology to compete with c-Si for large PV market deployment.

Another market opportunity for roll-to-roll printing of perovskite is leveraging the lightweight module market, including flexible modules, temporary installations and portable PV. It is expected that these portable products would sustain a higher market price on a $/W basis than a rooftop installed module. There is not good market knowledge on the scale of the opportunity in the lightweight module market and this is recommended as a subject of further research.

Costing: III-V on silicon using mechanical bonding

Tandems of III-V cells on silicon have been the subject of considerable interest for the possibility of accessing higher efficiencies. The increased efficiency allows for increases in complexity in the device design, and one approach to developing a III-V on silicon tandem that has been investigated within ACAP is mechanical bonding of a III-V cell to a c-Si cell.

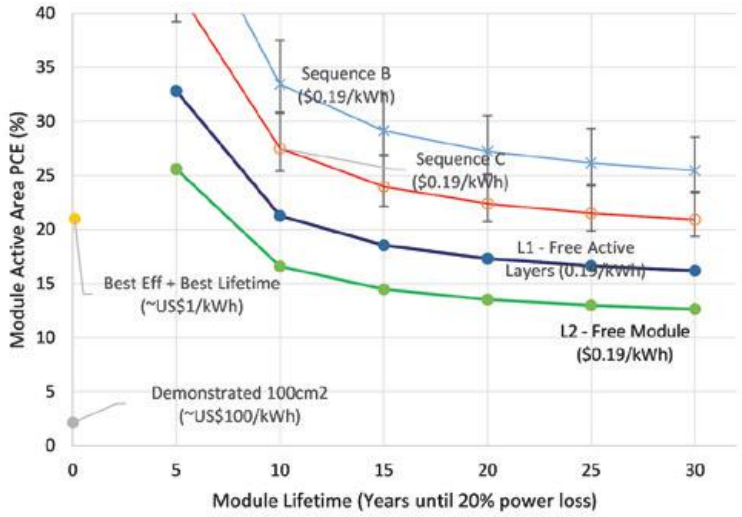

Figure PP4.1.2: Required module active area efficiency as a function of module lifetime for residential LCOE of USD 0.19/kWh (Chang et al., 2017).

In this cost analysis, the cost of the bonding step is assessed, with the costs of manufacturing both the top III-V cell and the bottom c-Si cell taken from other cost studies, including some work done by a project partner (NREL).

The analysis found that the costs of the III-V/Si module were driven by the III-V cell deposition cost, followed by the bonding cost. Significant changes are needed for the technology to be competitive with target LCOE. The analysis is supported by independent findings from NREL and the recommended way forward is to avoid the separate deposition and bonding process, and focus on the direct deposition of the III-V on the silicon bottom cell or to consider an alternative material for the top cell.

The high efficiency potential of tandem cell technologies opens new market opportunities where higher LCOE could be tolerated, such as space-constrained applications. From an analysis of the impact of module cost and efficiency on LCOE (see Figure PP4.1.3), it can be see that a 30% efficient module, would be competitive at 25c/kWh if the module manufacturing cost was close to $800/m^2$, while a 20% module would need to be produced at $500/m^2$ to be competitive at that LCOE.

Costing: silicon cell technology using LDSE

The most common manufacturing technology currently in production relies on modules assembled from silicon wafers processed into cells using screen print technologies to apply metal contacts. The manufacturing cost of the sequence was reported in the 2014 ACAP annual report and improved upon in 2015.

In the past year, the costing methodology has been applied to the evaluation of cost and production requirements of the laser doped selective emitter (LDSE) technology developed at UNSW. The LDSE technology was developed to reduce losses associated with the front contact process and reduce the demand for silver in the front contact, replacing it with a plated metal contact.

The costing analysis reveals that changing from Al-back surface field to LDSE increases the manufacturing cost per unit area. This is because of the added dopant application and laser processing, and the replacement of the front screen print with plating. Recent progress in screen printing technologies has reduced the demand for silver and reduced some of the near-term cost benefit associated with replacing silver with copper metallisation. While the area cost of the LDSE is higher, the efficiency enhancement returns the $/W cost to a comparable value. But with no significant improvement in $/W cost, there is no compelling reason to implement this technology on its own.

Further analysis is in progress of the manufacturing costing of PERC technologies, and a first analysis indicates a significant benefit is expected from adding LDSE to the PERC technology. LDSE is expected to have significant commercialisation potential in the future as the industry is moving from Al-BSF to PERC as the baseline process.

Summary

The manufacturing costing program continues to develop methods for assessing the manufacturing costing of new technologies, taking into account uncertainties associated with processes still under development and enabling identification of technology risks and priority areas for research.

Highlights

- Costing methodology developed that is well suited to early stage technologies.

- Innovative in that it allows for uncertainty in cost inputs.
- Aimed at informing research direction by identifying key cost drivers and key cost uncertainties.
- Helps prioritise cost and process development activities.

Future Work

In future years, we will extend the cost analysis to novel technologies under investigation within ACAP. Target areas for 2017, with early analysis showing promise include PERC, hydrogenation and CZTS. Analysis will be done to assess near-term opportunities for improvement and to guide research into the highest impact areas. The outcomes of the cost analysis will be compared with the U.S. Department of Energy SunShot module price targets.

References

Jones-Albertus et al., 2015, "Technology Advances Needed for Photovoltaics to Achieve Widespread Grid Price Parity"., Washington, D.C.: Department of Energy (DOE). Accessed January 2016, http://energy.gov/eere/sunshot/downloads/technology-advances-needed-photovoltaics-achieve-widespread-grid-price-parity.

Chang et al., 2017, "A Manufacturing Cost Estimation Method with Uncertainty Analysis and its Application to Perovskite on Glass Photovoltaic Modules", in press *Progress in Photovoltaics: Research and Applications*.

SunShot 2016, Dec 2016, "The SunShot Initiative's 2030 Goal", Accessed January 2017 https://energy.gov/sites/prod/files/2016/12/f34/SunShot%202030%20Fact%20Sheet-12_16.pdf.

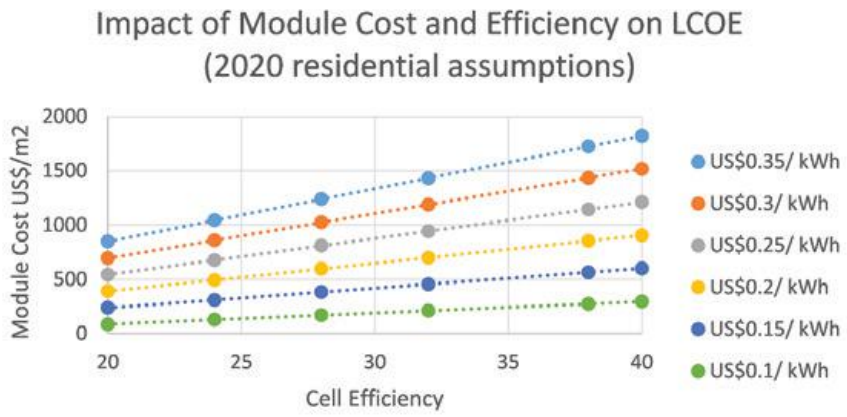

Figure PP4.1.3: Impact of cell efficiency and module manufacturing cost on LCOE with assumptions consistent with modelling by Jones-Albertus et al. that uses the anticipated SunShot 2020 residential scenario, where the baseline LCOE is US$0:09=kWh.

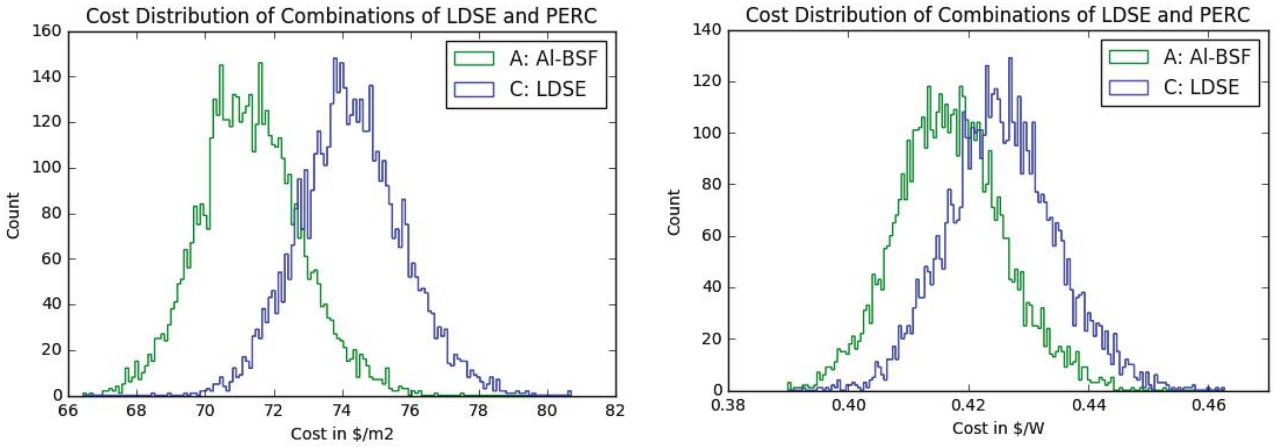

Figure PP4.1.4: Cost distribution of combinations of LDSE and PERC added to Al-BSF in (a) US$/m^2 and (b) US$/W.

PP5 Education Training and Outreach

Overview

Within the PP5 Education, Training and Outreach package, ACAP has specific targets for high quality publications and for the number of researchers in different categories that benefit from the infrastructural support it provides, as well as for the number and length of researcher exchanges. A significant number of outreach events is also targeted for each year. As well as major events such as those reported in the PP5 section of this annual report, other outreach activities in 2016 have included public lectures on material relevant to ACAP's activities, newspaper and magazine articles, and visits, information papers and presentations for policy developers and their advisors.

Of particular note for 2016 was the strong media interest arising from announcements through the year of world records for different ways of converting solar energy to electricity. ACAP even made to front page of the Sydney Morning Herald on 18 May 2016. ACAP finished the year with new efficiency records for perovskite cells announced on 2 December at the coupled ACAP and Asia Pacific Solar Research Conferences in Canberra. Integrating the conferences with the ANU Solar Oration offered the opportunity to be enthused and recharged by the Solar Century's Jeremy Leggett.

Again in 2016, there was very strong international interest in the articles by ACAP researchers in leading journals. A remarkably high number of these were "Hot Papers" and "Highly Cited Papers", as identified by the Thomson-Reuters' Web of Science. See Section 2 of this report for further information. In general, interest in and citations of AUSIAPV/ACAP's work have grown considerably over the year.


The facts on a 'Google tax'

Sydney's fashion fiesta

The Sydney Morning Herald

INDEPENDENT. ALWAYS.

ASIC inquiry Transcripts revealed

ANZ staff accused of fixing bank rates

Scientists get their moment in the sun

From wannabe 'gangster' to terror suspect

Election 2016: Full coverage of the campaign News, Pages 4-7

Figure PP5.1: Front page of the Sydney Morning Herald of 18 May 2016, featuring Dr Mark Keevers of the UNSW node.

The ACAP nodes continue to educate the future practitioners and researchers and educators to support the necessary rapid expansion of the national and global photovoltaics industry and to develop more effective educational tools.

PP5.1 Multi-Node Activities

PP5.1a Annual ACAP Conference

Lead Partner
UNSW

Oral Presenters
Dr Nancy Haegel (NREL), Prof Udo Bach (Monash), Dr Hasitha Weerasinghe (CSIRO), Dr Mei Gao (CSIRO), Mr Jincheol Kim (UNSW), Mr Mathias Rothmann (Monash), Mr The Duong (ANU), Dr Di Yan (ANU), Dr Catherine Chan (UNSW), Dr Dani Stoltzfus (UQ), Ardalan Armin (UQ), Jegadesan Subbiah (UoM), Valerie Mitchell (UoM), Prof Martin Green (UNSW), Carolyn Goonrey (ARENA), Prof Andrew Blakers (ANU), Dr Anita Ho-Baillie (UNSW), Prof Gavin Conibeer (UNSW), Prof David Jones (UoM), Prof Paul Meredith (UQ), Dr Nathan Chang (UNSW), Dr Richard Corkish (UNSW)

Poster Presenters
CSIRO: Doojin Vak, Régine Chantler, Mathilde Fievez, Clément Aury
UoM: Kyra Schwarz, Bolong Zhang, Nicolau Saker Neto, Thomas Fabig, Paul Geraghty, Calvin Lee

Monash: Iacopo Benesperi, Liangcong Jiang, Jianfeng Lu, Gaveshana Sepalage, Rebecca Milhuisen, Wenchao Huang
UQ: Ravi Nagiri, Aren Yazmaciyan, Shanshan Zhang
UNSW: Alison Lennon, Stephen Bremner, Ziv Hamieri, Xiaojing Hao, Xiaojing Hao

Funding Support
ARENA / ACAP

Aim

ACAP holds an annual research conference near the end of each year in order to keep ARENA and its National Steering Committee informed, and to exchange research results, enhance collaboration and reinforce one-on-one contacts between students and staff from the different nodes.

The program includes an oral summary of progress and plans for each node by its leader as well as oral and poster presentations of technical progress from staff and student researchers.

Progress

The 2016 conference, the fourth, ran with a public forum on Day One, integrated with the final day of the Third Asia-Pacific Solar Research Conference (Annual APVI Conference – see section PP5.1b, below), followed by a closed workshop for ACAP participants on Day Two.

The ACAP proceedings began with a plenary presentation from invited guest speaker Dr Nancy Haegel, Director of the Materials Science Center at the US National Renewable Energy Laboratories entitled "Terawatt-Scale Photovoltaics: Trajectories and Challenges".

The plenary session was followed by two technical presentations from each of the six nodes, describing detailed progress in selected tasks from within the ACAP program.

Over lunch, attendees at both conferences read and discussed the showcase posters invited from each node.

Day Two followed with an ARENA presentation and summary presentations of progress in each of the Program Packages. The seventh ACAP National Steering Committee meeting and the fourteenth Management Committee meeting were held on the afternoon of the second day of the conference.

Highlights

- UNSW's announcement of new confirmed efficiency records for large area perovskite solar cells: 12.08% for a 16 cm^2 cell
- 18% efficiency rating on a 1.2 cm^2 single perovskite cell
- 11.5% for a 16 cm^2 four-cell perovskite mini-module

Figure PP5.1a.1: The 2016 ACAP Conference was integrated with the Asia-Pacific Solar Research Conference (see PP5.1b) at the Australian National University (Photo: A. Abrahams).

Future Work

The next ACAP Conference will be held in coordination with the fourth Asia-Pacific Solar Research Conference, in Melbourne in December 2017. The first day will again overlap with the final day of the Asia-Pacific Solar Research Conference and the ACAP presentations on that day will form a special session of the broader conference.

PP5.1b Annual APVI Conference

Lead Partner
UNSW

ACAP Team
Staff and students of all nodes

Academic Partners
All nodes

Industry Partner
Australian Photovoltaics Institute (APVI)

Aim

The APVI's Asia-Pacific Solar Research Conference aims to provide a forum for development and discussion of content specific to Australia and its region, and an opportunity to foster collaboration between institutes, and to promote engagement between industry and academics. ACAP partners with the APVI to support the development of the conference program through participation in its organisation and through scheduling ACAP presentations at the conference.

Progress

The third Asia-Pacific Solar Research Conference was held on 29 November – 1 December 2016 at

Figure PP5.1b.1: Student prizes for Best Poster for Gaveshana Sapalage (Monash), Best Paper for Johanna Bowyer (UNSW) and for Women in Solar Best Poster for Yu Jiang (UNSW) were presented by Steve Blume (left), President of the Australian Solar Council (Photo: R. Passey).

Figure PP5.1c.1: The third APVI Asia-Pacific Solar Research Conference.

the Australian National University, Canberra, ACT. Representatives of three ACAP nodes, ANU, UNSW and Monash University were involved in the organising committee. Staff and students from the nodes participated in academic review committees and contributed papers and posters to the conference. The conference drew nearly 300 participants from academia, government and industry, and ran parallel streams covering such areas as organic PV, PV devices, solar heating and cooling, policy and field experience.

Highlights

- Solar Oration: Jeremy Leggett (Solar Century).
- Plenary speakers Day Two: Prof Gus Nathan (University of Adelaide), Dr Nathan Steggel (Windlab), Prof Brian Schmidt (ANU), Ms Lara Olsen (Tesla Australia).
- Plenary Speakers Day Three: Dr Nancy Haegel, (NREL), Prof Klaus Vajen (University of Kassel), Mr Bob Burton (Fossil Futures).
- Coordinated to run a parallel stream with the annual ACAP Conference as a knowledge-sharing event.

PP5.1c APVI Engagement

Lead Partner
UNSW

ACAP Team
UNSW: A/Prof Renate Egan, Dr Richard Corkish, Dr Anna Bruce
ANU: Prof Andrew Blakers
Monash: Dr Jacek Jaseniek

ACAP Student
Sharon Young

Industry Partners
APVI: Dr Renate Egan, Dr Rob Passey

Funding Support
ACAP and APVI subscribers and supporters, including ARENA

Progress

The Australian Photovoltaics Institute (APVI) is one of the more effective vehicles for Australian policy development through its focus on data, analysis and collaborative research. ACAP became a founding “Large Organisation” member of the Australian Photovoltaics Institute (APVI) and ACAP partners have been active members of APVI throughout 2016.

ACAP collaborators contributed to and participated in a number of outreach events including:

- Australian representation on the Executive Committee for the International Energy Agency, PV Power Systems
- APVI Cost Reflective Pricing Workshop, held in Sydney in June 2016
- the co-hosting of a Solar Oration at ANU in November 2016
- third APVI Asia-Pacific Solar Research Conference in December 2016 (see PP5.1b).

This series of events and activities brought together solar researchers, industry partners and advocates, and created media attention for ACAP and ARENA.

Highlights

- The third Asia-Pacific Solar Research Conference was held in conjunction with the ACAP, ASTRI and ECI annual meetings. With the theme of information, collaboration and integration, the event brought close to 300 participants to ANU.
- The Solar Oration, hosted by ANU in parallel brought Jeremy Leggett, author and advocate for solar, to Australia to raise awareness of the impact and opportunity in renewable energy.

Future Work

- Ongoing representation on the Executive Committee for the International Energy Agency, PV Power Systems, including hosting of the Executive Committee meeting in Melbourne in late 2017.
- Participation in the fourth APVI Asia-Pacific Solar Research Conference in December 2017.

PP5.1.f Coursework Education

Lead Partner
UoM

UoM Team
Dr David J. Jones, Prof Andrew B. Holmes, Dr Wallace Wong
UNSW Team
Dr Alison Lennon, Dr Santosh Shrestha, Dr Ivan Perez-Wurfl, Prof Alistair Sproul, Prof Darren Bagnall

UQ Team
UQ academic staff

CSIRO Team
Dr Fiona Scholes, Dr Gerry Wilson, Dr Doojin Vak, Dr Hasitha Weerasinghe, Dr Mei Gao, Ms Jyothi Ramamurthy, Dr Andrew Scully, Mrs Régine Chantler, Dr Anthony Chesman, Dr Kallista Sears, Dr Noel Duffy

Monash Team
Assoc Prof Jasieniak

Funding Support
ARENA, ACAP, UoM

Aim

Capacity building for the next generations of photovoltaics researchers.

Progress

- All the nodes are involved in undergraduate and postgraduate education as capacity building for the next generations of photovoltaics researchers. Of particular note for 2016:
- 30 students participated in the undergraduate course, “Nanoscience: Synthesis”, run by the School of Chemistry and Molecular Bioscience at UQ
- the UoM node continues to deliver a Masters course in “Organic Electronics”
- UNSW’s BE (honours) in “Photovoltaics and Solar Energy” and BE (honours) in Renewable Energy streams were reviewed by Engineering Australia and re-accredited
- Arizona State University’s “Advanced PV Manufacturing” course was offered as a short course at UNSW in 2015 and present plans are to run it every three years to ensure each student has the opportunity to take the course.

Highlight

- Solar activities listed as one of the top ten research areas in Sustainability at UoM.

Future Work

- The undergraduate course, “Nanoscience: Synthesis” at UQ is expected to be offered again in 2017.

Reference

https://pursuit.unimelb.edu.au/features/making-any-surface-solar

PP5.2 UNSW-Led Activities

PP5.2b Sunswift, Sunsprint, MiniSprint, Solar Boat Race, Solar Pursuit

Lead Partner
UNSW

UNSW Team
Mr Robert Largent, Dr Richard Corkish

UNSW Students
Simba Kuestler, Emmy Tran, Connor O’Shea, Ravi Raj, Hayden Smith, Sam O’Brien, Gabriel Mendoza, Adam Joffe, Nabi Genc, Tom Dransfield, James Anderson, William Green, Brian Ling, Cze Ying Goh, Michelle Seeto, Jason Chan, Tim Williamson, Keith Ly, Hamal Shah, ELizabeth Scott, Matthew Holohan, Syed Ahmed, Courtney Morris, Kevin Kam, Izzan Khalzani, Branden Lim, Eben Brebner, Alexander Gu, Kelvin Tan, Sam Wemyss

Academic Partners
North Sydney Institute of TAFE, CSIRO, participating secondary and primary schools

Industry Partners
Thales, Core Builders, Solbian, Sunpower, Leap Australia, Graphique Solutions, JGID, Weatherzone, Nova Systems, Activ, UNSW ARC Clubs and Societies, Comply Serve, Downer, Green Power, Altium, Bunnings, Coilcraft, Mo Milling, 3M, Addcom Contact Solutions, Calm Aluminium, Benelec, Quickstep, Trio Test & Measurement, Keysight Technologies, Solgen, NSW Office of Environment and Heritage, Bathurst Regional Council, Sydney Dragway, Marulan Dirt and Tar Circuits, Hunter Valley Electric Vehicle Festival, Atlassian, SESA, Sydney Motor Sport Park, Moir Group, EV West, CST Composites, ADR Compliant Services, Akubra, British Racing Motors, High Technology Control, Joviam, TeXtreme, TomTom, Velo

Funding Support
UNSW Faculty of Engineering, UNSW School of Photovoltaic and Renewable Energy Engineering, ARC@UNSW, UNSW School of Computer Science and Engineering

Aim

Sunswift and Sunsprint and related activities enthuse and engage school and university students in science and engineering and are a major outreach activity for ACAP. Inspiring the public is another of the team's core aims.

Progress

The Sunswift team in 2016 has been focused on its mission of making "eVe", Australia's first road-legal solar sports car while designing its next generation car. The team has also spent considerable time attending and hosting public events as well as talking to schools throughout New South Wales.

The vast majority of the work required for "road legal" status has been completed and the process only awaits feedback from consultants on two component regulations, before we move on to the final Single Uniform Type Inspection. A long and complex process is coming to completion: registration as a car designer and manufacturer, alongside an entity that can issue new car VIN numbers; building the car to meet the Australian road standards; completion of all dynamic tests required by the regulations; compiling over 100 pages of summary documents to demonstrate compliance; feedback and discussions; on-site inspection of the vehicle by the NSW road authority; granting of compliance plates; and registration with state authorities.

Only once every four years the Sunswift student team has a chance to design and make a new car.

The next, 6th generation, car is set to be groundbreaking, but details remain confidential. Based on the combined experience of five previous cars, the next will be a practical yet exceptional vehicle. This means more passengers, more connectivity, more control, more comfort and, of course, more innovation.

The seven-day 2016 NSW Regional Outreach Tour was an opportunity to show school students and the general public the amazing opportunities in engineering and sustainable technology; generate media coverage for supporters, including ACAP; and train for the 2017 Bridgestone World Solar Challenge. Thousands of students participated in workshops, where they built, raced and refined mini solar cars. The tour precipitated 43 media stories, with media value of $31,482, reaching an audience of 96,161. Sunswift's social media platforms also performed well – with Facebook alone reaching over 15,000 people that week. Throughout the tour, every team member was actively involved in fleet radio communication, staged practice emergency scenarios, adhering to strict timelines and fulfilling their designated roles for the 2017 Bridgestone World Solar Challenge.

Despite 2016 being the "quiet phase" of Sunswift's four-year cycle, since details of the new car are confidential, it still received considerable coverage from a range of outlets surrounding its road-legal efforts and Outreach Tour. Events which significantly involved Sunswift in 2016 included: 2016 UNSW O-Week; filming of eVe in action for an upcoming Imax film; National Geographic Track Day; Engineering and Science Student Parent Night; CeBIT Industry Event; National Manufacturing Week (Sydney); UNSW High School Information Day; UNSW ENGSOC Projects Fair; Western Sydney Model Show; The Gadget Expo; Australian Solar Council Presentation; Energy Future Conference; WomENgineering; and the Nura Gili Winter School Program.

2016 Schools outreach events included: Kambala School; Wenona School; Sydney Boys High; Redlands; Sunsprint Workshop at Georges River Grammar; ASPIRE Dubbo; Sydney Grammar; and the above-mentioned Outreach Tour.

Media outlets that covered Sunswift in 2016 included:

- Television and Radio: Channel 7; NBN News (Port Macquarie Region); Prime 7 (Tamworth Region); NBN News (Tamworth Region); Win News (Orange Region); Prime 7 (Orange Region); Channel 9; ABC Radio (Mid-North Coast); ABC Radio (New England North West); ABC (Western Plains); 2SM Radio network; 2BS Radio (Bathurst Region); BRockfm (Bathurst Region).
- Print and Online: *Mosman Daily*; *Business Insider Australia*; *Port News*; *Central Western Daily*; *Scimex.org*; *Daily Liberal*; *Molong Express*; *Southern Courier*; *Gizmodo*; *Armidale Express*; *Northern Daily Leader*; *Western Advocate*; *Coonabarabran Times*.

Figure PP5.2b.1: Sunswift at a school outreach in 2016.

Figure PP5.2b.2: Primary students enjoy the thrill of the race.

Figure PP5.2b.3: The Model Solar Boat Competition.

- Facebook: Over 5,200 page likes; average reach > 10,000/week; top single post reach of 8,400.
- Twitter: Over 2,000 followers; 380 impressions/day; 21,000 impressions in one month.
- Linkedin: Over 500 page likes; top post > 200 likes.
- Youtube: Most popular video had over 71,000 views.
- Flickr: Over 10,500 photos available.
- Instagram: Over 1,200 followers.

The SunSprint Solar Challenge is a collection of age-appropriate solar races designed for K–12 school students. The event encompasses the SunSprint Model Solar Challenge (years 7–12), MiniSprint (two categories: K–6 and 7–12), Solar Boats (K–6 and 7–12) and the Solar Pursuit (using MiniSprint-style cars and is open to all, including teachers). The event is held on the first Saturday in September.

The SunSprint Model Solar Car Challenge is a photovoltaics project–based learning event designed for high-school students. Solar cars are designed and built according to specifications provided by the Australian-International Model Solar Challenge (AIMSC), a national organisation overseeing and linking all of the state events. These specifications provide design criteria that, when followed, allow students all over Australia to build model solar cars that are uniformly competitive with respect to design, cost and use of materials. The students contribute ideas, inspiration, time and money. The average SunSprint vehicle costs over $600 and takes the team over four months to design and build. Many schools throughout NSW have allowed final-year Design and Technology students to adopt SunSprint as their year-long major project, as SunSprint addresses several aspects of the curriculum.

The MiniSprint Model Solar Car Challenge and the Model Solar Boat Challenge are offshoot events allowing primary school students to design and build solar vehicles and

then experience the thrill of competition. The MiniSprint competitors start with a kit containing all of the important parts of the solar car, which can be constructed in an evening by means of soldering, gluing and taping.

The Model Solar Boat Competition requires much more student design than the MiniSprint category. The boats can be made of any material and can use almost any size or combination of solar cells and motors. The challenge for younger competitors is to get their boats to float right-side up and to move through the water successfully in competition with others.

The Pursuit Race has MiniSprint style cars chase each other around a single lane oval track until one of the cars catches up and touches the other. Participants are K – 12 with categories for primary and secondary school.

Winners in 2016 were:

- SunSprint (100m figure-eight track) – Strathfield South High School 1st and 3rd place with Moorebank High School coming in 2nd place;
- MiniSprint (20m track) - 1st place Callaghan College, 2nd place Kincoppal and 3rd place Casula Public School;
- MiniSpirnt Boats - 1st, 2nd & 3rd Casula Public School;
- Pursuit Race (20m oval track) - 1st place Casula Public School and 2nd place Wenona.

Highlights

- Imminent "road-legal" status for eVe;
- Outstanding engagement of school and university students in science and engineering.

Future Work

- The next, 6th generation, car will be based on the combined experience of five previous cars, meaning more passengers, more connectivity, more control, more comfort and, of course, more innovation;
- The team will compete in the Bridgestone 2017 World Solar Challenge;
- SunSprint Solar Challenge.

PP5.2f Lunchtime Public Seminar Series

Lead Partner
UNSW

ACAP Team
UNSW: Prof Martin Green, Prof Stuart Wenham, Prof Thorsten Trupke, Dr Udo Romer, Dr Rob Nicholls, Dr Murad Tayebjee, Dr Mattias Juhl, Dr Dirk König
UQ: Prof Paul Meredith
ANU: Dr Hieu Nguyen

ACAP Students
UNSW: Rhett Evan, James Hazelton
ANU: Thomas Allen

Academic Partners
FOM Institute AMOLF: Albert Polman
Colorado School of Mines: Brian Gorman
University of Oxford: Laura Herz
Arizona State University: Delia Saenz
KRICT, UNIST: Sang Il Seok
University of Warwick: John Murphy
Universidade Federal de Santa Catarina: Lucas Nascimento
Loughborough University: Paul Rowley
NREL: William Tumas, Anthony Burrell
UC Berkeley: Jessie Knapstein
MIT: Mallory Jensen
University of Sydney: Joe Dong
Catalonia Institute for Energy Research: Paul Pistor
Shanghai Jiao Tong University: Yong Li, Ruzhu Wang
Imperial College London: Ned Ekins-Daukes
Indian Association for the Cultivation of Science: G.P. Das
RMIT University: Alan Pears
Helmholtz-Zentrum Berlin: Sebastian W. Schmitt
University College London: Michael Grubb
Industry Partners
DuPont: Daniel Inns
Todae Solar: JJ Ferrandis
Barefoot Power: David Hind
China Sunergy: Jun Lv
UTS: Scott Kelly
IEA-PVPS: Gaëtan Masson
Sinton Instruments: Ron Sinton
Solar entury: Jeremy Leggett
Ecoult: John Wood

Aims

- Public dissemination of research progress and results.
- Foster collaboration between research institutes.
- Allow researchers to be informed about relevant issues outside their narrow research topics.

Progress

The UNSW School of Photovoltaic and Renewable Energy Engineering, with ACAP support and involvement, hosts a series of lunchtime seminars by visitors and local researchers. In 2016, a wide range of very interesting presenters from all around the world were involved. Many of the speakers consented to audio/video recording of their sessions and subsequent web access, thus creating a significant and persistent education and outreach resource.

Highlight

15 November 2016 – Ron Sinton – Sinton Instruments, "Implementation of advanced solar-cell analysis at cell test"

Reference

Public Research Seminars, www.engineering.unsw.edu.au/energy-engineering/public-research-seminars

PP5.2l AQF Level 9 Specialisation of the Master of Engineering Science

Lead Partner
UNSW

UNSW Team
Dr Santosh Shrestha, Dr Anna Bruce, A/Prof Alistair Sproul, Prof Darren Bagnall

Aim

- Improve program quality and consistency through compliance with Australian Quality Framework (AQF) Level 9 program criteria.
- Improve the quality of the postgraduate programs in photovoltaic and renewable energy engineering.

Progress

This project has been completed. The UNSW School of Photovoltaic and Renewable Energy Engineering (SPREE) has introduced and delivered Master of Engineering Science streams in Photovoltaic and Solar Energy SOLACS8338 and Renewable Energy SOLADS8338. They are two-year (full-time) programs and are compliant with AQF Level 9 program criteria.

Proposals are being prepared for a Master of Engineering in Photovoltaic and Renewable Energy. This program, when approved, will be accredited by Engineers Australia.

Highlight

Establishment and delivery of Master and Graduate Diploma of Engineering Science degrees in Photovoltaic and Solar Energy and Renewable Energy.

Future Work

This project has been completed.

PP5.2n WIRE

Lead Partner
UNSW

UNSW Team
A/Prof Renate Egan, Prof Darren Bagnall

UNSW Students
Kate Lindsay, Belinda Lam

PP5.2n.1: WIRE team.

Funding Support
ARENA, UNSW

Aim

WIRE was established in 2010 to inform, educate and empower current and future female photovoltaics and renewable energy students.

Progress

WIRE provides a fun and casual environment for students across all stages of their degree programs. Members are able to socialise and support each other by means of various activities, networking events and excursions, thus enhancing their perspectives on various renewable energy fields.

These events foster strong friendship ties between industry associates and the UNSW School of Photovoltaic and Renewable Energy Engineering. Such ties provide members with a support system, both at university and once they enter the workforce.

In 2016, WIRE held regular meetings and networking events. We also held an industry networking evening in which three industry members from various companies and positions were invited to discuss the topic "Developing your career" and their experiences. All events are aimed at creating opportunities and include Q&A sessions allowing students to gain an insight into future careers. The society also hosted social events for members to meet their fellow students at a board games event at a campus restaurant and fortnightly picnics.

Future Work

WIRE will continue to support the female students to engage with industry in the very positive setting of the Paris Agreement and Australia's commitments to Mission Innovation.

PP5.2p National Research Infrastructure Roadmap

Lead Partner
UNSW

UNSW Team
Dr Richard Corkish, Dr Bram Hoex

ACAP Team
All nodes

Aim

Raise the profile of photovoltaics in the National Research Infrastructure Plan to increase funding opportunities.

Progress

The Chief Scientist for Australia, Dr Alan Finkel AO, is leading the development of the 2016 Roadmap and the process is managed by the Department of Education and Training (Australian Government, 2016). He is supported by an Expert Working Group comprising eminent Australians with experience and knowledge of the research and innovation system. ACAP made a submission (Corkish and Hoex, 2016) during the consultation on the National Research Infrastructure Capability Issues Paper and participated in the Sydney face to face consultation on 19 August 2016.

The ACAP submission highlighted the history and potential environmental and economic benefits for photovoltaics research in Australia. Australia has been leading the world in solar cell device efficiency for most of the last four decades and device efficiency is the simplest and most direct path to lower cost solar electricity (Fraunhofer ISE, 2015). The report listed 26 past entrepreneurial outcomes from ACAP institutions.

The Draft 2016 National Research Infrastructure Roadmap was developed and released for comment on 5 December 2016, with some reference to solar energy.

Highlight

Collation of 26 past entrepreneurial outcomes from ACAP institutions.

References

Australian Government, Department of Education and Training, 2016, 2016 National Research Infrastructure Roadmap, www.education.gov.au/2016-national-research-infrastructure-roadmap.

Corkish, R. and Hoex, B., 2016, ACAP submission, https://submissions.education.gov.au/Forms/National-Research-Infrastructure-Capability-Issues-Paper-Submissions/Documents/Australian%20Centre%20for%20Advanced%20Photovoltaics.pdf.

Fraunhofer ISE, 2015, "Current and Future Cost of Photovoltaics – Long-term Scenarios for Market Development, System Prices and LCOE of Utility-Scale PV Systems", a study on behalf of Agora Energiewende.

PP5.7 CSIRO-Led Activities

Lead Partner
CSIRO

CSIRO Team
Dr Fiona Scholes, Dr Gerry Wilson, Dr Doojin Vak, Dr Hasitha Weerasinghe, Dr Mei Gao, Ms Jyothi Ramamurthy, Dr Andrew Scully, Mrs Régine Chantler, Dr Anthony Chesman, Dr Kallista Sears, Dr Noel Duffy

Monash Team
Dr Jacek Jasieniak

Academic Partners
Monash University Art Design and Architecture (MADA); Monash University Business School; University of Technology Sydney (UTS); Georgia Institute of Technology

Funding Support
ACAP, CSIRO

Aim

CSIRO continues to be committed to participating in the community to advance awareness of photovoltaic research. In the context of ACAP, CSIRO promotes photovoltaic technologies via numerous education, training and outreach activities with an emphasis on printed solar film technology. We engage in a range of knowledge-sharing activities both domestically and internationally.

Progress

Following a major facelift in 2016, CSIRO's Flexible Electronics Laboratory showroom has continued to function as an exciting destination for CSIRO visitors. In

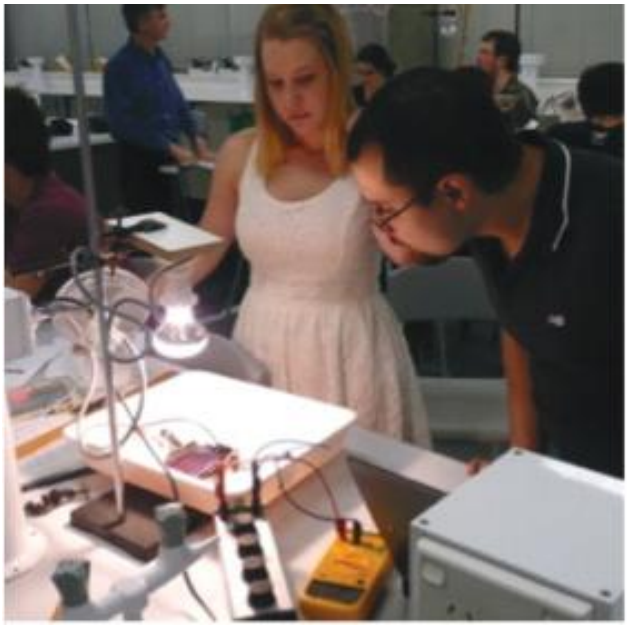

Figure PP5.7.1: Conducting experiments using CSIRO printed organic solar films by undergraduate students at UTS.

2016, some 53 tours of the laboratory were conducted, which included visitors from various high profile research institutions (e.g. Chinese Academy of Sciences), Australian SMEs and larger businesses (e.g. through the CEO Institute) as well as government representatives (e.g. Victorian Department of Environment, Land, Water and Planning).

Following the supply of 100 additional printed solar film modules to University of Technology Sydney (UTS) in 2015, the CSIRO team continued to contribute to the UTS inquiry-oriented learning program in 2016, participating in the UTS undergraduate physics program via their lecture and practical program (Figure PP5.7.1).

After the tremendous success of our initial collaboration in 2015, CSIRO was again involved as "client" to Monash University industrial design undergraduates. With a better developed project brief and improved understanding of engaging with industrial designers, the CSIRO team worked with the students to develop concepts which utilise and highlight the distinct advantages of printed solar films. The students created aesthetic prototypes which contributed to an end-of-year exhibition (Figure PP5.7.2). These may later be developed into functional prototypes to further explore potential paths to market for printed PV.

CSIRO was also involved in initiating a new collaboration with Monash University Business School through the Monash MBA program. CSIRO (Scholes, Ramamurthy, Chesman) and Monash (Jasieniak) ACAP partners worked with a team of four MBA students for their final "experiential learning" project, and together explored potential business cases for printed solar films. The students delivered a comprehensive presentation and report, including suggestions for possible paths to commercialisation for printed PV technology.

The CSIRO team continued its engagement with local public events, participating in Melbourne Knowledge Week (Figure PP5.7.3), the Scientists and Mathematicians in Schools (SMiS) program, and National Science Week at Queen Victoria Market.

In terms of ACAP-supported academic outreach activities, Dr Mei Gao and Dr Doojin Vak presented at the 2016 MRS Spring meeting and then visited the laboratories of Prof Samuel Graham and others at Georgia Institute of Technology. This visit continued to build on previous interactions, which ultimately resulted in support for a project through the ACAP Collaboration Grant scheme in 2016. In addition, CSIRO was invited to be one of the international partners in Georgia Tech's proposal for "Solution to Global Energy Conversion Needs". Prof Graham also visited CSIRO's Flexible Electronics Laboratory in late 2016 and spent several days working with the team in CSIRO's laboratories to gain a better understanding of how printed solar films are fabricated. In addition to their visit to Georgia Tech, Dr Mei Gao and Dr Doojin Vak also explored other opportunities with visits to MIT, Case Western Reserve University and Eastman Chemicals during the same trip.

With additional support from a CSIRO Julius Career Award, Dr Doojin Vak also spent three months in Korea, visiting several Korean universities and government agencies, and delivering numerous presentations to potential collaborators in both academia and industry.

Highlights

- The CSIRO Flexible Electronics Laboratory hosted 53 tours for visitors from high profile research institutions, industry and government.
- Continued relationship building through another ACAP-supported visit of CSIRO researchers to Georgia Tech resulted in a project funded by the ACAP Collaboration Grant scheme (Dr Hasitha Weerasinghe).
- A second round of collaboration between CSIRO and Monash Industrial Design students resulted in exciting new design concepts for future exploitation.

References

CSIRO blog post: https://blog.csiro.au/printed-solar-designs-a-bright-idea/.

Monash University Art Design and Architecture, Design Exhibition 2016.

Figure PP5.7.2: Prototype concepts incorporating flexible solar films created by Monash University industrial design students.

Figure PP5.7.3: CSIRO team at Melbourne Knowledge Week.

6. AUSIAPV International Activities

Overview

The Australia–US Institute for Advanced Photovoltaics (AUSIAPV) encompasses the local activities of the Australian Centre for Advanced Photovoltaics (ACAP) as well as international collaborations with US-based partner organisations. The AUSIAPV program is directed at the highest level through an International Advisory Committee, with representatives from the key partners in Australia and the US, with engagement fostered through the development of collaborative research programs and the annual AUSIAPV/ACAP conference.

Since late 2015 and through 2016 the organisation has had three rounds of small grants to researchers based at ACAP nodes and 17 of them were underway before the end of this reporting year and their progress reports are included in this chapter, along with those of the previously established collaborations.

A paper based on the Power Cube collaboration (Section 6.1), which established a new record of efficiency in excess of 40% in late 2014, was again selected for an Opening Plenary presentation at the European Photovoltaic Solar Energy Conference, this time in June 2016 in Hamburg. Two new world records for solar energy conversion arising from this project were certified in 2016 and an exceptional mirror reflectance over the 400–1800 nm range was also certified.

Specific project activities that leverage the benefits of the AUSIAPV relationship also include key projects in Section 6.2 regarding the development of dye-sensitised solar cells in partnership with the University of California Los Angeles, in which a PBDTTT-EFT:ICBA homo-tandem solar cell is demonstrated with a power conversion efficiency of 9% and an ultra-high open circuit voltage of 1.93 V, and Section 6.3 as part of the Foundation Program to Advanced Cell Efficiency II (FPACE II) as well as a collaboration under the US Department of Energy SunShot Inititiave, where UNSW is involved in a program led by Arizona State University.

The AUSIAPV collaboration described in Section 6.4 is a long-standing one that records the current status of a whole range of photovoltaic technologies in the maintenance and publication of Solar Cell Efficiency Tables and that reported in Section 6.5, a project with new collaborating organisation, PV Lighthouse, has grown into a leading tool for teaching photovoltaics manufacturing globally.

Many of the hot topics of the advancing silicon cell technology are being addressed by the collaboration grants. UNSW and NREL work together to develop reliable plated metallisation processes, to replace the silver-based printed contacts used for most solar cells, for the metal grids of silicon heterojunction cells and full-area electrodes for polysilicon (poly-Si) selective carrier contact cells, as reported in Section 6.6. Sections 6.7 and 6.9 describe another silicon cell partnership, ANU with the University of California Berkeley, Lawrence Berkeley National Laboratory, including the Molecular Foundry, a founding collaborating US research organisation. In the former project the contacts are primarily used to separate the electrons and holes and over 19% efficiency has been achieved, and in the latter more than 20% has been achieved with full-area rear contacts on n-type cells. ANU works with the Georgia Institute of Technology and the University of Central Florida (Section 6.10) to improve double-sided pyramidal texturing for improved light trapping in silicon cells. An ANU researcher visited NREL in 2016 and will visit again in 2017 to take advantage of their advanced silicon materials luminescence characterisation tools (Section 6.11). The topic for Section 6.15 is the analysis, by UNSW and the US National Institute of Standards and Technology (NIST), of the cost performance of thin, flexible silicon solar cells under portable conditions, and the understanding of performance-limiting mechanisms of accidental impurities in silicon cells are furthered by UNSW with the University of North Carolina Charlotte (Section 6.18) and UNSW with Arizona State University (Section 6.19). Low-thermal-stress laser tools for processing of junctions and contacts are being developed by UNSW and NIST in the project in Section 6.20.

Other grants support the combination of III-V and silicon cells into higher efficiency tandem structures. Section 6.8 describes a project in which ANU and NREL works together to develop mechanically stacked III-V/silicon tandem cells for compatibility with concentrating lenses developed for the ARENA-supported Micro Urban Solar Integrated Concentrators (MUSIC) project. UNSW works with Ohio State University to optimise the design of silicon cells to partner with GaAsP, using powerful simulation programs (Section 6.16).

Thin-film materials and devices have also been supported by small collaboration grants. CSIRO has been working with Stanford University and Georgia Institute of Technology to quantitatively analyse the cohesion between the printed layers of large-area flexible perovskite and organic solar modules in the project discussed in Section 6.12 and UoM and NREL apply time-resolved microwave conductivity to better understand organic semiconductors (Section 6.13). Melbourne

University, Princeton University and Georgia Institute of Technology, as described in the next section, are developing methods to screen organic materials for the useful singlet diffusion process. Section 6.21 describes the partnership of UNSW and Arizona State University to improve light trapping, to enhance the absorption of thin cells.

Lastly, Section 6.17 expands on efforts of UNSW and NREL to develop and apply credible costing and cost comparison methods for the manufacture of different sorts of solar cells.

In addition to the specific activities captured in this chapter, many of the reports already presented as detailed research reports also involve collaborations with US partners. These include the silicon tandem cell reported in PP1.3a and section 6.16, where well-established collaborations with institutes such as NREL, Arizona State University, Ohio State University, Colorado School of Mines, Yale University and University of Delaware are complemented by industry partner contributions from key players in the semiconductor foundry industries including Epistar Corp., Veeco and Amberwave, plus other partners from around the world.

Finally, the education, training and outreach activities reported in PP5 include a wide range of international interactions, such as the World Solar Challenge which is, arguably, the biggest and most stimulating international congregation of solar engineering students in the world, the ACAP Conference, regular and special public lectures, and partnership arrangements in teaching and on-line learning, such as the development and delivery of courses between institutes in the US and Australia.

6.1 Improved Sunlight to Electricity Conversion Efficiency: Above 40% for Direct Sunlight and Above 30% for Global

Lead Partner
UNSW

UNSW Team
Dr Mark Keevers, Prof Martin Green, Dr Jessica Yajie Jiang

UNSW Student
Bruno Concha Ramon

NREL Team
Dr Keith Emery, Larry Ottoson, Tom Moriarty

Industry Partners
RayGen: Ian Thomas, John Lasich
Spectrolab: Dr Richard King (now ASU)
Trina Solar: Dr Pierre Verlinden, Yang Yang, Xueling Zhang
AZUR SPACE: Werner Bensch

Funding Support
ASI/ARENA, AUSIAPV, NREL, Spectrolab, RayGen, Trina Solar, AZUR SPACE, UNSW

Aim

The original aim of the project was to design, fabricate and test a proof-of-concept, prototype spectrum splitting CPV module demonstrating an independently confirmed efficiency above 40%. The combination of such a spectrum splitting or "Power Cube" receiver and a CPV power tower system (Figure 6.1.1) has the potential to reduce the cost of utility-scale photovoltaics. With the targeted record performance level achieved in 2014, the project was extended in 2015 to target 42% CPV module efficiency and over 30% efficiency for a non-concentrating, flat-plate implementation of the approach. As a contribution to the AUSIAPV program, NREL has provided extensive independent testing of module performance and advice on module design.

Progress

Prototype design

The original prototype design was based on reflective concentration optics, a custom bandpass (spectrum splitting) filter, and two 1 cm^2 high efficiency commercial CPV cells, one Si and the other a triple-junction III-V cell, each mounted on a concentrator cell assembly (CCA) and a water-cooled heatsink, with an optional reflective secondary optical element (SOE) to improve flux uniformity. The mechanical design – based on optomechanical components – was iterated to achieve a lightweight, robust and fully adjustable structure, enabling optimisation about all critical linear and rotation axes. More design details are given in the 2013, 2014 and 2015 ACAP Annual Reports. A photograph of the actual system under testing at UNSW in 2014 is shown in Figure 6.1.2.

The triple-junction cell used in the prototype was a commercial Spectrolab concentrator cell (C3MJ+ cell, nominally 39.2% efficient at 500 suns–concentration, mounted on a ceramic substrate), while the Si cell was a SunPower back-contact cell of circa 1998 vintage (nominally 26% efficient at 200 suns), mounted on a

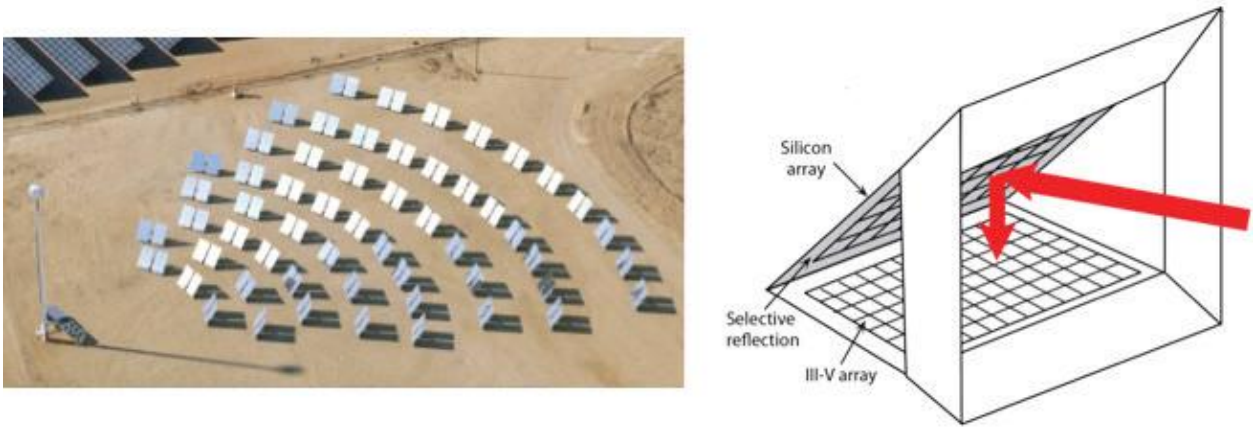

Figure 6.1.1: Photovoltaic power tower: (a) A heliostat field directs sunlight to a central tower housing a dense photovoltaic array receiver in the CPV system being developed by RayGen (artist's impression; image courtesy of RayGen); (b) Possible design of an advanced receiver implementing the demonstrated improvements at scale.

ceramic substrate and encapsulated under glass by ENEA, Italy, followed by MgF_2 anti-reflection coating (ARC) at UNSW. This combination gave a record 40.4% efficiency in testing at NREL at the end of 2014, the first demonstrated conversion of sunlight to electricity with efficiency over 40%.

Improved parabolic mirror

A key feature of the present approach is the energy selective bandpass filter custom-designed by Omega Optical Inc., which performed almost ideally. In particular, reflection was close to 100% at the desired wavelengths. This stimulated the first design modification. This was to replace the "enhanced silver" parabolic mirror simulating the heliostat field output by a dielectric mirror, custom-designed by Omega Optical based on design principles suggested by Dr Keevers. Figure 6.1.3 shows the measured reflection, exceptionally close to 100% over the entire wavelength range.

This mirror may set a new record for high reflectance over solar wavelengths, with independent measurements by NIST (US National Institute of Standards and Technology) confirming R = 99.7% ± 0.2% over the 400–1800 nm range. An improved version of the 287 cm^2 aperture area prototype using this improved parabolic mirror was independently tested at NREL's outdoor test facility in Colorado, again in a four-terminal configuration with efficiency of 40.6% ± 2% at air mass 1.5 certified, a new world record for a system of this size.

One-sun module

The project was extended in 2015 to investigate how the spectrum splitting approach could be applied to standard non-concentrating solar modules that have to respond to sunlight from a wide range of incident angles. The approach adopted was based on an earlier UNSW discovery (Mills and Guitronich, 1978) of the near-ideal angular response properties of glass prisms. The module concept is shown in Figure 6.1.4. Light reflected from the first cell along the prism hypotenuse is channelled to the second cell.

Our present design uses prisms with a 30° apex angle. In this design, this approximately halves the area of III-V cells required while maintaining an acceptance angle of 118° for on-axis light to hit both cells, with better performance for skew rays (Mills and Guitronich, 1978). An apex angle of 42° gives the full 180° acceptance angle, if required (e.g. for collecting albedo light), while 22° apex angle gives a still useful 93° acceptance angle, such as might be useful in low concentration systems such as the SunPower C7 tracker. All incident light hits at least one cell, in any case.

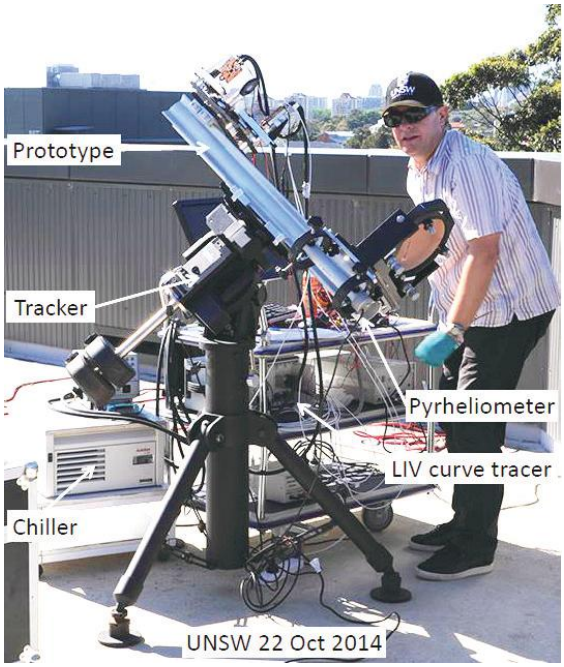

Figure 6.1.2: The prototype under testing at UNSW on 22 October 2014 with an efficiency of over 40% measured on that day.

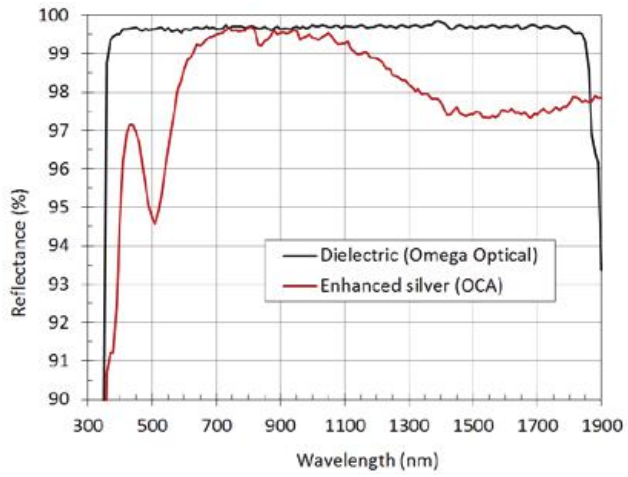

Figure 6.1.3: Measured reflection from the new dielectric mirror, showing 99.7% ± 0.2% over the 400–1800 nm range, certified at NIST.

The economics of III-V cells for one-sun use is reported in a recent NREL study (Woodhouse and Goodrich, 2013). Reference case costs are $13.60/W, or $3.40/cm^2, consistent with volume prices of III-V concentrator cells – too high for the present approach to be economic. However, NREL suggests these costs could considerably reduce in the medium- to long-term to $2.40/W, where the present approach starts looking interesting. Ultimately, NREL speculates costs as low as $0.50 per Watt may be feasible, making the approach of definite interest. Alternatively, cells other than III-V may be used. For example, 28% efficiency has already been reported for perovskite cells combined with Si in a split-spectrum tandem, although stability and durability are key issues here.

For our initial module, given the cells available, it was decided to implement the same design as in Figure 6.1.4 but with the III-V and silicon cell positions reversed with the final minimodule shown in Figure 6.1.5, being held by Dr Keevers. The 4 cm x 8 cm III-V cells were GaInP/GaInAs/Ge triple-junction cells designed for one-sun application (Bett et alia, 2009), acquired from Azur Space while the 4 cm x 4 cm Si cells were high performance interdigitated back contact (IBC) cells specially fabricated by Trina Solar for the project with antireflection (AR) coating optimised for the narrow band illumination involved.

An AR coating was also deposited on the illuminated face of the single prism forming the minimodule and a bandpass reflector designed by Omega Optical deposited on the long face, prior to the attachment of the III-V cell to this face (bandpass reflection rather than transmission used in this case). This reflects light roughly in the 900–1050 nm range, which is steered by the prism onto the silicon cell.

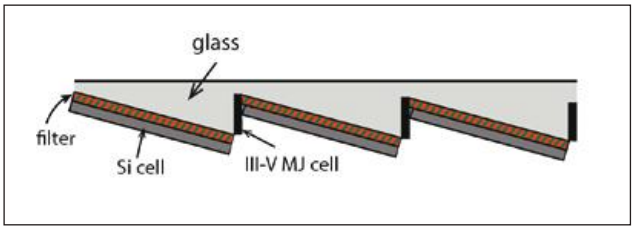

Figure 6.1.4: Initial one-sun module design concept where prisms are used to steer light reflected from one cell to the second for a wide range of incidence angles.

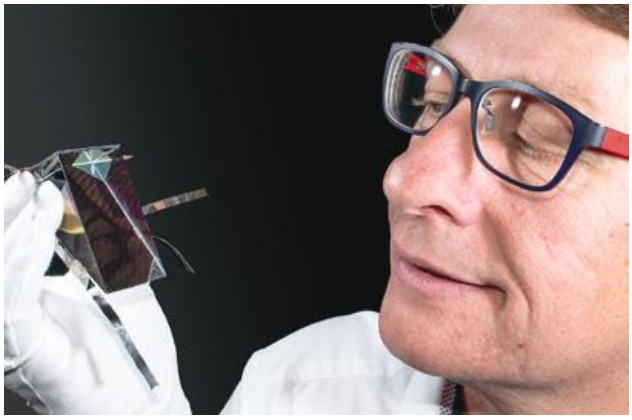

Figure 6.1.5: Dr Mark Keevers holding the record one-sun minimodule, with a III-V cell supplied by Azur Space along the prism hypotenuse combined with an Si cell supplied by Trina Solar. An efficiency of 34.5% was certified at NREL.

An efficiency of 34.5% in a four-terminal configuration was independently confirmed in April 2016 by NREL for the 28 cm^2 minimodule, the highest ever one-sun measurement for a solar module of this size, far above the previous record of 24.1% (albeit for an appreciably larger area module). Presently, the approach is being used to fabricate a much larger 800 cm^2 device with similarly high efficiency targeted.

Highlights

- Paper based on this work selected for opening plenary presentation at the most recent 2016 European Photovoltaic Solar Energy Conference in Munich.
- New world record of 40.6% certified at NREL for a 287 cm^2 concentrator system.
- New world record of 34.5% certified at NREL for a 28 cm^2 non-concentrating minimodule.
- Exceptional mirror reflectance of 99.7% ± 0.2% over the 400–1800 nm range certified at NIST.

Future Work

Further refinement of the concentrator prototype design is expected to allow an efficiency of 42% to be demonstrated, increasing the margin over the alternative

CPV and solar thermal approaches. Applying a similar approach to a standard non-concentrating, flat-plate module is expected to result in confirmation of record efficiency well over 30% for an 800 cm² module in 2017.

References

Mills, D. and Giutronich, J., 1978, "Ideal Prism Solar Concentrators", *Solar Energy*, vol. 21, p. 423.

Woodhouse, M. and Goodrich, A., 2013, "Manufacturing Cost Analysis Relevant to Single-and Dual-Junction Photovoltaic Cells Fabricated with III-Vs and III-Vs Grown on Czochralski Silicon" (Presentation), NREL Report No. NREL/PR-6A20-60126.

6.2 Dye-Sensitised Solar Cells

Lead Partner
Monash

Monash Team
Prof Yi-Bing Cheng

Monash Student
Wenchao Huang

Academic Partner
University of California Los Angeles, Prof Yang Yang

Funding Support
ACAP, ARENA, ARC, Monash

Aim

Due to the thinness of the active layer, the light absorption is a critical issue to limit the further improvement in organic photovoltaic OPV device performance. In order to use the solar radiation more efficiently, a promising approach is to use tandem solar cells combining two photoactive layers to improve the light absorption. The aim of this project is to collaborate with UCLA to develop highly efficient tandem organic solar cells.

Progress

As the interconnection layer in the fabrication of tandem cells requires a heat treatment, the use of highly thermal stable front sub-cells plays an important role in developing high performance tandem solar cells. The key aspects of the work in this report is to: (1) understand the relationship between morphology, photophysics, device performance and thermal stability in the single-junction organic solar cell; and (2) develop highly efficient organic homo-tandem solar cells.

The polymer poly[[2,6'4,8-di(5-ethylhexylthienyl) benzo[1,2-b;3,3-b]dithiophene]3-fluoro-2[(2-ethylhexyl) carbonyl]thieno[3,4-b]thiophenediyl] (PBDTTT-EFT),

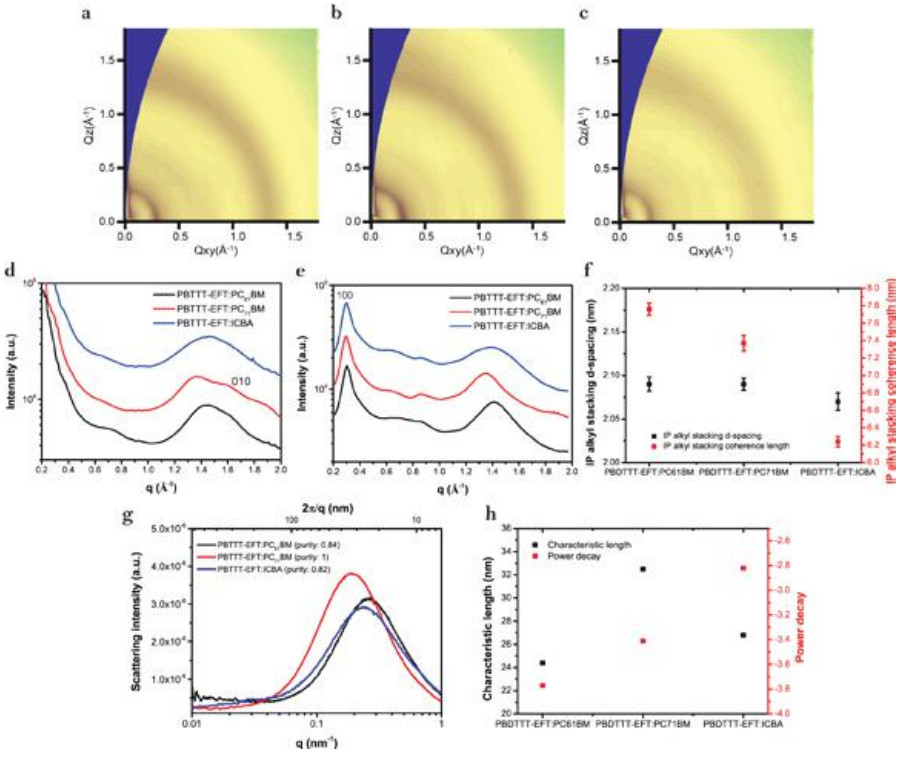

Figure 6.2.1: Morphological studies of various polymer:fullerene blends. Two-dimensional (2-D) grazing incident wide angle scattering (GIWAXS) patterns of (a) PBDTTT-EFT:PC61BM, (b) PBDTTT-EFT:PC71BM, and (c) PBDTTT-EFT:ICBA. Line profiles of various PBDTTT-EFT:PC71BM blends cut from 2-D GIWAXS patterns: (d) out-of-plane (OOP) direction, and (e) in-plane (IP) direction; (f) lamellar d-spacing and coherence lengths, fit from line profiles (e); (g) Lorentz-corrected R-SoXS profiles of various PBDTTT-EFT:fullerene blends (scattering profiles were taken at the X-ray energy of 284 eV); and (h) fit parameters from R-SoXS scattering profiles.

also called PTB7-Th, in particular has recently attracted intense attention due to the excellent device performance in both polymer/fullerene and polymer/polymer solar cells. Here, we demonstrate the correlation between morphology, device performance and thermal stability in polymer/fullerene solar cells based on different fullerene acceptors (PC71BM and ICBA) blended with the low bandgap polymer PBDTTT-EFT. Morphology is characterised with Ggazing incidence wide angle X-ray scattering (GIWAXS) and resonant soft X-ray scattering (R-SoXS), which together reveal that the PBDTTT-EFT:ICBA blend exhibits a lower polymer crystallinity, lower fullerene domain purity, and smaller fullerene domain size compared to PDBTTT-EFT:PC71BM blends, as shown in Figure 6.2.1. Although the highly mixed morphology has led to the geminate and non-geminate recombination (confirmed by transient absorption and transient photovoltage decay measurement), it is important to prevent the unfavourable coarsening upon heat treatment.

As shown in Figure 6.2.2, when the ICBA blend is annealed at 90°C, the device efficiency experiences a slight increase at the initial stage (within 5 minutes) because the annealing of the ICBA promotes further phase separation leading to larger and purer ICBA domains The device exhibits a slight decrease in its efficiency only after 10 minutes annealing because the coarsening of fullerene domain results in the poor exciton separation. In contrast, the device based on PBDTTT-EFT:PC71BM has very poor thermal stability. A rapid decrease of efficiency is observed, dropping 26% after 1 minute of thermal annealing. Device efficiency continuously decreases as a function of annealing time, exhibiting only half of its initial value after 20 minutes of thermal annealing.

Based on the good thermal stability, the PBDTTT-EFT:ICBA blend is a promising candidate for use in tandem solar cells. The use of a homo-tandem architecture however is able to increase light absorption in the cell without suffering the severe recombination that would occur in a thick single-junction cell. As shown in Figure 6.2.3(a), an architecture of ITO/PEIE/active layer/MoO_3/PEDOT:PSS/ZnO/PEIE/active layer/MoO_3/Ag is used in our homo-tandem solar cell with both front and rear sub-cell made of the PBDTTT-EFT:ICBA blend. Figure 6.2.3(b) shows J-V curve characteristics of homo-tandem solar cells. A power conversion efficiency of 9% has been achieved in this device, with a short circuit current of 9.6 $mAcm^{-2}$ and an ultra-high open circuit voltage of 1.93 V, which is the highest open circuit voltage reported for a double-junction organic tandem cell. It also should be noted that tandem solar cells are able to output an efficiency of over 8.5% at an operating voltage of 1.5 V, which shows potential for application in driving a water splitting system.

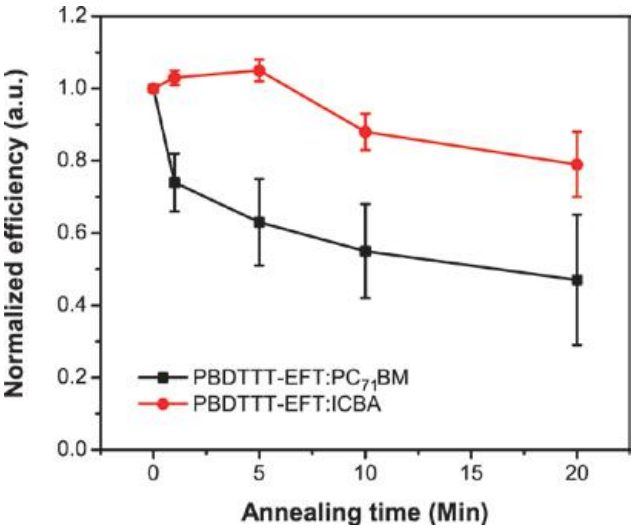

Figure 6.2.2: Normalised device efficiency as a function of annealing time. The blend films were annealed at 90°C.

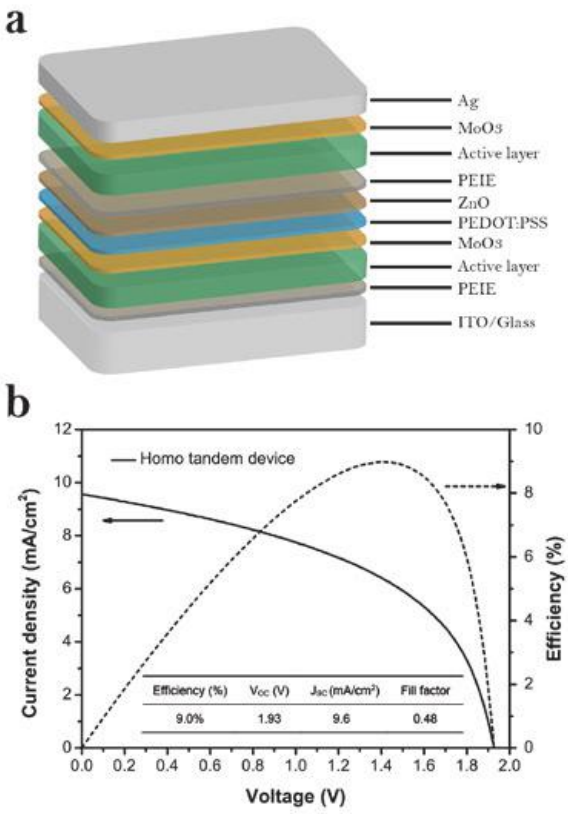

Figure 6.2.3: (a) Schematic double-junction device architecture. The front sub-cells are fabricated by PBDTTT-EFT:ICBA blends; and (b) Device performance of homo-tandem solar cells.

Highlights

- Understanding the correlation between morphology, photophysics and device performance in blends of polymer PBDTTT-EFT with different fullerene acceptors.
- Due to the highly mixed morphology, the PBDTTT-EFT:ICBA blends exhibit enhanced thermal stability compared to other blends.
- A homo-tandem PBDTTT-EFT:ICBA tandem solar cell is demonstrated with a power conversion efficiency of 9% and an ultra high open circuit voltage of 1.93 V.

Future Work

1. Develop advanced metal oxide interfacial layers to further improve the efficiency of single-junction solar cells.
2. Understand the effect of underlying substrate on the morphology of polymer blends.
3. Explore non-fullerene acceptors to replace fullerene acceptors to improve both device efficiency and stability in organic tandem solar cells. Due to the complementary absorption spectra, the application of non-fullerene acceptors is able to maximise the short circuit current of the sub-cell.

Reference

Huang, W. et al., 2017, Adv. Energy Mater., 1602197.

6.3 Carrier Selective Contacts for Boosting Silicon Solar Cell Efficiency

Lead Partner
UNSW

UNSW Team
A/Prof Stephen Bremner, Dr Anita Ho-Baillie

UNSW Student
Jing Zhao

Academic Partners
Arizona State University, A/Prof Stuart Bowden, Prof Christiana Honsberg

Aim

The aim is to develop novel device structures for ultrathin crystalline silicon (c-Si) solar cells based on "carrier selective contacts". UNSW contributes device modelling (e.g. using Sentaurus TCAD), materials deposition (e.g. spin coating), characterisation and integration of selected wide bandgap materials including transition metal oxides (e.g. NiO_x, VO_x) as carrier selective contacts for the novel silicon cell structure as part of a collaborative effort.

Progress

NiO_x and VO_x films were prepared on silicon substrates by a sol-gel dip coating method. Spin coating offers a low-cost, low temperature and easy method to achieve thin and uniform NiO_x/VO_x coatings. Atomic force microscope images of optimised layers are displayed in Figure 6.3.1. The optical constants (complex refractive index, n and k) in the wavelengths range of 380–1680 nm measured by spectra ellipsometer were extracted with double Tauc-Lorentz oscillators model for NiO_x and triple Lorentz oscillators model for VO_x. The optical bandgap is determined from the energy intercept by extrapolating

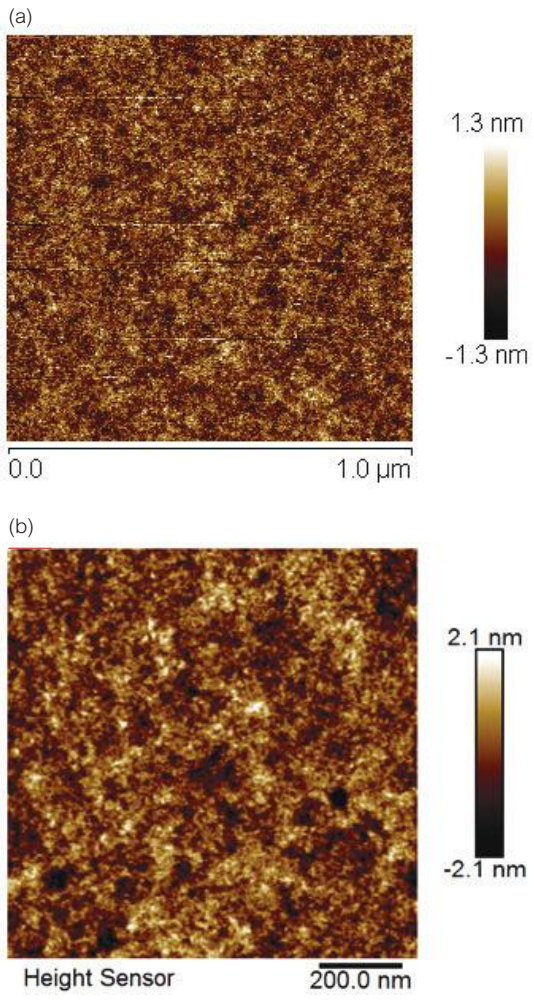

Figure 6.3.1: Atomic force microscope images of NiO_x (a) and VO_x (b). The root mean square roughness (RMS) values obtained for NiO_x and VO_x are around 0.518 and 0.469 nm, respectively.

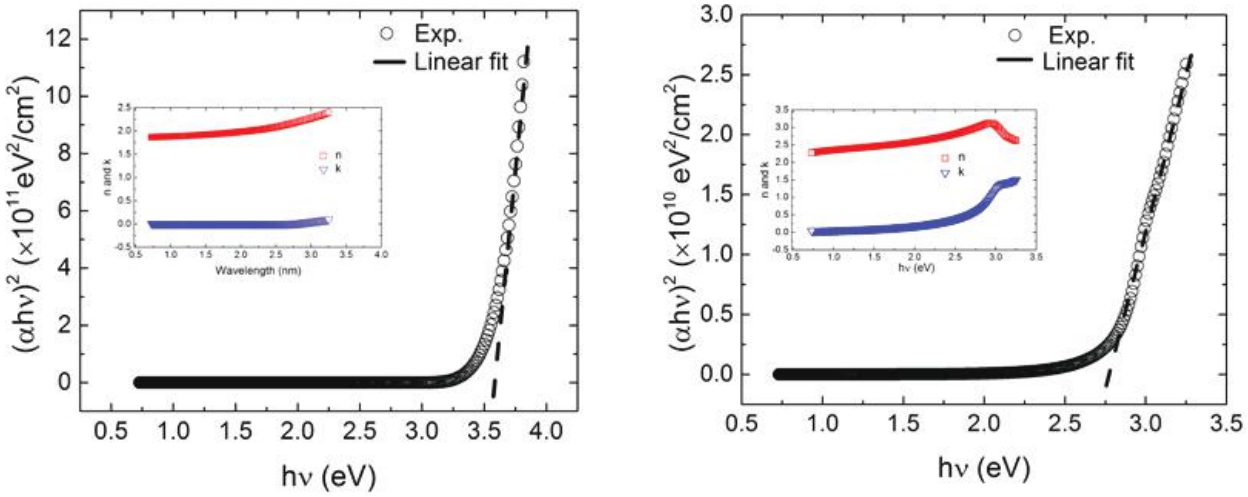

Figure 6.3.2: Plots of $(ahv)^2$ and hv (Inset: Complex refractive index n and k) of (a) NiO_x and (b) VO_x.

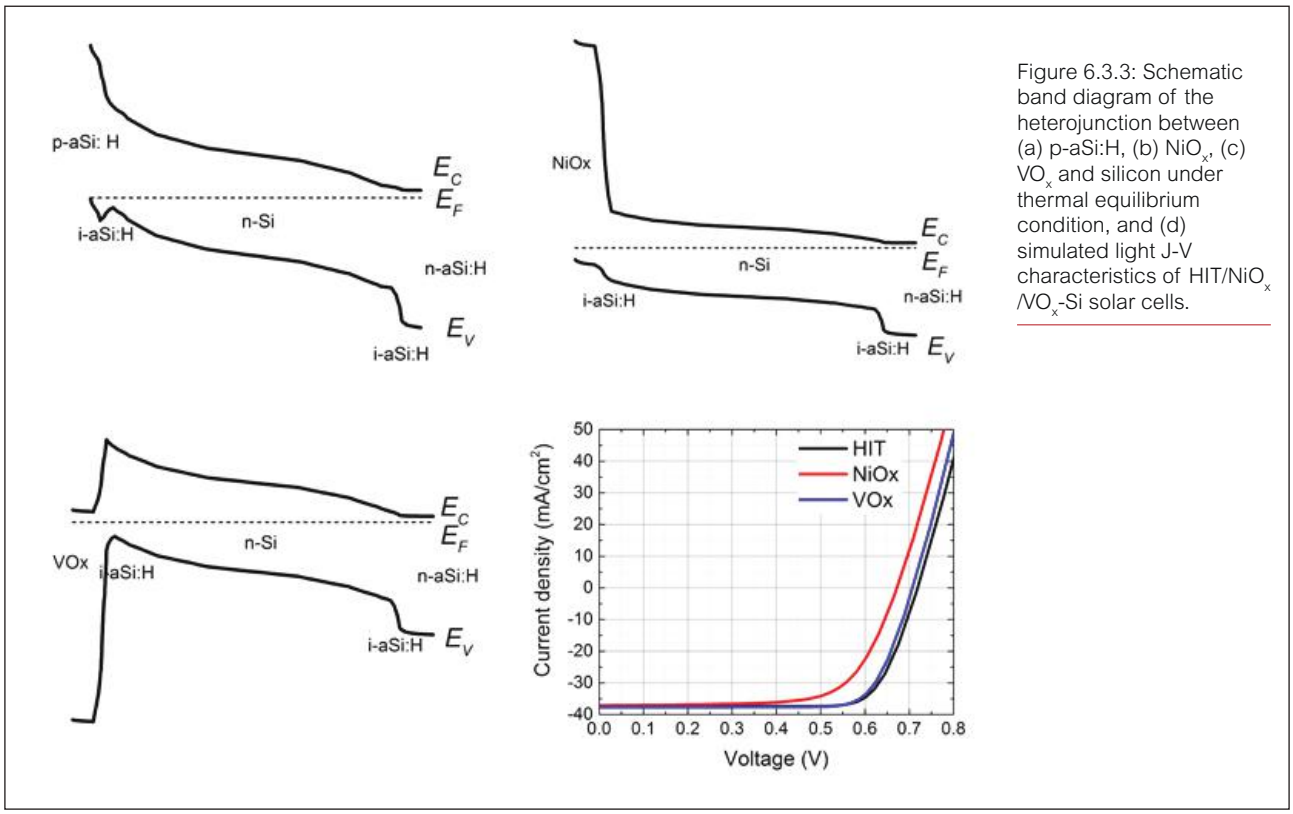

Figure 6.3.3: Schematic band diagram of the heterojunction between (a) p-aSi:H, (b) NiO_x, (c) VO_x and silicon under thermal equilibrium condition, and (d) simulated light J-V characteristics of HIT/NiO_x/VO_x-Si solar cells.

the linear portion of the plot of the square of (absorption coefficient multiplied by photon energy) versus photon energy hv to absorption coefficient equals to zero. The results are shown in Figure 6.3.2, in our case, the optical bandgap for NiO_x is estimated to be 3.6 eV and 2.7 eV for VO_x agreeing well with other reported values. The work function of each transition metal oxide (TMO) was also measured using Kelvin Prove Force Microscope (KPFM). This procedure resulted in an estimated work function of 4.85 eV for NiO_x and 5.15 eV for VO_x.

A predictive model for NiO_x/VO_x-silicon CSC solar cells that accepts electrical and optical properties of NiO_x/VO_x has also been developed using Sentaurus technology computer-aided design (TCAD). The parameters obtained by characterisation, along with those in the literature, were used as inputs for this model allowing the band diagram and Light JV of p-aSi:H/NiO_x/VO_x-Si solar cells to be plotted. As shown in Figure 6.3.3, a salient feature is the asymmetry of conduction/valence band offsets at the interface between p-aSi:H/NiO_x/VO_x and n-Si, which makes it possible to achieve high conversion efficiency

without the use of heavy doping in the silicon. The large barrier for electrons resulting from the band bending in n-Si and the conduction band offset at the conduction band edges blocks the transport of electrons, while the comparatively small valence band offset facilitates holes to transit through p-aSi:H/NiO_x or the oxygen vacancy-derived defect states in VO_x to the front contact.

According to our TCAD heterojunction model, the conversion efficiency can reach up to 17.24% and 20.66% for NiO_x and VO_x CSC solar cells, respectively. Importantly, the device performance can be further improved by the modification of the TMO like the thickness and stoichiometry.

Highlights

- TCAD-based heterojunction model developed, allowing for entering of experimentally obtained parameter values.
- High quality, smooth layers of NiO_x and VO_x layers by sol-gel methods have been obtained.

Future Work

Obtaining information about the carrier selective nature of these layers has begun with transfer length model measurements, however the interface to the silicon has proven problematic, a common issue for TMO-based CSC approaches. The inclusion of a thin amorphous silicon (a-Si) layer between the TMO and silicon is underway, with high quality passivating a-Si being provided by our collaborators at ASU. In parallel with this effort, we will be depositing thin aluminium oxide layers to be sandwiched between the TMO and silicon. This will be done by atomic layer deposition at UNSW, with aluminium oxide proven to give excellent surface passivation. It is expected that this will allow a better assessment to be made of the viability of the NiO_x and VO_x layers for use in CSCs. Further experiments to give more detailed information on the transport of carriers through these layers, particularly through defect energy levels, is being investigated as well.

6.4 Solar Cell Performance Documentation

Lead Partner
UNSW

UNSW Team
Prof Martin Green, Dr Anita Ho-Baillie

NREL Team
Keith Emery, Dr Dean Levi

Academic Partners
Fraunhofer Institute, JRC Ispra, AIST Japan

Funding Support
ACAP

Aim

To improve accuracy and quality of photovoltaic device measurement and reporting.

Progress

A long-standing research collaboration between UNSW and NREL, now being conducted as an AUSIAPV collaborative project, involves the reliable documentation of the current status of the whole range of photovoltaic technologies worldwide. This is by the biannual publication of the "Solar Cell Efficiency Tables" in the Wiley journal, *Progress in Photovoltaics*.

By enforcing guidelines for the inclusion of solar cell efficiency results into these Tables, this not only provides an authoritative summary of the current state of the art but also ensures measurements are reported on a consistent basis. One criterion that has been important to enforce has been that results be independently certified at one of a limited but increasing number of "designated test centres", generally of a national facility status, with a certified measurement capability and additionally involving international "round robin" testing.

This rigour has been important particularly as new device technologies come to the fore and groups relatively inexperienced with cell testing suddenly are thrust into the limelight. The other important role has been in developing measurement standards when international standards are not available. Figure 6.4.1 shows standards in this category developed for defining the area used for efficiency determination for experimental laboratory cells.

Several results from the AUSIAPV/ACAP program have set new world standards and are featured in these Tables. In 2016, this included a new record efficiency for a concentrating photovoltaic submodule, increasing performance levels to 40.6%, as well as for a non-concentrating one-sun minimodule, increasing this to 34.5%. New records were also set for CZTS cell performance, with 7.6% confirmed for a 1 cm^2 device early in 2016, increased to 9.5% for a smaller device later in the year. New world records for large-area perovskite performance were also confirmed over the year although only one, 11.5% for a 16 cm^2 minimodule, matched with the categories reported in these Tables. ACAP partner, Trina Solar, also featured prominently, setting a new world record for commercially dominant multicrystalline cells, with 21.3% reported for a large-area commercially sized device based on the UNSW-developed PERC (Passivated Emitter and Rear Cell) approach.

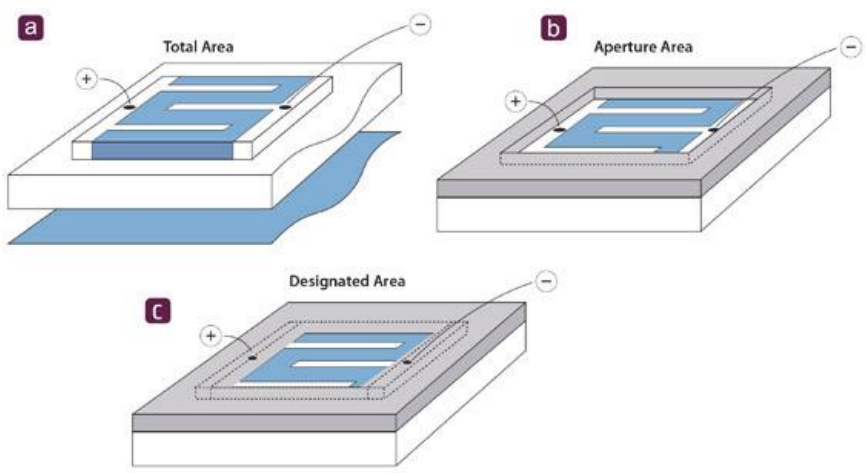

Figure 6.4.1: Cell area definitions: (a) Total area; (b) Aperture area; (c) Designated illumination area.

The Tables are widely used and referenced by the photovoltaic research community. According to the ISI Web of Knowledge, the eight versions prepared since 2013 under the banner of AUSIAPV have all been among the most cited papers published since then in the engineering discipline worldwide.

Highlight

- Value of Tables validated by exceptionally high citation rates.

Future Work

Publish two updated versions of the Tables during 2017.

6.5 PV Manufacturing Education

Lead Partner
UNSW

UNSW Team
Dr Bram Hoex

UNSW Student
Chris Whipp

QESST Team
Prof Stuart Bowden, Dr Andre Augusto

Industry Partner
PV Lighthouse

Funding Support
ACAP, UNSW

Aims

Many students come to UNSW wanting to learn how solar cells are manufactured. However, silicon solar cell manufacturing involves a diverse range of processing, ranging from chemical etching, plasma physics and metal alloying to screen printing. Understanding all of these processes, and how they interact in a production line, is challenging, to say the least, especially when it is not possible to take students to see a cell production line. Combined with the need for students to learn how to optimise a process with so many interrelated steps, a major educational challenge arises. To address this challenge, in 2001–2002 Professor Stuart Wenham and Dr Anna Bruce from the School of Photovoltaic and Renewable Energy Engineering at UNSW developed a simulation of the production of screen-printed silicon solar cells, called the Virtual Production Line (VPL).

In 2014, PV Factory (a cloud-based simulation platform) was developed through an ACAP-supported collaboration involving PV Lighthouse, UNSW and Arizona State University as a teaching application that could engage PV and Solar Energy Engineering students as they learned about how solar cells are made. This platform utilised revised versions of many of the earlier algorithms developed for VPL. Hosting of the simulation in the cloud has made it simpler for students to use the simulation – with the software hosted in the cloud there is no limitation regarding downloads nor version control. Cloud-based delivery has also enabled the implementation of leaderboards where students can compete with their classmates and users across the world to achieve the highest cell efficiency. PV Factory was released to the public in January 2015 and can be accessed at: https://factory.pvlighthouse.com.au.

PV Factory has attracted more than 9,000 unique users since its inception and is currently used in at least five universities in their teaching programs (including UNSW and ASU). PV Factory has processed over 200,000 solar cell batches and has produced more than 2.2 million solar cells. Hence, it is clear that PV Factory has been found to be extremely useful in international PV manufacturing education.

Progress

In 2016 the focus has been on planning a revision of the content delivery of PV manufacturing education. After a critical review of the course content in close consultation with the students at UNSW, it has been decided to establish an online Wiki complemented by tailored videos and animations illustrating the various processes involved in PV manufacturing.

Highlights

The PV Factory platform has been running consistently for over two years now and is formally used by five universities worldwide to run classes in their PV education programs.

Future Work

A joint UNSW–ASU project will commence in 2017 to "technology enhance" the content delivery to complement the PV Factory platform.

References

Abbott, M., et al., 2015, 42nd IEEE Photovoltaic Specialists Conference, New Orleans.

Lennon, A., et al., 2015, IEEE International Conference on Teaching, Assessment, and Learning for Engineering (TALE), Zhuhai, China, p. 267.

Whipp, C., 2016, "Upgrading PV Factory as an Educational Tool", BSc Thesis, UNSW.

6.6 Metal Plating for Next Generation Silicon Solar Cells

Lead Partner
UNSW

UNSW Team
A/Prof Alison Lennon, Dr Udo Römer

ACAP Team
Dr Paul Stradins, Dr Mathew Page, Dr Manuel Schnabel

Academic Partner
National Renewable Energy Laboratory (NREL)

Funding Support
ACAP

Aim

The objective of this project is to develop reliable plated metallisation processes for the metal grids of silicon heterojunction cells and full-area electrodes for polysilicon (poly-Si) selective carrier contact cells. The project will develop both the plating processes (guided by optical modelling) for the two technologies and the measures of process reliability that will be required (e.g. adhesion of the plated metal and determination of possible penetration of the metal through barrier layers).

Progress

In 2016 our partners at NREL deposited their poly-Si contacts on the rear side of cell precursors, fabricated at UNSW. Following the poly-Si deposition process an indium tin oxide (ITO) layer has to be deposited at the solar cells' rear surface serving as: (i) a mirror for long wavelength light; (ii) a capping layer for the thin poly-Si layer; and (iii) a conductive seed layer for the following plating process. Unfortunately, our colleagues at NREL faced various problems with their ITO deposition tool and had to design and fabricate a new sample holder specifically for the cells used in this project. As the ITO layer is an important part of the cell structure and is required for the plating process, no plating experiments have been conducted to date.

Nevertheless, the optical properties of different ITO layers (that can be deposited by NREL) have been measured on small test samples and optical simulations have been conducted in order to optimise the thickness of the ITO layer and to investigate the influence of different metallisation schemes on the optical properties and thus on the short circuit current of the solar cells.

Figure 6.6.1 shows the simulated current density for two ITO layers developed at NREL, compared to two ITO layers from literature, for different ITO layer thicknesses of each. In all cases, Ag has been used as a rear reflector, covering the ITO layer. It is shown that using an ITO layer can increase the current density of the solar cell by > 0.1 $mAcm^{-2}$, even when using Ag as the rear reflector metal.

Figure 6.6.2(a) shows the simulated current density for different rear metals on top of the optimised ITO layer, again for different ITO thicknesses. A strongly reduced current density can be observed for typical seed metals used for Cu plating, like Ni and W. The results are approximately the same, regardless if these seed metals are assumed to be 3 μm thick or only 50 nm thick and capped with a 3 μm thick Cu layer. For these metals, the application of an ITO layer between metal and solar cell

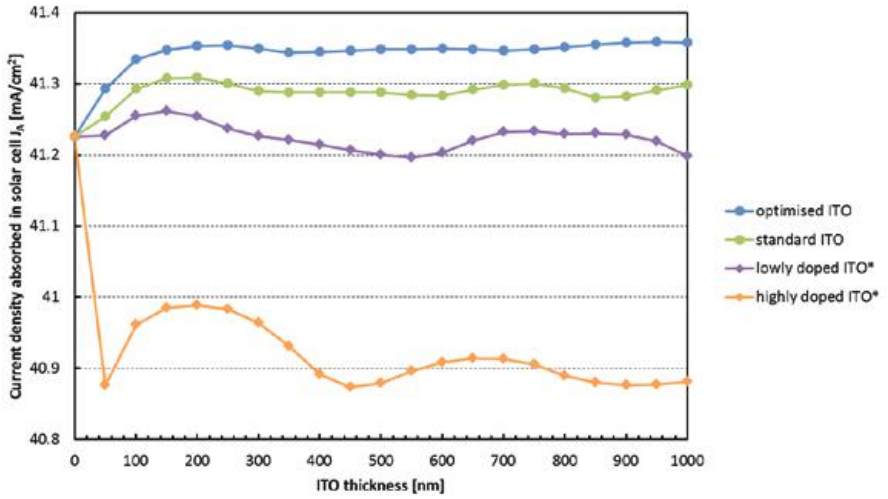

Figure 6.6.1: Optical simulation of simplified solar cell structures featuring 70 nm SiN_x, 180 μm Si, 2 nm SiO_2, 50 nm poly-Si, ITO, and 3 μm Ag.

(a)

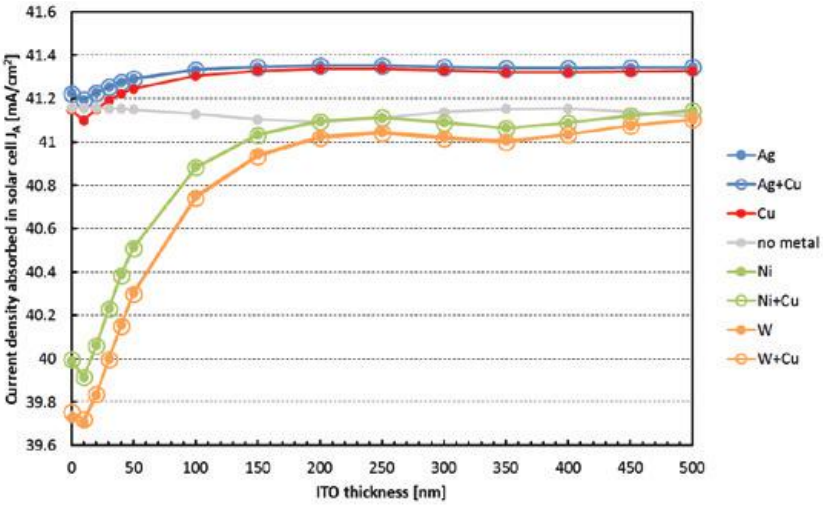

(b)

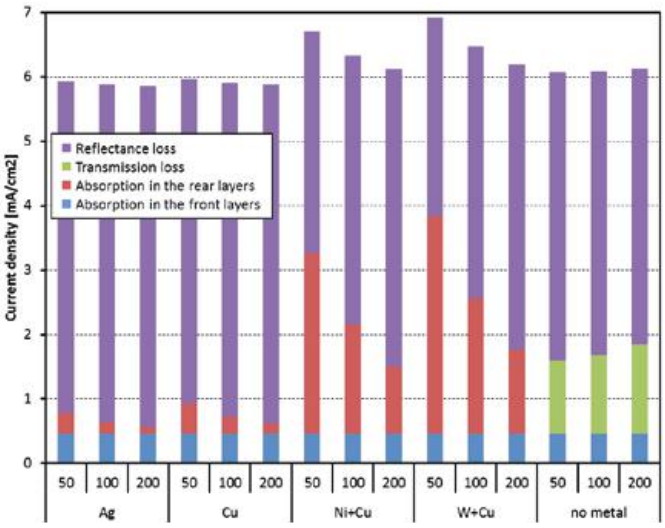

Figure 6.6.2: (a) Optical simulation of simplified solar cell structures featuring 70 nm SiN_x, 180 μm Si wafer, 2 nm SiO_2, 50 nm poly-Si, ITO, and either 3 μm metal or 50 nm metal capped with 3 μm Cu; and (b) Impact of the different current loss mechanisms.

has a much stronger impact on the current density, than for the Ag or Cu metallised cells.

Figure 6.6.2(b) shows that the observed current loss differences are, as expected, caused by parasitic absorption in the rear layers. Holman et al., 2013 have shown that even when using a good rear reflector like ITO, the thickness of this layer also is important in order to reduce the parasitic absorption of the rear metals. This is especially true for solar cells featuring a textured front side, as this will cause a large part of the light to impact the rear surface at small incident angles, leading to total internal reflection at the Si/ITO interface and therefore also to evanescent waves that penetrate the ITO layer and depending on the thickness of the ITO layer to absorption in the metal layer. Even though the parasitic absorption of Ni and W can be reduced by using an optimised ITO layer, the direct plating of Cu on ITO turns out to be a simpler solution in terms of optical performance.

Highlights

- Fabrication of solar cells featuring poly-Si rear contacts, only lacking the step of ITO deposition and metal plating.
- Optical simulation of solar cell structure and analysis of impact of the ITO thickness and different metallisation schemes on the rear reflectance.

Future Work

- Complete fabrication of the cell precursors by sputtering ITO.
- Establish an ITO sensitisation process suitable for Cu plating of the cells.
- Characterise the fabricated solar cells: investigate contact resistance of plated metal, compare optical properties with simulations, investigate adhesion properties and determine possible Cu penetration through the ITO layer after thermal treatment.
- Fabricate a second batch of optimised solar cells refining problems identified in the first batch of cells.

Reference

Holman, Z.C., Filipč, M., Descoeudres, A., De Wolf, S., Smole, F., Topič, M. and Ballif, C., 2013, "Infrared light management in high-efficiency silicon heterojunction and rear-passivated solar cells", Journal of Applied Physics, 113, 013107.

6.7 Dopant-Free Crystalline Silicon Solar Cells

Lead Partner
ANU

ANU Team
Prof Andres Cuevas, Dr Yimao Wan, Mr Chris Samundsett

ANU Students
Thomas Allen, PeiTing Zheng

USA Partners
Team
Professor Ali Javey (UCB, LBNL), Dr James Bullock (UCB, LBNL)
University of California Berkeley (UCB), Lawrence Berkeley National Laboratory (LBNL, including the Molecular Foundry)

Aim

This collaboration with UCB, extended to EPFL in Switzerland, has demonstrated silicon solar cells that implement functional materials with an extremely high or low work function, such as sub-stoichiometric molybdenum oxide (MoO_x) and lithium fluoride (LiF_x), to create hole-selective and electron-selective contacts on c-Si. These materials not only remove the fundamental limitations associated with doped silicon, but can also be deposited at low temperatures (≤ 200°C) in simple, full-area architectures, greatly reducing the cost and complexity of fabrication. The project has led to the demonstration of dopant-free silicon solar cells with full-area passivated contacts and a conversion efficiency close to 20%. It has also led to an n-type Si solar cell with a partial-area rear contact structure, with an efficiency of 20.6%.

Progress

A salient characteristic of solar cells is their ability to separate photo-generated electrons and holes by providing two different pathways of asymmetrical conductivity, thus "easing" them towards their respective contacts. All commercially available crystalline silicon (c-Si) solar cells achieve this by doping the near-surface regions of the wafer or overlying silicon-based films, such as hydrogenated amorphous silicon. Despite being commonplace, this doping approach is known to be hindered by a host of optoelectronic losses and technological limitations specific to heavily doped silicon (or amorphous silicon). A paradigm shift to circumvent these issues involves the replacement of doped-silicon conductors with alternative materials that form "carrier-selective" contact structures on c-Si. In this project we have successfully developed and implemented dopant-free heterocontacts for both electrons and holes, using alkali metal fluorides and metal oxides, respectively, resulting in competitive efficiencies approaching 20%. Furthermore, the simplified architectures inherent to this approach allow cell fabrication in only seven low-temperature (≤ 200°C), lithography-free steps – a marked improvement on conventional doped-silicon high-efficiency processes, highlighting potential improvements

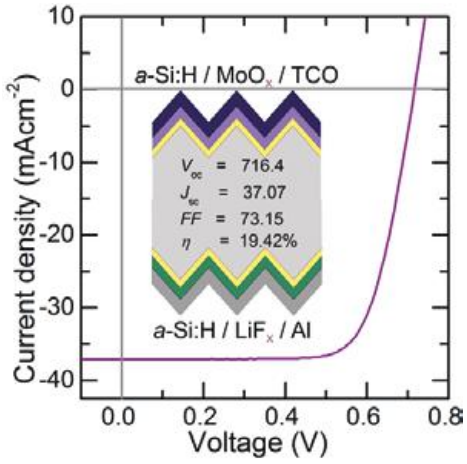

Figure 6.7.1: Current density versus voltage for n-type cell with LiF_x/Al contact

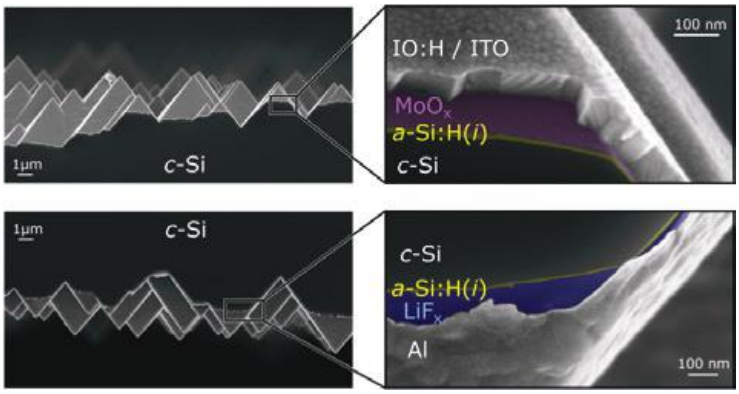

Figure 6.7.2: Superacid passivation of textured crystalline silicon surfaces.

on both sides of the cost-to-performance ratio for c-Si photovoltaics.

This project has facilitated a strong collaboration between the Cuevas research group at ANU and the Javey research group at UCB. Since both groups already had collaborations with the Ballif–De Wolf group at EPFL, the project has both assisted and benefited from it as well. It is also worth mentioning that this collaboration project forms part of a broader strategy that also includes ACAP project PP1.2b on passivated contacts and collaboration project PP6.9, also with UCB. Given the relatively small amount of funding available within the "main" project (PP1.2b), these two collaboration projects have been extremely useful. The present project (PP6.7) has allowed us to dedicate specific resources and funding to the collaboration, enabling work that would otherwise have been impossible. To gain a global picture of how effective this collaboration has been, it would be appropriate to read the annual reports (2016) for projects PP1.2b and PP6.9, where additional work and publications are described.

Given that before the start of this project we had developed hole-selective contacts based on molybdenum oxide (Bullock et al., 2015), in this project we have placed special emphasis on the complementary electron-selective contacts. Whereas MoO_x has still been used within this project to fabricate the dopant free asymmetric heterocontact (DASH) solar cell, we have investigated materials like lithium fluoride, calcium (reported in project PP1.2b), magnesium fluoride and magnesium oxide (the last two reported in project PP6.9), to make n-type cells either with a full-area rear contact or with a partial-area rear contact (PaRC). The latter devices reproduce on n-type silicon, the advanced cell structure that is becoming increasingly popular on p-type silicon. Within this project we have convincingly demonstrated these novel n-type Si PaRC devices, with efficiencies above 20%.

As an ancillary work, we have developed a new chemical method for a temporary, quasi-stable passivation of silicon wafer surfaces, in order to facilitate the characterisation of their electronic quality. Such characterisation of the bulk electronic properties of silicon is essential to select high quality wafers and to monitor and optimise the fabrication of high efficiency solar cells, such as those presented below.

Lithium fluoride electron contacts for high efficiency n-type crystalline silicon solar cells

Low-resistance contact to lightly doped n-type crystalline silicon (c-Si) has long been recognised as technologically challenging, due to the pervasive Fermi-level pinning effect. This has hindered the development of certain devices such as n-type c-Si solar cells made with partial rear contacts (PRC) directly on the lowly doped c-Si wafer. In this project we have demonstrated a simple and robust process for achieving mΩcm² scale contact resistivities on lightly doped n-type c-Si via a lithium fluoride/aluminium contact. The realisation of this low-resistance contact has enabled the fabrication of a first-of-its-kind high-efficiency n-type PRC solar cell. The electron contact of this cell was made to less than 1% of the rear surface area, reducing the impact of contact recombination and optical losses, and permitting to achieve a conversion efficiency greater than 20% in the initial proof-of-concept stage. The implementation of the LiF_x Al contact eliminates the need for the costly high temperature phosphorus diffusion, typically implemented in such a cell design to nullify the issue of Fermi-level pinning at the metal/semiconductor interface. The timing of this demonstration is significant, given the ongoing transition from p-type to n-type c-Si solar cell architectures, together with the increased

adoption of advanced PRC device structures within the c-Si photovoltaic industry.

Dopant-free, asymmetric heterocontact (DASH) silicon solar cells

In this project we have demonstrated the DASH cell concept – a simple, low temperature c-Si solar cell featuring dopant-free heterocontacts. A key enabling factor has been the development of a novel c-Si/a-Si:H(i)/LiFx/Al electron-selective heterocontact to complement a recently developed MoO_x hole-selective heterocontact. Proof-of-concept device efficiencies with a conversion efficiency approaching 20% have been achieved, supported by a high V_{OC} of 716 mV and low contact resistance at both the electron and hole heterocontacts. This represents a significant improvement on the state of the art for the dopant-less approach (from η of ~14% to ~20%) bringing the DASH architecture into the competitive realm of industrially applicable technologies such as doped-amorphous silicon heterojunctions (SHJ) and conventional dopant-diffused architectures. The versatility and simplicity of the DASH approach can potentially benefit more advanced solar cell architectures. In particular, dopant-free interdigitated back contact and dopant-free bifacial (using, for example, LiF_x transparent conductive oxide contacts) solar cells are both logical extensions of this work. The advancement past the limitations of single bandgap c-Si cells towards a monolithic tandem cell structure can also be facilitated by the use of transparent, dopant-free carrier-selective contacts for a c-Si bottom cell. Put simply, the DASH system developed here can be viewed as a toolbox for a wide range of c-Si solar cell architectures, providing opportunities for facile fabrication of high efficiency device structures at low temperatures.

Superacid passivation of crystalline silicon surfaces

The reduction of parasitic recombination processes commonly occurring within the silicon crystal and at its surfaces is of primary importance in crystalline silicon devices, particularly in photovoltaics. We have explored a simple, room-temperature treatment, involving a non-aqueous solution of the superacid bis(trifluoromethane) sulfonimide, to temporarily deactivate recombination centres at the surface. We have shown that this treatment leads to a significant enhancement in optoelectronic properties of the silicon wafer, attaining a level of surface passivation in line with state-of-the-art dielectric passivation films. Finally, we have demonstrated its advantageous application to carrier lifetime and process cleanliness monitoring, establishing its compatibility with large area photoluminescence imaging in the process.

Highlights

- Silicon cells with a partial-area rear contact using LiF_x (20.6% efficient).
- A high efficiency (19.4%) solar cell with dopant-free asymmetric heterocontacts (DASH), using intrinsic amorphous silicon, molybdenum oxide MoO_x, and lithium fluoride, LiF_x.

References

Bullock, J., et al., 2015, J. Photovoltaics 5, 1591.

Bullock, J., Hettick, M., Geissbühler, J., Ong, A.J., Allen, T., Sutter-Fella, C.M., Chen, T., Ota, H., Schaler, E.W., De Wolf, S., Ballif, C., Cuevas, A. and Javey, A., 2016, "Efficient silicon solar cells with dopant-free asymmetric heterocontacts", Nature Energy, 1, 15031.

Bullock, J., Kiriya, D., Grant, N., Azcatl, A., Hettick, M., Kho, T., Phang, P., Sio, H., Yan, D., MacDonald, D., Quevedo-Lopez, M., Wallace, R., Cuevas, A. and Javey, A., 2016, "Superacid passivation of crystalline silicon surfaces", ACS Appl. Mater. Interfaces, 8(36), 24205–24211.

Bullock, J., Wan, Y., Hettick, M., Geissbühler, J., Ong, A.J., Kiriya, D., Yan, D., Allen, T., Peng, J., Zhang, X., Sutter-Fella, C.M., Wolf, S.D. Ballif, C., Cuevas, A. and Javey, A., "Survey of dopant-free carrier-selective contacts for silicon solar cells", IEEE 43rd Photovoltaic Specialists Conference (PVSC), 0210-0214.

Bullock, J., Zheng, P., Jeangros, Q., Tosun, M., Hettick, M., Sutter-Fella, C.M., Wan, Y., Allen, T., Yan, D., Macdonald, D., De Wolf, S., Hessler-Wyser, A., Cuevas, A. and Javey, A., 2016, "Lithium Fluoride Based Electron Contacts for High Efficiency n-Type Crystalline Silicon Solar Cells", Adv. Energy Mater., 1600241, doi:10.1002/aenm.201600241.

6.8 GaAs/Si Elongate Tandem Cells for Moderate Concentration

Lead Partner
ANU

ANU Team
Dr Matthew Stocks, Prof Andrew Blakers

Academic Partner
NREL

Funding Support
ARENA, ANU, NREL

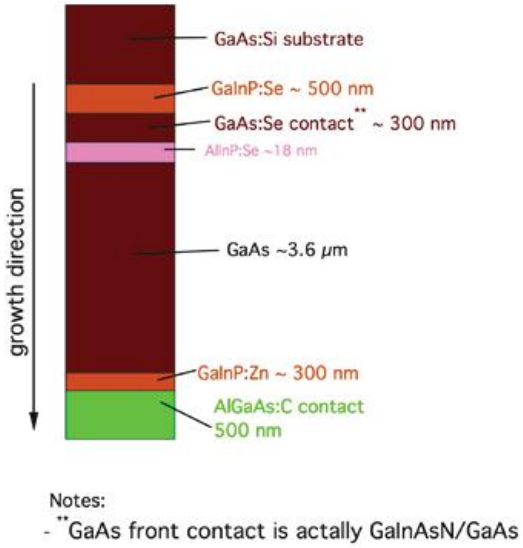

Figure 6.8.1: Cross-section of the GaAs cell precursor.

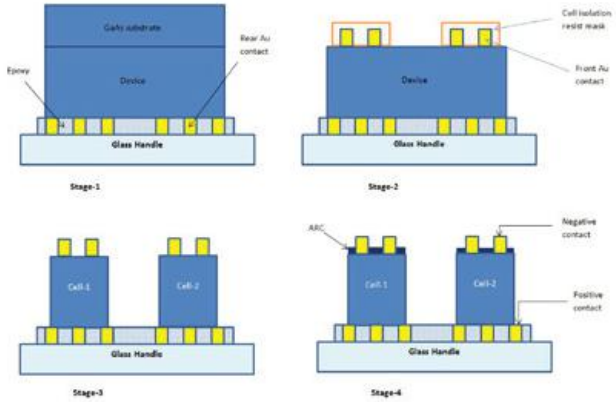

Figure 6.8.2: Schematic of GaAs cell processing.

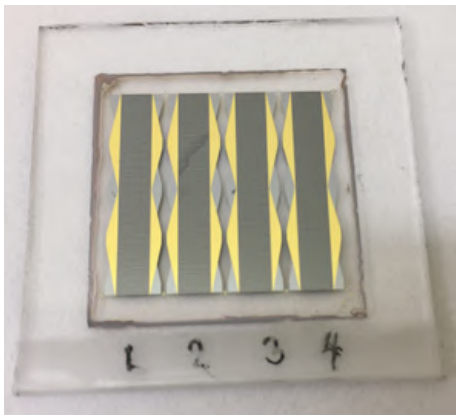

Figure 6.8.3: Image of the completed cells.

Aim

Demonstrate the potential of mechanically stacked tandems to increase silicon module efficiency.

Progress

GaAs cell development has been undertaken in collaboration with NREL. NREL grew the active layers for the GaAs device as per Figure 6.8.1. This structure is inverted in the final cell configuration. The precursor was 25 mm x 25 mm.

Subsequent cell processing was undertaken at ANU. This process involved deposition of the bottom contacts, mounting on glass, selectively removing the GaAs substrate, deposition of the top contact and subsequent isolation. This sequence is shown schematically in Figure 6.8.2. The cell has top and bottom grids on the 20 mm long by 0.3 mm wide active area to enable sub-bandgaps to pass through the cells. Top and bottom contacts are accessible via the top surface of the device with the interleaved contacts on the cell edge. Images of complete devices can be seen in Figure 6.8.3. The cell dimensions and grid have been designed to be compatible with the moderate concentration linear compound parabolic concentrator lenses developed for the Micro Urban Solar Integrated Concentrators (MUSIC) project.

The cells have demonstrated efficiencies up to 23%. Cell voltage and fill factor have been as expected (1.057 V and 84%) however currents have been low. It is not clear if this is a calibration error due to the silicon reference (different bandgap) or a cell issue. While reflection measurements show that the optics look okay, EQE measurements have not been clear due to difficulties contacting the cell (see below). If the device current achieves the expected levels, then these GaAs cell efficiencies should exceed 26% and tandem combinations with silicon should be comfortably greater than 30%

Contacting issues have prevented the measurement of the cells in a tandem configuration. The metal contacts have titanium as the intermediate layer to ensure adhesion of the gold to the cell. This resulted in titanium as the accessible surface on the completed devices (see grey edge contacts in Figure 6.8.3). Attempts to attach wires to these contacts have not yet been successful. Additional trials are underway on different contacting methods but may require an additional deposition step to deposit a less reactive metal on the surface of the lower contact pads.

Highlight

- Processing of the first GaAs cells at the ANU.

Future Work

- Modification of the cell process to increase current and improve contacting.
- Testing of the GaAs/Si tandem under moderate concentration.

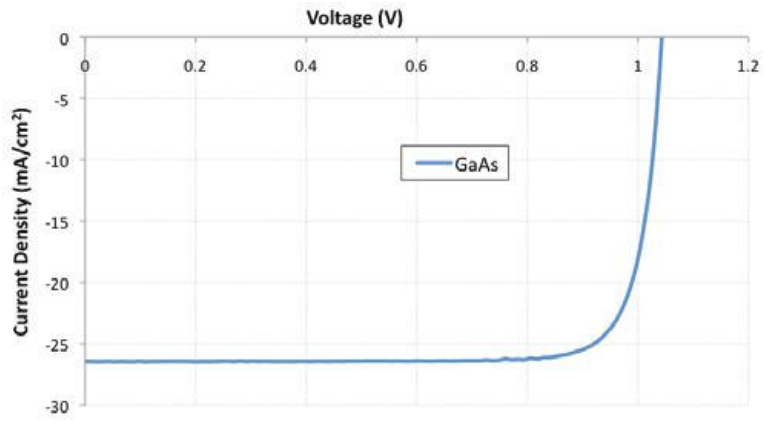

Figure 6.8.4: Current voltage curve of the GaAs top cell.

6.9 Advanced Hole-Selective Contacts to Replace Boron Diffusion

Lead Partner
ANU

ANU Team
Dr Yimao Wan, Prof Andres Cuevas, Mr Chris Samundsett, Dr Jie Cui, Ms Josephine McKeon

ANU Students
Thomas Allen, Peiting Zheng, Di Yan, Xinyu Zhang

ACAP Team
Dr James Bullock, Dr Mark Hettick, Professor Ali Javey (UCB, LBNL)
Academic Partners
University of California Berkeley (UCB), Lawrence Berkeley National Laboratory (LBNL, including the Molecular Foundry)
Funding Support
ARENA

Aim

One of the major factors limiting the further advancement of n-type low-cost silicon solar cells is the high temperature boron diffusion step, which causes a severe degradation in silicon material quality, with a reduction in bulk carrier lifetime by a factor of three. The advent of hole-selective heterocontacts offers a solution to the problem, plus additional advantages, including lower processing temperatures, a reduced requirement in cleanliness and a simpler fabrication procedure. This project aims to: (i) survey and trial a number of simple hole-selective contact (HSC) schemes; and (ii) transfer the most successful of these to low-cost silicon solar cells.

Progress

The screening trial of several possible candidates for HSC has been completed at ANU showing the following materials have promisingly low contact resistivity for holes: MoO_x, WO_x and NiO_x. The first proof-of-concept cells based on both p-type and n-type substrates were also fabricated using the abovementioned three candidates, demonstrating that MoO_x and WO_x have great potential to replace boron diffusions, providing ohmic contact to p-type Si and junction (rectifying) contact to n-type Si substrates. Screening trials are also ongoing at UCB, focusing on MoO_x, WO_x and VO_x, complementing the absence of capability in evaporating VO_x at ANU. Proof-of-concept cells will also be fabricated at a later stage.

Although the specific goal of this project is to develop HSCs for solar cells, its generic objective is to contribute to the new field of dopant-less solar cells, complementing work done in a companion collaboration project (PP6.7) and in the host project on passivated contacts PP1.2b. In that broader context, there has been a window of opportunity during 2016 to develop two new electron-selective contacts based on magnesium fluoride and magnesium oxide. Both are briefly described below. Further details can be found in the corresponding papers, published in *Advanced Energy Materials* and *ACS Applied Materials Interfaces*.

Passivated electron-selective contacts based on magnesium fluoride

Magnesium fluoride is well known for its optical, rather than electronic, properties. In this study we present a novel application to form the electron contact of silicon solar cells. The passivated electron contact is composed of deposited layers of amorphous silicon (~ 6.5 nm),

magnesium fluoride (~ 1 nm) and aluminium (~ 300 nm). X-ray photoelectron spectroscopy revealed a work function of 3.5 eV for the MgF_2/Al stack, significantly lower than that of aluminium itself (~ 4.2 eV), thus enabling an ohmic contact to n-type c-Si. The optimised contact structure exhibits a sufficiently low contact resistivity of ~76 $m\Omega cm^2$, together with a very low contact recombination current density of ~ 10 $fAcm^{-2}$. Its implementation as a full-rear contact of n-type Si solar cells led to a 20.1% proof of concept device with a high open circuit voltage of 687 mV.

Magnesium oxide electron-selective contacts

A high Schottky barrier (> 0.65 eV) for electrons is typically found on lightly doped n-type crystalline silicon (c-Si) wafers for a variety of contact metals. This behaviour is commonly attributed to the Fermi-level pinning effect and has hindered the development of n-type c-Si solar cells, while its p-type counterparts have been commercialised for several decades, typically utilising aluminium alloys in full-area, and more recently, partial-area rear contact configurations. Here we demonstrate a highly conductive and thermally stable electrode composed of a magnesium oxide/aluminium (MgO_x/Al) contact, achieving moderately low resistivity ohmic contacts on lightly doped n-type c-Si. The electrode, functionalised with nanoscale MgO_x films, significantly enhances the performance of n-type c-Si solar cells to a power conversion efficiency of 20%, advancing n-type c-Si solar cells with full-area dopant-free rear contacts to a point of competitiveness with the standard p-type architecture. The low thermal budget of the cathode formation, its dopant-free nature and the simplicity of the device structure enabled by the MgO_x/Al contact open up new possibilities in designing and fabricating low-cost solar cells.

Highlights

- 20.1% n-type silicon solar cell with an a-Si:H/MgF_2/Al full-area rear passivated contact.
- 20% n-type silicon solar cell with an MgO_x/Al full-area contact.

Future Work

- Explore the contact properties by vanadium oxide (VO_x) evaporated at UCB.
- Prototype cell fabrication using MoO_x, WO_x and VO_x at UCB.
- Improve cell performance of MoO_x by optimising the HSC layers in reducing both recombination and contact resistivity.
- Write up a journal and conference paper to wrap up the work.

References

Wan, Y., Samundsett, C., Bullock, J., Hettick, M., Allen, T., Yan, D., Peng, J., Wu, Y., Cui, J., Javey, A. and Cuevas, A., 2016, "Conductive and Stable Magnesium Oxide Electron-Selective Contacts for Efficient Silicon Solar Cells"", Adv. Energy Mater., 1601863.

Wan, Y., Samundsett, C., Bullock, J., Allen, T., Hettick, M., Yan, D., Zheng, P., Zhang, X., Cui, J., McKeon, J., Javey, A. and Cuevas, A., 2016, "Nanoscale magnesium fluoride electron–selective contacts for crystalline silicon solar cells", ACS Appl. Mater. Interfaces, 8(23), pp 14671–14677.

Wan, Y., Samundsett, C., Bullock, J., Yan, D., Allen, T., Zheng, P., Zhang, X., Cui, J., McKeon, J. and Cuevas, A., 2016, "Magnesium fluoride based electron-selective contact", 43rd IEEE Photovoltaic Specialists Conference (PVSC), 2540–2542.

6.10 Advanced Light Trapping for High Efficiency Si Cells

Lead Partner
ANU

ANU Team
Prof Andrew Blakers, Dr Soe Zin

Academic Partners
Georgia Institute of Technology (GIT), USA
University of Central Florida (UCF) (added following Dr Zin's move to UCF)

Funding Support
ARENA, ANU, GIT

Aim

Light trapping in most high efficiency silicon solar cell designs entails a textured front surface and a planar rear surface. Silicon solar cells incorporating double-sided pyramidal texture (DST) are capable of superior light trapping. However, the DST structure increases surface recombination. Modifying the rear texture in DST cells has the potential not only to improve light trapping significantly by more effective scattering, but also reduces surfaces, leading to increased cell conversion efficiency. Improved, highly effective and low-cost methods of light trapping will be developed that are compatible with very low surface recombination rates (5 $fAcm^{-2}$). This work will build upon and optimise existing work in modifying DST devices that has yielded very good light trapping and low surface recombination rates.

Progress

This project commenced in April 2016. Progress to date includes: a one-week visit to Australia from Dr Ajay D Upadhyaya (GIT) and Professor Ajeet Rohatgi; fabrication and measurement of samples at ANU; measurement of these samples at GIT and also at UCF; and diffusion of UCF samples at ANU.

Highlights

- One- week visit to Australia by two GIT academics.
- Sample exchanges.

Future Work

- Further characterisation and analysis of samples.
- Write up project report.

6.11 Advanced Luminescence Studies of Si Wafers and Cells

Lead Partner
ANU

ANU Team
Prof Daniel Macdonald, Dr Hieu Nguyen

Academic Partner
National Renewable Energy Laboratory (NREL), USA

Funding Support
ARENA, ANU, NREL

Aim

This project aims to combine complementary expertise at ANU and NREL in Colorado, in the field of luminescence characterisation of materials for solar cells. In particular, the advanced high resolution luminescence methods developed at NREL for thin-film photovoltaic materials will be applied to some outstanding challenges in silicon photovoltaics, especially in relation to understanding key defects in silicon solar cells.

Progress

This two-year project commenced in July 2016. Progress to date includes a one-week visit to NREL by Dr Hieu Nguyen from ANU in August 2016, during which time he familiarised himself with the numerous high resolution tools available at NREL. Detailed plans for the initial experiments during Dr Nguyen's subsequent nine-month visit to NREL, commencing in April 2017, have been drawn up in consultation with our colleagues at NREL. Sample preparation and pre-characterisation at ANU is now well underway.

Highlights

- One-week visit to NREL by Dr Hieu Nguyen in August 2016.
- Detailed plans and sample preparation for subsequent nine-month visit in 2017 are largely complete.

Future Work

During Dr Nguyen's nine-month visit to NREL in 2017 we aim to achieve three technical objectives:

1. Cathodoluminescence (CL) mapping of defects in silicon wafers. Courtesy of the fact that the luminescence excitation is achieved by a beam of electrons, rather than photons, CL allows much higher spatial resolution for mapping luminescence from semiconductors. Here we aim to apply the ultra-high resolution CL mapping capabilities at NREL to study luminescence from dislocations, grain boundaries and precipitated impurities in silicon wafers.

2. Low temperature photoluminescence (PL) spectroscopy. At temperatures below 20K, many important impurities and defects in silicon, such as Fe and Cr, emit sub-bandgap luminescence at unique wavelengths. The PL spectroscopy system at NREL can access temperatures as low as 4K, in comparison with our system at ANU which can only reach 78K. We will apply such low temperature PL spectroscopy at NREL to a range of silicon samples prepared and pre-characterised at ANU.

3. Time-resolved photoluminescence (TRPL). The TRPL system at NREL allows direct measurement of carrier lifetimes as low as several nanoseconds, which are very difficult to measure with the standard techniques used for silicon. Here we aim to apply TRPL to measure lifetimes in a range of dielectric materials and heavily doped layers of silicon solar cells, which at low temperatures emit luminescence at distinct wavelengths.

6.12 De-Cohesion Analysis of Printed Solar Modules

Lead Partner
CSIRO

CSIRO Team
Dr Fiona Scholes, Dr Gerry Wilson, Dr Hasitha Weerasinghe, Dr Doojin Vak, Dr Mei Gao, Ms Régine Chantler

AUSIAPV Partner: Stanford University Team
Prof Reinhold H Dauskardt

AUSIAPV Partner: Stanford University Student
Nick Rolston

AUSIAPV Partner: Georgia Institute of Technology Team
Prof Samuel Graham

Funding Support
ARENA, CSIRO, Stanford, Georgia Institute of Technology

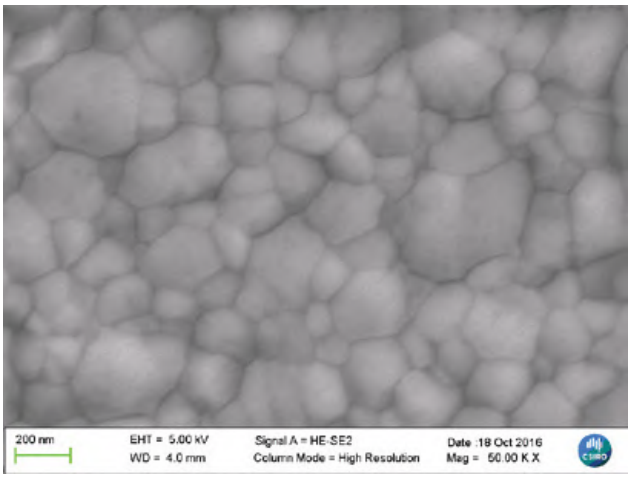

Figure 6.12.1: Roll-to-roll printed perovskite films using slot-die printing method.

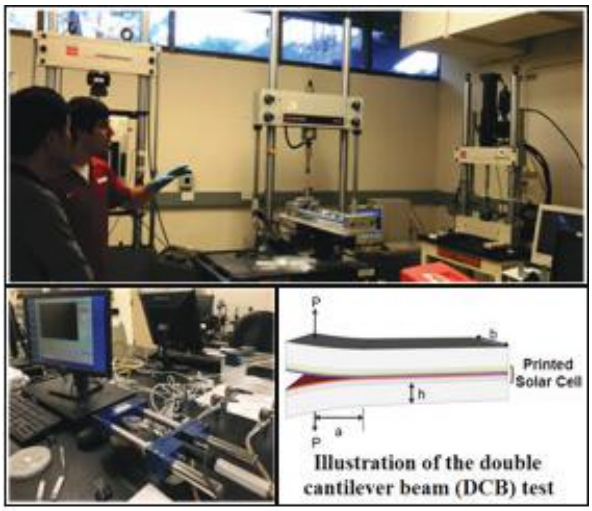

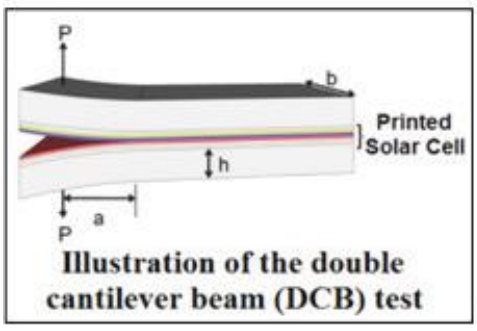

Figure 6.12.2: Schematic representation of the double cantilever beam (DCB) test for mechanical fracture analysis of printed solar cells (P = load, a = crack length, h = beam thickness, d = beam width).

Aim

The aim of this project, in collaboration with Professor Reinhold Dauskardt's research group at Stanford, is to quantitatively analyse the cohesion between the printed layers of large-area flexible perovskite and organic solar modules employing newly developed quantitative mechanical analysis systems.

Progress

Over the first three to four months of the project, the CSIRO team focused on producing efficient perovskite solar cell (PSC) devices on flexible polymer substrates using roll-to-roll (R2R) printing methods under ambient conditions. Several printing trials were conducted to optimise each printed layer of these devices. Flexible PSC devices with power conversion efficiencies (PCEs) over 10% were achieved.

R2R-printed structures fabricated to different stages (i.e. PET|ITO|ZnO|perovskite, PET|ITO|ZnO|perovskite|PEDOT:PSS, PET|ITO|ZnO|perovskite|PEDOT:PSS|MoO_3|Ag) were prepared in the same manner as completed devices and were sent to Stanford for mechanical fracture analysis using their double cantilever beam (DCB) set-up. The objective of these DCB studies was to investigate the effect of additives used during printing the perovskite layer on the interlayer cohesion between the printed layers. Preliminary experiments have been completed by the team at Stanford, with early results indicating that multiple cation perovskite has a lower fracture energy than single cation perovskite.

Some of these R2R-printed perovskite devices have been sent to Georgia Tech for mechanical bending and fracture studies.

Highlights

- Flexible perovskite solar cell devices with PCE >10% have been achieved and subjected to mechanical fracture analysis.
- Preliminary results suggest that multiple cation perovskite has lower fracture energy than single cation perovskite.

Future Work

We will continue to further improve the efficiency of flexible, R2R-printed PSC devices by introducing alternative electrode materials and further optimising device preparation conditions. Evaluation of these printed PSC systems using mechanical fracture analysis facilities available at Stanford will continue. It is also expected that comparative aging experiments will be performed, by storing the printed films under different environmental conditions. Furthermore, lifetime studies on the encapsulated PSC devices/modules followed by DCB tests will be carried out.

6.13 Determining Charge Lifetime and Mobility Dynamics in Organic Semiconductors for Photovoltaic Applications

UoM Team
A/Prof Trevor Smith, Dr Wallace Wong, Dr David Jones

UoM Student
Ms Kyra Schwarz

NREL/Department of Chemistry and Biochemistry at University of Colorado Boulder, USA Team
Prof Garry Rumbles, Dr Obadiah Reid

Funding Support
AUSIAPV, ARC, UoM, NREL

Aims

- Conduct time-resolved microwave conductivity measurements on new high performance OPV materials.
- Construct a novel long timescale transient absorption spectroscopy system and conduct measurements of these materials under the lowest possible light fluence conditions to determine excited state kinetics in the absence of multi-excitonic effects.
- Acquire expertise in the use of time-resolved microwave conductivity (TRMC) with a view to future implementation of this method in Australia to assist the broader photovoltaic community

Progress

Funding for a TRMC system was secured through a successful ARC LIEF grant to Smith, Jones, Wong, Ghiggino and colleagues at Monash and RMIT. Smith visited NREL and Professor Garry Rumbles to inspect their state-of-the-art TRMC apparatus and long timescale transient absorption system. The features of the NREL TRMC system, designed and constructed largely by Dr Obadiah Reid, were assessed.

A unique, long timescale transient absorption apparatus is under construction in the Melbourne node, and is in the final stages of implementation and optimisation. Recently published work by our group (Schwarz et al.) has identified the urgent need for TA measurements with low pulse fluences on timescales significantly longer than the 1 ns currently achievable. This apparatus will enable such measurements on our new materials.

Highlights

- Successful ARC LIEF grant funding for TRMC apparatus
- Construction of long timescale transient absorption apparatus based on a high repetition rate, low pulse energy laser system, is nearing completion.

Future Work

TRMC equipment will be purchased in 2017. Professor Garry Rumbles and/or Dr Obadiah Reid will visit Melbourne during 2017 to help with the selection of the optimal system. TRMC measurements will be performed at NREL setting baseline levels in terms of parameters such as sensitivity and time-resolution that the new instrument must reach.

The long timescale transient absorption apparatus will be used to investigate the excited state dynamics of new materials being synthesised in the Jones and Wong groups.

References

Geraghty, P.B., Lee, C., Subbiah, J., Wong, W.W.H., Banal, J.L., Jameel, M.A., Smith, T.A. and Jones, D.J., 2016, “High performance p-type molecular electron donors for OPV applications via alkylthiophene catenation chromophore extension”, Beilstein J. Org. Chem., 12, 2298–2314.

Schwarz, K.N., Geraghty, P.B., Jones, D.J., Smith, T.A. and Ghiggino, K.P., 2016, “Suppressing sub-nanosecond bimolecular charge recombination in a high performance organic photovoltaic material”, J. Phys. Chem. C., 120 (42), 24002–24010.

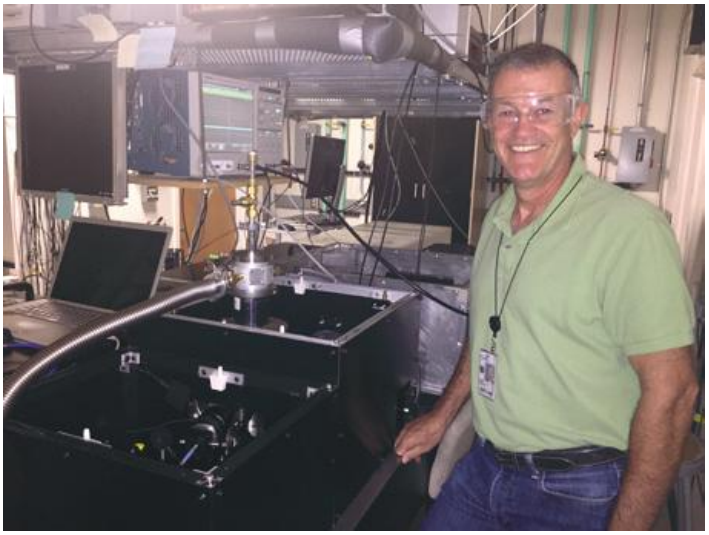

Figure 6.13.1: Professor Garry Rumbles, NREL, showing his TRMC instrument during a visit by Associate Professor Trevor Smith.

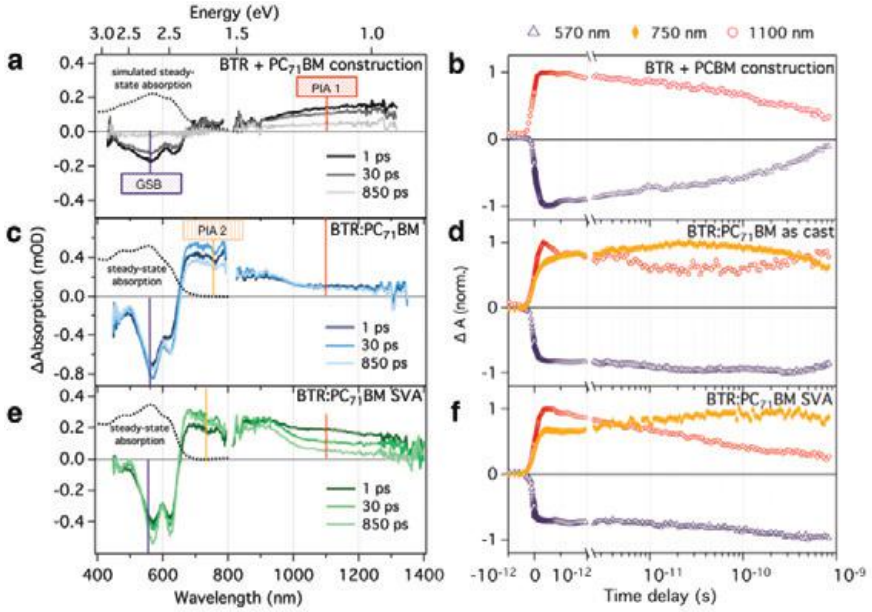

Figure 6.13.2: Thin-film transient absorption measurements with 400 nm excitation at 6 μJcm^{-2} of new high performance materials (Schwarz et al., 2016).

6.14 Screening Singlet Fission in Organic Semiconductors for Photovoltaic Applications

UoM Team
Dr David Jones, Prof Ken Ghiggino, A/Prof Trevor Smith, Dr Lars Goerigk

UoM Students
Ms Kyra Schwarz, Ms Saghar Masoomigadarzi

US Academic Partners
Princeton University (Prof Greg Scholes), Georgia Institute of Technology, USA (Prof Seth Marder)

Funding Support
AUSIAPV, UoM, Princeton

Aims

- Develop a reliable spectroscopic screening method for detecting singlet fission in organic semiconducting materials.
- Investigate the application of time-resolved 2-D spectroscopy for characterising singlet fission.
- Screen existing organic semiconductor materials library and new organic materials from AUSIAPV partners for singlet fission

Progress

Smith, Schwarz and Jones all visited the Scholes laboratory at Princeton University during 2016 to discuss techniques suited to the investigation of singlet fission processes in new materials. In particular, the merits and disadvantages of the use of ultrafast spectroscopy for detecting the existence and dynamics of singlet fission were assessed. PhD student, Kyra Schwarz, spent some time in the Scholes laboratory gaining expertise in the ultrafast techniques, and discussing with fellow students the intricacies of such experiments.

Recently, new design criteria have been suggested for the development of high performance singlet fission materials. Surprisingly, a number of high performance OPV materials synthesised in Dr Jones' laboratory closely matched the requirements, therefore we initiated a primary theoretical screening program using high level DFT theory and TD-DFT to examine known molecules, and calculate their energy levels. None of the synthesised materials had appropriate energy levels, i.e. $E(S_1) \geq 2E(T_1)$, and were not further examined. The developed theoretical protocols have allowed us to pre-screen new materials targeted for synthesis.

New candidate singlet fission materials have been identified, designed and synthesised, and are currently being characterised spectroscopically. A method of studying candidate materials using low temperature, near infrared emission (probing the energy of the triplet state by detecting phosphorescence) has been established and indications are that triplet energy levels of at least some of these new materials are appropriate for singlet fission. Further work in this area is underway.

Professor Greg Scholes visited Melbourne and a workshop was held featuring several speakers from the USA and UoM staff and students, highlighting areas of joint interest and providing a forum for discussion of recent findings.

6.14.1: UoM PhD student Kyra Schwarz visiting the Frick Chemistry Laboratories, Princeton University, October 2016.

6.14.2: A selection of attendees at a joint USA–UoM workshop, 12 December 2016.

Dr David Jones will be visiting Georgia Tech in 2017 furthering synthesis and characterisation of new materials.

Highlights

- Establishment of near infrared emission apparatus for detecting low energy phosphorescence at 77K from candidate materials.
- New candidate materials designed, synthesised and being characterised.
- Ultrafast laser spectroscopy experiments underway on new materials.
- Joint USA–UoM workshop held at University House, UoM.

Future Work

Time-resolved near infrared techniques will be developed and new candidate materials studied to confirm triplet state emission and dynamics of excited state behaviour.

2-D ultrafast spectroscopy measurements will be applied on new candidate materials and results correlated with ultrafast transient absorption measurements. Computational predictions of energy levels and rates to be finalised and compared with experimental results. This will lead to the design of additional candidate materials that will be characterised spectroscopically.

6.15 Thin Silicon Solar Cells for Portable Applications

Lead Partner
UNSW

UNSW Team
Dr Ivan Perez-Wurfl

ACAP Team
Dr Brian Dougherty

Academic Partners
Brian Dougherty, Mechanical Engineer, Engineering Laboratory, National Institute of Standards and Technology (USA)

Industry Partners
Solbian Energie Alternative S.r.l., Luca Bonci

Funding Support
ACAP, NIST (in-kind), Solbian (in-kind)

Aims

- Evaluate the electrical and thermal performance of the cells and modules under various outdoor and portable conditions.
- Analyse the cost-performance of flexible silicon solar cell modules under portable conditions.
- Develop test methods and protocols for benchmarking portable modules.

Progress

This project was originally intended to study ultrathin silicon on steel modules. When it was confirmed that said modules would be unavailable for this study, a variation in the proposal was submitted to ACAP. The variation was authorised on 30 August 2016. The proposed variation was to perform the same studies proposed in the first proposal but applied to a different type of flexible panels.

Dr Ivan Perez-Wurfl has replaced Dr Binesh Puthen-Veettil as the principal investigator for this project. A good relationship has been established with Solbian, a company that produces commercial flexible high efficiency modules. Unfortunately, as the ultrathin silicon solar cells were not available for testing, our partners at NIST had to postpone any studies planned for this project until 2017. It will proceed as planned in the new year.

Solbian has sent 10 single cell samples for preliminary optical and electrical testing that will be done at UNSW. We are also in the process of rescheduling experiments at NIST.

Highlights

- A project variation was proposed and authorised.
- Funds for the project have been preserved.
- The project will commence in 2017.

Future Work

- Test of Solbian single cell panels to clarify tests to be performed at NIST.
- Perform tests on Solbian panels as per project proposal.

6.16 Design Optimisation of Silicon Sub-Cells in GaAsP/Si

Lead Partner
UNSW

UNSW Team
A/Prof S. Bremner, Dr A. Ho-Baillie, Dr H. Mehrvarz, Prof M. Green

UNSW Student
Chuqi Yi

Academic Partner
Ohio State University

Ohio State University Team
Dr T. Grassman, Prof S. Ringel

Funding Support
ARENA

Aim

The aim of this project is to determine the optimum design for an active silicon substrate operating as the bottom sub-cell in a III-V/Si multi-junction solar cell. This must be done with a process flow compatible with III-V growth.

Progress

A Sentaurus TCAD model for the simulation of both p- and n-type wafer designs has been successfully developed satisfying the requirements for Milestone 1.1. Initial results for a p-type wafer design confirmed the findings of previous work done by us, looking at the influence of the interface of the GaP and silicon, as well as the emitter diffusion profile (Almansouri et al., 2015). Simulation results are presented in Figure 6.16.1(b), below, for a rear junction PERL style design silicon solar cell operating under a 1.7 eV filtered spectrum shown in Figure 6.16.1. A cross-section summary of the structure, which has not been previously modelled to the best of our knowledge, is provided in Figure 6.16.1(a). As can be seen in the simulated results for the external quantum efficiency the thickness of the cell can have a significant effect on device performance, dependent on the bulk minority carrier lifetime. This is a crucial point for the rear junction approach since a thin silicon wafer can complicate epitaxial growth, with the large lattice mismatch accommodated across the structure leading to significant bowing if the silicon is not thick enough to mechanically absorb the mismatch strain. This model will be used to incorporate experimental results to determine which design offers the best potential performance overall.

Development of a full process flow has also been undertaken with investigations of methods for preserving the minority carrier lifetime in the silicon during subsequent III-V epitaxy. The use of silicon nitride has been reported as an effective barrier layer (Zhang et al., 2016) and our efforts have focused on this approach. Silicon nitride layers of different thicknesses were deposited by plasma-enhanced chemical vapour deposition on silicon wafers with a thermally grown 26 nm silicon dioxide layer (see Figure 6.16.2). All samples were heated to 600°C under ultra-high

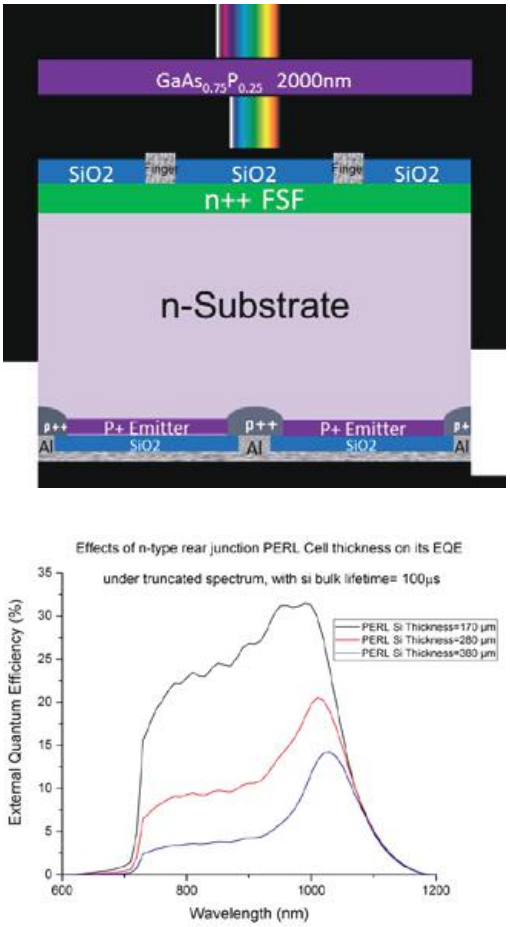

Figure 6.16.1: (a) Cross-section of 1.7 eV filtered rear junction silicon solar cell modelled using Sentaurus TCAD, consisting of an n-type silicon wafer with rear boron diffusion emitter and a phosphorus diffusion front surface field; and
(b) Simulated external quantum efficiency for the rear junction device in Figure 6.16.1(a). The thickness of the cell has been varied for a bulk minority carrier lifetime of 100 micro-seconds. This sort of lifetime is at the low end of what will be used in a final device.

vacuum and left for 4.5 hours before being ramped down to room temperature. This was to mimic typical temperatures and timing for growth of III-V material appropriate for the final structures proposed. As shown in Table 6.16.1, the lifetime for the 25 nm nitride layer sample has been reduced, but for all the layers thicker than this the lifetime was either not affected or improved. We suspect this is due to hydrogen from the nitride diffusing into the silicon. When these samples were subsequently taken through a thermal process similar to that reported in the first report of high quality GaP on Si growth by MBE (Grassman et al., 2009) (peak temperature of 800°C, due to the need to thermally clean the silicon surface prior to epitaxy) the lifetimes were catastrophically reduced. Interestingly, a 366 nm silicon dioxide layer also provided lifetime protection to 600°C, but again for higher temperatures the lifetime was compromised.

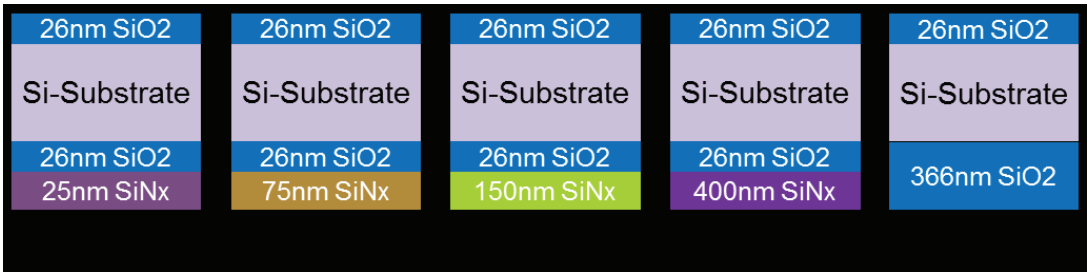

Figure 6.16.2: Test samples for lifetime protection of silicon wafers undergoing ultra-high vacuum thermal treatment. All havea thermally grown silicon dioxide layer, with four samples having 26 nm front and back and with varying silicon nitride thicknesses on the rear surface. A 366 nm silicon dioxide sample was also included for comparison.

Highlights

- Sentaurus TCAD model of standard polarity PERL silicon solar cell under a 1.7 eV filtered spectrum developed with results produced to drive first designs.
- Sentaurus TCAD model of a rear junction PERL type silicon solar cell design using an n-type wafer under a 1.7 eV filtered spectrum developed. This model will be used to assess critical design parameters like wafer thickness.
- First results for silicon nitride capping prior to III-V epitaxy indicate the ability to preserve minority carrier lifetime beyond temperatures seen for bare silicon. Preservation for temperatures up to 600°C has been demonstrated for typical epitaxial growth times (4.5 hours).

Future Work

Current simulation efforts are focused on fully integrating the multi-junction device including a tunnel junction (a tunnel junction model has been developed) – this was not possible in previous PC1D simulation models. A typical final device with a conventional PERL silicon solar cell design is summarised in Figure 6.16.3. Rear surface texturing and its impact on the silicon cell performance as well as overall multi-junction devices will be undertaken. In parallel the inclusion of a rear a-Si layer for passivation and to form a non-diffused rear junction is also under development with models for a-Si / crystalline silicon HIT devices having been developed.

Optimisation of lifetime preservation strategies will continue with the highest processing temperatures, of 800°C, being probed. The approach is to view the silicon nitride as a sacrificial layer that will provide a processing time window, during which the degradation is to a level that does not impact the underlying silicon. Investigations of nitride thickness and the amount of time that the silicon can be at elevated temperatures are returning the first initial results at the time of writing.

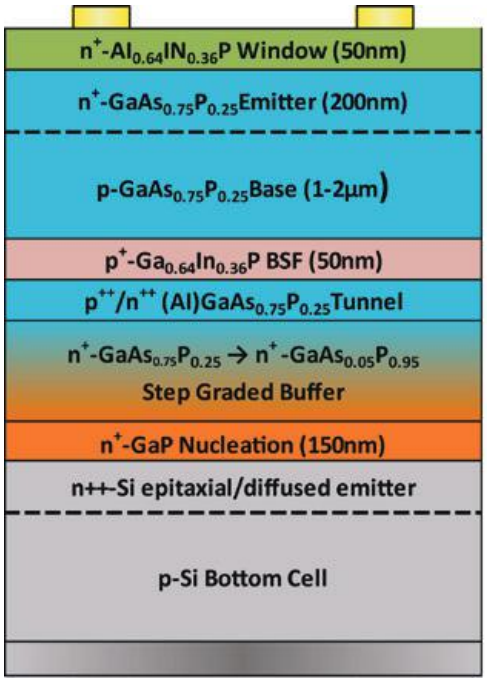

Figure 6.16. 3: Final device structure for a conventional PERL silicon bottom cell with GaAsP top cell. A buffer layer to allow transition from silicon to III-V material is included as well as an AlGaAsP-based tunnel junction for electrical connection between the top and bottom cells.

References

Almansouri, I., et al., 2015, "Designing bottom silicon solar cells for multijunction devices," IEEE Journal of Photovoltaics, 5(2), 683–690.

Grassman, T., et al., 2009, "Control and elimination of nucleation-related defects in GaP/Si(001) heteroepitaxy", Applied Physics Letters, 94, 232106.

Zhang, C., et al., 2016, "Hetero-emitter GaP/Si Solar Cells with High Si Bulk Lifetime," IEEE Photovoltaic Specialist Conference, 1950–1953.

Sample #	SiNx Thickness (nm)	Lifetime with only Oxide (µm)	Lifetime Before MBE heat up (with oxide and Nitride) (µs)	Lifetime After first MBE heat up (µs)	Lifetime After second MBE heat up (µs)
1	25	154.27	220.77	108.62	-
2	75	182.99	195.85	290.82	28.71
3	150	122.08	151.91	345.51	28.63
4	400	164.3	210.2	219.30	31.68
5	366 oxide only	49.68	-	48.03	10.15

Table 6.16.1: Summary of results for lifetime preservation samples in Figure 6.16.2. Samples underwent a 4.5 hour thermal soak at 600°C, with only the thinnest silicon nitride layer not protecting the lifetime. When a full thermal treatment up to ~800°C was used all samples saw a catastrophic decrease in lifetime.

6.17 Cost Evaluation of Emerging PV Technologies

Lead Partner
UNSW

UNSW Team
Dr Anita Ho-Baillie, A/Prof Renate Egan, Prof Martin Green

UNSW Student
Nathan Chang

ACAP Team
CSIRO, Monash

Academic Partners
NREL

Overview

A key criterion for progressing a technology from research to commercialisation is an accurate projection of the manufacturing cost. For emerging technologies many things change with scale, with location and over time and so the performance and cost in high volume production can only be estimated. Nevertheless, well-informed analysis is required and provides the basis for making useful decisions while recognising and estimating this uncertainty.

This project combines the world-leading technical expertise and close links to manufacturing at UNSW in Australia with the established credibility in techno-economic analysis at NREL. The formal collaboration will reinforce established relationships and knowledge sharing in the area of manufacturing costing and techno-economic analysis.

Aims

The project will deliver well-informed analysis of manufacturing costs for key ACAP technologies to assist in guiding research directions and decision making.

This project aims to deliver outcomes consistent with PP4 and is aligned with NREL objectives in techno-economic analysis. Further, the project fosters international collaboration to enable well-informed cost evaluation of emerging PV technologies by combining the world-leading technical expertise and close links to manufacturing at UNSW in Australia with the established credibility and expertise in techno-economic analysis at NREL in the USA.

Deliverable 1: A draft paper reporting the results of costing of perovskites on glass, suitable for publication in a peer-reviewed journal, submitted for internal review at UNSW and NREL.

Deliverable 2: A paper reporting the costing of silicon contacting technologies, suitable for publication in a peer-reviewed journal, submitted for internal review at UNSW and NREL.

Deliverable 3: A cost modelling report on the two technologies sufficient to meet the requirements of the Year Four milestone for PP4.

Progress

Energy from photovoltaics is increasingly competitive in many markets, yet studies point to the need for continuous improvements in efficiency and cost to provide increased market share and to create new markets. Incremental changes in efficiency and cost are expected to continue to drive down the prices of the incumbent technologies: silicon and, to a smaller extent, CdTe. Further, opportunities exist for step-change through new materials and structures motivates research in new materials such as the organohalide perovskites, and new structures, such as tandem solar cell devices.

Manufacturing cost estimations can be very helpful even in this early stage of process development, because they can identify areas of cost improvement that are necessary to bring the technology to commercialisation, as well as show the potential of the technology once it has

overcome certain barriers. Working on cost improvement in parallel with performance issues should also reduce the total time to commercialise a technology.

Traditionally costing is applied to mature technologies, where input values are reasonably well known. For developing technologies, many of the input values are unknown and assumptions must be made. The team at ACAP has developed novel approaches that permit the consideration of a range of allowed values for each cost parameter in order to carry out uncertainty analysis. This approach delivers outputs that can be used to focus research and development resources on the key cost drivers, as illustrated in the flow chart in Figure 6.17.1.

To develop the uncertainty analysis, a nominal value is recorded as the best estimate of the input parameter, while low and high values represent the uncertainty range. The impact of the uncertainty in each parameter is assessed using Monte Carlo analysis. Typically, 5,000 scenarios are generated, and each input parameter is independently assigned a random value according to a "two half normal distribution", where the median of the distribution is the nominal estimate, and the 10th and 90th percentile marks provide the low and high estimates respectively.

The distribution of the cost results from each scenario is evaluated to indicate the uncertainty of the calculated results and delivers a probability distribution for the total module manufacturing cost. This probability distribution can be used to compare different proposed sequences to assess the impact of a proposed change. This probability distribution can then be used to provide a figure of merit of the cost impact of assumptions and uncertainties in the model.

This costing methodology can be carried out iteratively, as processes and knowledge develop, producing cost estimates relatively quickly. The approach offers the advantage of an early identification of key cost drivers and areas of cost uncertainty. It can be used to indicate that a different process sequence needs to be considered, or that further work is required to refine some cost uncertainties.

To permit a market readiness assessment and to allow comparison with more mature module technologies, a $\$/W_p$ value can be derived from reported and forecast module efficiency for the developing technology. Further, for the end customer, the \$/W data for the module alone is insufficient to calculate the market value of the technology. Other factors such as the lifetime of the module and the additional costs of mounting, connecting and maintaining a system need to be combined to give the levelised cost of electricity (LCOE) in \$/kWh. To assess the efficiency and lifetime requirements, an LCOE calculator is then used to compare the proposed technology with LCOE values for different markets.

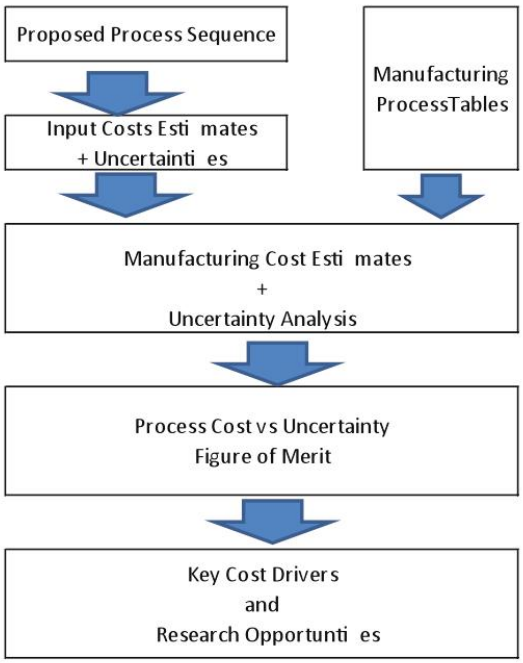

Figure 6.17.1: Flow chart of the approach used in this work.

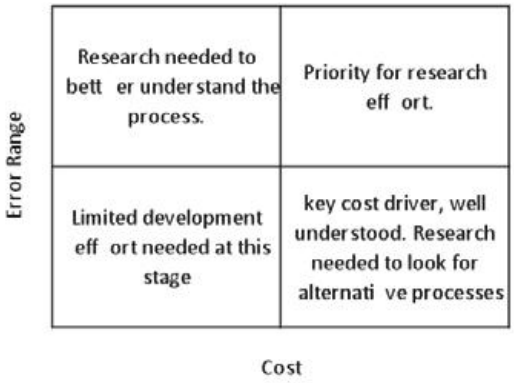

Figure 6.17.2: Matrix used to assess necessary research intensity.

The combination of manufacturing costing in $\$/m^2$ and the uncertainties in that costing, along with market comparisons of \$/W and LCOE can be used to inform research directions for an emerging technology.

Deliverable 1. Perovskites on glass: Perovskites based on methylammonium lead iodide have demonstrated remarkable efficiency of over 20% in small laboratory cells using potentially low-cost solution deposition methods. It is typically assumed that, because this material can be made using a solution-based process, it will have a very low manufacturing cost. This task explored the reported process conditions, identifying opportunities for focusing further research on contacting and substrate technologies. Further work is planned to extend this to the costing of perovskite printing (roll-to-

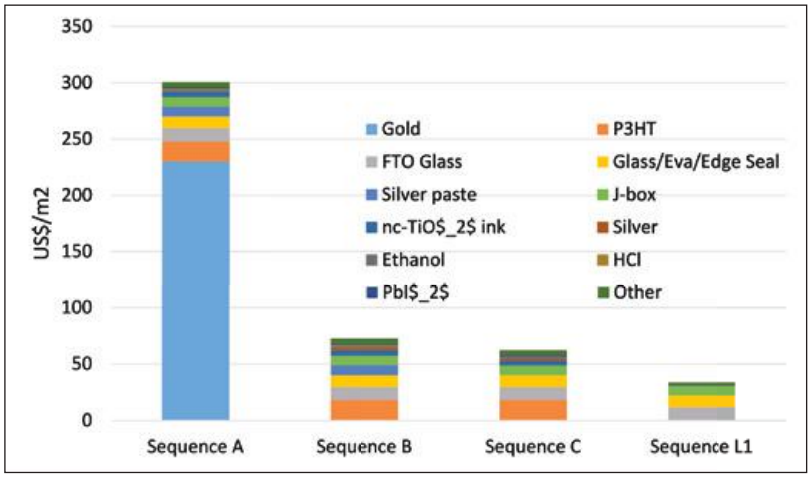

Figure 6.17.3: Perovskite on glass materials: costing for four sequences assessed.

roll) in partnership with Monash and CSIRO. Detailed reporting is provided in the PP4 section of this report.

Deliverable 2. Silicon contacting technologies: Research within ACAP continues to demonstrate improved efficiencies within the dominant silicon solar cell technology sequence. These improvements are made through advances in front and rear contact technologies, as well as materials improvements. Leveraging the learning and expertise of the extensive silicon manufacturing costing program at NREL, this task delivers an update on the costing analysis to document the PERC manufacturing process, in consultation with our manufacturing partners (recognising commercial sensitivity).

In this project, the costing methodology has been applied to the evaluation of cost and production requirements of the laser-doped selective emitter (LDSE) technology developed at UNSW and reported in PP4 and will be extended to combining LDSE to the PERC technology, n-type silicon and advanced hydrogenation technologies being commercialised at UNSW.

Deliverable 3: The team has had a paper accepted for publication that describes the novel cost modelling methodology. The technique takes into account uncertainties associated with processes still under development and enables identification of technology risks and priority areas for research.

Highlights

The manufacturing costing task has developed a novel method for assessing the manufacturing costing of new technologies.

This project has established and developed a working relationship with Michael Woodhouse and Daniel Chung at NREL.

Future Work

The project will be extended to allow for completion of costing in the silicon technologies and a site visit to NREL by postgraduate student Nathan Chang.

Reference

Chang, N., et al., 2017, "A Manufacturing Cost Estimation Method with Uncertainty Analysis and its Application to Perovskite on Glass Photovoltaic Modules", in press, Progress in Photovoltaics: Research and Applications.

6.18 Studying Thermal Effects of B-O Related Light-Induced Degradation

Lead Partner
UNSW

UNSW Team
Dr Brett Hallam

UNSW Student
Moonyong Kim

Academic Partners
University of North Carolina Charlotte (UNCC), Prof Abasifreke Ebong

Funding Support
ARENA, ARC, UNCC (In-kind)

Figure 6.18.1: (a) Photo of the installed bench and light-tight enclosure for in situ QSS-PC measurements during B-O related degradation; (b) Photo of the inside of the enclosure with the Sinton Instruments WCT-120 QSS-PC lifetime tool and an LED-based bias light.

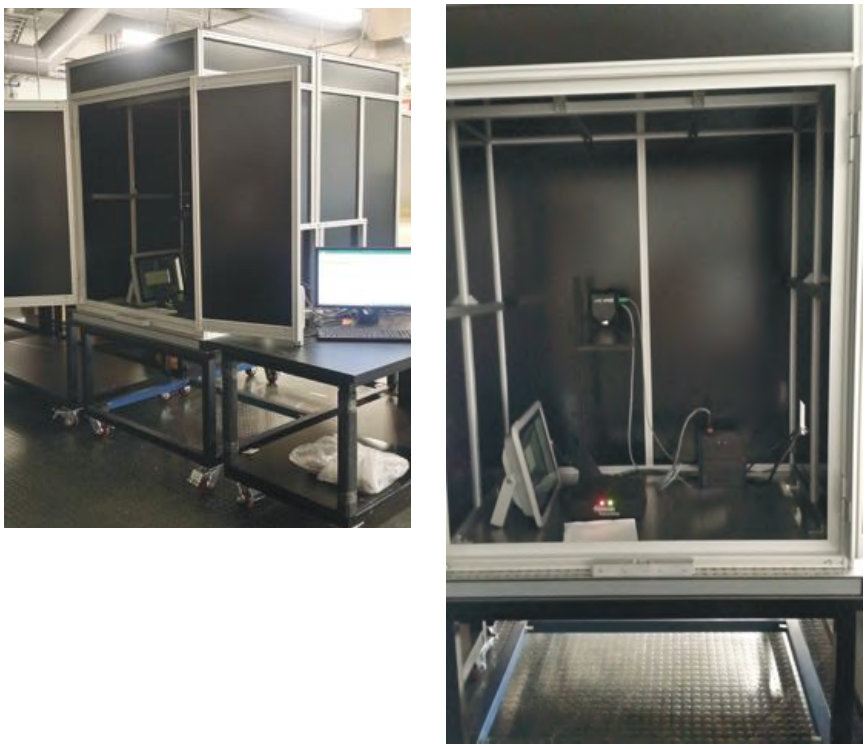

Aims

- Determine effect of thermal processing on modulating defect concentrations and ability to mitigate light-induced degradation.
- Reduce the effects of light-induced degradation by > 50% by optimising thermal firing profiles for silicon solar cells.
- Develop characterisation tools for investigating light-induced defects in silicon solar cells and other recombination active defects in low-quality silicon.

Progress

A light-tight enclosure was purchased and installed in the R&D lab of the Solar Industrial Research Facility (SIRF), to enclose a Sinton Instruments WCT-120 quasi-steady-state photoconductance tool. Figure 6.18.1(a) shows a photo of the installed bench and light-tight enclosure with in situ degradation capabilities. Figure 6.18.1(b) shows the inside of the enclosure with the Sinton Instruments WCT-120 tool and LED-based bias light (~0.1 sun intensity).

A macro-enabled spreadsheet was developed to automatically trigger the Sinton Instruments spreadsheet at predetermined intervals to take a QSS-PC measurement. The code automatically time-stamps the files such that the duration of light-soaking is recorded for subsequent analysis.

In situ lifetime measurements have been obtained during B-O degradation. Example curves are shown in Figure 6.18.2 (Kim, 2017) on the influence of thermal annealing in modulating the fraction of fast and slow degradation.

This work has provided further evidence of a single defect being responsible for B-O related degradation, representing a major leap forward in the understanding of the B-O defect. This work was also submitted to the 2017 Silicon PV Conference (Hallam, 2017).

Highlights

- QSS-PC measurement with in situ degradation capabilities established.
- Thermal processing observed to modulate the fraction of fast and slow boron-oxygen degradation, giving strong evidence of a single defect being responsible.

Future Work

Future work will investigate the influence of high temperature processing in modulating the defect precursor concentration and therefore reduce the extent of B-O related light-induced degradation. Thermal processing will be performed in a custom built rapid thermal processing (RTP) unit at UNCC and in a conventional belt firing furnace at UNSW to determine the activation energy and attempt frequency of the thermal reduction in the defect precursor concentration. In situ degradation and long-term stability testing of these will be performed at UNSW. We will also investigate the use of a subsequent rapid illuminated hydrogenation process to passivate the remaining defects in the silicon.

A trip to work with Professor Abasifreke Ebong at the UNCC is scheduled for the first two weeks of May 2017 to fabricate cells with varied thermal processes during

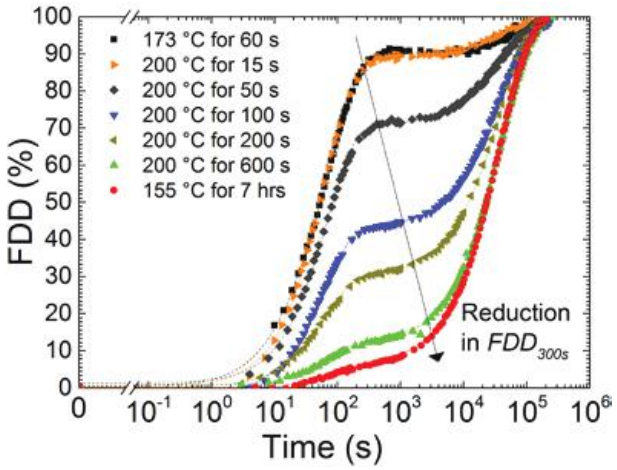

Figure 6.18.2: Example of in situ lifetime degradation curves of light soaking time versus the fractional defect density (FDD) of B-O defects compared to full degradation at an excess carrier concentration of $\Delta n=9.1x10^{15}/cm^3$.

fast-firing to investigate the effect of high temperature processing in reducing the B-O defect concentration. Professor Ebong is currently preparing samples to send to UNSW for testing with in situ lifetime and voltage monitoring.

References

Hallam, B. et al., 2017, "New Insights into Boron-Oxygen Related Degradation",. In preparation for Silicon PV / SOLMAT conference.

Kim, M., et al., 2017, "Modulating the extent of fast and slow boron-oxygen related degradation in Czochralski silicon by thermal annealing: Evidence of a single defect", accepted for Journal of Applied Physics, 18th January 2017.

6.19 Origin of Interface Defect Levels for High Efficiency Silicon Solar Cells

Lead Partner
UNSW

UNSW Team
Dr Ziv Hameiri

UNSW Students
Robert Dumbrell, Yan Zhu, Shuai Nie

Academic Partners
Arizona State University, Dr Mariana Bertoni
Funding Support
UNSW MREII, ARC DECRA

Aims

The project started only at the end of 2016.

- Installation of contactless capacitance-voltage measurement system at UNSW.
- Building a temperature and injection dependent lifetime spectroscopy system at UNSW.

Progress

A contactless capacitance-voltage measurement system was installed at UNSW and the building of the temperature and injection dependent lifetime spectroscopy system at UNSW was completed. The first design of experiment (DoE) was developed and approved by both the UNSW and ASU teams. An ASU student arrived at UNSW during January 2017 for a four-month research visit and a Taste-of-Research undergraduate student was engaged to work on the project over the 2016–17 summer break.

Highlights

- Installation of contactless capacitance-voltage measurement system at UNSW.
- Building the temperature and injection dependent lifetime spectroscopy system at UNSW.
- A great ToR student joined the UNSW team to be involved in the project.

Future Work

Measurement of samples according to DoE and proposal.

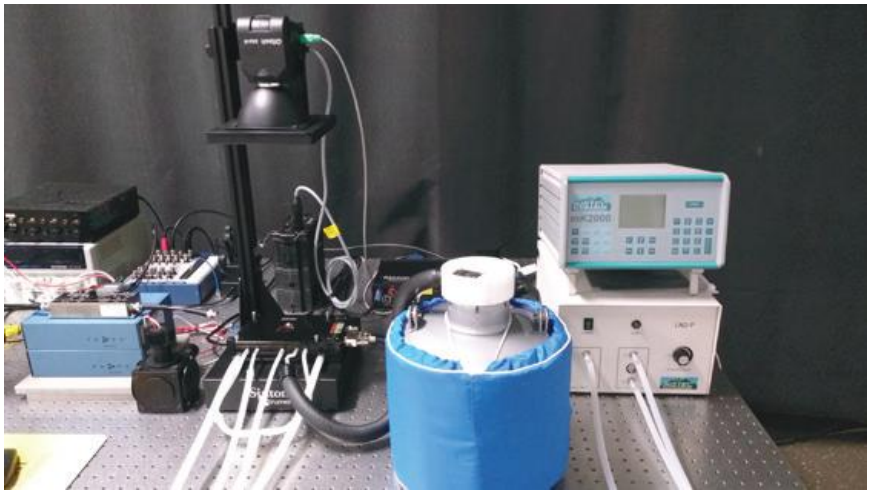

Figure 6.19.1: The temperature and injection dependent lifetime spectroscopy system at UNSW

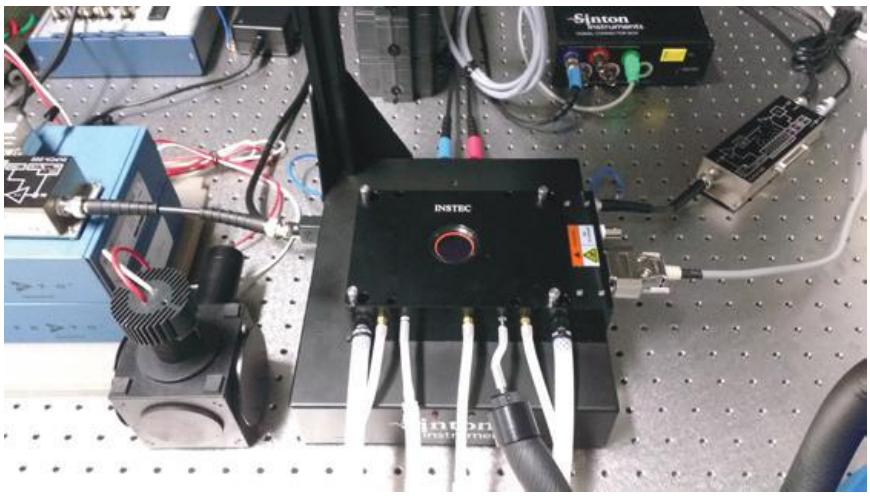

Figure 6.19.2: The contactless capacitance-voltage measurement system at UNSW

6.20 Developing Laser Processed Large-Area Front Deep Junctions and Heterojunction Passivated Back Contacts

Lead Partner
UNSW

UNSW Team
Dr Ivan Perez-Wurfl

UNSW Students
Tian Zhang, Zibo Zhou

Academic Partners
NIST (USA), Dr Brian Simonds

Funding Support
ACAP, NIST (in-kind)

Aims

The main goal of this project is to develop a dual-beam laser annealing system to fabricate deep front junctions on silicon wafers with reduced thermal stress. The system relies on a fixed large-area laser and a scanning, variable-area laser beam. The reduction in stress is achieved by increasing the substrate temperature prior to melting and by controlling the heating and cooling rates. Furthermore, by varying the pre-melting substrate temperature as well as the power, area and scan speed of the scanning line laser, we can controllably investigate melting depth, bulk silicon dislocation density, doping profile and surface morphology. A unique advantage of this dual-beam laser system is its ability to reach pre-melting substrate temperatures higher than 700°C (limit of the line-laser set-up at UNSW). This dual-beam laser annealing system should be able to create deep emitters in a matter of

seconds for investigating deep and low-doped junctions with the accompanying laser-induced thermal stress effects.

The second part of this project is to further demonstrate the application of lasers on silicon solar cell fabrication using a nanosecond pulsed laser to fabricate poly-Si/tunnelling SiO_2/Si heterojunction passivated back contacts. The pulsed laser could potentially eliminate damage to the ultrathin tunnelling SiO_2 passivation layer from traditional furnace annealing. A transient reflectance measurement can be used to monitor the crystallisation of amorphous silicon and the fast transient laser melting process.

Progress

Overall, we have completed or partially completed three of the four project aims put forward for this proposal, namely:

- Establish a robust high power dual-beam laser annealing/melting system (completed).
- Demonstrate 3–10 um deep junction with low thermal stress in a device (partially completed).
- Fabricate laser processed poly-Si/tunnelling SiO_2/Si heterojunction passivated back contacts (partially completed).

We have built a dual- beam laser system in the Applied Physics Division at the National Institute of Standards and Technology (Figure 6.20.1). The system was built on a portable optical stage, which is equipped with one stationary 500 W continuous wave 1070 nm laser (OVEN) for substrate heating and another scanning quasi-continuous wave (QCW) 1070 nm laser (SCAN) for silicon melting. The substrate temperature can be monitored in real time using an OMEGA pyrometer. An advantage of the contactless substrate heating is the ability to reach high temperatures. We have been able to controllably maintain the temperature of 1.5 cm x 3 cm silicon substrates at temperature between 700°C and 960°C.

To control the hardware built, a LabVIEW program was developed to remotely control and monitor process parameters, including substrate temperature, heating and cooling rate, waiting time before scan laser firing, the power, scan speed and ramp up/ramp down of power of the scan laser. The current system is suitable for samples as large as 1.5 cm x 3 cm which allow a processing area of 0.7 cm x 3 cm. However, by simply upgrading the OVEN laser head to 10 kW (available at NIST) and modifying the beam shaping optics, larger silicon substrates could be accommodated.

Several batches of samples were fabricated and characterised to investigate the formation of deep junction using the above described dual-beam laser system. Using Sirtl defect etching (HF/CrO_3) of polished cross-sections, we have demonstrated junction depths as large as 45 μm as shown in Figure.6.20.2(d). The junction location determined using the Sirtl etching is consistent with the junction location as shown by EBIC (see Figure.6.20.2(a)–(c)). However, it is notable that there is a large density of defects (proportional to the density of pits in the figure) induced by thermal stress appearing during the laser scanning. In particular, the silicon region that did not melt, shows the highest density of defects. By increasing the substrate temperature from 700°C to 960°C, preliminary results show a reduction of thermally induced defects (see Figure.6.20.3). Another advantage of using a higher substrate temperature is the reduction of scan laser power needed to achieve Si melting opening the possibility of replacing the scan laser with a high energy line heating lamp.

Another achievement of this project is the construction and testing of a pulsed laser annealing set-up for ultrathin a-Si crystallisation to form heterojunction poly-Si/ultrathin SiO_2/Si contacts. A unique capability of the constructed set-up is the ability to monitor time resolved reflectance (TRR) with nanosecond resolution. Figure 6.20.4 shows the measured a-Si crystallisation dynamics during a 28 ns laser annealing process. We have preliminarily demonstrated the crystallisation without strong ablation by controlling the laser pulse energy. The examination of the electrical performance of these structures as carrier selective contacts requires further investigation.

Both samples prepared with deep junctions as well as those with poly-Si/ultrathin SiO_2/Si contacts have been demonstrated and partially studied. This is the partial completion of tasks B and C. Incorporating them into solar cells is a task that we have planned for the coming year to complete these aims.

Publications were the fourth aim of the project. We are working on the first publication and gathering information for the second publication proposed for this project. A third publication seems possible with the results we expect this year.

Implementation of COMSOL simulation models is underway. This was not an aim of the proposed project in 2016 but its need has become apparent. We believe that a reliable numerical model will improve our understanding of laser thermal dynamics. Also, a reliable model will speed up the optimisation of the laser annealing process parameters.

Highlights

<u>Construction of a dual-beam laser for deep junction formation</u>

- Dual-beam laser annealing system built on portable optical stage with capability of laser power being scaled up to 10 kW.

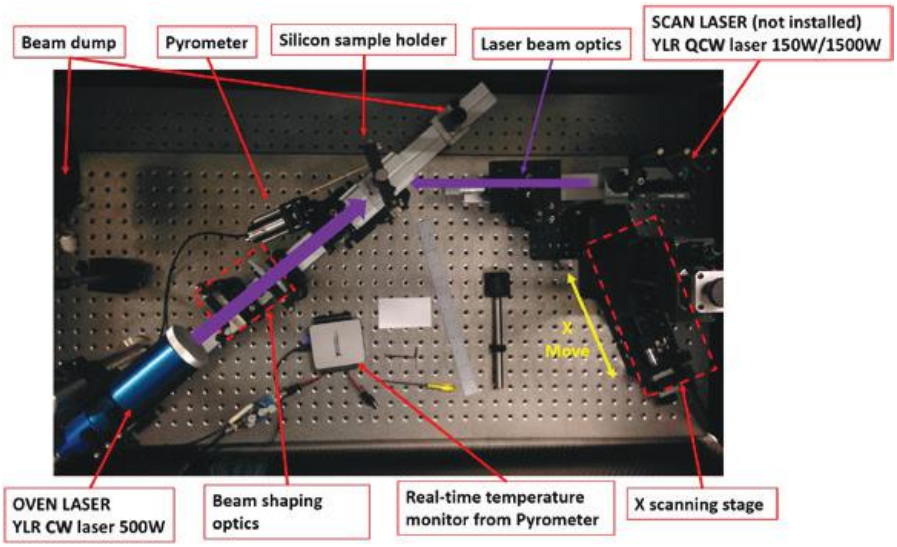

Figure 6.20.1: Dual-beam laser system.

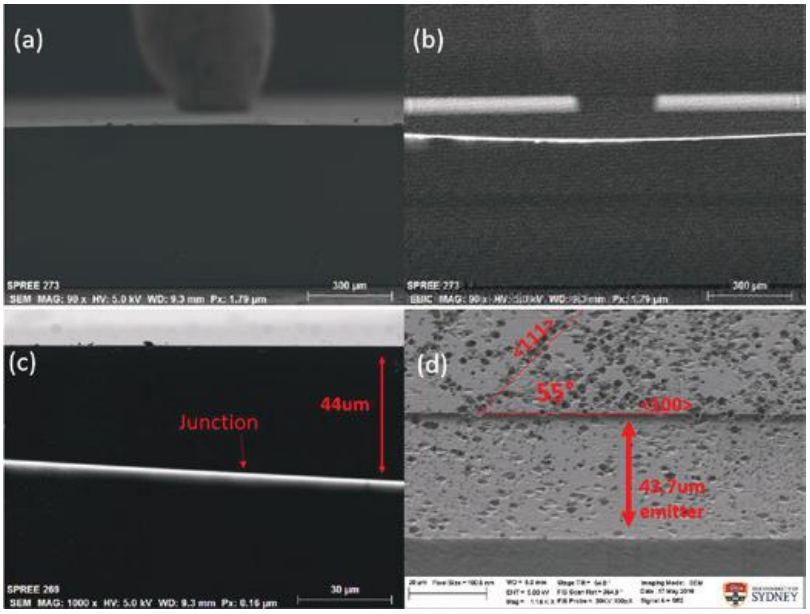

Figure 6.20.2: Deep junction.

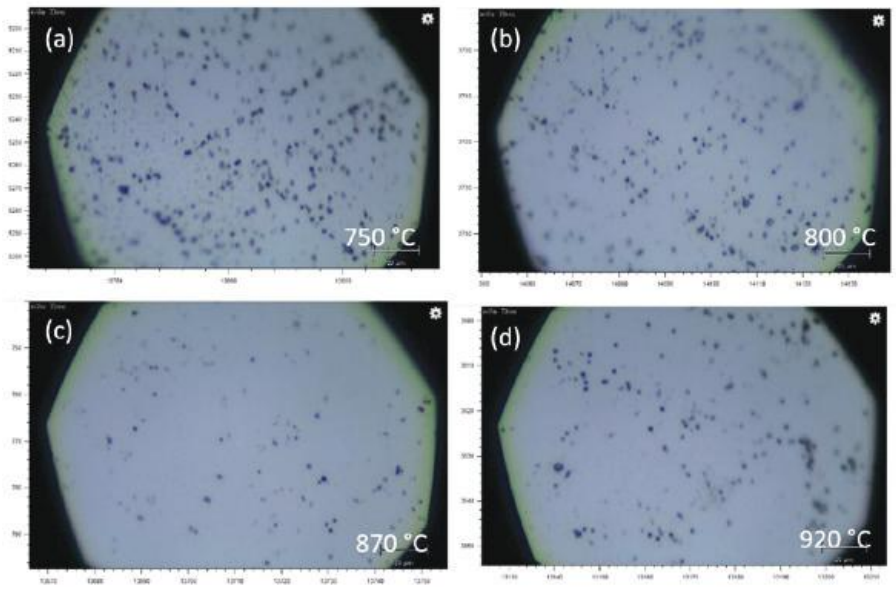

Figure 6.20.3: Bulk defects vs substrate temperature.

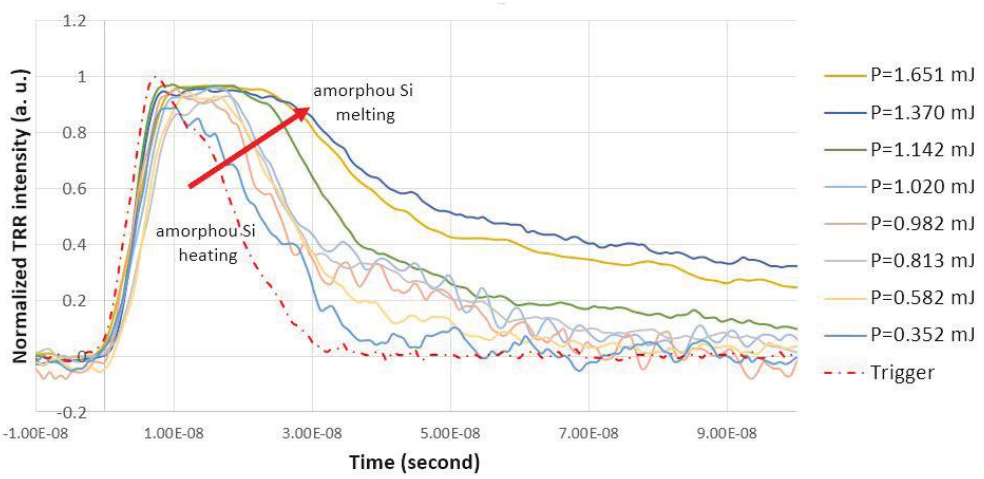

Figure 6.20.4: Transient reflectance.

- LabVIEW program is designed to perform automatic and remote annealing process control on a substrate temperature, heating/cooling rates and line-laser power and scan speed independently.
- Deep and sharp junctions 10–50 micrometres in depth have been fabricated.
- Reduced bulk defect density has been identified when a higher substrate temperature is used. However, an amount of thermal-induced dislocations and defects is still large compared to areas not treated by the laser.

Laser processed poly/tunnelling SiO_2/Si heterojunction

- Pulsed laser has been preliminarily demonstrated to be able to crystallise 20 nm highly doped a-Si:H without ablation to form a poly-Si/ultrathin SiO_2/Si heterojunction.
- Transient reflectance measurement has been implemented to monitor real-time pulsed laser annealing process.

Future Work

- The dual-beam laser system built up in NIST will be used to fabricate more silicon samples to achieve better control of the melting depth and to further investigate methods to reduce thermal stress.
- COMSOL models to be implemented for simulating silicon laser melting to better understand thermal dynamics.
- Full-area front deep junction by laser melting will be further processed into silicon solar cells.
- Write up and publish two journal papers on deep junction formation by dual-beam laser annealing.

We wish to highlight that progress on this project came to a halt as of mid-December 2016 as Dr Tian Zhang stopped working at UNSW to take a position at Monash University. Plans are in place to have Mr Zibo Zhou continue his work at NIST towards mid-2017.

6.21 Novel Light-Trapping Technique in Solar Cells

Lead Partner
UNSW

UNSW Team
Dr Supriya Pillai, Prof Martin A. Green, Dr Michael E. Pollard

UNSW Students
Claire E.R. Disney, Yuanchih Chang

Academic Partners
Arizona State University, Prof Christiana Honsberg

Funding Support
ACAP, ARENA, UNSW

Aim

An investigation of whether parasitic absorption in metals can compromise light absorption in cells and to clarify the future of plasmonic structures as potential light-trapping layers in solar cells.

Progress

Rear plasmonic structures have been proposed for light trapping and efficiency improvements demonstrated.

However a very common concern in relation to plasmonic structures for light trapping is the potential parasitic absorption in the metal itself. To understand the scattering and absorption process in the metal nanostructures, simulations were performed using Lumerical FDTD (finite difference time domain) software. The novel plasmonic structure proposed earlier where dielectric nanospheres are embedded in the metal on the rear of Si was the subject of the study. The key advantage of these nanotextured rear metal reflectors with nanospheres is that they couple the light-trapping enhancements offered by the metal nanoparticles (which has demonstrated photocurrent enhancements earlier), with the continuity of a rear mirror.

Figure 6.21.1 shows the calculated absorption in Ag and Al metals for 675 nm silica nanospheres with 800 nm period. This size was selected based on the optimised structures for a 2 μm thick Si absorber layer. Figure 6.21.2 shows the far-field scattering plots for this configuration along with a 500 nm case. The wavelengths selected were at resonance (peak absorption in metal) for the 500/675 nm nanosphere cases. These are both compared to the 200 nm case, for which these wavelengths are off-resonance. These results reveal that at resonance, though the overall fraction of light scattered back into Si is reduced, the fraction which is scattered at large angles is greatly increased. This large angle scattering also persists surrounding these resonances and between them, but at resonant wavelengths it acts as a counterbalance to the increased parasitic losses and thus allows the enhancement in absorption in Si to be maintained across a wide range of wavelengths. This scattering of light at larger angles increases the chance of light achieving multiple bounces and thus a greater chance that it will be absorbed in Si rather than escaping out of the front of the cell as is the case with planar rear metal reflectors.

Our study also found that excitation of plasmons at roughened Ag surfaces with sharp features can result in significant increases in absorption in metal and could prove detrimental to cell performance. However careful consideration of the geometry would ensure that the resultant light trapping provided by plasmonic structures could be beneficial to cell absorption.

Highlights

- The mechanisms linking these parasitic losses and absorption enhancements were identified.
- Our results clearly show that the large angle scattering provided by the plasmonic nanostructures is the reason for the enhanced absorption observed in the solar cells.

Future Work

Future work will investigate the effect of the plasmonic structures on thin films fabricated using nanosphere lithography.

Reference

Disney, C.E.R., et al., “Self-Assembled Nanostructured Rear Reflector Designs for Thin-Film Solar Cells”, ACS Photonics, 2015.

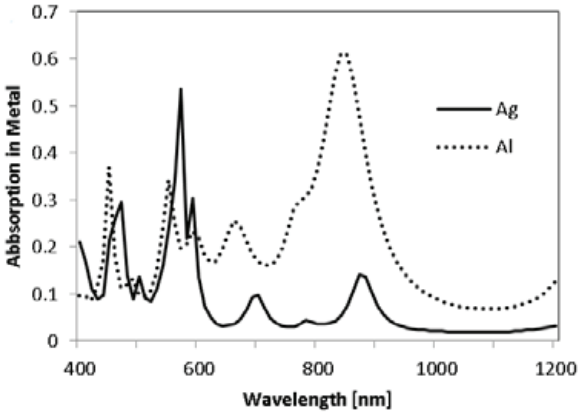

Figure 6.21.1: Absorption into Ag or Al reflector at the rear of Si with embedded arrays of 675 nm nanostructures and an 800 nm period.

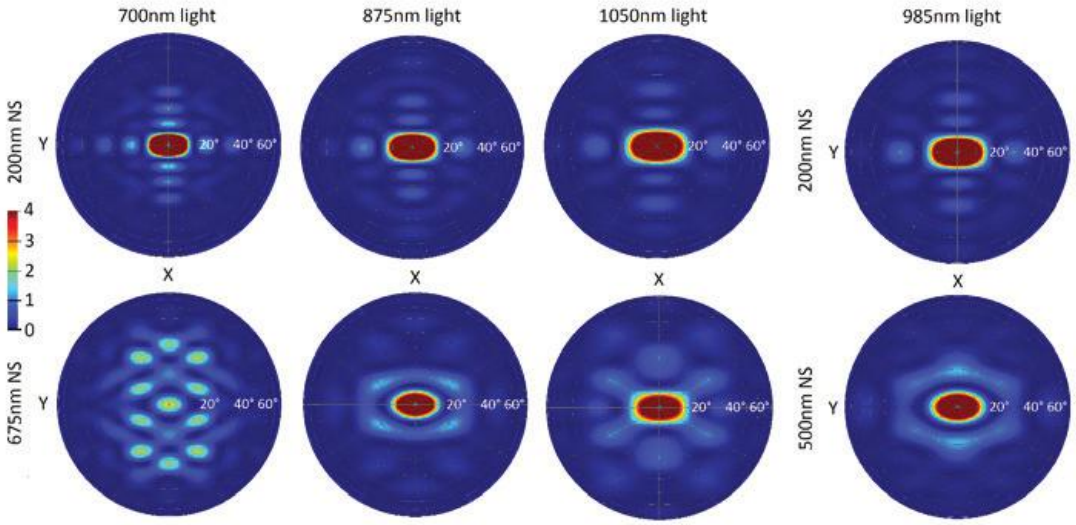

Figure 6.21.2: Far-field scattering plots showing the angles at which light is scattered back into the Si from the rear interface of the cell for an 800 nm array period with Ag. The wavelengths selected were at resonance for the 500/675 nm NS cases, and off resonance for the 200 nm NS case. The absorption plot for the 675 nm nanostructure case is shown in Figure 6.21.1.

7. Financial Summary

In December 2012, a grant of $33.1 million from the Australian Government through ARENA was announced to support the 8-year program of the Australia-US Institute for Advanced Photovoltaics (AUSIAPV). This support leveraged an additional $55.4 million cash and in-kind commitment from AUSIAPV participants taking the total value of the project to $88.5 million.

AUSIAPV commenced on 1 February 2013 after the signing of the Head Agreement between ARENA and UNSW, and with the receipt of letters of confirmation of participation under the terms of the Head Agreement by the other project participants. Collaboration Agreements with the Australian participants in the Australian Centre for Advanced Photovoltaics (ACAP) were completed on 1 July 2013.

An extension to the program, to undertake an Australian Solar PV Cell and Module Research Infrastructure Plan and Feasibility Study was signed in October 2014, generating an additional milestone, 4A. This project was completed and Milestone 4A was paid in October 2015. A further extension was formalised through Variation #4, executed in February 2016. It extended perovskites research in ACAP and generated two new Milestones (4B and 5B) for 2016 and others in subsequent years. Both the new 2016 Milestones were met and paid. The Milestone 5 payment from ARENA to UNSW was also paid, in July 2016. Disbursements were made to each node following confirmation of institutional cash contributions.

Good progress was made in 2014 - 2016 towards regaining the original budgetary expenditure timelines. A robust and transparent process to distribute collaboration funds was developed in 2015 and also implemented in a small first funding round in that year. Two larger, rounds were undertaken during 2016 and planning is underway for a fourth round in Q2 of 2017. All technical milestones for 2016 were achieved.

The breakdown by institution of the $11.3 million total cash and in-kind budget for 2016 is shown in Figure 7.1(a). The actual total 2016 cash and in-kind expenditure was $13.6 million and its breakdown is shown in Figure 7.1(b), with additional irrevocable cash commitments carried into 2017.

A new collaborating industry participant, Dyesol Pty. Ltd., joined during 2016 and a MoU was signed with the US National Institute of Standards and Technology.

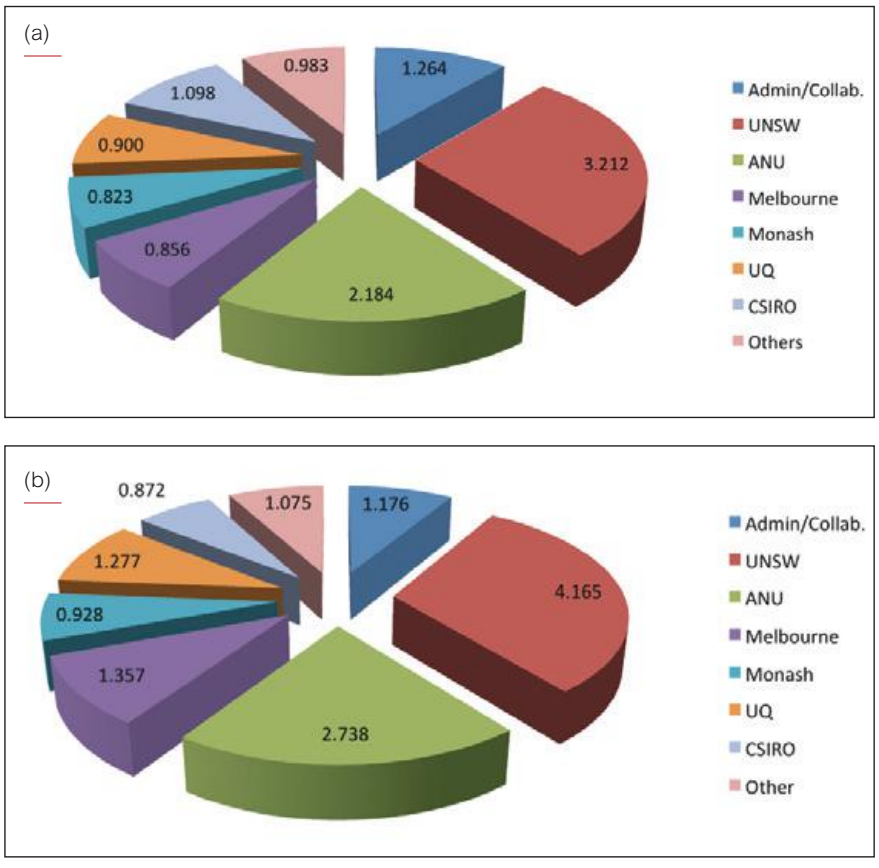

Figure 7.1: (a) Total AUSIAPV/ACAP cash and in-kind expenditure budget ($m) for 2016 broken down by institution; (b) Actual cash and in-kind expenditure ($m) breakdown by institution for 2016.

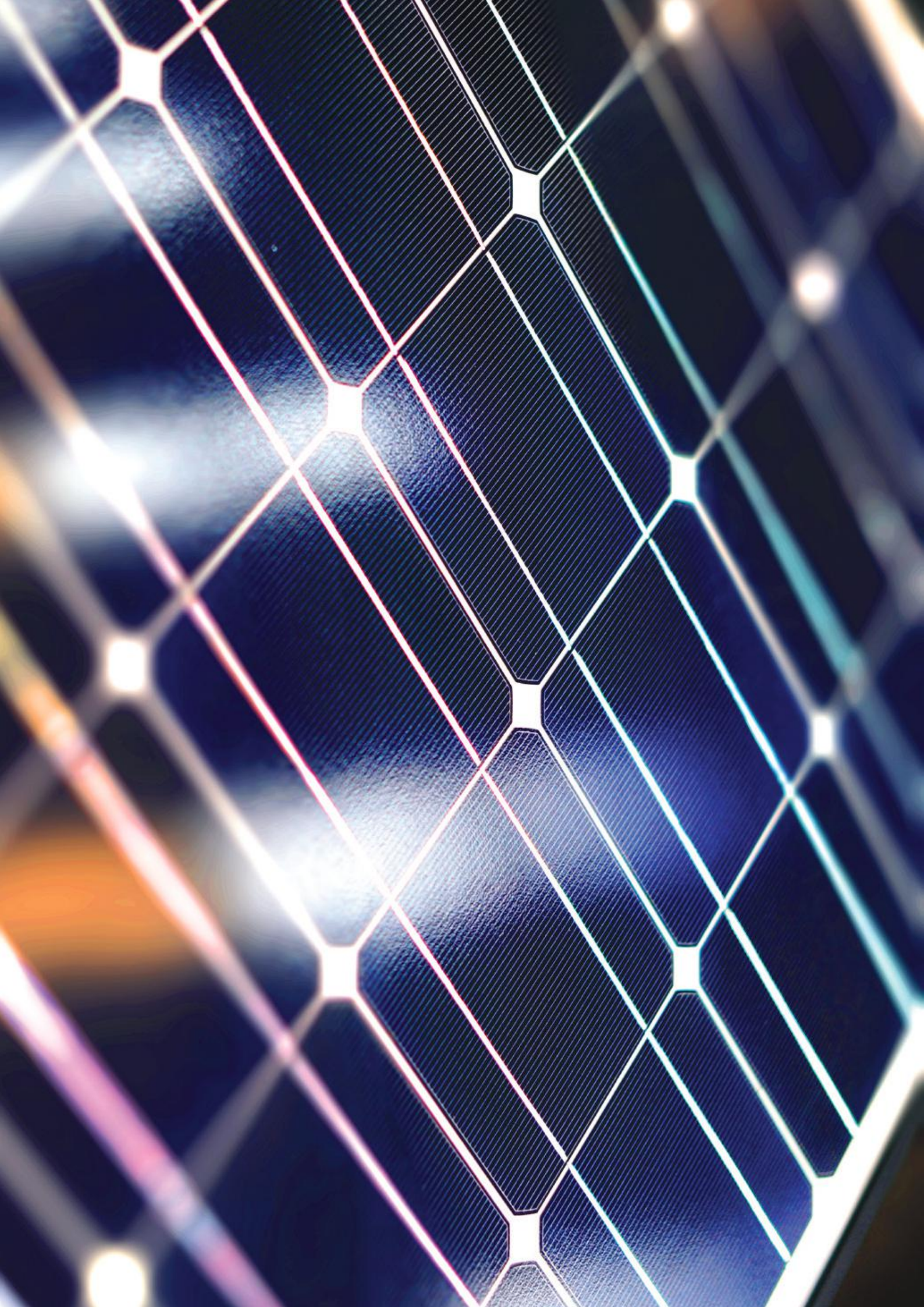

8. Publications

8.1 Books and Proceedings

Gordon, I., Conibeer, G., Krc, J., Slaoui, A., and Niki, S. (editors), "Proceedings of the 2015 E-MRS Spring Meeting Symposium C - Advanced Inorganic Materials and Structures for Photovoltaics", Solar Energy Materials and Solar Cells, Vol. 145, p. 83, 2016

Dupré, O., Vaillon, R. and Green, M.A., "Thermal Behavior of Photovoltaic Devices", Springer International Publishing, 2017 (DOI: 10.1007/978-3-319-49457-9) (ISBN 978-3-319-49456-2)

8.2 Book Chapters

Blakers, A. and Zin, N., "Silicon Solar Cell Device Structures", in Angèle Reinders, Pierre Verlinden, Wilfried van Sark, Alexandre Freundlich, "Photovoltaic Solar Energy: From Fundamentals to Applications", Wiley & Sons, ISBN: 978-1-118-92746-5, January 2017

Hoex, B., "Surface Passivation and Emitter Recombination Parameters", in Angèle Reinders, Pierre Verlinden, Wilfried van Sark, Alexandre Freundlich, "Photovoltaic Solar Energy: From Fundamentals to Applications", Wiley & Sons, ISBN: 978-1-118-92746-5, January 2017

Green, M.A., "Advanced Concepts", in Angèle Reinders, Pierre Verlinden, Wilfried van Sark, Alexandre Freundlich, "Photovoltaic Solar Energy: From Fundamentals to Applications", Wiley & Sons, ISBN: 978-1-118-92746-5, January 2017

Corkish, R., Lipinski, W. and Patterson, R., "Introduction to Solar Energy", in Solar Energy, World Scientific Series in Current Energy Issues, Vol. 2, Crawley, G. (ed.), World Scientific. ISBN: 978-981-4689-49-6, 2016

8.3. Patent Applications

Abbott, M., Wenham, S., Hamer, P., Hallam, B., "A method for processing silicon material", PCT/AU2016/050174, 2016

Abbott, M., Wenham, S., Hamer, P., Hallam, B., "A method for processing silicon material", National Phase (Non-PCT), Taiwan, 105107722, 2016

Green, M. Hao, X., Li, W., Huang, J., "A method of manufacturing a photovoltaic device", PCT, 2016

Hao, X., Liu, F., Cui, H., ; Liu, X., Liu, X., "A photovoltaic cell and a method of forming a photovoltaic cell", PCT/AU2016/050835, 2016

Hao, X., Liu, F., Huang, J. Yan, C. Sun, K., Green, M., "A method of forming a photovoltaic cell and a photovoltaic cell", Provisional, Australia, 2016902434, 2016

Lennon, A., Allen, V., "A method and an apparatus for treating a surface of a TCO material in a semiconductor device", Provisional, Australia, 2016900683, 2016

Lennon, A., Lu, Z., "A method of anodising a surface of a semiconductor device", PCT/AU2016/050027, 2016

Lennon, A., Ouyang, Z., "An electrochemical capacitor and an integrated energy-generation and energy-storage device", Provisional, Australia, 2016901511, 2016

Lennon, A., Yao, Y., Li, Z.; Hsiao, P.-C., Jiang, Y., Soederstroem, T., "A method for forming a contacting structure to a back contact solar cell", PCT, 2016

Lennon, A., Yao, Y., Li, Z.; Hsiao, P.-C., Jiang, Y., Soederstroem, T., "A method for forming a contacting structure to a back contact solar cell", National Phase (Non-PCT), Taiwan, 105122345, 2016

Mai, L., Wenham, S., Wenham, A., Hallam, B., Chan, C., Chong C.M., Chen, R., "Mitigating hydrogen-induced recombination (HIR) and contact resistance deterioration through the use of hydrogen sinks", Provisional, Australia, 2016904788, 2016

Mai, L., Wenham, S., Wenham, A., Hallam, B., Chan, C., Chong C.M., Chen, R., Chen, D., Fung, T., Kim, M., "Mitigating light-induced degradation (LID) in multicrystalline silicon solar cells", Provisional, Australia, 2016904785, 2016

Uddin, A., "A photovoltaic cell and a method of forming a photovoltaic cell", patent no. WO 2016/023064 A1.

Uddin, A., Elumalai, N., "A photovoltaic cell and a method of forming a photovoltaic cell", (Provisional, Australia, 2016904145, 2016Uddin, A., Elumalai, N., "A method of forming a light absorbing layer for a photovoltaic cell and a photovoltaic cell comprising the light-absorbing layer", Provisional, Australia, 2016904157, 2016

Wenham, S., Hallam, B., Einhaus, R., "A method for manufacturing a photovoltaic device", Provisional, Australia, 2016902733, 2016

Wenham, S., Hamer, P., Hallam, B., Sugianto, A.; Chan, C., Song, L., Lu, P.H., Wenham, A., Ly Mai, L., Chong, C.M., Xu, G.Q., Matthew Bruce Edwards, M., "Thermal processing in silicon", National Phase, China, 2014800421193, 2016

Wenham, S., Hamer, P., Hallam, B., Sugianto, A.; Chan, C., Song, L., Lu, P.H., Wenham, A., Ly Mai, L., Chong, C.M., Xu, G.Q., Matthew Bruce Edwards, M., "Thermal processing in silicon", National Phase, Europe, 14830301.9, 2016

Wenham, S., Hamer, P., Hallam, B., Sugianto, A.; Chan, C., Song, L., Lu, P.H., Wenham, A., Ly Mai, L., Chong, C.M., Xu, G.Q., Matthew Bruce Edwards, M., "Thermal processing in silicon", National Phase, South Korea, 10-2016-7004933, 2016

Wenham, S., Hamer, P., Hallam, B., Sugianto, A.; Chan, C., Song, L., Lu, P.H., Wenham, A., Ly Mai, L., Chong, C.M., Xu, G.Q., Matthew Bruce Edwards, M., "Thermal processing in silicon", National Phase, Singapore, 11201600284V, 2016

Wenham, S., Hamer, P., Hallam, B., Sugianto, A.; Chan, C., Song, L., Lu, P.H., Wenham, A., Ly Mai, L., Chong, C.M., Xu, G.Q., Matthew Bruce Edwards, M., "Thermal processing in silicon", National Phase, USA, 14/905711, 2016

Wenham, S., Hamer, P., Hallam, B., Sugianto, A.; Chan, C., Song, L., Lu, P.H., Wenham, A., Ly Mai, L., Chong, C.M., Xu, G.Q., Matthew Bruce Edwards, M., "High concentration doping in silicon", National Phase, Australia, 2014295816, 2016

Wenham, S., Hamer, P., Hallam, B., Sugianto, A.; Chan, C., Song, L., Lu, P.H., Wenham, A., Ly Mai, L., Chong, C.M., Xu, G.Q., Matthew Bruce Edwards, M., "High concentration doping in silicon", National Phase, Europe, 14828986.1, 2016

Wenham, S., Hamer, P., Hallam, B., Sugianto, A.; Chan, C., Song, L., Lu, P.H., Wenham, A., Ly Mai, L., Chong, C.M., Xu, G.Q., Matthew Bruce Edwards, M., "High concentration doping in silicon", National Phase, South Korea, 10-2016-7004555, 2016

Wenham, S., Hamer, P., Hallam, B., Sugianto, A.; Chan, C., Song, L., Lu, P.H., Wenham, A., Ly Mai, L., Chong, C.M., Xu, G.Q., Matthew Bruce Edwards, M., "High concentration doping in silicon", National Phase, Singapore, 11201600282S, 2016

Wenham, S., Hamer, P., Hallam, B., Sugianto, A.; Chan, C., Song, L., Lu, P.H., Wenham, A., Ly Mai, L., Chong, C.M., Xu, G.Q., Matthew Bruce Edwards, M., "High concentration doping in silicon", National Phase, USA, 14/905710, 2016

Wenham, S., Hamer, P., Sugianto, A.; Chan, C., Song, L., Lu, P.H., Wenham, A., Ly Mai, L., Chong, C.M., Hallam, B., Xu, G.Q., Matthew Bruce Edwards, M., "Advanced Hydrogenation of Silicon Solar Cells", China, 2016105440806, 2016

Wenham, S., Hamer, P., Sugianto, A.; Chan, C., Song, L., Lu, P.H., Wenham, A., Ly Mai, L., Chong, C.M., Hallam, B., Xu, G.Q., Matthew Bruce Edwards, M., "Advanced Hydrogenation of Silicon Solar Cells", USA, 15/204813, 2016

Wenham, S., Hamer, P., Sugianto, A.; Chan, C., Song, L., Lu, P.H., Wenham, A., Ly Mai, L., Chong, C.M., Hallam, B., Xu, G.Q., Matthew Bruce Edwards, M., "Thermal processing in silicon", Australia, 2014295817, 2016

Wenham, S., Wenham, A., Bagnall, D., Chen, R., Abbott, M., "Advanced hydrogen passivation that mitigates hydrogen-induced recombination (HIR) and surface passivation deterioration in PV devices", Provisional, Australia, 2016904784, 2016

Wenham, S., Wenham, A., Hallam, B., Chan, C., "Mitigating hydrogen-induced recombination (HIR) and contact resistance deterioration through the use of crystallographic defects or grain boundaries", Provisional, Australia, 2016904789, 2016

Wenham, S., Wenham, A., Hallam, B., Chan, C., Chen, R., "Auto-generation of the neutral charge state for hydrogen atoms in silicon for hydrogen passivation and mitigation of light-induced degradation (LID)", Provisional, Australia, 2016904787, 2016

Wenham, S., Wenham, A., Hallam, B., Chan, C., Chong, C.M., Chen, R., Abbott, M., Payne, D., "A method for processing silicon material", Provisional, Australia, 2016902198, 2016

Wenham, S., Wenham, A., Hallam, B., Chan, C., Chong, C.M., Chen, R., "Generation of neutral atomic hydrogen in silicon using photons to mitigate hydrogen-induced recombination (HIR) in PV devices", Provisional, Australia, 2016904786, 2016

8.4 Papers in Refereed Scientific and Technical Journals

Allen, T.G., Bullock, J., Zheng, P., Vaughan, B., Barr, M., Wan, Y., Samundsett, C., Walter, D., Javey A., and Cuevas, A., "Calcium contacts to n-type crystalline silicon solar cells", Progress in Photovoltaics: Research and Applications, 2016. DOI: 10.1002/pip.2838

Allen, T.G., Wan, Y. and Cuevas, A., "Silicon surface passivation by gallium oxide capped with silicon nitride", IEEE J. Photovoltaics, Vol.6, pp. 900-905, 2016, DOI: 10.1109/JPHOTOV.2016.2566881

Almansouri, I., Green, M.A., and Ho-Baillie, A., "The ultimate efficiency of organolead halide perovskite solar cells limited by Auger processes", Journal of Materials Research, Vol. 31(15), pp. 2197-2203, 2016

Armin, A., Yazmaciyan, A., Hambsch, M., Li, J., Burn, P.L., and Meredith, P., "Electro-optics of conventional and inverted thick junction organic solar cells", ACS Photonics, Vol. 2 (12), pp 1745-1754, 2015

Barugkin, C., Beck, F. and Catchpole, K., 2016, "Diffuse reflectors for improving light management in solar cells: a review and outlook", Journal of Optics, Vol. 19(1)

Barugkin, C., Paetzold, U., Catchpole, K., Basch A. and Carius, R., 2016, "Highly reflective dielectric back reflector for improved efficiency of tandem thin-film solar cells", International Journal of Photoenergy, Vol. 2016, Article ID 7390974, http://dx.doi.org/10.1155/2016/7390974

Battaglia, C., Cuevas A. and De Wolf, S., "High efficiency crystalline silicon solar cells: status and perspectives", Energy and Environmental Science, Vol. 9, pp. 1552-1576, 2016 DOI: 10.1039/c5ee03380b

Borgwardt, M., Wilke, M., Kampen, T., Mahl, S., Xiao, M.D., Spiccia, L., Lange, K.M., Kiyan, I.Y., Aziz, EF., 2016, "Charge transfer dynamics at dye-sensitized ZnO and TiO2 interfaces studied by ultrafast XUV photoelectron spectroscopy", Scientific Reports, Vol. 6, Article 24422

Borgwardt, M., Wilke, M., Kampen, T., Mahl, S., Xiao, M.D., Spiccia, L., Lange, K.M., Kiyan, I.Y., Aziz, EF., "Charge Transfer Dynamics at Dye-Sensitized ZnO and TiO2 Interfaces Studied by Ultrafast XUV Photoelectron Spectroscopy", Scientific Reports, Vol. 6, Article 24422, 2016

Boriskina, S.V., Green, M.A., Catchpole, K., Yablonovitch, E., Beard, M.C., Okada, Y., Lany, S., Gershon, T., Zakutayev, A., Tahersima, M.H., Sorger, V.J., Naughton, M.J., Kempa, K., Dagenais, M., Yao, Y., Xu, L., Sheng, X., Bronstein, N.D., Rogers, J.A., Alivisatos, A.P., Nuzzo, R.G., Gordon, J.M., Wu, D.M., Wisser, M.D., Salleo, A., Dionne, J., Bermel, P., Greffet, J.J., Celanovic, I., Soljacic, M., Manor, A., Rotschild, C., Raman, A., Zhu, L., Fan, S., and Chen, G., "Roadmap on optical energy conversion", Journal of Optics (United Kingdom), Vol. 18(7), 2016

Borojevic, N., Hameiri, Z., and Winderbaum, S., "Advanced optical modelling of dynamically deposited silicon nitride layers", Applied Physics Letters, Vol. 109, pp. 021903-021903, 2016

Bremner, S.P., Yi, C., Almansouri, I., Ho-Baillie, A., and Green, M.A., "Optimum band gap combinations to make best use of new photovoltaic materials", Solar Energy, Vol. 135, pp. 750-757, 2016

Bullock, J., Hettick, M., Geissbühler, J., Ong, A.J., Allen, T., Sutter-Fella, C.M., Chen, T., Ota, H., Schaler, E.W., De Wolf, S., Ballif, C., Cuevas A., and Javey, A., "Efficient silicon solar cells with dopant-free asymmetric heterocontacts", Nature Energy, Vol. 2, p. 15031, 2016. DOI: 10.1038/NENERGY.2015.31

Bullock, J., Kiriya, D., Grant, N., Azcatl, A., Hettick, M., Kho, T., Phang, P., Sio, H., Yan, D., MacDonald, D., Quevedo-Lopez, M., Wallace, R., Cuevas, A. and Javey, A., "Superacid passivation of crystalline silicon surfaces", ACS Appl. Mater. Interfaces, Vol. 8(36), pp 24205–24211, 2016 DOI: 10.1021/acsami.6b07822

Bullock, J., Zheng, P., Jeangros, Q., Tosun, M., Hettick, M., Sutter-Fella, C. M., Wan, Y., Allen, T., Yan, D., Macdonald, D., De Wolf, S., Hessler-Wyser, A., Cuevas, A. and Javey, A., "Lithium fluoride based electron contacts for high efficiency n-type crystalline silicon solar cells", Advanced Energy Materials, 1600241, 2016. doi:10.1002/aenm.201600241

Cao, W., Zhang, Z., Patterson, R., Lin, Y., Wen, X., Veetil, B.P., Zhang, P., Zhang, Q., Shrestha, S., Conibeer, G., and Huang, S., "Quantification of hot carrier thermalization in Pbs colloidal quantum dots by power and temperature dependent photoluminescence spectroscopy", RSC Advances, Vol. 6(93), pp. 90846-90855, 2016

Chan, K., Wright, M., Elumalai, N.K., Uddin, A.and Pillai, S., "Plasmonics in organic and perovskite solar cells: optical and Electrical Effects", Adv. Opt. Materials, ,DOI:10.1002/adom.201600698 (2016) (2016)

Chen, D., Edwards, M., Wenham, S., Hallam, B., Abbott, M., "Laser enhanced gettering of silicon substrates", Frontiers in Energy, Vol.11., pp. 23-31, 2016

Chen, R., Wang, S., Wenham, A., Shi, Z., Young, T., Ji, J., Edwards, M., Sugianto, A., Mai, L., Wenham, S., and Chong, C., "Plated Contacts for solar cells with Superior Adhesion Strength to Screen Printed solar cells", Frontiers in Energy, Vol., pp. 1-6, 2016

Chen, S., Wen, X., Huang, S., Huang, F., Cheng, Y-B., Green, M.A., and Ho-Baillie, A., "Light illumination induced photoluminescence enhancement and quenching in lead halide perovskite", Solar RRL, p. 1600001, 2016

Chen, S., Wen, X., Sheng, R., Huang, S., Deng, X., Green, M.A., and Ho-Baillie, A., "Mobile ion induced slow carrier dynamics in organic-inorganic perovskite CH3NH3PbBr3", ACS Applied Materials and Interfaces, Vol. 8(8), pp. 5351-5357, 2016

Chung, D., Mitchell, B., Weber, J.W., Yager, N., and Trupke, T., "Photoluminescence imaging for quality control in silicon solar cell manufacturing", MRS Advances, Vol., pp. 1-10, DOI: https://doi.org/10.1557/adv.2016.424 , 2016

Chung, S., Shrestha, S., Wen, X., Feng, Y., Gupta, N., Xia, H., Yu, P., Tang, J., and Conibeer, G., "Hafnium nitride for hot carrier solar cells", Solar Energy Materials and Solar Cells, Vol. 144, pp. 781-786, 2016

Conrad, B., Zhao, X., Li, D., Wang, L., Diaz, M., Soeriyadi, A.H., Lochtefeld, A., Gerger, A., Barnett, A., and Perez-Wurfl, I., "Window optimization enabling broadband double-layer antireflection coating for GaAsP/SiGe tandem on silicon", Solar Energy, Vol., 127, pp. 216-222, http://dx.doi.org/10.1016/j.solener.2016.01.019, 2016

Cui, J., Allen, T., Wan, Y., McKeon, J., Samundsett, C., Yan, D., Zhang, X., Cui, Y., Chen, Y., Verlinden P. and Cuevas, A., "Titanium oxide: a re-emerging optical and passivating material for silicon solar cells", Solar Energy Materials and Solar Cells, 2016 DOI:10.1016/j.solmat.2016.05.006

Deng, X., Wen, X., Huang, S., Sheng, R., Harada, T., Kee, T.W., Green, M., and Ho-Baillie, A., "Ultrafast carrier dynamics in methylammonium lead bromide perovskite", Journal of Physical Chemistry C, Vol. 120(5), pp. 2542-2547, 2016

Deng, X., Wen, X., Lau, C.F.J., Young, T., Yun, J., Green, M.A., Huang, S., and Ho-Baillie, A.W.Y., "Electric field induced reversible and irreversible photoluminescence responses in methylammonium lead iodide perovskite", Journal of Materials Chemistry C, Vol. 4(38), pp. 9060-9068, 2016

Wang, D., Wright, M., Elumalai N.K., and Uddin, A., "Stability of perovskite solar cells" Solar Energy Materials & Solar Cells 147 (2016) 255–275

Dkhissi, Y., Meyer, S., Chen, D.H., Weerasinghe, H.C., Spiccia, L., Cheng, Y.B., Caruso, R.A., "Stability comparison of perovskite solar cells based on zinc oxide and titania on polymer substrates", Chemsuschem, Vol. 9, pp. 687-695, 2016

Dkhissi, Y., Weerasinghe, H., Meyer, S., Benesperi, I., Bach, U., Spiccia, L., Caruso, R.A., Cheng, YB., "Parameters responsible for the degradation of CH3NH3PbI3-based solar cells on polymer substrates", Nano Energy, Vol. 22, pp. 211-222, 2016

Du, J.H., Jin, H., Zhang, Z.K., Zhang, D.D., Jia, S., Ma, L.P., Ren, W. C., Cheng, H.M., Burn, P.L., "Efficient organic photovoltaic cells on a single layer graphene transparent conductive electrode using MoOx as an interfacial layer", Nanoscale, Vol. 9, pp. 251-257, 2016

Duong, T., Grant, D., Rahman, S., Blakers, A., Weber, K.J., Catchpole, K.R. and White, T.P., "Filterless spectral splitting perovskite–silicon tandem system with >23% calculated efficiency", IEEE Journal of Photovoltaics, Vol. 6(6), p. 1432, 2016

Duong, T., Lal, N., Grant, D., Jacobs, D., Zheng, P., Rahman, S., Shen, H., Stocks, M., Blakers, A., Weber, K.J., White, T.P., and Catchpole, K.R., "Semitransparent perovskite solar cell with sputtered front and rear electrodes for a four-terminal tandem", IEEE Journal of Photovoltaics, Vol. 6, pp 679–687, 2016

Duong, T., Mulmudi, H.K., Shen, H., Wu, Y., Barugkin, C., Osorio Mayon, Y., Nguyen, H.T., Macdonald, D., Peng, J., Lockrey, M., Li, W., Cheng, Y-B., White, T.P., Weber, K., and Catchpole, K.R., "Structural engineering using rubidium iodide as a dopant under excess lead iodide conditions for high efficiency and stable perovskites," Nano Energy, http://dx.doi.org/10.1016/j.nanoen.2016.10.027 (2016).

Dupre, O., Vaillon, R., and Green, M.A., "Experimental assessment of temperature coefficient theories for silicon solar cells", IEEE Journal of Photovoltaics, Vol. 6(1), pp. 56-60, 2016

Dupre, O., Vaillon, R., and Green, M.A., "A full thermal model for photovoltaic devices", Solar Energy, Vol. 140, pp. 73-82, 2016

Elumalai, N., Mahmud, M., Wang, D., Uddin, A., "Perovskite solar cells: progress and advancements", Energies Vol. 9, p. 861, 2016

Elumalai, N.K. and Uddin, A., "Open circuit voltage of organic solar cells: an in-depth review", Energy and Environmental Science, Vol. 9(2), pp. 391-410, 2016

Elumalai, N.K. and Uddin, A., "Hysteresis in organic-inorganic hybrid perovskite solar cells", Solar Energy Materials & Solar Cells 157 (2016) pp476–509.

Fong, K.C., Padilla, M., Fell, A., Franklin, E., McIntosh, K.R., Teng, K., Blakers, A.W., Nebel- Yona, J. and Sachin, S., "Perimeter recombination characterization by luminescence imaging", IEEE Journal of Photovoltaics, Vol 6, pp 244 - 251, Jan 2016

Franklin, E., Fong, K., McIntosh, K., Fell, A., Blakers, A., Kho, T., Walter, D., Wang, D., Zin, N., Stocks, M., Wang, E.C., Grant, N., Wan, Y.M., Yang, Y., Zhang, X.L., Feng, Z.Q., Verlinden, P.J., 2016, "Design, fabrication and characterisation of a 24.4% efficient interdigitated back contact solar cell", Progress in Photovoltaics: Research and Applications, Vol. 24(4), pp. 411-427, DOI: 10.1002/pip.2556

Fu, X., Jacobs, D.A., Beck, F.J., Duong, T., Shen, H., Catchpole, K.R. and White, T.P., "Photoluminescence study of time- and spatial-dependent light induced trap de-activation in CH3NH3PbI3 perovskite films", Physical Chemistry Chemical Physics, Vol. 18(32), pp. 22557-22564, 2016.

Green, M.A., "Accurate expressions for solar cell fill factors including series and shunt resistances", Applied Physics Letters, Vol. 108(8), 2016

Green, M.A., "Australian photovoltaics research and development", ACS Energy Letters, Vol. 1(4), pp. 516-520, 2016

Green, M.A., "Commercial progress and challenges for photovoltaics", Nature Energy, Vol. 1, Article Number 15015, 2016

Green, M.A., Emery, K., Hishikawa, Y., Warta, W., and Dunlop, E.D., "Solar cell efficiency tables (Version 48)", Progress in Photovoltaics: Research and Applications, Vol. 24(7), pp. 905-913, 2016

Green, Martin A.; Emery, Keith; Hishikawa, Yoshihiro; et al., "Solar cell efficiency tables (version 47)", Progress in Photovoltaics, Vol. 24(1), pp. 3-11, 2016

Gupta, N., Veettill, B.P., Conibeer, G., and Shrestha, S., "Effect of substrate temperature and radio frequency power on compositional, structural and optical properties of amorphous germanium carbide

films deposited using sputtering", Journal of Non-Crystalline Solids, Vol. 443, pp. 97-102, 2016

Guse, J.A., Soufiani, A.M., Jiang, L., Kim, J., Cheng, Y.B., Schmidt, T.W., Ho-Baillie, A., and McCamey, D.R., "Spectral dependence of direct and trap-mediated recombination processes in lead halide perovskites using time resolved microwave conductivity", Physical Chemistry Chemical Physics, Vol. 18(17), pp. 12043-12049, 2016

Guse, J.A., Soufiani, A.M., Jiang, L.C., Kim, J., Cheng, Y.B., Schmidt, TW., Ho-Baillie, A., McCamey, D.R., "Spectral dependence of direct and trap-mediated recombination processes in lead halide perovskites using time resolved microwave conductivity", Physical Chemistry Chemical Physics, Vol. 18, pp. 12043-12049, 2016

Hallam, B., Abbott, M., Nærland, T., and Wenham, S., "Fast and slow lifetime degradation in boron-doped Czochralski silicon described by a single defect", Physica Status Solidi - Rapid Research Letters, Vol. 10(7), pp. 520-524, 2016

Hallam, B., Abbott, M., Nampalli, N., Hamer, P., and Wenham, S., "Influence of the formation-and passivation rate of boron-oxygen defects for mitigating carrier-induced degradation in silicon within a hydrogen-based model", Journal of Applied Physics, Vol. 119(6), 2016

Hambsch, M., Lin, Q., Burn, P. L., Meredith, P., "Efficient, monolithic large area organohalide perovskite solar cells", J. Mater. Chem. A, Vol. 4, pp. 13830-13836, 2016

Hameiri, Z., "Photovoltaics literature survey (No. 123)", Progress in Photovoltaics: Research and Applications, Vol. 24(1), pp. 133-136, 2016

Hameiri, Z., "Photovoltaics literature survey literature survey(No. 124)", Progress in Photovoltaics: Research and Applications, Vol. 24(2), pp. 269-271, 2016

Hameiri, Z., "Photovoltaics literature survey (No. 125)", Progress in Photovoltaics: Research and Applications, Vol. 24(3), pp. 405-407, 2016

Hameiri, Z., "Photovoltaics literature survey (No. 126)", Progress in Photovoltaics: Research and Applications, Vol. 24(4), pp. 584-587, 2016

Hameiri, Z., "Photovoltaics literature survey (No. 127)", Progress in Photovoltaics: Research and Applications, Vol. 24(6), pp. 899-902, 2016

Hameiri, Z., "Photovoltaics literature survey (No. 128)", Progress in Photovoltaics: Research and Applications, Vol. 24(8), pp. 1157-1161, 2016

Hameiri, Z., "Photovoltaics literature survey (No. 129)", Progress in Photovoltaics: Research and Applications, Vol. 24(10), pp. 1378-1381, 2016

Hamer, P., Hallam, B., Abbott, M., Chan, C., Nampalli, N., and Wenham, S., "Investigations on accelerated processes for the boron-oxygen defect in p-type Czochralski silicon", Solar Energy Materials and Solar Cells, Vol. 145, pp. 440-446, 2016

Han, J., Abbott, M.D., Hamer, P.G., Hoex, B., Wang, L., Lochtefeld, A., and Barnett, A.M., "Ultrathin silicon solar cell loss analysis", IEEE Journal of Photovoltaics, Vol. 6(5), pp. 1160-1166, 2016

Heilmann, M., Munshi, A.M., Sarau, G., Göbelt, M., Tessarek, C., Fauske, V.T., Van Helvoort, A.T.J., Yang, J., Latzel, M., Hoffmann, B., Conibeer, G., Weman, H., and Christiansen, S., "Vertically oriented growth of GaN nanorods on Si using graphene as an atomically thin buffer layer", Nano Letters, Vol. 16(6), pp. 3524-3532, 2016

Huang, C., Fu, N., Liu, F., Jiang, L., Hao, X., and Huang, H., "Highly efficient perovskite solar cells with precursor composition-dependent morphology", Solar Energy Materials and Solar Cells, Vol. 145, pp. 231-237, 2016

Huang, C., Liu, C., Di, Y., Li, W., Liu, F., Jiang, L., Li, J., Hao, X., and Huang, H., "Efficient planar perovskite solar cells with reduced hysteresis and enhanced open circuit voltage by using PW12-TiO2 as electron transport layer", ACS Applied Materials and Interfaces, Vol. 8(13), pp. 8520-8526, 2016

Huang, F.Z., Jiang, L.C., Pascoe, A.R., Yan, Y.F., Bach, U., Spiccia, L., Cheng, Y.B., "Fatigue behavior of planar CH3NH3PbI3 perovskite solar cells revealed by light onioff diurnal cycling", Nano Energy, Vol. 27, pp. 509-514, 2016

Huang, W.C., Chandrasekaran, N., Prasad, S.K.K., Gann, E., Thomsen, L., Kabra, D., Hodgkiss, J.M., Justin, M., Cheng, Y.B., McNeill., C.R., "Impact of Fullerene mixing behavior on the microstructure, photophysics, and device performance of polymer/Fullerene solar cells", ACS Applied Materials & Interfaces, Vol. 8(43), pp. 29608-29618, 2016

Jia, X., Puthen-Veettil, B., Xia, H., Yang, T.C.J., Lin, Z., Zhang, T., Wu, L., Nomoto, K., Conibeer, G., and Perez-Wurfl, I., "All-Silicon tandem solar cells: practical limits for energy conversion and possible routes for improvement", Journal of Applied Physics, Vol. 119(23), 2016

Jiang, Y., Almansouri, I., Huang, S., Young, T., Li, Y., Peng, Y., Hou, Q., Spiccia, L., Bach, U., Cheng, Y.B., Green, M.A., and Ho-Baillie, A., "Optical analysis of perovskite/silicon tandem solar cells", Journal of Materials Chemistry C, Vol. 4(24), pp. 5679-5689, 2016

Jiang, Y., Hao, M., Jiang, L., Liu, F., and Liu, Y., "Shape and stoichiometry control of bismuth selenide nanocrystals in colloidal synthesis", RSC Advances, Vol. 6(53), pp. 47840-47843, 2016

Jiang, Y., Pillai S. and Green, M.A., "Grain boundary effects on the optical constants and Drude relaxation times of silver films", Journal of Applied Physics, Vol. 120, p. 233109, 2016

Jiang, Y., Pillai, S., and Green, M.A., "Realistic silver optical constants for plasmonics", Scientific Reports, Vol. 6, 2016

Jiang, Y., Soufiani, A.M., Gentle, A., Huang, F., Ho-Baillie, A., and Green, M.A., "Temperature Dependent optical properties of CH3NH3PbI3 perovskite by spectroscopic ellipsometry", Applied Physics Letters, Vol. 108(6), 2016

Jiang, Y.J., Almansouri, I., Huang, S.J., Young, T., Li, Y., Peng, Y., Hou, Q.C., Spiccia, L., Bach, U., Cheng, Y.B., Greena, M.A., Ho-Baillie, A., "Optical analysis of perovskite/silicon tandem solar cells", Journal Of Materials Chemistry C, Vol. 4, pp. 5679-5689, 2016

Jiang, Y.J., Wen, X.M., Benda, A., Sheng, R., Ho-Baillie, A.W.Y., Huang, S.J., Huang, F.Z., Cheng, Y.B., Green, MA., "Time-resolved fluorescence anisotropy study of organic lead halide perovskite", Solar Energy Materials And Solar Cells, Vol. 151, pp. 102-112, 2016

Jin, X., Li, H., Li, D., Zhang, Q., Li, F., Sun, W., Chen, Z., and Li, Q., "Role of ytterbium-erbium co-doped gadolinium molybdate (Gd2(MoO4)3:Yb/Er) nanophosphors in solar cells", Optics Express, Vol. 24(18), pp. A1276-A1287, 2016

Juhl, M.K. and Trupke, T., "The Impact of voltage independent carriers on implied voltage measurements on silicon devices", Journal of Applied Physics, Vol. 120(16), pp. 165702-165702, 2016

Jumabekov, A.N., Della Gaspera, E., Xu, Z.Q., Chesman, A.S.R., van Embden, J., Bonke, S.A., Bao, Q., Vak, D. and Bach, U., "Back-contacted hybrid organic-inorganic perovskite solar cells", Journal Of Materials Chemistry C, Vol. 4, pp. 3125-3130, 2016

Kim, J., Yun, J.S., Wen, X., Soufiani, A.M., Lau, C.F.J., Wilkinson, B., Seidel, J., Green, M.A., Huang, S., and Ho-Baillie, A.W.Y., "Nucleation and growth control of HC(NH2)2PbI3 for planar perovskite solar cell", Journal of Physical Chemistry C, Vol. 120(20), pp. 11262-11267, 2016

Kim, M., Hamer, P., Li, H., Payne, D., Wenham, S., Abbott, M., and Hallam, B., "Impact of thermal processes on multi-crystalline silicon", Frontiers in Energy, Vol., pp. 1-10, 2016

Kim, Y.C., Jeon, N.J., Noh, J.H., Yang, W.S., Seo, J., Yun, J.S., Ho-Baillie, A., Huang, S., Green, M.A., Seidel, J., Ahn, T.K., and Seok, S.I., "Beneficial effects of PbI2 incorporated in organo-lead halide perovskite solar cells", Advanced Energy Materials, Vol. 6(4), 2016

König, D., "Number series of atoms, interatomic bonds and interface bonds defining zinc-blende nanocrystals as function of size, shape and surface orientation: analytic tools to interpret solid state spectroscopy data", AIP Advances, Vol. 6(8), 2016

Lai, Y., Zhao, L., Gao, C., Kang, L., Yan, C., Jiang, L., and Liu, F., "Fabrication of Cu2ZnSn(S,Se)4 thin film solar cells by selenization of reactively sputtered precursors", Materials Letters, Vol. 182, pp. 336-339, 2016

Lan, D. and Green, M.A., "Generalised distributed model of a solar cell: lateral injection effects and impact on cell design and characterisation", Solar Energy Materials and Solar Cells, Vol. 147, pp. 108-114, 2016

Lan, D. and Green, M.A., "Limiting efficiencies of GaIn/GaAs/Ge up-conversion systems: addressing the issue of radiative coupling", Applied Physics Letters, Vol. 109(12), 2016

Lan, D. and Green, M.A., "Photoluminescent and electroluminescent couplings in monolithic tandem solar cells", Progress in Photovoltaics: Research and Applications, http://dx.doi.org/10.1002/pip.2750, 2016

Lau, C.F.J., Deng, X., Ma, Q., Zheng, J., Yun, J.S., Green, M.A., Huang, S., and Ho-Baillie, A.W.Y., " CsPbIBr2 perovskite solar cell by spray-assisted deposition", ACS Energy Letters, Vol. 1(3), pp. 573-577, 2016

Li, D., Zhao, X., Wang, L., Conrad, B., Soeriyadi, A., Lochtefeld, A., Gerger, A., Barnett, A., and Perez-Wurfl, I., "Performance improvement for epitaxially grown SiGe on Si solar cell by optimizing the back surface field", Physica Status Solidi: Rapid Research Letters, Vol., 2016

Li, Y., Ouyang, S., Xu, H., Wang, X., Bi, Y., Zhang, Y., and Ye, J., "Constructing solid-gas-interfacial Fenton reaction over alkalinized-C3N4 photocatalyst to achieve apparent quantum yield of 49% at 420 Nm", Journal of the American Chemical Society, Vol. 138(40), pp. 13289-13297, 2016

Li, Z. and Lennon, A., "Patterned masking using polymers: insights and developments from silicon photovoltaics", International Materials Reviews, Vol. 61(6), pp. 416-435, 2016

Lin, Q., Armin, A., Burn, P.L., Meredith, P., "Near infrared photodetectors based on sub-gap absorption in organohalide perovskite single crystals", Laser Photonics Rev., Vol. 10(6), pp. 1047-1053, 2016

Lin, Q., Nagiri, R. C. R., Burn, P. L., Meredith, P., "Considerations for upscaling organohalide perovskite solar cells", Adv. Opt. Mater, DOI: 10.1002/adom.201600819, 2016

Lin, S., Feng, Y., Wen, X., Harada, T., Kee, T.W., Huang, S., Shrestha, S., and Conibeer, G., "Observation of hot carriers existing in Ag2S nanoparticles and its implication on solar cell application", Journal of Physical Chemistry C, Vol. 120(19), pp. 10199-10205, 2016

Liu, F., Jiang, Y., Yang, J., Hao, M., Tong, Z., Jiang, L., and Wu, Z., "MoS2 nanodot decorated In2S3 nanoplates: A novel heterojunction with enhanced photoelectrochemical performance", Chemical Communications, Vol. 52(9), pp. 1867-1870, DOI: 10.1039/C5CC09601D, 2016

Liu, F., Yan, C., Huang, J., Sun, K., Zhou, F., Stride, J.A., Green, M.A., and Hao, X., "Nanoscale microstructure and chemistry of Cu2ZnSnS4/CdS interface in kesterite Cu2ZnSnS4 solar cells", Advanced Energy Materials, Vol. 6(15), 2016

Liu, X., Feng, Y., Cui, H., Liu, F., Hao, X., Conibeer, G., Mitzi, D.B., and Green, M., "The current status and future prospects of kesterite solar cells: a brief review", Progress in Photovoltaics: Research and Applications, Vol. 24(6), pp. 879-898, 2016

Liu, X., Huang, J., Zhou, F., Liu, F., Sun, K., Yan, C., Stride, J.A., and Hao, X., "Understanding the key factors of enhancing phase and compositional controllability for 6% efficient pure-sulfide Cu2ZnSnS4 solar cells prepared from quaternary Wurtzite nanocrystals", Chemistry of Materials, Vol. 28(11), pp. 3649-3658, 2016

Liu, Z., Hao, X., Huang, J., Li, W., Ho-Baillie, A., and Green, M.A., "Diode laser annealing on Ge/Si (100) epitaxial films grown by magnetron sputtering", Thin Solid Films, Vol. 609, pp. 49-52, 2016

Lu, P.H.D., Lin, D., Wang, X., Lennon, A., and Wenham, S., "Laser doping through anodic aluminium oxide silicon solar cell", Solar Energy Materials and Solar Cells, Vol. 145, pp. 349-357, 2016

Lu, Z., Ouyang, Z., Grant, N., Wan, Y., Yan, D., and Lennon, A., "Manipulation of stored charge in anodic aluminium oxide/SiO2 dielectric stacks by the use of pulsed anodisation", Applied Surface Science, Vol. 363, pp. 296-302, 2016

Yan, L., Kah , K.H., and Uddin, A., "Dopamine-induced growth of Au and Ag nanoparticles on ITO substrate and their application in PCPDTBT-based polymer solar cell", plasmonics (2016) p1-7, (doi:10.1007/s11468-016-0270-x).

Ma, Q., Huang, S., Wen, X., Green, M.A., and Ho-Baillie, A.W.Y., "Hole transport layer free inorganic CsPbIBr2 perovskite solar cell by dual source thermal evaporation", Advanced Energy Materials, Vol. 6(7), 2016

MacQueen, R.W., Tayebjee, M.J.Y., Webb, J.E.A., Falber, A., Thordarson, P., and Schmidt, T.W., "Limitations and design considerations for donor-acceptor systems in luminescent solar concentrators: the effect of coupling-induced red-edge absorption", Journal of Optics (United Kingdom), Vol. 18(6), 2016

Mahmud, M.A., Elumalai, N.K., Upama, M.B., Wang, D., Chan, K. H., Wright, M., Xu, C., Haque, F. andUddin, A., "Low temperature processed ZnO thin film as electron transport layer for efficient perovskite solar cells", Solar Energy Materials and Solar Cells Vol. 159, pp. 251-264, 2017

Mahmud, M.A., Elumalai, N.K., Upama, M.B., Wang, D., Haque, F., Wright, M., Chan, K.H., Xu, C. and Uddin, A., "Enhanced stability of low temperature processed perovskite solar cells via augmented polaronic intensity of hole transporting layer" Physica Status Solidi - Rapid Research Letters, Vol. 10, pp. 882 - 889, http://dx.doi.org/10.1002/pssr.201600315

Mahmud, M.A., Elumalai, N.K., Upama, M.B., Wang, D., Wright, M., Sun, T., Xu, C., Haque, F., and Uddin, A., "Simultaneous enhancement in stability and efficiency of low-temperature processed perovskite solar cells", RSC Advances, Vol. 6(89), pp. 86108-86125, 2016

Mahmud, M.A., Elumalai, N.K., Upama, M.B., Wang, D., Wright, M., Chan, K. H., Xu, C., Haque, F. and Uddin, A., "Single vs mixed organic cation for low temperature processed perovskite solar cells", Electrochimica Acta, Vol. 222, pp. 1510-1521, 2016

Mitchell, B., Chung, D., and Teal, A., "Photoluminescence imaging using silicon line-scanning cameras", IEEE Journal of Photovoltaics, Vol. 6(4), pp. 967-975, 2016

Nattestad, A., Perera, I., Spiccia, L., "Developments in and prospects for photocathodic and tandem dye-sensitized solar", Journal Of Photochemistry And Photobiology C-Photochemistry Reviews, Vol. 28, pp. 44-71, 2016

Nomoto, K., Gutsch, S., Ceguerra, A.V., Breen, A., Sugimoto, H., Fujii, M., Perez-Wurfl, I., Ringer, S.P., and Conibeer, G., "Atom probe tomography of phosphorus- and boron-doped silicon nanocrystals with various compositions of silicon rich oxide", MRS Communications, Vol., pp. 1-6, 2016

Nomoto, K., Sugimoto, H., Breen, A., Ceguerra, A.V., Kanno, T., Ringer, S.P., Perez-Wurfl, I., Conibeer, G., and Fujii, M., "Atom probe tomography analysis of boron and/or phosphorus distribution in doped silicon nanocrystals", Journal of Physical Chemistry C, Vol. 120(31), pp. 17845-17852, 2016

Pakhuruddin, M.Z., Huang, J., Dore, J., and Varlamov, S., "Enhanced absorption in laser-crystallized silicon thin films on Textured Glass", IEEE Journal of Photovoltaics, Vol. 6(4), pp. 852-859, 2016

Pakhuruddin, M.Z., Huang, J., Dore, J., and Varlamov, S., "Light Absorption enhancement in laser-crystallized silicon thin films on textured glass", IEEE Journal of Photovoltaics, Vol. 6(1), pp. 159-165, 2016

Pascoe, A.R., Meyer, S., Huang, W.C., Li, W., Benesperi, I., Duffy, N.W., Spiccia, L., Bach, U., Cheng, Y.B., "Enhancing the optoelectronic performance of perovskite solar cells via a textured CH3NH3PbI3 morphology", Advanced Functional Materials, Vol. 26, pp. 1278-1285, 2016

Pascoe, A.R., Yang, M.J., Kopidakis, N., Zhu, K., Reese, M.O., Rumbles, G., Fekete, M., Duffy, N.W., Cheng, Y.B., "Planar versus mesoscopic perovskite microstructures: The influence of CH3NH3PbI3 morphology on charge transport and recombination dynamics", Nano Energy, Vol. 22, pp. 439-452, 2016

Payne, D.N.R., Chan, C.E., Hallam, B.J., Hoex, B., Abbott, M.D., Wenham, S.R., and Bagnall, D.M., "Acceleration and mitigation of carrier-induced degradation in p-type multi-crystalline silicon", Physica Status Solidi - Rapid Research Letters, Vol. 10(3), pp. 237-241, 2016

Payne, D.N.R., Chan, C.E., Hallam, B.J., Hoex, B., Abbott, M.D., Wenham, S.R., and Bagnall, D.M., "Rapid passivation of carrier-induced defects in p-type multi-crystalline silicon", Solar Energy Materials and Solar Cells, Vol. 158, pp. 102-106, 2016

Reineck, P., Brick, D., Mulvaney, P., Bach, U., "Plasmonic Hot Electron solar cells: The effect of nanoparticle size on quantum efficiency", Journal Of Physical Chemistry Letters, Vol. 7(20), pp. 4137-4141, 2016

Sheng, R., Wen, X., Huang, S., Hao, X., Chen, S., Jiang, Y., Deng, X., Green, M.A., and Ho-Baillie, A.W.Y., "Photoluminescence characterisations of a dynamic aging process of organic-inorganic CH3NH3PbBr3 perovskite", Nanoscale, Vol. 8(4), pp. 1926-1931, 2016

Shi, X., Prewett, P., Huq, E., Bagnall, D.M., Robinson, A.P.G., and Boden, S.A., "Helium ion beam lithography on Fullerene molecular resists for sub-10 nm patterning", Microelectronic Engineering, Vol. 155, pp. 74-78, 2016

Song, L., Wenham, A., and Wenham, S., "Low temperature Diffusion and its impact on hydrogenation", Solar Energy Materials and Solar Cells, Vol. 149, pp. 221-225, 2016

Soufiani, A.M., Tayebjee, M.J.Y., Meyer, S., Ho-Baillie, A., Sung Yun, J., McQueen, R.W., Spiccia, L., Green, M.A., and Hameiri, Z., "Electro- and photoluminescence imaging as fast screening technique of the layer uniformity and device degradation in planar perovskite solar cells", Journal of Applied Physics, Vol. 120(3), pp. 035702-035702(035707), 2016

Stolterfoht, M., Armin, A., Shoaee, S., Kassal, I., Burn, P.L., Meredith, P., "Slower carriers limit charge generation in organic semiconductor light-harvesting systems", Nature Communications, Vol. 7, 2016

Stolterfoht, M., Philippa, B., Shoaee, S., Jin, H., Jiang, W., White, R.D., Burn, P.L., Meredith, P., Pivrikas, A., "Charge transport without recombination in organic solar cells and photodiodes", Journal of Materials Chemistry C, Vol. 119, pp. 26866–26874, 2015

Stolterfoht, M., Shoaee, S., Armin, A., Jin, H., Kassal, I., Jiang, W., Burn, P., Meredith, P., "Electric field and mobility dependent first-order recombination losses in organic solar cells", Adv. Energy Mater., 1601379, 2016

Stoltzfus, D., Clulow, A.J., Jin, H., Burn, P.L., Gentle, I.R., "Impact of dimerization on phase separation and crystallinity in bulk heterojunction films containing non-Fullerene acceptors", Macromolecules, Vol. 49(12), pp. 4404−4415, 2016

Stoltzfus, D., Ma, C-Q., Nagiri, R.C.R., Clulow, A.J., Bäuerle, P., Burn, P.L., Gentle, I.R., Meredith, P."Thiophene dendrimer-based low donor content solar cells", Appl. Phys. Lett, Vol. 109, p. 103302, 2016

Sun, C., Rougieux, F.E. and Macdonald, D., "Reassessment of the recombination properties of aluminium-oxygen complexes in n- and p-type Czochralski-grown silicon", Physica Status Solidi B: Basic Solid State Physics, Vol. 253(10), pp. 2079-2084, 2016.

Sun, K., Liu, F., Yan, C., Zhou, F., Huang, J., Shen, Y., Liu, R., and Hao, X., "Influence of sodium incorporation on kesterite Cu2ZnSnS4 s fabricated on stainless steel substrates", Solar Energy Materials and Solar Cells, Vol. 157, pp. 565-571, 2016

Sun, K., Yan, C., Liu, F., Huang, J., Zhou, F., Stride, J.A., Green, M., and Hao, X., "Over 9% efficient kesterite Cu2ZnSnS4 solar cell fabricated by using Zn1–XCdxS Buffer Layer", Advanced Energy Materials, Vol. 6(12), 2016

Tan, H.L., Tahini, H.A., Wen, X., Wong, R.J., Tan, X., Iwase, A., Kudo, A., Amal, R., Smith, S.C., and Ng, Y.H., "Interfacing BiVO4 with reduced graphene oxide for enhanced photoactivity: a tale of facet dependence of electron shuttling", Small, Vol. 12(38), pp. 5295-5302, doi: 10.1002/smll.201601536, 2016

Tan, H.L., Wen, X., Amal, R., and Ng, Y.H., "BiVO4{010} and {110} relative exposure extent: governing factor of surface charge population and photocatalytic activity", Journal of Physical Chemistry Letters, Vol. 7(7), pp. 1400-1405, 2016

Tong, Z., Zhang, K., Sun, K., Yan, C., Liu, F., Jiang, L., Lai, Y., Hao, X., and Li, J., "Modification of absorber quality and Mo-back contact by a thin Bi intermediate layer for kesterite Cu2ZnSnS4 solar cells", Solar Energy Materials and Solar Cells, Vol. 144, pp. 537-543, 2016

Tong, Z.F., Yang, J., Yan, C., Hao, M.M., Liu, F.Y., Jiang, L.X., Lai, Y.Q., Li, J., and Liu, Y.X., "Synthesis of Cu2ZnSnS4 thin film from mixed solution of Cu2SnS3 nanoparticles and Zn ions", Transactions of Nonferrous Metals Society of China, Vol. 26(8), pp. 2102-2108, 2016

Upama, M. B., Wright, M., Elumalai, N. K., Mahmud, M. A., Wang, D., Chan, K. H., Xu, C., Haque, F., Uddin, A., "High performance semitransparent organic solar cells with 5% PCE using non-patterned MoO3/Ag/MoO3 anode", Current Applied Physics Vol. 17, pp. 298-305, 2017

Upama, M.B., Wright, M., Puthen-Veetil, B., Elumalai, N.K., Mahmud, M.A., Wang, D., Chan, K.H., Xu, C., Haque, F., and Uddin, A., "Analysis of burn-in degradation in organic solar cells using photothermal deflection spectroscopy", RSC Advances 6 (2016) p103899.

Upama, M.B., Wright, M., Elumalai, N.K., Mahmud, M.A., Wang, D., Chan, K.H., Xu, C., Haque, F. and Uddin, A., "optical modelling of P3HT:PC71BM semi-transparent organic solar cell", Optical and Quantum Electronics Vol. 49(28) 2017

Wan, Y., et al., 2016, "A magnesium/amorphous silicon passivating contact for n-type crystalline silicon solar cells", Appl. Phys. Lett. 109, 113901.

Wang, D., Wright, M., Elumalai, N.K., and Uddin, A., "Stability of perovskite solar cells", Solar Energy Materials and Solar Cells, Vol. 147, pp. 255-275, 2016

Wang, L., Conrad, B., Soeriyadia, A., Zhao, X., Li, D., Diaz, M., Lochtefeld, A., Gerger, A., Perez-Wurfl, I., and Barnett, A., "Current matched three-terminal dual junction GaAsP/SiGe tandem solar cell on Si", Solar Energy Materials and Solar Cells, Vol. 146, pp. 80-86, 2016

Wang, L., Li, D., Zhao, X., Conrad, B., Diaz, M., Soeriyadi, A., Lochtefeld, A., Gerger, A., Perez-Wurfl, I., and Barnett, A., "Current and efficiency improvement for a GaAsP/SiGe on Si tandem solar cell device achieved by light trapping techniques", Physica Status Solidi - Rapid Research Letters, Vol. 10(8), pp. 596-599, 2016

Wang, X., Hsiao, P.C., Zhang, W., Johnston, B., Stokes, A., Wei, Q., Fell, A., Surve, S., Shengzhao, Y., Verlinden, P., and Lennon, A., "Untangling the mysteries of plated metal finger adhesion: understanding the contributions from plating rate, chemistry, grid geometry, and sintering", IEEE Journal of Photovoltaics, Vol. 6(5), pp. 1167-1174, 2016

Wen, X., Huang, S., Chen, S., Deng, X., Huang, F., Cheng, Y.B., Green, M., and Ho-Baillie, A., "optical probe ion and carrier dynamics at the CH3NH3PbI3 interface with electron and hole transport materials", Advanced Materials Interfaces, Vol., 2016

Wen, X.M., Feng, Y., Huang, S.J., Huang, F.Z., Cheng, Y.B., Green, M., Ho-Baillie, A., "Defect trapping states and charge carrier recombination in organic-inorganic halide perovskites", Journal Of Materials Chemistry C, Vol. 4, pp. 793-800, 2016

Wright, M., Lin, R., Tayebjee, M.J.Y., Veettil, B.P., Jiang, Y., Liang, X., Uddin, A., and Conibeer, G., "Effect of blend composition on ternary blend organic solar cells using a low band gap polymer", Synthetic Metals, Vol. 212, pp. 142-153, 2016

Wu, L., Puthen-Veettil, B., Nomoto, K., Hao, X., Jia, X., Lin, Z., Yang, T.C., Zhang, T., Gutsch, S., Conibeer, G., and Perez-Wurfl, I., "Temperature dependent electroluminescence from all-Si-nanocrystal P-I-N diodes grown on dielectric substrates", Journal of Applied Physics, Vol. 119(6), 2016

Wu, W.Q., Chen, D.H., Huang, F.Z., Cheng, Y.B., Caruso, R.A., "Optimizing semiconductor thin films with smooth surfaces and well-interconnected networks for high-performance perovskite solar cells", Journal Of Materials Chemistry A, Vol. 4, pp. 12463-12470, 2016

Wu, W.Q., Chen, D.H., Huang, F.Z., Cheng, Y.B., Caruso, R.A., "Sub-100 degrees C solution processed amorphous titania nanowire thin films for high-performance perovskite solar cells", Journal Of Power Sources, Vol. 329, pp. 17-22, 2016

Wu, Y.L., Shen, H.P., Walter, D., Jacobs, D., Duong, T., Peng, J., Jiang, L.C., Cheng, Y.B., Weber, K., "On the origin of hysteresis in perovskite solar cells", Advanced Functional Materials, Vol. 36, pp. 6807-6813, 2016

Xia, H., Wen, X., Feng, Y., Patterson, R., Chung, S., Gupta, N., Shrestha, S., and Conibeer, G., "Hot carrier dynamics in HfN and ZrN measured by transient absorption spectroscopy", Solar Energy Materials and Solar Cells, Vol. 150, pp. 51-56, 2016

Xiang, W.C., Marlow, J., Bauerle, P., Bach, U., Spiccia, L., "Aqueous p-type dye-sensitized solar cells based on a tris(1,2-diaminoethane)cobalt(II)/(III) redox mediator", Green Chemistry, Vol.18, pp. 6659-6665, 2016

Xiao, M.D., Gao, M., Huang, F.Z., Pascoe, A.R., Qin, T.S., Cheng, Y.B., Bach, U., Spiccia, L., "Efficient perovskite solar cells employing inorganic interlayers", Chemnanomat, Vol. 2, pp.182-188, 2016

Xu, Q., Johnson, C., Disney, C., and Pillai, S., "Enhanced broadband light trapping in C-Si solar cells using nanosphere-embedded metallic grating structure", IEEE Journal of Photovoltaics, Vol. 6(1), pp. 61-67, 2016

Yan, C., Liu, F., Sun, K., Song, N., Stride, J.A., Zhou, F., Hao, X., and Green, M., "Boosting the efficiency of pure sulfide CZTS solar cells using the In/Cd-based hybrid buffers", Solar Energy Materials and Solar Cells, Vol. 144, pp. 700-706, 2016

Yan, L., Chan, K.H., and Uddin, A., "Dopamine-Induced Growth of Au and Ag nanoparticles on ITO substrate and their application in PCPDTBT-based polymer solar cell", Plasmonics, pp. 1-7, http://dx.doi.org/10.1007/s11468-016-0270-x, 2016

Yang, J., Ge, R., Zhang, Z., Chen, W., Wang, B., Feng, Y., Huang, S., Shrestha, S., Patterson, R., and Conibeer, G., "Theoretical investigation of carrier transfer by an optical contacting scheme for optoelectronic application", Journal of Applied Physics, Vol. 119(15), 2016

Yaung, K.N., Kirnstoetter, S., Faucher, J., Gerger, A., Lochtefeld, A., Barnett, A., and Lee, M.L., "Threading dislocation density characterization in Iii–V photovoltaic

materials by electron channeling contrast imaging", Journal of Crystal Growth, Vol. 453, pp. 65-70, 2016

Yoo, S., Sprafke, A., Lipiński, W., and Liu, J., "Feature issue introduction: Light, Energy and the Environment, 2015", Optics Express, Vol. 24(10), pp. A981-A984, 2016

Yu, Z., Perera, I.R., Daeneke, T., Makuta, S., Tachibana, Y., Jasieniak, J.J., Mishra, A ., Bauerle, P., Spiccia, L., Bach, U., "Indium tin oxide as a semiconductor material in efficient p-type dye-sensitized solar cells", NPG Asia Materials 2016, Vol. 8, e305, 2016

Yun, J., Huang, J., Teal, A., Kim, K., Varlamov, S., and Green, M.A., "Correlation of the crystal orientation and electrical properties of silicon thin films on glass crystallized by line focus diode laser", Thin Solid Films, Vol. 609, pp. 12-18, 2016

Yun, J.S., Seidel, J., Kim, J., Soufiani, A.M., Huang, S., Lau, J., Jeon, N.J., Seok, S.I., Green, M.A., and Ho-Baillie, A., "Critical role of grain boundaries for ion migration in formamidinium and methylammonium lead halide perovskite solar cells", Advanced Energy Materials, Vol. 6(13), 2016

Zeng, Y., Pan, X., Lu, B., and Ye, Z., "Fabrication of flexible self-powered UV detectors based on ZnO nanowires and the enhancement by the decoration of Ag nanoparticles", RSC Adv., Vol. 6(37), pp. 31316-31322, 2016

Zeng, Y., Ye, Z., Lu, B., Dai, W., and Pan, X., "Enhanced photoelectric performance in self-powered UV detectors based on ZnO nanowires with plasmonic Au nanoparticles scattered electrolyte", Applied Physics A, Vol. 122(4), 2016

Zhang, P., Feng, Y., Wen, X., Cao, W., Anthony, R., Kortshagen, U., Conibeer, G., and Huang, S., "Generation of hot carrier population in colloidal silicon quantum dots for high-efficiency photovoltaics", Solar Energy Materials and Solar Cells, Vol. 145, pp. 391-396, 2016

Zhang, T., Simonds, B., Nomoto, K., Veettil, B.P., Lin, Z., Wurfl, I.P., and Conibeer, G., "Pulsed KrF excimer laser dopant activation in nanocrystal silicon in a silicon dioxide matrix", Applied Physics Letters, Vol. 108(8), 2016

Zhang, X., Wan, Y.M., Bullock, J. Allen, T., Cuevas, A.et al., "Low resistance Ohmic contact to p-type crystalline silicon via nitrogen-doped copper oxide films", Appl. Phys. Lett. 109, 052102, 2016

Zhang, Y., Tayebjee, M.J.Y., Smyth, S., Dvoř ák, M., Wen, X., Xia, H., Heilmann, M., Liao, Y., Zhang, Z., Williamson, T., Williams, J., Bremner, S., Shrestha, S., Huang, S., Schmidt, T.W., and Conibeer, G.J., "Extended hot carrier lifetimes observed in bulk In0.265±0.02Ga0.735N under high-density photoexcitation", Applied Physics Letters, Vol. 108(13), 2016

Zhao, L., Di, Y., Yan, C., Liu, F., Cheng, Z., Jiang, L., Hao, X., Lai, Y., and Li, J., "In Situ growth of SnS absorbing layer by reactive sputtering for thin film solar cells", RSC Advances, Vol. 6(5), pp. 4108-4115, 2016

8.5 Conference Papers and Presentations

Allen, T., "Electron selective contacts – novel materials and approaches to contact formation", 3rd Workshop on passivation, Advanced passivation and Selective contacts, Ecole Polytechnique, Palaiseau, France, June 2016

Allen, T.G., Zheng, P., Vaughan, B., Barr, M., Wan, Y., Samundsett, C. and Bullock, J., "Low resistance TiO2-passivated calcium contacts to for crystalline silicon solar cells", 43rd IEEE Photovoltaic Specialists Conference, Portland, 6-10 Jun 2016, pp. 230-233

An, X., Teng, P., Mehrvarz, H., To, A., Li, H., Johnson, C., Hoex, B., and Barnett, A., "Empirical and Quokka simulated evidence for enhanced Voc due to limited junction area for high efficiency silicon solar cells", 43rd IEEE PVSC, Portland, U.S., 6-10 Jun 2016

Anderson, K., "An investigation of perovskite solar cells with active areas beyond 1cm2", 3rd Asia Pacific Solar Research Conference, Canberra, 29 Nov - 1 Dec 2016

Armin, A., "Scaling up solution processed thin film solar cells", 4th ACAP Conference and 3rd Asia Pacific Solar Research Conference, Canberra, 1 Dec 2016

Armin, A., Lin, Q., Kopidakis, N., Burn, P.L., and Meredith, P., "Filterless narrowband visible-NIR light detection", ICSM, China, 26 Jun - 1 Jul 2016

Aury, C., "Modification, characterisation and optimisation of printing equipment for solar cell fabrication", 4th ACAP Conference and 3rd Asia Pacific Solar Research Conference, Canberra, 1 Dec 2016

Bach, U., "Back-contact perovskite solar cells", 4th ACAP Conference and 3rd Asia Pacific Solar Research Conference, Canberra, 1 Dec 2016

Bach, U., "Back-contact perovskite solar cells", HOPV16, Swansea, UK, June 28 – July 1, 2016

Bach, U., "Dye-sensitized and perovskite solar cells", 5th International SolTech Conference, Munich, Germany, April 5 – 8, 2016

Bach, U., "Dye-sensitized and perovskite solar cells", Emerging Energy Technologies Summit and Exhibition, Melbourne, Australia, December 5 –7, 2016

Bach, U., "New electrolytes and semiconductors for dye-sensitized photocathodes", SPIE Photonics West OPTO, San Franscisco, California, February 13-18, 2016

Bach, U., “Perovskite back-contact solar cells”, Conference International Symposium on Next Generation Solar Cells and Solar Energy Conversion, Hsinchu, Taiwan, November 21-24, 2016

Bach, U., “Perovskite solar cells”, 3rd Asia Pacific Solar Research Conference, Canberra, 29 Nov - 1 Dec 2016

Bach, U., “Recent advances in perovskite solar cell research: semitransparent and flexible CH3NH3PbI3 solar cells and their stability”, 12th Workshop on the Future Direction of Photovoltaics, Tokyo, Japan, January 28-29, 2016

Barker , W., “Systematic determination of the most accurate method of QSSPC and PCD data analysis for n-type silicon wafers”, 3rd Asia Pacific Solar Research Conference, Canberra, 29 Nov - 1 Dec 2016

Barnett, A., Han, J., Hoex, B., Jiao, F., Johnson, C.M., Wang, L., An, X., and Lochtefeld, A., “Ultra-thin Silicon solar cell for lightweight steel roofs”, PVSEC-26, Singapore, 24-28 Oct 2016

Benesperi, I., “Polypyridyl iron complex as a hole transporting material for organic-inorganic perovskite solar cells”, 4th ACAP Conference and 3rd Asia Pacific Solar Research Conference, Canberra, 1 Dec 2016

Bennett, R., “Investigating practical approaches to fine control of perovskite morphology in large scale processing”, 3rd Asia Pacific Solar Research Conference, Canberra, 29 Nov - 1 Dec 2016

Black, L. Allen, T., McIntosh, K.R., and Cuevas, A., “Improved silicon surface passivation of APCVD Al2O3 by rapid thermal annealing”, Energy Procedia, Vol. 92, pp. 317-325, 2016

Boreland, M.B. and Evans, R., “Automated statistical algorithms to interpret root cause variance in photovoltaic cell manufacturing”, 32nd European Photovoltaic Solar Energy Conference and Exhibition, Munich, Germany, 20-24 Jun 2016

Borojevic, N., Hameiri, Z., and Winderbaum, S., “Advanced optical characterisation of industrial PECVD silicon nitride layers”, 32nd European Photovoltaic Solar Energy Conference and Exhibition, Munich, Germany, 20-24 Jun 2016

Bremner, S., “Connecting sub-cells in III-V on silicon multi-junction solar cells”, 4th ACAP Conference and 3rd Asia Pacific Solar Research Conference, Canberra, 1 Dec 2016

Bullock J., et al., “Dopant-free carrier selective contacts for silicon solar cells”, 43rd IEEE Photovoltaic Specialists Conference, Portland, 6-10 Jun 2016

Bullock, J., Wan, Y., Hettick, M., Geissbühler, J., Ong, A.J., Kiriya, D., Yan, D., “Survey of dopant-free carrier-selective contacts for silicon solar cells”, 43rd IEEE Photovoltaic Specialists Conference, Portland, 6-10 Jun 2016, 0210-0214

Chan, C., “Light-induced degradation mechanisms in multi-crystalline Si PERC cells”, 4th ACAP Conference and 3rd Asia Pacific Solar Research Conference, Canberra, 1 Dec 2016

Chang, N., “A manufacturing cost analysis method for early stage technologies”, 3rd Asia Pacific Solar Research Conference, Canberra, 29 Nov - 1 Dec 2016

Chang, Y., “Nanosphere lithography for fast and controlled fabrication of large area plasmonic nanostructures in thinthin filmfilm photovoltaics”, 3rd Asia Pacific Solar Research Conference, Canberra, 29 Nov - 1 Dec 2016

Chantler, R., “Designing the future of solar energy”, 4th ACAP Conference and 3rd Asia Pacific Solar Research Conference, Canberra, 1 Dec 2016

Cheng, Y.-B., “Control of nucleation and growth in organic–inorganic hybrid perovskite solutions”, International Symposium on Next Generation Solar Cells and Solar Energy Conversion, Hsinchu, Taiwan, November 21-24, 2016

Cheng, Y.-B., “Electron microscopy characterisation of CH3NH3PbI3”, 10th Aseanian Conference on Nano-Hybrid Solar Cells, Beijing, China, September 20-23, 2016

Cheng, Y.-B., “Flexible glass and printed optoelectronics”, 2016 International Forum on Advanced Materials, Nanjing, China, September 24-26, 2016

Cheng, Y.-B., “Flexible perovskite solar cells and their stability”, 1st International Energy and Environmental Materials Forum, Gold Coast, Queensland, February 2-6, 2016

Cheng, Y.-B., “Flexible perovskite solar cells and their stability”, International Symposium on Flexible and Stretchable Electronics, Huazhong University of Science and Technology, Wuhan, China, June 29-30, 2016

Cheng, Y.-B., “Microstructral characterisation and control for organic–inorganic hybrid perovskite solar cells”, 2nd International Symposium on Renewable Energy Technologies, Sydney, Australia, November 30 – December 4, 2016

Cheng, Y.-B., “Microstructural development and characterisation for perovksite solar cells”, 12th Workshop on the Future Direction of Photovoltaics, Tokyo, Japan, January 28-29, 2016

Cheng, Y.-B., “Microstructure and property comparison between planar and mesoscopic perovskite solar cells”, 6th China- Australia Joint Symposium on Energy and Biomedical Materials, Suzhou, China, January 6-9, 2016

Cheng, Y.-B., “Printing of flexible thin film solar cells”, Nature Conference on Flexible Electronics-Challenges and Opportunities, Nanjing, China, June 4-8, 2016

Cheng, Y.-B., “Printing of solar cells and technical challenges”, 6th Chinese Flexible and Printed Electronics Symposium, Changzhou, China, October 24-25, 2016

Cheng, Y.-B., “Stability Issues of perovskite solar cells”, 3rd Asia Pacific Solar Research Conference, Canberra, 29 Nov - 1 Dec 2016

Cheng, Y.-B., “Stability of perovskite solar cells under static and dynamic illumination conditions”, The 5th Sungkyun International Solar Forum, Seoul, Korea, May 25-27, 2016

Cheng, Y.-B., “Stability of perovskite solar cells”, Nature Conference on Materials for Energy, Wuhan, China, June 11-14, 2016

Conibeer, G., Shrestha, S., Bremner, S., Zhang, Y., Tayebjee, M., “Uncovering hot carrier cooling mechanisms in multiple quantum wells”, 26th Photovoltaic Science and Engineering Conference, Singapore, 24-28 October 2016

Conrad, B., Soeriyadi, A., Li, D., Wang, L., Zhao, X., Lochtefeld, A., Gerger, A., Perez-Wurfl, I., and Barnett, A., “Improved GaAsP/SiGe tandem on silicon outdoors and under concentration”, 43rd IEEE PVSC, Portland, U.S. , 6-10 Jun 2016

Cuevas, A., “Electron and hole selective contacts for simple, efficient silicon solar cells”, Annual Meeting of State Key Laboratory of PV Science & Technology, Trina Solar, China, May 2016.

Cuevas, A., “Selective contact materials for simple solar cells”, Fifth biennial conference of the Combined Australian Materials Societies,CAMS, Melbourne, Australia, Dec 2016.

Cuevas, A., “Surface passivating films and contacts for silicon solar cells”, 12th Workshop on the Future Direction of Photovoltaics”, organized by The Japan Society for Promotion of Science (JSPS), Tokyo, Jan. 2016

Cui J., et al., “Highly effective electronic passivation of silicon by ALD hafnium oxide (HfO2)”, 26th International Photovoltaic Science and Engineering Conference (“PVSEC-26”), Singapore October 2016

Cui, J. “Highly effective electronic passivation of silicon surfaces by atomic layer deposited hafnium oxide”, 3rd Asia Pacific Solar Research Conference, Canberra, 29 Nov - 1 Dec 2016

Cui, J., “Surface and contact passivation for simple, efficient silicon solar cells”, Photovoltaic Industry Workshop, SungKyunKwan University, Suwon, Korea, Sept 2016

Cui, J., et al., “Titanium Oxide (TiO2): A Re-emerging optical and passivating Material for silicon solar cells”, 6th Silicon PV Conference, Chambery, 2016

Daniel Jacobs, D., “Characterizing and explaining hysteresis behaviour in perovskite solar cells: device modelling with mobile ions”, 3rd Asia Pacific Solar Research Conference, Canberra, 29 Nov - 1 Dec 2016

Duck, B., “Correlated electroluminescence and photoluminescence as a perovskite thin film diagnostic tool”, 3rd Asia Pacific Solar Research Conference, Canberra, 29 Nov - 1 Dec 2016

Duck, B., “Outdoor PV energy yield prediction”, 3rd Asia Pacific Solar Research Conference, Canberra, 29 Nov - 1 Dec 2016

Dumbrell, R.W., Juhl, M.K., Li, M., Trupke, T., and Hameiri, Z., “Effective lifetime of full rear metallized cells by quasi-steady-state photoluminescence”, 26th International Photovoltaic Science and Engineering Conference, Singapore, 24-28 Oct 2016

Dunbar, R., “Comparison of efficiency measurement methods for perovskite solar cells”, 3rd Asia Pacific Solar Research Conference, Canberra, 29 Nov - 1 Dec 2016

Duong, T., “High efficiency perovskite-silicon tandem system: a roadmap toward 26%”, 4th ACAP Conference and 3rd Asia Pacific Solar Research Conference, Canberra, 1 Dec 2016

Duong, T., Grant, D., Rahman, S., Blakers, A., Weber, K., White T. and Catchpole, K. “High efficiency perovskite/silicon tandem cells with low parasitic absorption”, 43rd IEEE Photovoltaic Specialists Conference, Portland, 6-10 Jun 2016

Duong, T., Grant, D., Rahman, S., Blakers, A., Weber, K., White T. and Catchpole, K., “High efficiency perovskite/silicon tandem cells with low parasitic absorption”, IEEE 43rd Photovoltaic Specialist Conference, 5–10 June, 2016, Portland, Oregon, USA

Elumalai, N.K., Mahmud, A., Wang, D., Wright, M., Upama, M.B., Chan, K.H., Xu, C., Uddin, A., “Hysteresis and electrode polarization in normal and inverted hybrid perovskite solar cells”, 43rd IEEE Photovoltaic Specialists Conference, 5–10 June, 2016, Portland, Oregon, USA

Ernst, M., “Laser-processed large area interdigitated back contact silicon solar cells with high open-circuit voltage”, 3rd Asia Pacific Solar Research Conference, Canberra, 29 Nov - 1 Dec 2016

Fabig, F., “Preparation and characterization of mini-emulsion nanoparticle suspensions for organic photovoltaics”, 4th ACAP Conference and 3rd Asia Pacific Solar Research Conference, Canberra, 1 Dec 2016

Fievez, M., “One Step process for Printable perovskite thin-films Photovoltaics”, 4th ACAP Conference and 3rd Asia Pacific Solar Research Conference, Canberra, 1 Dec 2016”, 4th ACAP Conference and 3rd Asia Pacific Solar Research Conference, Canberra, 1 Dec 2016

Fong, K., “Simulation of Fill-factor Loss in IBC solar cells”, 3rd Asia Pacific Solar Research Conference, Canberra, 29 Nov - 1 Dec 2016

Fong, K.C., Blakers, A.W. et al, “Simulation of fill-factor loss in IBC solar cells”, Asia-Pacific Solar Research Conf, Australian National University, November 2016

Gao, M., “Roll to roll compatible process for printed perovskite solar cells”, 4th ACAP Conference and 3rd Asia Pacific Solar Research Conference, Canberra, 1 Dec 2016

Geraghty,P., “Understanding optoelectronic properties of high performance materials for OPV”, 4th ACAP Conference and 3rd Asia Pacific Solar Research Conference, Canberra, 1 Dec 2016

Goodarzi, M., “Modeling and characterization of multicrystalline silicon blocks by quasi-steady-state photoconductance”, 3rd Asia Pacific Solar Research Conference, Canberra, 29 Nov - 1 Dec 2016

Grant, D., “An optical study on material selection for perovskite/silicon 2-terminal tandem solar cells”, 3rd Asia Pacific Solar Research Conference, Canberra, 29 Nov - 1 Dec 2016

Green, M. ,“Solar PV technology roadmap”, Solar Energy 2016, Melbourne, 4-5 May 2016.

Green, M., “37% efficient one-sun minimodule and over 40% efficient concentrator submodules”, 32nd European Photovoltaic Solar Energy Conference, Munich, 20-24 Jun 2016.

Green, M., “Australian-Chinese co-operation in the development of the photovoltaic industry”, Australia-China Forum on Science and Technology, Brisbane, 28-30 Nov 2016.

Green, M., “Future developments in silicon cell technology”, Chinese State Key Lab Conference, Shanghai, 22 Nov 2016.

Green, M., “Global perspectives and insights on PV in China”, The Terawatt Workshop, Freiburg, Germany, 17-18 Mar 2016.

Green, M., “Potential of silicon-perovskite tandem solar cells”, Academic Board of the State Key Lab Annual Meeting/Workshop, Trina Solar, Changzhou, China, 26-27 May 2016.

Green, M., “Recent developments and Future Trends in Photovoltaics”, International Symposium on Renewable Energy Technologies, University of Technology, Sydney, 30 Nov – 4 Dec 2016.

Green, M., “Silicon tandem solar cells: challenges and potential”, 10th International Photovoltaic Power Generation Conference (SNEC), 24-26 May 2016.

Green, M., “Silicon-based tandem cells”, 2016 MRS Spring Meeting, Phoenix, USA, 28 March – 1 Apr 2016.

Green, M., “The potential of silicon-based tandem solar cells”, PV Conference and Exhibition of China (PVCEC 2016), Beijing, 19-21 Oct 2016.

Hameiri, Z., Borojevic, N., Mai, L., Kim, K., Nandakumar, N., and Winderbaum, S., “Development of lowlow-absorption and thermally-stable silicon nitride films for surface passivation of silicon solar cells”, 26th International Photovoltaic Science and Engineering Conference, Singapore, 24-28 Oct 2016

Hameiri, Z., Borojevic, N., Mai, L., Nandakumar, N., Kim, K., and Winderbaum, S., “Should the refractive index at 633 nm be used to characterize silicon nitride films?”, 43rd IEEE Photovoltaic Specialists Conference, Portland, 6-10 Jun 2016

Hamieri, Z., “Advanced temperature and injection dependent lifetime tester for defect identification”, 4th ACAP Conference and 3rd Asia Pacific Solar Research Conference, Canberra, 1 Dec 2016

Han, J., Abbott, M., Hamer, P., Hoex, B., Lochtefeld, A., and Barnett, A., “Ultra-thin silicon solar cell: flexibility, modeling and prediction”, 32nd European Photovoltaic Solar Energy Conference and Exhibition, Munich, Germany, 20-24 Jun 2016

Han, Y., Franklin, E., Zhang, X., Thomson A.and Wan, Y., “Rear passivation and point contacts formation by laser process through stacks of a-Si:H(i) and a-Si:B for high efficiency silicon solar cell”, 32nd European Photovoltaic Solar Energy Conference and Exhibition, Munich, Germany, 20-24 Jun 2016

Hao, X., “Defect control in mismatched Ge heteroepitaxy by laser annealing, towards a cost-effective virtual Ge substrate for high efficiency III-V solar cells”, 4th ACAP Conference and 3rd Asia Pacific Solar Research Conference, Canberra, 1 Dec 2016

Hao, X., “Towards 10% state-of-the-art abundant, environmentally friendly pure sulfide Cu2ZnSnS4 solar cells by engineering the Cu2ZnSnS4/buffer interface”, 4th ACAP Conference and 3rd Asia Pacific Solar Research Conference, Canberra, 1 Dec 2016

Ho-Baillie, A., Efficient perovskite solar cell by blow-drying, 4th ACAP Conference and 3rd Asia Pacific Solar Research Conference, Canberra, 1 Dec 2016

Huang, W., “Influence of Fullerene acceptor on the performance, microstructure and photophysics of low band-gap polymer solar cells”, 4th ACAP Conference and 3rd Asia Pacific Solar Research Conference, Canberra, 1 Dec 2016

Jacobs, D., et al. “Modelling of slow transient processes in organo-metal halide perovskites”, 2016 International Conference on Numerical Simulation of Optoelectronic Devices (NUSOD), 11-15 July 2016, Sydney

Jasieniak, J., “Ultrasonic spray deposition of TiO2 hole blocking layers for high efficiency hybrid perovskite solar cells”, 3rd Asia Pacific Solar Research Conference, Canberra, 29 Nov - 1 Dec 2016

Jiang, L., “Fatigue behavior of planar CH3NH3PbI3 perovskite solar cells revealed by light on/off diurnal cycling”, 4th ACAP Conference and 3rd Asia Pacific Solar Research Conference, Canberra, 1 Dec 2016

Jin, H. “Efficient organic solar cells with 3D NDI-based non-fullerene acceptors”, 3rd Asia Pacific Solar Research Conference, Canberra, 29 Nov - 1 Dec 2016

Jones, D., “Side-chain engineering In high performance p-type organic semiconductors for printed OPV”, 3rd Asia Pacific Solar Research Conference, Canberra, 29 Nov - 1 Dec 2016

Jones, T., “Efficient solid-state dye-sensitised solar cells modules”, 3rd Asia Pacific Solar Research Conference, Canberra, 29 Nov - 1 Dec 2016

Juhl, M.K., Lu, C., and Hameiri, Z., “Review of determination of the effective surface recombination coefficient from minority carrier lifetime measurements”, 26th International Photovoltaic Science and Engineering Conference, Singapore, 24-28 Oct 2016

Jumabekov, A., “Back-contacted hybrid organic-inorganic perovskite solar cells”, 3rd Asia Pacific Solar Research Conference, Canberra, 29 Nov - 1 Dec 2016

Kallista Sears, K., “Robust and flexible perovskite solar cells with roll-to-roll printed electrodes”, 3rd Asia Pacific Solar Research Conference, Canberra, 29 Nov - 1 Dec 2016

Kim, J., “Towards large area and high efficiency perovskite solar device by modified spin-coating process”, 4th ACAP Conference and 3rd Asia Pacific Solar Research Conference, Canberra, 1 Dec 2016

Kim, J.-E. and Vak, D., “Upscaling perovskite solar cells via one-step slot-die coating at controlled temperature”, 4th ACAP Conference and 3rd Asia Pacific Solar Research Conference, Canberra, 1 Dec 2016

Kim, K.H., Borojevic, N., Winderbaum, S., Duttaguptta, S., and Hameiri, Z., “Impact of deposition condition and thermal process on industrial PECVD AlOx AlOx layer for surface passivation”, 26th International Photovoltaic Science and Engineering Conference, Singapore, 24-28 Oct 2016

Kim, K.H., Hameiri, Z., and Winderbaum, S., “In-situ diagnostics of PECVD AlOx deposition by optical emission spectroscopy”, 26th International Photovoltaic Science and Engineering Conference, Singapore, 24-28 Oct 2016

Kim, K.H., Hameiri, Z., Borojevic, N., Duttagupta, S., and Winderbaum, S., “Outstanding as-deposited surface passivation by industrial PECVD Aluminum Oxide”, 43rd IEEE Photovoltaic Specialists Conference, Portland, 6-10 Jun 2016

Kim, M., Li, H., Payne, D., Wenham S., Hallam, B., Abbott, M., “Application of high efficiency emitters to multi-crystalline silicon”, 32nd European Photovoltaic Solar Energy Conference and Exhibition, Munich, Germany, 20-24 Jun 2016

Lau, C., “CsPbIBr2 perovskite solar cell by spray assisted deposition”, 3rd Asia Pacific Solar Research Conference, Canberra, 29 Nov - 1 Dec 2016

Lee, C., “Polarized optical microscopy on high-performing molecular organic semiconductors”, 4th ACAP Conference and 3rd Asia Pacific Solar Research Conference, Canberra, 1 Dec 2016

Lennon, A., “Low cost options for the metallization of high efficiency poly-Si passivated solar cells”, 4th ACAP Conference and 3rd Asia Pacific Solar Research Conference, Canberra, 1 Dec 2016

Lennon, A., “Metallisation metrology for reliable and durable silicon photovoltaic modules”, 3rd Asia Pacific Solar Research Conference, Canberra, 29 Nov - 1 Dec 2016

Li, H., Abbott, M., Hallam, B., Barnett, A., and Wenham, S., “Improvement of industrial phosphorus diffused emitters and impact on solar cell efficiencies”, 43rd IEEE PVSC, Portland, U.S., 6-10 Jun 2016

Limpert, S., Bremner, S., Conibeer, G., Anttu, N., and Linke, H., “Absorption in and scattering from single horizontal Au-contacted InAs/Inp heterostructure nanowires”, 2016/08/17/, 16th International Conference on Numerical Simulation of Optoelectronic Devices, Sydney, Australia, 11-15 Jul 2016

Liu, A., “Shallow Dopant(s) in silicon revealed by photoluminescence Spectra”, 3rd Asia Pacific Solar Research Conference, Canberra, 29 Nov - 1 Dec 2016

Liu, S., “Exploring the potential and limitations of interdigitated back contact solar cells using experimentally validated Quokka 3-D simulation”, 3rd Asia Pacific Solar Research Conference, Canberra, 29 Nov - 1 Dec 2016

Liu, Z., “The development of novel nanocluster-based buffer layers for multi-junction solar cells”, 3rd Asia Pacific Solar Research Conference, Canberra, 29 Nov - 1 Dec 2016

Lu, J., “Stabilizing the organic-inorganic perovskite with an ‘eclipsed’ arrangement structure: from

Van der Waals forces to chemical bonds", 4th ACAP Conference and 3rd Asia Pacific Solar Research Conference, Canberra, 1 Dec 2016

Lunardi, M., Ho-Baillie, A., Moore, S., Alvarez-Gaitan, J.P. and Corkish, R., "Life cycle assessment and energy payback time of perovskite/Si tandem solar cells", 3rd Asia Pacific Solar Research Conference, Canberra, 29 Nov - 1 Dec 2016

Ma, F., Li, M., and Hameiri, Z., "Advanced evaluation of surface passivation nonuniformity from photoluminescence imaging of undiffused lifetime samples", 26th International Photovoltaic Science and Engineering Conference, Singapore, 24-28 Oct 2016

Ma, Q., "Inorganic CsPbI2Br perovskite solar cells", 3rd Asia Pacific Solar Research Conference, Canberra, 29 Nov - 1 Dec 2016

Mahmud, M.A., Elumalai, N.K., Upama, M.B., Wang, D., Wright, M., Chan, K.H., Xu, C., Uddin, A., "Performance enhancement with doped P3HT in a low temperature solgel ZnO processed perovskite solar cell", 43rd IEEE Photovoltaic Specialists Conference, 5–10 June, 2016, Portland, Oregon, USA

Mahmud, M.A., Wright, M., Elumalai, N.K., Xu, C., Mahmud, M.A., Wang, D., Chan, K.H., Uddin, A., "Sensitization of PTB7:PC71BM organic solar cells by using Si-PCPDTBT", 43rd IEEE Photovoltaic Specialists Conference, 5–10 June, 2016, Portland, Oregon, USA

Meredith, P., "From molecules to MWs: solar PV research at UQ", School of Photovoltaics and Renewable Energy Engineering Seminar Series, UNSW Sydney, 2016

Meredith, P., "Organohalide perovskite photodetectors", Karlsruhe Institute of Technology Lecture Series, Germany, 20 Jun 2016

Meredith, P., Armin, A., Hambsch, M., Lin, Q., Burn, P.L., "Scaling physics of thin film solar cells", HOPV, Swansea, UK, 28 Jun - 1 Jul 2016

Meredith, P., Armin, A., Stolterfoht, M., Lin, Q., Burn, P.L., "Optoelectronics of thin film solar cells", Gordon Research Conference, Italy, 5 - 10 Jun 2016

Milhuisen, R., "Metal complex-based hole transport materials for thin film solar cells", 4th ACAP Conference and 3rd Asia Pacific Solar Research Conference, Canberra, 1 Dec 2016

Mitchell, V., "Amphiphilic block copolymers as organic photovoltaics: Towards industrially relevant solubilities", 4th ACAP Conference and 3rd Asia Pacific Solar Research Conference, Canberra, 1 Dec 2016

Mulmudi, H., "Investigating phase segregation in Rubidium based mixed cation perovskite solar cells using cathodoluminescence", 3rd Asia Pacific Solar Research Conference, Canberra, 29 Nov - 1 Dec 2016

Nagiri, R., "Morphology characterization of the active layer and interfaces in organic solar cells", 3rd Asia Pacific Solar Research Conference, Canberra, 29 Nov - 1 Dec 2016

Nagiri, R., "Morphology characterization of the active layer and interfaces in organic solar cells", 4th ACAP Conference and 3rd Asia Pacific Solar Research Conference, Canberra, 1 Dec 2016

Neto, N., "Desymmetrised building blocks for controlled synthesis of conjugated materials", 4th ACAP Conference and 3rd Asia Pacific Solar Research Conference, Canberra, 1 Dec 2016

Nguyen, H., "Detecting heavily-doped layers using micro-photoluminescence Spectroscopy", 3rd Asia Pacific Solar Research Conference, Canberra, 29 Nov - 1 Dec 2016

Park, J., Zi, O., Yan, C., Green M.A. and Hao, X., "Mechanical transfer of pre-annealed Ag nanowire network on ITO electrode for Cu2ZnSnS4 solar cells", 43rd IEEE Photovoltaic Specialists Conference, Portland, OR, 5-10 June 2016.

Peng, J., "Efficient Indium-Doped TiOx electron Transport layers for high-performance perovskite solar cells and perovskite-silicon tandems", 3rd Asia Pacific Solar Research Conference, Canberra, 29 Nov - 1 Dec 2016

Pheng, P., "N-type high-performance Multicrystalline and Quasi-Monocrystalline silicon Wafers with Lifetimes above 2ms", 3rd Asia Pacific Solar Research Conference, Canberra, 29 Nov - 1 Dec 2016

Ramamurthy, J., "Alternate Counter electrode", 3rd Asia Pacific Solar Research Conference, Canberra, 29 Nov - 1 Dec 2016

Römer, U., "The transport mechanism of carrier selective poly-Si / c-Si junctions – tunneling vs. pinholes", 3rd Asia Pacific Solar Research Conference, Canberra, 29 Nov - 1 Dec 2016

Rothmann, M., "Direct observation of intrinsic twin domains in tetragonal CH3NH3PbI3", 4th ACAP Conference and 3rd Asia Pacific Solar Research Conference, Canberra, 1 Dec 2016

Rougieux, F., "High efficiency Upgraded Metallurgical grade silicon cells", 3rd Asia Pacific Solar Research Conference, Canberra, 29 Nov - 1 Dec 2016

Schwarz, K., "Suppressing sub-nanosecond bimolecular charge recombination in a high performance organic photovoltaic material", 4th ACAP Conference and 3rd Asia Pacific Solar Research Conference, Canberra, 1 Dec 2016

Schwarz, K., "The Role of Spin and Nanoscale Morphology in an Organic Photovoltaic Heterojunction", 3rd Asia Pacific Solar Research Conference, Canberra, 29 Nov - 1 Dec 2016

Sepalage, G., “Solution-processed CuSCN as a hole transporting material and its implications on performance and stability of perovskite solar cells”, 4th ACAP Conference and 3rd Asia Pacific Solar Research Conference, Canberra, 1 Dec 2016

Shen, H. “Analysis of the hysteresis behaviour and response time of perovskite solar cells due to both perovskite film and electron transport material”, 3rd Asia Pacific Solar Research Conference, Canberra, 29 Nov - 1 Dec 2016

Shi, A., “Accelerated Lifetime Testing of Organic-Inorganic perovskite solar cells Encapsulated by Poly-isobutylene”, 3rd Asia Pacific Solar Research Conference, Canberra, 29 Nov - 1 Dec 2016

Simonds, B.J., Teal, A., Zhang, T., Hadler, J., Zhou, Z., Varlamov, S., and Perez-Würfl, I., “Dual-Beam Laser Thermal processing of silicon Photovoltaic Materials”, in Proceedings of SPIE - The International Society for optical Engineering, Laser Applications in Microelectronic and Optoelectronic Manufacturing (LAMOM) XXI, Beat Neuenschwander; Stephan Roth; Costas P. Grigoropoulos; Tetsuya Makimura, San Francisco, California, U. S. 13 Feb 2016 http://dx.doi.org/10.1117/12.2213583

Sio, H., “Recombination behaviour of p-type high performance multicrystalline silicon before and after phosphorus diffusion and hydrogenation”, 3rd Asia Pacific Solar Research Conference, Canberra, 29 Nov - 1 Dec 2016

Soeriyadi, A.H., Wang, L., Conrad, B., Zhao, X., Li, D., Lochtefeld, A., Gerger, A., Barnett, A., and Perez-Wurfl, I., “Spatially Resolved EI and PI Coupling of a Dual Junction solar cell”, 43rd IEEE PVSC, Portland, U.S. , 6-10 Jun 2016

Soeriyadi, A.H., Wang, L., Conrad, B., Zhao, X., Li, D., Lochtefeld, A., Gerger, A., Barnett, A., and Perez-Wurfl, I., “Solar cell Parameters Extraction of Subcells in a Dual Junction System through a Three Terminal Device Design”, PVSEC-26, Singapore, 24-28 Oct 2016

Song, N., Chen, J., Yan, C., Wen, X., Hao X. and Green, M.A., “Effect of a ZnS Intermediate layer on Properties of Cu2ZnSnS4 films from Sputtered Zn/CuSn Precursors on Si (100) Substrate”, 43rd IEEE Photovoltaic Specialists Conference, Portland, OR, 5-10 June 2016.

Soufiani, A., “Lessons Learnt from Spatially-resolved electro- and Photo-luminescence Imaging: Interfacial Delamination in CH3NH3PbI3 Planar perovskite solar cells upon Illumination”, 3rd Asia Pacific Solar Research Conference, Canberra, 29 Nov - 1 Dec 2016

Stocks, M. “Performance advantages of series-parallel connection of tandem solar cells”, 3rd Asia Pacific Solar Research Conference, Canberra, 29 Nov - 1 Dec 2016

Stoltzfus, D., “Thiophene dendrimer-based low donor content solar cells”, 4th ACAP Conference and 3rd Asia Pacific Solar Research Conference, Canberra, 1 Dec 2016

Subbiah, J., “Fabrication of efficient organic solar cells: Device optimization and scale-up”, 4th ACAP Conference and 3rd Asia Pacific Solar Research Conference, Canberra, 1 Dec 2016

Sun, C., “Activation Kinetics of the Boron-Oxygen defect in Compensated n- and p-type silicon Studied by high-Injection Micro-photoluminescence”, 3rd Asia Pacific Solar Research Conference, Canberra, 29 Nov - 1 Dec 2016

Sun, C., Nguyen, H.T., Rougieux, F.E., and Macdonald, D., “Characterization of Cu and Ni precipitates in n- and p-type Czochralski-grown silicon by photoluminescence”, 6th International Conference on Crystalline silicon Photovoltaics (SiPV), Chambery, France 2016

T. Allen T., et al., “Calcium-based electron contacts to n-type PERC cells”, European Photovoltaic Solar Energy Conference, Munich, 2016

T. Allen T., et al., “Low resistance TiO2-passivated calcium contacts to for crystalline silicon solar cells”, 43rd IEEE Photovoltaic Specialists Conference, Portland, 6-10 Jun 2016

Teymouri, A., “Transparent Conductive film for Emerging Heat-Sensitive Devices”, 3rd Asia Pacific Solar Research Conference, Canberra, 29 Nov - 1 Dec 2016

Teymouri, A., Pillai, S., Ouyang, Z., Hao X. and Green, M.A., “Promising hybrid graphene-silver nanowire transparent conductive electrode”, 43rd IEEE Photovoltaic Specialists Conference, Portland, OR, 5-10 June 2016.

To, A., “Advanced modelling of the recombination rate at inverted p+ silicon surfaces: A novel method for the extraction of fixed interface charge”, 3rd Asia Pacific Solar Research Conference, Canberra, 29 Nov - 1 Dec 2016

Uddin, A., “Optical modelling of semi-Transparent OPV Devices”, 16th International Conference on Numerical Simulation of Optoelectronic Devices, Sydney, Australia, 11-15 Jul 2016

Uddin, A., “Organic-inorganic Hybrid Photovoltaic Research and Achievement”, Energy Future Conference, UNSW Sydney, Australia, 4-6 July 2016.

Uddin, A., “Surface Plasmonic effects on Organic solar cells”, Nanotech conference -2016 Dubai, UAE, 21–23 April 2016.

Upama, M.B., Wright, M., Elumalai, N.K., Mahmud, M.A., Wang, D., Chan, K.H., Xu, C., Haque, F., Uddin, A., “Optical modelling of semi-transparent OPV devices”, NUSOD 2016, University of Sydney, 11–15 July 2016.

Vak, D., “Flexible electronics Capability at CSIRO”, 4th ACAP Conference and 3rd Asia Pacific Solar Research Conference, Canberra, 1 Dec 2016

Vargas Castrillon, C.A., Hameiri, Z.H., and Coletti, G.C., “Revision of the temperature Dependence of Iron-Acceptors Association Rate”, Photovoltaics science and engineering conference PVSEC-26, Singapore, 24-28 Oct 2016

Wan, Y., Samundsett, C., Bullock, J., Yan, D., Allen, T., Zheng, P., Zhang, X., Cui, J., “Magnesium fluoride based electron-selective contact”, 43rd IEEE PVSC, Portland, U.S. , 6-10 Jun 2016, pp. 2540-2542

Wang, D., Elumalai, N.K., Mahmud, M.A., Upama, M.B., Wright, M., Chan, K.H., Xu, C., Uddin, A., “Effect of PCBM film thickness on the performance of inverted perovskite solar cells”, 43rd IEEE Photovoltaic Specialists Conference, 5–10 June, 2016, Portland, Oregon, USA.

Wang, P., Wen, X., Shrestha, S., Conibeer, G., and Aguey-Zinsou, K., “Metal Hydrides as Hot Carrier solar cell Absorber”, in Proc. SPIE 9937, Next Generation Technologies for Solar Energy Conversion VII, 993707 Oleg V. Sulima; Gavin Conibeer, San Diego, California, U.S. 23 Sep 2016 doi:10.1117/12.2242400, 2016

Wang, S., Mai, L., Wenham, A., Hameiri, Z., Chan, C., Hallam, B., Sugianto, A., Chong, C.M., Ji, J., Shi, Z., and Wenham, S., “Laser Hydrogenation of Laser Doped and Grooved solar cells”, 32nd European Photovoltaic Solar Energy Conference and Exhibition, Munich Germany, 20-24 Jun 2016

Weerasinghe, H., “Encapsulation and De-cohesion Analysis of Printed Photovoltaics”, 4th ACAP Conference and 3rd Asia Pacific Solar Research Conference, Canberra, 1 Dec 2016

Weerasinghe, H., “Lifetime Assessment of Printed Photovoltaic Devices”, 4th ACAP Conference and 3rd Asia Pacific Solar Research Conference, Canberra, 1 Dec 2016

Wenham, A., Chong, C.M., Wang, S., Ji, J., Shi, Z., Mai, L., Sugianto, A., Wenham, S., Barnett, A., and Green, M., “Laser Formed Anchor Points for Copper Plating Adhesion on Al-Bsf and Perc cells”, 32nd European Photovoltaic Solar Energy Conference and Exhibition, Munich, Germany, 20-24 Jun 2016

Wenham, A.M., Chong, C.M., Wang, S., Chen, R., Ji, J., Shi, Z., Mai, L., Sugianto, A., Wenham, S., Barnett, A., and Green, M., “Copper Plated contacts for Large-Scale Manufacturing”, 43rd IEEE PVSC, Portland, U.S. , 6-10 Jun 2016

Wu, Y.-L., “Grain boundary characterization using Cathodoluminescence and photoluminescence mapping of large grained perovskite films”, 3rd Asia Pacific Solar Research Conference, Canberra, 29 Nov - 1 Dec 2016

Yan D., et al., “Passivating contacts for silicon solar cells with a double SiOx/SiNx interlayer”, 26th International Photovoltaic Science and Engineering Conference (“PVSEC-26”), Singapore October 2016

Yan, D., “Passivating contacts for silicon solar cells based on recrystallised amorphous silicon”, 4th ACAP Conference and 3rd Asia Pacific Solar Research Conference, Canberra, 1 Dec 2016

Yazmaciyan, A., “On The Role Of Fullerene Percolation Pathways In Charge Generation And Charge Extraction In Polymer: Fullerene Organic solar cells”, 4th ACAP Conference and 3rd Asia Pacific Solar Research Conference, Canberra, 1 Dec 2016

Yazmaciyan, A., “On The Role Of Fullerene Percolation Pathways In Charge Generation And Charge Extraction In Polymer:Fullerene Organic solar cells”, 3rd Asia Pacific Solar Research Conference, Canberra, 29 Nov - 1 Dec 2016

Ye, Q., “Rear thermally diffused point contact solar cell with dielectric breakdown”, 3rd Asia Pacific Solar Research Conference, Canberra, 29 Nov - 1 Dec 2016

Yoon, W., Lochtefeld, A., Kotulak, N., Scheiman, D., Barnett, A., Jenkins, P., and Walters, R., “Enhanced surface passivation of Epitaxially Grown Emitters for high-efficiency Ultrathin Crystalline Si solar cells”, 43rd IEEE PVSC, Portland, U.S. , 6-10 Jun 2016

Zafirovska, I., Juhl, M.K., Weber, J.W., Kunz, O., and Trupke, T., “Module inspection using line scanning photoluminescence imaging”, 32nd European Photovoltaic Solar Energy Conference and Exhibition (32nd EU PVSEC), Munich, Germany, 6-10 Jun 2016

Zhang, B., “Molecular insulated chromophores for luminescence solar concentrators”, 4th ACAP Conference and 3rd Asia Pacific Solar Research Conference, Canberra, 1 Dec 2016

Zhang, S., “Interface engineering of solution processed organohalide perovskite solar cells”, 4th ACAP Conference and 3rd Asia Pacific Solar Research Conference, Canberra, 1 Dec 2016

Zhang, S., “Interface engineering of solution processed organohalide perovskite solar cells”, 3rd Asia Pacific Solar Research Conference, Canberra, 29 Nov - 1 Dec 2016

Zhang, Z., “Using CsPbBr3 perovskite nanoparticles to boost the efficiency of PbSe quantum dot solar cells”, 3rd Asia Pacific Solar Research Conference, Canberra, 29 Nov - 1 Dec 2016

Zhang,X., Cuevas, A., Bullock, J., “Characterisation of sputtering deposited amorphous silicon films for silicon heterojunction solar cells”, 43rd IEEE PVSC, Portland, U.S. , 6-10 Jun 2016, pp. 0073-0076

Zheng, P., Rougieux, F.E., Samundsett, C., Yang, X., Wan, Y., Degoulange, J., Einhaus, R., Rivat, P., and Macdonald, D., "Simulation of 20.96% efficiency n-type Czochralski UMG silicon solar cell", 6th International Conference on Crystalline silicon Photovoltaics (SiPV), Chambery, France (2016)

Zhu, Y., Castrillon, C.V., Jensen, M.A., Juhl, M.K., Coletti, G., and Hameiri, Z., Defect characterization via temperature and injection dependent lifetime spectroscopy', 9th International Workshop on Crystalline silicon for Solar cells and 3rd Silicon Materials Workshop, Tempe, AZ, U.S. 10-12 Oct 2016

Zin, N., McIntosh, K., Kho, T., Franklin, E., Fong, K., Stocks, M., Wang, E.-C., Ratcliff, T. and Blakers, A., "Rounded rear pyramidal texture for high efficiency silicon solar cells", IEEE 43rd Photovoltaic Specialist Conference, 5–10 June, 2016, Portland, Oregon, USA

8.6 Theses

An, Xin Rui, "High performance thin silicon solar cells", PhD, UNSW, 2016

Baerhujin, Qiaoke, "Photoluminescence spectroscopy for understanding light management in solar cells", PhD, ANU, 2015

Banal, James, "Spectral downshifting by molecular aggregates in planar concentrators for solar energy conversion", PhD, UoM, 2016

Bhargava, Rishabh, "Dual-function smart electrolytes for novel design of dye-sensitized solar cells", Masters, MONASH, 2016

Borojevic, Nino, "Novel texturing and patterning techniques for silicon solar cells", PhD, UNSW, 2016

Chandrasekharan, Ajeesh, "Low Optical Gap Materials for organic solar cells - Research and Application", PhD, UQ, 2015

Chen, Jian, "Kesterite thin film solar cell fabricated by sulphurising sputtered metallic/metal-sulphide precursor",

Han, Jianshu, "Fabrication and analysis of ultra-thin Si solar cell", PhD, UNSW, 2016

Huang, Wenchao, "Understanding the relationship between morphology and device performance in organic solar cells", PhD, Monash, 2016

Jia, Xuguang, "All silicon .tandem solar cell: optical characterization, practical energy conversion limitation and possible routes for improvement", PhD, UNSW, 2016

Jiang, Wei, "Complementary materials for tandem organic solar cells", PhD, UQ, 2015

Jiang, Yajie, "Optical properties for photovoltaics: silver and perovskite", PhD, UNSW, 2015

Kim, Il Ku, "Light detection and harvesting systems using organic semiconductors", PhD, UQ, 2016

Lan, Dongchen, "Light absorption and emission in photovoltaic devices", PhD, UNSW, 2016

Li, Xin, "Development of organic photodetector materials", PhD, UQ, 2016

Li, Yang, "A new optical modelling framework for photovoltaic devices", PhD, UNSW, 2016

Li, Zhongtian, "Aerosol patterned rear contact silicon solar cells", PhD, UNSW, 2016

Lin, Qianqian, "Opto-electronics of perovskite solar cells and photodetectors", PhD, UQ, 2016

Lin, Shu, "Investigation of silver sulfide nanoparticles for hot carrier solar cell absorber", PhD, UNSW, 2016

Liu, Xiaolei, "Molybdenum back contact treatment for Cu2ZnSnS4 solar cells", PhD, UNSW, 2016

Lu, Zhong, "Use of anodic aluminium oxide for contacting silicon solar cells", PhD, UNSW, 2016

McKinley, Arnold Fredric, "The physics and mathematical theory of nano-scaled ring resonators and loop antennas", PhD, ANU, 2014

Pakhuruddin, Mohd, "Development of light-trapping schemes in evaporated laser-crystallised silicon thin-film solar cells on glass superstrates", PhD, UNSW, 2016

Pascoe, Alexander, "Charge transport and recombination in hybrid organic-inorganic solar cells", PhD, Monash, 2016

Paz, Simon, "Tridentate and macrocyclic cobalt Complexes as Redox Mediators in p-Type Dye-sensitised solar cells", Hons., Monash, 2016

Rodriguez, John, "Aerosol jet etched solar cells", PhD, UNSW, 2016

Shu, Lin, "Investigation of silver sulfide nanoparticles for hot carrier solar cell absorber", PhD, UNSW, 2016

Sio, Hang Cheong, "Carrier recombination in multicrystalline silicon: a study using photoluminescence imaging", PhD, ANU, 2015

Song, Aaron, "Functional conjugated polymers – from design to devices", PhD, UoM, 2016

Song, Ning, "Epitaxial Growth of Cu2ZnSnS4 thin films for tandem solar cells", PhD, UNSW, 2015

Stolterfoht, Martin, "Charge generation and transport phenomena in disordered organic semiconductors and photovoltaic diodes", PhD, UQ, 2016

Vu, Kuyen, "Toward the synthesis of semi-conducting brush polymer for organic solar cells", Masters, UoM, 2016

Wang, Haotian, “Large area organic solar cells: fabrication and optimization”, Masters, UoM, 2016.

Wang, Kai, “Theoretical study of time-resolved photoluminescence from silicon wafers and bricks”, PhD, UNSW, 2016

Western, Ned, “Hydrogen passivation of silicon solar cells”, PhD, UNSW, 2016

Wu, Lingfeng, “Silicon nanocrystal solar cells on dielectric substrates”, PhD, UNSW, 2016

Xia, Hongze, “Theoretical study and characterisation of hot carrier solar cell materials”, PhD, UNSW, 2016

Xiao, Manda, “High performance hybrid thin film solar cells”, PhD, Monash, 2016

Yang Chien-Jen Terry, “Transparent conducting aluminium doped zinc oxide for silicon quantum dot solar cell devices in third generation photovoltaics”, PhD, UNSW, 2016

Yun, Jae Sung, “Material and electrical properties of liquid phase crystallised silicon r-film solar cells on glass”, PhD, UNSW, 2015

Zhao, Xin, “Design, fabrication, characterization and optimization of SiGe solar cell in a GaAsP/SiGe dual junction solar cell system”, PhD, UNSW, 2016

Zhou, Fangzhou, “An investigation into carbon intermediate layer at CZTS/Mo back contact and the effect of RTP conditions on CZTS-based thin film solar cells” , Masters, UNSW, 2016

Obituary for Professor Leone Spiccia

14.03.1957 – 18.12.2016

It is with great sadness that we note the passing of Professor Leone Spiccia. Leone was an ACAP chief investigator and led the Monash node together with his colleagues Professor Yi-Bing Cheng and Professor Udo Bach.

Leone graduated with a BSc (Hons) and gained a PhD from the University of Western Australia. He worked as a postdoctoral fellow at the universities of Calgary, Neuchatel and the ANU, before being appointed to a lectureship in Chemistry at Monash University in 1987. Leone rose rapidly to Senior Lecturer (1994), Reader (1999) and then Professor in 2006. He also acted as Deputy Head of Chemistry from 2003 to 2006 and Deputy Dean from 2006 to 2008.

Leone held visiting professorships at the Heidelberg University and the École Polytechnique Fédérale de Lausanne and was recently a specially appointed Professor in the Catalyst Research Centre at Hokkaido University in Japan. His awards include the Burrows Award of the Inorganic Division of the Royal Australian Chemical Institute (RACI), a Discovery Outstanding Researcher Award of the ARC, a Helmholtz International Fellowship, an Alexander von Humboldt Senior Research Fellowship and the H.G. Smith Medal of the RACI.

With Leone we lost an amazing friend, colleague, supervisor and mentor. His ideas and discoveries shaped the research fields in which he was active from solar energy to cancer therapy.

Through our future involvement in ACAP we vow to keep his legacy alive for years to come.

Australian Centre for Advanced Photovoltaics
Australia-US Institute for Advanced Photovoltaics

UNSW Sydney NSW 2052 Australia

Tel +61 2 9385 4018
Fax +61 2 9662 4240
Email: acap@unsw.edu.au

www.ausiapv.net.au
www.acap.net.au

Director: Scientia Professor Martin Green

Acknowledgements

Written and compiled by
Australian Centre for Advanced Photovoltaics
Australia-US Institute for Advanced Photovoltaics

Photos, figures and graphs
Courtesy of Centre staff, students and others

Cover image by Yajie Jiang
EBSD orientation map of the grain structure of Ag film annealed at 400 degree for 10 minutes. Different grain orientations are highlighted with various colours. The twin/grain boundaries are marked in black lines. A high density of twins is randomly located within normal grains.